PREMIER REFERENCE SOURCE

Dental Computing and Applications

Advanced Techniques for Clinical Dentistry

Andriani Daskalaki

Dental Computing and Applications:
Advanced Techniques for Clinical Dentistry

Andriani Daskalaki
Max Planck Institute for Molecular Genetics, Germany

Medical Information Science
REFERENCE

MEDICAL INFORMATION SCIENCE REFERENCE
Hershey · New York

Director of Editorial Content: Kristin Klinger
Senior Managing Editor: Jamie Snavely
Managing Editor: Jeff Ash
Assistant Managing Editor: Carole Coulson
Typesetter: Carole Coulson
Cover Design: Lisa Tosheff
Printed at: Yurchak Printing Inc.

Published in the United States of America by
Information Science Reference (an imprint of IGI Global)
701 E. Chocolate Avenue, Suite 200
Hershey PA 17033
Tel: 717-533-8845
Fax: 717-533-8661
E-mail: cust@igi-global.com
Web site: http://www.igi-global.com/reference

and in the United Kingdom by
Information Science Reference (an imprint of IGI Global)
3 Henrietta Street
Covent Garden
London WC2E 8LU
Tel: 44 20 7240 0856
Fax: 44 20 7379 0609
Web site: http://www.eurospanbookstore.com

Library of Congress Cataloging-in-Publication Data

Dental computing and applications : advanced techniques for clinical dentistry / Andriani Daskalaki, Editor.
p. cm.
Summary: "This book gives insight into technological advances for dental practice, research and education, for general dental clinician, the researcher and the computer scientist"--Provided by publisher. Includes bibliographical references and index.
ISBN 978-1-60566-292-3 (hardcover) -- ISBN 978-1-60566-293-0 (ebook) 1. Dental informatics 2. Dentistry--Data processing. 3. Dentistry--Technological innovations. I. Daskalaki, Andriani, 1966- RK240.D446 2009 617'.075--dc22

2008045881

British Cataloguing in Publication Data
A Cataloguing in Publication record for this book is available from the British Library.

Editorial Advisory Board

Table of Contents

Section II
Software Support in Oral Surgery

Section III
Software Support in Tissue Regeneration Proceeders in Dentistry

Section IV
Software Support in Dental Implantology

Section V
Software Support in Clinical Dental Management and Education

Detailed Table of Contents

These results prompted Vogel to conduct the registration and fixation of the mandible position under defined pressure (10 to 30 N), creating a final method of measurement which gives objective, reproducible and documentable results. The existent system—DIR®System—is on the market, consisting of: Measuring sensor, WIN DIR software, digital multichannel measuring amplifier, plan table with step motor, carrier system and laptop.

Section II
Software Support in Oral Surgery

This chapter discusses the requirements of an image analysis tool designed for dentistry and oral and maxillofacial surgery focussing on 3D-image data. As software for the analysis of all the different types of medical 3D-data is not available, a model software based on VTK (visualization toolkit) is presented. VTK is a free modular software which can be tailored to individual demands. First, the most important types of image data are shown, then the operations needed to handle the data sets. Metric analysis is covered in-depth as it forms the basis of orthodontic and surgery planning. Finally typical examples of different fields of dentistry are given.

This chapter shows how large improvement in image quality can be obtained when radiographs are filtered using adequate statistical models. In particular, it shows that impulsive noise, which appears as random patterns of light and dark pixels on raw radiographs, can be efficiently removed. A switching median filter is used to this aim: failed pixels are identified first and then corrected through local median filtering. The critical stage is the correct identification of the failed pixels. We show here that a great improvement can be obtained considering an adequate sensor model and a principled noise model, constituted of a mixture of photon counting and impulsive noise with uniform distribution. It is then shown that contrast in cephalometric images can be largely increased using different grey levels stretching for bone and soft tissues. The two tissues are identified through an adequate mixture derived from histogram analysis, composed of two Gaussians and one inverted log-normal. Results show that both soft and bony tissues are clearly visible in the same image under wide range of conditions. Both filters work in quasi-real time for images larger than five Mega-pixels.

offered to universities and scientific community. They can enter into collaboration by contributing to the Dental Digital Library knowledge base. In return, access would be granted for educational and research purposes, thus stimulating knowledge and information exchange. In the future, similar benefits may be mutually exchanged with regulatory bodies and Standards Development Organizations (SDOs).

The present chapter deals with the introduction and implementation of rapid prototyping technologies in medical and dental field. Its purpose is to overview the advantages and limitations derived, to discuss the current status and to present the future directions, especially in dental sector. Furthermore, a flow-chart is outlined describing the procedure from the patient to the final 3-D object, presenting the possibles alternatives in the process. Finally, an example is presented, decribing the process of the construction of high accurate surgical guided templates in dental implantology, through rapid prototyping.

In this chapter, we report the minimal set of characters from the Unicode Standard that is sufficient for the notation of human dentition in Zsigmondy-Palmer style. For domestic reasons, the Japanese Ministry of International Trade and Industry expanded and revised the Japan Industrial Standard (JIS) character code set in 2004 (JIS X 0213). More than 11,000 characters that seemed to be necessary for denoting and exchanging information about personal names and toponyms were added to this revision, which also contained the characters needed for denoting human dentition (dental notation). The Unicode Standard has been adopted for these characters as part of the double-byte character standard, which enabled, mainly in eastern Asian countries, the retrieval of human dentition directly on paper or displays of computers running Unicode-compliant OS. These countries have been using the Zsigmondy-Palmer style of denoting dental records on paper forms for a long time. We describe the background and the application of the characters for human dentition to the exchange, storage and reuse of the history of dental diseases via e-mail and other means of electronic communication.

Foreword

Dental Science, like much of the evolution of human civilization, progresses in steps that are often the result of the complex relationship between science, empirical knowledge, and advances in technology. Over the years some of these have been peculiar to dentistry, but most of the time they have been part of wider movements, associated with the driving impact of discoveries and technological development. In the history of science there have been leaps forward linked to improvements in observation, such as the telescope and the microscope, or in measurement with the invention of accurate time pieces. Perhaps no development (since Aristotle laid the foundations of modern science nearly two and a half millennia ago) has had such a far reaching and in-depth impact on scientific thinking, research and practice as the advent of the computer. Computing has modified our perception, the sense and use and interpretation of time and enabled scientists to perform existing procedures far faster and more accurately than ever; it has allowed them to make a reality of things they had only dreamed of before; and perhaps of greater consequence and more excitingly, it has often stimulated them to perceive and focus on their subject with new eyes; to see it on a different scale from a completely different perspective.

The almost meteoric speed of improvements in hardware following Moore's Law and the parallel developments in software have meant that previously unimaginable amounts of computing power are now available to scientists and practitioners in a form that can be carried around in a briefcase. The burgeoning development of "cloud computing" currently underway means that the individual at their practice, in the laboratory, in office or at home, will soon have the power of a mainframe computer at their fingertips. Thus, quantitative and qualitative information can be gathered via constantly developing resources, tools and support to create a much more realistic and detailed picture of health and disease.

Dentistry is a particularly complex and sophisticated applied science; every problem to be solved is as unique as the individual, no two faces, two mouths or even two teeth are identical. To navigate from observation to diagnosis and then to the most appropriate therapeutic solution in a situation with multiple variables and degrees of freedom, the dentist has to draw on scientific knowledge from a wide range of specialist disciplines. This knowledge has to be combined with experience and judgement and the resulting diagnosis and treatment planning implemented in the form of therapy by means of the clinical wisdom and manual dexterity accrued through years of training and practice. Furthermore, in many cases the success of the final result will also depend on the dentist's sense of colour and aesthetics.

This book amply illustrates how the use of computing related technology in dentistry has expanded beyond statistical number crunching and information retrieval to make an imaginative and creative contribution to almost every aspect of dental science. In some of these areas, digital technology may go much further than enhancing current approaches and technologies and fundamentally change many of the factors that make up the way the subject is conceived. Scientific knowledge from other areas such as engineering and mathematics and biology can now be more easily applied to dental and oral and maxillofacial problems. Computers will not only transform the way dentists will work in the near future, they also have the potential to reformulate the ways that we think about many aspects of our continuously broadening and deepening medical discipline.

It is a privilege and a pleasure to write a foreword to a book that makes a significant contribution to the shape of things to come in dentistry. Contributions in this book illustrate the progress that has been made in applying computing to such diverse areas and topics as chephalometric, 3D-time, finite element and image analyses, 3-D reconstruction and guided surgery, modelling and shrinkage and stress of materials, intraoral registration, tissue engineering of teeth, clonogenic assays, health records, a library for dental biomaterials, rapid prototyping , unicode characters for human dentition and even virtual dental practices and environments. All of these document the creativity and persistence of dedicated scientists pursuing the goal of unravelling the dynamics of living structures and functions and supporting problem solving processes and management in oral and maxillofacial surgery, oral radiology, restorative and prosthetic dentistry, orthodontics, endodontics, dental implantology and practically every field of dental practice, research and education.

The dentist of the future will have new and powerful tools to help in the processes of diagnosis, analysis, calculation, prediction and treatment. Computing and its related technologies will help dentists to work faster, with greater knowledge and awareness of the situation they are dealing with to implement solutions that are more effective and have a more certain prognosis. With such a complex and multifaceted science however, the role of the individual practitioner in selecting, orchestrating and implementing this array of exciting new possibilities will be enhanced, but remain unchallenged.

Petros Koidis
December 2008

***Petros Koidis** was born in Kozani, Greece 1957. He is professor and chairman of the Department of Fixed Prosthesis and Implant Prosthodontics at the School of Dentistry in the Aristotle University of Thessaloniki, in Greece and, since 2007 he is visiting professor in the School of Dentistry at the University of Belgrade, in Serbia. He is a graduate of Aristotle University of Thessaloniki, where he conducted his PhD in temporomandibular disorders. He obtained the degree of Master of Science at The Ohio State University (Columbus, USA), where he was also trained in Advanced Fixed and Removable Prosthodontics. His research interests include the links of prosthetic rehabilitation, biomaterials, temporomandibular disorders and computer-aided design and engineering. He is internationally renowned for his scientific work, having published over than 100 articles and having presented them in over than 170 meetings and conferences, for which he is the recipient of several awards and honors.*

Preface

Computer and Information Technology have transformed society and will continue to do so in the future. An increasing number of dentists use a variety of computer technologies, including digital intraoral cameras and paperless patient records.

The topic of dental computing is related to the application of computer and information science in dentistry. Dental computing produces an increasing number of applications and tools for clinical practice. Dental computing support research and education, and improvements in these areas translate into improved patient care. Dentists must keep up with these developments to make informed choices. Dental computing present possible solutions to many longstanding problems in dental practice, research, and program administration, but it also faces significant obstacles and challenges. The dental computing experts in this book conducted literature reviews and presented issues surrounding dental computing and its applications.

The aim of the book is to gain insight into technological advances for dental practice, research, and education. We aimed this book at the general dental clinician, the researcher, and the computer scientist.

ORGANIZATION OF THE BOOK

The book is roughly divided into five sections:

Section I: Software Support in Clinical Dentistry, introduces the basic concepts in the use of computational tools in clinical dentistry. Chapter I starts with a brief introduction of geometric morphometric (GM) methods, including procrustes superimposition, principal component analysis. This chapter discusses the principles and guidelines of CT technology used in dentistry. Finally, the Viewbox software is described, a tool that enables practical application of sophisticated diagnostic and research methods in Orthodontics. Chapter II presents a toolchain including image segementation, registration and 3D visualization that allows a time series analysis based on DICOM CT images. Chapter III describes the shrinkage concepts that will improve clinical understanding for management of shrinkage stress, and help design and assess polymerization shrinkage research. Chapter IV describes a computer-controlled systems for registration the position of the mandible.

Section II: Software Support in Oral Surgery, serves as a comprehensive introduction to computational methods supporting oral surgery. Chapter V discusses the requirement of an image analysis tool designed for dentistry and oral and maxillofacial surgery focussing on 3D-image data. Chapter VI shows how large improvements in image quality can be obtained when radiographs are filtered using adequate statistical models. Chapter VII provides information related to 3D reconstructions from few projections in Oral Radiology.

Section III: Software Support in Tissue Regeneration Proceeders in Dentistry, provides examples of application supporting research in regeneration dentistry. Chapter VIII deals with overcoming the drawbacks of the currently available tooth replacement techniques by tissue engineering, the success achieved in it at this stage and suggestions on the focus for future research. Chapter IX introduces a cost-effective and fully automatic bacterial colony counter which accepts digital images as its input.

Section IV: Software Support in Dental Implantology, describes informatic tools and techniques which can serve as a valuable aide to implantology procedures. In Chapter X the author describes a new system for guided surgery in implantology. Chapter XI summarizes latest results on developing software tools for improving imaging and graphical modelling techniques in computerized dental implatology. Chapter XII covers published Finite Elements Analysis (FEA) literature on dental implant research in the material properties, simulation of bone properties and anatomy, mechanical behaviour of dental implant components, implant dimensions and shape, design and properties of prosthetic reconstructions, implant placement configurations, discussion on the limitations of FEA in the study of biological systems –recommendations for further research.

Section V: Software Support in Clinical Dental Management and Education, includes five chapters. Chapter XIII presents a systematic review about EDRs (Electronic Dental Records), describes the current status of availability of EDR systems, implementation and usage and establish a research agenda for EDR to pave the way for their rapid deployment. Chapter XIV describes the haptic dental simulator developed at the University of Illinois at Chicago. Chapter XV describes a digital Library for dental biomaterials. Chapter XVI provides insight into the implementation of rapid prototyping technologies in medical and dental field. Chapter XVII describes the background and the application of the characters for human dentition to the exchange, storage and reuse of the history of dental diseases via e-mail and other means of electronic communication. In Chapter XVIII, the authors focus on a virtual tooth drilling system whose aim is to aid dentists, dental students and researchers in getting acquainted with the handling of drilling instruments and the skills and challenges associated with cavity preparation procedures in endodontic therapy.

The book "*Dental Computing and Applications: Advanced Techniques for Clinical Dentistry*" contains text information, but also a glossary of terms and definitions, contributions from more than 36 international experts, in-depth analysis of issues, concepts, new trends, and advanced technologies in dentistry. While providing the information that is critical to an understanding of the basic of dental informatics, this edition focuses more directly and extensively than ever on applications of dental computing.

The diverse and comprehensive coverage of multiple disciplines in the field of dental computing in this book will contribute to a better understanding all topics, research, and discoveries in this evolving, significant field of study. This book provides information for both informatic researchers and also medical doctors in obtaining a greater understanding of the concepts, issues, problems, trends, challenges and opportunities related to this field of study.

In shaping this book, I committed myself to making the textbook as useful as possible to students and advanced researchers coping with the demands of modern medical research. I hope will make this book a helpful tool-not only for the student who needs an expert source of basic knowledge in dental informatics, but also for the advanced researcher who needs clear, concise, and balanced information on which to conduct his research

Thanks to a very hard-working editorial advisory board of scientists, excellent authors who fulfilled our invitations, and a very efficient publisher providing clear procedures and practices for a quality production, readers may now enjoy chapters on some of the major ideas that have concerned computing and its applications in dentistry.

Andriani Daskalaki
Max Planck Institute for Molecular Genetics, Germany

REFERENCES

American Dental Association Survey Center. (1997). *Survey of current issues in dentistry: Dentists' computer use*. Chicago: American Dental Association: 1998.

Eisner, J. (1999). The future of dental informatics. *Eur J Dent Educ*, *3*(suppl 1), 61–9.

Schleyer, T., & Spallek, H. (n.d.). Dental informatics. A cornerstone of dental practice. *J Am Dent Assoc*, *132*(5), 605-613.

Acknowledgment

I have received generous encouragement and assistance from my former teachers in the Dental School, University of Athens.

I gratefully acknowledge the efforts of the anonymus reviewers, who made a great number of pertinent and constructive comments that helped me to improve the book significantly.

I sincerely acknowledge the help of all persons involved in the collation and review process of this book, without whose support the project would not have been satisfactorily completed.

I wish to express my appreciation to my colleagues, Prof. Petros Koidis, from The Universitry of Thessaloniki, Dr. Athina Lazakidou from the University of Peloponnese, and Dr. Cathrin Dressler from Laser- und Medizin-Technologie GmbH, Berlin, who, as experts in their fields, have helped me with constructive criticism and helpful suggestions.

Special thanks also go to the publishing team at IGI Global, and especially Kristin M. Klinger whose contributions throughout the whole process from inception of the initial idea to final publication have been invaluable. In particular to Julia Mosemann, Joel Gamon, who continuously prodded via e-mail for keeping the project on schedule and to Jan Travers, whose enthusiasm motivated me to initially accept his invitation for taking on this project.

Last but not least, I am grateful to my father, Dimitrios Daskalakis, for his unfailing support and encouragement.

In closing, I wish to thank all of the authors for their insights and excellent contributions to this handbook.

Andriani Daskalaki
Max Planck Institute for Molecular Genetics, Germany
January 2009

Section I

Software Support in Clinical Dentistry

Chapter I
Software Support for Advanced Cephalometric Analysis in Orthodontics

Demetrios J. Halazonetis
National and Kapodistrian University of Athens, Greece

ABSTRACT

Cephalometric analysis has been a routine diagnostic procedure in Orthodontics for more than 60 years, traditionally employing the measurement of angles and distances on lateral cephalometric radiographs. Recently, advances in geometric morphometric (GM) methods and computed tomography (CT) hardware, together with increased power of personal computers, have created a synergic effect that is revolutionizing the cephalometric field. This chapter starts with a brief introduction of GM methods, including Procrustes superimposition, Principal Component Analysis, and semilandmarks. CT technology is discussed next, with a more detailed explanation of how the CT data are manipulated in order to visualize the patient's anatomy. Direct and indirect volume rendering methods are explained and their application is shown with clinical cases. Finally, the Viewbox software is described, a tool that enables practical application of sophisticated diagnostic and research methods in Orthodontics.

INTRODUCTION

Diagnostic procedures in Orthodontics have remained relatively unaltered since the advent of cephalometrics in the early 30's and 40's. Recently, however, the picture is beginning to change, as advances in two scientific fields and dissemination of knowledge and techniques to the Orthodontic community are already making a discernible impact. One field is the theoretical domain of geometric morphometrics (GM), which provides new mathematical tools for the study of shape, and the other is the technological field of computed tomography (CT), which provides data for three-dimensional visualization of craniofacial structures.

This chapter is divided into three main parts. The first part gives an overview of basic mathematical tools of GM, such as Procrustes superimposition, Principal Component Analysis, and sliding semilandmarks, as they apply to cephalometric analysis. The second part discusses the principles of CT, giving particular emphasis to the recent development of cone-beam computed tomography (CBCT). The final part reports on the Viewbox software that enables visualization and measurement of 2D and 3D data, particularly those related to cephalometrics and orthodontic diagnosis.

GEOMETRIC MORPHOMETRICS

Geometric morphometrics uses mathematical and statistical tools to quantify and study shape (Bookstein, 1991; Dryden & Mardia, 1998; Slice, 2005). In the domain of GM, shape is defined as the geometric properties of an object that are invariant to location, orientation and scale (Dryden & Mardia, 1998). Thus, the concept of shape is restricted to the geometric properties of an object, without regard to other characteristics such as, for example, material or colour. Relating this definition to cephalometrics, one could consider the conventional cephalometric measurements of angles, distances and ratios as shape variables. Angles and ratios have the advantage that they are location- and scale-invariant, whereas distances, although not scale-invariant, can be adjusted to a common size. Unfortunately, such variables pose significant limitations, a major one being that they need to be of sufficient number and carefully chosen in order to describe the shape of the object in a comprehensive, unambiguous manner. Consider, for example, a typical cephalometric analysis, which may consist of 15 angles, defined between some 20 landmarks. It is obvious that the position of the landmarks cannot be recreated from the 15 measurements, even if these have been carefully selected. The information inherent in these shape variables is limited and biased; multiple landmark configurations exist that give the same set of measurements. A solution to this problem (not without its own difficulties) is to use the Cartesian (x, y) coordinates of the landmarks as the shape variables. Notice that these coordinates are also distance data (the distance of each landmark to a set of reference axes), so they include location and orientation information, in addition to shape. However, the removal of this 'nuisance' information is now more easily accomplished, using what is known as Procrustes superimposition.

Procrustes Superimposition

Procrustes superimposition is one of the most widely used methods in GM (Dryden & Mardia, 1998; O'Higgins, 1999; Slice, 2005). It aims to superimpose two or more sets of landmarks so that the difference between them achieves a minimum. There are various metrics to measure the difference between two sets of landmarks, but the most widely used is the sum of squared distances between corresponding points, also known as the Procrustes distance. Therefore, Procrustes superimposition scales the objects to a common size (various metrics can be used here as well, but centroid size (Dryden & Mardia, 1998) is the most common) and orientates them to minimize the Procrustes distance. The remaining difference between the landmark sets represents shape discrepancy, as the nuisance parameters of orientation and scaling have been factored out.

In Orthodontics, superimposition methods are widely used for assessment of growth and treatment effects. When comparing a patient between two time points, the most biologically valid superimposition is based on internal osseous structures that are considered stable, or on metallic implants (Björk & Skieller, 1983). However, this is not possible when comparing one patient to another. Although such a comparison may, at first sight, be considered a rare event, or even pointless, it is essentially the basis of every cephalometric analysis performed for diagnostic evaluation at the start of treatment. Measuring angles and distances and comparing these to average values of the population is equivalent to superimposing our patient to the average tracing of the population and noting the areas of discrepancy. The problem of finding the most appropriate superimposition is not easy and GM can offer a new perspective (Halazonetis, 2004). Figure 1 shows cephalometric tracings of 4 patients superimposed by the traditional cranial base Sella-Nasion superimposition and the Procrustes superimposition. The cranial base method makes it very difficult to arrive at a valid interpretation of shape differences between these patients, because the location of points S and N within the structure is the only factor driving the superimposition. Apparent differences in the position of other points may be due more to the variability of points S and N within the shape than to variability of the other points.

The Procrustes distance of a patient to the average of the population is an overall measure of the distinctiveness of the patient's shape. It can be used to judge the extent of craniofacial abnormality and it can give a measure of treatment success; if the Procrustes distance after treatment is smaller than before, then the patient has approached the population average (assuming this is our target). Similarly, it can be used in treatment planning to evaluate various treatment alternatives by creating shape predictions and comparing their Procrustes distances. The prediction with the smallest Procrustes distance relative to the average of the population may be selected as the best treatment choice. This method of treatment planning is not diagnosis-driven but prediction-driven and could be a solution in those cases where diagnostic results are conflicting or difficult to interpret.

Figure 1. Cephalometric tracings of 4 patients. Left: superimposed on Sella-Nasion line. Right: superimposed by Procrustes superimposition.

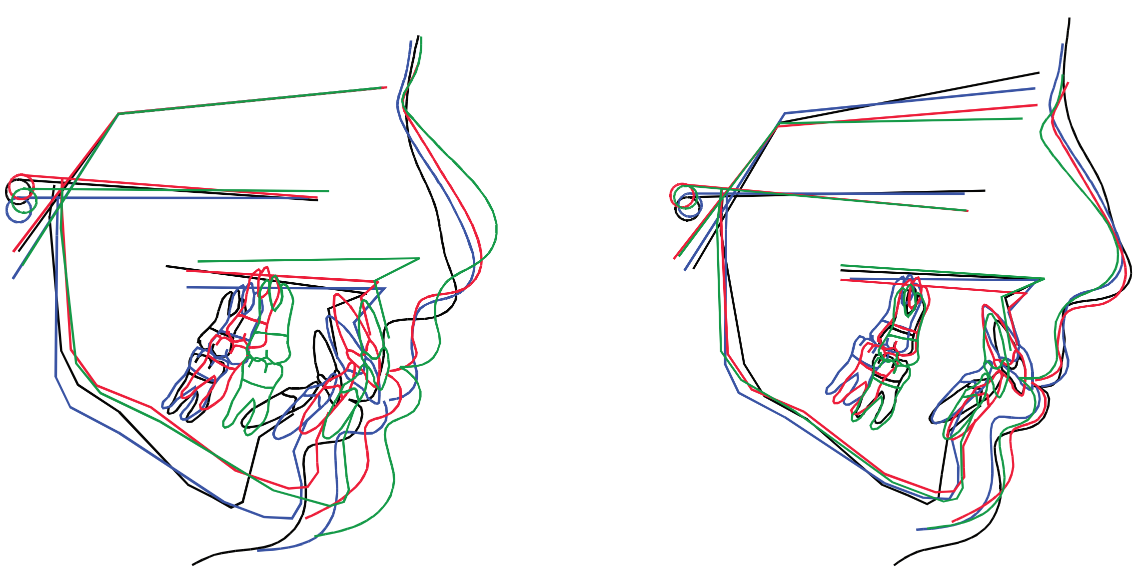

Shape Variables and Principal Component Analysis

Assume that we use Procrustes superimposition to superimpose a cephalometric tracing of a patient on the average of the population. Each cephalometric point will not coincide exactly with the corresponding point of the average tracing but will be a distance away in the x and y direction. These small discrepancies constitute the shape variables and are used for calculation of the Procrustes distance, as explained above. For each point of the shape we will have two such variables (dx and dy), giving a rather large total number of variables to deal with in statistical tests, but, most importantly, to get a feeling of the underlying patterns in our data. However, since all the points belong to the same biological entity, it is expected that there will be correlations between the positions of the points, due to structural and functional factors. Using the statistical tool of Principal Component Analysis (PCA) we can use these correlations to transform our original shape variables into new variables that reveal the underlying correlations and their biological patterns (O'Higgins, 1999; Halazonetis, 2004; Slice, 2005). The variables produced by PCA (Principal Components, PC) can be used for describing the shape of our patient in a compact and quantitative manner. A few principal components are usually sufficient to describe most of the shape variability of a sample, thus constituting a compact and comprehensive system of shape description that could be used for classification and diagnosis.

Semilandmarks

The discussion on shape assessment has thus far made the implicit assumption that the landmarks used for defining the shape of the patients are homologous, i.e. each landmark corresponds to a specific biological structure, common between patients. Although we define most landmarks to follow this rule, sometimes landmarks are placed along curves (or surfaces) that do not have any discerning characteristics to ensure homology. The landmarks merely serve the purpose of defining the curve and their exact placement along the curve is not important. In such cases, the landmarks are considered to represent less information and are called semilandmarks (Bookstein, 1997). Since the exact placement of semilandmarks is arbitrary to some extent, differences in shape between patients may appear larger than actual. In such cases, the semilandmarks can be adjusted by sliding them on the curve or the surface they lie on, until differences are minimized (Bookstein, 1997; Gunz et al., 2005).

COMPUTED TOMOGRAPHY

Computed tomography was invented in the early 1970's by Godfrey Hounsfield, who later shared the Nobel Prize in Medicine with Allan Cormack, developer of the mathematical algorithms for reconstruction of the data. The development of computed tomography (CT), which revolutionized medical diagnosis in the 70's and 80's, had a barely noticeable effect in Dentistry, mainly because of the cost of the procedure and the high amount of radiation. However, the recent development of cone-beam computed tomography (CBCT) and the manufacturing of 'dental' CBCT machines is beginning to make a large impact in all areas of dental practice, including implant placement and orthodontic diagnosis (Sukovic, 2003; Halazonetis, 2005). Orthodontic practices and university clinics in the US and other countries are phasing out the conventional radiographic records, consisting of a lateral cephalogram and a panoramic radiograph, and substituting CBCT images. Although radiation to the patient is higher, many believe that the higher diagnostic information more than compensates.

Data

The data from a CT examination can be though of as many 2-dimensional digital images stacked one on top of the other, to produce a 3-dimensional image, or 'volume'. Each image has pixels that extend in 3-dimensions and are called 'voxels'. The whole 'volume' is typically 512x512 in the x- and y-directions and can extend to 300 or more slices in the z-direction, giving a total count of more than 80 million voxels.

Because each voxel represents x-ray attenuation, the voxels do not have colour information; data are represented by an 8-bit or 12-bit number, so a voxel value ranges from 0 to 255 or from 0 to 4095. The higher the value, the more dense the tissue represented by the voxel. Voxel values are sometimes converted to Hounsfield units (HU). In this scale, air is assigned a value of -1000 HU and water a value of 0 HU. Values of other materials are assigned by linear transformation of their attenuation coefficients. Bone has a HU value of 400 and above.

Cone-Beam Computed Tomography in Orthodontics

Advantages and Limitations

There are two main questions to consider when assessing CBCT imagining in Orthodontics. One is whether CBCT is preferable to the conventional records of a lateral cephalogram and a panoramic radiograph, and second, whether CBCT is advantageous relative to a medical CT examination. Various factors come into mind for both of these questions, including quantity and quality of diagnostic information, radiation hazard, cost, acquisition time, ease of access to the machine and ease of assessment of data. Although some of these factors may be determinative in some circumstances (e.g. no CT machine available in area of practice), the most important ones are related to diagnostic information, radiation concerns and data evaluation.

Diagnostic Information

Three-dimensional information is undoubtedly better than the 2-D images of the conventional cephalogram and panoramic radiographs. There is no superposition of anatomical structures and the relationship of each entity to the others is apparent in all three planes of space. The superiority of 3D images has been demonstrated in cases of impacted teeth, surgical placement of implants and surgical or orthodontic planning of patients with craniofacial problems, including clefts, syndromes and asymmetries (Schmuth et al., 1992; Elefteriadis & Athanasiou, 1996; Walker et al., 2005; Cevidanes et al., 2007; Cha et al., 2007; Van Assche et al., 2007; Hwang et al., 2006; Maeda et al., 2006). However, the fact that 3D images are superior does not imply that they should substitute 2D images in every case (Farman & Scarfe, 2006). The clinician should evaluate whether the enhanced information is relevant and important on a case-by-case basis, just as the need for a cephalometric or panoramic radiograph is evaluated.

One factor that may be limiting in some cases is the restricted field of view of CBCT machines. The first models could image a severely limited field, just enough to show the mandible and part of the maxilla, up to the inferior orbital rims. Newer models allow large fields, but it is still not possible to image the entire head (Figure 2 and Figure 8). Additionally, the time taken to complete the scan may be more than 30 seconds, a factor that could introduce blurring and motion artifacts.

Another limiting factor is the resolution of the images. A periapical radiograph can give a very clear view of the fine bony trabeculae in the alveolar process. Panoramic radiographs and cephalograms can also show such details, but CBCT data have a voxel size of approximately 0.4 mm in each direction resulting in a comparatively blurred picture, not to mention a multitude of artifacts that reduce image quality severely.

Figure 2. Restricted field of view in CBCT image, even though machine was set to widest possible. In this instance, the extent towards the back of the head barely includes the mandibular condyles. Data rendered in Viewbox.

Radiation Exposure

Numerous investigations have been conducted to measure radiation exposure to CT examinations. One of the most widely used measures is the equivalent dose (or effective dose), which measures the biological effect of radiation. The equivalent dose is calculated by multiplying the absorbed dose by two factors, one representing the type of ionizing radiation and the other mainly representing the susceptibility of the biological tissue to the radiation. The unit of measurement is the sievert (Sv). Natural background radiation incurs about 2400 μSv per year. According to the United Nations Scientific Committee on the Effects of Atomic Radiation (UNSCEAR) 2000 Report to the General Assembly, "the average levels of radiation exposure due to the medical uses of radiation in developed countries is equivalent to approximately 50% of the global average level of natural exposure. In those countries, computed tomography accounts for only a few per cent of the procedures but for almost half of the exposure involved in medical diagnosis." (UNSCEAR, 2000) Table 1 reports the equivalent dose from various medical examinations, including conventional CT, CBCT and cephalometric and panoramic radiography.

Data Evaluation

An aspect that is seldom discussed in relation to the advent of CBCT in orthodontic diagnosis is data evaluation. The assessment of the data obtained by a CBCT examination represents some difficulties compared to conventional examinations. These difficulties arise because the dentist or orthodontist may not be trained for this task and because extra facilities are needed (computers

Table 1. Effective dose from various sources and time equivalent to natural background radiation. Data compiled from Shrimpton et al. (2003), Ngan et al. (2003), Ludlow et al. (2003, 2006), Tsiklakis et al. (2005) and Mah et al. (2003).

Source	Effective dose	Time equivalent
Natural background radiation	2400 μSv	12 months
Medical CT (head examination)	1500 μSv	7.5 months
CBCT	50-500 μSv	1-10 weeks
Panoramic radiograph	10-20 μSv	1.5-3 days
Cephalometric radiograph	3-5 μSv	12-20 hours

and software). Furthermore, normative data may not be available, making it difficult to differentiate the normal from the pathological, or, to assess the degree of discrepancy from the average of the population.

3D Cephalometrics

The rather fast introduction of CBCT imaging in Orthodontics seems to have taken the field unprepared. The more than 70 years of 2D conventional cephalometrics seems so ingrained that recent papers in the literature concentrate on evaluating methods that create simulations of 2D cephalograms from the 3D CBCT data (Moshiri et al., 2007; Kumar et al., 2008), thus trying to retain compatibility with old diagnostic methods instead of seeking to develop something new. Very little thought seems to have been invested into recognizing and assessing the capabilities of this new medium as well as the significant differences between it and 2D cephalometrics. Consider, for example, the ANB measurement, which aims to assess anteroposterior discrepancy between the maxilla and mandible. A direct transfer of this measurement to 3D seems without problems until one realizes that an asymmetry of the mandible will move point B laterally, thus increasing the ANB angle, without there being any change in anteroposterior mandibular position in relation to the maxilla. Similar problems crop up with other measurements. A 3D cephalometric analysis should be developed starting from a complete overhaul of current practices and should probably incorporate geometric morphometric methods for assessment of shape. Currently no such analysis exists, although efforts have been made, mostly in the lines described previously (Swennen et al., 2006). Thus, whereas CBCT imaging is increasingly used, most of the available information remains unexploited; evaluated either in a qualitative manner, or by regressing to 2D.

A major difficulty hindering progress, besides the conceptual problems of the third dimension, is the lack of normative data. The standards of the historical growth studies are of little use and ethical considerations do not allow such studies to be carried out with the ease there were done in the early years of cephalometrics. However, the large number of CT examinations done all over the world for other medical and diagnostic reasons constitute a pool of data that could provide invaluable information if they could be gathered and systematically analysed.

Image Interpretation and Artifacts in CBCT

A significant difficulty in the clinical application of CBCT images is the lack of training in their interpretation. Dental Schools and Orthodontic Departments are starting to add courses in computed tomography but it will be many years until the knowledge and skills permeate to faculty members and practicing clinicians. Some of the most common methods of viewing CT data are described in the next section of this chapter. Below we mention a few of the most important artifacts that occur in all forms of CT imaging but are most apparent in CBCT (Barrett & Keat, 2004). The difference in artifact level between medical CTs and dental CBCTs is large and image quality is considerably lower in CBCTs.

Noise

Noise can be produced by many factors including stray and scatter radiation and electromagnetic interference. The lower the radiation level, the higher the noise will be. Thus, CBCT images usually have more noise than medical CTs. Noise can be reduced by the application of various smoothing filters, but at the expense of loss of image detail.

Streaking Artifacts

Streaking artifacts are caused by very dense materials, usually dental amalgams, restorations or metal crowns and bridges (Figure 3). They are due to a complete absorption of x-ray radiation, thus allowing no signal to reach the detectors. Various algorithms exist to reduce such artifacts but it is very difficult to abolish them.

Ringing Artifacts

These appear as concentric circles centred at the centre of the image (Figure 4). They are due to differences in detector sensitivity and can be reduced by calibration of the machine.

Beam Hardening - Cupping Artifacts

X-ray beams are composed of photons of a wide range of energies. As an x-ray beam travels through the patient, its intensity is reduced due to absorption, but this reduction is not uniform over the energy range, because lower energy photons are absorbed more rapidly than high energy photons. The result is a change in energy distribution of the beam (also known as beam hardening). Therefore, a beam that passes through a thick portion of the patient's body will have proportionately more of its low energy photons absorbed and will ap-

Figure 3. Streaking artifacts due to highly radiopaque metal prosthesis. Notice that streaks radiate from the metal source and extend to the edges of the image (arrows).

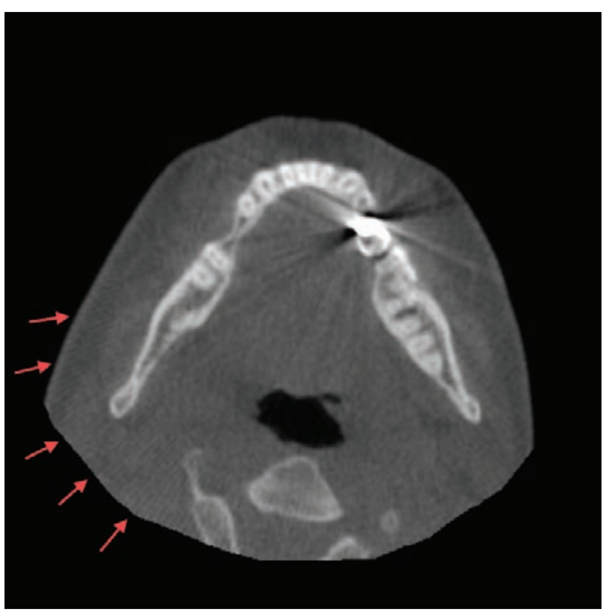

Figure 4. Ringing artifacts. Image from a micro-CT machine showing rat tooth embedded in fixing material. Note concentric rings due to detector mis-calibration.

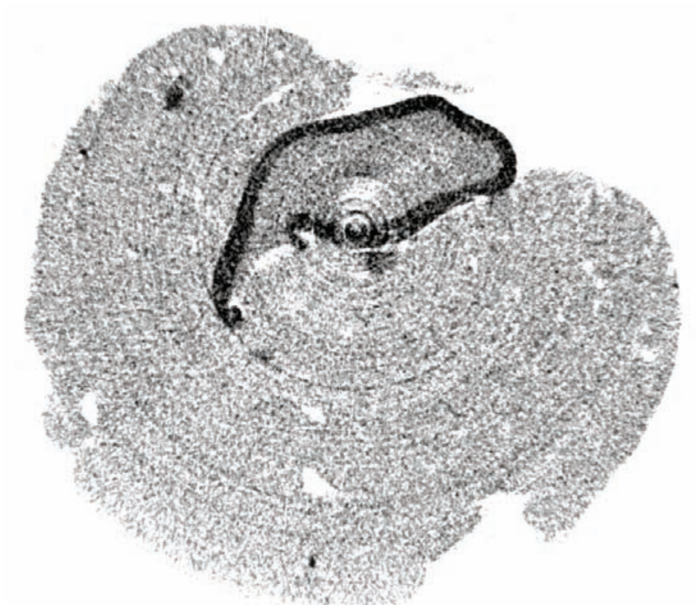

Figure 5. An axial slice of a CBCT image. The profile of voxel values along the line shows the characteristic cupping artifact due to beam hardening. The profile is not smooth due to noise.

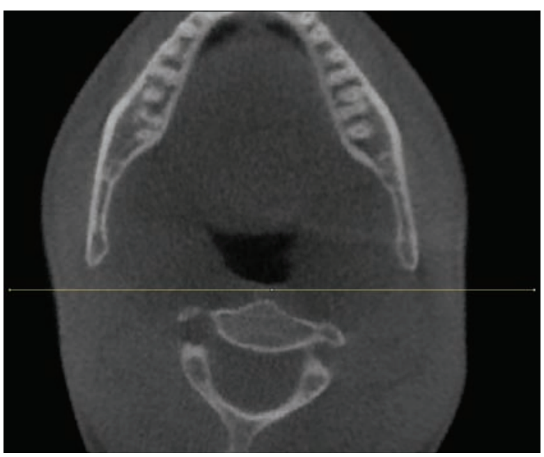

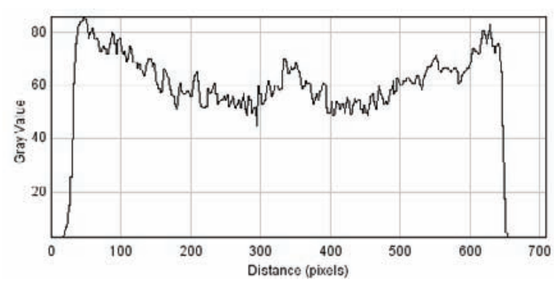

pear to the detectors to be more energetic than expected. A more energetic beam is interpreted by the machine as a beam having passed through less dense material. Thus, the internal portion of the patient's body will appear darker, producing a characteristic 'cupping' profile of voxel values along the line of the beam (Figure 5). Cupping artifacts widen the range of voxel values that correspond to the same tissue type and make volume segmentation and rendering more difficult.

Partial Volume Averaging

Voxels are not of infinitesimal size but extend in spatial dimensions, usually having a size of 0.3 to 0.6 mm in each direction. If a voxel happens to be located at the interface between two (or more) different tissues, then its value will be the average of those tissue densities. Depending on the relative proportion of each tissue, the voxel could have any value between the values of the two tissues. The partial volume averaging effect (PVAE) is thus a problem of resolution; the larger the voxel size the more the effect. The voxel size commonly used in CT imaging is large enough to create artifacts in numerous areas of the craniofacial complex. The paper-thin bone septa of the ethmoid bone may completely disappear, leaving an image of soft tissue surrounding empty spaces with no osseous support. Similarly, the cortical bone covering the roots of teeth may be too thin and be confused with soft-tissue, thus giving the impression of dehiscence. Pseudo-foramina are sometimes seen on calvarial bones, especially in infants, whose bones are very thin.

PVAE is especially significant when taking measurements, because measurements entail the placement of landmarks on the interface between anatomical structures, the area that PVAE affects most.

The Partial Volume Averaging effect should not be confused with the Partial Volume Effect (PVE). This artifact occurs when the field of view is smaller than the object being imaged, so it is seen predominantly in CBCTs. The parts of the object outside the field of view absorb radiation and through shadows on the detectors, but this happens only for part of the image acquisition (otherwise the whole object would be visible). This extraneous information cannot be removed by the reconstruction algorithm and shows as artifacts, usually manifesting as streaks or inconsistent voxel densities. PVE artifacts are also known as projection data discontinuity–related artifacts (Katsumata, 2007) and are particularly troublesome in limited field of view CBCT images (Figure 6).

Artifact Effect on Voxel Value Distributions

As explained above, each voxel represents the density of the tissue at the voxel's position. The voxel value is used for a multitude of purposes, from rendering (explained below) to segmentation and measurements. Volume segmentation is the process of subdividing the volume into tissue types so that anatomical structures can be identified and measurements taken. Depending on its

Figure 6. Axial slice of anterior part of the maxilla showing impacted canine. PVE artifacts are evident.

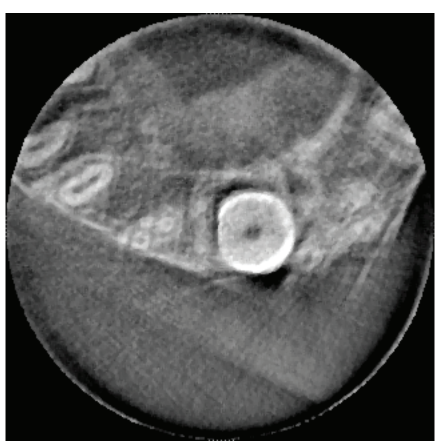

value, a voxel can be classified as belonging to a particular tissue type such as bone, muscle, skin, etc. However, tissues are not completely homogeneous, 'noise' may be present and artifacts (e.g. PVE and cupping) may shift voxel densities from their true value. Thus, each tissue type does not contain voxels that have exactly the same value. Instead, voxels of a particular tissue span a range of values. Volume segmentation requires that the density ranges of the various tissue types do not overlap, so that cut-off points (thresholds) can be established that will divide the voxels without misclassification. This requirement is frequently violated and the distribution of bone density values and soft-tissue values overlap each other. As Figure 7 shows, there is no threshold value that can separate the two tissues without any misclassifications. This problem is especially apparent in CBCT imaging compared to medical CT and affects volume rendering as well (see below).

VOLUME RENDERING

Volume rendering is the process of visualizing the volume data as an image on the computer screen (Halazonetis, 2005). The volume data constitutes a rectangular three-dimensional grid of voxels, the value of each voxel representing the radiographic density of the tissue at the corresponding position. For this discussion, it helps to consider the whole volume as an object in 3-dimensional space, floating behind the computer screen, the screen being a window into this space. We know the density of the object at specific coordinates and we wish to reconstruct an image of the object from this

Figure 7. A CBCT axial slice showing a section of the mandible. Due to artifacts, the soft-tissues on the buccal side of the mandible have comparable densities to the bone on the lingual side. The green line is the iso-line for a threshold value that is appropriate for segmenting the lingual part of the mandible but not for the labial part. Conversely, the red line represents a higher threshold, appropriate for the denser bone of the outer mandibular surface, but not for the lingual. Voxel size is 0.42 x 0.42 x 0.60 mm.

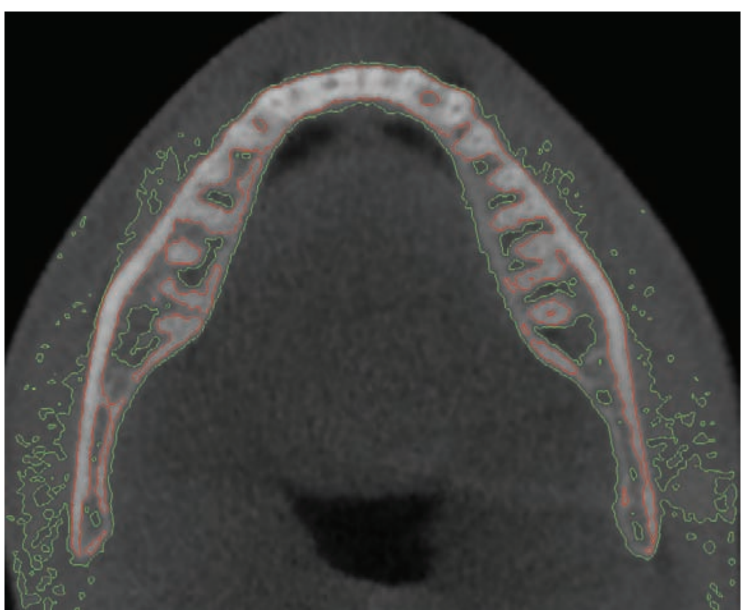

information. There are two main methods to do this, direct volume rendering, where the values of the voxels are directly converted into colour values for the pixels of the computer screen, and indirect volume rendering, where the voxel values are first converted into data describing a geometrical object, which is then rendered on the screen, usually with the help of dedicated graphics hardware.

Direct Rendering: Transfer Function

Direct volume rendering can be accomplished in a multitude of ways (Marmitt, 2006) but the easiest to describe and understand is ray-casting. Ray-casting uses the analogy of an object floating behind the computer screen. Since the screen is our window to the 3-dimensional world, the colour of each pixel will depend on the objects that lie behind it. A straightforward approach assumes that from each screen pixel starts a ray that shoots towards the object. As the ray pierces the object and traverses through it, it takes up a colour that depends on the tissues it encounters along its way. The colours are arbitrary and are usually assigned according to the voxel values. For example, to show bone in white and soft tissue in red we could assign white to the pixels whose ray encounter voxels of a high value and red to the pixels whose ray encounter voxels of a low value. To show bone behind soft tissue we additionally assign opacity according to voxel value. Voxels of low value could have a low opacity, so that the ray continues through them until it encounters high-value voxels. In this way, the final colour assigned to the pixel will be a blend of red and white. This method of ray casting can produce high quality renderings of CT data (Figure 8A).

There are a few details that need to be mentioned. First, the value of a voxel represents the value at a specific point in space. Mathematically, this point has no spatial extent, so the rays that are spawn from the screen pixels may penetrate the volume without encountering a voxel. The solution to this problem is that the ray is sampled at regular intervals along it. At each sampling point on the ray, the required value is interpolated from the neighbouring voxel points. There are numerous ways of interpolating a voxel value. The fastest is tri-linear interpolation, where only the 8 immediate neighbours are taken into account, but other methods, using a larger neighbourhood, may produce better results. In any case, the calculated value is only an approximation of the true value. Another factor that may lead to artifacts in the rendered image is the frequency of sampling along the ray. Too large a sampling distance may result in skipping of details and loss of smooth gradients (Figure 9).

As was mentioned above, the colour and opacity at each sampling point along the ray is arbitrarily set, usually dependent on the calculated voxel value or tissue density. In general, the mapping of the voxel values to colour and opacity is called the transfer function. Most commonly this is a one-dimensional transfer function, meaning that colour and opacity are a function of one variable only, voxel value. However, more complex transfer functions are possible (Kniss et al., 2002). A two-dimensional transfer function can map tissue density and gradient of tissue density (difference of density between neighbouring voxels), making it possible to differentiate areas at the interface between tissues (Figure 10).

Direct Iso-Surface Rendering

This method also uses ray casting, but instead of accumulating colours and opacities as the ray traverses through the volume, it detects the position where the ray crosses a specific threshold of voxel density (Parker et al., 1998). The threshold has been set by the user and corresponds to the boundary between two tissues (e.g. soft-tissue and bone, or air and soft-tissue). Such boundaries that represent a specific voxel density are called iso-surfaces. Figure 8B shows two iso-surfaces rendered by ray casting. The skin iso-surface has

Figure 8. Rendering of a CBCT dataset. (a) Ray casting using a transfer function. (b) Iso-surface rendering of two iso-surfaces (soft-tissues transparent). (c) Average intensity ray casting (simulation of conventional radiograph). (d) MIP (maximum intensity projection). Data from NewTom 3G, rendered in Viewbox.

Figure 9. Artifacts produced from too large a sampling step during ray casting. Left: large sampling step leading to slicing artifacts. Right: high-quality rendering using 4 times smaller step size. Medical CT data.

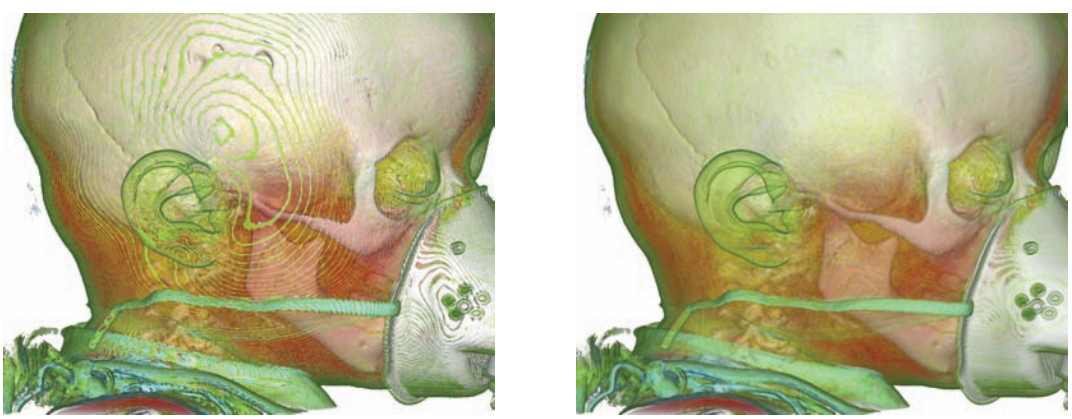

Figure 10. (a) Two-dimensional histogram of CT volume data. Horizontal axis is voxel density, increasing from left to right. Vertical axis is voxel gradient. Arches are characteristic of low-noise data and represent voxels that lie on tissue boundaries. (b) and (c) Transfer functions mapping voxel densities and gradients to colours and opacities. The transfer function of (c) was used for rendering of Figure 9.

(a)

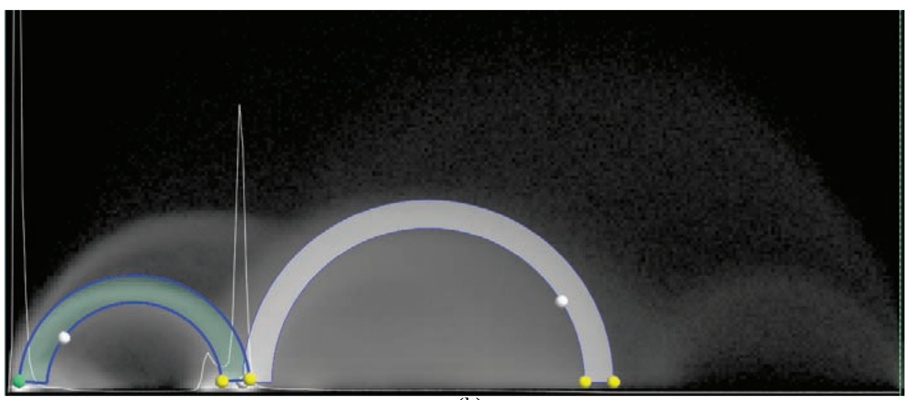

(b)

(c)

been rendered semi-transparent, in order to show the skeletal structures underneath.

Average Intensity Ray Casting

This method calculates the average density of the voxels that each ray passes through and creates an image that approximates the image that would be produced by conventional radiographic techniques (Figure 8C). In Orthodontics, average intensity rendering can create simulated cephalograms from CBCT data, to be used for conventional cephalometric analysis.

Maximum Intensity Projection

Maximum Intensity Projection (MIP) is a ray-casting technique that shows the densest structures that each ray encounters as it travels through the CT volume (Figure 8D). MIP rendering can be useful to locate and visualize dense objects, such as metal foreign objects or blood vessels infiltrated with radio-dense enhancing material, or to identify areas of bone perforation and fractures.

Indirect Rendering

Indirect rendering uses the CT data to create a geometric object that is then rendered on the screen. The object is, most commonly, an iso-surface, i.e. a surface that represents the interface between areas of a higher density value and areas of a lower density value. The points that lie on the iso-surface have all a density equal to a specified threshold, called the iso-value. It can be shown mathematically that an iso-surface is continuous (except at the edges of the volume) and closes upon itself. Such a surface can be approximated by a large number of triangles, usually calculated from the voxel data using the Marching Cubes algorithm or one of its variants (Lorensen & Cline, 1987; Ho et al., 2005). The resulting triangular mesh can be rendered very quickly using the graphics hardware of modern personal computers (Figure 11).

Advantages of indirect rendering include the speed of rendering and the capability to easily place points on the mesh for measurements or to compute volume and area, and to splice and manipulate the mesh in order to simulate surgical procedures. Meshes can also be used for computer-aided manufacturing of 3D objects, either biological structures for treatment planning, or prostheses and implants. However, meshes do not represent the biological structures as well as direct rendering because the iso-surface that is used to construct them does not necessarily represent the boundary of a tissue, due to artifacts of CT imaging.

Figure 11. Indirect rendering of volume by creation of triangular mesh. Left: Mesh rendered as a wireframe object. Middle: Mesh rendered as a faceted triangular surface. Right: Smooth rendering.

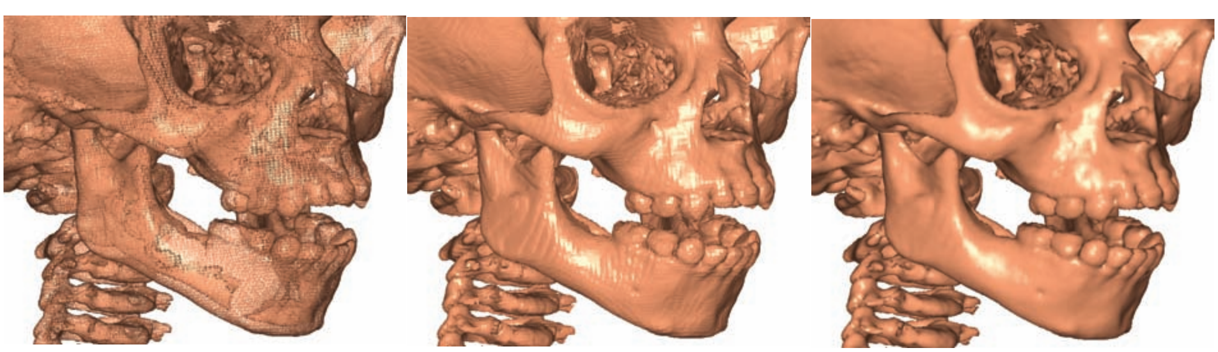

THE VIEWBOX SOFTWARE

The Viewbox software (www.dhal.com) (Figure 12) started as conventional 2-dimensional cephalometric analysis software for orthodontists in the early 1990's (Halazonetis, 1994). Recently it has been updated for 3-D visualization and analysis, including volume rendering and geometric morphometric procedures. Viewbox has been designed as a flexible system that can work with various kinds of 2D and 3D data, such as images, computed tomography data, surface data and point clouds. The software is built upon a patient-centric architecture and can handle various types of virtual objects, as detailed below.

Initially, when Viewbox development started, the only way to get cephalometric data into a computer was through an external digitizer tablet. The data were x and y point coordinates that were used for calculating the cephalometric measurements. Scanners and digital cameras were not widely available, nor did they have the specifications required for precise measurements. Therefore, objects such as digital images and CT data were not even considered. The focus was placed on developing a flexible user-defined system that could handle almost any type of measurements that might be required, either in conventional cephalometric analysis or any 2D measurement of diagnostic or experimental data (e.g. data from animal photographs or radiographs, measurement of dental casts, panoramic radiographs etc.). This system was based on the definition of Templates that incorporated all the data structures and information necessary to carry out the measurements and analyses specified by the user. A Template would include information on the points that were digitized, the measurements based on these points, the analyses (groups of measurements), types of superimpositions available, and so on. When analyzing a new cephalometric radiograph (or any other diagnostic record), the user would

Figure 12. The viewbox software

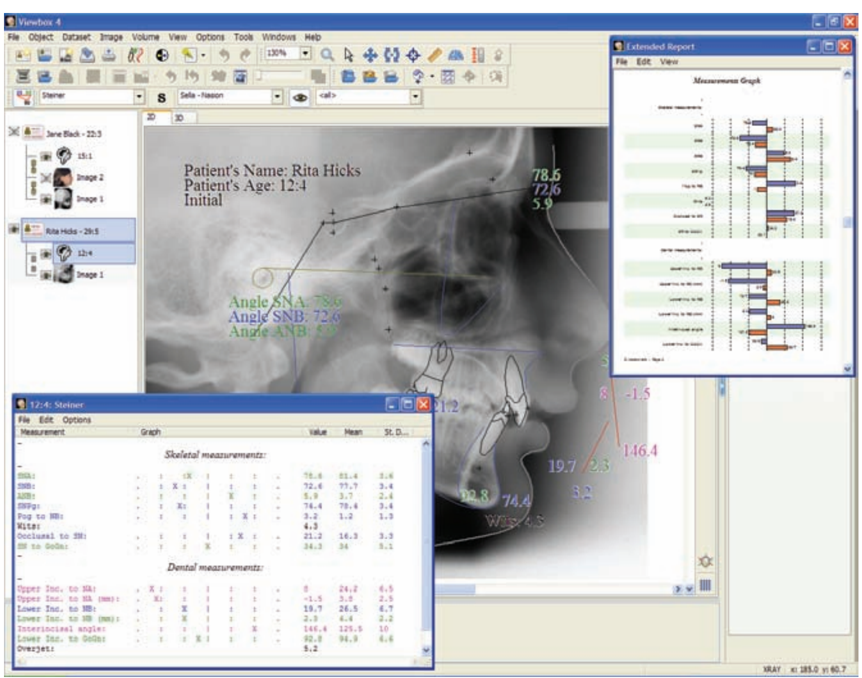

create a new Dataset based on a selected Template. The Dataset would consist of a collection of x and y coordinate data, mapped to the points of the Template. The coordinate data would be filled by the user by digitizing the radiograph and the measurements would be calculated using the functions specified in the Template's definition. This architecture enabled a system that was completely user-definable with no rigid built-in restrictions. The user could specify measurement types, normal values, types of superimpositions, names and number of digitized points and other such data, making it possible to build completely customized solutions to any 2D analysis task. Datasets contained nothing more than the coordinates of the digitized points, making it easy and fast to store and retrieve data, as the main bulk of information was in the Template structure, which needed to be loaded only once.

With the progress in imaging devices and the fall in price of transparency scanners, digitization of radiographs on-screen soon became an attractive alternative. Viewbox was updated to be able to load digital images and communicate with scanners. Digitization could be performed by clicking on the points of the digital image on screen. Thus, a new object, the Image, was added to the Viewbox inventory. Images were accompanied by functions for image enhancement and manipulation. Soon afterwards, functions that would aid the user in locating the landmarks on the images were added (Kazandjian et al., 2006), as it was evident in the literature that landmark identification errors were probably the largest source of numerical errors in cephalometric analysis (Baumrind & Frantz, 1971; Houston et al., 1986).

The latest step in Viewbox development came with the increasing use of CBCT machines in the orthodontic practice and the realization that 3D data will dominate clinical diagnosis and treatment planning in the future. This is now evident by the steady penetration of 3D models in orthodontic practices, the increasing use of 3D facial photographs and the use of 3D CT data and stereolithography models for diagnosis and treatment planning of challenging cases (Halazonetis, 2001). Thus, Viewbox has been redesigned by adding more internal objects, such as meshes, and volumes, and a 3D viewer for the visualization of these objects. The 2D viewer has been retained for backward compatibility, but it may be removed in the future when the 3D viewer inherits all its capabilities, as it will serve no real use. Viewbox is now a patient-centric system and includes the types of 'objects' described in the part "key terms and definitions".

Images can be viewed both in a 2D viewer and a 3D viewer. Images can be adjusted to enhance perception of difficult to see structures. In addition to basic capabilities such as image inverse, brightness, contrast and gamma adjustment, Viewbox includes more sophisticated histogram techniques, such as adaptive histogram stretching, adaptive histogram equalization and contrast limited adaptive equalization (Figure 13). Furthermore, using a combination of such techniques, together with transparent blending of two images, it is possible to do structural superimposition of two radiographs, as proposed by Björk & Skieller (1983), in order to assess growth and treatment effects (Figure 14).

When digitizing points on images, Viewbox can detect brightness levels and assist in accurate landmark placement by locking on abrupt brightness changes, which usually correspond to bony or soft-tissue outlines (Kazandjian et al., 2006), (Figure 15).

Mesh

A mesh is a surface composed of triangular elements, each element consisting of 3 vertices and a face. A mesh has connectivity information so it is possible to determine if the surface is composed of separate detached objects.

Meshes can be loaded from files (common file types are supported, including OBJ, PLY and STL) or can be created from volumes using a variant

Figure 13. Image enhancement. (a) Original image. (b) Gamma adjustment. (c) Adaptive histogram equalization. (d) Contrast limited adaptive histogram equalization (CLAHE)

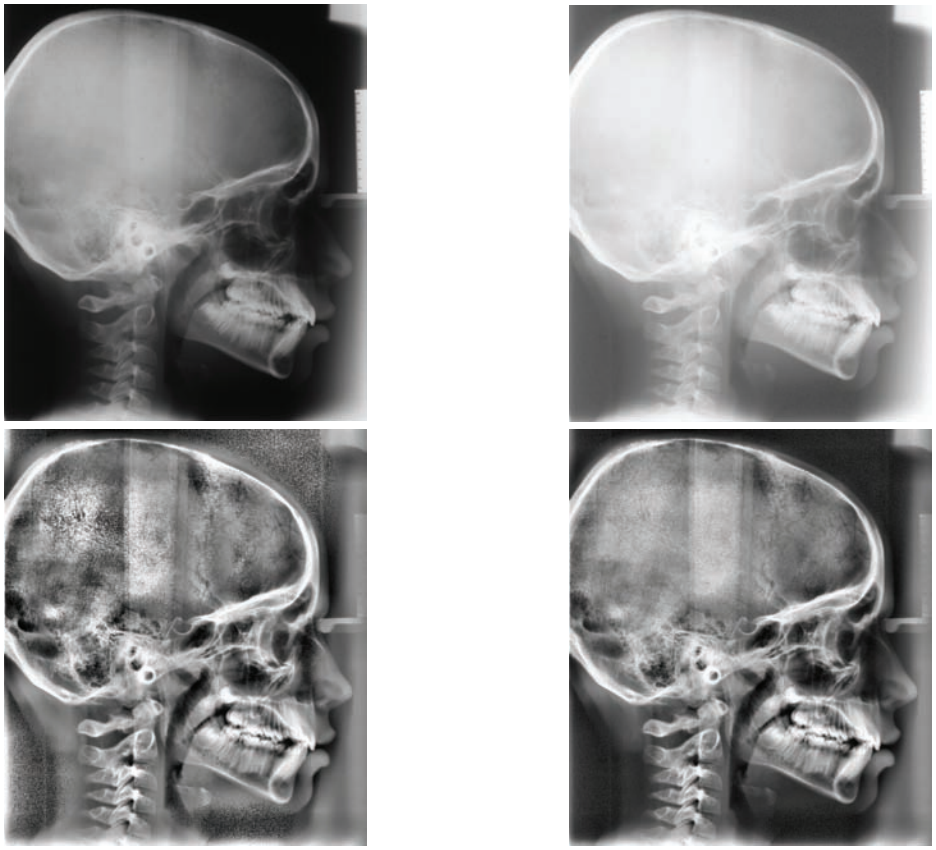

Figure 14. Structural superimpositioning using blending of transparent images. Left: Before superimposition, one radiograph is rendered in red and the other in green, after a CLAHE filter has been applied to both. Right: After manual registration most of the cranial base structures are yellow, signifying a good fit.

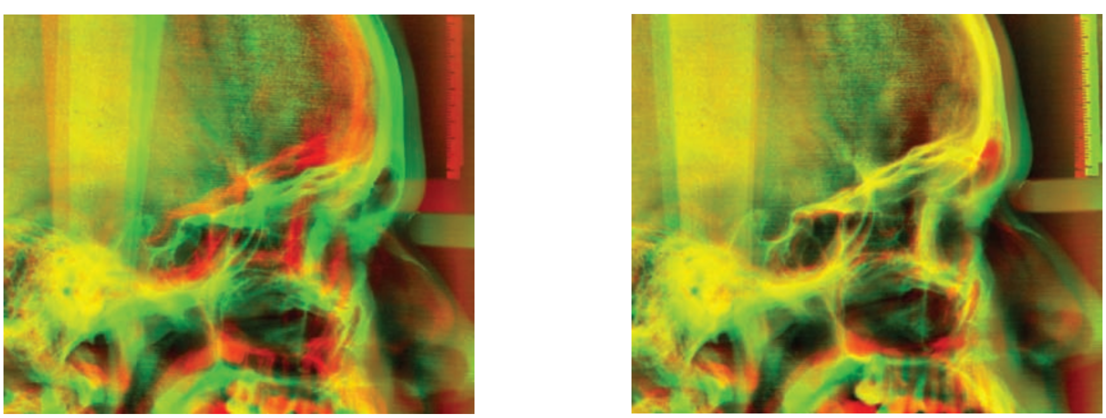

Figure 15. Edge detection feature in Viewbox. Red circle is the mouse position. Green line is the direction along which edge detection is attempted. Blue line shows the detected edge. This corresponds to a zero-crossing of the second derivative of brightness, as shown in the inset graph.

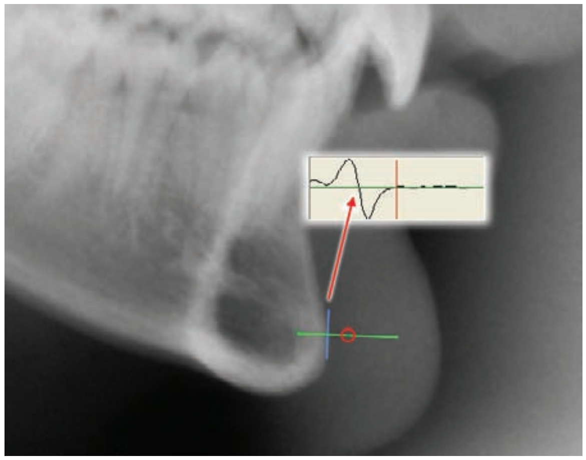

of the marching cubes algorithm (Lorensen & Cline, 1987). In orthodontics, meshes are used for rendering digital dental models, 3D digital photographs of the face and objects created from CT scans (Figure 16, Figure 17, Figure 11).

Meshes are drawn using OpenGL routines and they can be rendered as a faceted surface, a wireframe object (showing only the outlines of the triangles) or a smooth surface (Figure 11). Viewbox contains basic mesh manipulation routines such as cropping, smoothing and decimation (reducing the number of triangles). Additionally, meshes can be registered on each other by using best fit methods.

Digitizing Points and Curves

The multiple objects supported by Viewbox make it a flexible system for digitizing patient records as well as data from other sources such as scanned bones, fossils, animal specimens, individual teeth, etc. Points can be digitized by clicking on the object on-screen; this method is supported for images, meshes, points clouds, slices and volumes rendered with iso-surface rendering. Additionally, curves can be placed on objects. Curves are smooth lines (cubic splines), usually located on edges of images or ridges of a 3D object, whose shape is controlled by points placed along them.

Curves can be used for measuring the length of a structure or the surface area, in cases of a closed flat curve. However, the main usage is for automatic location of landmarks. For example, if a curve is drawn along the outline of the symphysis on a lateral cephalogram, Viewbox can locate points Menton, Gnathion, Pogonion, B point and other such landmarks, by using the definitions of these points. For instance, Menton will be automatically located on the most inferior point of the curve, ‘inferior’ being a direction specified either absolutely (i.e. along the y-axis of the coordinate system) or relative to another cephalometric plane of the patient (e.g. perpendicular to Frankfurt horizontal, as defined by points Porion and Orbitale). Automatic point location can be helpful for reducing error in point identification, especially for points that are defined relative to a particular reference direction, such as points defined by phrases like ‘the most anterior’, ‘the

Figure 16. A laser-scanned plaster model imported as a triangular mesh. The holes in the model are areas that were not visible to the laser light.

Figure 17. 3D photograph imported as a mesh, rendered as a wireframe model, a smooth surface and a textured surface.

Figure 18. Left: A slice cutting through a CBCT volume. The slice can be moved along a user-adjustable path, shown here by the green line. Right: The slice image.

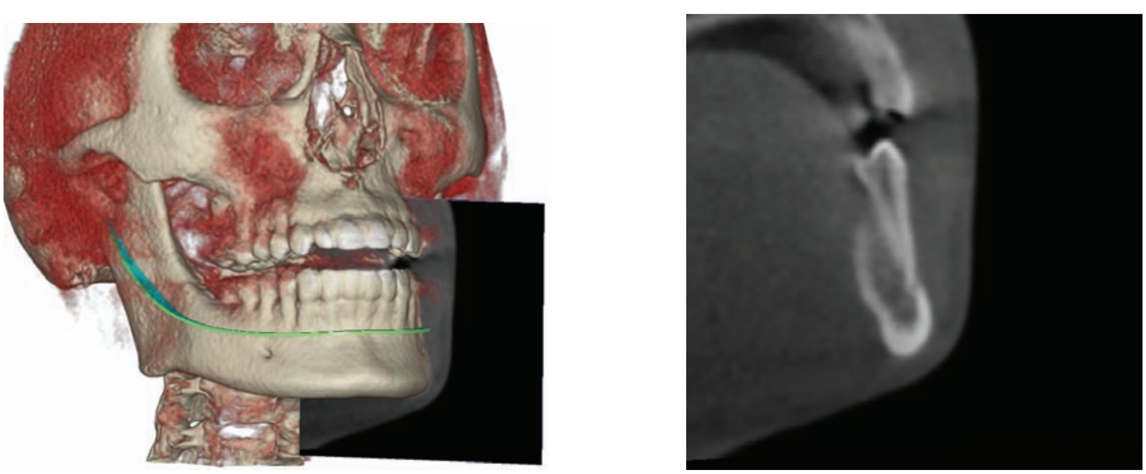

most superior', etc. Also, points defined relative to the curvature of a structure can be located in the same way. An example of this type is point Protuberance Menti (Ricketts, 1960), defined as lying on the inflection point (point of zero curvature) of the outline of the alveolar process between B point and Pogonion.

Curves are also used for placing semilandmarks and letting them slide. As described previously, semilandmarks do not encode biological information by their position along the curve, because there are no discernable features on the curve. The biological information is in the shape of the curve; as long as this shape reflects the underlying biological structure, the semilandmarks' precise location is irrelevant. However, since the semilandmarks will be used for shape comparison, we need to ensure that discrepancies in their position between patients or specimens does not affect our results. This can be accomplished by first automatically distributing them along the length of a curve, at predefined intervals, and then sliding them on the curve, until the Procrustes distance, or some other metric of shape similarity relative to a reference template, is reduced to a minimum. This ensures that no extraneous shape variability is introduced by incorrect semilandmark placement. Viewbox supports sliding semilandmarks on both curves and surfaces (meshes) in 3D (Figure 19).

In addition to digitized points and curves, Viewbox provides for geometrically derived landmarks such as midpoints, projections of points on lines, extensions of lines, centroids, etc.

Measurements

There are more than 40 measurement types available. These include direct measurements based on the position of points (e.g. various distances and angles), compound measurements (e.g. sum, difference, product of other measurements), measurements between datasets (e.g. the distance between one point of one dataset to a point of another dataset, useful for measuring changes due to growth or treatment) and basic morphometric measurements (e.g. Procrustes distance).

For each measurement the user can define normal values (average and standard deviation) for arbitrary age ranges. This enables Viewbox to show measurements colour-coded, so that it is immediately apparent which measurements are outside the normal range of the population (Figure 20).

Figure 19. Points placed on mesh created from CT data. Most of the points are sliding semilandmarks.

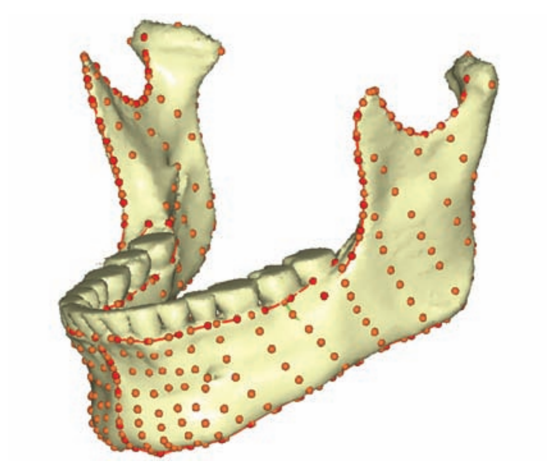

Figure 20. Cephalometric analysis on radiograph using colour-coded measurements to signify deviations from average.

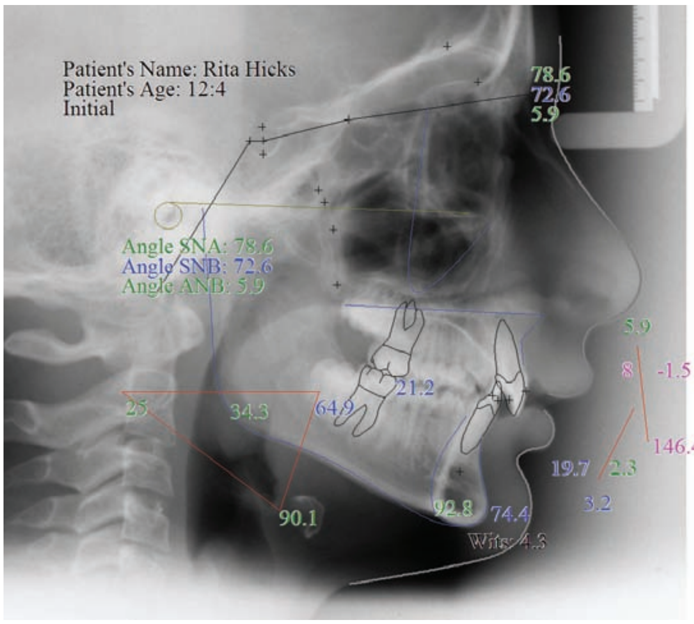

Figure 21. Impacted canine as seen from three different views of a 3D rendering of a CBCT scan

Research Tools and Clinical Use

Viewbox is a comprehensive system incorporating features useful for research projects but also for clinical applications. For research, the most significant is the ability to define points and measurements to suite almost any 2D or 3D task. Measurements and raw point coordinates can be exported to a text file for statistical evaluation in any statistics software. The average of a population can be computed, using any conventional superimposition or Procrustes. Morphometric functions give access to basic GM tools, including sliding semilandmarks on curves and surfaces in 2D and 3D.

In addition to the commonly found features of conventional cephalometric software, clinically valuable are the 3D rendering capabilities for CT data. These allow CT visualization on personal computers at a quality equal to that attainable on dedicated hardware of CT machines (although at a significantly lower speed). Such visualization can be very valuable for treatment planning of patients with craniofacial anomalies, for locating impacted teeth or for assessing the position of teeth within the jaws and to each other (Figure 21). For quantitative assessment, landmarks can be placed on such data and measurements taken, thus enabling 3D analyses. Surface data from laser-scanners or other devices can be imported, allowing the simultaneous visualization of dental casts, facial scans and CT images. The combined data can be used for virtual surgical treatment planning. Because the data are 3D, this method produces more accurate and representative predictions, both of the bony relationships and of the soft-tissue shape.

Other Software and Hardware

Software for 3D cephalometric analysis are in rapid development. Dolphin Imaging (www.dolphinimaging.com) has extended its cephalometric software to import CBCT data, produce various visualizations, including renderings simulating conventional cephalograms and panoramic radiographs, and take measurements in 3D. Medicim (www.medicim.com) have a 3D cephalometric module and a surgical treatment planning module that enables prediction of soft-tissue response to surgical procedures using a mathematical model.

Digital dental models have established themselves as an alternative to plaster. The three main companies that provide the service of converting impressions or plaster casts to digital data are Geo-Digm Corp. (www.dentalemodels.com), OrthoCAD (www.orthocad.com) and OrthoProof (www.orthoproof.nl). Each company provides its own software that enables viewing, measurements, and virtual setups.

Facial scans are the third data type that completes the picture. Various technologies are used, including laser scanning and stereophotogrammetry (Halazonetis, 2001). Companies actively working in this field include Breuckmann (www.breuckmann.com), Dimensional Imaging (www.di3d.com), Canfield Scientific (www.canfieldsci.com) and 3dMD (www.3dmd.com).

CONCLUSION

As computed tomography and sophisticated shape measuring tools permeate the fields of Orthodontic diagnosis and treatment, software support will become more and more important in everyday clinical practice. Development of such software is slow and difficult. Efforts should be applied to produce user-friendly systems so that our patients can benefit. However, software development may not be the critical factor in dissemination of these methods. Postgraduate Orthodontic programmes should place more emphasis on teaching geometric morphometrics and the techniques of computed tomography and research needs to be conducted for gathering normative 3D data as well as for developing new 3D cephalometric analyses.

ACKNOWLEDGMENT

Thanks to Alexandros Stratoudakis, Panos Christou, Christos Katsaros and Michael Coquerelle for providing CT data and meshes for the images. This work was supported by the EVAN project (European Virtual Anthropology Network) MRTN-CT-2005-019564, a Marie Curie Research Training Network. All images in this chapter were produced by the Viewbox software.

REFERENCES

Barrett, J. F., & Keat, N. (2004). Artifacts in CT: Recognition and avoidance. *Radiographics, 24,* 1679-1691.

Baumrind, S., & Frantz, R. C. (1971). The reliability of head film measurements. 1. Lamdmark identification. *American Journal of Orthodontics, 60,* 111-127.

Björk, A., & Skieller, V. (1983). Normal and abnormal growth of the mandible. A synthesis of longitudinal cephalometric implant studies over a period of 25 years. *European Journal of Orthodontics, 5,* 1-46.

Bookstein, F. (1991). *Morphometric tools for landmark data: geometry and biology.* Cambridge: Cambridge University Press.

Bookstein, F. L. (1997). Landmark methods for forms without landmarks: morphometrics of group differences in outline shape. *Medical Image Analysis, 3,* 225-243.

Cevidanes, L. H., Bailey, L. J., Tucker, S. F., Styner, M. A., Mol, A., Phillips, C. L., Proffit, W. R., & Turvey, T. (2007). Three-dimensional cone-beam computed tomography for assessment of mandibular changes after orthognathic surgery. *American Journal of Orthodontics and Dentofacial Orthopedics, 131,* 44-50.

Cha, J-Y., Mah, J., & Sinclair, P. (2007). Incidental findings in the maxillofacial area with 3-dimensional cone-beam imaging. *American Journal of Orthodontics and Dentofacial Orthopedics, 132,* 7-14.

Dryden, I. L., & Mardia, K. V. (1998). *Statistical shape analysis.* Chichester, U.K.: John Wiley & Sons.

Elefteriadis, J. N., & Athanasiou, A. E. (1996). Evaluation of impacted canines by means of computerized tomography. *International Journal of Adult Orthodontics and Orthognathic Surgery, 11,* 257-264.

Farman, A. G., & Scarfe, W. C. (2006). Development of imaging selection criteria and procedures should precede cephalometric assessment with cone-beam computed tomography. *American Journal of Orthodontics and Dentofacial Orthopedics, 130,* 257-265.

Gunz, P., Mitteroecker, P., & Bookstein, F. L. (2005). Semilandmarks in Three Dimensions. In D. E. Slice (Ed.), *Modern morphometrics in physical anthropology* (pp. 73-98). New York: Kluwer Academic / Plenum Publishers.

Halazonetis, D. J. (1994). Computer-assisted cephalometric analysis. *American Journal of Orthodontics and Dentofacial Orthopedics, 105,* 517-521.

Halazonetis, D. J. (2001). Acquisition of 3-dimensional shapes from images. *American Journal of Orthodontics and Dentofacial Orthopedics, 119,* 556-560.

Halazonetis, D. J. (2004). Morphometrics for cephalometric diagnosis. *American Journal of Orthodontics and Dentofacial Orthopedics, 125,* 571-581.

Halazonetis, D. J. (2005). From 2D cephalograms to 3D computed tomography scans. *American Journal of Orthodontics and Dentofacial Orthopedics, 127,* 627-637.

Ho, C. C., Wu, F. C., Chen, B. Y., Chuang, Y. Y., & Ouhyoung, M. (2005). Cubical marching squares: adaptive feature preserving surface extraction from volume data. *Computer Graphics Forum, 24,* 537-545.

Houston, W. J. B., Maher, R. E., McElroy, D., & Sherriff, M. (1986). Sources of error in measurements from cephalometric radiographs. *European Journal of Orthodontics, 8,* 149-151.

Hwang, H. S., Hwang, C. H., Lee, K. H., & Kang, B. C. (2006). Maxillofacial 3-dimensional image analysis for the diagnosis of facial asymmetry. *American Journal of Orthodontics and Dentofacial Orthopedics*, *130*, 779-785.

Katsumata, A., Hirukawa, A., Okumura, S., Naitoh, M., Fujishita, M., Ariji, E., & Langlais R. P. (2007). Effects of image artifacts on gray-value density in limited-volume cone-beam computerized tomography. *Oral Surgery, Oral Medicine, Oral Pathology, Oral Radiology, and Endodontics, 104*, 829-836.

Kazandjian, S., Kiliaridis, S., & Mavropoulos, A. (2006). Validity and reliability of a new edge-based computerized method for identification of cephalometric landmarks. *Angle Orthodontist*, *76*, pp. 619-24.

Kniss, J., Kindlmann, G., & Hansen, C. (2002). Multi-Dimensional Transfer Functions for Interactive Volume Rendering. *IEEE Transactions on Visualization and Computer Graphics, 8*, 270-285.

Kumar, V., Ludlow, J., Cevidanes, L., & Mol, A. (2008). In vivo Comparison of Conventional and Cone Beam CT synthesized Cephalograms. *Angle Orthodontist, 78*, 873-879.

Lorensen, W. E., & Cline, H. E. (1987). Marching Cubes: A High Resolution 3D Surface Construction Algorithm. *Computer Graphics, 21*, 163-169.

Ludlow, J. B., Davies-Ludlow, L. E., & Brooks, S. L. (2003). Dosimetry of two extraoral direct digital imaging devices: NewTom cone beam CT and Orthophos Plus DS panoramic unit. *Dentomaxillofacial Radiology, 32*, 229-234.

Ludlow, J. B., Davies-Ludlow, L. E., Brooks, S. L. & Howerton, W.B. (2006). Dosimetry of 3 CBCT devices for oral and maxillofacial radiology: CB Mercuray, NewTom 3G and i-CAT. *Dentomaxillofacial Radiology, 35*, 219-226.

Maeda, M., Katsumata, A., Ariji, Y., Muramatsu, A., Yoshida, K., Goto, S., Kurita, K., & Ariji, E. (2006). 3D-CT evaluation of facial asymmetry in patients with maxillofacial deformities. *Oral Surgery, Oral Medicine, Oral Pathology, Oral Radiology, and Endodontics, 102*, 382-390.

Mah, J. K., Danforth, R. A., Bumann, A., & Hatcher, D. (2003). Radiation absorbed in maxillofacial imaging with a new dental computed tomography device. *Oral Surgery, Oral Medicine, Oral Pathology, Oral Radiology, and Endodontics, 96*, 508-513.

Marmitt, G., Friedrich, H., & Slusallek, P. (2006). Interactive Volume Rendering with Ray Tracing. *Eurographics State-of-the-Art Report 2006*, Vienna. Retrieved April 12, 2008, from http://graphics.cs.uni-sb.de/Publications/2006/eg2006star_vrt.pdf

Moshiri, M., Scarfe, W. C., Hilgers, M. L., Scheetz, J. P., Silveira, A. M., & Farman, A. G. (2007). Accuracy of linear measurements from imaging plate and lateral cephalometric images derived from cone-beam computed tomography. *American Journal of Orthodontics and Dentofacial Orthopedics, 132*, 550-560.

Ngan, D. C., Kharbanda, O. P., Geenty, J. P., & Darendeliler, M. A. (2003). Comparison of radiation levels from computed tomography and conventional dental radiographs. *Australian Orthodontic Journal, 19*, 67-75.

O'Higgins, P. (1999). Ontogeny and phylogeny: some morphometric approaches to skeletal growth and evolution. In M.A.J. Chaplain, G.D. Singh, J.C. McLachlan (Ed.), *On growth and form. Spatiotemporal pattern formation in biology* (pp. 373-393). New York: John Wiley & Sons.

Parker, S., Shirley, P., Livnat, Y., Charles Hansen, C., & Sloan, P. P. (1998). Interactive ray tracing for isosurface rendering. In *IEEE Visualization '98*, pp. 233–238.

Ricketts, R. M. (1960). A foundation for cephalometric communication. *American Journal of Orthodontics, 46,* 330-357.

Schmuth, G. P. F., Freisfeld, M., Koster, O., & Schuller, H. (1992). The application of computerized tomography (CT) in cases of impacted maxillary canines. *European Journal of Orthodontics, 14,* 296-301.

Shrimpton, P. C., Hillier, M. C., Lewis, M. A., & Dunn, M. (2003). Doses from Computed Tomography (CT) examinations in the UK – 2003 Review. *National Radiological Protection Board*. Retrieved March 16, 2008, from http://www.hpa.org.uk/radiation/publications/w_series_reports/2005/nrpb_w67.pdf

Slice, D. E. (2005). Modern morphometrics. In D. E. Slice (Ed.), *Modern morphometrics in physical anthropology* (pp. 1-45). New York: Kluwer Academic / Plenum Publishers.

Sukovic, P. (2003). Cone beam computed tomography in craniofacial imaging. *Orthodontics & Craniofacial Research*, *6*(Suppl 1), 31-36.

Swennen, G. R. J., Schutyser, F., & Hausamen, J. E. (2006). *Three-dimensional cephalometry. A color atlas and manual*. Berlin: Springer-Verlag.

Tsiklakis, K., Donta, C., Gavala, S., Karayianni, K., Kamenopoulou, V., & Hourdakis, C. J. (2005). Dose reduction in maxillofacial imaging using low dose Cone Beam CT. *European Journal of Radiology, 56,* 413-417.

UNSCEAR, United Nations Scientific Committee on the Effects of Atomic Radiation. (2000). *Sources and effects of ionizing radiation, Report to the General Assembly, with scientific annexes*. Report Vol. I. Retrieved February 18, 2008, from http://www.unscear.org/unscear/en/publications/2000_1.html

Van Assche, N., van Steenberghe, D., Guerrero, M. E., Hirsch, E., Schutyser, F., Quirynen, M. & Jacobs, R. (2007). Accuracy of implant placement based on pre-surgical planning of three-dimensional cone-beam images: a pilot study. *Journal of Clinical Periodontology, 34,* 816-821.

Walker, L., Enciso, R., & Mah, J. (2005). Three-dimensional localization of maxillary canines with cone-beam computed tomography. *American Journal of Orthodontics and Dentofacial Orthopedics, 128,* 418-423.

KEY TERMS

Dataset: A dataset is a collection of points and curves that have been placed on an object. The dataset contains the coordinates of the digitized points and the coordinates of the controlling points of the curves (cubic splines).

Image: Digital images have become the most common method of entering diagnostic data for digitization and measurement. The most prevalent file formats in dentistry include JPEG, TIFF and DICOM. Viewbox can communicate directly with scanners using the TWAIN interface.

Patient: This is the fundamental object, representing a patient or specimen. It holds the name, gender and date of birth of the patient as well as the 'child' objects, such as datasets, images or CT data.

Point Cloud: Point clouds are collections of 3D points. Point clouds can be acquired from a surface digitizer or can be created from meshes. Point clouds contain no information regarding the shape of the surface from which they were collected and for this reason their usefulness is limited.

Slice: A slice is used to create a 2D image by taking an arbitrary cross-section through a volume or a mesh (Figure 18).

Template: Datasets are based on Templates. A template can be thought of as an exemplary dataset, containing all the information required to measure and analyze the object. The most common dataset in orthodontics is related to analysis of a lateral cephalogram and contains the conventional cephalometric points and measurements. However, templates are completely user-definable, so they can be created for whatever purpose is desired. Examples include templates for measuring dental casts, facial photographs, osseous structures from CTs, etc.

Volume: Volumes contain data from CTs or MRIs. They are regular rectangular 3D arrays of voxels. Each voxel holds a single value representing the density of the tissue at that location. Volumes can be rendered in various ways, as previously described.

Chapter II
A New Software Environment for 3D-Time Series Analysis

Jörg Hendricks
University of Leipzig, Germany

Gert Wollny
Universidad Politécnica de Madrid, Spain

Alexander Hemprich
University of Leipzig, Germany

Thomas Hierl
University of Leipzig, Germany

ABSTRACT

This chapter presents a toolchain including image segmentation, rigid registration and a voxel based non-rigid registration as well as 3D visualization, that allows a time series analysis based on DICOM CT images. Time series analysis stands for comparing image data sets from the same person or specimen taken at different times to show the changes. The registration methods used are explained and the methods are validated using a landmark based validation method to estimate the accuracy of the registration algorithms which is an substantial part of registration process. Without quantitative evaluation, no registration method can be accepted for practical utilization. The authors used the toolchain for time series analysis of CT data of patients treated via maxillary distraction. Two analysis examples are given. In dentistry the scope of further application ranges from pre- and postoperative oral surgery images (orthognathic surgery, trauma surgery) to endodontic and orthodontic treatment. Therefore the authors hope that the presented toolchain leads to further development of similar software and their usage in different fields.

INTRODUCTION

In this chapter, the authors present and validate a toolchain that allows the analysis of changes in a patient or specimen based on a series of DICOM CT images taken at different times by using image segmentation, voxel based rigid and non-rigid registration, as well as 3D visualization. This time series analysis of medical images enables the full three-dimensional comparison of two or more data sets of the same person or specimen, e.g., the comparison of pre- and post treatment CT images. Such analysis helps to understand the underlying processes, that arise, for instance, from treatment.

One prominent example of treatment inducing changes of shape in patients is distraction osteogenesis (a method to correct severe maxillary hypoplasia or retrusion). In clinical practice, this planning is often based on computer tomography (CT) scans and the surgeon's experience. Planning these procedures can be difficult if complex three-dimensional changes are to be performed (Berti et al., 2004), and as a first step towards an improved treatment planning, a thorough understanding of what is achieved and how the different structures have been moved is needed. Here a better understanding of the structural changes induced by the surgical therapy is desirable as a first step. Given a thorough understand of the procedure, a superior treatment planning and outcome could be achieved.

In dentistry, the scope of the presented toolchain generally ranges from pre- and postoperative oral surgery images (orthognathic surgery, trauma surgery) to endodontic and orthodontic treatment as well as the analysis of growth. The new tool is already part of our operation planning and visualization software. We concentrated on the time series analysis of routinely acquired pre- and postoperative CT-images of patients who were treated via maxillary distraction osteogenesis as no studies regarding the analysis of the complex three-dimensional mid-facial movements are available (Hierl et al., 2005). Furthermore, incorrect treatment planning may lead to a malpositioned midface and may necessitate further surgical intervention. At the end of this chapter we give some examples of the results of the time series analysis performed. Finally validation of the registration methods is performed. This means showing that our registration algorithm applied consistently succeeds with an average error acceptable for the application. In the near future the toolchain will be improved and integrated into a multifunctional planning tool. Furthermore, the range of data files will be enlarged. By now only DICOM files from CT or CBT (cone beam tomography) can be loaded. In the future polygon-based surfaces should be included, too.

A Short Review of Time Series Medical Image Analysis

The time series analysis of medical images has a long history and its importance in medical treatment is undisputed. Most of the time series analyses have to be done manually and therefore they are dependent on the expertise and objectiveness of the observer. In the last years the tools for image registration have been improved and methods were developed to analyze images automatically. Historically, image-registration has been classified as being "rigid" (where images are assumed to be of objects that simply need to be rotated and translated with respect to one another to achieve correspondence) or "non-rigid" (where either through biological differences or image acquisition or both, correspondence between structures in two images cannot be achieved without some localized stretching of the images). Usually the first step in an automatic analysis of serial medical images includes rigid registration, to eliminate positional differences of the patients during image acquisition. As mentioned above the transformations applied to the images are restricted to rotation and translation by rigid registration. Consequently these transformations are not able to deal with local variations between the images, but only with global ones. A high number of methods based on rigid registration were introduced in recent years. Most investigations focused on neurological patients and therefore on the registration of MR images to detect and assess lesions or volumetric changes of brains. For example Lemieux et al. investigated epilepsy patients or Fox et al. patients suffering from Alzheimer's disease.

The next step to quantify deformations usually is the non-rigid registration. Therefore non rigid registration adds local variability to the registration process and the structural change over time can be described by a non-rigid registration transformation. An overview of the large variety of registration approaches has been given by many authors. For more aspects of image registration, the reader is referred to other reviews; there is good technical coverage in Lemieux et al., (1998), Fox et al., (2000), Crum et al. (2004), Hill et al. (2001), Brown (1992), Lester and Arridge (1999), Maintz and Viergever (1998) and Zitova and Flusser (2003), reviews of cardiac applications in Makela et al. (2002), nuclear medicine in Hutton et al. (2002), radiotherapy in Rosenman et al. (1998), digital subtraction angiographies in Meijering et al. (2003) and brain applications in Toga and Thompson (2001) and Thompson et al. (2000). In summary, the analysis of medical images is an active research area and they are used in many medical fields.

A Short Review of Validation Methods

Estimation of accuracy of registration algorithms is a substantial part of the registration process. Without quantitative evaluation, no registration method can be accepted for practical utilization. Therefore validation of the methods used is necessary. It usually means that a registration algorithm applied to typical data in a given application consistently succeeds with a maximum (or average) error acceptable for the application. For feature based approaches in which the information of structure, such as landmarks, curves and surfaces, is used a real-world error can be calculated, which for landmark methods expresses the distance between corresponding landmarks post-registration. For rigid-registration this form of validation has been studied intensively and it has been found that an average registration error for the whole volume can be estimated from knowledge of the landmark positions (Fitzpatrick et al., 2003). The most comprehensive case-study for the validation of rigid-body registration is probably the Vanderbilt University project (West et al., 1997). Validation of non-rigid, local and elastic registration methods is still at the beginning. That is because such an analysis is not generally possible for non-rigid techniques so although the error at landmarks can be established, the error in other parts of the volume is dependent on the transformation model and must be estimated using other means. In voxel-based approaches the registration itself usually cannot inform the user of success or failure, as the image similarity measure is not related to real-world error in a simple way. For these problems, validation is usually performed by making additional measurements post-registration or showing that an algorithm performs as desired on pairs of test images for which the transformation is known. One common approach is to identify corresponding landmarks or regions independently of the registration process and establish how well the registration brings them into alignment (Collins et al., 1997. Woods et al., 1998). In summary, the validation of registration, especially non-rigid registration is a nontrivial problem, partially because the errors can occur in each stage of the registration process and partially because it is hard to distinguish between registration inaccuracies and actual physical differences in the image contents. Important is to choose a validation method that gives an average error that can account for the calculation of values of interest in the investigation performed with the respective application.

Description of Tools and CT Scanning

This chapter deals with workflow and explains the tools used for time series analysis. All pre- and postoperative CT scans were taken with a spiral CT (Siemens volume zoom plus) with contiguous slices, thickness 1mm, no overlapping, without gantry tilting, collimation 1 mm, 512 x 512 matrix. All CT data were stored in DICOM file format and transferred to a hard drive with a Linux-based personal computer running the new software. The following steps were then conducted: The CT data were converted to Vista file format and the images were segmented, that is, to assign material labels to the image voxel. That way soft tissue was separated from bony structure with the function of grayscale thresholding. Metallic implants and orthodontic devices may cause artifacts, which might result in spikes in after visualization. These implants or devices were removed manually in the segmented geometry. The segmented input images were then rigidly registered to correct differences in position and orientation. Then non rigid-registration was conducted to quantify differences between the pre- and postoperative images describing the structural change. An overview in given in the graphic below.

Before describing our registration method the terminology used is explained. When two images are being registered one is conventionally regarded as static and defining a frame of reference and the other is transformed (*i.e.* translated, rotated, scaled, sheared, warped) to bring corresponding features into alignment. The static image is variously known as the target, reference

Image 1.

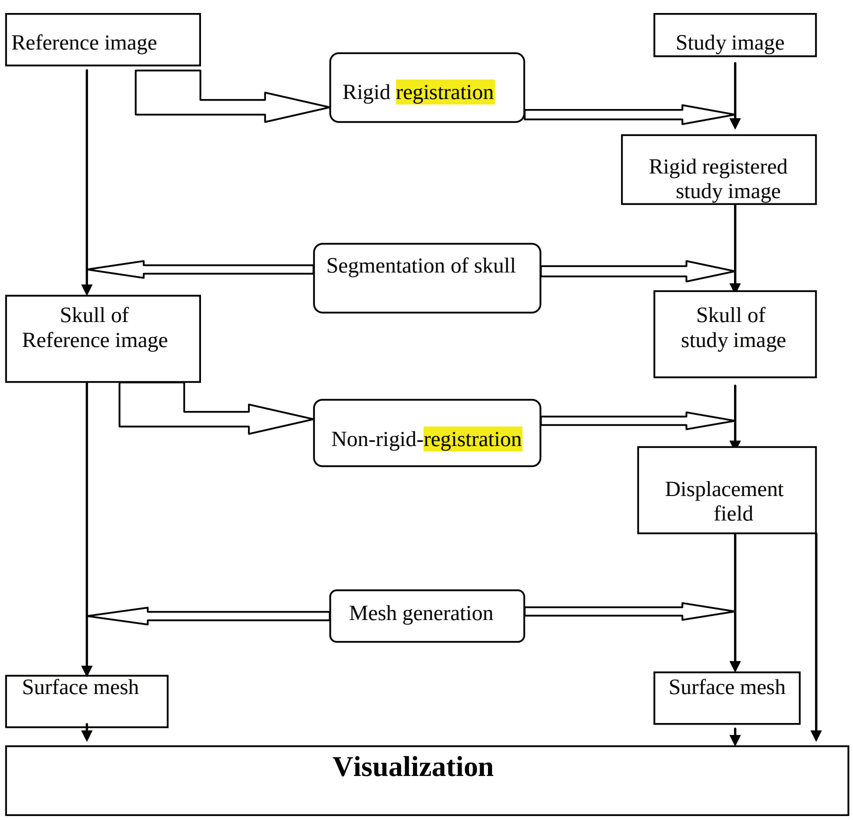

or baseline image. We use reference image. The image undergoing transformation is then known as the source, floating, repeat or study image. We use study image the criterion used to register two images can be known as the similarity measure or the objective or cost function. The term cost function is used. The geometrical transformation that maps features in one image to features in another is known as the transformation, deformation field, displacement field or warp.

The registration aims at transforming a study image S with respect to a reference image R by means of a transformation T (Θ (Θ is the set of possible transformations), so that structures at the same coordinates in both images finally represent the same object. In practice, this is achieved by finding a transformation T_{reg} which minimises a cost function F_{cost}, while constraining the transformation through the joint minimisation of an energy term E(T):

$$T_{reg} := \arg\min_{T \in \Theta} \left(F_{cost}(S_T, R) + {}_{K}E(T) \right) \qquad (1)$$

The cost function F_{cost} accounts for the mapping of similar structures. E(T) ensures topology preservation, which is necessary to maintain structural integrity in the study image, and it thus introduces a smoothness constraint on the transformation T_{reg}. The parameter K is a weighting factor that balances registration accuracy and transformation smoothness. By restricting the set of possible transformation Θ to rigid transformations, i.e. to rotation and translation, topology is preserved per se, we may set K = 0 and rigid registration is obtained by minimizing the cost function F_{cost}. CT images are normalised by the Hounsfield *scale*, mapping similar materials to similar intensities. Therefore, we obtain rigid registration by minimising the *Sum of Squared Differences* (SSD)

$$\mathbf{F_{cost}}(\mathbf{S},\mathbf{R}) := \int_{\Omega} (\mathbf{S}\,(\vec{x}) - \mathbf{R}\,(\vec{x}))\mathbf{2}\,\mathbf{d}\vec{x} \qquad (2)$$

using a modified *Marquardt-Levenberg* algorithm (Thevenaz et al., 1995). If Θ is not restricted, we require K > 0 and we target for *non-rigid registration*. In voxel based approaches for non rigid registration, as we used, the cost function F_{cost} is derived from local or global image intensity similarity measures. The advantage of these methods lies in the independence of human interaction which makes voxel based approaches the tool of choice when it comes to the automatic analysis of large sets of data. Like proposed by Christensen (1994), we employ *fluid dynamics* as energy constraint E(T) - since it allows for large deformations - and we minimize SSD (2).Surface based rendering was used to visualize the shape changes of the skull. By using the marching tetrahedra algorithm the skull surface was extracted from the segmented and rigidly registered data sets (Ning and Bloomenthal, 2001). The shape change described by the non-rigid registration is displayed as arrows or by a colouring scheme. The arrows ending at the surface display at each point the corresponding deformation vector. For the colouring scheme outward-pointing normals were coded in blue, inward pointing in red. Colour intensity reflected its magnitude and the colour scale is given in mm (see Figure 1). For further information about the registration method see Wollny (2004).

Description of Validation

Landmarks were picked manually for validation purposes using a volume rendering visualization method. 36 anatomical soft and hard tissue landmarks on the patients faces had been predefined which showed mostly a high reproducibility (landmark pick error ≈ 1 mm). Exceptions were mouth angle, gnathion, medial kanthus, upper lip (philtrum edge) and glabella. These points showed deviations up to 3mm when selected by different observers or in different images. In order to pick the landmarks on bone and skin we used a self-developed 3D-texture based iso-surface

Figure 1. Visualization of maxillary advancement in a modified quadrangular manner. Colour-coded display, the colour depth resembles the distance. Displacement vectors are shown, too. By clicking on any point of the surface, the amount of the appropriate displacement is shown in mm scale.

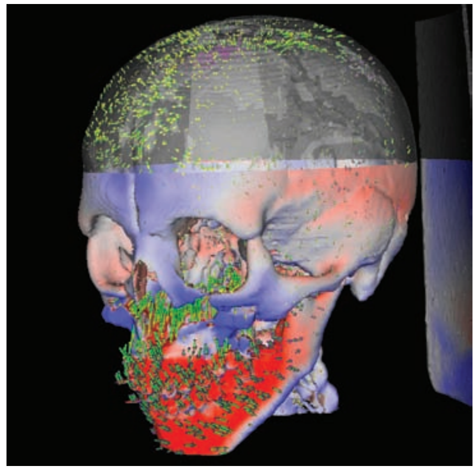

Figure 2. Iso-surface browser tool to pick landmarks on bone and skin. By moving the lever on the far left, the surface can be changed according to Hounsfield units.

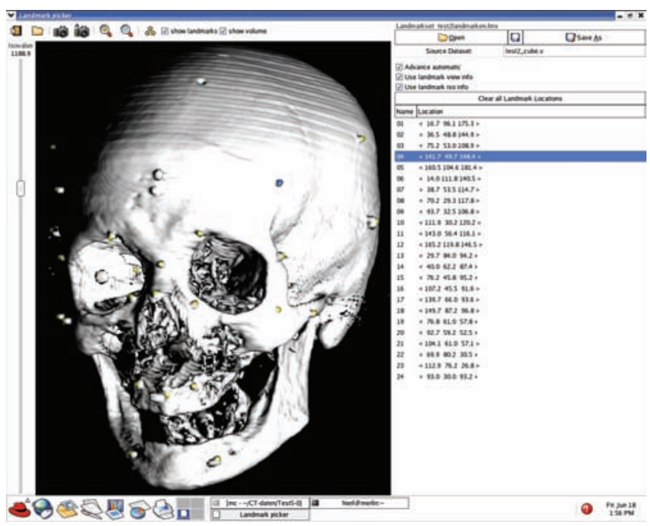

browser that allows an intuitive interactive change between soft tissue and bone (see Figure 2). The landmarks are listed in Table 1.

Patients and Skulls Used for Validation

For the validation of the rigid registration we used one human skull, one porcine skull and two rabbit skulls and for the registration of the non-rigid registration the pre- and postoperative CT-images of 19 patients suffering from cleft lip and palate which were treated via maxillary distraction osteogenesis (RED system, Martin Co. Tuttlingen, Germany). We chose 4 cadaver heads of different size in order to prove whether or not the CT-data size influences the accuracy of the method.

Table 1. Landmark definition list

<u>Midface:</u>	
Anterior nasal spine (= Nasospinale)	most anterior point
Bregma	intersection of sagittal and coronar sutures
Ear lobule	most caudal contact point of the lobulus and the adjacent skin
Exokanthion (=lateral kanthus)	soft tissue lateral kanthal border
Endokanthion (=medial kanthus)	soft tissue medial kanthal border
Glabella	most anterior point between superciliar arches in midsagittal plane
Orbitale (= Infraorbital rim)	lowest point on infraorbital rim
Lambda	intersection of sutura lambdoidea and sutura sagittalis in midsagittal plane
Nasion (bone)	midpoint of suture between frontal and nasal bones
Nasion (skin)	deepest point of the concavity overlying the frontonasal suture
Nasal Tip (= Pronasale)	most anterior point of nasal skin
Nostril (Piriforme aperture)	most inferior-lateral point of piriforme aperture
Opisthion	most posterior point of Foramen magnum in midsagittal plane
Prostion	transition point of the alveolar process and the dental crowns between (= intradentale superior / Alveolare) the two upper incisors
Supraorbitale (=supraorbitale rim)	most anterior-superior border of superior orbital rim
Fronto-zygomatic suture point (= frontomalare temporale)	most lateral point of frontozygomatic suture
<u>Mandible</u>	
Lower lip (Angulus oris)	most lateral point
Mental foramen (= Mentale)	most caudal point
Gnathion Bone (~ Menton)	most anterior-inferior point of chin symphysis
Gonion	mandibular angle point (postero-inferior)
Upper Lip Philtrum	upper lip vermillion border at the philtrum lines
Coronoid process (= Coronion)	most superior point

20 micro titanium screws (1.5 mm Ø; Martin Co. Tuttlingen, Germany) were implanted into the porcine skull, 9 micro titanium screws into each rabbit skull and 24 micro titanium screws in the human skull. The distances between the center of all screw heads were measured with a precision slide gauge (see Figure 3). The number of screws implanted depended on the skulls size and the screws were placed on areas of the skulls that cover the whole skull surface and should therefore allow all over examination. The skulls were CT-scanned in th eaboce mentioned manner and maxillary osteotomies of the skulls were performed. Then the advanced maxillae were fixed with titanium miniplates. The pig and human skull were displaced in two steps each followed by CT-scanning and the rabbit skulls once (see Figure 4). After the displacements the distances between the screw heads were measured again.

Figure 3. Manual measurement of the distance between the screw heads of the human skull

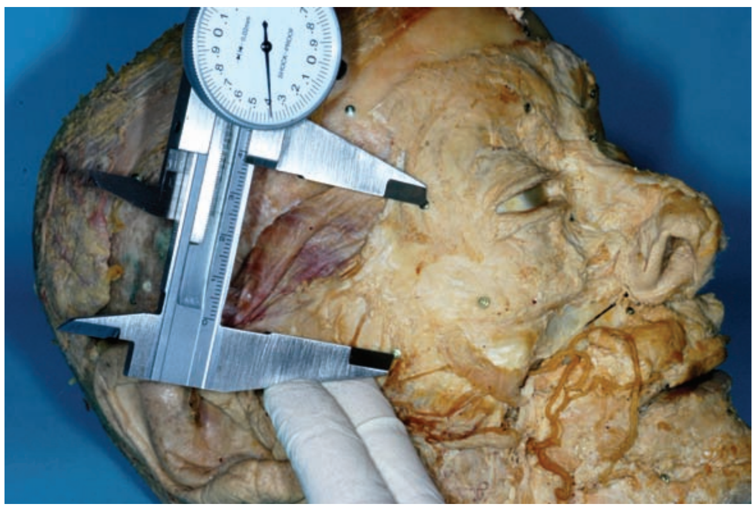

Figure 4. Processed and visualized CT scan of pig cadaver with titanium micro scews, osteotomy an forward displacement of the anterior maxilla. The screws and miniplates are framed in red and yellow.

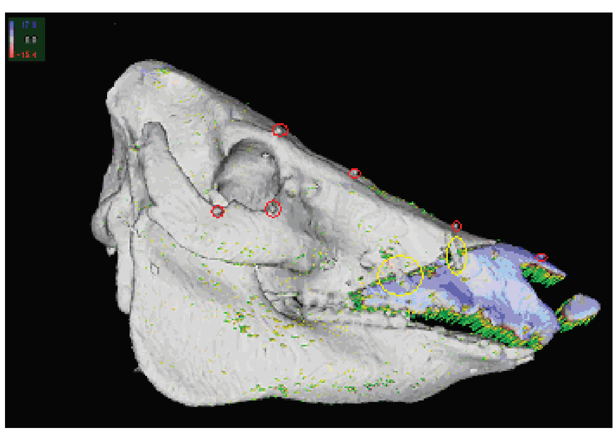

Error Calculation

The visualization and rigid registration method were validated by comparing the values of the manually measured distances between the screws heads in the cadavers and the values of the calculated distances between the screw heads in the visualized segmented and rigidly registered images. The distances were calculated in this manner:

$$\sqrt{((x_1-x_2)^2+(y_1-y_2)^2+(z_1-z_2)^2)}$$

$\mathbf{x_{1.}\ x_{2.}\ y_{1.}\ y_{2.}\ z_{1.}\ z_2}$ are the coordinates of the screw heads in the three-dimensional images. In the same manner the deviations between the distances of the coordinates of the anatomical landmarks found in the non-rigidly registered images and the coordinates of the correspondent landmarks found in the reference images with the distances of the coordinates of the anatomical landmarks in the study image and the coordinates of the correspondent landmarks found in the reference images were quantified to validate the voxel based non-rigid registration.

RESULTS

Validation of Rigid Registration and Visualization Method

The validation of the rigid registration and visualization method showed very good results. The calculated distances between the screw heads and the manually measured distances between the screw heads showed no statistically significant difference ($P > 0.05$, t-test). The measurements on the pig skull showed an average deviation of 1.31 mm (with a range between 0.1 mm and 2.9 mm) after the first displacement and an average deviation of 0.88 mm (with a range from 0.1 mm and 2.3 mm) after the second displacement. The standard error was 1.56 % and 0.98 % (344 measurements) (see Table 2). The average deviation of the distances between the screw heads of the human skull was

Table2. Comparison of measured and calculated distances for the pig skull. Distances are given in mm.

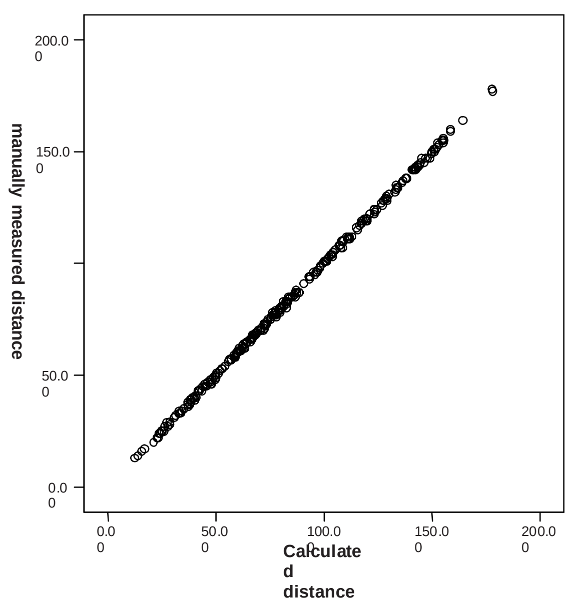

0.68 mm (with a range between 0.1 mm and 1.6 mm) after the first displacement and 0.64 mm (with a range between 0.1 mm and 1.5 mm) after the second displacement. The standard error was 0.6 % and 0.5 %) (456 measurements). The rabbit skulls showed average deviations of 0.5 mm (with a range between 0.1 mm and 1.2 mm) and 0.33 mm (with a range between 0.1 mm and 1.1 mm). The standard error was 1.52 % and 1.17 % (144 measurements). These derivations correspond with errors that may be implied because of the given image resolution of 1 mm^3 and some errors that occur with the measurement via slide gauge that can explain the outlier.

Validation of Non-Rigid Registration

The landmark based validation of the non-rigid registration showed an average deviation of 2.13 mm. The median was 1.6 mm (range between 0.1 mm and 6.8 mm). 70 distances between the anatomical landmarks of the 545 distances collected showed derivations above 4 mm which means that < 13 % of the results were outlying the accuracy of the method of measurement. In average the non-rigid registration error for each distance at the selected landmarks was far below 4 mm. This error range corresponds again to errors that may be introduced because of the image resolution of 1 mm^3 and a landmark pick error of ≈ 1 mm per data set. As mentioned above some landmarks showed higher deviation, when selected by different persons and in different images like mouth angle, gnathion, medial kanthus, upper lip (philtrum edge) and glabella. The landmark pick error for these landmarks was up to 3 mm. The percentage error i is not given because of the falsification caused by the landmark pick error as well. But there was no error dependency from the length of the distance moved noticeable. The average error, standard deviation and landmark pick error for each landmark is given in Table 3. It is important to note that valid and invalid displacement vectors can be discerned easily, because

Figure 5. The displacement vectors for the for. mentale and tub. mentale are starting and ending on the appropriate surface mesh whereas the displacement vector for the spina nasalis ant. displays an registration error, the arrow protrudes over the surface of the study image that is shown transparent in this example

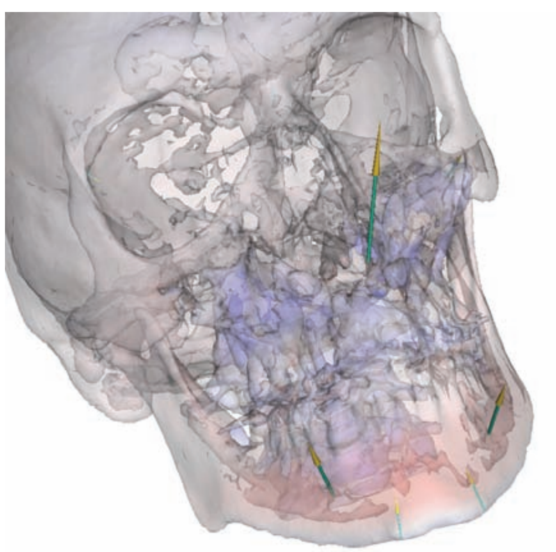

Table 3. Average error, standard deviation and corresponding landmark pick error of the distances between the anatomical landmarks considered for validation of the non-rigid registration (mm). (l)=left side, (r)= right side

Landmark name	average error in mm	standard deviation	landmark pick error
Bregma	2.04	1.50	1
Mouth angle (l)	3.55	1.59.	3
Mouth angle (r)	3.40	1.66	3
Earlobe (l)	2.13	1.27	1
Earlobe (r)	1.65	0.99	1
Foramen mentale (l)	2.15	1.74	1
Foramen mentale (r)	1.70	1.10	1
Fronto-zygomatico suture (l)	1.21	0.77	1
Fronto-zygomatico suture (r)	1.23	0.85	1
Glabella	2.19	1.62	3
Gnathion	3.30	0.14	1
Gonion (l)	1.75	1.27	1
Gonion (r)	2.70	1.62	1
Lower lip (l)	2.27	0.91	2
Lower lip (r)	2.26	1.39	2
Infraorbital rim most caudal point (l)	1.75	0.92	1
Infraorbital rim most caudal point (r)	1.66	0.76	1
Lambda	3.05	1.71	3
Lateral kanthus (l)	1.70	1.50	1
Lateral kanthus (r)	1.65	1.57	1
Medial kanthus (l)	3.55	0.77	3
Medial kanthus (r)	3.40	0.98	3
Nasal tip	1.68	1.03	1
Nasion (bone)	2.26	1.42	1
Nasion (skin)	1.88	1.09	1
Nose tip	1.60	1.27	1
Nostril (l)	2.43	1.42	1
Nostril (r)	2.54	1.67	1
Opisthion	0.75	0.38	1
Coronoid process (l)	0.89	0.36	1
Coronoid process(r)	1.24	1.04	1
Prostion	2.92	1.66	1
Anterior nasal spine	2.71	1.75	1
Supraorbital rim (l)	1.84	1.47	1

continued on following page

Table 3. continued

Supraorbital rim (r)	1.95	0.88	1
Upper lip (l) (philtrum edge)	2.55	1.68	2
Upper lip (r) (philtrum edge)	2.55	1.38	2

all starting and ending points of the vectors are located on the appropriate pre- and postoperative mesh surface. So erroneous vectors of anatomical landmarks can be easily recognized and be taken out of the analysis (see Figure 5).

CLINCAL EXAMPLE FOR TIME SERIES ANALYSIS OF PATIENTS WHO WERE TREATED VIA MAXILLARY DISTRACTION

Analysis of Soft Tissue Changes Following Maxillary Distraction Osteogenesis

In one study the soft tissue changes following maxillary distraction osteogenesis were investigated (Hierl et al., 2007). Therefore with the aid of the novel toolchain, the relation between soft and hard tissue changes was analyzed in a group of patients treated at the Leipzig University Department of Oral and Maxillofacial surgery. The patient group consisted of 20 patients, who were treated via maxillary distraction osteogenesis from 2002 to 2004. 18 suffered from cleft lip and palate, age ranged from 10 to 63 years, the average age was 24 years. The same system (RED II and Leipzig retention plate; Martin Medizintechnik, Tutlingen, Germany) was used for all patients. The RED II System includes an external, halo frame based distractor and a miniplate system for bony anchorage. After a subtotal modified quadrangular osteotomy, the distraction procedure started on the 4^{th}-5^{th} day after surgery. Advancement was 1mm/day until an overcorrection of 15-20 % was achieved. The distraction period was followed by a consolidation period, which lasted 4-8 weeks depending on age and dentition. The preoperative CT scans for the time series analysis were taken 3-5 weeks before surgery. The postoperative scans 2-4 weeks after removal of the distraction device. Scanning was performed with the same scanner used for the data of validation (Siemens volume zoom plus scanner). Slice thickness was the same (1mm without overlapping). The pre- and postoperative CT scans were then processed with the toolchain. A limited number of easy to locate landmarks was chosen. Those landmarks were anterior nasal spine, columella base, nasion (bone and soft tissue), piriforme aperture right and left, alar base right and left, zygomatic prominence right and left (bone and soft tissue). The interdependence of hard and soft tissue was evaluated by way of Wilcoxon test. Furthermore the distance between the coordinates of corresponding soft and hard tissue landmarks was computed. This data served as a control measurement for the displacement vectors as again pre- and postoperative data were statistically compared with Wilcoxon test. The analysis showed an average bony displacement in the piriforme aperture region of 8.1 mm with a soft tissue displacement of 8.1 mmwith a soft tissue displacement of 8.0 mm. Regarding zygomatic prominence displacement distances lay at 8.6 mm (bone) and 8.3 mm (soft tissue). No statistical significant difference could be noted. The average soft tissue depth over bony landmarks ranged between 13-16 mm. There was no statistical significant difference between pre- and postoperative data seen.

Analysis of a Trauma Patient

In this chapter we give a short overview of the time series analysis of the data of a patient who had a posttraumatic malposition of the zygomatic bone that needed to be corrected and a defect of the frontal bone which led to the opening of the frontal sinus and had to be closed. The operation included a bone augmentation from the parietal to the frontal bone as well as a lift of the right zygomatic bone. The operation was done via a coronal incision and three miniplates were used for osteosynthesis. Furthermore the patients right eye was lost due to the accident and the eye prosthesis was displaced inferiorly due to the malpositioned zygoma. Reposition of the zygoma led to a correct position of the prosthesis. The pictures below show the computed and visualized data of that patient (Figure 6 -8). A description of what is seen is given below each picture.

DISCUSSION

In this study we presented a novel tool chain that allows time series analysis to assess soft and hard tissue changes by mid-facial distraction treatment. To our knowledge this is the first software that allows a three-dimensional time series analysis of pre- and postoperative CT data sets in this manner. At first there is to say, that both validation methods show some problems caused by the image resolution of 1 mm^3 per data set, but higher resolution also means higher radiation exposure and for our purposes this accuracy is adequate. If the tool chain is used for other surgical procedures that require higher accuracy a new validation might be required. For example cone beam x-ray CT data may be used. The validation of the rigid registration and visualization method showed no statistically significant difference between the manually measured distances and the calculated distances in the visualized and rigidly registered images of the four cadaver heads ($P > 0.05$). In total 944 measurements were made. The standard error was found between 0.5 % and 1.56 %. These results demonstrate high accuracy for the visualization and rigid registration method. The sample size for the validation of the rigid registration was small with four cadaver heads or even with ten when counting the skulls again after displacement, but because of the very small deviations between the skulls there may be no other results expected by higher sample sizes. Minor limitations of the analysis method can be found in the limitation of voxel based non-rigid registration. Not all reasons for that are now known. On the one hand, especially landmark based validation is difficult, because in some cases the disease pattern (e. g. cleft lip and palate) makes the identification of important landmarks of the mid-facial area (like, e. g., the corners of the mouth, the upper lip, the prostion or the spina nasalis anterior) difficult or even impossible. Therefore it might be necessary to optimize the landmark based visualization, especially when using data of patients suffering from diseases, that influence the structure and shape of the face. A similar problem that structures are present in one image which are not present in the other definitely causes that the non-rigid registration based on fluid dynamics tends to misregister. These specific geometry problems of the intricate bony structure of the human midface occur because some bony parts of the midface get thinner during the distraction and therewith their intensity in the CT-data, this might lead to a loss of these parts in the study image and consequently these parts are not incorporated in the non-rigid registration process so that some structures are registered to wrong parts of the skull. To overcome such limitations, it might be useful to combine voxel based approaches with landmarks to restrict the transformation at certain points. We hope to improve the registration results by adding sparse landmark information to the registration criterion. By now outlier can be easily recognized when regarding displacement vectors of anatomical landmarks and can then be taken

Figure 6. Preoperative CT. The yellow coloured bone displays the bone deficiency of the frontal bone and the descent of the zygomatic bone left. Furthermore the eye-prosthesis is visible in the right orbit.

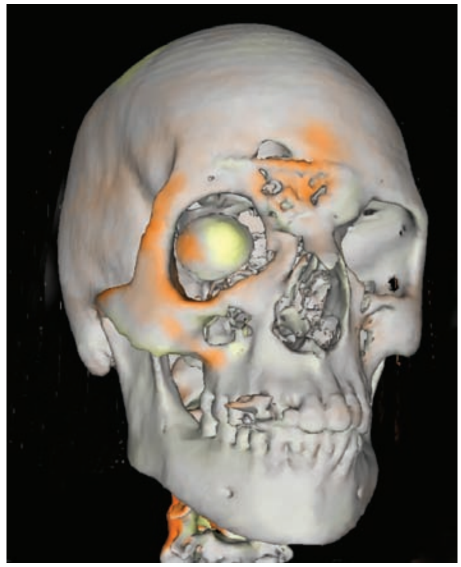

Figure 7. This image shows the computed and visualized postoperative patient data. Good to see is the donor site of the parietal bone right (dark blue) and the augmented bone on the frontal bone where the defect was before. Furthermore the successful upward movement of the zygomatic bone is indicated by the red colour. Furthermore the miniplates can be seen.

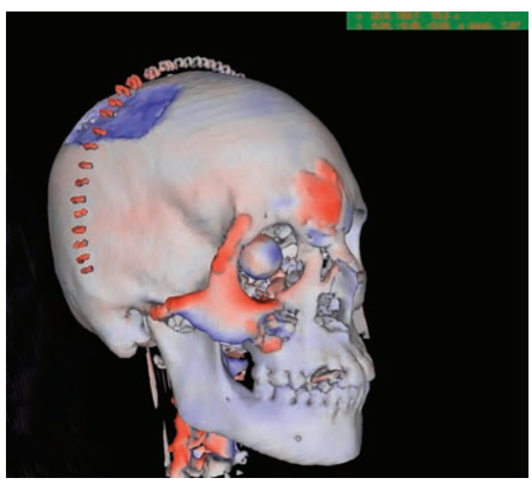

Figure 8. The arrows clarify the structural movements. The bone graft donor site at the parietal bone and the frontal bone augmentation are clearly noticeable. The upward movement of the zygomatic bone is again demonstrated by the red colored parts of the zygomaticarch and bone. The arrows in the left orbit show the movement of the eye prosthesis.

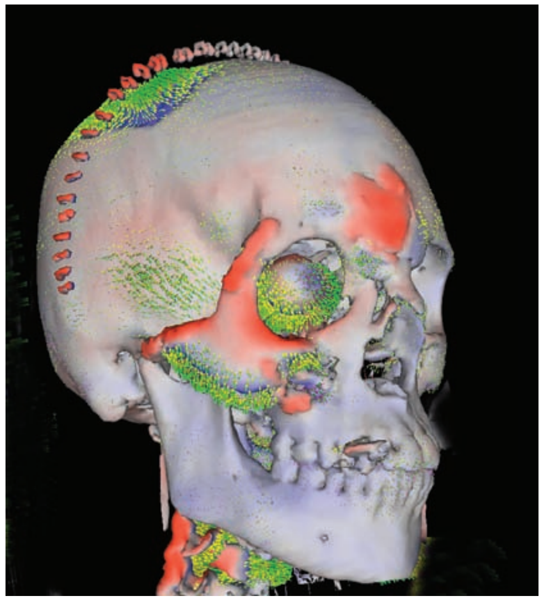

out of the analysis. In near future the toolchain will be used for time series analysis of other patient data. Especially orthodontic and endodontic treatment of patients will be analysed with cone beam tomography data and the surgical treatment of more trauma patients will be assessed.

REFERENCES

Berti, G., Fingberg, J., Hierl, T., & Schmidt, J. G. (2004). An interactive planning and simulation tool for maxillo-facial surgery. In T. M. Buzug & T. C. Lueth (Eds.), *Perspectives in image-guided surgery* (pp. 872-879). World Scientific Publishing.

Brown, L. G. (1992). A survey of image registration techniques. *Computing Surveys, 24*, 325–76.

Christensen, G. E. (1994). *Deformable shape models for neuroanatomy*. DSc.-thesis, Server Institute of Technology, Washington University, Saint Louis.

Collins, D. L., Evans, A. C. (1997). Animal: validation and applications of nonlinear registration-based segmentation. *Int J Pattern Recogn Artificial Intelligence, 11,* 1271–94.

Fitzpatrick, J. M., & West, J. B. (2001). The distribution of target registration error in rigid-body point-based registration. *IEEE Trans Med Imaging*, *20*, 917–27.

Fox, N.C., Cousens, R., Scahill, R. J., Harvay, R. J., Rossor, M. N. (2000). Using serial registered brain magnetic resonance imaging to measure disease progression in Alzheimer disease. *Archive of Neurology, 57*(3), 339-344.

Hierl, T., Wollny, G, Hendricks, J., Berti, G., Schmidt, J. G., Fingberg, J., & Hemprich, A.

(2005). 3D-Analysis of soft tissue changes following maxillary distraction osteogenesis. In T. M. Buzug, K. Prüfer, K. Sigl, J. Bongarz, P. Hering, & G. Willems (Eds.), *Reconstruction of Soft Facial Parts.* Police and Research. Luchterhand Publishers. BKA Series 31-2.

Hill, D. L. G, Batchelor, P. G., Holden, M., & Hawkes, D. J. (2001). Medical image registration. *Physics in Medicine and Biology, 46*, R1–R45.

Kak, A. C., & Slaney, M. (2001). *Principles of Computerized Tomographic Imaging.* Philadelphia, PA: Society of Industrial and Applied Mathematics.

Lemieux, L., Wiehmann, U.C., Moran, N. Fl., Fish, D. R., Shorvon, S. D. (1998). The detection and significance of subtle changes in mixed brain lesions by serial MRI scan matching and spaitial normalisation. *Medical Image Analysis, 3*(2), 227-242.

Lester, H., & Arridge, S. R. (1999). A survey of hierarchical non-linear medical image registration. *Pattern Recognition, 32*,129–49.

Maintz, J. B. A., & Viergever, M. A. (1998). A survey of medical image registration. *Med Image Anal, 2,* 1–36.

Makela, T., Clarysse, P., Sipila, O., Pauna, N., Pham, Q. C., Katila, T., et al. (2002). A review of cardiac image registration methods. *IEEE Trans Med Imaging, 21*, 1011–21.

Ning, P., & Bloomenthal, J. (1991). An evaluation of implicit surface tilers. *Computer Graphics, 13*(6), 33-41.

Pluim, J. P., Maintz, J. B., & Viergever, M. A. (2003). Mutual-information-based registration of medical images: a survey. *IEEE Trans Med Imaging, 22*(8), 986-1004. Review.

Thevenaz, P., Ruttimann, U. E., & Unser, M. (1995). Iterative multi-scale registration without landmarks. In B. Werner (Ed.), *Proceedings of the 1995 IEEE International Conference on Image Processing (ICIP`95), III,* 228-231. Los Alamitos, CA, 23-26.

Wollny, G. (2004). Analysis of changes in temporal series of medical images. *MPI Series for Human Cognitive and Brain Sciences, 43.* Leipzig, Germany.

Zitova, B., & Flusser, J. (2003). Image registration methods: a survey. *Image Vision Comput, 21*, 977–1000.

KEY TERMS

Maxillary Distraction Osteogenesis: Method to correct severe mid-facial hypoplasia and retrognathia

Non-Rigid Registration: Method to quantify deformations between images

Rigid Registration: Method to eliminate positional differences of the patients during image acquisition

Time Series Analysis: Analysis of data sets taken at different times

E: Energy term

F_{cost}: Cost function

K: Weighting factor

R: Registration image

S: Study image

$T_{(reg)}$: Transformation (for registration)

Θ: Set of possible transformations

Ω: Continous image domain

CBT: Cone beam tomography

CT: Computer tomography

DICOM: Digital Imaging and Communications in Medicine

MR(T): Magnetic resonance (tomography)

RED: Rigid external device

SSD: Sum of squared differences

Chapter III
Relationship Between Shrinkage and Stress

Antheunis Versluis
University of Minnesota, USA

Daranee Tantbirojn
University of Minnesota, USA

ABSTRACT

Residual stress due to polymerization shrinkage of restorative dental materials has been associated with a number of clinical symptoms, ranging from post-operative sensitivity to secondary caries to fracture. Although the concept of shrinkage stress is intuitive, its assessment is complex. Shrinkage stress is the outcome of multiple factors. To study how they interact requires an integrating model. Finite element models have been invaluable for shrinkage stress research because they provide an integration environment to study shrinkage concepts. By retracing the advancements in shrinkage stress concepts, this chapter illustrates the vital role that finite element modeling plays in evaluating the essence of shrinkage stress and its controlling factors. The shrinkage concepts discussed in this chapter will improve clinical understanding for management of shrinkage stress, and help design and assess polymerization shrinkage research.

WHAT IS SHRINKAGE STRESS?

The concept of shrinkage stress is intuitive. The notion that stresses arise if a composite filling shrinks inside a tooth is not difficult to convey. The actual assessment of shrinkage and its effects, however, has turned out to be complex and is often a source of confusion. Shrinkage became an issue in dentistry when resin-based composites were introduced as restorative materials (Bowen, 1963), and has remained a persistent concern since. The main difference between resin-based composite and the classic amalgam restorations was adhesion to the tooth structure. Bonding of composite restorations enabled more conservative cavity designs that no longer relied on undercuts for retention and thus preserved more tooth tissue. Unlike unbonded amalgam fillings, an adhesive composite restoration becomes an integral part of the tooth structure. This allows recovery of the original distribution of masticatory loads in a treated tooth. Hence, a composite "filling" actually restores structural integrity lost by decayed tooth tissue and during the process of cavity preparation (Versluis & Tantbirojn, 2006). However, by becoming a more integral part of the load-bearing tooth structure, changes in the composite, such as shrinkage, will also be transferred into the tooth structure causing so-called *residual* stresses.

The origin of shrinkage is the formation of a polymer network during the polymerization reaction. This process results in a denser material, where the density change is manifested in volumetric contraction or shrinkage. Where the composite is bonded to the tooth, the tooth structure will confine the dimensional changes. This leads to the generation of shrinkage stresses in both the restoration and tooth. Under normal clinical conditions, shrinkage movement is so small that it is practically imperceptible. However, the effects of shrinkage may show up indirectly in clinical symptoms. Shrinkage stress has been associated with enamel crack propagation, microleakage and secondary caries, voids in the restoration, marginal loss, marginal discrepancy, and post-operative sensitivity (Jensen & Chan, 1985; Eick & Welch, 1986; Unterbrink & Muessner, 1995). It should be pointed out that none of these clinical symptoms are actually stresses, and their correlation with shrinkage stresses, if any, is not obvious. Furthermore, clinical symptoms are seldom caused by only one factor. Therefore, the precise correlation of these symptoms with polymerization shrinkage is debatable and remains an area of investigation.

To understand the contributions of polymerization shrinkage under clinical conditions, the nature of shrinkage stress has to be studied. The scientific method for studying any subject is creating a theoretical "model" of reality that expresses the current understanding. Subsequently, such models are tested with precise observations and measurements, and if needed, amended or replaced based on new insights. In this chapter, a progression of shrinkage models will be used to discuss advances in dental shrinkage stress research.

SHRINKAGE STRESS MODEL: CORRELATION WITH SHRINKAGE

The most simple model for shrinkage stress is that the residual stress is related to shrinkage. This intuitive model is based on the observation that without shrinkage there will be no shrinkage stress. The observation is subsequently extrapolated into a positive correlation between shrinkage and stress, because it appears credible that when shrinkage increases, shrinkage stress increases too. This intuitive model is probably the most common and practical expression of our understanding of the nature of polymerization shrinkage stress. Manufacturers, clinicians, and researchers alike have the same initial response when confronted with shrinkage data: "a composite with higher shrinkage values must cause higher stresses". To validate this model, the relationship between shrinkage and stress will be considered more closely.

It is important to clearly distinguish between shrinkage and stress. A shrinkage value α is a dimensional change which is defined as the amount of change divided by the original dimension:

$$\alpha = (d_1 - d_0) / d_0 = \Delta d / d_0 \qquad (1)$$

where d_0 is the original dimension, d_1 the dimension after shrinkage, and Δd is the dimensional change. Note that α is dimensionless, and often reported as percentage. The amount of shrinkage can be determined in a physical experiment in which a material dimension before and after polymerization are measured. If it were true that shrinkage stress is directly correlated with shrinkage, shrinkage stress can be assessed by ranking the shrinkage values. In effect, this assumption implies that shrinkage stress would be a material property independent of the restoration environment or geometry.

Unlike shrinkage, stress cannot be measured directly in an experiment. Stress is a calculated engineering factor that expresses how a force is distributed inside a material. However, stress is related to physical deformation or strain, which can be measured experimentally. The most simple relationship between stress σ and strain ε is a uniaxial (i.e., one-dimensional) linear elastic correlation with the elastic modulus E:

$$\sigma = E\,\varepsilon\ [\mathrm{N/m^2}] \qquad (2)$$

An elastic modulus is a material property, which means that it has a constant value for each material, and expresses the inherent stiffness of a material. Since shrinkage can be considered as a form of strain, this relationship illustrates that shrinkage stress is not only a function of the shrinkage but also depends on the elastic modulus.

Applying the insight that shrinkage stress depends on both shrinkage and elastic modulus is not intuitive anymore. It requires a calculation that involves another mechanical property. Still, in a new shrinkage stress model based on Eq (2), residual stress may seem to remain a simple expression, that is easily calculated by the product with the elastic modulus and again can be ranked as if it were a material property. Unfortunately, simple Eq (2) is only valid for one-dimensional conditions. In reality, shrinkage and shrinkage stress are three-dimensional. Hence, the definition of stress requires a set of six equations (three normal stresses σ and three shear stresses τ), which under isotropic conditions becomes:

$$\sigma_{xx} = E\,/\,((1+\nu)(1-2\nu))\ ((1-\nu)\varepsilon_{xx}+\nu(\varepsilon_{yy}+\varepsilon_{zz})) \qquad (3a)$$

$$\sigma_{yy} = E\,/\,((1+\nu)(1-2\nu))\ ((1-\nu)\varepsilon_{yy}+\nu(\varepsilon_{xx}+\varepsilon_{zz})) \qquad (3b)$$

$$\sigma_{zz} = E\,/\,((1+\nu)(1-2\nu))\ ((1-\nu)\varepsilon_{zz}+\nu(\varepsilon_{xx}+\varepsilon_{yy})) \qquad (3c)$$

$$\tau_{xy} = E\,/\,(2\ (1+\nu))\ \gamma_{xy} \qquad (3d)$$

$$\tau_{yz} = E\,/\,(2\ (1+\nu))\ \gamma_{yz} \qquad (3e)$$

$$\tau_{zx} = E\,/\,(2\ (1+\nu))\ \gamma_{zx} \qquad (3f)$$

where the x-y-z indices denote x-y-z directions, γ are the shear strains, and ν is the Poisson's ratio representing the lateral-axial strain ratio. Note that isotropic conditions mean that the mechanical properties (i.e., E and ν) are the same in all directions, which is a reasonable assumption for a particle-filled resin-based composite. Clearly, the three-dimensional reality makes predicting shrinkage stresses much more difficult. Taking into account six stress components simultaneously cannot be considered intuitive anymore. Solving these expressions to obtain the shrinkage stress will require considerably more effort.

The most comprehensive solution to calculate these complex stress conditions is by using finite element analysis. This engineering tool provides a system to solve the necessary constitutive equations and continuity requirements. Finite element analysis solves stress and strain patterns in a complex structure by dividing it into smaller "elements" that are much simpler to calculate. By calculating those elements all together simultaneously, the whole structure is solved. This simultaneous solution of many elements requires considerable computing power. With the availability of powerful computer systems and improvements in user friendly graphical interfaces, finite element analysis has become widely accessible to dental researchers (Korioth & Versluis, 1997). Finite element analysis has played a driving role in the current state of polymerization shrinkage research and thinking. This chapter will use finite element analysis to test and discuss shrinkage stress models, and show the powerful and unique insight a finite element analysis approach offers when trying to resolve the effects of polymerization shrinkage stress in dentistry.

Using finite element analysis, the original intuitive shrinkage stress model can be easily tested. **Figure 1** shows a finite element model of a buccal-lingual cross-section in a premolar with a deep Class II MOD (mesio-occluso-distal) restoration. The tooth is restored with a composite for which the shrinkage and elastic modulus values were varied. **Figure 1A** was filled with a typical restorative composite with a shrinkage value of 1.8%. The resulting residual shrinkage stresses in the restoration are shown according to a linear color scale. Yellow and orange colors are high stresses, purple and blue are low stresses. In **Figure 1D** the cavity was restored with a composite with only half the amount of shrinkage (1.0%). Such impressive improvement in shrinkage can, for example, be achieved by increasing the filler content and thus reducing resin volume. Since fillers do not shrink during polymerization, a lower resin content generally decreases shrinkage values. A practical analogy of this example is the comparison between a conventional and packable composite, where the increased filler content in a packable composite reduces shrinkage values. The intuitive shrinkage stress model would anticipate lower shrinkage stresses for the composite that shrinks less. However, comparison between **Figures 1A** and **1D** shows that the shrinkage stresses are virtually the same because, along with a reduction in shrinkage, the elastic modulus increased. Increasing filler content generally increases elastic modulus. Therefore, the benefit of decreased shrinkage may be cancelled out by the increase in elastic modulus. **Figures 1B** and **1C** show the effect on shrinkage stresses when one property at the time is varied. This example illustrates that shrinkage stress cannot be assessed based only on shrinkage, but must include other composite properties as well in the evaluation. It also shows that even a very simple finite element model can test common shrinkage stress behavior, and can integrate different material properties in a multi-dimensional condition to determine the relationship between shrinkage and stress.

Figure 1. Residual shrinkage stress distributions in composite restorations with different shrinkage (α) and elastic modulus (E) values. Colors show stress levels (modified von Mises equivalent stress) according to a linear scale.

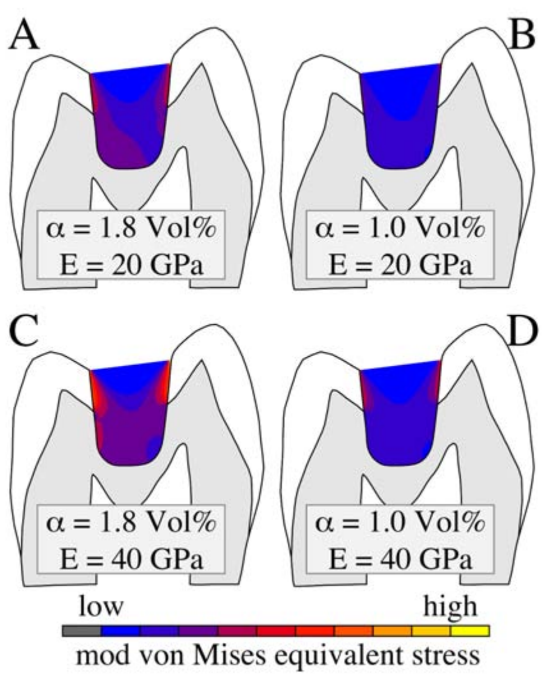

SHRINKAGE STRESS MODEL: C-FACTOR

Finite element analysis has only relatively recently become an integral part of shrinkage stress research. The acceptance of numerical analysis has been slow in a dental materials research environment that has traditionally been the domain of laboratory methods. Moreover, clinical relevance has also been an important quality for dental research. It is therefore not surprising if there is a strong desire for simple shrinkage stress models that can be assessed experimentally and are easily applied to clinical conditions. One of the models that has become very popular in dentistry is the so-called C-factor (Feilzer et al., 1987). A C-factor or "configuration" factor is the ratio of bonded to free surface area. This model states that a composite restoration with a high C-factor (e.g., Class I or Class V) will have higher shrinkage stresses than a restoration with a lower C-factor (e.g., Class II or Class IV). The model is based on experimental observations in which cylindrical composite samples were attached to a load-cell and cured. Given a constant diameter, increasingly higher shrinkage forces will be recorded when the cylinder length is reduced (**Figure 2A**). This observation was explained by the relative increase of bonded to free surface area, which was subsequently extrapolated to cavity configurations where a higher ratio of bonded surfaces should also increase shrinkage stresses. It is true that shrinkage stress is affected by the amount of shrinkage constraints, as was predicted by Bowen who stated that restorations with large free surfaces were likely to develop less shrinkage stress (Bowen, 1967). The simplicity and practicality of the C-factor model is certainly attractive. Firstly, because it implies that stress can be measured experimentally, basically using the relationship:

$$\sigma = F / A \tag{4}$$

where F is the load measured by the load-cell and A is the cross-sectional area of the cylindrical test sample. Note that a load-cell does not measure shrinkage *stress*, but rather a reaction *force* in axial direction. Secondly, because the C-factor model assumes that stress measured in simple shaped test specimens (cylinders) can be applied to more complex restorations, merely using the ratio between the bonded and unbonded surface areas.

Using finite element analysis the C-factor model is easily tested. The graph in **Figure 2A** shows the axial reaction forces that a load-cell measures for different lengths of cylindrical shaped composite samples. The graph shows an increasing reaction force with decreasing cylinder length (i.e., increasing C-factor). The graph also shows the nominal stress, calculated using Eq (4). However, the finite element analysis offers a more comprehensive three-dimensional stress solution. The graph in **Figure 2A** shows the average stress determined as the average of all axial stress components in the whole cylindrical specimen. The average stress level turns out to be about twice as high as the nominal stress value. Although the nominal and average axial stress values are significantly different, they follow the same trend as the axial force output of the load-cell, which increases when the cylinder length is reduced. This appears to validate the C-factor model, at least qualitatively.

However, the assumption of uniaxial stress is only valid if a cylinder is infinitely long and if the shrinkage would take place only in axial direction (i.e., along the longitudinal cylinder axis). In reality, stress conditions are not one-dimensional due to the finite cylinder length and the three-dimensional nature of shrinkage itself. According to Eq (3), there are six stress components that should be considered. These six stress components are calculated by the finite element analysis, but it is not convenient to plot all indivually for each cylinder length. Since it is the combined effect of these six components that determine the overall stress state in the composite, they are often integrated into one value using a specific criterion. A popular criterion is the von Mises criterion. **Figure 2B** shows the stress distribution in the cylinders using a modified von Mises criterion. It

Figure 2. C-factor model and shrinkage stress prediction. (a) Cylindrical test specimens to measure axial forces. (b) Shrinkage and stress distribution in cylindrical specimens. (c) Analogy of C-factors in stylized cavities. (d) Shrinkage and stress distribution in cavities assuming rigid walls. (e) Shrinkage and stress distributions in cavities assuming non-rigid walls. Dashed curves in graphs are stress distributions of the cylindrical specimens for comparison. Shrinkage deformation shown 100-times enlarged.

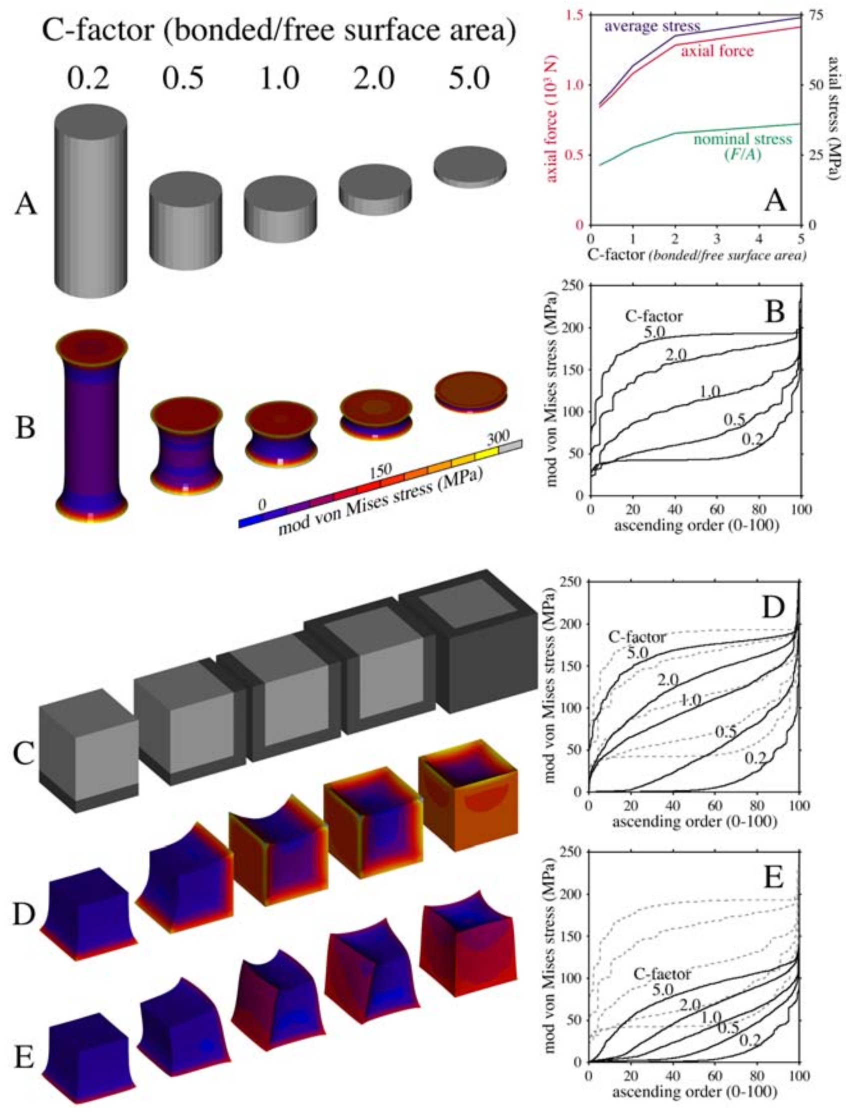

modifies the original von Mises criterion to take into account the difference between compressive and tensile strength (de Groot et al., 1987; Versluis et al., 1997). The figure shows a gradient of stress values in the composite cylinders rather than one nominal "shrinkage stress". The yellow and orange colors indicate that there are high stress concentrations close to the bonded areas and the blue and purple colors indicate lower stress values along the free surfaces. Clearly, shrinkage stress in the composite is not a single or nominal value as implied by a C-factor shrinkage stress model.

To further test the validity of the C-factor shrinkage stress model, shrinkage stresses were simulated in cubical cavity shapes, where an increasing number of bonded walls represent different clinical preparation types (**Figure 2C**). Since the bonding conditions and shapes are different, direct comparison of stress patterns between the cavity configurations and between the cavities and cylinders is problematic. However, stress values themselves can be compared since in this case the objective is to test the validity of the C-factor model for extrapolation of shrinkage stresses between different configurations. Stress values are compared by collecting all stress values from the cylindrical and simulated restoration configurations, and plotting them in ascending order in the graphs of **Figures 2B** and **2D**. The graphs show that for exactly the same composite properties, the cylindrical and cubical composite geometries generate different shrinkage stresses for identical C-factors. Apparently, stress is not only determined by mechanical properties and bonded surface area, but geometry also affects shrinkage stresses. Stresses calculated with one geometry can therefore not be simply extrapolated to another geometry.

Additionally, the C-factor model only distinguishes between "bonded" and "unbonded" areas. Since it does not identify the substrate to which the composite is bonded, an infinitely stiff substrate or undeformable cavity wall is implied. **Figure 2E** shows the stress curves if the simulated restoration would have been bonded to a deformable cavity wall, such as enamel and dentin. The figure shows that the stresses again change substantially when the bonding substrate changes. Stress thus not only depends on the composite attributes, but also on the properties of the substrate.

Again, using a simple finite element analysis, a very popular shrinkage stress model that extrapolates one physical aspect of shrinkage stress generation to predict stress values, could be easily tested. The finite element model demonstrated some crucial shrinkage stress insights. First, shrinkage stress is not a single nominal value, but a location dependent distribution consisting of a whole range of values. Secondly, this location dependent distribution of shrinkage stresses depends on geometry. Thus, changing the geometry changes the shrinkage stresses. Thirdly, even if one could determine every quality of a composite restoration, such as composite properties and restoration configuration, it would still not provide all necessary information to determine the shrinkage stresses in a restoration. Shrinkage stress cannot be determined without consideration of the response of the structure to which a composite is bonded. To understand shrinkage stresses, it is imperative to consider the whole restored tooth structure.

SHRINKAGE STRESS MODEL: RESTORATION SIZE

A third shrinkage stress model to be discussed here is the assumption that large restorations shrink more than small restorations, implying that large restorations will generate more shrinkage stresses. This shrinkage stress model has often crept into shrinkage stress discussions. It is another example of a mostly intuitive shrinkage concept, which is usually incorrectly rationalized by the perception that large restorations "shrink more". Unlike the first intuitive concept that correlated shrinkage and stress, and the second C-factor model that based shrinkage stresses on one configuration measure, discussion of this model requires consideration of multiple facets. Because the size of a restoration affects multiple factors concerning the whole tooth structure, the implication of this model is more complex than the former simple deduction models.

The first facet to examine is the definition of shrinkage. Shrinkage is a dimensionless ratio (Eq. 1), often reported as a percentage. Shrinkage is thus per definition independent of size. Given the same geometry and boundary conditions, 5% shrinkage in a large restoration causes the same shrinkage stresses as 5% shrinkage in a small restoration. This can be simply illustrated using finite element analysis by scaling a stylized tooth-restoration model up or down in **Figure 3A**. The figure shows no change in shrinkage stress values and distribution. Although this example decisively demonstrates that shrinkage and thus shrinkage stress is not higher in larger restorations, what happens to the shrinkage stresses when a small and large restoration are compared in a same sized tooth? In such case the mechanical response of to the restoration shrinkage will be different. Cutting a large cavity means a larger loss of tooth tissue, and hence more weakening of the tooth crown than from a small cavity. As a result, the larger restoration is bonded to a less rigid structure compared to a smaller restoration. A weakened tooth structure will be less capable of constraining composite shrinkage and thus the restoration will experience lower shrinkage stresses than if the tooth would have retained more rigidity, like with a smaller restoration (**Figure 3C**). Contrary to the popular notion, it can thus be concluded that, given the same shrinkage properties, a larger restoration will have lower shrinkage stresses in the restoration itself than a smaller restoration.

But this is not the final word about this shrinkage stress model, because there is another facet to shrinkage stresses in a restoration. Observing the stress distributions in **Figure 3C** shows that shrinkage stresses are not confined to the restoration and its interface with the tooth, there are also shrinkage stresses generated inside the restored tooth. Compared to the smaller restoration, the tooth with the larger restoration has lost more of its rigidity, i.e., its resistance to deformation. Therefore, the tooth with the larger restoration will deform more easily and consequently will be higher stressed than it would have been with a smaller restoration. Shrinkage stress is thus not only in the restoration, but also applies to the tooth. It cannot be emphasized enough that when shrinkage stresses are evaluated, both sides of the tooth-restoration complex should be taken into consideration, because lower stresses in the restoration may go along with higher stresses in the tooth.

The example above assumed the same shrinkage properties in the large and small restorations. This is a reasonable approximation for auto-curing systems. Such systems could be assumed to be independent of restoration size if temperature effects are neglected. Shrinkage behavior for light-activated composites, on the other hand, may not be independent of restoration size. Due to light attenuation effects that cause diminishing light intensities deeper inside a light-cured material, the polymerization reaction at the restoration surface will develop more rapidly and result in a higher degree of cure compared to composite deeper inside a restoration. The consequences of this effect will be more pronounced in large restorations than in small ones. As a result, compared to a large restoration, a small restoration will cure faster and more thoroughly, resulting in a higher overall shrinkage (**Figure 3B**). Therefore, again contrary to the popular notion, a large restoration of light-activated composite material may shrink less under the same conditions and thus generate less shrinkage stresses rather than more. Not because large restorations “shrink less” but because a large restorations may not be cured as thoroughly as smaller ones. This example demostrates that determination of accurate shrinkage values is a prerequisite for accurate residual stress calculations.

SHRINKAGE VALUE

Until now, a generic shrinkage term has been used to describe the amount of polymerization contraction. Although shrinkage stress may not be linearly correlated to shrinkage, the shrink-

Figure 3. Effect of restoration size on residual shrinkage stresses. (a) Auto-curing composite. (b) Light-activated composite. (c) Quarter view of molar restored with small and large Class I restoration. Von Mises equivalent stress is shown.

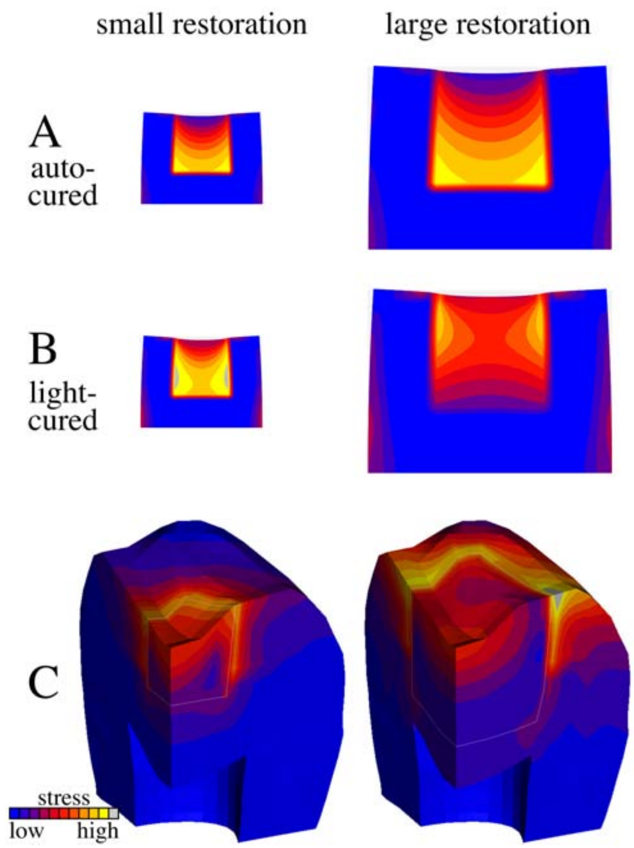

age value is still the most important factor for polymerization shrinkage stress because without shrinkage there would be no shrinkage stress. Assessing shrinkage stresses thus requires determination of shrinkage values. This section will examine shrinkage values and how they relate to shrinkage stresses.

According to Eq (1), shrinkage can be measured as the change in dimensions. Shrinkage can be determined in both volume and distance measurements. These provide volumetric and linear shrinkage, respectively. Given the reasonable assumption that composites shrinkage is isotropic, linear shrinkage *L* can be converted into volumetric shrinkage *V*:

$$V = 3L - 3L^2 + L^3 \tag{5a}$$

If the shrinkage value is low, the higher order terms become small enough to be neglected, resulting in the convenient expression:

$$V = 3L \tag{5b}$$

Consequently, linear shrinkage can be converted into volumetric shrinkage:

$$L = V / 3 \tag{5c}$$

For 9% volumetric shrinkage, 3% linear shrinkage is obtained with Eq (5c), where the correct value is about 3.1%. Since most composites shrink considerably less, the simple conversion is a good approximation for dental applications.

Shrinkage values have been measured in many ways. One common technique is to measure displaced volume, in which a composite sample is immersed in a liquid and cured (Penn, 1986). The shrinkage volume can be calculated by measuring the displaced liquid. A shrinkage value obtained with such method can be called the *total shrinkage*, because it measures the entire amount of dimensional change of the composite during polymerization. It should be noted that any technique that restricts free contraction cannot be considered a pure measurements of total shrinkage, because some of its shrinkage movement was prevented. The origin of shrinkage is the formation of a polymer network. Therefore, total shrinkage is primarily a function of degree of cure. Furthermore, effective density can also be affected by network organization. It has been suggested that curing regimens can affect the network distribution, and thus network structures are not necessarily comparable at the same degree of cure. However, the effects on the total dimensional change seem to be small. Therefore, good rule of thumb remains that the same composite with the same degree of cure should produce similar values for total shrinkage.

While the shrinkage value is the origin of shrinkage stresses, calculation of the stress using this factor has to be carried out with caution. **Figure 4A** shows a premolar with a composite restoration where stress and deformation been calculated using a typical 3% total shrinkage value. The figure shows how the composite shrinkage within the cavity has deformed the tooth structure, pulling the buccal and lingual cusps together by about 200 μm. Such a large deformation, which exceeds the thickness of a human hair, is unlikely to be realistic since it should be visible by the naked eye and there would have been many sightings in clinical practice. A shrinkage model in which shrinkage stresses are calculated using the total shrinkage value is thus likely incorrect.

Bowen has pointed out that not all polymerization shrinkage causes shrinkage stresses (Bowen, 1963). When a composite cures, it is transformed from a viscous paste to an essentially solid material. In the viscous state, flow of the composite can relax shrinkage stresses without a buildup of residual shrinkage stresses (Bausch et al., 1982).

Figure 4. Residual polymerization stress distributions and deformation calculated with three different shrinkage models: (a) elastic, (b) viscoelastic, and (c) pre/post-gel. Green outline is the original contour before polymerization shrinkage.

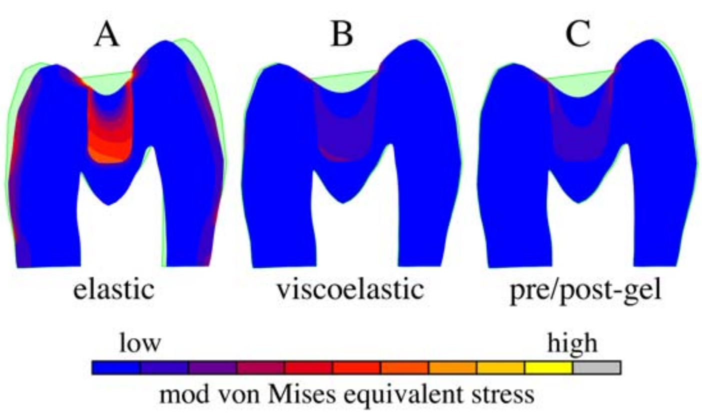

Residual stresses will only be generated when the composite material cannot timely relax anymore, which happens when a more rigid polymer network structure has developed. In other words, shrinkage stress is generated when the composite material behaves solid enough to transfer stresses. The problem with the calculation used in **Figure 4A** was that the material was considered elastic (i.e., no plastic flow) throughout the polymerization reaction, completely disregarding viscous and viscoelastic effects. **Figure 4B** shows the stress and deformation calculated with a viscoelastic composite model. It shows the same amount of total shrinkage but significantly lower stress and a tooth deformation (approximately 40 μm intercuspal distance change) that is within a realistic range of cusp-flexure values (Pearson & Hegarty, 1989; Suliman et al., 1993; Panitvisai & Messer, 1995; Meredith & Setchell, 1997; Alomari et al., 2001; Tantbirojn et al., 2004). Calculating the shrinkage stress is thus not a linear elastic calculation, where the end result is determined independently of the polymerization process by the final shrinkage and modulus values. The unrealistic assumption of an elastic model is easily exposed by finite element analysis, which demonstrates that shrinkage stress assessment must include the time-dependent shrinkage and modulus development as they evolve during a polymerization process.

The dynamic process is a significant complication for studying polymerization shrinkage. Most test methods for material property determination are designed for steady-state materials. However, properties of composite that describe their mechanical response change rapidly during the polymerization reaction. To record such changes requires methods that can capture complete material behavior instantaneously and continuously. Viscoelastic behavior goes through fundamental changes during polymerization. Simply said, its response shows initially a Maxwell type behavior (spring and dashpot in series) and transforms to a predominantly Kelvin-Voight type behavior (spring and dashpot parallel) behavior during polymerization (Dauvillier et al., 2001, 2003). Since there is often not sufficient experimental data available to accurately calculate this complex transformation, alternative methods that measure effective shrinkage values have been proposed for shrinkage stress assessment.

SHRINKAGE STRESS MODEL: EFFECTIVE SHRINKAGE

The concept of an effective shrinkage value divides the total shrinkage into a pre- and post-gel contribution (Bausch et al., 1982; Davidson & de Gee, 1984):

$$\alpha_{total} = \alpha_{pre\text{-}gel} + \alpha_{post\text{-}gel} \qquad (5)$$

The pre-gel shrinkage $\alpha_{pre\text{-}gel}$ can be considered the amount of shrinkage during polymerization when the composite is still viscous, and thus represents the shrinkage that does not generate shrinkage stresses. Post-gel shrinkage $\alpha_{post\text{-}gel}$ is the shrinkage component after a composite has become solid enough to generate shrinkage stresses. Shrinkage stress therefore originates only from the post-gel shrinkage portion. Post-gel shrinkage can thus be considered the effective shrinkage with regard to the shrinkage stress. The transition point between the pre- and post-gel shrinkage has been called the gel-point. Note that this gel-point term is defined to describe a mechanical response, and does not necessarily coincide with similar terms used in polymer science. The formulation of the pre-and post-gel shrinkage model has led to a search for the gel-point. However, the accurate determination of the gel-point has remained elusive. It should be noted that the pre- and post-gel model is a simplification of the viscoelastic process. It is unlikely that the development of viscoelastic properties will show a well-defined point, as has been discussed in detail by Versluis et al., (2004a). Nevertheless, the general concept of an effective shrinkage value has turned out to be very illustrative and practical.

Effective shrinkage has been measured using a strain gauge method (Sakaguchi et al., 1997). In this method, a composite sample is attached to a strain gauge and cured. Strain gauges are sensors consisting of a very thin metallic wire-frame encapsulated in a glass-fiber reinforced epoxy-phenolic resin film. Strain gauges are based on the principle that the electrical resistance of the metal wire increases with increasing strain (deformation). When the attached composite shrinks, it deforms the embedded wire-frame in the strain gauge. The resulting change in resistance can be measured and shrinkage strain is obtained. Since the composite can only deform the strain gauge when it is solid enough to generate stresses, a strain gauge measures per definition the effective shrinkage or post-gel shrinkage.

Application of the pre- and post-gel shrinkage model in a finite element analysis (**Figure 4C**) shows that, while the total shrinkage is the same as in **Figure 4A**, the calculated shrinkage stress and resulting tooth deformation is similar to the viscoelastic model (**Figure 4B**). The post-gel shrinkage value thus includes the viscoelastic history during polymerization. It has been shown that using post-gel shrinkage values, tooth deformation and thus likely shrinkage stress can be closely approximated (Versluis et al., 2004b). The advantage of using this method is that the analysis becomes quasi-linear, simplifying the measurement and solution of an otherwise fully nonlinear analyses of viscoelastic composite properties.

Another advantage of the pre- and post-gel shrinkage model is that it makes it easier to conceptualize effects of reaction kinetics on the shrinkage stress. An example is the discussion in the dental literature about the question if shrinkage stress is affected by the curing light intensity. The reason that this issue has not been resolved may be due in part to experimental data that show no effect of curing light intensity on the shrinkage value, from which some have concluded that there will also be no effect on the shrinkage stress. As discussed above, light curing to the same degree of cure will cause a similar polymer network density and thus total shrinkage value, irrespective of the used light intensity. However, total shrinkage does not predict the shrinkage stress, because it is the amount of effective or post-gel shrinkage that generates the residual stresses. The amount of viscous flow, and thus the pre- and post-gel shrinkage, is determined by the kinetics of the polymerization process. It is conceivable that a high light intensity increases the rate at which a rigid network is formed, and thus accelerates the occurrence of the "gel-point". Because the total shrinkage for a particular composite is constant at the same degree of cure, a gel-point that occurs earlier in the polymerization process reduces pre-gel shrinkage and increases post-gel shrinkage. Higher curing light intensities, especially during the early polymerization reaction, increases the effective shrinkage and therefore shrinkage stresses. Using the strain gauge method it has been confirmed that curing light-intensity affects the value of the effective shrinkage (Versluis et al., 1998, 2004a; Sakaguchi & Berge, 1998). Light-curing to a similar degree of cure at different light-intensities resulted in different effective shrinkage values. Curing at lower light-intensities decreased the effective shrinkage values, which will reduce shrinkage stresses if other conditions are comparable, while higher light-intensities increase the effective shrinkage. Note that experimental observations like these have led to the introduction of ramp-cure or step-cure regimens on commercial curing light sources (Kanca & Suh, 1999; Suh et al., 1999; Bouschlicher & Rueggeberg, 2000). The post-gel shrinkage concept has turned out to be a useful factor to develop an understanding of the development and calculation of shrinkage stresses.

From the examination of shrinkage values, it can be concluded that (a) not all shrinkage generates stresses and (b) not all curing regimens generate the same amount of residual stresses. The calculation of shrinkage stresses has become more complex since the evolving viscoelastic effect must be taken into account. While the final shrinkage may be a constant value in a thoroughly cured restoration, the effective or post-gel shrinkage can vary depending on local reaction kinetics. While the consequences of this complexity may be overwhelming for an intuitive approach, finite element analysis is perfectly suited to integrate and apply comprehensive local, time-dependent, and nonlinear behavior into one shrinkage stress analysis. This section about the shrinkage value showed that finite element analysis is not only for calculating stresses, but its use also advances understanding of the shrinkage value itself. Although total shrinkage remains the most commonly reported property to characterize a composite's shrinkage stress quality, finite element analysis has clearly demonstrated its limitations. Total shrinkage does not reflect shrinkage stress behavior, which is much better characterized by the effective or post-gel shrinkage.

AFTER THE SHRINKAGE: RELAXATION

Most of a polymerization reaction in a light-activated composite typically takes place within the first 10 seconds, after which it continues at a decreasing rate. Shrinkage strain development has been shown to continue for more than 24 hours. Although elastic behavior dominates in a cured composite resin, the material still exhibits some viscoelastic behavior after it has been fully cured. Viscoelastic effects in cured composites are thought to relax residual stresses over an extended period of time. This process is enhanced by viscoelastic properties of the tooth tissues, which in effect also reduce residual shrinkage stresses over time (Kinney et al., 2003). Furthermore, environmental conditions may cause stress relaxation due to water sorption and consequently hygroscopic expansion, while the composite modulus may undergo a slow deterioration due to solubility and matrix softening effects (Momoi & McCabe, 1994; Oysaed & Ruyter, 1986). It is not known to which extend such stress relaxation happens under clinical conditions. **Figure 5** shows cuspal deformation in an in vitro experiment for a molar with a Filtek Supreme (3M ESPE, St Paul, MN) Class II MOD restoration after polymerization, and after 4 and 8 weeks in water. The initial cuspal deformation due to polymerization shrinkage stresses substantially decreased after 4 weeks in water, and had continued the decrease 8 weeks later for this composite material. Shrinkage stresses calculated for composite restorations are therefore probably most acute immediately after curing. The fact that any harmful stresses may relax over time does not diminish the requirement that the tooth-restoration complex must survive the initial period, probably spanning more than a week for restorative composites, because debonding caused by initially high stresses is not restored when residual stresses relax. Consideration and management of shrinkage stresses therefore remains necessary.

THE ROLE OF SHRINKAGE EXPERIMENTS

The previous sections discussed the relationship between polymerization shrinkage and shrinkage stresses. It was demonstrated that shrinkage stress is not a composite or restoration property, but is a local value determined by a number of factors involving both the composite and the surrounding environment. It was stated that stress cannot be measured experimentally, but is a calculated engineering factor. It was shown that when all contributing factors are taken into account, the calculation of shrinkage stress has become so complex that the only comprehensive solution is using finite element analysis. This brings up the question if there is any role left for experimental shrinkage research. Finite element analysis must be considered an integration system. It offers an environment in which basic material properties are integrated according to universal physical laws. It cannot predict polymerization shrinkage, but calculates shrinkage stress based on external input of physical material behavior obtained from experimental measurements using a shrinkage model designed by the operator. The validity of any finite element model of shrinkage must also be checked against reality using experimental measurements, because using finite element analysis does not ensure validity of a shrinkage model. Clearly, experiments remain a vital component of any shrinkage research. To better understand the role of experiments in research, it is important to distinguish between two types of experiments: basic experiments to provide input for the shrinkage model and simulation experiments for validation of the shrinkage model.

Basic experiments must determine properties independent of geometry. This allows their application in other systems than the one in which they were measured. For example, elastic modulus is a basic property while cusp flexure is not. Cusp flexure involves the overall stiffness of a tooth, which includes various material properties, geometry, boundary conditions, and even the location where the flexure was measured. It is only valid for that tooth under the exact same conditions. However, elastic modulus can be applied to calculate the flexure in any tooth shape, and is thus considered a basic property. The measuring of cuspal flexure is an example of a simulation experiment. It can be used to test the shrinkage

Figure 5. Residual shrinkage stress relaxation due to hygroscopic expansion, shown as reduction in tooth deformation. (a) Digital image of an Mesial-Occlusal-Distal slot preparation in an extracted upper molar. (b) Deformation pattern at buccal and lingual cusps due to residual shrinkage stresses from the composite restoration immediately after curing. (c,d) Cuspal deformation decreased after 4 and 8 weeks immersion in water. Negative values represent inward movement of cuspal surface.

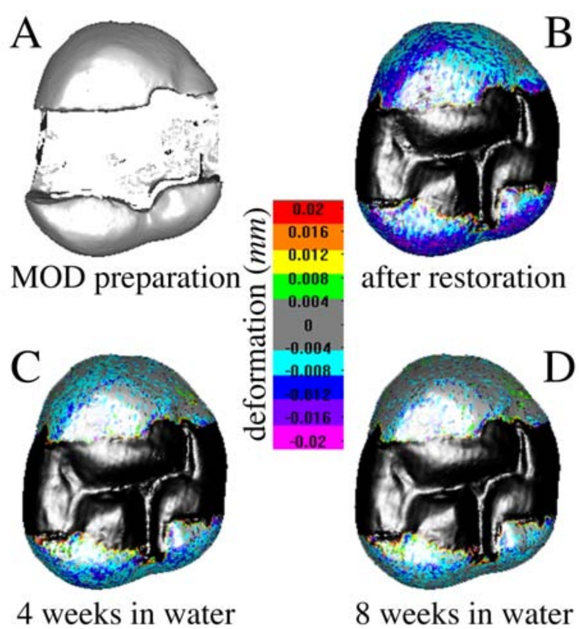

model, because instead of isolating a single property, flexure is the result of multiple interacting properties. If the shrinkage model recreates those interactions correctly, it will replicate the flexure in a similar tooth system. If that is the case, the model is considered validated.

Based on the previous discussions, it is clear that the ultimate value of these two categories of shrinkage experiments is accomplished if used in conjunction with finite element analysis. Without a system to integrate basic shrinkage properties, such properties have little value beyond arbitrary material ranking, because they cannot predict shrinkage stress by themselves. Similarly, without finite element analysis, simulation experiments also have limited predictive value, because they only apply to the one test condition and even in those unique conditions they cannot provide actual shrinkage *stress* values.

Still, the dental literature shows various examples of alleged shrinkage stress experiments. Measuring techniques in those publications typically involve load cells, strain gauges, or cusp flexure measurements. However, none of those techniques actually measures stress but rather an arbitrary deformation from which a nominal load value can be derived at best. For example, measuring shrinkage "stresses" using load cells assumes a homogeneous uniaxial stress distribution. Such nominal stress value does not do justice to the spectrum of actual stress values, and has limited application because it cannot be associated with other shapes or conditions since stress is not a material property.

Shrinkage measurement, on the other hand, can be considered a basic property, that can be determined independent of shape as a change in density. One may notice that light-activated composites do have a size dependency, simply because they depend on curing light attenuation. However, this means that shrinkage should be determined locally as a function of curing conditions, such as the applied light-intensity. Similarly, it can been argued that shrinkage depends on strain rate, where a heavily constrained composite results in a different shrinkage development. Determination of basic properties is obviously not synonymous with a "simple" property or experiment. Shrinkage behavior may require a strain rate dependent property determination, where the transient properties must be determined as a function of the strain rate. Clearly, any meaningful utilization of such increasingly complex material model reconfirms the necessity of using numerical methods such as finite element analysis, which in return are completely dependent on experimental shrinkage research for input and validation.

HOW CAN POLYMERIZATION SHRINKAGE BE MODELED?

Finite element analysis of polymerization shrinkage can be achieved at different levels of complexity. Finite element modeling of shrinkage can be as accurate and complex as the available input data allows. The limitations for modeling shrinkage and its effects are determined by the abilities of the modeler, the details of the supporting experimental data, and the access to computational and software resources. It is not the intention of this chapter to teach finite element analysis. However, a few comments will be made regarding the modeling of shrinkage.

Polymerization shrinkage is basically densification, which results in a volumetric change. Few finite element programs offer specific polymerization shrinkage options but all should support an option for thermal expansion. Shrinkage can be modeled using the thermal expansion option, applying the linear shrinkage value as a coefficient of thermal expansion. Material contraction is achieved by lowering the temperature in the model. To accommodate time-dependent shrinkage, temperature changes can be applied as a function of time. During polymerization not only a dimensional change takes place, but there is also a change in viscoelastic properties.

These can be applied simultaneously along with the density changes.

Modeling the viscoelastic changes is not trivial. It has been discussed in previous sections that there is a fundamental transformation in viscoelastic response. Since shrinkage stresses depend on the history of shrinkage and viscoelastic development, only a correctly modeled transformation can accurately determine the shrinkage stress outcome. Unfortunately, due to the complexity of the experimental determination, there is still little data available to describe the complete time-dependent constitutive behavior during polymerization for all dental composites. Furthermore, not all numerical software is easily adapted for modeling the transformation, because it has not been a common concern in general engineering where the software is developed. However, it has been shown that a pre- and post-gel shrinkage model can serve as a simple method to estimate polymerization shrinkage stresses. Using pre- and post-gel shrinkage values approximates the nonlinear behavior in a quasi-linear analysis with a minimum of two time increments.

During pre-gel increments, a very low elastic modulus and high Poisson's ratio can simulate the nearly stress-free mostly-plastic flow, while the final elastic modulus and Poisson's ratio in combination with the post-gel shrinkage are applied to generate the effective residual shrinkage stresses. Since the composite deformation during the pre-gel increments is simulated in an elastic model, it is imperative to ensure its viscous stress relaxing effect when progressing to post-gel modeling. There are various options to accomplish this. For example, by using an element switch. In this method, pre- and post-gel behavior is modeled by two different but overlapping elements that share the same nodes. The elements can be activated/deactivated accordingly. This method ensures that the post-gel elements inherit the pre-gel shrinkage deformation without their elastic memory.

Since the contribution of the pre-gel shrinkage simulation on the shrinkage stresses calculated using this method is negligible, it may sometimes be unnecessary to model the pre-gel shrinkage for the calculation of shrinkage stresses. However, this assumes a homogeneous polymerization reaction inside the composite material, which occurs in an auto-curing composite system. For light-activated composites, shrinkage development is not homogeneous. Time and location of pre- and post-gel shrinkage development will affect the outcome of the calculated shrinkage stresses. To simulate those conditions, each location (i.e., each element, or better yet, each element integration or gauss point) should be given its own time-dependent pre- and post-gel material response based on the local light intensity.

The results of finite element analysis should be validated, especially when shrinkage models become more intricate. Validation is not to prove the validity of the proven concept of numerical analysis, but rather the modeling performance of the operator. Results of a finite element analysis should be critically tested against other models (convergence and alternative condition testing to ensure that final conclusions do not depend on the mesh distribution or other anomalies) and other data, preferably from simulation experiments, to assure that the shrinkage model and consequently the results are realistic. It should be noted that validation is not based on exact duplication of experimental values. Even experimental values do not replicate exactly. However, it is the similarity in behavior and magnitude that indicates a positive validation.

SUMMARY: THE ROLE OF FINITE ELEMENT ANALYSIS IN SHRINKAGE RESEARCH

The role of finite element analysis in polymerization shrinkage stress research was highlighted in this *Chapter*. Tracing some of the most popular shrinkage models, it was shown that the use of even very simple finite element models can prevent simplistic and potentially misleading shrinkage stress concepts that may hamper progress. Application of finite element analysis does not only facilitate better insight in shrinkage stress concepts, it also helps designing research experiments and provides a system in which the experimental polymerization shrinkage data can be integrated.

A finite element approach does not replace experimental shrinkage research, but instead completes it. Individual composite properties such as shrinkage or nominal stress values derived from simulation experiments cannot be extrapolated to shrinkage stresses. However, in combination with finite element analysis, such experiments contribute vital information for polymerization shrinkage stress research.

It was demonstrated that the more is learned about shrinkage stresses, the more complex its assessment becomes. Starting from a simple initial concept in which shrinkage stress was simply considered a property of the composite, it was shown in a number of shrinkage model refinements that stress depends on a large number of factors. These factors include the composite restoration as well as the tooth structure to which it is attached and the interfacial conditions.

Beyond the modeling of polymerization shrinkage effects discussed in this chapter, the finite element approach can be seamlessly extended to study how such residual stresses interact with other clinical conditions, such as thermal and masticatory load cycles, and to design and test shrinkage stress management actions such as cavity design and incremental filling techniques.

It is important for continued progress in shrinkage research that shrinkage stress is not considered by itself, but is applied within more comprehensive systems. Actions undertaken to control shrinkage stresses may impact other aspects. For example, liners have been advocated to reduce shrinkage stresses. Bonding to a compliant ("soft") liner material "absorbs" the shrinkage deformation, reducing resistance encountered by the shrinking composite and thus generating less residual stresses. However, the long-term success of a composite restoration is ultimately determined by its ability to survive the oral function. Lining a cavity with compliant materials may reduce shrinkage stresses, but it could also prevent recovery of a tooth's original stiffness and thus mechanical performance. Finite element analysis is perfectly suited to accommodate the study of such aggregated conditions, integrating the shrinkage model with other challenges that are encountered in an oral environment.

The final chapter about polymerization shrinkage stress has not been written. Ongoing research continues to contribute corrections and refinements of our current insight of the process and clinical impact. Due to its versatility as a powerful integration system, finite element analysis is most likely to remain a vital analysis tool that will continue to drive this progress and apply new insights along the way that improve clinical decisions.

REFERENCES

Alomari, Q. D., Reinhardt, J. W., & Boyer, D. B. (2001). Effect of liners on cusp deflection and gap formation in composite restorations. *Operative Dentistry, 26,* 406-411.

Bausch, J. R., de Lange, K., Davidson, C. L., Peters, A., & de Gee, A.J. (1982). Clinical significance of polymerization shrinkage of composite resins. *Journal of Prosthetic Dentistry, 48*, 59-67.

Bouschlicher, M. R., & Rueggeberg, F. A. (2000). Effect of ramped light intensity on polymerization force and conversion in a photoactivated composite. *Journal of Esthetic Dentistry, 12,* 328-339.

Bowen, R. L. (1956). Use of epoxy resins in restorative materials. *Journal of Dental Research, 35,* 360-369.

Bowen, R. L. (1963). Properties of a silica-reinforced polymer for dental restorations. *Journal of the American Dental Association, 66,* 57-64.

Bowen, R. L. (1967). Adhesive bonding of various materials to hard tooth tissues. VI. Forces developing in direct-filling materials during hardening. *Journal of the American Dental Association, 74,* 439-445.

Dauvillier, B. S., Aarnts, M. P., & Feilzer, A. J. (2003). Modeling of the viscoelastic behavior of dental light-activated resin composites during curing. *Dental Materials, 19,* 277-285.

Dauvillier, B. S., Hübsch, P. F., Aarnts, M. P., & Feilzer, A. J. (2001). Modeling of viscoelastic behavior of dental chemically activated resin composites during curing. *Journal of Biomedical Materials Research, 58,* 16-26.

Davidson, C. L., & de Gee, A. J. (1984). Relaxation of polymerization contraction stresses by flow in dental composites. *Journal of Dental Research, 63*, 146-148.

Eick, J. D., & Welch, F. H. (1986). Polymerization shrinkage of posterior composite resins and its possible influence on postoperative sensitivity. *Quintessence International, 17,* 103-111.

Feilzer, A. J., De Gee, A. J., & Davidson, C. L. (1987). Setting stress in composite resin in relation to configuration of the restoration. *Journal of Dental Research, 66,* 1636-1639.

de Groot, R., Peters, M. C. R. B., de Haan, Y. M., Dop, G. J., & Plasschaert, A. J. M. (1987). Failure stress criteria for composite resin. *Journal of Dental Research, 66,* 1748-1752.

Jensen, M. E., & Chan, D. C. N. (1985). Polymerization shrinkage and microleakage. In G. Vanherle, & D.C. Smith (Eds.), *Posterior composite resin dental restorative materials* (pp. 243-262). Utrecht, The Netherlands: Peter Szulc Publishing Co.

Kanca, J. 3rd, & Suh, B. I. (1999). Pulse activation: Reducing resin-based composite contraction stresses at the enamel cavosurface margins. *American Journal of Dentistry, 12,* 107-112.

Kinney, J. H., Marshall, S. J., & Marshall, G. W. (2003). The mechanical properties of human dentin: a critical review and re-evaluation of the dental literature. *Critical Reviews in Oral Biology and Medicine, 14,* 13-29.

Korioth, T. W. P., & Versluis, A. (1997). Modeling the mechanical behavior of the jaws and their related structures using finite element (FE) analysis. *Critical Reviews in Oral Biology and Medicine, 8,* 90-104.

Meredith, N., & Setchell, D. J. (1997). In vitro measurement of cuspal strain and displacement in composite restored teeth. *Journal of Dentistry, 25,* 331-337.

Momoi, Y., & McCabe, J. F. (1994). Hygroscopic expansion of resin based composites during 6 months of water storage. *British Dental Journal, 176,* 91-96.

Oysaed, H., & Ruyter, I. E. (1986). Composites for use in posterior teeth: mechanical properties tested under dry and wet conditions. *Journal of Biomedical Materials Research, 20,* 261-271.

Panitvisai, P., Messer, H. H. (1995). Cuspal deflection in molars in relation to endodontic and restorative procedures. *Journal of Endodontics, 21,* 57-61.

Pearson, G. J., & Hegarty, S. M. (1989). Cusp movement of molar teeth with composite filling materials in conventional and modified MOD cavities. *British Dental Journal, 166,* 162-165

Penn, R. W. (1986). A recording dilatometer for measuring polymerization shrinkage. *Dental Materials, 2,* 78-79.

Sakaguchi, R. L., Versluis, A., & Douglas, W. H. (1997). Analysis of strain gauge method for measurement of post-gel shrinkage in resin composites. *Dental Materials, 13,* 233-239.

Sakaguchi, R. L. & Berge, H. X. (1998). Reduced light energy density decreases post-gel contraction while maintaining degree of conversion in composites. *Journal of Dentistry, 26,* 695-700.

Suh, B. I., Feng, L., Wang, Y., Cripe, C., Cincione, F., & de Rijk, W. (1999). The effect of the pulse-delay cure technique on residual strain in composites. *Compendium of Continuing Education in Dentistry, 20*(2 Suppl), 4-12.

Suliman, A. A., Boyer, D. B., & Lakes, R. S. (1993). Interferometric measurements of cusp deformation of teeth restored with composite. *Journal of Dental Research*, *72*, 1532-1536.

Tantbirojn, D., Versluis, A., Pintado, M. R., DeLong, R., & Douglas, W. H. (2004). Tooth deformation patterns in molars after composite restoration. *Dental Materials, 20,* 535-542.

Unterbrink, G. L., & Muessner, R. (1995). Influence of light intensity on two restorative systems. *Journal of Dentistry, 23,* 183-189.

Versluis, A., Tantbirojn, D., & Douglas, W. H. (1997). Why do shear bond tests pull out dentin? *Journal of Dental Research*, *76,* 1298-1307.

Versluis, A., Tantbirojn, D., & Douglas, W. H. (1998). Do dental composites always shrink toward the light? *Journal of Dental Research, 77*, 1435-1445.

Versluis, A., Tantbirojn, D., & Douglas, W.H. (2004a). Distribution of transient properties during polymerization of a light-initiated restorative composite. *Dental Materials, 20,* 543-553.

Versluis, A., Tantbirojn, D., Pintado, M. R., DeLong, R., & Douglas, W. H. (2004b) Residual shrinkage stress distributions in molars after composite restoration. *Dental Materials, 20*, 554-564.

Versluis, A., & Tantbirojn, D. (2006). Filling cavities or restoring teeth? *Journal of Dental Sciences*, *1*, 1-9.

KEY TERMS

Elastic Modulus: A material property that plays an important role in the amount of residual shrinkage stress because it describes the relationship between stress and strain (deformation).

Finite Element Analysis: A numerical method developed to compute physical responses, based on subdivision of a (structural) system into smaller, simple shaped, interconnected elements.

Polymerization Shrinkage: Material contraction that takes place during a polymerization reaction. Resin-based composites shrink when conversion of monomers results in a polymer network with a more compact structure.

Shrinkage Model: A theoretical model that expresses the relationship between polymerization shrinkage and shrinkage stress based on scientific observations. Shrinkage models are used to assess shrinkage stresses and develop clinical procedures to minimize their effects.

Shrinkage Relaxation: The decrease in initial residual shrinkage stresses over time due to material and environmental effects such as viscoelasticity and hygroscopic expansion.

Shrinkage Stress: Stresses that are generated as a result of polymerization shrinkage. These can leave residual stresses in a restored tooth structure, in the composite material, and/or at the tooth-material interface.

Shrinkage Value: Quantification of polymerization shrinkage. The amount of shrinkage can been expressed in various terms, such as volumetric, linear, total, pre-gel, post-gel, and effective shrinkage.

Stress Concentration: A local area with increased stress level, e.g., at sharp corners or where materials with different elastic moduli meet. Stress concentrations are areas of increased risk for failure initiation because those stresses are most likely to exceed material strength properties first.

Chapter IV
An Objective Registration Method for Mandible Alignment

Andreas Vogel
Institut für Medizin- und Dentaltechnologie GmbH, Germany

ABSTRACT

This chapter introduces a computer-controlled method for mandible alignment. The exact positioning of the mandible in relation to the maxilla is still one of the great daily challenges in restorative dentistry. Between 1980 and 1991 long-term animal experimentation series about the performance of jaw muscles as well as temporomandibular joints were made at the University of Leipzig, Germany. Until today other studies of similar scale or approach can not be found in international literature. Miniature pigs were exposed to stress under unilateral disturbance of occlusion. Based on that morphological, histochemical and biochemical processings and some other functions were then analyzed. The studies proved that masticatory muscles play a vital role in the positioning of the mandible. Combining these findings with knowledge about support pin registration and the influence of masticatory force on the results of this method a computer-controlled registration method was developed. With the DIR®System exists a final method of measurement which gives objective, reproducible and documentable results.

INTRODUCTION

The exact positioning of mandible is still one of the common challenges in restorative dentistry. There are many methods that are being taught when it comes to bite registration, and is frequently mentioned in international literature. Looking closer one discovers that truly objective guidelines for a reproducible methodology are missing. It is solely up to the manual and the individual varying skills of the dentist to determine the so called centric position. This situation reflects the fact that until now multiple definitions of the centric position can be found across different international publications. Sources in the past decades note the alignment of the temporomandibular joints (condyles) was referred on the correlation to the teeth row. Commendable works over the last years give a detailed overview over the manifold literature. The following brief compilation of attempts at a definition over the last hundred years are mainly based on the research of Von Schilcher (2004; referencing 409 international publications). The compilation covers all key stages of dentistry and within these stages illustrates the level of knowledge at a certain point in time. It does not lay to claim to be a source of completeness.

THE HISTORY

Early methods include Gysi (around 1900) referring to the "Gothic arch" and McCollumn (1921) adducting the hinge axis to determine the jaw relations. After this early period different definitions and ideas follow in ever accelerated successions. Jacobson, Sheppard et al. (1959) favor an intermediate (non-retral) position in which temporomandibular joints, teeth and muscles are in balance. Meanwhile Lauritzen et al. (1964) reclaims the terminal hinge axis. This continues 1966/67 (Mühlmann et al.), 1978 (Bauer et al.; Stuart), and 1986 (Gerber). In all cases all structural elements involved are being evaluated differently and the focus keeps shifting between temporomandibular joint and occlusion. In 1992 the Arbeitsgemeinschaft für Funktionsdiagnostik (AFG) (i.g. Working pool for function diagnostics) of the Deutsche Gesellschaft für Zahn-, Mund- und Kieferheilkunde (DGZMK) defines the condyles in centric position as "cranio-ventral, non-sideways shifted position of both condyles in physiological head-disc-positions as well as physiological load of the participating tissue". In 2006 Türp took on a critical review of over 80 works across the international literature, resulting in a comprehensive article about bite registration. He explicitly considers the horizontal and vertical jaw relationships separately and concludes that today's centric position is the desirable one. At the same time he realizes that "the problem within centric positioning of the condyles is not knowing in which exact position the condyle-head disc-complex is in relation to the temporal joint structures." All together he states that there is not a commonly accepted method for the registration of the position of the jaws. The overwriting commonality in all these attempts of pinpointing a definition is the reoccurrence of the sagittal and transverse alignment of the mandible as a central focus. Much less insight is given about the objective facts of the third plane, the vertical axis. The bottom line being that under exact scientific aspects, the role of the musculature as well as the nerval control are underrated.

BASIC RESEARCH OF THE OROFACIAL SYSTEM

In the early 1980's Dr. med. Andreas Vogel initiated an investigation by a work group at the Poliklinik für Prothetische Stomatologie at the University of Leipzig (in cooperation with the Anatomic Institutes of the Universities of Leipzig und Rostock, especially noting Gert Horst Schumacher as well as the Institut für Sportmedizin of the Deutsche Hochschule für Körperkultur —DHfK -, also Leipzig, all Germany). To gain deeper insight into these complex processes the group focused on the behavior of certain masticatory muscles and temproromandibular joints structures in relation to the occlusal system. The results of these investigations, which lasted over ten years, were conducted under varying statements of task and can be summarized as following:

- Highest priority needs to be awarded to the neuromuscular component within the orofacial system.
- The efficiency (chewing) as well as the matters of sensitiveness (tactile perception and

control) are being transmitted through the neuromuscular system.

In 2003, based on these findings, Vogel set parameters for a valid definition (speech at the 7. Prosthetic-Symposium, Berlin, Germany):

- Comprehensive knowledge in regards to physiology and morphology of all participating structures within a specific setting (statics).
- Comprehensive knowledge in regards to physiological reactions of all participating structures within specific settings (function).

While obtaining a greater understanding of the muscular elements' behavior insight into the behavior of the tempromandibular joint structures was gained as well. This is of considerable importance in regards to the diagnostic and therapeutic approach of dentist and therapist alike. Thus a concept could be developed in which, technical measurements, clinical diagnostics as well as therapy are based on an exact defined long-term animal experimentation series, combined with previously existing scientific findings. Until the 1980's the morphology of the temporomandibular joints was relatively well researched. The behavior of the masseter muscle was studied as well. Applying exact methods of basic research the team began an animal research series at the University of Leipzig. The chosen test animal was Mini-LEWE (a miniature pig), an internationally recognized breed for researching problems in dentistry. Both, control groups and the number of test animals were selected to produce meaningful results (statistics). The time span of the experiments was selected with the same intentions. The conduction of the experiments was standardized as well, so all subsequent research could be based on the exact same approach.

THE MASSETER MUSCLE

The task at hand was to maintain a consistent approach in order to properly analyze how a one-sided occlusal interference would influence the morphology of the masticatory muscles (interference of the occlusion through an elevated cast filling in the fourth and first premolar of the right maxilla). Ulrici's experiments on the masseter muscle (Leipzig, 1982) became the starting point of the series. Regular periodic measurements of the masticatory force—conducted with load cells—as well as muscle biopsies, which were run before the experiment began and were repeated 20 weeks after the start. The assayed tissue samples of the left and right masseter muscle were processed both biochemically and histochemically. Within the masseter muscle fast FT fibers (fast contraction, easily fatigable) are dominant—physiologically based on its function as elevator muscle—versus the slow ST fibers (long-term tasks). The one-sided occlusal interference leads to a significant mutation of the amount of fiber in favor to the slow ST fibers, in addition to a quantitative increase on the disturbed side.

The cross-sectional size of the FT fibers were measurably enlarged on the non-disturbed side, also, the amount of capillaries increased. On the disturbed side the enzyme activity decreased over the test period more than on the non-disturbed side. On the non-disturbed side the masticatory force increased significantly in relation to the disturbed side. The entire enzyme activity dropped substantially during the experiments, more so on the disturbed side. EMG measurement showed raised activity levels on the non-disturbed side. These results—most of all concerning the spectrum of fibers—are corresponding with the works of other scientists and prove clearly the direct relationship between the morphological criteria and functional claims. This could affirm the assumption that by pain in the orofacial system the masticatory muscles are of high significance.

THE TEMPOROMANDIBULAR JOINT

A particular research series (Händel, 1986) examined the impact of the same one-sided occlusal interference on the temporomandibular joint. Due to the unstable conditions caused by the different loads of pressure in the left and right temporomandibular joints, significant tissue changes were occurring in the cartilage surface area of the condyles, the discus articularis as well as in the lining of the fossa articularis.

THE LATERAL PTERYGOID MUSCLE

Encouraged by these results further animal experiments were being prepared. The aim of these research series was to expand on the previous approach with introduction of the areas temporalis muscle, the medial and lateral pterygoid as well as the temporomandibular joints (Ulrici, 1991). Special attention was given to the lateral pterygoid muscle since—as the literature indicated—no long-term experiments had been conducted on this subject yet. The unique quality of this deeply embedded and but not secured palpatable muscle lay in its origin within a single upper and lower inferior head. The upper and lower heads unite after an almost horizontally course and insert directly at the temporomandibular articulation capsule (over many years a subject of discussion in the anatomical field). These special anatomical features in combination with its resultant functions within the joint put the lateral pterygoid in the center of interest.

The experiments conducted at the University of Leipzig and its results are still of topic today. In all literature no evidence of comparable and equally fundamental research can be found, merely statements in regards to the special functional behavior of the upper or inferior head of the lateral pterygoid muscle and of the muscle at whole (Murray et al elsewhere this chapter).

As is known in the physiology of the muscles, the masseter muscle and the temporal muscle consist about 75% out of fast FT fibers. Similar values were found for the medial pterygoid muscle. Within these FT fibers with glycolid metabolism we at least have to differentiate between type IIA, type IIB and type II X. Type IIA are aerobic fibers that allow for an increase of the portion of ST fibers within itself. In contrast to the masseter, temporal and medial pterygoid muscles a higher portion (up to 70% in the literature) of the slow ST fibers is assumed in the lateral pterygoid muscle. This low amount of trainable FT fibers leads us to suspect that muscles with such a fiber spectrum will display more difficulties in adaptation. The experiment implemented unilateral interference caused morphological changes in the masseter muscle, the temporal muscle and pterygoid muscles as well as metabolism change when shifting the masticatory force to the opposite side. (Please note that a consistent terminology for fiber types does not exist, for example another designation for ST fibers is MyHC-I. Within this terminology MYHC-IIA equals the FT fiber type IIA and so forth. But most importantly we have to acknowledge that, due to their extremely difficult and varying tasks, masticatory muscles are completely different from all other skeletal muscles. At this point partially referring to studies about fiber-type composition of muscles conducted by Korfage, Koolstra, Van Eijden, also Goldsprink et al.)

The lateral pterygoid muscle is that muscle of mastication, reacting the most sensitive by displaying a significant increase of ST fibers on the disturbed side. In addition the cross-sectional size of both fiber types enlarged. An increased amount of capillaries were recorded on the disturbed side, meanwhile a decline of enzyme activity took place on the contra-lateral. The metabolism did not adjust according to the morphological processes. This metabolic disorder could be the possible cause for a heightened algesia of this muscle, keeping in mind that the reason of muscle pain in general is not resolved yet. Different theories, most notably

Figure 1.

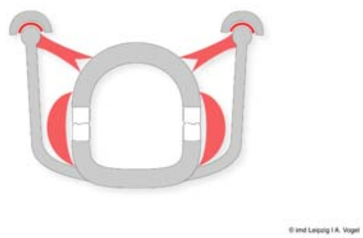

a. Accurate occlusion with joints and muscles in balance

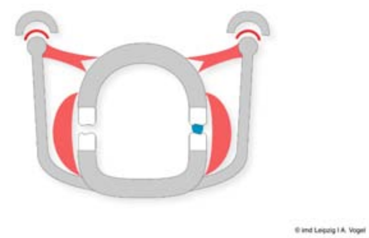

b. Implementation of a one-sided disturbance

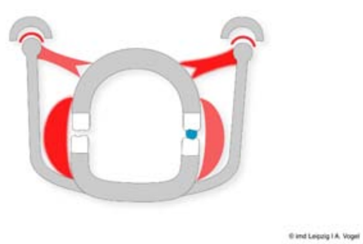

c. Masseter, temporalis and medial pterygoid muscle displaying a bigger alteration of the fiber spectrum at the opposite side then on the disturbed side several weeks after the implementation of a one-sided disturbance. Lateral pterygoid musclebeing more disturbed on the side with the elevated filling.

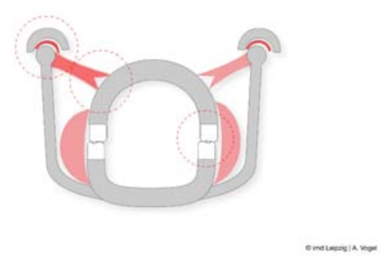

d. Lateral pterygoid muscle displaying a working hypertrophy on the opposite side after elimination of the disturbance, the temporomandibular joint being affected as well and the occlusion not being in the centric position. (All images © A.Vogel/imd)

metabolism disorder and mini lesions on muscle fibers are to be under consideration. After eliminating the disturbance the lateral pterygoid muscle continued to display further reactions in form of work-related hypertrophy on the non-disturbed side. This is a special reaction to the heavy load, induced by evasion, abrasion and the search for new habitual intercuspidation. The disturbance of the arthro-muscular balance was most pronounced after about 30 weeks. (The effects of one-sided occlusal disturbance most notably on the temporomandibular joint on the contra-lateral as described by Händel was confirmed.)

These long-term, carefully planned test series could prove that through purely mechanical shifts of the mandible reactions are being put in action.

These reactions lead to a buildup of new, adaptive reflex pattern of both, the chewing motion and the so called centric position. In practice this can be retrieved within the habitual intercuspidation, the result being an alteration of the masticatory muscles itself. Therefore the deepest impact was recorded in the lateral pterygoid muscle which corresponds with the fact that it is involved in all movements of the mandible, mainly determined by horizontal tasks and restrain as well as coordination. The insights of the 1980's and early 1990's correspond with the results of long-term EMG experiments on the lateral pterygoid muscle conducted at the Westmead Centre for Oral Health, University of Sydney. The tests on patients (electrode placement trajectory on the lateral pterygoid muscle under CT control) were run under varying tasks over a time span of about 10 years, focusing on both upper and inferior head of the lateral pterygoid muscle.

Amongst other things the effects of one-sided occlusal interference were verified by the Sydney team (Huang, Whittle and Murray, 2006): "IHPL (e.g. inferior head of lateral pterygoid) activity was significantly ($p < 0, 05$) increased with the occlusal alteration during the outgoing (movement from intercuspal position to approximately 5mm right) and return phases of laterotrusion. The other muscles demonstrated no change or a significant decrease activity. CONCLUSIONS: These findings suggest that a change to the occlusion on the working-side in the form of a steeper guidance necessitates an increase in IHPL activity to move the mandible down the steeper guidance." In 2007 Murray et al drew the conclusion that the lateral pterygoid is part of all masticatory movements and should be functionally considered a homogeneous muscle: "These studies have defined the detailed functional properties of, in particular, the lateral pterygoid muscle, whose physiology and function is not well understood. In summary, the data are consistent with the hypothesis previously proposed that the lateral pterygoid should be regarded as a system of fibers that acts as one muscle, with varying amounts of evenly graded activity throughout its entire range, and with the distribution of activity within the muscle being determined by the biomechanical demands of the task." The functional coherence of the lateral pterygoid was a premise of the Leipzig test series.

DEVELOPMENT OF A NEW MEASURING TECHNIQUE

After the Leipzig test series it was necessary to re-consider the value of the performance of the mastycatory musceles and notably of the lateral pterygoid muscle in dentistry based on the cognitions about muscles within the orofacial system in general, as well as the muscle-physiological features of singular participating muscles and their interactions. Hence grew an urgency to implement objective methods of measurement in the orofacial field, as applied decades before in other fields of medicine, only which could truly give justice to the complexity of this muscular system. Most of all these insights immediately impacted manual bite registration conducted in restorative dentistry.

In the following years, combining his knowledge of the results of the animal-based test series with the scientific overview of the multiple forms of the theme bite registration, Vogel began, within the framework of an interdisciplinary research complex, to develop an objective measurement technique which was to fulfill the following requirements: To develop a diagnostic method which allows for objective insight into different components of the masticatory system as well as the evaluation of all functional processes. To ensure that this method would deliver appropriate findings, assuming adequate medical capabilities, the actual state can be determined, and simultaneously allow conclusions towards the normal physiological behavior of the masticatory system - the target state. With this method, bite registration was finally awarded the significance in restorative dentistry that it deserves. It was necessary to capture and show objective basic biological and physiological parameters, so that a diagnostic as well therapeutic approach could be secured. Such a system also needed to objectively display a functional pattern of the neuromuscular system and evaluate further components of the orofacial system like the temporomandibular joint and occlusion, while also complying with the requirements of modern day measuring techniques in medicine. It also needed to produce easily replicable results for the dentist, dental technician and not least the patients participating in the recording processes.

As early as 1993 Vogel presented the prototype of a system which could comply with all of these requirements at the 42. annual meeting of the Deutsche Gesellschaft für Prothetik und Werkstoffkunde e.V. in Lübeck-Travemünde (Germany). In 1993, after perfecting the sensor technology and software as well as integrating a conductor system to fixate the obtained parameters for the mandible position, the system was introduced to the market (patent of the sensor: Vogel/Heinze/Wiesinger). It should be pointed out that the software contents were developed as the result of the above mentioned animal tests and their scientific findings. Besides these findings, based on a complex overview of the application of support pin registration, additional positions of the pin, which were not given attention earlier, were incorporated into the registration. At last a new type of handling for the registration of the mandible position was substantiated, including an entirely new form of bite registration under a defined masticatory force.

DIR® SYSTEM: DYNAMICS AND INTRAORAL REGISTRATION

Based on the learnings of this measuring system practice it became necessary to optimize essential parameters. In the field of sensor, amplifier and transition and fixation technology, new technical developments were integrated. A new addition was the capability not only to measure under defined masticatory force, but also to enable fixing under this force. Without modifications of the clinical contents the software was adjusted according to this optimized measurement technique and officially released under the name DIR® System in the last quarter of 2006. It was certified after MPG 93-42 EWG, Anhang 4, of the European Union standards.

The system operates on the principle of support pin registration. Alongside the records of the original pin position registration a combination of additional positions is being utilized in the readings. By doing this, a combination of two-dimensional functions, under high resolution, is made graphically transparent, visually rendering the actual neuromuscular commitment as well as the functional behavior of the structures of the temporomandibular joints. Vogel, Jüde, Jakstat proved that not only the position of the support pin but also the applied force influences the measurement results. In DIR® the integration of masticatory force is being applied in the 10 to 30 newton range, which corresponds to the performance parameter of masticatory musculature. Because of this strength-based muscle performance a third dimension is being indirectly included in the assessment. A positive side effect is that the measurements are being displayed in real time on a monitor. This allows for better self-control and increases concentration of the patient.

With the employment of this system it is, in particular in dentistry, intended to consolidate the occlusal conditions. This allows the dental practitioner to align the non-visible position of the temporomandibular joints as well as the force vectors of the adequate muscles in a physiologically optimal state, a set point, which then allows one to determine the correct occlusional conditions, the key factor for all restorative work. Subsequent necessary therapeutic measures, e.g.

Figure 2. Diagram of the elements of the DIR®System

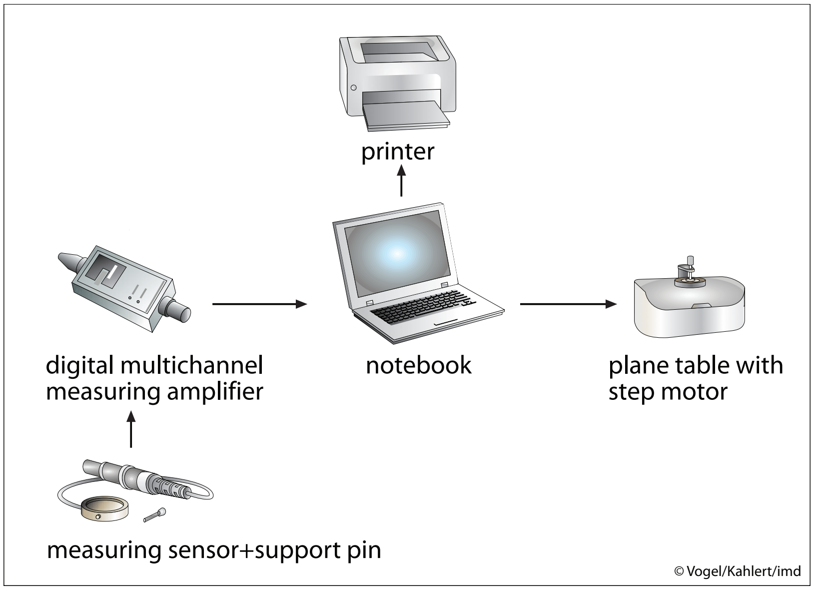

Figure 3. Support pin and sensor placed in plaster casts

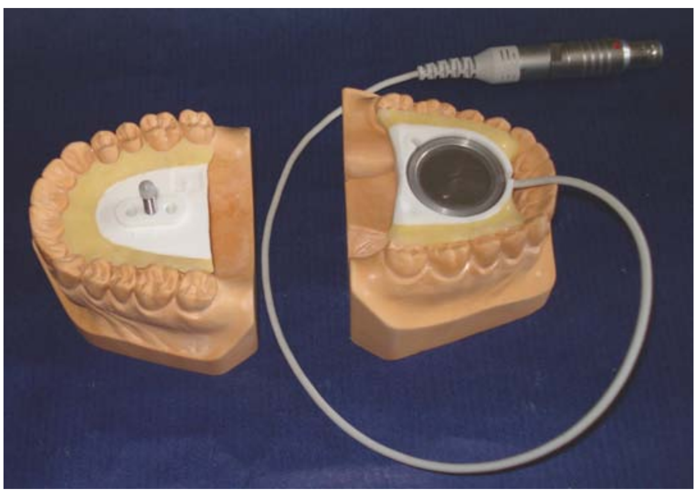

gnatho-orthopedic, and surgical concepts, can then be debated and planned. The aspect of occlusion in combination with reflex based occurrences alone, creates a significance which has not been achieved or demonstrated in any other field. The critical discourse surrounding this problem makes it essential to intensively analyze occlusion and also consider its relation to further aspects (e.g. spine, pelves) within these functional occurrences. This critical and all encompassing point of view inevitably raises other issues such as the theory of occlusion, programming of dental articulators and the calculation of specific planes. As it is the responsibility of the dentist to correctly position and occlusally fixate the mandible, Vogel is convinced that first and foremost a physiologically correct position of the mandible needs to be established before further medical disciplines can be taken into consideration. Once these procedures are accepted interdisciplinary collaboration (otorhinolaryngology, neurology, orthopedics, physical therapy, osteopathy) can begin and a number of new approaches for further assessment will open up. As already mentioned, it is imperatively necessary to continue the work in combination with exact and objective measurement technique from the already named areas of dentistry, so that in the future scientifically secured results, expressed by treatment strategies, can be handed to the practitioner.

FUNCTIONALITY OF THE DIR® SYSTEM

The preliminary concern when developing this new objective measurement technique was to consider varied parameters and to develop an instrument which would be highly relevant to a dental practice, most of all enabling the participating partners, dentist and dental technician, to share a collective and comprehensible point of view for necessary occlusal restoration.

The most integral technical components of DIR®-System – measuring technique for identification of the mandible position, are a new type of sensor, a new measurement amplifier, and new software which has been adjusted to match the new hardware as well as a highly precise transmission system. This combination allows to record the interference-free two-dimensional movements of the mandible in an very high resolution. The third aspect is that the under masticatory force conducted measurement is becoming an essential part of the assessment process.

The integration of the parameters movement and masticatory force with an electronic measuring process is new for bite registration in dentistry. It also allows for conclusions in regards to behavior of structures under functional aspects which were unknown until the present point in time.

Figure 4. Pin placed in the maxilla and sensor placed in the mandible of a patient`s mouth, both are fixed on patterns

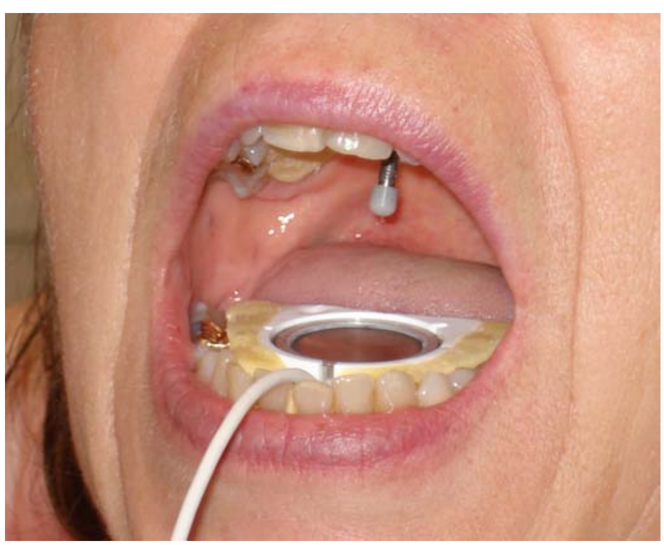

Figure 5. A computer-simulated image of an DIR® measurement

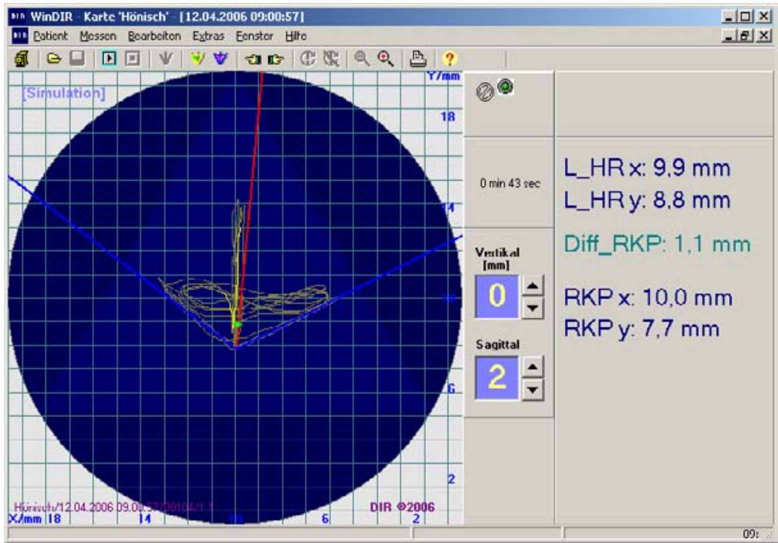

After approximately 15 years of deployment of this measurement technique into the everyday practice (in 2006 the former system was upgraded to become the DIR® System) it has become apparent that the approach created by Vogel has been validated, in multiple ways, in the clinical field today. The latest results in research in regards to support pin registration as well as in the area of morphology of the muscles validate the system approach:

In 2006 a study about the precision of intraoral support pin registration, presented in a dissertation by Natalie Weber, proved that this method can be assumed as accurate, having been a reoccurring topic of discussion in dentistry. In a group of 22 subjects of an average age of 22 and free of complaints, 88 percent resulted in an aberration of less than 0,5mm. The data reiterates the high level of accuracy of this method. The methodical specifications of this study–young test persons free of complaints–as well as its results–variations with each measurement in addition to a daily error rate, validate Vogel once more in one specific aspect of his approach to develop a new process for registering the position of the mandible: The pin registration is an acceptable method but has be to synchronized with the existing modern technical capabilities. Surprisingly Weber's thesis does not take the basic studies and subject-matter research by Kleinrok into consideration.

Vogel's second proposition, the significance of the chewing muscles and the temporomandibular joints has been recently affirmed. A study about the effects of masticatory force training on the masticatory musculature (dissertation, presented in 2002 by Regber) showed that the lateral pterygoid muscle reacted very differently compared to other masticatory muscles, a result which was underestimated by Regber. At this point we have to emphasize, once again, the results of the manifold EMG recordings of the lateral pterygoid muscle conducted at The University of Sydney, Australia. A new detailed case study (Janke, 2007) reports successful treatments of patients with TMD (temporomandibular disorder) based on measurement results of the DIR® System. After these measurements the habitual position (actual state) of the mandible was corrected into the physiological position (target state) with bite splints.

The main focus within the framework of dentistry should be to exactly determine position and value of the orofacial system, and clearly define its allotment within the human system. The aspect of the occlusion in combination with reflex actions create a level of significance which simply can not be reached or demonstrated in other medical disciplines. The critical dispute of this problem makes it necessary to research occlusion extremely intensively and to consider its functionality in relation to other aspects (e.g. spine, pelvis). This critical point of view inescapably follows suit —as mentioned above—with further problems for the practice: occlusion concepts, calculation of specific planes as well as the application of for example face-bows.

In addition the practice with DIR® System shows that, especially in the field of dentistry and dental technique, very different basic approaches are being applied. Based on the author's insights it is imperatively necessary in the field of physiotherapy to develop unified concepts and to deploy these in the educational system. As it is equally essential to further investigate certain areas in basic research (muscles, neural control, pain). It is desirable, through clearly defined transparent positions, to reach a crucial leap in quality (optimal function in terms of the patient) for the restorative occurrences within the occlusal system via integration of all involved structures of the body

It is highly positive that doctors from different fields are opening up to the subject matter and that successes of first interdisciplinary collaborations are being reported. It remains up to the commitment of further research teams to critically dispute such a complex subject matter and shed more light into such problems as TMD. Murray and his team came to the following results through yet another series of experiments based on EMG recordings: "Despite earlier reports to the contrary, both heads of the lateral pterygoid muscle appear to be electrically silent at the postural or resting jaw position, and therefore appear to play no role in the anteropersterior positioning ot the jaw at the postural position. An important role has also been demonstrated electromyographically for progressive changes in activity in the inferior head as the direction of horinzontal jaw force shifts from one side to the other. This suggests an important role for the lateral pterygoid muscle in the generation of side-to-side and protrusive jaw forces. The lateral pterygoid muscle is likely therefore to play an important role in parafunctional excursive jaw movements and also possibly a role in influencing jaw position in patients where the maxillomandibular relationship records change from session to session. The above data provide new insights into the normal function of the lateral pterygoid muscle. The proposal that the lateral pterygoid muscle plays some role in the aetiologoy of TMD needs now to be rigorously tested." The afore mentioned being in conjunction with Vogel.

FINAL REMARKS

From the perspective of dentistry and prosthetic dentistry the introduction of the DIR® System accounts for the permanently increasing need to bring transparency into the "black box" of bite registration. It is the concern of the author to bring security and improved capacity in regards to diagnostic and therapy for the dental practitioner before he or she decides on a certain therapy. This point of view manifests that in the future the results of restorative, gnatho-orthopedic and implantological treatments call for evalution from a different point of view (IAAID-Symposium 2006, R. Slavicek, G. Risse about gnatho-orthopedic treatment). Functions in the sense of physiological target values of the patient should concede a dominant role. It is no coincidence that in young patients recurrence or TMD occurs time-displaced after gnatho-orthopedic treatments. The results of restorative dentistry can lead to occlusional alteration or even non-physiological positioning of the axis of the teeth in relation to the force vectors of the musculature, which then again can lead to the already mentioned negative consequences.

It is therefore advised to always keep the function in perspective - in the interest of all, the patient, the dentist, therapist, and the dental technician. The parameters movement and masticatory force are being applied with the instantaneous goal to bring the moving structures (actual state) into an ideal physiological state (target state) for the object. The many internationally conducted experiments presented have created a good starting position for bringing more clarity into the oriofacial system and to begin solving many problems in dentistry. In addition to TMD many other controversial problems are being discussed. These issues will require the dental field to research further.

REFERENCES

Händel, L. (1986). *Experimentelle Untersuchungen am Miniaturschwein (Mini-LEWE) zur Auswirkung unilateraler Okklusionsstörungen auf die Mjorphologie der Strukturen beider Kiefergelenke (Ein Beitrag zur Ätiologie des Schmerz-Dysfunktions-Syndroms).* Leipzig: Dissertation zur Promotion A.

Hirsch, C., & John, M. (2003). Prävalenz kraniomandiblulärer Dysfunktion (CMD) bei Kindern und Jugendlichen. *Dtsch. Zahnärztl. Zeitschr, (DZZ)*, 10, 589-92.

Huang, B. Y., Whittle, T., & Murray, G. M. (2006). A working-side chang to lateral tooth guidance increases lateral pterygoid muscle activity. *Arch Oral Biol. 5*(8), 689-96.

Janke, A. T. W. (2007). *Auswirkung nach dem DIR-System vermessener okklusal adjustierter Aufbißschienen auf die Stellung der Halswirbelsäule bei CMD-Patienten*. Krems: M.A.-theses.

Korfage, J. A. M., Koolstra, J. H., Langenbach, G. E. J., & van Eijden, T. M. G. J. (2005). Fiber-type Composition of the Human Jaw Muscles - (Prat 1). Origin and Functional Significane of Fiber-type Diversity. *J Dent Res.*, *84*(9), 774-83.

Korfage et al. (2005). Fiber-type Composition of the Human Jaw Muscles– (Part 2). Role of Hybrid Fibers and Factors Responsible für Inter-individual Variation. *J Dent Re.*, *84*(9), 784-93.

Murray, G. M., Bhutada, M., Peck, C. C., Phanachet, I., Sae-Lee, D., & Whittle, T. (2007). The human lateral pterygoid muscle. *Arch Oral Biol.*, *52*(4), 377-80.

Murray, G. M., Phanachet, I., Uchida, S., &Whittle, T. (n.d.). The human lateral pterygoid muscle. A review of some experimental aspects and possible clinical relevance. *Austral dental Journal*, *49*(1), 2-8.

Regber, K. (2002). *Auswirkungen eines Kaukrafttrainings auf die Kaumuskulatur.* Freiburg i.Br.: Inaugural-Dissertation.

Türp, J. C., & Schindler, H.-J. (2002). Zum Zusammenhangt zwischen Okklusion und Myoarthropathien. *Schweiz. Monatsschr. Zahnmed*, *113*(9), 403-11.

Ulrici, V. (1982). *Experimentelle Untersuchungen am Miniaturschwein (Mini-LEWE) zur Auswirkung von unilateralen Okklusionsstörungen auf die Kaumuskulatur (Ein Beitrag zur Ätiologie des Schmerz-Dysfunktions-Syndroms).* Leipzig: Dissertation zur Promotion A.

Ulrici, V. (1991). *Die Veränderungen des arthromuskulären Gleichgewichts im orofazialen Organ durch unilaterale Interferenzen. Eine tierexperimentelle Untersuchung am* Minischwein. Leipzig: Habilitationsschrift.

Vogel, A., Jakstat, H., & Jüde, H.-D. (1990). Experimentelle Untersuchungen zum Einfluß der Registrierkraft auf das Ergebnis der Stützstiftregistrierung. *Dtsch. Stomatol., 40*, 363-65.

v. Schilcher, C. (2004). *Die Position des Condylus mandibulare – Eine kritische Literaturübersicht*. Würzburg: Inaugural-Dissertation.

Weber, N. A. (2006). *Untersuchung zur Präzision des intraoralen Stützstiftregistrates bei der Ermittlung der zentrischen Kieferrelation verglichen mit der maximalen Interkuspidationsposition funktionsgesunder Probanden*. Münster: Inaugural-Dissertation.

KEY TERMS

Bite Registration: Various methods to registrate the relationship of the maxilla and the mandible

DIR®System: An obejctive method to record the mandible alignment to gain the centric position

Intraoral Recording: Recording the mandible position relating to the maxilla

Lateral Pterygoid Muscle: A masticatory muscle, which lays in the depth and can not be palpated properly

Mandible Alignment: Positioning of the mandible in relation to the maxille

Masticatory Force: Force developed by closing the theeth rows under power

Masticatory Muscles: System of muscles for opening and closing the mandiblel, for chewing, swallowing and articulation

Section II
Software Support in Oral Surgery

Chapter V
Requirements for a Universal Image Analysis Tool in Dentistry and Oral and Maxillofacial Surgery

Thomas Hierl
University of Leipzig, Germany

Heike Hümpfner-Hierl
University of Leipzig, Germany

Daniel Kruber
University of Leipzig, Germany

Thomas Gäbler
University of Leipzig, Germany

Alexander Hemprich
University of Leipzig, Germany

Gert Wollny
Universidad Polytéchnica de Madrid, Spain

ABSTRACT

This chapter discusses the requirements of an image analysis tool designed for dentistry and oral and maxillofacial surgery focussing on 3D-image data. As software for the analysis of all the different types of medical 3D-data is not available, a model software based on VTK (visualization toolkit) is presented. VTK is a free modular software which can be tailored to individual demands. First, the most important types of image data are shown, then the operations needed to handle the data sets. Metric analysis is covered in-depth as it forms the basis of orthodontic and surgery planning. Finally typical examples of different fields of dentistry are given.

INTRODUCTION

Image analysis is routinely performed in all fields of dentistry, ranging from 2D X-ray analysis to the investigation of plaster model casts in orthodontics or the planning of surgical procedures based on CT data. In daily practise, different image analysis tools are used which have been designed for specialized needs, in many instances one programme for one single task. This is especially true for 3D images where landmark based analysis methods are often used. Ways to handle these data will be shown in this chapter.

IMAGE DATA IN DENTISTRY

During the last decades, image analysis in dentistry was mostly confined to 2D bitmap images. Typical examples have been:

- Plain X-rays → cephalometric analysis in orthodontics, caries diagnostics, endodontics etc.
- Photographs → facial analysis in oral and maxillofacial surgery and orthodontics

The advent of 3D-scanning technologies has brought a wealth of new image data to dentistry. CT-scanning, magnetic resonance imaging (MRI), cone beam tomography, and optical scanning (e. g. laser scanning, fringe projection or stereophotogrammetry) are now widely used. A short and incomplete list of reasons why such data is acquired includes:

- Optical scanning of dental crowns for prosthodontic work (CAD-CAM design and production of crowns and bridgework)
- CT and CBT for implant surgery (ranging from planning of implant position to surgical navigation during implant placement)
- CT, MRI, and optical scanning for 3D cephalometry
- Optical scanning of dental plaster casts in orthodontics
- CT, MRI, and optical scanning in epithetics (i. e. generating artificial missing facial parts after tumor surgery, accidents or due to syndromic diseases)

A key issue of most 3D scanners is the use of proprietary file formats with an inconsistent export possibility into common file formats. Most software functions of the programmes which come alongside the scanners, however, are confined to these proprietary file formats. This implies that missing import filters are limiting the use of these programmes in daily practise. Commercially used software is free of such constraints but rarely adapted to the needs of dental professionals, is rather expensive and requires profound training.

REQUIREMENTS FOR A "UNIVERSAL" IMAGE ANALYSIS TOOL

An ideal image analysis tool should appeal to the typical software used by medical professionals (i.e. the look and feel of standard office software). Functions and drop down menus should be named in plain words, mathematical terms should be used sparsely. Regarding the data to be analysed, import filters for typical 2D and 3D format files should be available. These include:

- Bitmap formats (BMP, JPEG, …)
- Rdiologic images (DICOM standard)
- Polygon based surface data derived from optical scanners (STL, VRML, OBJ, …)

Regarding the 3D image files export filters are required for special tasks. This includes production of rapid prototyping (RP) specimens for implant templates, epithetics or alloplastic implants (Ono et al. 2000). The most important format is STL, which is the standard language of RP-machines. Other export formats like VRML are useful in case of surgical planning if virtual skulls or bone segments are created which will undergo surgery. For DICOM data export formats are needed if the data have to be processed as the original DICOM data should not be changed (this is a key point of this format to keep the inherent medical information).

For 2D images typical pre-analysis procedures include cropping, rotation, mirroring, colour changes and correction of contrast and brightness. Here a multitude of software solutions exists, and most tasks can be performed with any of them. In the majority, analysis of dental images is concerned with metric measurements. After calibration to the real distances landmarks are used to define distances, angulations, proportions to create new landmarks with new distances and so on. Furthermore parallel and perpendicular lines will have to be created. In the 2D world special orthodontic software exists to solve these requirements. Here a most important factor is how intuitive the analysis can be done and the time needed. Being able to perform an analysis in the shortest possible time will be a key issue in clinical practise and will define the use of any software. Also the database should allow easy access to the data for statistical analysis.

In the 3D world the situation is more complicated. As mentioned above many programmes are confined to special formats. Converting formats may lead to loss of information like an export from OBJ to STL format looses facial texture information. Programmes may read DICOM data or polygon data. The key asset of 3D data is the possibility to have a look from all sides. Thus pre-analysis features have to include:

- Moving the object (pan)
- Rotating the object
- Zoom capability

CT, MRI and CBT data may be inspected by way of image stacks, that means looking at individual slices within the scanned specimen. These planes may be parallel to the scanners gantry or perpendicular forming orthogonal x, y, z planes. Furthermore so-called oblique planes may be created which may lie in any direction. In case of 3D reconstruction, the image data has to be segmented (i. e. using a threshold to define which grey-scale values will be shown) to confine the displayed image to the structures to be analysed. This works easy with CT images due to the wide range of the Hounsfield scale, somewhat worse for CBT data and most complicated for MRI data. Anatomical structures may be displayed via volume or surface rendering. Regarding metric analysis, 3D images are much more difficult than 2D ones. As the object may move, the chosen landmarks have to stick. As the landmarks lie on the surface of the object, thresholding becomes a major issue analysing CT or CBT images. Changing the threshold changes the geometry und thus the landmark coordinates (that way the threshold boundaries should be stated in scientific work using segmentation procedures). A coordinate system has to be set up to attribute x, y, and z values to calculate distances or define lines, angles and planes. More elaborate features in processing 3D-data sets include clipping, adding different aspects, loading different data-sets and manipulate them independently, or performing boolean operations (Hierl et al. 2006).

As mentioned above, image analysis can be landmark-based. In dental and medical applications, the use of landmarks is widely accepted as most areas of interest show distinct landmarks which are routinely used in clinical language to describe these specimens. As therapeutical approaches are orientated on these landmarks, too, metrical information about these landmarks is more or less self-explaining for the medical practitioner. Using 3D cephalometric measurements is the method of choice in cases of asymmetry or severe pathology (Kragskov et al. 1997). On the contrary, using complex ways of analysis like thin-spline-analysis (Bookstein 1996) or landmark-free methods, which describe shape changes may lead to a general understanding but can rarely be utilized for therapy. Therefore the focus of this chapter will lie on a conventional approach with stress on 3D datasets. Image analysis of time series (for example comparing pre- and posttherapeutical images) using registration procedures is an important feature, too, but is not dealt within this chapter.

DESIGN OF A MODEL SOFTWARE

As mentioned above, an ideal, low-priced software for analysing medical 3D data is hard to find. On the other hand, open projects to furnish the background for such software have been developed. Most famous are VTK (visualization toolkit; www.vtk.org, www.paraview.org for parallel computing) and ITK (NLM insight toolkit; www.itk.org) which deliver modules for data processing and visualization that are publicly available and can be combined freely. Furthermore, modules not available by now can be written by and shared with the huge VTK community. Based on VTK, a software designed for dental and medical image analysis is presented. Schroeder et al. (2006) serve for further reading on VTK. A most important feature is usability, therefore close contact between clinicians and software programmers is suggested.

First step is choosing the image formats to be read. For 2D and 3D images, the following formats were selected: 2D: BMP, JPEG, PNG, for 3D: DICOM, STL, VRML, OBJ, 3ds.

Second step is to integrate basic functions. This implies 3D rendering of DICOM images as well as functions like zooming, rotation or panning. Independent clipping planes and thresholding to segment DICOM images are needed, too. To facilitate segmentation, buttons for typical pre-set

Figure 1. Four window display of a CT data set. The use of crosshairs allows landmark placement anywhere. The sella landmark is shown in the midst of sella turcica.

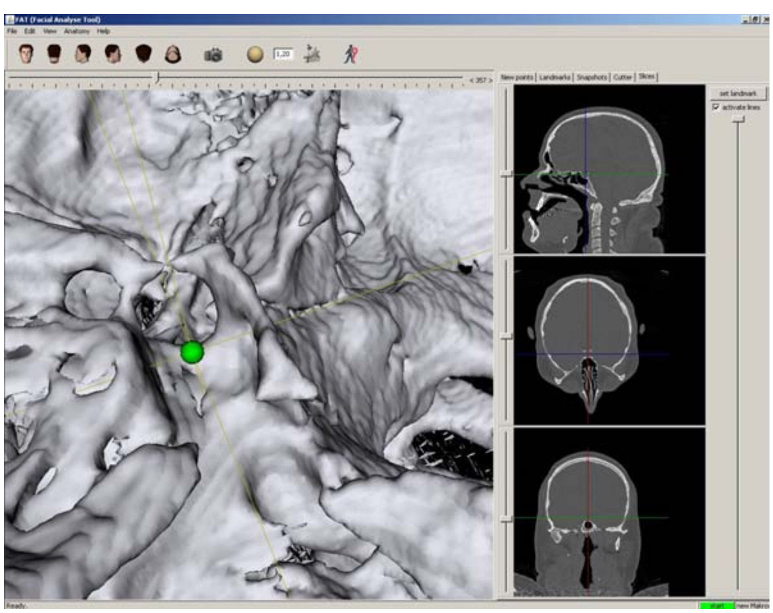

values for soft tissue surface display and bony segmentation are integrated decreasing the need for manual segmentation. In medical CT scanning an often neglected problem is the orientation of the scanner´s gantry. Tilting of the gantry plane is done to avoid exposition of the lenses. During 3D reconstruction most software programmes will not correct the gantry which will lead to gross distortion of the rendered object by displacement of all axial slices in the z-plane. Automatic gantry tilt correction can be implemented in VTK and is a useful feature.

For metrical analysis, a hierarchical procedure was chosen. First step is to select the appropriate landmarks. These may be anatomical ones in case of cephalometry and orthodontics and here an open, self-defined library to choose the ones needed is helpful. Landmarks may be select by way of different means. E. g. by direct placement on the thresholded CT image, by way of using crosshairs, or by using a maximum intensity projection to reduce a 3D image to a 2D one, in which exact landmark placement can be easier. Figure 1 shows the use of crosshairs, which is important for landmarks that do not lie on the surface of the investigated object. Furthermore the coordinates of the individual landmarks must be available for further use (Figure 2). This allows processing of the data. In case of cephalometry, Euclidian distance matrix analysis (Lele and Richtsmeier 2001) or finite element methods (Lozanoff and Diewert 1989) may be performed that way.

Having chosen the landmarks, the trigonometric operations follow. Figure 3 shows possible operations, ranging from defining distances, different ways to construct planes, proportions, angulations, to perpendicular distances, lines or planes. In addition these operations may define new points etc, which can serve as a basis for further measurements (Figure 4). So, an intricate

Figure 2. Facial scan taken by an optical scanner. Import format is VRML. Anatomic landmarks have been placed on the surface. The individual coordinates are displayed instantly and may be used for further processing. On the far left of the table the landmark is given, then a short definition follows. Below right the location of the highlighted landmark is shown.

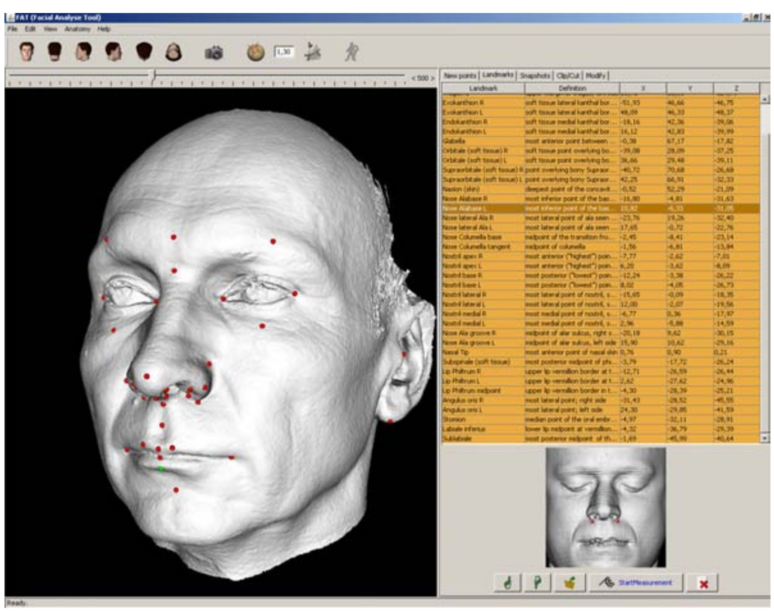

Figure 3. Construction table for trigonometric operations. Any operations can be performed by inserting the appropriate landmarks. Each result is shown and stored in a spreadsheet.

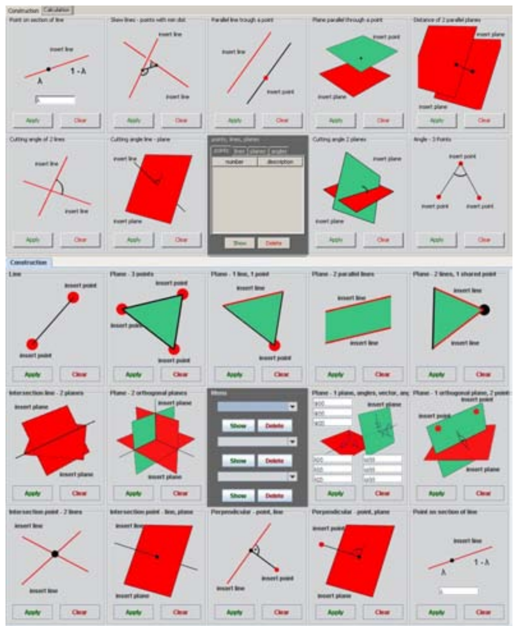

Figure 4. Pathway for a landmark based analysis. Generated objects can be used for further analysis. This way, complex metrical analysis is possible.

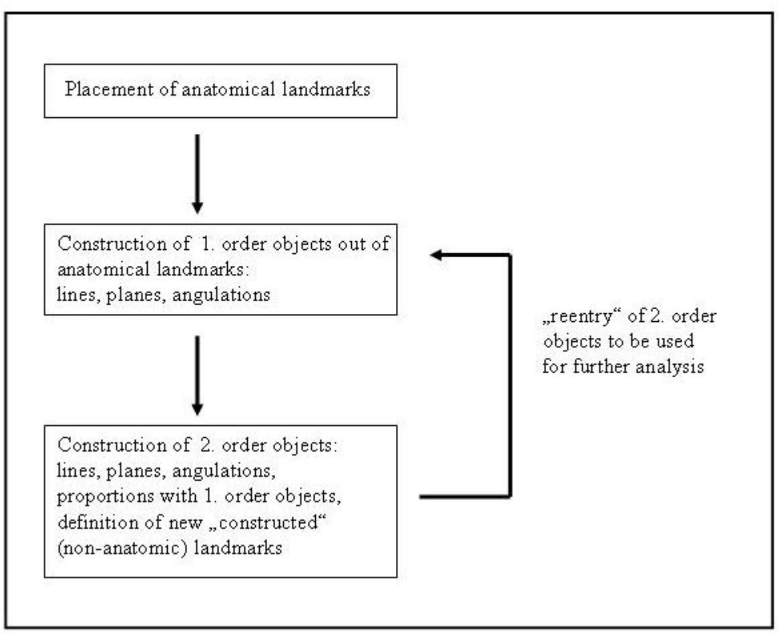

trigonometric analysis can be performed. In the end a spreadsheet with all the information for that individual specimen is given. The construction table has to be self-explaining. In this example a drag and drop function to allocate the landmarks and picking from a table are possible. Finally analyses are created which resemble batch programmes. In the end, an appropriate analysis is selected for the data, the landmarks are loaded automatically and the only work is to place the landmarks in the correct order. After the last landmark has been placed, the result of the full analysis is given in a spreadsheet ready for export to a statistical software programme. In addition, the landmark coordinate data can be saved, too. Thus the correct position of the landmarks may be re-evaluated or more landmarks may be added for a new analysis.

By way of segmentation, objects can be created. Adding multiple objects to a scene and handling them independently allows planning operations like surgery, orthodontic therapy or prosthodontics (Figure 5).

Boolean operations with objects will be necessary to construct CAD-CAM facial implants (Figure 6), epithetic prostheses, or in prosthodontics .

Being able to inspect intersections of multiple datasets will also allow the investigation of occlusion using virtual model casts.

Export filters are necessary to allow further work with the generated data. For practical reasons VRML and STL seem reasonable. This way objects can be created by way of rapid prototyping or used for further work (Figure 7). If finite element methods need to be applied, segmentation and export functions are needed for preprocessing of the data, too (Remmler et al. 1998).

SOFTWARE VALIDATION

Any kind of software used for medical investigations needs validation. Different ways have been suggested. Human skulls have been used in

Figure 5. Virtual try-on of an internal mandibular distraction device on a patient´s skull. Virtual operations help in shortening operation room times and can improve surgical outcome.

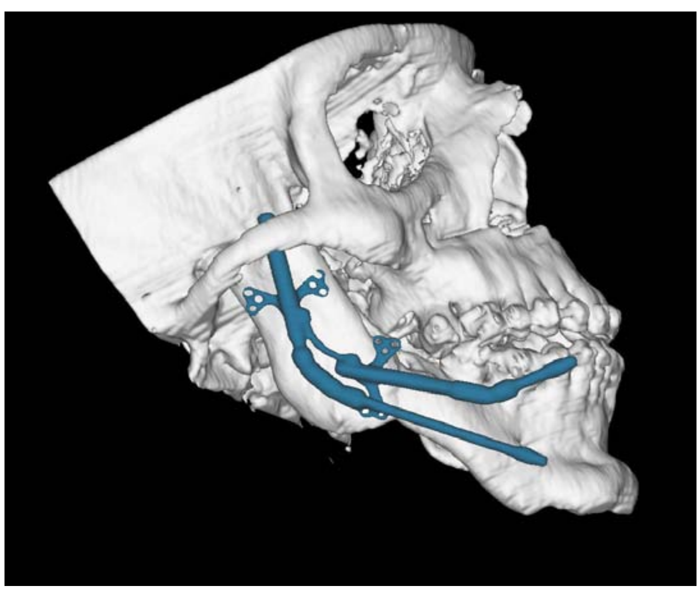

Figure 6. Planning of a CAD-CAM generated alloplastic implant by fusion of two objects. Pink: patient´s situation with traumatic nasoethmoidal and frontal deficiency; deep yellow: skull segment taken from a skull library. Both objects are superpositioned and fused. Afterwards the patients´ object will be subtracted and the implant object will remain. Only minor work to correct the transition to the patient skull will be necessary. Segmented VRML data is used for these operations.

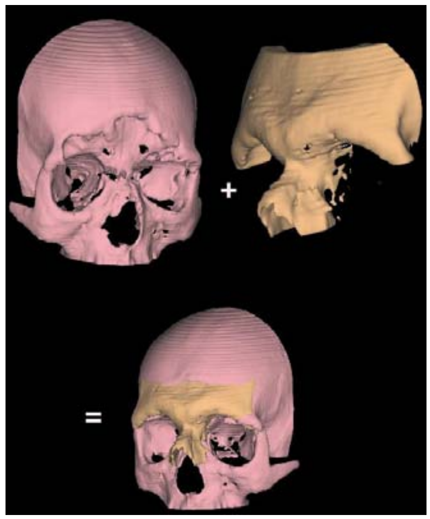

Figure 7. Surgical template for implant placement generated via rapid prototyping. Here the STL export filter has been used to create a FDM specimen.

many instances as they resemble best the intricate anatomy and the data set may show problems with import functions, 3D-reconstruction, segmentation, and trigonometric measurements. A common way is measuring distances on the real skull and compare the results with measurements on the virtual object (Hildeboldt and Vannier 1988). Distances on the real skull can be taken with a 3D-digitizer or with precision callipers. In our validation study, a precision calliper was used. To minimize errors due to landmark identification, titanium micro-screws were inserted on 22 landmarks before CT-scanning of the skull. Statistical analysis of 48 measurements showed not significant difference (CT parameters: 1 mm slicing, contiguous slices, Ø deviation real skull – vs. virtual skull 1 % of the measurements which equalled 0.24 mm. Students t test, $p < 0.01$) (Figure 8).

CLINCAL APPLICATION

A typical application of dental image analysis is investigating a dental arch. Plaster casts are taken routinely and conventional analysis was done by placing a Perspex plate with an etched metric grid over the crowns. For precise measurements reflection microscopes or callipers were used. Now optical scanning will furnish a precise virtual model with no risk of loosing information due to fractures of the brittle plaster cast. Having set up a metric analysis the file is loaded and the appropriate landmarks are placed. Then the batch programme will calculate all pre-defined measurements automatically. As the virtual model can be zoomed, moved, or rotated freely, an analysis can be performed in short time (Figure 9).

Figure 8. Software validation. Measurements between titanium micro screw markers (red dots) are performed on the real and virtual skull. Using micro screws diminishes landmark location errors.

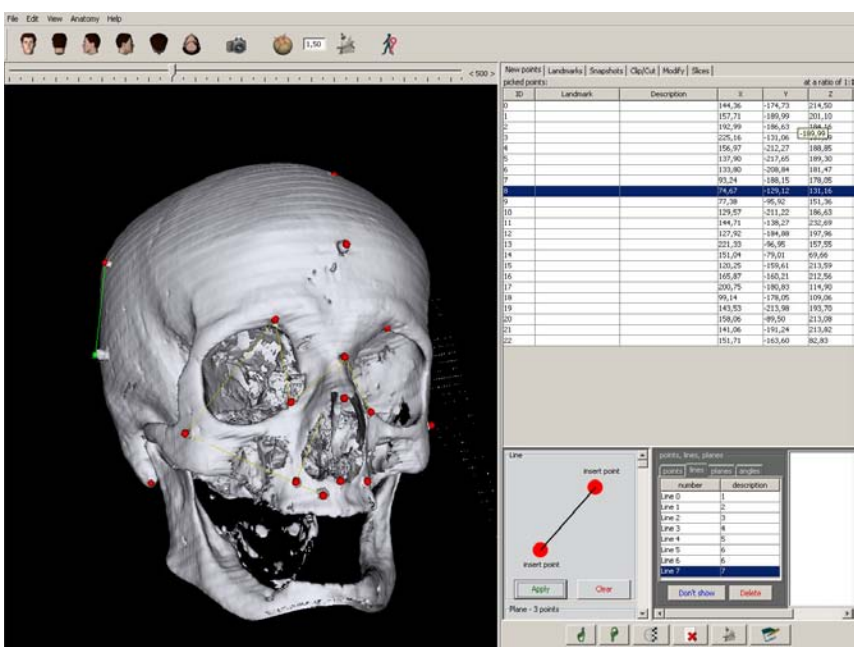

Figure 9. 3D-analysis of a dental plaster cast. Import format is STL. Note the high quality of the laser-scanning process. On the left landmarks, a midsagittal symmetry plane, and distances from cuspids to the reference plane are shown. Right a grid has been placed for quick visual reference.

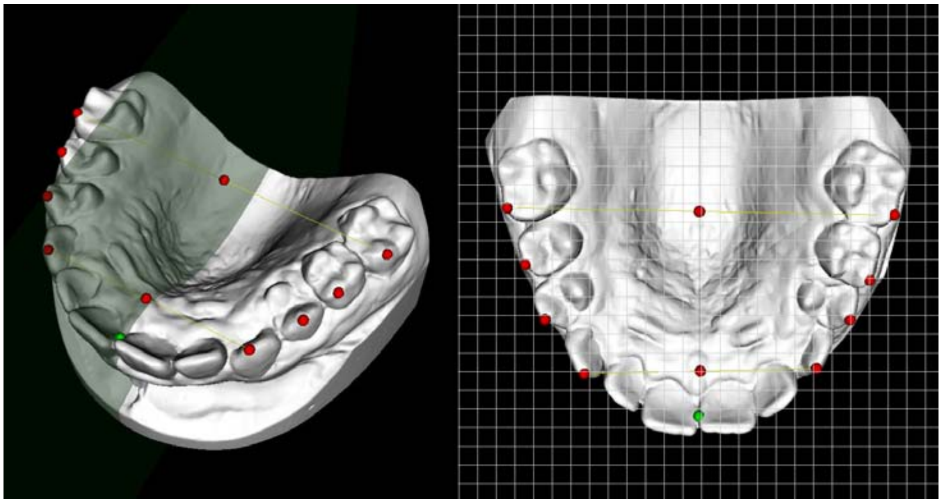

ADDITIONAL FEATURES

Of course the above mentioned features cover only parts of dental image analysis. Measuring areas and volumes is important and will have to be included. That way manual segmentation of regions with little contrast difference is possible, too. Registration procedures are also integrated but will not be discussed within this chapter.

CONCLUSION

With the increase in image data in dentistry and medicine analysis tools become more and more important. Especially the possibility to scan objects three-dimensionally increases the need for powerful instruments. As commercially available software by now lacks special features or has drawbacks in workflow, a solution to overcome these problems is using free software. VTK is presented as a possible solution. It offers a wealth of modules which can be used for almost all tasks in dental image analysis. Thus close cooperation between informatics and medical departments is an ideal way to generate software up to the clinicians need. As these features will be communicated freely, it sounds reasonable to expect that commercial software will be developed, which will incorporate these features.

REFERENCES

Bankman, I. A. (2000). *Handbook of medical imaging*, London: Academic press.

Bookstein, F. L. (1996). Biometrics, biomathematics and the morphometric synthesis. *Bull Math Biol, 58,* 313-65.

Hammond, P. (2008). The use of 3D face shape modelling in dysmorphology. *Arch Dis Child, 92*, 1120-1126.

Hierl, Th., Wollny, G., Schulze, F. P., Scholz, E., Schmidt, J. G., Berti, G., Hendricks, J., & Hemprich, A. (2006). CAD-CAM implants in esthetic and reconstructive craniofacial surgery. *J Comp Information Tech, 14,* 65-70.

Hildebolt, C. F., & Vannier, M. W. (1988). Three-dimensional measurement accuracy of skull surface landmarks. *Am J Phys Anthropol*, *76*, 497-503.

Lele, S., & Richtsmeier, J. T. (2001). *An invariant approach to statistical analysis of shapes.* London: Chapman and Hall-CRC press.

Kragskov, J., Bosch, C., Gyldensted, C., & Sindet-Pedersen, S. (1997). Comparison of the reliability of craniofacial anatomic landmarks based on cephalometric radiographs and three-dimensional CT scans. *Cleft Palate Craniofac J, 34,* 111-116.

Lozanoff, S., & Diewert, V. (1989). A computer graphics program for measuring two- and three-dimensional form changes in developing craniofacial cartilages using finite element methods. *Comp Biomed Res, 22,* 63-82.

Ono, I., Abe, K., Shiotani, S., & Hirayama, Y. (2000). Producing a full-scale model from computed tomographic data with the rapid prototyping technique using the binder jet method: a comparison with the laser lithography method using a dry skull. *J Craniofac Surg, 11,* 527-537.

Remmler, D., Olson, L., Duke, D., Ekstrom, R., Matthews, D., & Ullrich, C. G. (1989). Presurgical finite element analysis from routine computed tomography studies for craniofacial distraction: II. An engineering prediction model for gradual correction of asymmetric skull deformities. *Plast Reconstr Surg, 102,* 1395-1404.

Schroeder, W., Martin, K., & Lorensen, B. (2006). *The visualization toolkit. An object-oriented approach to 3D graphics.* Clifton Park: Kitware

Swennen, G. R., Schutyser, F., Barth, E. L., De Groeve, P., & De Mey, A. (2006). A new method of 3-D cephalometry Part I: the anatomic Cartesian 3-D reference system. *J Craniofac Surg, 17,* 314-325.

Yu, I. H., & Wong, Y. K. (2008). Evaluation of mandibular anatomy related to sagittal split ramus osteotomy using 3-dimensional computed tomography scan images. *Int J Oral Maxillofac Surg, 37,* 521-528.

KEY TERMS

CAD-CAM: Computer-aided design and computer-aided manufacturing. Describes the use of software tools for design activities. Afterwards computer systems are used to control the tools during product manufacturing.

CBT: Cone-beam tomography. Radiologic method to acquire 3D data sets.

Cephalometry: The measurement of the human head. Standard procedure in orthodontics, anthropology, forensic medicine and maxillofacial surgery.

DICOM: Digital imaging and communications in medicine. Standard for the management of medical imaging.

FDM: Fused deposition modelling. A rapid prototyping procedure.

OBJ: An open geometry definition file format

RP: Rapid Prototyping. Automatic construction of physical objects using solid freeform fabrication.

STL: Standard triangulation language or surface tesselation language. Standard language for rapid prototyping and CAD.

VRML: Virtual reality modeling language. A common language to describe 3D objects, widely used in the internet.

Chapter VI
Denoising and Contrast Enhancement in Dental Radiography

N. A. Borghese
University of Milano, Italy

I. Frosio
University of Milano, Italy

ABSTRACT

This chapter shows how large improvement in image quality can be obtained when radiographs are filtered using adequate statistical models. In particular, it shows that impulsive noise, which appears as random patterns of light and dark pixels on raw radiographs, can be efficiently removed. A switching median filter is used to this aim: failed pixels are identified first and then corrected through local median filtering. The critical stage is the correct identification of the failed pixels. We show here that a great improvement can be obtained considering an adequate sensor model and a principled noise distribution, constituted of a mixture of photon counting and impulsive noise with uniform distribution. It is then shown that contrast in cephalometric images can be largely increased using different grey levels stretching for bone and soft tissues. The two tissues are identified through an adequate mixture derived from histogram analysis, composed of two Gaussians and one inverted log-normal. Results show that both soft and bony tissues become clearly visible in the same image under a wider range of conditions. Both filters work in quasi-real time for images larger than five Mega-pixels.

INTRODUCTION

Principled statistical models have been introduced in the imaging field as an effective alternative to classical linear and non-linear filtering. The first efficient statistical algorithms were first introduced in the fields of astrophysics (Lucy 1974, Richardson 1974) and PET imaging (Shepp and

Vardi 1982). In these pioneering works the Poisson nature of the noise was first taken into account explicitly in the filtering stage. This leads to the formulation of a non-linear problem, where the cost function is named Kullback-Liebler divergence or Csizar divergence (Csizar 1991). Its minimization can be carried out efficiently through the *Expectation Maximization* algorithm, that is an iterative approach for estimating the parameters of a statistical model. EM iterates between the computation of an Expectation function, which describes the expected value of the negative log-likelihood over a set of latent variables, and the Maximization of this function, which allows adjusting the values of the parameters (Bishop 2006).

It was soon clear that considering an adequate model of the noise, much better results could be obtained. The price to be paid was a large increase in computational time. This was an obstacle to extend more principled statistical approaches to real problems and only few attempts were made in this direction (Geman and Geman 1984) until the last decade, in which computational power has made feasible this approach.

In this chapter, it is shown how using principled statistical models, two of the major problems in radiographic imaging can be reliably solved: impulsive noise removal, which is a common problem for any digital radiograph, and contrast enhancement in cephalometric radiography, where the anatomical structures of both soft and bone tissue have to be both clearly visible in the same image (Figure 1).

The method described in the first part of this chapter is based on the observation that two are the main noise components on a radiograph. The first one, called impulsive noise, shows up as a random pattern of light and dark pixels, which changes from image to image. It may be attributed to transient failures of the A/D converter or communication over the bus of the sensor. The second noise component is due to the emission statistics of the X-ray photons, which is considered typically Poisson (Webb 1988). Impulsive noise badly affects both readability of images and further processing. Therefore, before providing the radiograph to the clinician, this noise component has to be corrected, often in a transparent way, at the driver level.

The classical approach to impulsive noise removal is based on a two stages procedure: pulses are detected first and then the image is filtered only in correspondence of the failed pixels; a local median filter is used to avoid the modification of any pixel but the failed ones. This approach has been named switching median filtering (Alparone Baronti and Carla 1995).

However, as shown in Figure 2 and Table I, the number of false positives identified by traditional switching median filters (consider for instance the *Rank Conditioned Filter* (RCF) by Alparone Baronti and Carla 1995) is quite large with a consequent significant low-pass filtering effect and loss of details. This has suggested developing better schemes for pulse identification.

In particular, Gaussian models were introduced in (Miller and Thomas 1976) to reliably identify pulses in the image, and the model has been extended to mixture of Gaussians in (Saeed, Rabiee, Kar, Nguyen 1997) to model different signal and noise distributions. However, none of these approaches takes into account the true statistics of the noise.

In the first part of this chapter we show how, taking this into account along with an adequate model of the sensor, a pulse detector can be derived, which outperforms all the existing methods, for digital radiography. The filter was named RaIN, which stands for *Radiographic Impulsive Noise* filter (Frosio and Borghese, 2009). It is based on the definition of an adequate statistical model, constituted of a mixture of impulsive and photon counting noise. The corresponding likelihood function is efficiently maximized through EM.

Mixture models can be used not only to build a reliable pulse detector, but also to describe the statistical distribution of the grey levels inside a single radiograph, and a cephalometric image in

Figure 1. In panel (a), a raw cephalometric image is shown. The same image is shown: in panel (b) after the application of UM (mask size 26 x 26, gain 3); after GC ($\gamma = 0.5$) + UM in panel (c); after HE + UM in panel (d); after STF ($\gamma_{Bone} = 0.25$, $\gamma_{Soft} = 1.25$, TP = 52) + UM in panel (e). The rectangle highlighted in panel (e) is shown in panel (f) at a higher magnification rate (100 x 100 pixels are shown here); notice the presence of impulsive noise in this area.

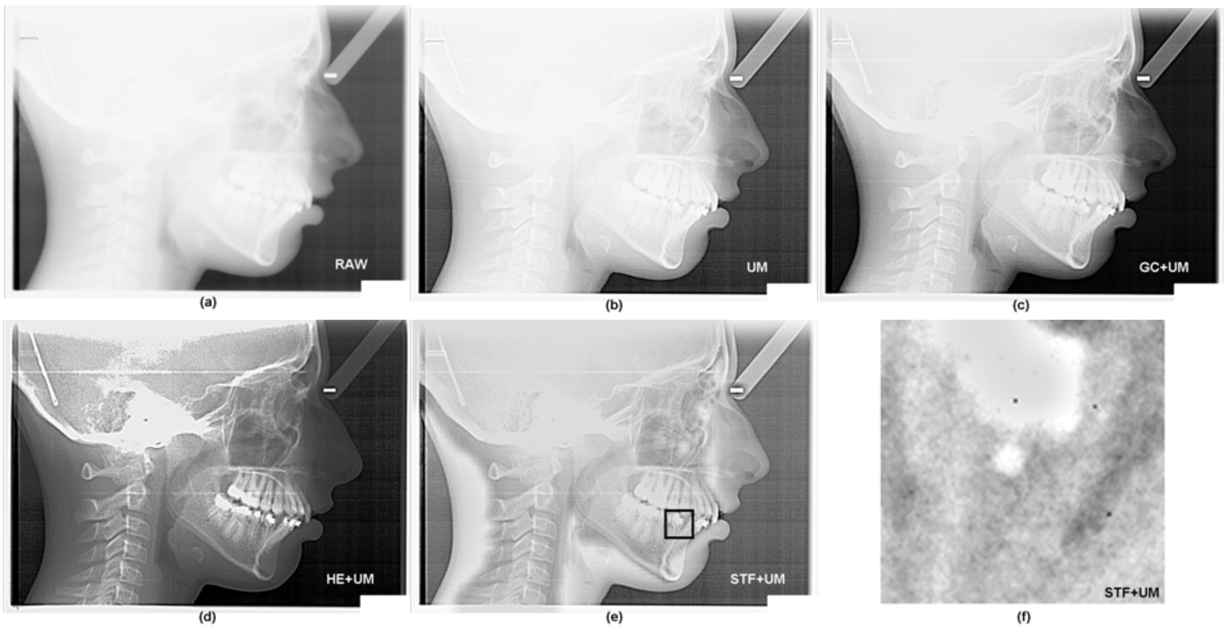

particular. This imaging modality is widely used by dentists, surgeons, and maxillofacial radiologists for diagnosis, surgical planning, and implant evaluation (Moyers 1988). Because of the very different absorption coefficients of the soft and bone tissues, underexposure of bone and overexposure of soft-tissue often occur. A clear visualization of both types of tissue is therefore hardly achieved in the same radiograph and contrast enhancement becomes necessary to increase the visibility of the interesting anatomical structures.

In the second part of this chapter, we show that a mixture of two Gaussians and one Log-normal can be used to reliably cluster such an image into three main classes: background, soft tissue and bone tissue. Background pixels are discarded whereas a large contrast increase for both soft and bone tissues can be achieved by applying a gamma transform with different γ values to the pixels belonging to the two classes. To speed-up processing, a look-up table and multi-resolution processing have been implemented which make the filter operation fully compatible with the interactive visualization rates required by clinical use (Frosio, Ferrigno and Borghese 2006). The filter, named *Soft Tissue Filter* (STF), has proven very effective under for a wide range of images; it outperforms the traditional contrast enhancement algorithms like *Gamma Correction* (GC), *Histogram Equalization* (HE) and *Unsharp Masking* (UM). A typical result is shown in Figure 1.

IMPULSIVE NOISE REMOVAL

Impulsive noise is removed through a switching median filter, whose efficiency is maximum if the failed pixels only are identified. In the following we derive the theory and the methodology, which lead to a very efficient pulse detector.

Sensor and Noise Model

The transfer function of a radiographic sensor can be described by a simple, linear model (Yaffe and Rowlands 1997):

$$g_{n,i} = G \cdot p_{n,i} \tag{1}$$

where G is the sensor gain, $g_{n,i}$ is the noisy grey level and $p_{n,i}$ is the noisy number of photons reaching the i[th] cell of the sensor. More refined models could be used; these may incorporate for instance non-linearity or hystheresis (Jaffe and Rowlands 1997). However, as sensors producers try to maximize linearity, sensors of the last generations can be accurately described by (1).

As $p_{n,i}$ in (1) describes an X-ray photon counting process, it obeys Poisson statistics (Webb 1988). Therefore $g_{n,i}$ can be considered a random variable whose *Probability Density Function* (pdf), p_{PC}, is given by:

$$p_{PC}\left(g_{n,i} \mid g_i\right) = \frac{1}{G} \cdot \left[\left(\frac{g_i}{G}\right)^{\frac{g_{n,i}}{G}} e^{-\frac{g_i}{G}} \right] \Bigg/ \left[\left(\frac{g_{n,i}}{G}\right)! \right] \tag{2}$$

where g_i is the noise free grey level value of the i[th] pixel. We explicitly observe that photon counting noise is characterized by the fact that its variance increases linearly with the grey levels, while in the Gaussian model the variance is constant over the entire grey levels range. Adopting a Gaussian noise model instead of the correct one produces therefore an under/overestimate of the noise power associated to the different grey levels.

On the sensor, impulsive noise adds to photon counting noise. We assume that it destroys any information about the original grey level of the failed pixels. It is also assumed that it can be described by a uniform distribution, but any other pdf could be accommodated into the model. Under these hypotheses, the following mixture model is derived (Frosio and Borghese, 2009):

$$\begin{cases} p\left(g_{n,i} \mid g_i\right) = P_{PC} \cdot p_{PC}\left(g_{n,i} \mid g_i\right) + P_{Imp} \cdot p_{Imp}\left(g_{n,i} \mid g_i\right) \\ 0 \le P_{PC} \le 1, \quad 0 \le P_{Imp} \le 1, \quad P_{PC} + P_{Imp} = 1 \end{cases} \tag{3}$$

where $p_{Imp}(g_{n,i}|g_i)$ is the pdf of the impulsive noise; P_{PC} and P_{Imp} are respectively the probability that a pixel is corrupted by photon counting or impulsive noise.

Other forms of noise could be considered in equation. (3), like thermal, read-out, or quantization noise. However, for a well constructed and calibrated radiographic sensor, these components should be much smaller than photon counting and impulsive noise (Miller and Thomas 1976). We also assume that the noise on each pixel is not correlated with that on adjacent ones, that is noise is white. Since the 40s (Fano G. 1947), it was known that the power of the photon counting noise measured on the sensor is usually smaller than the theoretically expected value (the ratio between the measured and the expected noise power is known as Fano's factor). This fact was attributed to the finite width of the *Point Spread Function* (PSF) of the sensor. Here, we suppose that PSF width is sufficiently small to neglect this effect. Experimental results demonstrate that, at least for the identification of the pixels corrupted by impulsive noise, this assumption is not critical.

In equations (3) the independent unknowns are the rate of photon counting noise, P_{PC}, and the sensor gain, G. The impulsive noise rate, P_{Imp}, is derived from P_{PC} as the two probabilities add to one. The noise free image g_i, is also not known; however such an image can be approximated by filtering the noisy image with a median filter. For the derivation and a more detailed analysis, see (Frosio and Borghese, 2009).

Figure 2. The same portion of radiograph depicted in Fig. 1f is shown here after treatment with: RaIN ($G = 0.1904$, $P_{Imp} = 0.135\%$) (a); RCF 3x3 (d); RCF 13x13 (g); CSAM (j); BEM (m). All these images were filtered with STF+UM before visualization. Panels (b), (e), (h), (k) and (n) show the pulses corrected by each filter in this area. In panels (c), (f), (i), (l) and (o), the pulses corrected on the entire image of Figure 1 are plotted.

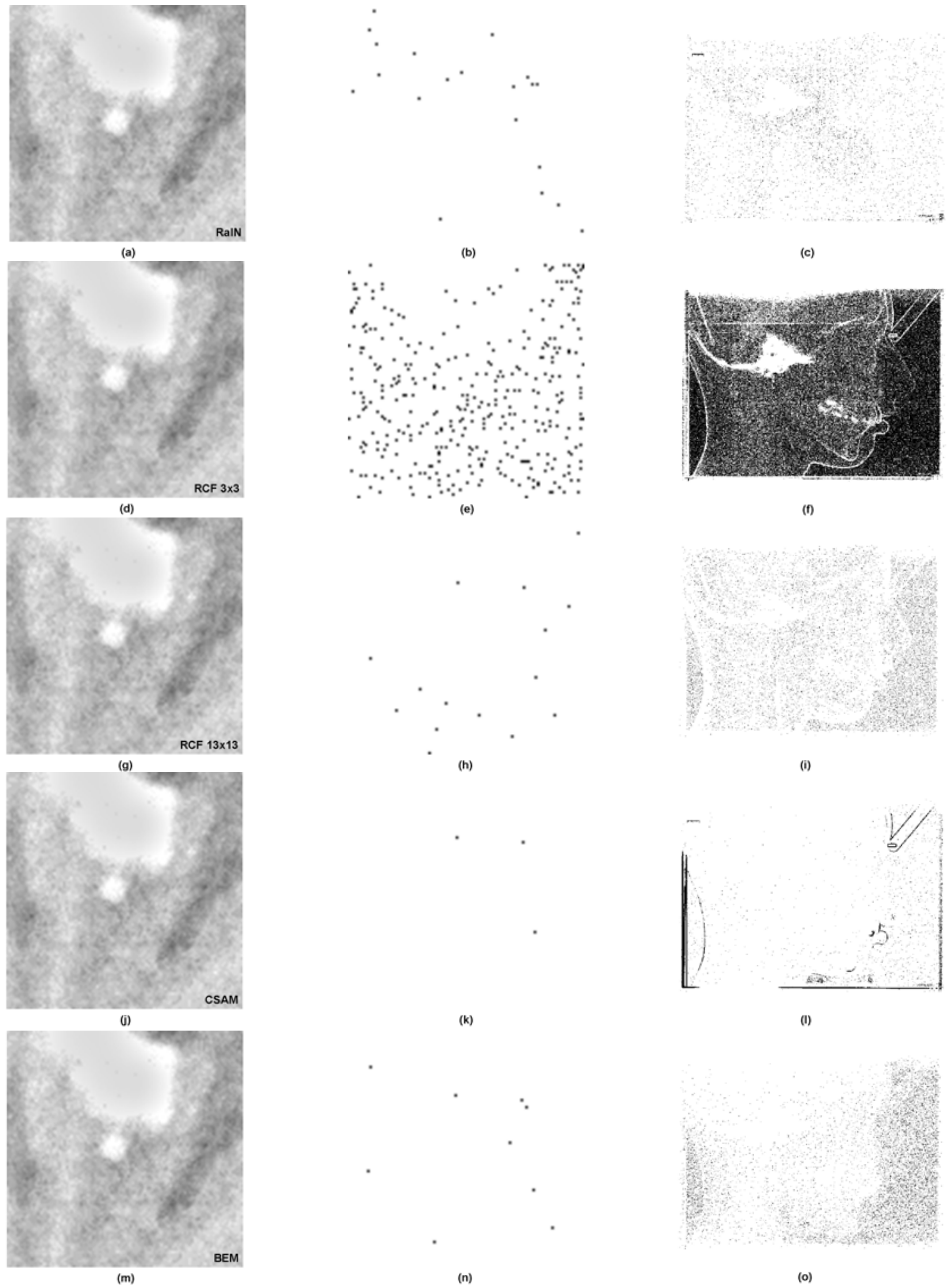

Parameters Estimate

Considering that the grey level values assumed by the pixels are uncorrelated, the likelihood of G and P_{PC}, $L(G, P_{PC})$. is the product of the probabilities of all the measured grey values, each computed through equation (3). The unknown parameters can be estimated by minimizing the negative log likelihood function, $f(G, P_{PC})$ (Weiss 2002), which is shown in Box 1 (Equation 4).

Using the Stirling's approximation for the factorial term, equation (4) becomes continuous and it can be minimized through any standard optimization technique for non linear functions. In particular the EM approach was adopted (Frosio Abati and Borghese 2008) to speed up the optimization for this particular model.

This technique is based on splitting each iteration of the optimization procedure into two sub-steps: expectation and maximization. The rationale is that the maximization would be easier if one could know whether one sample derives from the impulsive or photon counting component; this information is coded in EM introducing a set of latent, unobservable random variables, **z**, which code this information. In the expectation step, the Expectation function is built: at the kth iteration, this can then be written as the expected value of the negative log likelihood with respect to **z**, $Q(\mathbf{z}|G,P_{PC})$. For our model, it can be written as shown in Box 2 (Equation 5) where ^ indicates the estimate of P_{PC}, P_{Imp}, $p_{PC}(g_{n,i}|g_i)$ and $p_{Imp}(g_{n,i}|g_i)$ obtained at the (k-1)th iteration. In the kth Maximization sub-step, $Q(\mathbf{z}|G,P_{PC})$ is maximized by setting its derivatives with respect to G and P_{PC} equal to zero. This leads to the EM updating equations, which, for our model, are:

$$\begin{cases} G = -2 \cdot \dfrac{\displaystyle\sum_{i=1}^{N} \frac{\hat{p}_{PC}\left(g_{n,i} \mid g_i\right) \cdot K_i}{\hat{p}\left(g_{n,i} \mid g_i\right)}}{\displaystyle\sum_{i=1}^{N} \frac{\hat{p}_{PC}\left(g_{n,i} \mid g_i\right)}{\hat{p}\left(g_{n,i} \mid g_i\right)}} \\ P_{PC} = \displaystyle\sum_{i=1}^{N} \frac{\hat{P}_{PC} \cdot \hat{p}_{PC}\left(g_{n,i} \mid g_i\right)}{\hat{p}\left(g_{n,i} \mid g_i\right)} \bigg/ N \end{cases} \qquad (6)$$

Box 1. Equation 4

$$f\left(G, P_{PC}\right) = -\ln\left[L\left(G, P_{PC}\right)\right] = -\sum_{i=1}^{N} \ln\left[p\left(g_{n,i} \mid g_i\right)\right] =$$
$$= -\sum_{i=1}^{n} \ln\left\{P_{PC} \cdot p_{PC}\left(g_{n,i} \mid g_i\right) + P_{\text{Imp}} \cdot p_{Imp}\left(g_{n,i} \mid g_i\right)\right\} =$$
$$= -\sum_{i=1}^{n} \ln\left\{P_{PC} \cdot \frac{1}{G} \cdot \left[\left(\frac{g_i}{G}\right)^{\frac{g_{n,i}}{G}} e^{-\frac{g_i}{G}}\right] \bigg/ \left[\left(\frac{g_{n,i}}{G}\right)!\right] + P_{\text{Imp}} \cdot p_{Imp}\left(g_{n,i} \mid g_i\right)\right\}$$

Box 2. Equation 5

$$Q\left(z \mid G, P_{PC}\right) = \sum_{i=1}^{N}\left\{\frac{\hat{P}_{PC} \cdot \hat{p}_{PC}\left(g_{n,i} \mid g_i\right)}{\hat{p}\left(g_{n,i} \mid g_i\right)} \cdot \ln\left[P_{PC} \cdot p_{PC}\left(g_{n,i} \mid g_i\right)\right] + \ldots\right.$$
$$\left.\ldots + \frac{\hat{P}_{\text{Imp}} \cdot \hat{p}_{\text{Imp}}\left(g_{n,i} \mid g_i\right)}{\hat{p}\left(g_{n,i} \mid g_i\right)} \cdot \ln\left[P_{\text{Imp}} \cdot p_{\text{Imp}}\left(g_{n,i} \mid g_i\right)\right]\right\}$$

where:

$$\begin{cases} \hat{p}_{PC}\left(g_{n,i} \mid g_i\right) = \dfrac{H_i}{\sqrt{G}} e^{K_i/G} \\ K_i = g_{n,i} \cdot \left[\ln\left(g_i\right) - \ln\left(g_{n,i}\right)\right] + g_{n,i} - g_i \\ H_i = \dfrac{1}{\sqrt{2\pi \cdot g_{n,i}}} \end{cases} \quad (7).$$

To reduce the computational burden of (6), K_i and H_i can be computed only once, before starting optimization.

Iterative computation of (6) minimizes (4) (Figure 3). It is assumed that convergence is reached when the estimated parameters change less than 10^{-5} between two consecutive iterations. This requires on average 6 iterations of the EM algorithm, for a total of 0.125s on a Mobile Toshiba Intel Core Duo @ 2 GHz, 2G RAM. For sake of comparison, using standard optimization techniques (for instance steepest descent plus line search), the same accuracy is obtained only after 17 iterations, that require 0.61 seconds on the same machine.

Switching Median Filtering

At the end of the minimization step, all the pixels that satisfy:

$$\left[P_{PC} \cdot p_{PC}\left(g_{n,i} \mid g_i\right)\right] < \left[P_{Imp} \cdot p_{Imp}\left(g_{n,i} \mid g_i\right)\right] \quad (8)$$

are recognized as pulses and substituted with the median value of a 3x3 window centred in those pixels; all the other pixels are left unaltered.

Time required to filter a Cephalometric and a Panoramic radiograph is 2.21s and 1.92s respectively. Time was measured on a Mobile Toshiba Intel Core Duo @2GHz, 2G RAM. To reduce the computational load of each iteration, a limited number of pixels (one over sixteen) has been used to evaluate equation (6). As the image contains a very large number of pixels (>4M), this do not bias the estimate of the parameters, but it does reduce the computational time.

SOFT TISSUE FILTERING

Aim of Soft-tissue filtering is to increase the contrast of the anatomical structures of both soft

Figure 3. The negative log likelihood function, f, is plotted versus the number of iterations, for the RaIN filter in panel (a) and for the STF in panel (b). The steep descent is clearly observable. Panel (c) represents the histogram of the image shown in Figure 1 (black dashed line), matched by the mixture model (red dotted line); the three components of the mixture models, each weighted by its probability, are plotted using a blue, dash-dotted line.

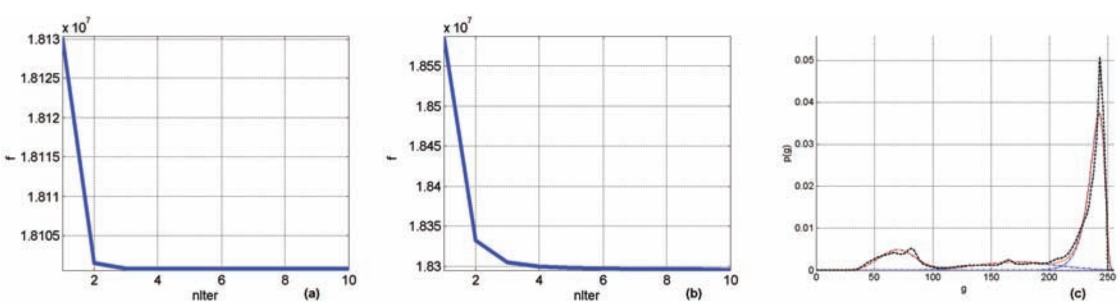

and bone tissues by applying a power law, called gamma correction, with a coefficient adapted to each single pixel. The power function can be written, in its general form, as:

$$g'(i,j) = (N_{GL} - 1)\left[\frac{g(i,j)}{N_{GL} - 1}\right]^{\frac{1}{\gamma(i,j)}} \qquad (9)$$

where *g(i,j)* is the grey level of the pixel *(i,j)* in the original image and *g'(i,j)* is its value transformed by the power function with exponent $\gamma(i,j)$. N_{GL} is the number of grey levels of the original image. We explicitly notice that such transformation leaves unaltered the grey levels 0 and $N_{GL}-1$.

The core of STF is the fitting of the cephalometric image histogram through an adequate mixture model of three components: one for the background, one for the soft tissue and one for the bony tissue. This mixture model allows an efficient and reliable separation of the three image components.

Histogram Description

First, pixels which are not associated to the image formation process are removed. These are the pixels at the border and those associated to possible logotypes. The histogram of the image, *h(g)*, is then computed on all the remaining pixels and then low-pass filtered with a moving average filter (the filter width is seven sampled for the image of Figure 3c).

The shape of *h(g)* has been carefully analyzed, by superimposing the histograms of many images taken with different exposure conditions and different patients' anatomical structures. This has allowed us choosing the most adequate mixture (Frosio, Ferrigno and Borghese 2006). Three main grey-level distributions can be identified in all the cephalometric images. The first one is associated to the background and it presents two small peaks, one close to the other (Figure 3c). This double-peak can be ascribed to the AEC control system, which generates a light band in the right part of the radiographs; however, the difference between these two distributions turns out to be statistically not significant and a single component can be used to model the background. The other two peaks are associated to bone and soft tissue. Soft-tissue is distributed approximately following a Gaussian distribution; bone tissue presents usually an asymmetrical shape, with a sharp descent in the right side of the peak. For this reason an inverted log-normal distribution seems more adequate to represent the bone tissue. We explicitly remark that the position, the width and the probability of the distributions associated to each component largely vary with the patient and with exposure conditions. Nevertheless the three-peaks structure of the histogram can be reliably fitted in all the images.

As can be appreciated in Figure 3c, mixture models can estimate a probability density that has a complex shape such that of the multimodal histogram shown here, using a restricted number of parameters (nine in this case): the mean and standard deviation of the two Gaussian components, two parameters for the inverted log-normal and three mixing parameters (one for each component of the mixture). More formally, we use the following pdf to describe the histogram:

$$p(g) = \sum_{j=1}^{M} p_j(g \mid j) \cdot P(j) \qquad (10)$$

with the constraint the sum of the probabilities of the each of the three components, *P(j)*, adds to one:

$$\sum_{j=1}^{M} P(j) = 1 \qquad 0 \le P(j) \le 1 \qquad (11)$$

The pdf of the first two components is a Gaussian, with mean equal to μ_j and standard deviation equal to σ_j:

$$p_j(g \mid j) = \frac{1}{\sqrt{2\pi}\sigma_j} \cdot \exp\left(-\frac{(g-\mu_j)^2}{2\sigma_j^2}\right) \qquad (12)$$

The inverted log-normal distribution can be written as:

$$p(x)=\frac{1}{\sqrt{2\pi}\cdot\sigma\cdot(N_{GL}-x)}\cdot\exp\left\{-\frac{\left[\ln(N_{GL}-x)-\mu\right]^2}{2\sigma^2}\right\} \quad (13)$$

and it is defined only for $x < N_{GL}$. Its mean and standard deviation are easily derived from the μ and σ parameters (see Frosio, Ferrigno, Borghese 2006, for details).

For all the three pdfs, the following:

$$\int p_j(g\mid j)\,dx=1,\forall j \quad (14)$$

holds. The unknown parameters, that identify the mixture, can be computed maximizing the likelihood of the parameters for the given image. Maximization is carried out more efficiently minimizing the negative log-likelihood, which in this case is:

$$f=-\ln L=-\sum_{j=1}^{N}\ln p_j(g)=-\sum_{j=1}^{N}\ln\left\{p_j(x\mid j)P(j)\right\} \quad (15)$$

where N is the number of pixels. A closed-form solution for computing the parameters in Eq. (15) is not available, so iterative algorithms have to be adopted. The most efficient machinery, also in this case, is represented by EM. Maximum speed up of the Maximization step is achieved considering that, for a digital radiography, the grey level assumed by each pixel belongs to a limited set (typically 256 grey levels for 8 bit images, or 4096 grey levels for 12 bit images). Since different pixels with the same grey level give the same contribution to parameters update, they can be grouped together. Following these observations we can derive the following updating equations:

$$\mu_j^{new}=\frac{\sum_{g=0}^{N_{GL}-1}P^{old}(j\mid g)\cdot g\cdot H_{1F}(g)}{\sum_{g=0}^{N_{GL}-1}P^{old}(j\mid g)\cdot H_{1F}(g)} \quad (16a)$$

$$\left(\sigma_j^{new}\right)^2=\frac{\sum_{g=0}^{N_{GL}-1}P^{old}(j\mid g)\cdot\left(g-\mu_j^{new}\right)^2\cdot H_{1F}(g)}{\sum_{g=0}^{N_{GL}-1}P^{old}(j\mid g)\cdot H_{1F}(g)} \quad (16b)$$

for the two Gaussian components;

$$\mu_j^{new}=\frac{\sum_{g=0}^{N_{GL}-1}P^{old}(j\mid g)\cdot\ln(N_{GL}-g)\cdot H_{1F}(g)}{\sum_{g=0}^{N_{GL}-1}P^{old}(j\mid g)\cdot H_{1F}(g)} \quad (17a)$$

$$\left(\sigma_j^{new}\right)^2=\frac{\sum_{g=0}^{N_{GL}-1}P^{old}(j\mid g)\cdot\left[\ln(N_{GL}-g)-\mu_j^{new}\right]^2\cdot H_{1F}(g)}{\sum_{g=0}^{N_{GL}-1}P^{old}(j\mid g)\cdot H_{1F}(g)} \quad (17b)$$

for the inverted lognormal component, and

$$P(j)^{new}=\frac{1}{N}\sum_{g=0}^{N_{GL}-1}P^{old}(j\mid g)\cdot H_{1F}(g) \quad (18)$$

for the mixing parameters. Their full derivation is reported in (Frosio, Ferrigno, Borghese 2006). We also notice that the term $\sum_{g=0}^{N_{GL}-1}P^{old}(j\mid g)\cdot H_{1F}(g)$ is common to updating equations (16-18), and therefore, it can be computed only once for each iteration.

To obtain a reliable estimate and maximize convergence speed, the parameters are initialized to their mean value, computed on a set of beta-test images. However, initialization is not critical: positioning the three components equally spaced in the grey level domain, and setting the variance of the three components to $N_{GL} / 10$, produces only a slight increase in the optimization time.

Assuming as stopping criterion that the negative log-likelihood does not decrease by less than 10^{-6} % of its value between two consecutive iterations, the final parameters are obtained in about 50 iterations, with a computational time of less than 50ms for the same machine used to compute the parameters of the RaIN filter. The much shorter computational time here, is due to the number of equations that should be evaluated in each iteration: one for each pixel for RaIN (> 4M equations), and one for each grey level for STF (= 256).

After minimization of equation (15), the Gaussian component with the lowest mean value corresponds to background, the one with the intermediate mean value is associated to soft tissue, and the inverted log-normal describes bone tissue.

At this stage the threshold that separates soft from bone structures, $Th_{Bone,}$ can be set so that the following function is minimized in Eq. 19 (see Box 3)that is the probability of wrongly classifying as soft-tissue a pixel belonging to bony tissue and vice-versa. This produces a very robust separation of bone and soft-tissue into two clusters.

Gamma Map and Local Gamma Correction

We can now apply gamma correction (Eq. 9) to each pixel in position *(i.j)*: in particular, we chose two different nominal values for *γ(.)*, one for the soft and one for the bone tissue:

$$\gamma(i,j) = \gamma_{Bone} \quad \text{iff} \quad g(i,j) \le Th_{Bone} \qquad (20a)$$

$$\gamma(i,j) = \gamma_{Soft\_Tissue} \quad \text{iff} \quad g(i,j) > Th_{Bone} \qquad (20b)$$

These values have to be set, having in mind that a γ value lower than one makes bone structures clearly visible, but soft tissue darkens and tends to mix with the background, while values greater than one are used to recover overexposed soft tissue, but they compress the dynamic range in bone regions.

If we apply such a gamma correction, that adopts only two distinct γ values, we would come up with sharp edge artifacts as we do not take into account that the transition between bone and soft tissue is usually larger than one pixel. Therefore, the resulting γ map has to be smoothed to avoid strong artifacts, as shown in Figure 6a.

To smooth the transition a binary γ map is first created, $\Gamma_b(.)$; this map contains either the value γ_{Soft_tissue} or γ_{Bone} according to the pixel classification coming out from equation (19). The final γ map applied to the radiograph, $\Gamma_f(.)$, is obtained by first downsampling $\Gamma_b(.)$, averaging the gamma values inside not overlapping squares of *TP* x *TP* dimension, then applying a moving average, 3x3, low-pass filter to the low resolution γ map, and

Box 3. Equation 19

$$\int_0^{Th_{Bone}} p_{bone}\left(g \mid j=3\right)P\left(j=3\right)dg + \int_{Th_{Bone}}^{N_{GL}} p_{soft\_tissue}\left(g \mid j=2\right)P\left(j=2\right)dg$$

lastly upsampling the filtered map to the original resolution through a bilinear interpolation scheme (Frosio Ferrigno and Borghese 2006).

Lastly, to take advantage of the full grey levels range, linear stretching is applied to the image histogram before local gamma correction. This allows eliminating the small number of pixels with very high grey levels; as a consequence, the image contrast is increased. Gamma correction, is then applied, resulting in the following transformation:

$$g'(i,j) = \begin{cases} (N_{GL}-1)\cdot\left[\dfrac{g(i,j)}{G_{Max}}\right]^{\frac{1}{\Gamma_f(i,j)}}, & g(x,y) < G_{Max} \\ (N_{GL}-1), elsewhere \end{cases} \tag{21}$$

where G_{Max} is the maximum significant grey level, defined as the minimum between the maximum number of grey levels, N_{GL}-1, and the grey level equal to the mean of the inverted log-normal plus two of its standard deviations as shown in Box 4 (Eq. 22).

Maximum speed-up of the algorithm is achieved by implementing Eq. (21) through a *look-up table* (LUT): Γ_f(i,j) is discretized into N_V values, Γ_0, ..., Γ_{N_V-1}. For each grey level, g_p, $0 \le p \le N_{GL}-1$, and for each gamma value, Γ_k, $0 \le k \le N_V-1$, the corrected level, g'_p, is computed through Eq. (21) and stored in the LUT, whose size is therefore N_{GL} x N_V. Each pixel g(i,j) is then corrected by accessing the LUT in position [g(i,j), Γ(i,j)]:

As total processing time is extremely short (less than 1s for an image of 5M pixels, on a Mobile Toshiba Intel Core Duo @2GHz, 2G RAM), interactive use of the filter is possible: the user can select in real time the preferred filter parameters, changing them interactively until a subjectively optimal visualization is achieved.

RESULTS

Impulsive Noise Removal

To evaluate the capability of the RaIN filter to correctly spot the pixels in which impulsive noise is present, we have used a set of 200 simulated images. These have dimension of 512 x 512 pixels at 12bpp and contain geometrical objects of different shapes, grey level and dimensions (cf. Figure 4a and 4b), filtered with a low-pass moving average filter with a large mask (from 33x33 to 49x49 pixels) to obtain low frequency (LF) images, and medium size mask (from 17x17 to 31x31 pixels), to obtain medium frequency (MF) images, whose frequency content is similar to that of a typical panoramic image. Impulsive noise was then added to these images with a rate of 0.1%, 0.2%, 0.5% or 1%.

The efficiency of the filter was evaluated by the *Selectivity* (Se), which describes the rate of failed pixels identified, and the *Positive Predictive Value* (PPV), that is the rate of failed pixels correctly identified with respect to the total number of identified pixels (Fawcett 2003). These indexes are computed as:

$$PPV = \frac{TP}{TP + FP} \tag{23a}$$

$$Se = \frac{TP}{TP + FN} \tag{23b}$$

Box 4. Equation 22

$$\min\left[N_{GL}-1, N_{GL}-1-\exp\left(\mu+\frac{\sigma^2}{2}\right)+\sqrt{\exp(\sigma^2+2\mu)\cdot(\exp(\sigma^2)-1)}\right]$$

Figure 4. Two simulated radiographs from the dataset used for the validation of the RaIN filter. An image with medium frequency content is shown in panel (a); an image with low frequency content is shown in panel (b).

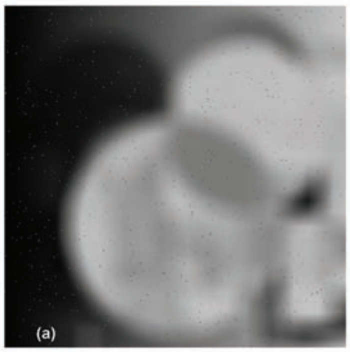

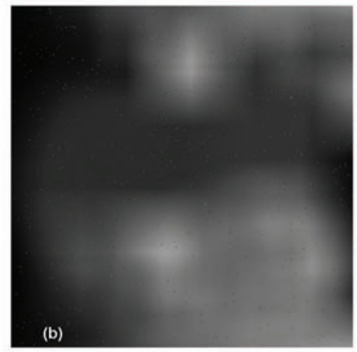

where *TP*, *TN*, *FP* and *FN* indicate the number of true positive/negative and false negative and false positive pixels. A pixel is a *true positive* (or, respectively, *true negative*) if it is correctly classified as a pulse (or, respectively, not pulse). A pixel erroneously classified as a pulse (not a pulse) constitutes a *false positive* (*false negative*).

The values of Se and PPV are reported in Table I. The RaIN filter spots more than 90% for both MF and LF images at all the corruption rates, meaning that, given a corruption rates of 0.1%, less than 27 pixels are left uncorrected in the image (on a total of 262 pulses). Moreover, a qualitative analysis of the undetected pulses reveals that these are compatible with the statistics of photon counting noise: their classification as pulses can be questioned, since even a human observer could not spot such pixels.

Results were compared with standard switching median filters, in particular with RCF (Alparone, Baronti, Carla 1995). A 3x3 and a 13x13 window was considered. RCF 3x3 achieves a slightly higher Se, but its PPV is extremely low confirming the poor ability of this filter to discriminate the failed pixels from the correct ones. In the best case (impulsive noise rate of 1%), PPV is equal to 11.45%: 19,004 pixels are erroneously spotted, leading to a potentially unacceptable image modification. Increasing the filter width to 13x13, PPV increases (it raises from 2.09% to 77.04% for LF images corrupted by impulsive noise of 0.2%), at the expense of a decrease in the ability to locate the failed pixels (Se drops from 95.41% to 69.61% on the same data).

RaIN produces superior results also when compared with other advanced filter, either statistically based like the BEM filter (Saeed, Rabiee, Kar and Nguyen, 1997) or based on refined deterministic image processing like the CSAM filter (Pok, Liu and Nair 2003). A more detailed account of quantitative results can be found in (Frosio and Borghese, 2009).

We have then evaluated the ability of the RaIN filter to spot failed pixels on real radiographs on the field. To this aim we have considered a set of 16 cephalometric images, 2437x1561 pixels at 12bpp, and 10 panoramic images, 1310x2534 pixels, at 12 bpp, acquired using the Orthoralix 9200 DDE™ System; the impulsive noise corruption rate did not exceed 0.2% for this apparatus. We have increased the contrast in the images, according to the clinical practice, by applying a gamma transform with $\gamma = 0.5$ followed by UM (Polesel, V., Ramponi, G., Mathews, V. J. 2000) with a mask size of 3x3 and a gain of 3. As shown in Figure 1f, pulses are clearly visible on these

Table 1. Selectivity and Positive Predictive Value measured for the images of the simulated dataset, for different pulse corruption rates, for the different filters analyzed.

		Se			
	Pulses%	**0.1%**	**0.2%**	**0.5%**	**1%**
RCF 3x3	**MF images**	95.43%±1.59%	95.75%±0.83%	95.58%±0.49%	93.74%±0.31%
	LF images	96.70%±0.82%	96.29%±1.22%	95.41%±0.80%	94.32%±0.57%
RCF 13x13	**MF images**	80.11%±2.24%	77.45%±1.42%	66.67%±2.11%	54.40%±1.57%
	LF images	83.63%±1.66%	79.87%±1.94%	69.61%±1.93%	57.18%±1.88%
CSAM	**MF images**	85.98%±1.19%	86.15%±1.92%	86.38%±1.81%	85.57%±1.02%
	LF images	88.20%±1.61%	87.12%±2.32%	87.22%±1.01%	87.28%±1.30%
BEM	**MF images**	89.09%±0.93%	88.74%±2.06%	88.26%±1.41%	85.77%±1.20%
	LF images	90.06%±2.30%	89.64%±1.69%	89.10%±1.08%	87.21%±0.68%
RaIN	**MF images**	94.08%±1.44%	94.28%±1.70%	94.80%±0.96%	95.05%±0.47%
	LF images	94.27%±1.06%	93.96%±1.58%	94.52%±0.68%	94.70%±0.70%

		PPV			
	Pulses%	**0.1%**	**0.2%**	**0.5%**	**1%**
RCF 3x3	**MF images**	1.43%±0.23%	2.51%±0.48%	6.84%±2.32%	11.45%±1.34%
	LF images	1.00%±0.11%	2.09%±0.33%	5.12%±0.63%	8.85%±0.94%
RCF 13x13	**MF images**	49.61%±9.05%	64.10%±12.29%	85.47%±5.01%	92.18%±2.61%
	LF images	54.74%±10.37%	77.04%±6.65%	89.69%±3.71%	94.17%±2.64%
CSAM	**MF images**	68.15%±22.86%	78.20%±22.19%	86.38%±13.12%	94.24%±6.43%
	LF images	41.52%±24.77%	57.63%±26.63%	81.38%±12.67%	87.65%±11.35%
BEM	**MF images**	65.72%±9.62%	78.27%±5.36%	91.15%±2.95%	96.54%±0.92%
	LF images	55.69%±4.49%	74.01%±4.55%	89.66%±2.23%	94.93%±1.12%
RaIN	**MF images**	97.55%±0.99%	97.61%±0.70%	98.05%±0.37%	98.32%±0.34%
	LF images	89.06%±16.70%	92.41%±9.39%	93.98%±7.74%	95.53%±4.53%

images. All the radiographs were processed by the RCF 3x3, RCF 13x13, CSAM, BEM and the RaIN filter, thus producing a total of 156 images, including the original un-filtered images; these images constituted the set used to asses the filtering results.

Evaluation was carried out by fifteen subjects expert to the field: seven dental surgeons operating in the day surgery unit of the University of Milano dental hospital, with at least three years of clinical experience and eight high level technicians employed in research and development in the dental radiographic field, with at least five years of experience. They were instructed to evaluate the presence of failed pixels in the images with a score between 0 and 3. 0 had to be assigned to images with no pulses, 1 if no more than two failed pixels were identified in no more than two analyzed areas, 2 if many pulses (> 2 pulses) were visible in a few areas of the image (≤ 2) or few pulses (≤ 2 pulses) were visible in several areas of the image (> 2). A score of 3 was assigned when more than 2 pulses were visible in many areas of the image. Each subject evaluated a subset of fifteen images, one at a time, randomly chosen in the images data set; he had unlimited amount of time and he was free to navigate it, zooming at 8x rate to better analyze the image locally. The score distribution is reported for each analyzed filter in Figure 5.

Figure 5. Score attributed to the images filtered with RaIN, BEM, CSAM, RCF 13x13 and RCF 3x3

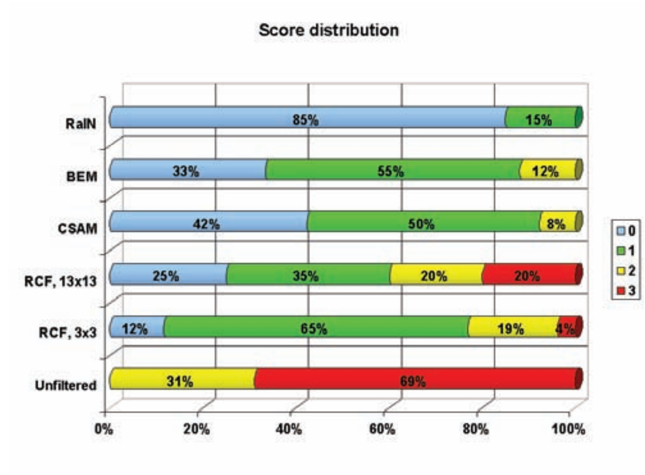

All the original radiographs received a score higher than or equal to 2: despite the low corruption rate, impulsive noise was clearly visible on them. On the other extreme, almost no pulse was spotted in the images processed with the RaIN filter, which obtains an average score of 0.19. RaIN filter corrects overall only 0.14% pixels, which is compatible with the nominal corruption rate of 0.2% of these images.

RCF 3x3 corrects as many as 4.73% of the pixels of a radiograph, on the average. Nevertheless it was not able to clear efficiently impulsive noise as it leaves a significant amount of failed pixels undetected (mean score of 1.1). RCF 13x13 corrects a lower number of pixels (0.23% of the total number of pixels), but it also leaves an even higher number of failed pixels undetected (mean score of 1.5). *CSAM* and *BEM* filters have similar performances: they produce an average score of 0.71 correcting, respectively, 1.67% and 0.80% pixels on the average.

Soft Tissue Filtering

The filter was extensively tested in the clinical field. The feedback obtained from dentists and maxillofacial surgeons during clinical trials was very positive. All of them observed a large increase in the readability of the radiographs filtered using the standard parameters. Moreover, they appreciated being able to modify the filter parameters interactively so as to obtain the best subjective visualization results.

The generalized large improvement in the visibility of both soft tissue and bony anatomical structures (cf. Figure 1) was achieved under a wide range of exposures, including underexposed (cf. Figure 6c) and overexposed radiographs (cf. Figure 6e). When underexposure occurs, the grey level range of the bony pixels is compressed and structures become poorly visible; on the other hand, in overexposed images, soft tissue tends to merge with the background. STF is able to improve the visibility of image details in both bone and soft tissues, in both types of images (cf. Figures 6d and 6f).

The default values used for the three filter parameters, γ_{Soft_Tissue}, γ_{Bone} and TP, are respectively $\gamma_{Bone} = 0.25$, $\gamma_{Soft\_Tissue} = 1.5$, and $TP = N_{ROW} / 36$, where N_{ROW} is the number of row of the radiograph. These parameters allow good results under a wide variety of exposures and are used to

Figure 6. The same radiograph shown in Figure 1 is shown in panel (a) after the application of STF when no downsampling and filtering is applied to the gamma map (γBone = 0.25, γSoft = 1.5, TP = 0). Notice the brisk transition between bony and soft tissue. The same image, when a parameter setting different from the standard one is adopted, is shown in panel (b): γBone = 0.15, γSoft = 2, TP = 104. A raw underexposed radiograph is shown in panel (c) and in panel (d) after the application of STF with γBone = 0.15, γSoft = 1.2, TP = 104. A raw, slightly overexposed radiograph is shown in panel (e) and in panel (f) after the application of STF with (γBone = 0.5, γSoft = 2, TP = 52). Notice the clear visibility of both soft-tissue and bone structures for the filtered images. UM was applied after STF to images in panels a, b, d, and f.

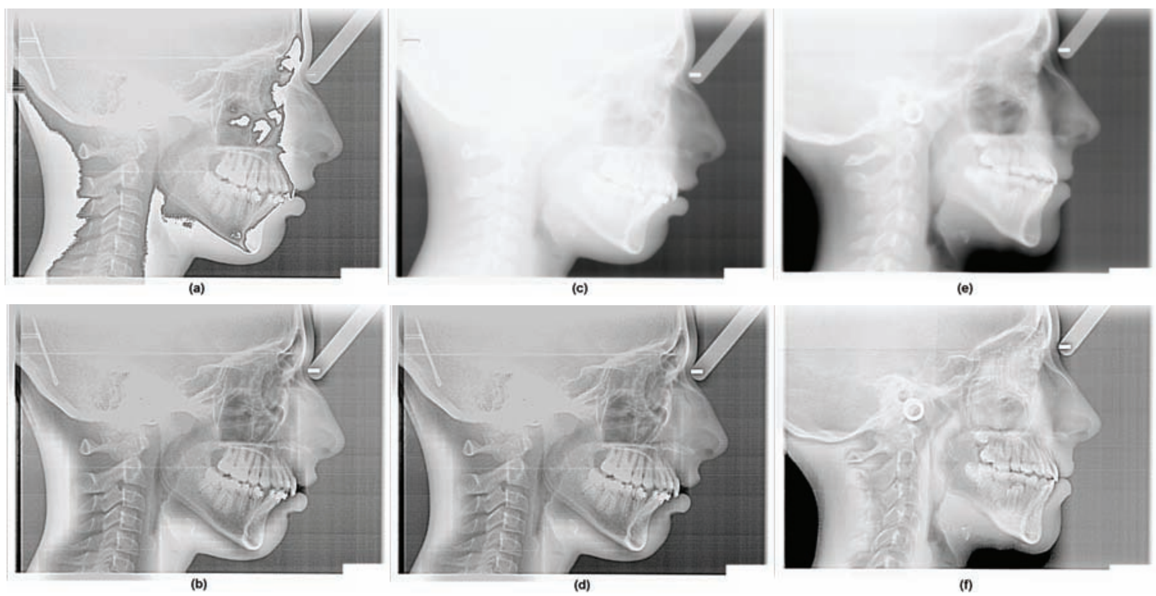

produce image in Figure 1e. However, thanks to STF processing speed, the clinician can modify the parameters interactively until he can find his best image quality, subjectively (cf. 6b). Moreover, $\gamma_{Bone} < 0.25$ and $\gamma_{Soft\_Tissue} > 1.5$, allow recovering image highly under or overexposed (Figures 6d and 6f).

Besides extensive qualitative evaluation, quantitative evaluations has been carried out. To this aim eighteen lateral 1871 x 2606 pixels cephalometric images, acquired with Orthoralix 9200 DDE®, have been used. A large debate is active on the most adequate metric to evaluate image quality. In our case, as the aim is to make the elements of two clusters clearly visible in the image without introducing any spatial artifact, two indexes seem the most adequate. The first one is the local contrast of the anatomical structures, which is a critical parameter associated to the ability to identify small anatomical details (Webb 1994). Local contrast was evaluated, selecting a window of 80 x 80 pixels, centered on the left-most molar in the radiograph, and measuring the following quantity:

$$C = \frac{o - b}{b} \qquad (24)$$

where o and b are defined as the 75th and 25th percentiles, respectively, of the histogram of the grey levels inside the window. The window was positioned manually on each image. The contrast enhancement effect was quantified dividing the local contrast measured in the filtered image by that measured in the original one. The second index is the Shannon entropy (Dhawan, Buelloni, and Gordon 1986) , which is defined as:

$$H = -\sum_{g=0}^{N_{GL}-1} p(g)\log_2(p(g)) \qquad (25)$$

where *p(g)* is the probability of grey level *g* occurring in the image. In order to compare the processing effect on a population of images with widely divergent H values, normalized entropy was adopted. This is defined as the ratio of the entropy of the filtered image to that of the original image. It quantifies the decrease/increase of the information contained in the filtered image with respect to the original one, taking in account only the distribution of the grey levels.

Both HE and GC reduce sensibly the entropy to 81% and 87% respectively, showing that they both reduce the information content in the image, as it is evident observing the limited grey level dynamics in Figures 1c and 1d. The local contrast is greatly increased for both filters to 1468% and 430% respectively. However, it should be remarked that this contrast increase is paid with a large loss of resolution in the grey levels dynamics, which, overall, produces images of less quality as features are outlined more poorly.

UM, on the contrary, increases both the entropy (to 104%) and the local contrast (116% of the original contrast). This effect can be ascribed to the edge enhancement introduced by the high pass filter used by UM. However, UM produces little increase in contrast in those regions where the grey levels are most uniform (for instance, the skull area) as in these regions the gradient is small and therefore high pass filtering has a small effect. However, these are the regions where the need of contrast increase is maximum as the visibility threshold increases with the grey level (Webb 1994).

The entropy of a radiograph treated with STF remains almost constant (98% of the initial entropy), while the contrast is raised more than four times, by 404% of the original contrast, on the average. These two characteristics largely improve the visibility of the anatomical features of both the bone and soft tissue. The contrast enhancement effect achieved by STF is therefore obtained through an optimal coding of the image grey levels, which does not imply any information loss.

It should be remarked that STF is equivalent to a local non-linear stretching of the grey-levels dynamic range: the dynamic range of both soft and bony tissue is enlarged, leading to increased visibility of anatomical structures of the two tissues. As a consequence, in the filtered images, bone and soft tissue may share some grey levels, as can be observed in Figures 1e and 6. Although this may be critical for some applications, such as analyzing bone density or investigating tumors, it holds little importance when the clinician has to identify anatomical features precisely, locate alterations in the patient's anatomy or visualize post-operative aesthetic modifications.

CONCLUSION

Statistical models are becoming crucial to the development of effective noise reduction and quality improvement. This is particularly true in radiographic imaging, where the often implicitly adopted Gaussian noise model, is a poor approximation of the noise statistics. We have shown here that using more principled models, better results can be obtained in a reasonably amount of processing time.

REFERENCES

Alparone T., Baronti S., & Carla R. (1995). Two-dimensional rank-conditioned median filter. *IEEE Trans. Circuits Syst. II*, *42*(2), 130-132.

Bishop C. (2006). *Pattern recognition and machine learning.* Springer Verlag.

Csiszar I., (1991). Why least squares and maximum entropy? An axiomatic approach to inference for linear inverse problems. *Annals of Statistics, 19,* 2032-66.

Dhawan, A. P., Buelloni, G., & Gordon, R. (1986). Enhancement of mammographic features by optimal adaptive neighborhood image processing. *IEEE Trans. Med. Imag., MI-5*, 8–15.

Fano, U. (1947). Ionization yield of radiations. II. The fluctuations of the number of ions. *Phys. Rev., 72,* 26-29.

Fawcett, T. (2003). *ROC graphs: Notes and practical considerations for data mining researchers.* Tech report HPL-2003-4. HP Laboratories, Palo Alto, CA.

Frosio I., Abati S., & Borghese N. A. (2008) An expectation maximization approach to impulsive noise removal in digital radiography. *Int. J. Computer Assisted Radiology and Surgery.*

Frosio I., & Borghese N. A. (2008). Statistical based impulsive noise removal in digital radiography. *IEEE Trans. on Medical Imaging, 28*(1), 3-16.

Frosio I., Ferrigno G., & Borghese N. A. (2006). Enhancing digital cephalic radiography with mixture models and local gamma correction. *IEEE Trans. Medical Imaging, 25*(1), 113-121.

Garnett, G., Huegerich, T., Chui, C., & He, W. (2005), A universal noise removal algorithm with an impulse detector, *IEEE Trans. Image Processing, 14*(11), 1747-1754.

Geman, S., & Geman, D. (1984). Stochastic relaxation, Gibbs distributions, and the Bayesian restoration of images. *IEEE Trans. Patt. Anal. And Mach. Intell., 6*(6), 721-741.

Gonzalez, W. (2008). *Digital image processing.* 3rd edition. Prentice Hall.

Jaffe, M. J., & Rowlands, J. A. (1997). X-ray detectors for digital radiography. *Phys. Med. Biol., 42,* 1–39.

Lucy, L. (1974). An iterative technique for the rectification of observed distribution. *Astron. J., 79,* 745-754.

Miller, J. H., & Thomas, J. B. (1976). The detection of signals in impulsive noise modeled as a mixture process. *IEEE Trans. on Communications*, (pp. 560-3).

Moyers, R. E. (1988). *Handbook of orthodontics.* Chicago: Year Book Medical Publisher.

Pok, G., Liu J. C., & Nair A. S. (2003). Selective removal of impulsive noise based on homogeneity level information. *IEEE Trans. Image Processing, 12*(1), 85-92.

Polesel, V., Ramponi, G., & Mathews V. J. (2000). Image enhancement via adaptive unsharp masking. *IEEE Trans. Image Processing, 9*(3), 505-510.

Richardson W. H. (1972). Bayesian-based iterative method of image restoration. *J. Opt. Soc. Amer., 62,* 55-59

Saeed, M., Rabiee, H. R., Kar, W. C., & Nguyen, T. Q. (1997). Bayesian restoration of noisy images with the EM algorithm. In *Proceedings of the ICIP 1997,* (pp. 322-5).

Shepp, L. A., & Vardi, Y. (1982). Maximum likelihood reconstruction for emission tomography. *IEEE Trans. Med. Imag., 1,* 113-122.

Webb, S. (1988). *The Physics of medical imaging.* Adam Hilger, Bristol-Philadelphia-New York, (pp. 29-32, 571-576).

Weiss, N. A. (2002). *Introductory statistics.* Addison Wesley, sixth edition.

KEY TERMS

Contrast Enhancement: Contrast enhancement is a procedure aimed to increase the contrast of an image, improving the visibility of small details in the image.

Expectation Maximization: This is a very efficient, iterative, optimization procedure specifically tailored for the estimate of the parameters of a statistical model.

Gamma Transform or Correction: Gamma transform is a parametric, monotone grey level transformation expressed as a power function. It allows the contrast for a limited set of grey values to be increased, at the expense of decreasing it for the others. For values of the γ parameter higher or smaller than 1, the contrast enhancement effect is obtained for the darker / brighter grey levels.

Impulsive Noise: Impulsive noise is described by a random value with a variance much higher than that of the original signal. In imaging, it can be observed as a random pattern of very dark and bright pixels. The number of failed pixels in digital radiography is usually small (<1%).

Mixture Model: Mixture models are linear combination of probability density functions that allow describing complex distributions of random variables using a limited set of parameters.

Poisson Noise: Poisson noise is associated to any photon counting process like that occurring in digital imaging. It follows the Poisson statistics. In this model the noise variance increases linearly with the average number of photons.

Photon Counting Noise: In this chapter, photon counting noise refers to the noise on a grey level radiograph. Its variance increases linearly with the average grey level. The formulation is slightly different from that of a Poisson distribution.

Soft Tissue Filter: “Soft Tissue Filter” refers to a wide class of image processing algorithms, whose aim is to increase the contrast of the anatomical structures of both the soft and bone tissue.

Chapter VII
3D Reconstructions from Few Projections in Oral Radiology

Ralf K. W. Schulze
Klinikum der Johannes Gutenberg-Universität, Mainz, Germany

ABSTRACT

Established techniques for three-dimensional radiographic reconstruction such as computed tomography (CT) or, more recently cone beam computed tomography (CBCT) require an extensive set of measurements/projections from all around an object under study. The x-ray dose for the patient is rather high. Cutting down the number of projections drastically yields a mathematically challenging reconstruction problem. Few-view 3D reconstruction techniques commonly known as "tomosynthetic reconstructions" have gained increasing interest with recent advances in detector and information technology.

INTRODUCTION

Three-dimensional (3D) imagery has been gaining ever increasing attention during the last decade. Since human beings are familiar with a 3D world surrounding them, representing image information also in 3D is a natural desire. This holds true particularly in medical radiography, where more or less complex structures are visualized for the purpose of diagnosis or sophisticated treatment procedures. Established techniques for radiographic 3D reconstruction such as Computed Tomography (CT) including its most recent extension, Cone Beam CT (CBCT) are based on an extensive set of projections from all around the object. Also, the imaging geometry of each and every projection has to be precisely known a priori, requiring large-scale scanners and sophisticated hardware technology. Obviously, since the x-ray dose is directly related to the number of projections, techniques using multiple projections administers a rather high dose to the patient. In Germany the increasing patient dose over the last decade is attributed to the increasing number of CTs (Bundesamt für Strahlenschutz, 2004). Dose considerations as well as other practical aspects such as flexibility, costs or availability have been the driving forces for the development of alternative techniques. If one drastically cuts down the number of input projections, then obviously the dose will also be reduced considerably. Such an approach, however, poses major challenges for the 3D reconstruction process, since the lack of input information renders the reconstruction problem at least instable. The reconstruction problem itself is a classical "inverse problem", where the results of actual observations (i.e. the projection data) are used to infer the values or the parameters characterizing the system under investigation. This chapter will summarize the most important techniques to tackle the very challenging problem of few-view 3D reconstruction. To begin with, we shall briefly resume the physical principles of radiographic image formation and the mathematical background of established 3D imaging techniques, such as CT.

RADIOGRAPHIC PROJECTION AND 3D RECONSTRUCTION FROM MULTIPLE PROJECTIONS

The projection value measured by any x-ray sensitive receptor follows the well-known Lambert-Beer law:

$$I_1 = I_o e^{-\int \mu(x,y,z)dl} \qquad (1)$$

with I_1 defining the intensity behind an absorber and I_0 the input intensity, respectively. The parameters μ and d denote the mass absorption coefficient and the thickness of the absorber. We aim to estimate μ as shade of gray at discrete instances to obtain a reliable representation of the object.

In 1917, the Austrian mathematician Johann Radon discovered that the two-dimensional (2D) distribution of properties of an object may be obtained from an *infinite number* of line integrals sampled through the object. Mathematically, a function $f(x,y)$ can be completely described by the complete number of straght line integrals through the support of $f(x,y)$, i.e.

$$f(x,y) = \int_{-\infty}^{+\infty} f\left[x(l), y(l)\right] dl \qquad (2)$$

The famous method predominantly applied for image reconstructions in CT-scanners uses this formula in a process termed "Filtered Backprojection (FBP)". Assuming parallel x-rays, the relationship between the projection data (P) and the object are given by:

$$P(\Theta,t) = \int_{-\infty}^{+\infty}\int_{-\infty}^{+\infty} f(x,y)\,\delta\,(x\cos\Theta + y\sin\Theta - t)\,dxdy \qquad (3)$$

where Θ denotes the projection angle and t the detector position in the beam (Fig. 1). Diracs delta function δ is required to define the line interval. The CT image reconstruction problem is to compute $f(x,y)$ given $P(\Theta,t)$. Note, that the term "$x\cos\Theta + y\sin\Theta - t$" in equation (3)" represents a line equation (e.g. green "ray-line" in Fig. 1), (Beyerer & Leon, 2002) the sum of which the integrals are sampled. In other words, the measured data on the image receptor represent the integrals over a finite number of lines connecting the x-ray source with the detector cells.

We can easily see from eqs. (2) and (3), that the inversion of the Radon transform, i.e. the inverse Radon transform, which is a standard procedure in CT, in theory requires an infinite number of line integrals (photon counts) to be measured. A good approximation, however may also be obtained

*Figure 1. An x-ray (green line) traverses an object located in the **x,y**-coordinate system at the position **t** of the detector (blue line) in the **Θ, t**-coordinate system. The intensity profile (gray plot) acquired by parallel x- rays is displayed adjacent to the detector line.*

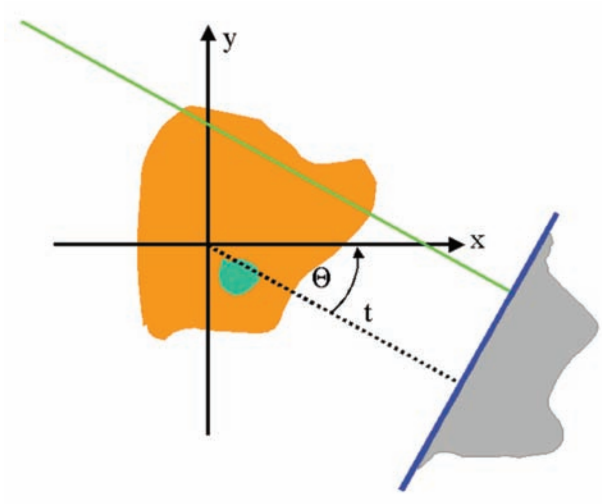

from a sufficient number of measurements. Also, eqs. (2) and (3) imply that the directions of the line integrals should cover the entire range. Both requirements give rise to a rather high radiation dose for the patient. Hence, methods requiring less input information, i.e. less radiation dose, may provide a useful alternative for some diagnostic tasks. This, however, violates the mathematical foundation stated above. Consequently, we are looking for methods requiring by far less input information, i.e. only few radiographic projections, to obtain a reliable estimate of the object under investigation. In addition, the projections may not come from all around the object, rather the angle they suspend is limited (i.e. $< \pi$). This combination yields a mathematically "ill-posed" inverse problem. Methods had to be found allowing for a reasonably accurate estimation of the 3D object, when the input information, i.e. the projection data alone are not sufficient to solve the problem.

In the remainder of this chapter we will briefly discuss the most important techniques developed to solve this ill-posed inverse problem which we will further refer to as "few-view limited-angle" reconstruction.

HISTORICAL BACKGROUND

The first researcher introducing an approach to recover depth information from few projections acquired at different geometries was Ziedses des Plantes in 1932 (Ziedses, 1932). The so called "Planigraphie" was later refined by Miller (Miller, McCurry, & Hruska, 1971) and Grant (Grant, 1972), who also coined the term "tomosynthesis". The latter today is often used as a general term for techniques basing on few-view radiographic 3D reconstruction (for an in depth overview see (Dobbins & Godfrey, 2003)). Before the introduction of fast and highly efficient digital radiographic detectors in the late 1990s, a widespread employment of tomosynthesis was impeded by the lengthy and cumbersome procedure required in clinical applications. Novel acquisition technol-

Figure 2. Projection scenarios ranging from dense source positions (black spots) distributed in a full circle (A) around the object (gray circle) to sparse arbitrarily orientated positions (F). The complexity of the reconstruction problem increases from A to F. The detector positions are assumed opposite the respective source positions.

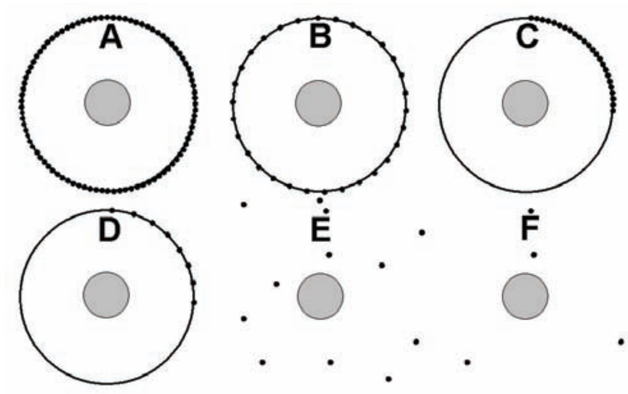

ogy, however, resulted in a variety of research approaches to establish tomosynthesis as a "viable clinical adjunct to CT" (Dobbins et al., 2003). Indeed, the introduction of digital image receptors gave rise to a boost of interest in the technology. Some authors extend and generalize the term "tomosynthesis" for all techniques attempting to reconstruct 3D-information from few projections which may or may not be distributed over a narrow angle. Tomosynthetic techniques have successfully been investigated in a variety of medical apllications such as a angiography (Dorsaz, Dorsaz, & Doriot, 2000; Fencil & Metz, 1990; Hoffmann et al., 1997; Hoffmann, Wahle, Pellot-Barakat, Sklansky, & Sonka, 2000; Metz & Fencil, 1989), hand imaging (Duryea, Dobbins, & Lynch, 2003), pulmonary imaging (Sone et al., 1995), mammography (Suryanarayanan et al., 2000; Wu, Moore, Rafferty, & Kopans, 2004; Zhang et al., 2006; Zhang et al., 2007) and dental imaging (Groenhuis, Webber, & Ruttimann, 1983; Kolehmainen et al., 2003; Niinimäki, Siltanen, & Kolehmainen, 2007; Siltanen et al., 2003; Webber, Horton, Tyndall, & Ludlow, 1997). In the following we will have a look on the methods which have been developed to solve the tomosynthetic reconstruction problem.

RECONSTRUCTION METHODS

The Few-View Limited-Angle Inverse Problem

From Figure 2 we get a good impression, what the nature of the problem is like. Obviously, we aim to solve the problem in instances, where projections of the object are not available from all around the object, and, in addition, are only limited in numbers (Fig. 2, C to F). In the worst and most general case, the projections may be taken in an arbitrary source motion (Fig. 2, E and F). It is well known that in all settings except of the one depicted in Fig.1A, FBP does not work properly to solve the reconstruction problem (see, e.g. (Mueller, Yagel, & Wheller, 1999; Siltanen et al., 2003)).

In tomosynthesis, typically relatively few projections are obtained from a limited angle, often from a circular array of source positions above the object. Hence, tomosynthetic reconstruction cannot rely on an inverse Radon transform. Instead, the classical reconstruction algorithm in tomosynthesis is based on a simple shift-and-add procedure. If only negligible magnification differences between projections occur, slices parallel to the detector surface can be reliably reconstructed by simply shifting the object images in relation to their distance to the detector and subsequently adding their intensities. Thereby, object images are added when appropriately shifted into focus, while at the same time images of out-of-plane structures are blurred. For an instructive illustration the reader is referred to (Dobbins et al., 2003; Webber et al., 1997). The disadvantage of this rather simple backprojection technique is, that it requires the source to be traversed within a plane parallel to the (stationary) detector plane (Wu et al., 2004). To accomplish for less constrained acquisition geometries, Webber and colleagues introduced Tuned Aperture Computed Tomography (TACT) in the 1990ies (Webber et al., 1997), which enables determination of the acquisition geometry from *a posteriori* by using fiducial markers. While shift-and-add reconstructions are simple and require little computational effort, their quality suffers from tomographic blur from structures outside the plane of interest. Deblurring procedures have been established implementing either spatial frequency filtering or algorithms more exactly correcting for blur by solving for blurring functions on planes adjacent to the one under reconstruction (Dobbins et al., 2003).

A conceptually completely different approach addressing the reconstruction problem is described in the following. It is important to realize, that in the discrete case, the measured intensity value in an image pixel may be interpreted as the sum of intensity values of all voxels in the path of that beam. This brings us to a convenient way to formulate the problem. Let **x** store values of unknown intensities in an $(N \times 1)$ column vector of all $N = n^3$ volume elements (voxels) in an $n \times n \times n$ reconstruction grid. The $R \times 1$ column vector **b**, composed of $R = MR_m$ intensity values of b_i pixels, represents the pixel intensities measured in M projections. The elements a_{ij} of the $R \times N$ weight matrix **A** represent the contribution of the ray r_i passing through pixel b_i on voxel v_j. We may formulate the following system of equations modeling the projection:

$$a_{11}x_1 + a_{12}x_2 + \ldots + a_{1n}x_n = b_1$$

$$a_{21}x_1 + a_{22}x_2 + \ldots + a_{2n}x_n = b_2$$

$$\vdots$$

$$a_{m1}x_1 + a_{m2}x_2 + \ldots + a_{mn}x_n = b_m,$$

or

$$\mathbf{Ax} = \mathbf{b} \tag{4}$$

Each eq. can be interpreted as a radiographic projection through the voxel grid, with b_i representing the “ray-sum” of a “ray” of finite width matching the width of the detector pixels.

It is important to realize, that the weights a_{ij} are of utmost importance for the solution, since they link the known pixel intensities to the unknown voxel intensities. Also note, that the entries in **b** correspond to the number of all pixels available and defines the overall number of equations available in (4). This in turn means, that for the few-view case we are interested in, the matrix **A** is sparse since only few entries will be nonzero. Consequently, there is no exact solution and eq. system (4) is underdetermined. It may be solved using numerical methods in the sense of an optimization problem. It is obvious from the definition of **A**, due to its huge $(R \times N)$ dimension efficient strategies to handle it are necessary.

The techniques to obtain the entries in **x** from eq. system (4) can be summarized under the general term “Algebraic Reconstruction Techniques (ART). Originally, ART defined the application of Kazcmarz’s algorithm (Kaczmarz, 1937) to find a best-fit solution of (4).

ALGEBRAIC RECONSTRUCTION ALGORITHMS

The Classical ART-Algorithm

As an extension to the Kaczmarz method for solving linear systems, ART in its classical form had been introduced by Gordon et. al. in 1970 (Gordon, Bender, & Hermann, 1970). ART refers to an iterative process implementing the system of linear eqs. (4) as the projection model. Starting from an initial guess volume vector $\mathbf{V}^0$ (e.g. all entries set to zero), the goal of ART is to identify those voxel-grid entries, that represent the best approximation given the projection values $\mathbf{b}$. A projection value b^k is computed according to the present state of $\mathbf{V}$ and the difference between b^k and b_i is distributed back (backprojected) onto the voxels $\mathbf{V}^0$ to obtain $\mathbf{V}^{k+1}$. Each update of the voxel grid (iteration) consists of a projection step, the calculation of a correction factor and a backprojection step. Mathematically, the basic concept may be illustrated by considering the eq. system (4) as a set of equations where each eq. defines a hyperplane in an N-dimensional space. If an exact solution to the system exists, all hyperplanes intersect in one single point representing that solution (Kak & Slaney, 1988). The Kaczmarz idea is illustrated in Fig. 3 for the simplified two-dimensional case of three equations (lines). Starting point is an arbitrary initial guess (v_0 in Fig. 3), which is then projected onto the first hyperplane (line in Fig. 3) and the resulting point reprojected onto the second hyperplane and so forth. The voxels are updated after one eq. is processed. After processing all eqs., one iteration is finished. If a single solution exists, this procedure will converge to this solution. For an excellent review of the technique the reader is referred to (Kak et al., 1988).

In the few-view case, however, de facto an infinite number of solutions is possible. Yet the procedure introduced above will always converge to a solution $\mathbf{V}^S$ that minimizes $\left|\mathbf{V}^0 - \mathbf{V}^S\right|$ (Tanabe, 1971). ART introduces artifacts (salt and pepper

Figure 3. Consider three line equations, the intersection of which is the desired solution. This sketch illustrates the geometric interpretation of the Kaczmarz procedure. Due to errors in the data the lines do not actually intersect. Starting from an arbitrary initial guess v_0 is projected onto the starting line. This procedure is repeated with all equations until convergence in a "closest point" fashion is reached. Obviously, the speed of convergence is triggered by the angle subtended by the lines.

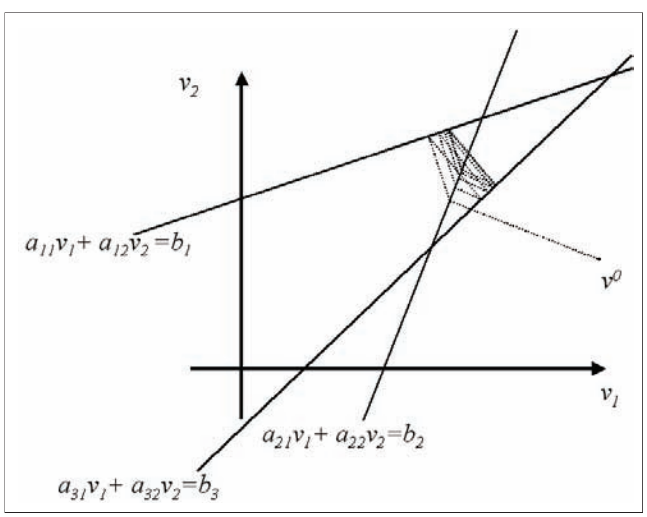

noise) due to the mostly crude approximation of the weighting factors a_{ij}, which cause inconsistencies in the system of linear equations. Due to the sequential updating process of the voxels ray after ray, these artifacts are additionally emphasized. Another source of error is induced by the diverging paths of x-rays from the source towards the detector (Mueller, 1998). Thus, the ray density in the voxel grid decreases from source to detector, resulting in a relative undersampling of voxel slices close to the detector. One well-known consequence is aliasing, typically appearing as Moire patterns in the reconstruction.

Numerous modifications of algebraic reconstruction algorithms have been suggested since its introduction in 1970 (Gordon et al., 1970) The most prominent representatives are Simultaneous Iterative Reconstruction Technique (SIRT) and Simultaneous Algebraic Reconstruction Technique (SART). While the classical ART algorithm proceeds each ray-sum separately, SIRT averages over all ray-sums in one projection before the backprojection and thus produces smoother results at the cost of a slower convergence (Kak et al., 1988). SART was developed (Andersen & Kak, 1984) in an attempt to combine the advantages of ART and SIRT. SART updates the volume analogously to SIRT, however, a weighted sum is used to update each voxel and voxels are interpolated by bilinear functions. More recent work suggests that the latter is responsible for the better performance of SART with respect to artifact suppression (Mueller, 1998). An additional advantage of SART is the highly parallel structure of its main computations lending itself very well for implementation on graphic processors to speed up reconstruction process (Mueller, 1998). Interestingly, an in depth analysis of classical ART by Mueller revealed that ART can be modified to produce equally artifact-reduced reconstructions as SART (Mueller, 1998).

Further modifications of ART include implementation of solvers computing more than one hyperplane or even all hyperplanes simultaneously, such as the Conjugate Gradient (CG) algorithm (Shewchuk, 1994) to reach faster convergence. Regularizations of the linear system such as the well-known Thikonov-regularization (Tikhonov, 1963) or minimization of the Total Variation Norm may be used to constrain the solution. Also, a non-negativity constraint in **x** may be applied to model the physical fact that the attenuation is necessarily positive.

STATISTICAL RECONSTRUCTION METHODS

Apart from the deterministic approach introduced above one may model the inverse problem from a statistical point of view, assuming the unknown x_{ij} as a random variable following some appropriate probability distribution function. This allows for an explicit modeling of noise and measurement statistics. Following the seminal paper of Siltanen et al. (Siltanen et al., 2003) we consider the following linear model in analogy to eq. (4):

$$\mathbf{Ax} + \varepsilon = \mathbf{b} \qquad (5)$$

Here $\mathbf{x} \in \mathbf{R}^m, \mathbf{b} \in \mathbf{R}^n$ and $\varepsilon \in \mathbf{R}^n$ are vectors containing random valued variables and ε represents Gaussian distributed error. However, the statistical formulation does not depend on a Gaussian approximation (Siltanen et al., 2003). In terms of probabilities, the desired object probability density can be expressed by the prior density p_{pr} and the noise probability density p_{noise} as:

$$p(\mathbf{x} \mid \varepsilon) = p_{pr}(\mathbf{x})\, p_{noise}(\varepsilon) \qquad (6)$$

Now we make use of extra knowledge we have on the imaging process by estimating the probability densities p_{pr} and p_{noise} in an appropriate form to substitute our lack of knowledge caused by the limited number of projections and the limited angular range. p_{noise} can be estimated from analyzing phantom x-ray projections. In p_{pr}, also termed "prior", we accumulate all *a priori* information on the object under investigation we have (and which we are able to formulate mathematically!). It is of utmost importance, that p_{pr} is not obtained from the measurements **b**. The proper formulation of the prior is the fundamental part of the statistical inversion procedure. As Siltanen points out "rule of thumb is that typical image vectors (say, of some existing library) should have high prior probability (density) while atypical or impossible ones should have low or negligible probability" (Siltanen et al., 2003).

The posterior probability density $p(\mathbf{x})$ we are looking for given the measurements **b** is obtained by the well-known Bayes theory:

$$p(\mathbf{x}\,|\,\mathbf{b}) = \frac{p(\mathbf{x},\mathbf{b})}{p(\mathbf{b})} = \frac{p_{pr}(\mathbf{x})\,p(\mathbf{b}\,|\,\mathbf{x})}{p(\mathbf{b})} \qquad (7)$$

Where $p(\mathbf{b})$ is the marginal density of **b** and essentially represents a normalization constant. The posterior density $p(\mathbf{x}\,|\,\mathbf{b})$, according to the Bayesian theory, is the solution of the inverse problem since it expresses our belief in the distribution of **x** based on the measurements **b** plus the a priori information contained in the prior density p_{pr}. Obviously, solving eq. (7) requires efficient searching strategies over a large-dimensional space, which is computationally demanding. For instance, the volume based on the posterior density is computed from the Maximum A Posteriori Estimate (MAP):

$$p(\mathbf{x}_{MAP}\,|\,\mathbf{b}) = \max\; p(\mathbf{x}\,|\,\mathbf{b}) \qquad (8)$$

which is an optimization problem. For detailed introduction of statistical inversion theory with focus on dental imaging the reader is referred to (Kolehmainen et al., 2003; Kolehmainen et al., 2006; Siltanen et al., 2003).

APPLICATIONS IN ORAL RADIOGRAPHY

In oral radiology, Webber and colleagues were the first researchers addressing (Groenhuis et al., 1983; Webber & Messura, 1999) and finally solving practical issues of tomosynthesis (Webber, 1994; Webber et al., 1997; Webber, 1997). Webbers patented technique TACT has often been used experimentally to address various clinical tasks in oral radiology (Abreu, Tyndall, & Ludlow, 2001; Abreu, Tyndall, Ludlow, & Nortje, 2002; Chai, Ludlow, Tyndall, & Webber, 2001; Liang, Tyndall, Ludlow, & Lang, 1999; Morant, Eleazer, Scheetz, & Farman, 2001; Nair, Tyndall, Ludlow, May, & Ye, 1998; Nair, Nair, Gröndahl, Webber, & Wallace, 2001a; Nair et al., 2001b; Shi, Han, Welander, & Angmar-Månsson, 2001; Tyndall, Clifton, Webber, Ludlow, & Horton, 1997). Also, it has even been applied successfully *in vivo* where it proved to be superior over conventional 2D-radiography with respect to diagnostic information (Webber et al., 1999). While TACT in its original version computes reconstructions as stacks of 2D planar slices using the shift-and-add algorithm (Webber et al., 1997), more elaborate modifications for artifact suppression were also applied (Nair et al., 2001c; Nair et al., 2001b; Nair et al., 2001a; Nair, Nair, Gröndahl, & Webber, 2002; Nair, Gröndahl, Webber, Umadevi, & Wallace, 2003). Artifact reduction, i.e. deblurring of the planes reconstructed, had been thoroughly addressed in a seminal paper by the tact inventors (Ruttimann, Groenhuis, & Webber, 1984). In the early years of the new millennium, two important papers were published introducing statistical inversion reconstruction for dental applications (Kolehmainen et al., 2003; Siltanen et al., 2003). The authors demonstrated, that inclusion of *a priori* knowledge on the object under investigation indeed improves the quality of few-view limited-angle reconstructions (Kolehmainen et al., 2003). The prior information consisted of a positivity prior in combination with a total variation prior (Kolehmainen et al., 2006). Interestingly, this work was the basis for an innovative radiographic device brought on the market some years later (see: http://www.vt-cube.com). This radiographic unit combines panoramic radiography with few (11) projections acquired over a narrow angle (± 21°) to generate transversal slices through the mandible or maxilla (Hyvönen, Kalke, Lassas, Setälä, & Siltanen, 2008). It is, however, important to realize that the cross sections generated with the technique based on statistical (i.e. Bayesian) inversion fundamentally differ from cross sections acquired by relatively simple tomographic motion blur. The latter technique has been established much earlier, and can be obtained using a normal radiographic film.

Our working group is also working in the field of 3D reconstruction from few projections. In contrast to the approaches described before all of them relying on a circular (section) acquisition geometry, our intention was to use projections from arbitrary geometries. The rational for our approach was the fact, that using conventional x-ray devices, e.g. intra-oral x-ray tubes, without any further equipment, de facto a random acquisition geometry will result. By means of a particular registration method (Schulze, Brüllmann, Röder, & d'Hoedt, 2004), we were able to develop a framework for computing volumetric datasets from such arbitrary projections (Schulze et al., 2008). For examples we refer to our website www.rsm3d.de.

Obviously, the radiation dose will be low with this technique, and the image quality seems to be appropriate e.g. for implantological preoperative planning. Also, simply due to ever increasing hardware potential, it seems reasonable to assume that research in the field of 3D reconstruction from

Figure 4. Acquisition geometry of the novel imaging device combining panoramic and cross sectional reconstructions. After exposure of a conventional panoramic radiograph on the direct digital image receptor with an individual splint containing small radioopaque reference objects, 11 additional projections are obtained roughly orthogonally to the panoramic geometry. By combination of the projection information from both acquisitions after registration by means of the reference objects, cross sections are computed using a statistical reconstruction approach. The cross sections may be interpreted as volumetric data lacking information in certain directions which are determined by the limited angular sampling range (modified from (Hyvönen et al., 2008)).

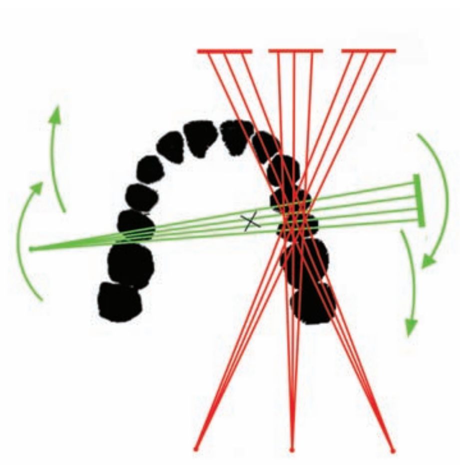

few projections continues to be very active. Thus it is very likely that we will experience further advances in reconstruction mathematics, resulting in a higher quality of the volumetric data.

CONCLUSION

The marketing of the panoramic device implementing statistical inversion reconstruction was a first step towards novel 3D technologies basing on incomplete input information. In mammography, the technical state of the art is even more advanced (Rantala et al., 2006; Suryanarayanan et al., 2000; Suryanarayanan et al., 2002; Wu et al., 2004; Wu, Moore, & Kopans, 2006; Zhang et al., 2006; Zhang et al., 2007) and systems ready to enter the market have proved their sensitivity already. It is evident, that tomosynthetic reconstruction offers a great potential for the future. Owing to the lack of input information inherent in these techniques, however, few-view limited-angle reconstruction methods will never match image quality of CT. Nevertheless, their flexibility in combination with their dose and cost reduction potential will establish them as alternative niche techniques appropriate for specific diagnostic tasks. As Dobbins and Godfrey point out in their in depth review, they potentially "provide a low-dose, low-cost method of volumetric imaging that can be easily performed as an adjunct to conventional radiography" (Dobbins et al., 2003). Future will answer the question, whether these innovative volumetric reconstruction techniques will really manage to occupy this diagnostic niche.

REFERENCES

Abreu, M. jr., Tyndall, D. A., & Ludlow, J. B. (2001). Generation of TACT image slices using different reconstruction algorithms: Effects on natural caries detection. *Oral Surgery, Oral Medicine, Oral Pathology, Oral Radiology, and Endodontology, 92,* 576-581.

Abreu, M. jr., Tyndall, D. A., Ludlow, J. B., & Nortje, C. J. (2002). Influence of the number of basis images and projection array on caries detection using tuned aperture computed tomography (TACT). *Dentomaxillofacial Radiology, 31,* 24-31.

Andersen, A. H., & Kak, A. C. (1984). Simultaneous algebraic reconstruction technique (SART): A superior implementation of the ART algorithm. *Ultrasonic Imaging, 6,* 81-94.

Beyerer, J., & Leon, F. P. (2002). Die Radontransformation in der digitalen Bildverarbeitung. *Automatisierungstechnik, 50,* 472-480.

Bundesamt für Strahlenschutz (2004). *Unterrichtung durch die Bundesregierung. Umweltradioaktivität und Strahlenbelastung im Jahr 2004* Bundesdruckerei Berlin, Germany.

Chai, U. Dom, Ludlow, J. B., Tyndall, D. A., & Webber, R. L. (2001). Detection of simulated periodontal bone gain by digital subtraction radiography with tuned-aperture computed tomography. The effect of angular disparity. *Dentomaxillofacial Radiology, 30,* 92-97.

Dobbins, J. T., & Godfrey, D. V. (2003). Digital x-ray tomosynthesis: current state of the art and clinical potential. *Physics in Medicine and Biology, 48,* 65-106.

Dorsaz, P.-A., Dorsaz, L., & Doriot, P. A. (2000). The effect of image distortion on 3-D reconstruction of coronary bypass grafts from angiographic Views. *IEEE Transactions on Medical Imaging, 19,* 759-762.

Duryea, J., Dobbins, J. T., & Lynch, J. A. (2003). Digital tomosynthesis of hand joints for arthritis assessment. *Medical Physics, 30,* 325-333.

Fencil, L. E., & Metz, C. E. (1990). Propagation and reduction of error in three-dimensional structure determined from biplane views of unknown orientation. *Medical Physics, 17,* 951-961.

Gordon, R., Bender, R., and Hermann, G. T. (1970). Algebraic reconstruction techniques (ART) for three-dimensional electron microscopy and X-ray photography. *Journal of Theoretical Biology, 29,* 471-481.

Grant, D. G. (1972). Tomosynthesis: A three-dimensional radiographic imaging technique. *IEEE Transactions on Biomedical Engineering, 19,* 20-28.

Groenhuis, R. A. J., Webber, R. L., & Ruttimann, U. E. (1983). Computerized tomosynthesis of dental tissues. *Oral Surgery, 56,* 206-214.

Hoffmann, K. R., Wahle, A., Pellot-Barakat, C., Sklansky, J., & Sonka, M. (2000). Biplane x-ray angiograms, intravascular ultrasound, and 3D visualization of coronary vessels. *International Journal of Cardiac Imaging, 15,* 495-512.

Hoffmann, K. R., Williams, B. B., Esthappan, J., Chen, S.-Y. J, Caroll, J. D., Harauchi, H. et al. (1997). Determination of 3D positions of pacemaker leads from biplane angiographic sequences. *Medical Physics, 24,* 1854-1862.

Hyvönen, N., Kalke, M., Lassas, M., Setälä, H., & Siltanen, S. (2008). Three-dimensional x-ray imaging using hybrid data collected with a digital panoramic device. *submitted (see http://www.siltanen-research.net/publications.html, June 2008).*

Kaczmarz, S. (1937). Angenäherte Auflösung von Systemen linearer Gleichungen. *Bulletin international de l'Académie Polonaise des Sciences et des Lettres A, 35,* 355-357.

Kak, A. C., & Slaney, M. (1988). *Principles of computerized tomographic imaging.* New York: IEEE Engineering in Medicine and Biology Society.

Kolehmainen, V., Siltanen, S., Järvenpäa, S., Kaipio, J. P., Koistinen, P., Lassas, M. et al. (2003). Statistical inversion for medical x-ray tomography with few radiographs: II. Application to dental radiology. *Physics in Medicine and Biology, 48,* 1465-1490.

Kolehmainen, V., Vanne, A., Siltanen, S., Järvenpäa, S., Kaipio, J. P., Lassas, M. et al. (2006). Parallelized Bayesian inversion for three dimensional dental x-ray imaging. *IEEE Transactions on Medical Imaging, 25,* 218-228.

Liang, H., Tyndall, D. A., Ludlow, J. B., and Lang, L. A. (1999). Cross-sectional presurgical implant imaging using tuned aperture computed tomography (TACT). *Dentomaxillofacial Radiology, 28,* 232-237.

Metz, C. E., & Fencil, L. E. (1989). Determination of three-dimensional structure in biplane radiography without prior knowledge of the relationship between the two views: Theory. *Medical Physics, 16,* 45-51.

Miller, E. R., McCurry, E. M., & Hruska, B. (1971). An infinite number of laminagrams from a finite number of radiographs. *Radiology, 98,* 249-255.

Morant, R. M., Eleazer, P. D., Scheetz, J. P., & Farman, A. G. (2001). Array-projection geometry and depth discrimination with tuned aperture computed tomography for assessing the relationship between tooth roots and the inferior alveolar canal. *Oral Surgery, Oral Medicine, Oral Pathology, Oral Radiology, and Endodontology, 2001, 91,* 252-259.

Mueller, K. (1998). *Fast and accurate three-dimensional reconstruction from cone-beam projection data using algebraic methods.* Dissertation, The Ohio State University.

Mueller, K., Yagel, R., & Wheller, J. W. (1999). Anti-aliased three-dimensional cone-beam reconstruction of low-contrast objects with algebraic methods. *IEEE Transactions on Medical Imaging, 18,* 519-537.

Nair, M. K., Gröndahl, H.-G., Webber, R. L., Umadevi, P., & Wallace, J. A. (2003). Effect of iterative restoration on the detection of artificially induced vertical radicular fractures by Tuned Aperture Computed Tomography. *Oral Surgery, Oral Medicine, Oral Pathology, Oral Radiology, and Endodontology, 96,* 118-125.

Nair, M. K., Nair, U. P., Gröndahl, H.-G., & Webber, R. L. (2002). Accuracy of tuned aperture computed tomography in the diagnosis of radicular fractures in non-restored maxillary anterior teeth - an in vitro study. *Dentomaxillofacial Radiology, 31,* 299-304.

Nair, M. K., Nair, U. P., Gröndahl, H.-G., Webber, R. L., & Wallace, J. A. (2001a). Detection of artificially induced vertical radicular fractures using tuned aperture computed tomography. *European Journal of Oral Sciences, 109,* 375-379.

Nair, M. K., Seyedain, A., Agarwal, S., Webber, R. L., Nair, U. P., Piesco, N. P. et al. (2001b). Tuned aperture computed tomography to evaluate osseous healing. *Journal of Dental Research, 80,* 1621-1624.

Nair, M. K., Seyedain, A., Webber, R. L., Nair, U. P., Piesco, N. P., Agarwal, S. et al. (2001c). Fractal analyses of osseous healing using tuned aperture computed tomography images. *European Radiology, 11,* 1510-1515.

Nair, M. K., Tyndall, D. A., Ludlow, J. B., May, K., & Ye, F. (1998). The effects of restorative material and location on the detection of simulated recurrent caries. A comparison of dental film, direct digital radiography and tuned aperture computed tomography. *Dentomaxillofacial Radiology, 27,* 80-84.

Niinimäki, K., Siltanen, S., & Kolehmainen, V. (2007). Bayesian multiresolution method for local tomography in dental x-ray imaging. *Physics in Medicine and Biology, 52,* 6663-6678.

Rantala, M., Vänskä, S., Järvenpäa, S., Kalke, M., Lassas, M., Moberg, J. et al. (2006). Wavelet-based reconstruction for limited-angle x-ray tomography. *IEEE Transactions on Medical Imaging, 25,* 210-216.

Ruttimann, U. E., Groenhuis, R. A. J., & Webber, R. L. (1984). Restoration of digital multiplane tomosynthesis by a constrained iteration method. *IEEE Transactions on Medical Imaging, 3,* 141-148.

Schulze, R., Brüllmann, D. D., Röder, F., & d'Hoedt, B. (2004). Determination of projection geometry from quantitative assessment of the distortion of spherical references in single-view projection radiography. *Medical Physics, 31,* 2849-2854.

Schulze, R., Heil, U., Weinheimer, O., Groß, D., Bruellmann, D. D., Thomas, E. et al. (2008). Accurate registration of random radiographic projections based on three spherical references for the purpose of few-view 3D reconstruction. *Medical Physics, 35,* 546-555.

Shewchuk, J. R. (1994). An introduction to the conjugate gradient method without the agonizing pain. *Unpublished Work, (http://www.cs.cmu.edu/~quake-papers/painless-conjugate-gradient.pdf, June 2008).*

Shi, X.-Q., Han, P., Welander, U., & Angmar-Månsson, B. (2001). Tuned-aperture computed tomography for detection of occlusal caries. *Dentomaxillofacial Radiology, 30,* 45-49.

Siltanen, S., Kolehmainen, V., Järvenpäa, S., Kaipio, J. P., Koistinen, P., Lassas, M. et al. (2003). Statistical inversion for medical x-ray tomography with few radiographs: I. General theory. *Physics in Medicine and Biology, 48,* 1437-1463.

Sone, S., Kasuga, T., Sakai, T., Kawai, T., Oguchi, K., Hirano, F. et al. (1995). Image processing in the digital tomosynthesis for pulmonary imaging. *European Radiology, 5,* 96-101.

Suryanarayanan, S., Karellas, A., Vedantham, S., Baker, S. P., Glick, S. J., D'Orsi, C. J. et al. (2002). Evaluation of linear and nonlinear tomosynthetic reconstruction methods in digital mammography. *Academic Radiology, 8,* 219-224.

Suryanarayanan, S., Karellas, A., Vedantham, S., Glick, S. J., D'Orsi, C. J., Baker, S. P. et al. (2000). Comparison of tomosynthesis methods used with digital mammography. *Academic Radiology, 7,* 1085-1097.

Tanabe, K. (1971). Projection method for solving a singular system of linear equations and its applications. *Numerische Mathematik, 17,* 203-214.

Tikhonov, A. N. (1963). Solution of incorrectly formulated problems and the regularization method. *Soviet Mathematics - Doklady, 4,* 1035-1038.

Tyndall, D. A., Clifton, L., Webber, R. L., Ludlow, J. B., & Horton, R. A. (1997). TACT imaging of primary caries. *Oral Surgery, Oral Medicine, Oral Pathology, Oral Radiology, and Endodontology, 84,* 214-225.

Webber, R. L. (1994). Self-calibrated tomosynthetic, radiographic-imaging system, method and device. US Patent [5,539,637]. USA.

Webber, R. L. (1997). Self-contained tomosynthetic, radiographic-imaging system, method and device. US Patent [5,668,844]. USA.

Webber, R. L., Horton, R. A., Tyndall, D. A., & Ludlow, J. B. (1997). Tuned-aperture computed tomography (TACT). Theory and application for three-dimensional dento-alveolar imaging. *Dentomaxillofacial Radiology, 26,* 53-62.

Webber, R. L., & Messura, J. K. (1999, November 11). An in vivo comparison of diagnostic information obtained from tuned-aperture computed tomography and conventional dental radiographic imaging modalities. *Oral Surgery, Oral Medicine, Oral Pathology, Oral Radiology, and Endodontology., 88,* 239-247.

Wu, T., Moore, R. H., & Kopans, D. B. (2006). Voting strategy for artifact reduction in digital breast tomosynthesis. *Medical Physics, 33,* 2461-2471.

Wu, T., Moore, R. H., Rafferty, E. A., & Kopans, D. B. (2004). A comparison of reconstruction algorithms for breast tomosynthesis. *Medical Physics, 31,* 2636-2647.

Zhang, Y. G., Chan, H.-P., Sahiner, B., Wei, J., Goodsitt, M. M., Hadjiiski, L. M. et al. (2006). A comparative study of limited-angle cone-beam reconstruction methods for breast tomosynthesis. *Medical Physics, 33,* 3781-3795.

Zhang, Y. G., Chan, H.-P., Sahiner, B., Wu, Y.-T., Zhou, C., Ge, J. et al. (2007). Application of boundary detection information in breast tomosynthesis reconstruction. *Medical Physics, 34,* 3603-3613.

Ziedses, B. G. (1932). Eine neue Methode zur Differenzierung in der Röntgenographie (Planigraphie). *Acta Radiologica, 13,* 182-192.

KEY TERMS

Few-View: Limited amount of projection data, more precisely a total number of appr. 5 to 20 projections.

Inverse Problem: Deriving values of some system under investigation from observed data.

Limited Angle: Angle subtended between the projections of less than π.

Oral Radiography: Diagnostic radiography as related to oral, perioral tissues and the entire dentomaxillofacial region.

Radiographic Projection: Process of two-dimensional radiographic image formation, where the (flat) detector measures incident photons that emerge from an x-ray source and traverse the object under investigation.

Tomosynthetic Reconstruction: Synonym for reconstruction of three-dimensional information on the object under investigation from few-projections obtained from a limited projection angle.

Volume Reconstruction: Reconstruction of three-dimensional information on the object under investigation.

Section III
Software Support in Tissue Regeneration Proceeders in Dentistry

Chapter VIII
Advances and Trends in Tissue Engineering of Teeth

Shital Patel
Swinburne University of Technology, Australia

Yos Morsi
Swinburne University of Technology, Australia

ABSTRACT

Tooth loss due to several reasons affects most people adversely at some time in their lives. A biological tooth substitute, which could not only replace lost teeth but also restore their function, could be achieved by tissue engineering. Scaffolds required for this purpose, can be produced by the use of various techniques. Cells, which are to be seeded onto these scaffolds, can range from differentiated ones to stem cells both of dental and non-dental origin. This chapter deals with overcoming the drawbacks of the currently available tooth replacement techniques by tissue engineering, the success achieved in it at this stage and suggestion on the focus for future research.

INTRODUCTION

The occurrence of children born with missing primary and/or adult teeth (hypodontia) is momentous (Nunn *et al*) and tooth loss resulting due to various pathological conditions like periodontal disease, dental caries, trauma, or a variety of genetic disorders affects most adults around the world. As per Mooney *et al*, periodontal disease is one of the most significant oral health problems in the U.S. (35% of the U.S. population is estimated to have periodontitis, and 80% of these also suffer from gingivitis).

Although there are several materials, which are used to replace lost tooth structures, none can completely replace the lost functions. Thus, as compared to endodontic treatment, tooth transplantation, and dental implants, the *de novo* regeneration of dental tissues might be a better approach in restorative dentistry (Zhang *et al*). John Hunter carried out homologous transplantation of teeth in humans, which was a common technique in the United Kingdom during the eighteenth century. According to him, if teeth were transplanted from a "sound and healthy" person, they might last for years. However, there is a possibility of transmitting infections in some cases; which was also discussed by him (Schultheiss *et al*). Present day technique of dental implant is more prone to mechanical and biological failure as compared to the natural dentition. In addition to this, they require a minimum level of bone, which makes its use limited in cases of severe bone loss (Ferreira *et al*). Also these techniques can elicit an immune stimulated host rejection response.

As the innate, biological tooth is better equipped to deal with biological threat and mechanical loading, the long-term goal of dental research is to develop methods of tooth replacement biologically. The ideal way of tooth replacement is to create a new, natural tooth from autologous human tissues. Progress in the field of tissue engineering and stem cell biology make it now feasible to investigate ways to make this become a reality. Ferreira *et al* have talked of several different methods that have been proposed to achieve biological tooth replacement. These include stimulation of the formation of a third dentition, the construction of a tooth by bioengineering the different component parts separately, seeding of tooth shaped biodegradable scaffolds with stem cells and producing embryonic-like tooth primordia from cultured cell populations. Each of these approaches has advantages and disadvantages.

TISSUE ENGINEERING APPROACH

Tissue engineering (TE) is a multidisciplinary area that integrates the principles of engineering and biological sciences to develop a biological substitute, which can be used to repair, regenerate or replace parts of the body.

A general approach of TE involves the use of temporary porous three-dimensional scaffolds to: (a) define the complex anatomical shape of the tissue, (b) guide the proliferation and differentiation of seeded cells and (c) provide mechanical support for the cells (Morsi *et al*). Thus scaffold plays a key role in tissue engineering by providing the initial extracellular matrix required to support the growth and proliferation of cells.

Various techniques are available for manufacturing the three-dimensional scaffolds that are dependent on the optimal scaffold required for the application on hand. The ideal scaffold should posses following characteristics: (i) the rate of scaffold degradation should be in accordance to the rate of tissue growth, (ii) the surface of the scaffold should be conductive to cell attachment, growth and differentiation, (iii) possess required pore size and interconnectivity for tissue integration, vascularisation and transfer of nutrients and waste removal, (iv) have adequate mechanical strength and flexibility to suit intended application, (v) possess high surface area to volume ratio and (vi) the scaffold should be easy to process and be manufactured in a cost effective manner.

The design of an ideal scaffold has to be accompanied by the selection of a suitable material. Several synthetic biodegradable polymers, such as polyglycolic acid (PGA), polylactic acid (PLA) and their copolymers, natural materials like collagen, fibrin and alginate are the most commonly used materials as scaffolds for tissue engineering applications. Irrespective of the type of material used and its application, it should be biocompatible, easy to modify, should have structural stability, and should be versatile, biodegradable and malleable.

The techniques being used for manufacturing 3D scaffold for TE has undergone considerable changes in the last decade and these techniques are continuously being evolved to accommodate the specific requirements of individual organ or tissue of interest such as pore size, interconnectivity and mechanical strength. The techniques for 3D scaffold fabrication can be divided into two categories: conventional methods and newer manufacturing technologies such as rapid prototyping. Further research into both approaches will lead to significantly new processes by overcoming the drawbacks of the current available techniques (Morsi *et al*).

CONVENTIONAL TECHNIQUES

Various conventional processing techniques have been developed to build porous structures from synthetic scaffold materials. These techniques can be broadly divided into the ones that involve addition of particles/porogens and those based on concepts of phase separation. Solvent casting-particulate leaching, gas foaming, melt molding are some of the examples of the former and the latter includes emulsification, freeze-drying and liquid-liquid phase separation. The phase separation techniques can be used to incorporate biological components into a scaffold.

- **Solvent casting-particulate leaching:** This technique involves dissolving a polymer like polylactic-co-glycolic acid (PLGA) or PLLA in a solvent such as chloroform or methylene chloride in a petri dish or a mold and adding porogen to it. Usually salt particles such as sodium chloride, tartrate or citrate of regulated size are used as porogens for this purpose. The salt particles can then be leached out by immersion in water. Porosity and pore size obtained are dependent upon the particle size and salt weight fraction. Pore diameters of 100-500 µm and porosities of 87-91% have been reported (Bartolo *et al*).
- **Gas foaming:** Here the melted polymer is saturated with blowing agent such as carbon dioxide at high pressure. This high-pressure gas is then brought back to atmospheric level thus rapidly decreasing the solubility of the gas in the polymer. With decreasing solubility of gas, the mixture is quenched so that the physical state of the material can be set. This generates nucleation and gas bubbles of various sizes varying from 100-500 µm within the polymer. Scaffolds with pore sizes of 200 – 300 µm and porosities of up to 93% can be created by this technique (Morsi *et al*).
- **Melt molding:** In meld molding, a teflon mold of the required shape is filled up with powdered polymer and porogen of specific diameter. This mold is then heated above the glass-transition temperature of the polymer while applying pressure to the mixture. As a result, the polymer particles bind together. Immersing it in water leaches the porogen component out and the scaffold is then dried. Thus a porous scaffold of desired/required shape can be obtained by melt molding technique.
- **Emulsification:** Polymer such as PLGA is dissolved in a solvent and mixing of ultrapure water to it produces an emulsion. This emulsion is cast in a mold and quenched in liquid nitrogen. Solvent and water are removed by freeze-drying process. Porosities up to 95% and pore sizes of 13-35 µm can be achieved using this technique.
- **Freeze-drying:** Here scaffolds can be produced from synthetic as well as natural polymers such as collagen. Synthetic polymers are dissolved in solvents like glacial acetic acid or benzene. The polymeric solution is then frozen and freeze-dried, resulting in a porous matrix. The freezing of the collagen solution results in the formation of ice crystals and this in turn forces the collagen

molecules to aggregate into the available interstitial spaces. Ethanol dehydrates the frozen collagen and ice crystals formed are removed by freeze-drying. The pore size of the scaffold is determined by the freezing rate and pH whereby a high freezing rate produces smaller pores (Morsi *et al*).

- **Liquid-liquid phase separation:** In this fabrication technique polymers are dissolved in solvents that have low melting point and are easy to sublime. A small amount of water may be required to work as a non-solvent in order to induce phase separation. The polymer solution is cooled below the melting point of the solvent and vacuum dried for some days for the solution to undergo complete solvent sublimation. The cooling parameters for the solution are important as they determine the morphology of the resultant scaffold. This method can produce scaffolds with porosities of up to 90% and pores of approximately 100 μm (Morsi *et al*).
- **Fibre meshes:** Here non-woven scaffolds are produced from polymers by the use of textile technology. Difficulties in obtaining good pore size, high porosity and low mechanical strength limit the use of this technique (Morsi *et al*, Bartolo *et al*).

However, the use of harsh organic solvents for dissolving polymers and other chemicals required by the fabrication process may produce toxic by-products, which greatly limits their application. In addition, the pore size, distribution and interconnectivity cannot be precisely controlled, as these processing techniques (excluding phase separation and fibre meshes) are dependent on a randomly distributed pore generator to form the pores within the scaffold. The lack of proper porosity and interconnectivity might prevent the cells from migrating deep into the scaffold when seeded and thus rendering the goal of tissue-engineered tissue/organ futile.

RAPID PROTOTYPING TECHNIQUES

Rapid prototyping techniques may be able to address some of the limitations encountered by the conventional techniques. They would help in building three-dimensional scaffold of desired shape using layered manufacturing strategies according to computer-aided design (CAD) without the preparation of molds (Pfister *et al*). There are various types of rapid prototyping techniques: stereolithography, selective laser sintering (SLS), fused deposition modelling (FDM), three-dimensional printing (3D printing), bioprinting, ink jet printing, three-dimensional bioplotting (3D bioplotting) (Pfister *et al*, Sachlos *et al*).

Stereolithography produces scaffolds directly from the CAD model; by solidifying the surface of a liquid photo polymer layer by layer with the help of a laser beam. Irradiation can be done by two ways in this process. The first one is the mask-based method wherein an image is transferred to a liquid polymer by irradiating through a patterned mask. The irradiated part of the liquid polymer is then solidified. In the second method, polymer structures are produced by direct writing process using a focused UV beam (Bartolo *et al*). This process is highly accurate in scaffold production.

SLS uses a laser emitting infrared radiation, which selectively heats the powder material just beyond its melting point. The laser traces the shape of each cross-section of the model to be built, thereby sintering powder in a thin layer. In addition, it also supplies energy that not only fuses neighbouring powder particles, but also bonds each new layer to ones previously sintered. For polymeric powders, the sintering process takes place in a sealed heated chamber at a temperature near the melting pointing filled with gases like nitrogen or argon. After each layer is solidified, the piston over the model retracts to a new position and a fresh layer of powder is supplied by means of a mechanical roller. The powder, which remains unaffected by the laser, works as a natural support for the model and remains in place until the model is complete (Bartolo *et al*).

Crump developed this extrusion-based rapid prototyping technique, commercially known as FDM in 1989 (Bartolo *et al*). Here, the computer converts the virtual object, created by CAD or computer tomography (CT) scan or magnetic resonance imaging (MRI), into a sequence of slices that are used to build, layer by layer, the corresponding real three-dimensional (3D) object (Pfister *et al*). FDM enables complex yet accurate shapes to be constructed with high mechanical stability. It offers high degree of control over shape, pore interconnectivity and porosity of scaffolds and a high resolution of 250 μm (Morsi *et al*).

Sachs *et al* developed 3D printing at the Massachusetts Institute of Technology in 1989 (Bartolo *et al*). The 3D printing is a layered fabrication process whereby sliced 2D profile of a model determined by CAD file is transformed to a STL file and printed onto a fresh layer of powder (natural polymers such as starch, dextran and gelatin) via deposition of a suitable water-based binder from the inkjet printhead. Though this technique enables the production of scaffolds at a fast pace as compared to the FDM technique, it lacks the precision and mechanical strength of FDM.

Bioprinting incorporates biological components such as living cells into the scaffold produced. Thus it has the ability to produce viable tissue (Morsi *et al*). Unlike the above techniques, 3D bioplotting can process a astonishingly wide range of different materials, including polymer melts, thermostat resins, polymer solutions, pastes with high filler contents, cement, and even bioactive polymers such as proteins. It can also be used to design and fabricate hydrogels with complex architectures and internal substructures (Pfister *et al*).

The creation of scaffolds for dental applications requires specific characteristics and precision of the tissue to be captured and ideally these scaffolds should be tailored to individual patients, which can be achieved using rapid prototyping techniques. A novel CAD system of structures based on convex polyhedral units called *Computer Aided System for Tissue Scaffolds or CASTS* has been created for use with this technology for TE applications. CASTS consists of a basic library of units. Each open-cellular unit is a unique configuration of linked struts. Various shapes can be obtained by assembling these units. Along with an algorithm, that permits the designer to identify the unit cell and the required dimensions, the system is able to generate a structure that is suitable for the intended TE application automatically. The shape and spatial arrangement of the structures can easily be altered by changing the parameters. The major advantage of CASTS is the elimination of dependence on user skills. Many different scaffolds of controllable architecture and desired properties can be designed from a small range of basic units (Naing *et al*).

CURRENT RESEARCH

One of the aims of tissue engineering is to create biological substitutes for transplantation. As scaffolding plays a vital role in the neo-tissue formation, selection of the biomaterial is very important. Synthetic biodegradable polymers like PGA, poly L-lactic- ε-caprolactone copolymer, polyglycolic acid-poly L-lactic acid copolymer (PGA/PLLA) and so on have been used for scaffold fabrication for dental applications as they do not carry the risk of pathogen transmission and immunorejection. On top of this, they degrade and resorb after fulfilling the scaffolding function, thereby eliminating the long-term inflammation and complications associated with foreign body reactions (Ma *et al*). Several studies have been carried out using synthetic biodegradable scaffolds like PGA/PLLA, PLGA, and PGA, some of which are listed in Table 1.

Both Buurma *et al* and Mooney *et al* have used non-woven PGA fibres as scaffold for their study. Young *et al* used PGA/PLLA and PLGA for tooth scaffolds. These were prepared with the use of polyvinylsiloxane (PVS) tooth molds in the shape of human incisors and molars. They used solvent casting-particulate leaching technique wherein the solvent used was chloroform and the porogen was sodium chloride. Duailibi *et al* produced biodegradable PGA and PLGA scaffolds by using the method suggested by Young *et al*. Lee *et al* produced PLGA by mold casting technique using sucrose as a porogen. Thus most studies have been carried out using conventional technique for scaffold preparation. However, scaffolds should be produced based on patient's requirements by using CASTS and RP techniques like 3D printing and 3D bioplotting.

Natural synthetic materials like collagen sponge have also been used as biocompatible and biodegradable scaffolds for tooth tissue engineering (Table 1). Collagen sponge has a number of advantages as it is similar in composition to the extra cellular matrix, it has low immunogenicity and cytotoxicity, and it has the efficiency with which it can form different shapes. It favors cell attachment and is chemotactic to cells. The pore structure of collagen sponge is ideal for the colonization of seeded cells. Furthermore, collagen sponge is reported to enhance bone formation by promoting the differentiation of osteoblasts. The features of collagen sponge suggest that it has the potential to provide an ideal scaffold for tooth-tissue engineering (Sumita *et al*).

The collagen sponge used by Sumita *et al* and Honda *et al* is made from the collagen extracted from porcine skin and contained 75% (dry weight) type I atelocollagen and 25% type III atelocollagen. They produced it using freeze-drying technique (Sumita *et al*). As previously mentioned, the foam structure design of the scaffold thus produced prevents the cells from migrating further into the scaffold. Thus, Sachlos *et al*, designed novel collagen scaffolds, which contained predefined internal architecture anticipated to support the transfer of nutrients and waste products, thereby favoring the migration and growth of cells throughout the scaffold. They used phase-change ink-jet deposition rapid prototyping technique and critical point drying technique. The moulds produced contained predefined and reproducible features as small as 200 µm (Sachlos *et al*).

Type of cells also plays a very important role in production of biological substitutes for tissue engineering. Several studies have been carried out using dental derived pulp fibroblasts and cell obtained from third molar tooth buds. In most studies for regeneration of tooth structures, porcine third molar tooth buds have been used (Table 1). Previously differentiated cells like endothelial cells, smooth muscle cells, fibroblasts etc were used for seeding the scaffolds for tissue engineering applications. However, with the progress in the field of stem cell biology, the cells, which have the capacity to differentiate, are being used increasingly.

Mooney *et al* carried out *in vitro* studies by seeding adult human dental pulp fibroblasts on biodegradable PGA fibers for a period of 60 days. Buurma *et al* showed that adult human dental pulp and gingival cell populations attached to biodegradable PGA scaffolds, synthesized and secreted type I collagen, cellular fibronectin and may express genes implicated in transducing bone morphogenetic protein signals after subcutaneous implantation in immuno-compromised mice. Young *et al* dissociated porcine third molar tooth buds into single-cell suspensions and seeded them onto the biodegradable PGA/PLLA scaffolds and then implanted into the omenta of athymic rats for 20-30 weeks. Duailibi *et al* implanted single-cell suspensions obtained from molar tooth buds from three- to seven-day-post-natal Lewis rat pups and seeded onto biodegradable PGA/PLGA into the omenta of adult Lewis rats. They found that four day post-natal tooth bud cells were optimal for tooth tissue engineering. They also demonstrate that bioengineered rat teeth develop more quickly than bioengineered pig teeth. The single cell suspensions used in the above experiments

Table 1. Selected tissue engineering applications for tooth

Process	**Authors**	**Application**	**Findings**	**Validation**
Fiber mesh	Mooney *et al* (1996)	Adult human dental pulp fibroblasts PGA fibres	Formation of new tissue resembling dental pulp	*In vitro*
Fiber mesh	Buurma *et al* (1999)	Adult human dental pulp fibroblasts, human gingival fibroblasts PGA fibres	Expression of genes indicative of a capacity to produce extracellular matrix	*In vivo*
Solvent casting-particulate leaching	Young *et al* (2002)	Porcine third molar tooth buds PGA-PLLA	20, 25 and 30 weeks post-implantation, recognizable crown structures exhibiting distinct coronal and apical organization with recognizable cusps and root tips are formed	*In vivo*
Solvent casting-particulate leaching	Duailibi *et al* (2004)	3 to 7 day-post-natal rat tooth buds PGA/PLGA	12 weeks post-implantation, crowns containing dentin, pulp and enamel are formed	*In vivo*
Solvent casting-particulate leaching	Young *et al* (2005)	Porcine third molar tooth buds, porcine bone marrow progenitor cells PGA-PLLA	Formation of tooth crown and rudimentary root structures containing pulp, dentin, enamel, alveolar bone, and PDL-like collagen type III connective tissue, and bone constructs consisting of immature and compact bone after 12 weeks of implantation	*In vivo*
Freeze-drying	Honda *et al* (2006)	Porcine third molar tooth buds Collagen sponge	Significantly greater alkaline phosphatase activity	*In vitro*
			After 20 weeks, the implants attained the structural characteristics of individual teeth	*In vivo*

continued on following page

Table 1. continued

Process	Authors	Application	Findings	Validation
Freeze-drying	Sumita *et al* (2006)	Porcine third molar tooth buds	Superior cell retention and enhanced alkaline phosphatase activity observed in collagen sponge scaffold as compared to PGA mesh scaffold	*In vitro*
		Collagen sponge and PGA mesh	Higher proportion of calcified tissue in regenerated teeth in the collagen sponge scaffold than the PGA mesh scaffold	*In vivo*

suggest that mammalian tooth buds may retain a cell-autonomous development program, even when dissociated into single-cell suspensions and grown in culture (Duailibi *et al*). Young *et al* demonstrated the utility of a hybrid tooth-bone TE approach for eventual clinical treatment of tooth loss accompanied by alveolar bone resorption. Unlike the above studies, Honda *et al* used dental epithelium and mesenchyme from porcine third molar teeth enzymatically separated and dissociated into single cells to seed collagen scaffold. Mesenchymal cells obtained were seeded onto the surface of the collagen scaffold and epithelial cells were then plated on top so that the two cell types were in direct contact with each other. These constructs were evaluated *in vitro* and *in vivo* by implanting in immuno-compromised mice for a period of 6-20 weeks. Sumita *et al* proved that collagen is a better scaffold for tooth TE as compared to PGA fibre mesh. They used porcine third molar tooth bud cells onto these scaffolds and cultured them *in vitro* to evaluate the cell adhesion and alkaline phosphatase activity. They also carried out in vivo studies by implanting these seeded scaffolds in the omenta of immuno-compromised rats and evaluating the tooth formation up to 25 weeks. The results obtained suggest that collagen sponge scaffold enhances initial cell attachment, cell differentiation and consequently the formation of calcified tissue.

FUTURE DIRECTIONS

Sterilization Methods

Various sterilisation techniques like use of ethylene oxide, gamma irradiation, and plasma sterilization are usually being used for the purpose of disinfecting the biomaterials used. 75% ethanol is also used for the purpose of sanitizing the biomaterial. These may play an important role in tissue formation. Ethylene oxide may be toxic to the cells if not completely removed. Gamma irradiation has shown to change the properties of PGA, mainly by increasing its cristallinity, making it more brittle, and by quicker weight loss (Mol). Nevertheless, cell growth and matrix production by the cells seeded onto gamma-irradiated scaffolds were not influenced. It still seemed that the cells were less dedifferentiated (Mol). Moreover, it is a costly process and requires an isolated site for safe operation. Plasma sterilization is a useful surface treatment as it uses UV photons to destroy micro-organisms (Mol). But it still has to be seen whether this is a suitable method for sterilizing scaffolds and whether the UV photons do not disrupt the surface of the polymer (Mol). Sterilization using high frequency microwaves seems to be a novel way of sterilization of biomaterials. It has been found to retain the native mechanical strength of the tissue (pericardium). Further studies need to be done to test its suitability.

Scaffold Improvements

The extracellular matrix (ECM) is a complex cross-linked network of proteins and glycosaminoglycans. It is like a naturally available scaffold in the body which acts as an architectural support that organizes cells in space, provides them with biochemical signals that regulate cellular behaviour, and separates one tissue type from another. The extracellular environment is significant for the control of the behaviour of every cell in all tissues. Cell-ECM interactions are mutual and very dynamic. Cells constantly receive and process information about the environment and respond accordingly and they often remodel their ECM as per their requirement. Numerous factors contribute to the nature of cells' interactions with other cells, growth factors, extracellular matrix proteins, and matricellular proteins. All of these components act collectively to regulate cell-surface protein activity, intracellular signal transduction, and subsequent gene expression, that lead to proliferation, migration, differentiation, programmed cell death, modulation of cytokines and growth factor activities and formation of complex tissues. Thus these interactions need to be considered while designing the tissue analogues (Ritter *et al*).

Chen *et al* explored the effect of biomaterial on tooth germ cell adhesion and proliferation *in vitro.* They evaluated the effects of cell–surface interactions of tooth germ cells on biomaterials with various surface hydrophilicities. Their results demonstrated that tooth germ cells attached and grew preferentially on moderately hydrophilic biomaterials. Moreover, cellular viability was proportional to the adhesion ratio (Chen *et al*). Incorporation of biological components such as proteins, growth factors etc into the scaffolds to make bioactive scaffolds is another direction of future research.

For the tissue-engineered tooth to resemble the native tissue, it also needs to be vascularised and also needs nerve regeneration.

Alternative Cell Sources

Studies have been carried out using the stem cells from dental origin. Ohazama *et al* have carried out studies using embryonic stem cells, neural stem cells, and adult bone-marrow-derived cells. This resulted in the development of tooth structures, showing that an embryonic primordium can grow in its adult environment. These results thus provide a noteworthy advance toward the construction of artificial embryonic tooth primordia from cultured cells that can be used to replace missing teeth following transplantation into the adult mouth (Ohazama *et al*).

CONCLUSION

TE is being increasingly used in medical research due to its flexibility and ability to generate tissues/organs as good as or even better than the natural ones. Most studies have been carried out using scaffolds produced by conventional techniques, further research needs to be focused on the use of RP techniques as these can capture the specificity and can accurately design the scaffolds tailored to individual patients. Progress in stem cell research can be very useful in tooth tissue engineering. Commercialisation of tissue-engineered tooth is still far away, however, this approach is very promising and efforts should certainly be made towards its commercialisation.

REFERENCES

Ohazama, S. A. C. M., Miletich, I., & Sharpe, P. T. (2004). Stem-cell-based tissue engineering of murine teeth. *J Dent Res*, *83*(7), 518-522.

Pfister, A., R. D. L., Laib, A., Bner, U. H., Schmelzeisen, R., Lhaupt, R. M. (2004). Biofunctional rapid prototyping for tissue-engineering applications: 3D bioplotting versus 3D printing. *Journal of Polymer Science: Part A: Polymer Chemistry, 42*, 624-638.

Ritter, A. B., S. R., & Michniak, B. B. (2005). Tissue Engineering. In S. R. Aurthur, B. Ritter, & B. B. Michniak (Eds.), *Biomedical engineering principles* (p. 596). CRC Press, Taylor & Francis Group.

Buurma, B., & Rutherford, R. B. (1999). Transplantation of human pulpal and gingival fibroblasts attached to synthetic scaffolds. *Eur J Oral Sci., 107*(4), 282-289.

Ferreira, C. F. (2007). Biological tooth replacement and repair. *Journal of Oral Rehabilitation, 34*, 933-939.

Young, C. S., Vacanti, J. P., Honda, M., Bartlett, J. D., & Yelick, P. C. (2002). Tissue engineering of complex tooth structures on biodegradable polymer scaffolds. *J Dent Res, 81*(10), 695-700.

Young, C. S., Rose Asrican, H. A., Ravens, M., Troulis, M. J., Kaban, L. B., Vacanti, J. P., & Yelick, P. C. (2005). Tissue-engineered hybrid tooth and bone. *Tissue Engineering, 11*(9/10), 1599-1610.

Mooney, D. J., C. P., James Piana, and Bruce Rutherford. (1996). Engineering dental pulp-like tissue in vitro. *Biotechnol. Prog., 12*, 865-868.

Schultheiss, D., D. A. B., Jorg Wefer, Udo Jonas. (2000). Tissue engineering from Adam to the zygote: Historical reflections. *World J Urol, 18*, 84-90.

Sachlos, E., N. R., C. Ainsley, B. Derby, J.T. Czernuszka. (2003). Novel collagen scaffolds with predefined internal morphology made by solid freeform fabrication. *Biomaterials, 24*, 1487-1497.

Nunn, J. H., N. E. C., T. J. Gillgrass, R. S. Hobson, N. J. Jepson, J. G. Meechan, and F. S. Nohl. (2003). The interdisciplinary management of hypodontia: background and role of paediatric dentistry. *British Dental Journal 194*, 245–251.

Naing, M. W., C. K. C. a. K. F. L. (2008). Computer aided tissue engineering scaffold fabrication. In P. B. Bopaya Bidanda (Ed.), *Virtual prototyping & Bio manufacturing in medical applications* (pp. 67-85). Springer.

Duailibi, M. T., S. E. D., C.S. Young, J.D. Bartlett, J.P. Vacanti, and P.C. Yelick. (2004). Bioengineered teeth from cultured rat tooth bud cells. *J Dent Res 83*(7), 523-528.

Honda, M. J., S. T., Yoshinori Sumita, Hiroshi Sagara, Minoru Ueda. (2007). The sequential seeding of epithelial and mesenchymal cells for tissue-engineered tooth regeneration. *Biomaterials*, 680-689.

Min Lee, J. C. Y. D., Benjamin M. Wu. (2005). Scaffold fabrication by indirect three-dimensional printing. *Biomaterials. 26*, 4281-4289.

Mol, A. (2005). *Functional tissue engineering of human heart valve leaflets.* The Netherlands: Eindhoven University of Technology.

Bartolo, P. J., H. A. A., Rodrigo A. Rezende, Tahar Laoui and Bopaya Bidanda. (2008). Advanced process to fabricate scaffolds for tissue engineering. In P. B. Bopaya Bidanda (Ed.), *Virtual prototyping & Bio manufacturing in medical applications* (pp. 149-170). Springer.

Ma, P. X., R. Z. (2001). Microtubular architecture of biodegradable polymer scaffolds. *J Biomed Mater Res, 56*, 469-477.

Chen, R-S., Y.-J. C., Min-Huey Chen, Tai-Horng Young. (2007). Cell-surface interactions of rat tooth germ cells on various biomaterials. *Journal of Biomedical Materials Research Part A, 83*, 241–248.

Zhang, W., X. F. W., J.G.C. Wolke, Z. Bian, M.W. Fan And J.A. Jansen. (2005). Differentiation ability of rat postnatal dental pulp cells in vitro. *Tissue Engineering, 11*(3/4), 357-368.

Morsi, Y. S., C. S. W. a. S. S. P. (2008). Conventional manufacturing processes for three-dimensional scaffolds. In P. B. Bopaya Bidanda (Ed.), *Virtual prototyping & Bio manufacturing in medical applications* (pp. 129-148). Springer.

Sumita, Y., M. J. H., Takayuki Ohara, Shuhei Tsuchiya, Hiroshi Sagara, Hideaki Kagami, Minoru Ueda. (2006). Performance of collagen sponge as a 3-D scaffold for tooth-tissue engineering. *Biomaterials, 27,* 3238–3248.

KEY TERMS

Computer Aided System for Tissue Scaffolds: This is a novel technology that enables the application of advanced CAD system based on convex polyhedral units.

Phase Separation: It is the transformation of a homogenous system into more than one phase. It is one of the ways of scaffold preparation.

Porogen: It is a chemically inert and high temperature resistant porous polymeric material which can be used for a wide variety of applications. For the purpose of scaffold preparation, normally sodium chloride particles of specific diameter are used as porogens.

Scaffolds: A supporting structure for cells and tissue to grow on. A scaffold will provide the physical structure that guides the cells to grow to the right anatomical shape.

Stem Cells: They are found in almost all multi-cellular organisms. They are the kind of cells which have the ability to renew themselves and differentiate into a variety of specialized cell types.

Sterilization: This is a process that destroys (kills) all living micro-organisms by the use of different chemicals, temperature, high pressure steam or irradiation.

Tissue Engineering: A multidisciplinary area which integrates the principles of engineering and biological sciences to develop a biological substitute, which can be used to repair, regenerate or replace parts of the body.

Chapter IX
Automated Bacterial Colony Counting for Clonogenic Assay

Wei-Bang Chen
University of Alabama at Birmingham (UAB), USA

Chengcui Zhang
University of Alabama at Birmingham (UAB), USA

ABSTRACT

Bacterial colony enumeration is an essential tool for many widely used biomedical assays. This chapter introduces a cost-effective and fully automatic bacterial colony counter which accepts digital images as its input. The proposed counter can handle variously shaped dishes/plates, recognize chromatic and achromatic images, and process both color and clear medium. In particular, the counter can detect dish/plate regions, identify colonies, separate aggregated colonies, and finally report consistent and accurate counting result. The authors hope that understanding the complicated and labor-intensive nature of colony counting will assist researchers in a better understanding of the problems posed and the need to automate this process from a software point of view, without relying too much on specific hardware.

INTRODUCTION

Numerous dental diseases such as dental caries and periodontal diseases are closely related with the bacteria in our oral cavity. Taking dental caries as an example, dental caries is well-known a multi-factor disease, which occurred with both fermentable dietary carbohydrate and dental plaque bacteria. The *Mutans Streptococci*, one of the bacteria strains in our oral cavity, has been implicated as a major etiological agent of dental caries. Hence, it is critical to know what bacterial strains and the amount of them that are in the collected oral samples, such as the saliva and plaque samples. To identify and quantify the microbes in a sample, one of the most widely accepted function assay in both clinical and research laboratories, is the clonogenic assay (a.k.a. colony forming assay).

The clonogenic assay is achieved by pouring a liquefied sample containing microbes onto agar plates, incubating the survived microbes as the seeds for growing the number of microbes via binary fission to form colonies (colony forming unit, CFU) on the plates. The bacteria species can be distinguished by growing them on different selective medium, and the quantification for the amount of viable microbes in the sample can be measured by enumerating the number of colony on the plate, since each viable microbe can grow and become a colony. In this way, the identity and the quantity of the bacteria in a given sample can be determined. With this diagnostic tool, we can monitor the progress of the disease and even to indicate the susceptibility of future occurrence of the disease. Moreover, it also provides a basis to determine proper antibiotic agents used in medical treatment. Without a doubt, this assay is broadly used in biomedical examinations, food and drug safety test, environmental monitoring, and public health (Liu, Wang, Sendi, & Caulfield, 2004).

Though clonogenic assay is very useful, there exists a bottleneck that limits its throughput. The technical hurdle occurs at the final step, the colony enumeration step in the assay since it is a time consuming and labor intensive process. The reason is that there might exist hundreds or thousands of colonies in a Petri dish, but the counting process is manually performed by well-trained technicians. In Figure 1 (a) and (b), we show a typical 100mm Petri dish with hundreds of colonies grown in it.

In addition to the low throughput problem, the consistency is another issue. The manual counting is an error-prone process since the results tend to have more subjective interpretation and mostly rely on persistent practice, especially when a vast number of colonies appear on the plate (Chang, Hwang, Grinshpun, Macher, & Willeke, 1994). Thus, it is very important to have consistent criteria to avoid the fluctuations in results.

In order to increase the throughput and to provide consistent and accurate results, colony counting devices were invented in the market (Dahle, Kakar, Steen, & Kaalhus, 2004). We reviewed these counters available on the market (Advanced Instruments, ; Barloworld Scientific

Figure 1. (a) Mutans Streptococci grown in a 100mm Petri dish with Mitis-Salivarius agar; (b) Escherichia Coli grown in a 100mm Petri dish with LB agar; (c) The hierarchical structure of objects in a bacterial colony image.

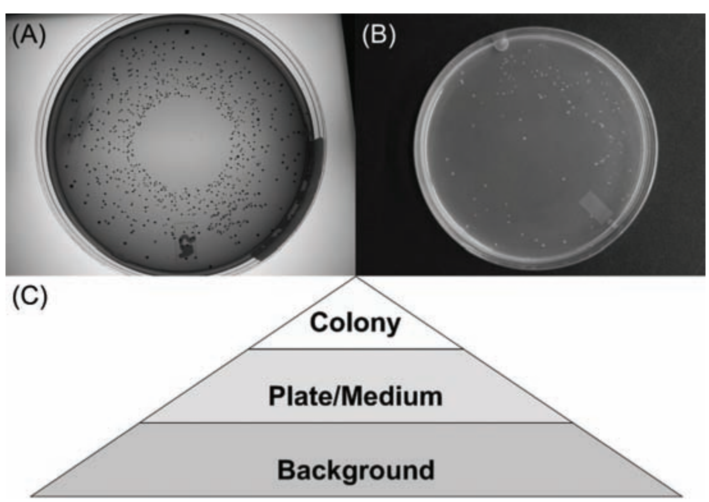

; BioLogics ; ChemoMetec ; Colifast ; Neutec Group ; Oxford Optronix ; Perceptive Instruments ; Progen Scientific ; Synbiosis) and classified them into two categories.

The first kind of counter, the automatic digital counters (Barloworld Scientific), is widely used in most laboratories. However, they are not truly automatic since they require operators to identify each colony with a probe so that the sensor system can detect and register each count. Obviously, this kind of counter still heavily depends on the routine manual counting, and is of no use in solving the problems aforementioned.

The second type of counter is semi-automatic or automatic counters. Some counters of this type may require users to manually specify the plate/dish area and to provide parameters prior to the actual enumeration process (Niyazi, Niyazi, & Belka, 2007). Besides, some of them may need operators to manually adjust the threshold values in order to handle dishes/plates that differ from their default settings. In addition, most automatic counters can only process one Petri dish at a time. In such cases, human operators are still heavily involved in the operation, and it is thus not efficient for high-throughput processing of plates/dishes.

In addition to the high-throughput processing concern, the affordability is another issue. Most automatic counters are often very expensive since they are equipped with dedicated image capturing hardware for acquiring high quality images to optimize counters' efficiency and performance. Besides, some automatic counters can only accurately detect colonies by growing bacteria on special growth medium with fluorogenic substrates (Dee et al., 2000). The substrates are utilized by bacteria and are metabolized into fluorescent product that can be used to locate colonies. These systems are extremely sensitive, and are good for detecting micro-colonies. However, the disadvantages are that it is costly to add fluorogenic substrates in the medium, and a sensitive instrument is also required to detect the fluorescence signal. Hence, the affordability of this kind of equipment is still questionable for most of laboratories due to the economical inefficiency of these high cost equipments in the market. For some laboratories that need to perform a large amount of enumeration tasks, more than one high-throughput counter are needed to fit their needs. Thus, the colony enumeration device poses a significant budgetary challenge to many laboratories (Putman, Burton, & Nahm, 2005).

Further, the robustness and applicability of the existing automatic counters is another concern. Laboratories have needs to use various types of dishes and plates in their examinations. However, most of the commercial counters are designed for measuring 60-150mm Petri dish and thus lack the flexibility for accommodating plates with different sizes and shapes. In addition, some existing counters use only binary images for detecting colonies. Plenty of important characters of the colony, such as color, are lost for identifying the genus of the bacteria.

Nowadays, digital image capture devices such as digital cameras and flatbed scanners, become more popular and affordable. Hence, it motives us to use these devices to obtain high-quality images for counting bacterial colonies. In this chapter, we use photos taken by digital cameras with various settings as our input images, and then, make an attempt to recognize colonies in those images. Our goal is to provide an inexpensive, software-based solution for alleviating those problems aforementioned. The proposed colony enumeration system is designed and implemented to work in a fully automatic manner such that it can process various types of plates and correctly detect bacterial colonies without users' intervention. Thus, time and money can be saved for laboratories to do more important tasks.

In the rest of this chapter, we first introduce the system architecture and the proposed methods, then demonstrate the experimental results, and finally summarize and conclude this chapter.

METHODS

The proposed bacterial colony enumeration system simulates the human recognition behavior that progressively identifies objects in an image based on the hierarchical layout of major objects in a bacterial colony image. The natural hierarchy of objects in a bacterial colony image consists of three layers, including the background, the plate/medium region, and the colonies. We illustrate the hierarchical layout of a bacterial colony image in Figure 1 (c). More specifically, the bacterial colony enumeration system first separates the plate/medium region from the background, and then, recognizes the bacterial colonies in the identified plate/medium region.

There are four major steps in the proposed bacterial colony enumeration system: dish/plate region detection, colony recognition, clustered colony separation, and finally, the colony enumeration. The main technique used in the proposed system is object segmentation. In particular, the proposed segmentation technique distinguishes foreground objects, such as dish regions or colonies, from their corresponding background by minimizing the intraclass variance and maximizing the interclass variance. In this chapter, we introduces a progressive segmentation method which is based on the recursive use of a widely adopted clustering and thresholding method called Otsu's method (Otsu, 1979). This method is used to find a proper threshold value for separating pixels into foreground and background classes in the target region (regions-of-interest). Once all colonies on the plate are recognized, we can simply count the number of remaining segments in the image as the estimated number of bacterial colonies on the plate/dish. In the remaining of this section, we will introduce in details the proposed bacterial colony enumeration system.

Dish/Plate Region Detection

The first step in this system is to detect the dish/plate region in a given image. The goal is to reduce the operator's workload by eliminating the process of manually specifying the target dish/plate region in the image. To make the dish/plate region more conspicuous from the background, the contrast-limited adaptive histogram equalization (CLAHE) is first performed on the converted grayscale images which operates on small regions called tiles in the images rather than the entire image (Zuiderveld, 1994). The contrast of each tile is enhanced and the neighboring tiles are then combined using bilinear interpolation to eliminate artificially induced boundaries.

Following the histogram equalization, we apply the Otsu's segmentation algorithm on the contrast enhanced image to detect the dish/plate region as a target region. However, because of the varying intensity of the target object (dish/plate region), there may form some small holes inside the target plate region. Those small holes are then filled by adopting a morphology-based method, and the target region can thus be consolidated. Sometimes, this method may also detect some smaller objects outside the target region due to the existence of noise in the background region. These isolated small objects are also removed by our algorithm on the basis of the assumption that the target region should occupy the majority (and central) part of the image. With the above operations, the target plate/dish regions can be correctly detected most of the time. We demonstrate the effectiveness of our automatic dish/plate region detecting algorithm in the experimental results (as shown in Figure 3). The experimental results show that our proposed counter can detect dish/plate regions very effectively, regardless of the size and shape of the dish/plate. Thus, the proposed system is flexible enough to be used for handling various kinds of dishes and plates.

Colony Recognition

The second step in our proposed architecture is colony recognition. The purpose of this step is to isolate colonies in the dish/plate, identify clustered colonies, and separate clustered colonies for subsequent colony enumeration.

Before actually performing the colony recognition, we have noticed that bacterial colony images can be classified into two groups based on their color characteristics. For those images with abundant color information, we call them chromatic images. On the contrary, for those images with less color information, we call them achromatic images.

Figure 1 (A) and (B) shows black *Mutans Streptococci* colonies grown in the 100mm Petri dish with the blue Mitis-Salivarius agar, and white *Escherichia Coli* colonies grown in the 100mm Petri dish with the clear LB agar, respectively. These two images exemplify the chromatic image and the achromatic image. Since these two types of images are quite dissimilar in their color characteristics, it is more appropriate to handle chromatic and achromatic images in different ways.

In order to distinguish chromatic images from the achromatic ones, we examine the standard deviation of average RGB values from each color channel. The smaller the standard deviation is, indicating a relatively low variation of colors, the higher the possibility that the image is achromatic. After grouping images into the two groups (chromatic/achromatic) by their embedded color information, we are now ready to apply different algorithms on extracted dish/plate regions to isolate colonies.

For chromatic images, we not only use Otsu's method (Otsu, 1979) to separate colonies from medium, but also adopt color similarity in HSV (Hue-Saturation-Value) color space to facilitate the colony boundary detection (Ma & Zhang, 1998). This is essential since a simple global threshold cannot extract all colonies due to the existence of artifacts such as scratches, dusts, markers, bubbles, reflections, and dents in the image. Equation 1 shows the calculation of color similarity in the HSV color space.

$$
\begin{aligned}
CS_{ij} &= 1 - \frac{1}{\sqrt{5}}\sqrt{\left(x_j - x_i\right)^2 + \left(y_j - y_i\right)^2 + \left(z_j - z_i\right)^2} \\
x_i &= S_i \times \cos\left(H_i \times 2\pi\right) \\
y_i &= S_i \times \sin\left(H_i \times 2\pi\right) \\
z_i &= V_i
\end{aligned} \qquad (1)
$$

where CS_{ij} is the color similarity of two pixels *i* and *j*. H, S, and V are the hue, saturation, and value of a pixel in the HSV color space.

The use of color similarity in colony boundary detection is based on the assumption that pixels inside a segment, no matter it is a colony segment or a dish/plate segment, have higher similarity values with its neighboring pixels, and pixels along the segment boundary have lower similarity values with their neighbors. For each single pixel, it is surrounded by eight neighboring pixels such that all nine pixels form a 3×3 window. We calculate the color similarity values between a pixel and its eight neighbors, and use the minimum similarity value to represent the maximum color difference with its neighbors. Thus, pixels within a segment have higher minimum similarity values. On the contrary, pixels on the boundary of a segment have lower values. After the calculation, the boundaries/edges are more evident, and all the minimum color similarity values form an intensity image. Thus, we can adopt the Otsu's method on the extracted dish/plate region in the enhanced intensity image to further distinguish the background (medium) from foreground objects (candidate colonies).

A much more challenging part in this research is to deal with achromatic images. Most of the existing colony counters have disappointing performance in handling achromatic images due to the low contrast between colonies and medium. In addition, the background artifacts look very similar to colonies in the clear agar, making it more difficult to discriminate the background artifacts from real colonies in the dish/plate.

To handle achromatic images, we develop a different method to alleviate the low contrast and artifacts problems. We also apply Otsu's segmentation algorithm to isolate colonies. However, Otsu's method is much less accurate in achromatic images due to the interference of artifacts. An additional noise removal step is developed for those achromatic images.

The color similarity measurement described earlier in this section cannot be applied since achromatic images lack color information. In this chapter, we proposed a new statistic approach to detect and remove those artifacts and successfully preserve only colonies. Our proposed statistic approach includes two steps. The first step is to remove those relatively large artifacts. We collect the sizes of all objects detected by Otsu's method from the dish/plate region, and generate frequency distribution with log base of those size values. Colonies of similar size should occupy the high frequency segment in this distribution, and the frequencies for those very large artifacts should be very low. By this assumption, we can remove those large size objects. The next step is to remove those smaller artifacts which are about the same size as the colonies in the dish/plate. In this step, the area size is not a good determinant since the area size range of those small artifacts has a significant overlap with that of colonies. Instead, we consider the intensity distribution of the dish/plate region as a two-peak distribution which consists of the distribution of medium pixels (background) and distribution of colonies pixels (foreground). Those small artifacts belong to background distribution; however, they have overlapped with the colony distribution. Therefore, we assume that colonies should be significantly different in intensity values comparing with their surrounding background, and it is very likely that those small artifacts have similar intensity values to their surrounding pixels. Based on this assumption, we examine each small object including colonies by hypothesis testing. In the hypothesis testing, we use the mean of surrounding pixel values as null and test if the mean of object pixel values has significant difference with the null, at the significance level of $\alpha = 0.01$.

Colony Separation

After most of the artifacts being removed from both chromatic and achromatic images, the remaining foreground objects are considered to be colonies. Ideally, each of these isolated foreground objects corresponds to one single colony. However, such an object may correspond to more than one colony because several colonies may cluster together. Therefore, there is a need to split them in order to obtain the correct colony count. To separate the aggregated colonies, we consider the intensity

Figure 2. An example of the Watershed algorithm performed on clustered colonies

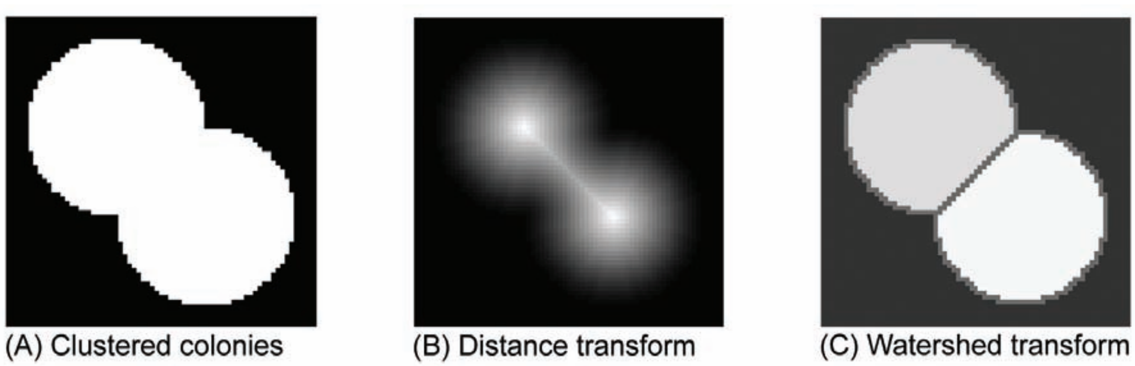

gradient image as topological surfaces (Vincent & Soille, 1991), thus the Watershed algorithm can be applied to divide clustered colonies in the image just as water flood in a topographical surface. We demonstrate how Watershed algorithm works in Figure 2. Figure 2 (a) shows a binary image that simulates two clustered colonies; Figure 2 (b) presents the distance transform of the binary image in Figure 2 (a); Figure 2 (c) illustrates the Watershed transform successful splitting the clustered colonies. After applying the Watershed algorithm, almost all colony segments have been separated and identified and are ready for the colony enumeration step.

Colony Enumeration

After all colonies are properly separated and identified, the final step is to acquire the total number of viable colonies by adding up the number of the remaining objects that have been identified as colonies.

EXPERIMENTAL RESULTS

To test the robustness of this counting system, we use five different digital cameras as the image acquiring devices in our experiments to obtain bacterial colony images for bacterial colony enumeration. The five digital cameras include a Sony DSC T100 Digital Camera (8.0-megapixel) with a resolution of 3264 × 2448, a Nikon D50 Digital SLR Camera (6.0-megapixel) with a resolution of 3008 × 2000, a Canon PowerShot A95 Camera (5.0-megapixel) with a resolution of 2592 × 1944, a Sanyo DSC-J1 Camera (3.2-megapixel) with a resolution 1600 × 1200, and an Asus P525 PDA cell phone built-in camera (2.0-megapixel) with a resolution 1600 × 1200.

Additionally, Petri dishes with two different types of medium and bacteria strains are used in our experiments. The first type of images is obtained from the Department of Pediatric Dentistry at the University of Alabama at Birmingham. This type of plate contains blue color Mitis-Salivarius agar which is used for isolating *Mutans Streptococci*. These acid-producing bacteria are commonly seen in our oral cavity, and have been implicated as a major etiological agent that attack tooth enamel minerals and cause dental caries. The second type of plate is obtained from the Division of Nephrology, Department of Medicine, University of Alabama at Birmingham. This type of plates contains the clear LB agar which is widely used in laboratories for growing *Escherichia Coli*.

Dish/Plate Region Detection

In this experiment, we compare the proposed dish/plate detection algorithm with Otsu's segmentation algorithm. Some sample segmentation results are demonstrated in Figure 3 (A). We evaluate the performance of the proposed dish/plate detection algorithm and Otsu's method by applying both algorithms on 300 images, including 36 chromatic images and 264 achromatic images. The performance is measured by the satisfaction rate which is defined in Box 1 (Eq. 2).

The overall satisfaction rates for the proposed method and Otsu's method are 89.0% and 36.3%, respectively. For the 36 chromatic images, the satisfaction rates for the proposed method and Otsu's method are 86.1% and 0%, respectively. For the 264 achromatic images, the satisfaction rates for the proposed method and Otsu's method are 89.4% and 41.3%, respectively. It is obvious that the proposed method outperforms Otsu's method in dish/plate region detection. We summarized the satisfaction rates for both methods in Figure 3 (b).

Colony Recognition

In this Section, the performance of this system on colony recognition is evaluated. It is more reasonable to discuss the counter performance on

Box 1. Equation 2

$$\frac{\text{Number of images that dish/plate regions are correctly detected}}{\text{Total number of images}} \times 100\%$$

Figure 3. Performance comparison for dish/plate region detection

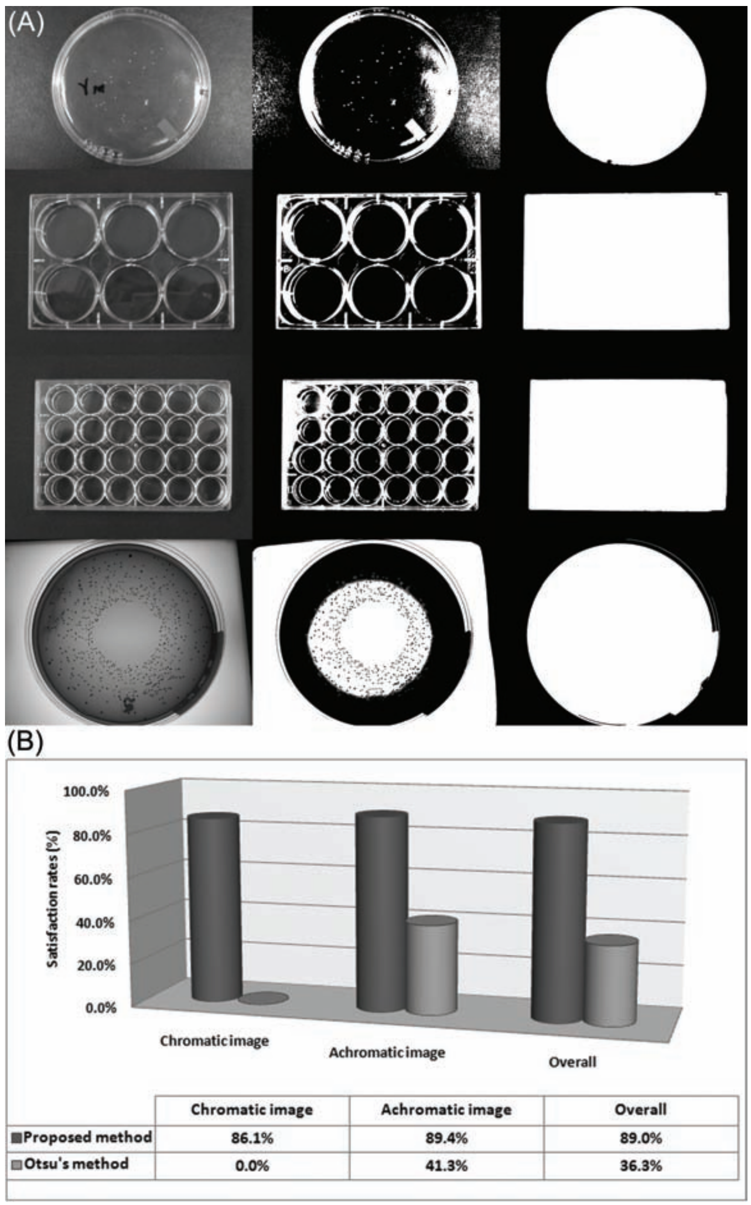

	Chromatic image	Achromatic image	Overall
Proposed method	86.1%	89.4%	89.0%
Otsu's method	0.0%	41.3%	36.3%

chromatic and achromatic images separately in this experiment since the characteristics of them are quite different. We compared the proposed counter (P.C.) with the Clono-Counter (C.C.) which is reported by Niyazi in 2007 (Niyazi et al., 2007). We apply both counters on 10 chromatic images and 30 achromatic images. The enumeration results are then compared with the ground truth for calculating the precision, recall, and F-measure values.

For chromatic images, the precision values of the P.C. and C.C. methods are 0.97±0.04 and 0.56±0.24, respectively; their recall values are 0.89±0.07 and 1.00±0.01, respectively; their F-measure values are 0.92±0.03 and 0.69±0.19, respectively. Table 1 shows the performance comparison on chromatic images.

To evaluate the robustness of the proposed counter (P.C.) on achromatic images, we conduct the following two experiments, and compare the performance of P.C. with that of C.C.

In the first experiment, we test the proposed counter (P.C.) on 30 achromatic images. The performance of the P.C. and C.C. methods on these achromatic images are summarized in Table 1. From Table 1, we can observe that the P.C. significantly outperforms the C.C. method. The average precision, recall, and F-measure values of the P.C. method are 0.69±0.30, 0.87±0.09, and 0.72±0.18, while the corresponding values of C.C. are 0.00±0.00, 0.00±0.00, and 0.00±0.00, respectively.

In the second experiment, we further apply the proposed method on 30 different achromatic images taken from the same dish, but with different background surfaces, zooms, and lighting conditions. We measure the precision, recall, and F-measure of the proposed counter. The average precision, recall, and F-measure on the 30 achromatic images are 0.95±0.04, 0.80±0.04, and 0.87±0.02, respectively. The results of the consistency analysis show the proposed system is quite consistent since the variance of enumeration results from the same dish is small.

Colony Separation

In recognizing colonies, there are some clustered colonies that need to be further divided into separate colonies. As mentioned earlier, we adopt the Watershed algorithm to solve this problem and found it effective in splitting clustered colonies according to our experimental results. An example of the splitting result with the use of Watershed algorithm is given in Figure 4.

In our experiment, we checked the performance of the Watershed algorithm on 19 randomly selected segments with clustered colonies which actually contain 98 colonies. After applying the Watershed algorithm, we obtain 96 colonies. Only 2 overlapped colonies are missed in the splitting process. It is worth mentioning that the Watershed algorithm is an integral part of the proposed system, where each step contributes to the better performance of the subsequent steps.

Table 1. Performance comparison on chromatic and achromatic images

Image Type	Method	Precision	Recall	F-measure
Chromatic	P.C.	0.97±0.04	0.89±0.07	0.92±0.03
	C.C.	0.56±0.24	1.00±0.01	0.69±0.19
Achromatic	P.C.	0.69±0.30	0.87±0.09	0.72±0.18
	C.C.	0.00±0.00	0.00±0.00	0.00±0.00
Overall	P.C.	0.76±0.28	0.88±0.08	0.77±0.18
	C.C.	0.14±0.27	0.25±0.44	0.17±0.31

Figure 4. An example of colony separation

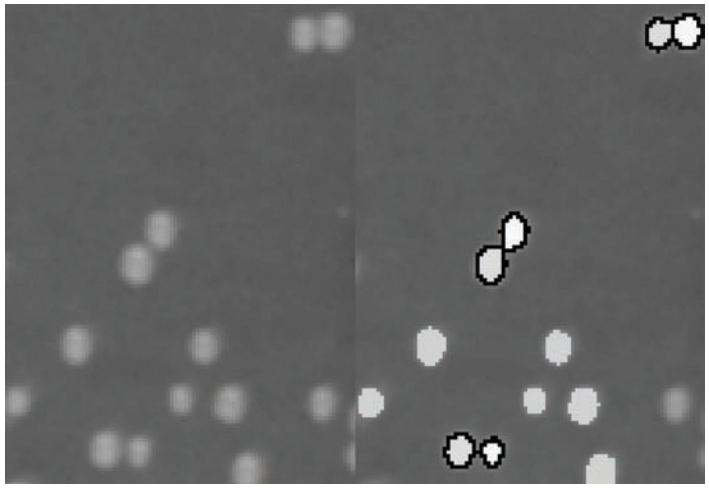

DISCUSSIONS AND CONCLUSIONS

In this chapter, we introduce a robust and effective automated bacterial colony enumeration system. The proposed system has the ability to identify various types of dish/plate in images, and then recognize colonies in the identified dish/plate region. The morphology of the colony segment is checked for distinguishing clustered colonies from single colonies. To obtain the accurate number of colonies, the Watershed transform is then applied to separate the aggregated colonies. After these steps, the number of colonies can be enumerated as the total number of segments in the image.

The most challenging part in this study is to handle achromatic images, since colonies look very similar to the clear medium (background). In addition, there exist a lot of noises on the plate such as bubbles, small scratches, and small markers. These round-shaped objects also look very similar to colonies and it is often hard to tell whether or not they are colonies even by human eyes. This makes the colony isolation task extremely difficult. The experimental results show the proposed system addresses these challenges and demonstrates reasonable performance on both chromatic and achromatic images.

It is worth mentioning that this study has the following contributions. First, the proposed counter can handle various kinds of dish/plate, including round and rectangular shaped dishes/plates, which is a very desirable feature. Second, we use general digital camera images as its input, and there is no need to purchase expensive and dedicated image acquiring devices. The third contribution is that our counter can distinguish chromatic from achromatic images and process both color and clear medium. In addition, since our counter is a fully automated, software-centered colonies counter, all the user needs to do is to take the pictures of the dishes/plates and leave the remaining job to the counter. Users are no longer involved in the tedious and time-consuming process of selecting the target area or providing values for parameters. Moreover, the performance of the proposed counter is promising for both chromatic and achromatic images. The above desirable features make this enumeration system very flexible and attractive to laboratories. Laboratories can save precious time and allocate limited budget on more important tasks.

Though the performance of our proposed bacterial colony enumeration system is very promising, there are still some remaining issues. In the future, we will put more effort on distinguishing the colony from noises in achromatic images. We may introduce more colony features such as color, texture, and topology to improve colony recognition. Another issue in this study is that bacterial colonies may have different shapes as well as colors in the real world; however, currently we can only handle clustered colonies which are composed of round-shaped colonies with Watershed algorithm. The ultimate goal is to accurately differentiate various bacteria species grown in the same dish and correctly enumerate the colonies for each bacteria species. We believe it will have great benefit for clinical dental studies.

ACKNOWLEDGMENT

This research of Dr. Chengcui Zhang is supported in part by NSF DBI-0649894 and UAB ADVANCE program through the sponsorship of the National Science Foundation.

REFERENCES

Advanced Instruments. *QCount and Color QCount*. Retrieved March 23, 2008, from http://www.aicompanies.com/

Barloworld Scientific. *Stuart SC6*. Retrieved March 23, 2008, from http://www.barloworld-scientific.com/

BioLogics. *AccuCount*. Retrieved March 23, 2008, from http://www.biologics-inc.com/

Chang, C. W., Hwang, Y. H., Grinshpun, S. A., Macher, J. M., & Willeke, K. (1994). Evaluation of counting error due to colony masking in bioaerosol sampling. *Appl Environ Microbiol*, *60*(10), 3732-3738.

ChemoMetec. *NucleoCounter*. Retrieved March 23, from http://www.chemometec.com/

Colifast. *Colifast Rapid Microcolony Counter*. Retrieved March 21, 2008, from http://www.colifast.no

Dahle, J., Kakar, M., Steen, H. B., & Kaalhus, O. (2004). Automated counting of mammalian cell colonies by means of a flat bed scanner and image processing. *Cytometry A*, *60*(2), 182-188.

Dee, S. W., Aas, R. S., Skjanes, K., Hermansen, L. F., Samset, I. D., Reitehaug, E., et al. (2000, Jan 1). *Development of a rapid system for monitoring total microbial load (HPC) in distribution systems and raw waters*. Paper presented at the Water Quality Technology Conference, Salt Lake City, UT.

Liu, X., Wang, S., Sendi, L., & Caulfield, M. J. (2004). High-throughput imaging of bacterial colonies grown on filter plates with application to serum bactericidal assays. *J Immunol Methods*, *292*(1-2), 187-193.

Ma, W.-Y., & Zhang, H. (1998). Content-based image indexing and retrieval. In B. Furht (Ed.), *Handbook of multimedia computing*. Boca Raton, FL: CRC Press.

Neutec Group. *Flash and Grow automatic colony counter*. Retrieved March 23, 2008, from http://www.neutecgroup.com/

Niyazi, M., Niyazi, I., & Belka, C. (2007). Counting colonies of clonogenic assays by using densitometric software. *Radiat Oncol*, *2*(4).

Otsu, N. (1979). A thresholding selection method from gray-scale histogram. *IEEE Trans. on Systems, Man, and Cybernetics*., *9*(1).

Oxford Optronix. *ColCount*. Retrieved March 23, 2008, from http://www.oxford-optronix.com/

Perceptive Instruments. *Sorcerer Colony Counter*. Retrieved March 23, 2008, from http://www.perceptive.co.uk/

Progen Scientific. *Schuett ColonyQuant automatic colony counter*. Retrieved March 23, 2008, from http://www.progensci.co.uk/

Putman, M., Burton, R., & Nahm, M. H. (2005). Simplified method to automatically count bacterial colony forming unit. *J Immunol Methods*, *302*(1-2), 99-102.

Synbiosis. *aCOLyte and ProtoCOL SR/HR*. Retrieved March 23, 2008, from http://www.synbiosis.com/

Vincent, L., & Soille, P. (1991). Watersheds in digital spaces: an efficient algorithm based on immersion simulations. *IEEE Trans. on Pattern Analysis and Machine Intelligence*, *13*(6), 583-598.

Zuiderveld, K. (1994). Contrast limited adaptive histogram equalization. In *Graphics gems IV*, (pp. 474-485): Academic Press Professional, Inc.

KEY TERMS

Bacterial Colony Counter: A manual, semi-automatic or automatic instrument used to enumerate the number of bacterial colonies on a plate.

Colony Forming Unit: Colony Forming Unit (CFU) is a measure of the number of viable microbes in microbiology. The theory behind is a single living microbe can grow and form a colony via binary fission.

Contrast Limited Adaptive Histogram Equalization (CLAHE): Contrast Limited Adaptive Histogram Equalization is a contrast enhancement method that performs on grayscale image. This method operates on small regions, called tiles, in the image, rather than the entire image. The contrast of each tail is enhanced by adopting histogram equalization.

HSV Color Space: HSV stands for Hue-Saturation-Value, which describe colors as points in a cylinder whose central axis ranges from black to white with neutral colors between them, where angle around the axis corresponds to “hue”, distance from the axis corresponds to “saturation”.

Image Segmentation: A process that partitions images into meaningful regions based on certain characteristics or properties such as intensity, color, shape, and/or texture.

Otsu’s Method: A thresholding technique used to determine an optimal threshold value for dividing data into two classes such that the intra-class variance is minimized and the inter-class variance is maximized.

Watershed Transformation: A morphological segmentation method that partitions images based on the gradient regardless of the shape and size of the object.

Section IV

Software Support in Dental Implantology

Chapter X
A New System in Guided Surgery:
The Flatguide™ System

Michele Jacotti
Private Practice, Italy

Domenico Ciambrone
NRGSYS ltd, Italy

ABSTRACT

In this chapter the authors describe a new system for guided surgery in implantology. The aim of this system is to have a "user friendly" computerized instrument for the oral surgeon during implant planning and to have the dental lab included in the decisional process. This system gives him the possibility to reproduce the exact position of the implants on a stone model; the dental technician can create surgical guides and provisional prosthesis for a possible immediate loading of the implants. Another objective of this system is to reduce the economic cost of surgical stents; in such a way it can be applied as a routine by the surgeon.

INTRODUCTION

In this chapter the authors present a new system of implant planning dedicated to guided surgery. They will explain the details of a process that leads from the elaboration of the digital data of a maxillary CT to the creation of surgical stents and provisional prosthesis.

They will try to organize the steps leading to a correct planning of the case and its realization from the surgical and prosthetical point of view.

Setting up the treatment plan.
Creation of the Flatguide™ diagnostic stent.
Acquisition of the digital CT.
OneScan Software 3D phase.
Flatguide™ Implant Planning.
Creation of the Real Volume.
Technical phase.
Surgical phase.
Prosthesic phase.

BRIEF HISTORY OF IMAGE DIAGNOSTIC IN IMPLANTOLOGY

The use of Dentascan in implantology goes back to the second half of the 80'. The first article dealing with the use of CT goes back to 1987.

After only one year, in 1988, the first article describing a system based on surgical stents based on CT appeared.

In the 90's there is the appearance of the first interactive Software for dentistry use.

After that, up to nowadays, one has noticed the more and more systematic appearance of:

- Systems utilizing known angle values and emergency points to be gauged by means of appliances and protractors.
- Robotic systems with radium-mat repere points on the diagnostic stents to gauge the difference between the capture plan and the diagnostic stent creation plan.
- Systems utilizing stereolithographic models to transfer the implant position onto the model;
- Double acquisition systems, with the stent and the maxillary CT with the stent to match the images.

THE NINE STEPS OF THE TECHNIQUE

Setting up the Treatment Plan

In the phase of the visit to the patient the clinician must start to elaborate treatment plans able to solve the needs of the patient himself.

It will be necessary to check the patient's general state of health, and the state of health of the oral cavity. The evaluation of the periodontal situation , in case the patient is not completely toothless, is of vital importance.

One starts from the phase of impressions, of the bite registration and of the facial arc if necessary.

Figure 1. Stent attached over the Flatguide™

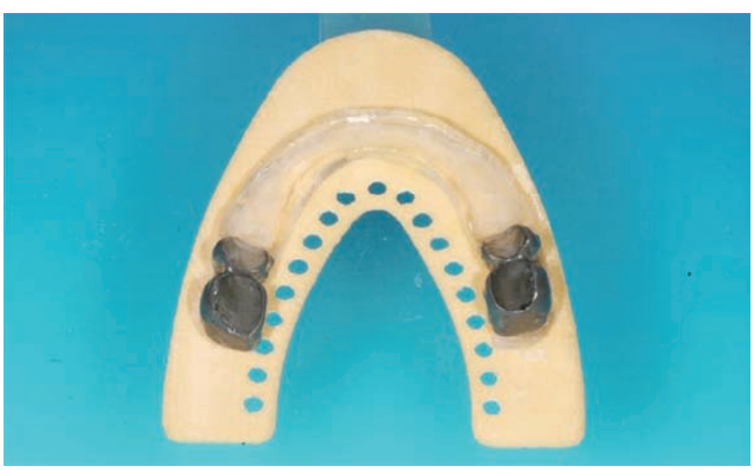

The dentist gives everything to the technician, including the patient's treatment plan.

Once the model has been mounted on the articulator, it twill be necessary to evaluate the feasibility of the project from the biomechanical, aesthetic and functional point of view.

Creation of the Flatguide™ Stent

Once the treatment plan has been established, the technician will realize a diagnostic wax-up reproducing the prosthetic planning on the model. On these data the technician will prepare a diagnostic stent.

One of the peculiar characteristics of the Flatguide™ system is that no kind of particular stent is used. The clinician can go on using the kind of stent he has always used: with barium sulphate teeth, with teeth brushed with dental amalgam powder, or without any specific property.

The only demand that needs attention is to glue a Flatguide™ over the stent. (Figure 1)

Acquisition of CT

The patient must undergo the CT wearing the Flatguide™ stent.

It is necessary to verify that the stent perfectly adheres to the residual teeth or to the mucosa, in the case of a completely edentulous patient. It is of primary importance that the stent in the oral cavity can be always reproducible.

It is advisable to spread some silicon on the Flatguide™ and ask the patient to close his teeth so that the stent is fixed in the correct position..

The dentist must verify that the patient is able to wear the stent by himself in the correct position.

The patient must go to a radiologist centre equipped to supply the CT data in digital form, usually on CD. The axial section data are saved in DICOM format (Digital Imaging and Communications in Medicine).

The DICOM standard is public and its definition is accessible to everybody. It allows the interchange of information between different makers' equipments, server and PC, specific for the biomedical field.

The DICOM data will then be treated by dedicated software.

OneScan 3D Software

The OneScan 3D (www.3dmed.it) software is a program for implant diagnosis and planning based on digital data. It is the only program including the Flatguide™ function.

The functioning of the software subverts the usual characteristics of the various CT based interactive systems. With this system one starts from an automatic 3D reconstruction modifying the acquisition plan if necessary and thus obtaining an insertion of the axial images to perfect the next phase, that is the reconstruction curve of the panorex sections.

Like all the most advanced software, OneScan 3D includes a series of functions, such as the marking of the alveolar nerve, a database of the implants and the abutments and the possibility to evaluate tissue densitometry.

Instead, the three advanced characteristics that differentiate it from the other software are:

- **3D reconstruction:** All the program operations are interactive and based on a real time 3D rendering. The OneScan 3D shows the volume of data acquired through a normal CT scan in an photorealistic way by using the Windows standard PC platform and the most widely used graphical cards (either ATI or nVIDIA). The volume is rendered by setting the proper opacity to each voxel to show the patient's tissues, as selected by the dentist, setting a visible range of values in the Hounsfield scale. The result is enforced by applying to the visible voxels a colormap

Figure 2. 3D reconstruction of the mandibular jaw with OneScan 3D

that better represents the visible tissues and then some lighting effects to obtain a photorealistic rendered image (Figure 2).

All the operations on the volume are in real time.

All the opacity and Hounsfield visibility settings can be changed on-line with an immediate visible result; it is then possible to skim through the tissues filtering their density, pass from soft tissues to hard tissues, from the mucosa to the teeth.

The volume can be “clipped” to analyze the anatomy cross-sections in a realistic way to examine structures of anatomic interest from inside

The overall volume transparency can be set to distinguish details of the different tissues of different density; for example to view the teeth roots while the volume is fully rendered

As well as in other software products, it is the possible to segment the model on various plans, axial and cross sectional, perform any type of measurements on them including density profile along an arbitrary segment

The OneScan 3D software has a simple but powerful “virtual 3D brush” to help the dentist in cleaning the volume from all possible artefacts (say scattering)

- **STL generator:** The OneScan 3D can generate an *stl. file representing the volume rendered as from the current filter settings. This kind of file is used by the firms that deal with prototypization to produce sterelithographic or sintherized three dimensional models.
- **Flatguide™ function:** The function that primarily characterizes the software. Its functioning is described in the next chapter.

Flatguide™ Planning

After loading the digital data with the OneScan 3D software, one goes on with implant planning:

To simplify the planning operation, the volume is first “calibrated” by graphically correcting possible anatomy’s pitch and roll due to a wrong patient’s position during the scan.

The most correct position for the implants is chosen, verifying, if it is there, the position of the prosthetic element reproduced by the diagnostic stent.

Figure 3. Implant planning with the Flatguide™, reconstructed in 3D

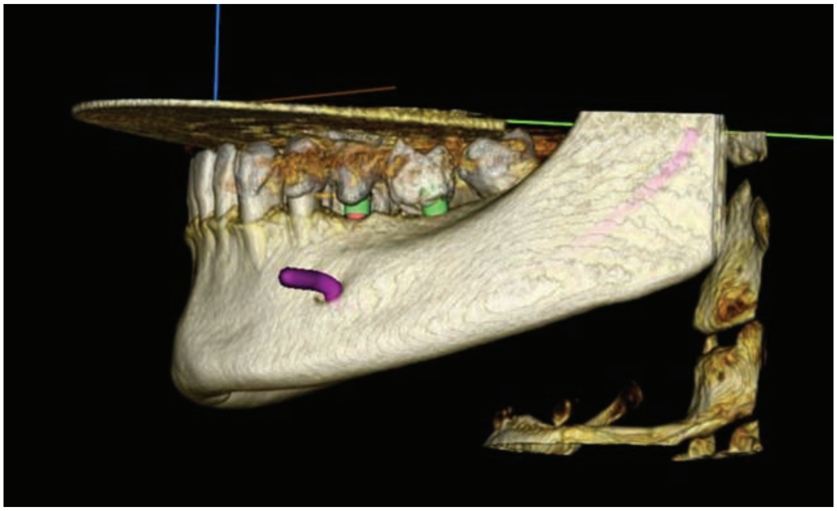

Figure 4. The virtual volume fitting over the Flatguide™

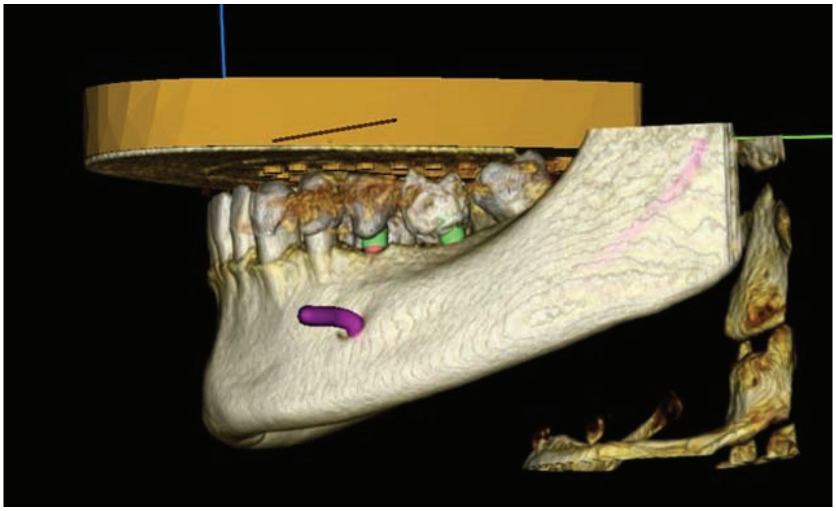

The implant diameter and length are optimized.

The planning effected on cross sectional and panorex is checked on the 3D (Figure 3).

Remember that the 3D image does not suffer from dimensional changes created by a wrong design of the reconstruction curve. The usual panning a zooming tools on all the projections help in this phase. As mentioned, using the "clipping" tool it is possible to section the images to check the implant relations with structures of anatomic interest from inside.

Once the implants are correctly positioned, one goes on with the "virtual stent" phase. The software scans all the axial sections searching for the Flatguide™ holes, and positions them in the next window. After finding the Flatguide™ spatial position it positions a Virtual Volume with the same horseshoe shape, with pins in the place of lingual holes above the Flatguide™ . The Virtual Volume is then shown over the rendered volume. The precision of the automatic positioning, in terms of fitting between the Flatguide™ holes and parallelism between the Flatguide™ and the Virtual Volume layers, is usually very high. The best result can be obtained if all the artefacts have been reduced or removed (virtual 3D brush) and if the volume has been correctly calibrated (see above) to put the Flatguide™ on a seamless horizontal plane (Figure 4).

In case the position of the Volume on the Flatguide™ is not perfect, it is possible to modify it manually orientating the Virtual Volume in space until it ties in perfectly with the Flatguide™. Once again, all the manual adjustment operation are visual and in real time.

Once the correct position of the Virtual Volume on the Flatguide™ has been verified, the program is asked to create the holes on the guide. The software creates the extension of the implants to perforate the Virtual Volume (Figure 5).

Moreover the distance between the Flatguide™ and the fixture-abutment connection is automatically calculated. This measure will turn useful to the technician for the reproduction of the implant depth in the stone model as it gives him the mucosal thickness.

The last phase consists of exporting the Virtual Volume. The spatial position data of the holes inside the Virtual Volume is exported. The information is gathered in a very light file, weighing usually 1 o 2 Kbite. This file is sent by e-mail to the Service Centre that will create the Real Volume. In the OneScan 3D local archive the information relevant to the submitted request is stored; all the Real Volume production and delivery phases are tracked through the Internet.

The result of the planning activity can be reported in an automatically generated *pdf report document than can include dentist's annotations, snapshots from the OneScan 3D operation and/or images coming from any source. The report automatically includes all the images to better visually describe the implants and their position, both in 2D and in 3D.

Creation of the Real Volume

The data sent by e-mail to the Service Centre are elaborated by CAD-CAM software. Trough this

Figure 5. Implant extension perforating the virtual volume

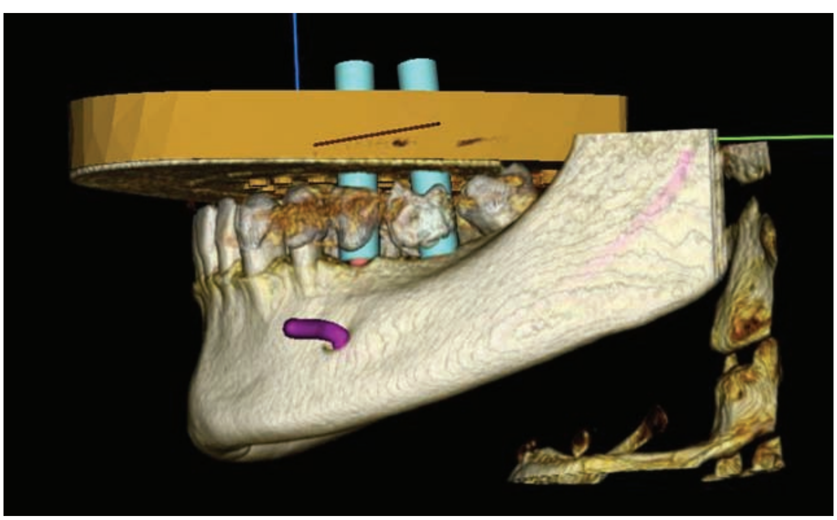

process it is possible to identify the holes reproducing the prolongation of the implant axis in the defined space of the Virtual Volume.

By means of the CAD-CAM technology, the Real Volume, in plastic material, with the reproduction of the implant holes will be obtained.

Inside the holes metal sleeves are inserted, that will be useful to the technician in the successive phase.

The Real Volume is sent to the implantologist by courier.

Technical Phase

As we said above, the dental technician figure is vital in the whole process, from the diagnosis to the prosthesis. As in every team work, the dental lab is involved in every phase.

In the technical phase the technician will receive the Real Volume. The Real Volume will be coupled to the Flatguide™, glued onto the diagnostic stent and positioned on the patient's stone model.

With appropriate drills, one goes through the Real Volume sleeves piercing the Flatguide™, the diagnostic stent and the stone model below (Figure 6).

In this way the correct implant position and axis are created. With a calibrated rod, the implant analog will be positioned inside the stone model, reproducing the distance between the Flatguide™ and the implant head calculated by the software in order to get also the exact depth.

As to the creation of a surgical stent there are two choices:

The more economical and quicker solution that can be used also by the dentist without the technician's support is to pierce the diagnostic stent after superimposing the Real Volume onto the Flatguide™. In the holes created by the appropriate drill some surgical steel sleeves are inserted and the stent will turn from a diagnostic stent to a surgical stent. This system, the quickest and most economic one does not allow the application of depth stops for the mills. The implantologist can avail himself of a spatial guide for the implants, but not for their depth, which he will measure by means of mills with depth notches.

The most complex, but also the costliest solution is to pierce the stone model too, position the

Figure 6. Real volume over the Flatguide™, with the sleeves and the calibrated rod

implant analog in the established spots and depth and use the stone model for the creation of a new surgical stent. With this system, as the implants have the right depth, it is possible to create a stent with depth stops for the mills. All the metal sleeves are positioned in the stent at the same height, usually 10 mm from the implant, including the sleeve thickness. In this way the stent becomes compatible with kits of commercially available surgical drills. For every implant length there will be a proper drill that works as long as it is.

By choosing the second solution, the more refined one, the technician has at his disposal the stone model reproducing the exact position of the implants and the thickness of the mucosa. On this model it is possible to realize any kind of provisional prosthesis, a single tooth, a small bridge, a full arch, and the Toronto bridge prosthesis.

It is important to notice that the system does not assume to supply perfectly correct prosthesis without any kind of tension when positioned in the patient's oral cavity.

One must take into account a certain degree of discrepancy between the implant virtual position on the model and the real position in the patient's cavity.

For this reason it is suggested to create provisional prosthesis with wider preparations so that they can be relined directly in the patient's mouth.

Surgical Phase

The surgical phase takes benefit from the spatial information extracted from the planning and applied to the stent through the Flatguide™ system.

In accordance with his needing the dental technician will prepare stents with different characteristics. Being an open system, without constraints, the technician, based on the dentist instructions, will prepare surgical stents with vertical holders in case he uses drills with holders for flapless surgery, or simple steel guides for a conventional surgery with open flaps. (Figure 7, 8).

As already pointed out above, the Flatguide™ system requires a team work; each step is discussed in advance to optimize results, costs, benefits.

Prosthesic Phase

It is the latest phase, but not for importance.

Figure 7. Surgical stent in situ

Figure 8. Correct implant positioning

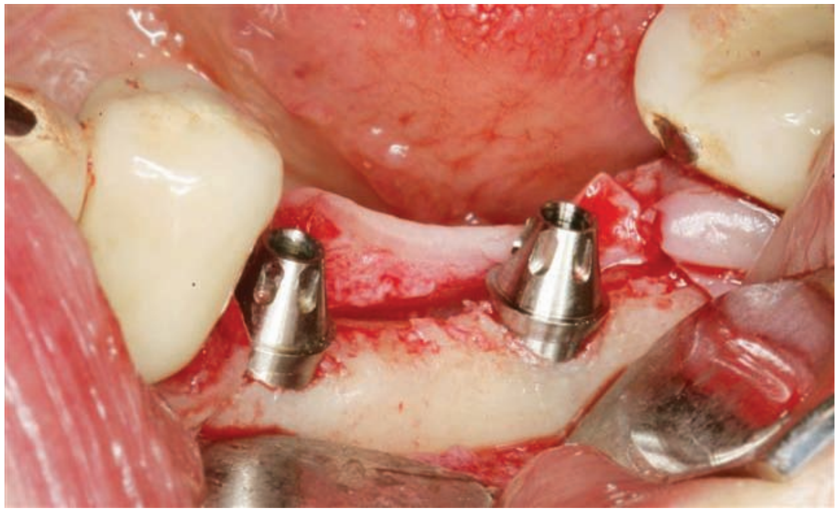

Figure 9. Provisional prosthesis, immediate loading

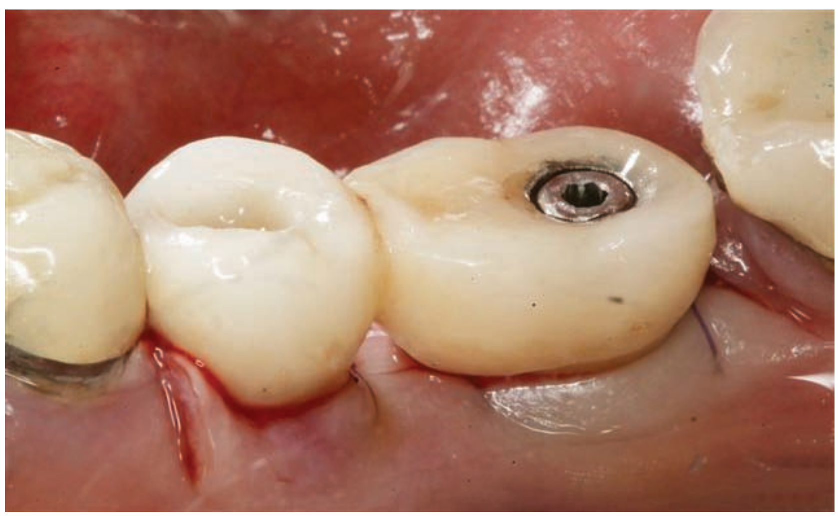

This is the objective of any interactive planning system: to have the prosthesis ended even before you begin the surgery phase!

With the Flatguide™ system it is possible to get the patient's stone model in which to insert the implant analogs each of them at the position and depth planned using the computer software.

On this model the technician can choose the suitable abutments and prepare the temporary prosthesis fitting the requirements coming from the implantologist (Figure 9, 10).

This systematic doesn't claim to provide a prosthesis with precision of 10th of a millimeter. The aim is to provide a stone model with implant analogs positioned in such a way to allow the technical to create provisionals slightly larger than the size of the implant's abutments. The provisional prosthesis, ranging from single crown, to the

Figure 10. Final ceramic restoration

bridge, to the Toronto type bridge prosthesis, will be relined directly in the patient's mouth.

Relining the prosthesis directly in the mouth of the patient, we will eliminate all the tensions we inevitably get by building a prosthesis on a model, stereolithographic or in stone, even before the surgery phase.

CONCLUSION

The Flatguide™ system, matched with OneScan 3D software, has revealed itself very simple to be used also for the General Practitioner. It does not need any calculation and the software is very immediate and self explaining; it has been studied to be used every day. The characteristic of not excluding the technician turns out to be added value. The technician starts cooperating in the diagnostic phase and ends in the definitive prosthesis phase, acting as part and parcel in every intermediate step. The quality of the images, particularly in 3D reconstructions, offers the clinician an excellent diagnostic instrument besides being useful in implant planning. It is therefore an excellent instrument of communication and marketing with the patients.

Last, but not least, the cost of a single stent is limited to the creation of a Real Volume, whose cost is today about 80-90€. With a limited cost it is possible to rehabilitate a whole arch.

REFERENCES

Balshi, S. F., Wolfinger, G. J., & Balshi, T. J. (2006). Surgical planning and prosthesis construction using computer technology and medical imaging for immediate loading of implants in the pterygomaxillary region. *Int J Periodontics Restorative Dent.* Jun, *26*(3), 239-47.

Campbell, D. J. (2001). The use of cross-sectional spiral tomography in the placement of implants. *N Z Dent J.* Jun, *97*(428), 49-51.

Cannizzaro, G., Leone, M., & Esposito, M. (2007). Immediate functional loading of implants placed with flapless surgery in the edentulous maxilla: 1-year follow-up of a single cohort study. *Int J Oral Maxillofac Implants.* Jan-Feb, *22*(1), 87-95.

Cheng, A. C., Tee-Khin, N., Siew-Luen, C., Lee, H., & Wee, A. G. (2008). The management of a severely resorbed edentulous maxilla using a bone graft and a CAD/CAM-guided immediately loaded definitive implant prosthesis: a clinical report. *J Prosthet Dent.*, *99*(2), 85-90.

Engelman, M. J., Sorensen, J. A., & Moy, P. (1988). Optimum placement of osseointegrated implants. *J Prosthet Dent, 59*(4), 467-73.

Frederiksen, N. L. (1995). Diagnostic imaging in dental implantology. Oral Surg Oral Med Oral *Pathol Oral Radiol Endod.* Nov, *80*(5), 540-54. Review.

Ganz, S. D. (2007). CT-derived model-based surgery for immediate loading of maxillary anterior implants. *Pract Proced Aesthet Dent.* Jun, *19*(5), 311-8; quiz 320, 302.

Jeffcoat, M. K. (1993). Application of digital radiography to implantology. *J Dent Symp.* Aug, *1*, 30-3.

Kupeyan, H. K., Shaffner, M., & Armstrong, J. (2006). Definitive CAD/CAM-guided prosthesis for immediate loading of bone-grafted maxilla: a case report. *Clin Implant Dent Relat Res.*, *8*(3), 161-7.

Lam, E. W., Ruprecht, A., & Yang, J. (1995). Comparison of two-dimensional orthoradially reformatted computed tomography and panoramic radiography for dental implant treatment planning. *J Prosthet Dent.* Jul, *74*(1), 42-6.

Maló, P., Rangert, B., & Nobre, M. (2005). All-on-4 immediate-function concept with Brånemark System implants for completely edentulous maxillae: a 1-year retrospective clinical study. *Clin Implant Dent Relat Res.*, 7(Suppl 1), S88-94.

Marchack, C. B. (2005). An immediately loaded CAD/CAM-guided definitive prosthesis: a clinical report. *J Prosthet Dent.* Jan, *93*(1), 8-12.

Marchack, C. B. (2007). CAD/CAM-guided implant surgery and fabrication of an immediately loaded prosthesis for a partially edentulous patient. *J Prosthet Dent.* Jun, *97*(6), 389-94.

Marchack, C. B. (2008). Complications of Computer-Aided-Design/Computer-Aided-Machining-Guided (NobelGuidetrade mark) Surgical Implant Placement: An Evaluation of Early Clinical Results. *Clin Implant Dent Relat Res.*

Reddy, M. S., Mayfield-Donahoo, T., Vanderven, F. J., & Jeffcoat, M. K. (1994). A comparison of the diagnostic advantages of panoramic radiography and computed tomography scanning for placement of root form dental implants. *Clin Oral Implants Res.* Dec, *5*(4), 229-38.

Rocci, A., Martignoni, M., & Gottlow, J. (2003). Immediate loading in the maxilla using flapless surgery, implants placed in predetermined positions, and prefabricated provisional restorations: a retrospective 3-year clinical study. *Clin Implant Dent Relat Res.*, 5(Suppl 1), 29-36.

Sanna, A., Molly, L., & Van Steenberghe, D. (n.d.). Immediately loaded CAD-CAM manufactured fixed complete dentures using flapless implant placement procedures: A cohort study of consecutive patients. *The Journal of Prosthetic Dentistry*, *97*(6), 331 – 339.

Van Steenberghe, D., Glauser, R., Blombäck, U., Andersson, M., Schutyser, F., Pettersson, A., & Wendelhag, I. (2005). A computed tomographic scan-derived customized surgical template and fixed prosthesis for flapless surgery and immediate loading of implants in fully edentulous maxillae: a prospective multicenter study. *Clin Implant Dent Relat Res.*, 7(Suppl 1), S111-20.

KEY TERMS

CAD: Computer-aided design is the use of computer technology to aid in the design and especially the drafting of a part or product. It is both a visual (or drawing) and symbol-based method of communications whose conventions are particular to a specific technical field. Nel software OneScan 3D viene utilizzata solo la componente visuale.

CAM: Computer-ided manufacturing is the use of computer-based software tools that assist engineers and machinists in manufacturing or prototyping product components. CAM is a programming tool that allows you to manufacture physical models using computer-aided design (CAD) programs. CAM creates real life versions of components designed within a software package. The Real Volume is creating using CAM techniques.

Computer Assisted Surgery: (CAS) represents a surgical concept and set of methods, that use computer technology for presurgical planning, and for guiding or performing surgical interventions. CAS is also known as computer aided surgery, computer assisted intervention, image guided surgery and surgical navigation, but these terms that are more or less synonyms with CAS.

CT: Computed tomography (CT) is a medical imaging method using tomography. Digital geometry processing is used to create a three-dimensional image of the inside of an object from a large series of two-dimensional X-ray images taken around a single axis of rotation. The word "tomography" is derived from the Greek *tomos* (slice) and *graphein* (to write).

DICOM: Digital **I**maging and **Co**mmunications in **M**edicine. Is a standard for handling, storing, printing, and transmitting information in medical imaging. It includes a file format definition and a network communications protocol. The communication protocol is an application protocol that uses CTP/IP to communicate between systems. DICOM files can be exchanged between entities that are able of receiving patient data in DICOM format.

Flapless Surgery: The surgery without opening flaps. The surgical template will drive the drill through the soft tissues and will stop the drill at the correct depth. It's a painless surgery, very well accepted by the patient.

Immediate Loading: When it is possible to give an adequate primary stability to the implants it is possible load them immediately. The implants stability is measured through the tightening torque. A value higher then 35N/cm will ensure the possibility to perform the implant. To do this the implantologist can perform some under-preparations of the site in order to increase the bone stability.

Implant Planning: The planning activity before a surgical intervention. It is usually performed over CT data. The best results can be obtained, today, through dedicated implantology software applications.

STL: Is a file format native to the stereolithography CAD software. This file format is supported by many software packages; it is widely used for rapid prototyping and computer-aided manufacturing. STL files describe only the surface geometry of a three dimensional object without any representation of colour, texture or other common CAD model attributes. The STL format specifies both ASCII and binary representations.

Chapter XI
Visualization and Modelling in Dental Implantology

Ferenc Pongracz
Albadent, Inc, Hungary

ABSTRACT

Intraoperative transfer of the implant and prosthesis planning in dentistry is facilitated by drilling templates or active, image-guided navigation. Minimum invasion concept of surgical interaction means high clinical precision with immediate load of prosthesis. The need for high-quality, realistic visualization of anatomical environment is obvious. Moreover, new elements of functional modelling appear to gain ground. Accordingly, future trend in computerized dentistry predicts less use of CT (computer tomography) or DVT (digital volume tomography) imaging and more use of 3D visualization of anatomy (laser scanning of topography and various surface reconstruction techniques). Direct visualization of anatomy during surgery revives wider use of active navigation. This chapter summarizes latest results on developing software tools for improving imaging and graphical modelling techniques in computerized dental implantology.

INTRODUCTION

In this chapter the author give his experiences gained developing visualization and graphical modelling tools in applications for computerized dental implantology. Intensive development efforts can be seen worldwide on the field of image-guided navigation systems applied in dental implantology. Several commercial products are available on European market (Simplant®, www.materialise.com; coDiagnostiX®, www.ivs-solutions.de; Denx®IGI, www.denx.com; ARTMA

Virtual Implant®, www.landsteiner.org; Galileos Implant Guide, www.sirona.de, Dental Planner, Albadent Inc.). Drawbacks and advantages of technology in dentistry and oral surgery for the last decade are surveyed by several laboratories (Siessegger et al, 2001, Ewers et al, 2005). The computerized implantology evolves into two directions: 1/ surgery support with prefabricated templates; 2/ active, image guided navigated drilling. In case of surgical template preparation of both the registration and drill calibration can be made outside of operation room in a stress-free environment. This improves accuracy; however, other problems like template fixing to patient's jaw, complete absence of interactive control of drill's orientation in space make the future of this method uncertain. In case of active, intraoperative navigation, the lack of experience, poor software support for synchronization of real and virtual environments sometimes overburden the surgeon. Future trend in computerized dentistry predicts less use of direct diagnostic imaging and more use of 3D visualization of anatomy (laser scanning of topography and various surface reconstruction techniques). Functional modelling is now possible with tooth surface database and simulation of occlusal properties (Pongracz and Bardosi, 2006). Modern visualization methods like resampling the slice sequence in CT and MR diagnostic volumes, combined views of surface topography and mesh surfaces support the modelling. These new approaches help in direct visualization of anatomy during surgery that revives wider use of active navigation in the future.

The accuracy of dental hand piece tracking in active navigation highly depends on the alignment method between diagnostic and surgical spaces (REGISTRATION) and the alignment procedure between tool's own coordinate space and the coordinate space of attached sensor (CALIBRATION). Well designed computational approach is needed for calibration of dental hand piece with small and unique geometry (Bardosi and Pongracz, 2007, Pongracz et al, 2007).

GRAPHICAL MODELLING

Data Sources

Conventional (CT) and cone beam computer tomography (CBCT) are generally used for 3 dimensional dental imaging. Recent results have controversial results regarding optimization of image characteristics (artifacts reduction versus density resolution) by using CT and CBCT technologies (Humpries et al, 2006, Katsumata et al, 2007). In our studies the patient imaging data are read in from both CT and CBCT sequences and stored as volumetric model (Xoran Technologies: i-CAT 3D Dental Imaging, GE Medical Systems: HiSpeed NX/i). Reslicing algorithm is frequently included to generate slice view in arbitrary cutting plane orientation. Bone surface models are created by isosurface raytracing algorithm or marching cubes algorithm. Mesh surfaces can be imported for adding gips model topography and realistic model of implants. The surface models can be clipped to see interaction of surfaces with volumetric data and visualize the details of interocclusal relationships.

Tooth Database

This is a really difficult issue because the fine, realistic details of intercusp relations are important for dental planning and their presence in the program gives an impression of the real environment for the dentist. The realistic graphics helps in navigating within the virtual scene for medical personnel even if he doesn't like working with computers. The CT imaging was performed on teeth of undamaged surfaces taken from the same cadaver skull. The teeth had no metal filling. The surface reconstruction was made by marching cubes (Lorensen and Cline, 1987) and decimator algorithms to find polygons and set their number to a reasonable level (Figure 1). The ideal positions and the 3D surface models of each tooth are stored and added during initialization (read in from compressed file package). Their locations are rendered to the standard dentition curve (represented as cubic spline connecting the surface centers of teeth). The coordinates are based on detailed anatomical description of articulation of dental curves and classification of the permanent dentition which are available for a long time (Massler and Schour, 1958). Local alignment and scaling of each tooth is possible within the ideal occlusal reference frame on separate panels for mesiodistal (transversal) and faciolingual (tangential) inclinations. These are related to the actual tangent and normal planes of the upper or lower dentition curves. Similar database has been created by others (Hassan et al, 2005, Krsek et al, 2007) but without using globally structured datasets based on ideal dental curves.

Dentition Planning

Latest effort in software development reveals that functional modelling is possible within the diagnostic environment with some novel graphical features (Pongracz et al, 2005, Pongracz and Bardosi, 2006). The goal is to simulate the function of articulator used in conventional design of prosthesis. The optimal dental occlusion is estimated according to the condition of centric occlusion i.e. after bringing occlusal surfaces of mandible and opposing maxillary arch into identical centered position. This identical position of occlusal surfaces is set by triangles in the program, and—after appropriate resampling (interpolation of images according to the triangles' normal vectors) of the CT volume—the diagnostic estimate for an ideal interocclusal relationship

Figure 1. Tooth surface database from cadaver teeth. Each tooth model was reconstructed from CT data with marching cubes algorithm and decimated to 5000 triangles. After reconstruction they were placed into a global coordinate space defined by occlusal triangles. The triangles for the upper and lower jaws are in the same position and size according to ideal centric occlusion. Spline curves, - crossing the occlusal triangles' vertices - added to initialize dentition curves. The shape of dentition curves is controlled by moving the triangles' vertices in 3 dimensions. Each tooth model can be locally moved, rotated relative to their initial location on dental curve. Each tooth has own anatomical coordinate space and their shape can be rescaled along any of local axes.

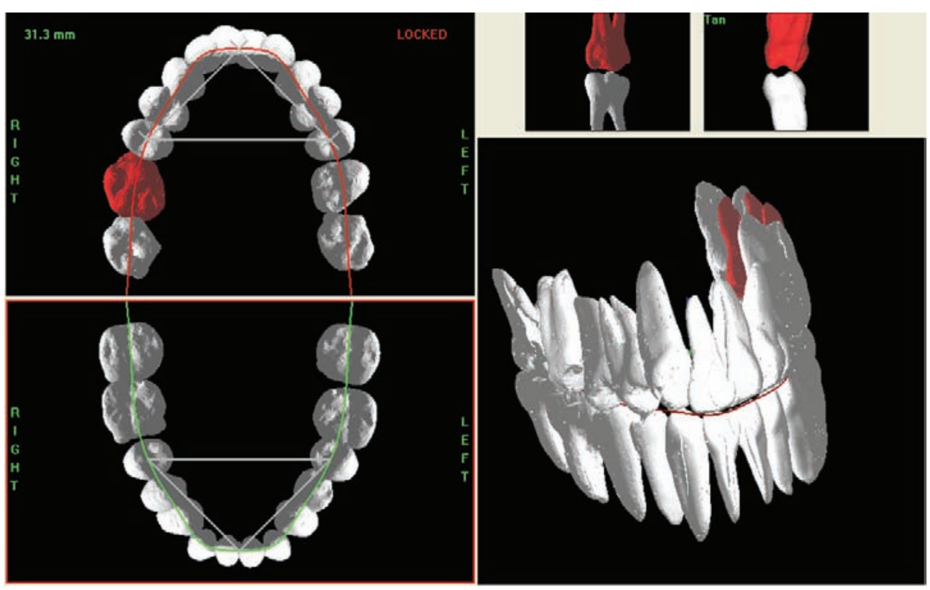

can be created (Figure 2). The original volume is divided into two subvolumes during resampling: first one is defined above the maxillary triangle and the second one is under the mandibular triangle. These two subvolumes are merged into a single one for analysing local relationships. This resampled volume now determines the common reference frame for all manipulation of tooth and implant models and helps in implant placement (Figure 3). Local alignment is made on separate planes for mesiodistal and faciolingual inclinations. These local views display the resampled image together with tooth models (from database) to predict small details for contact areas. The tooth models can be scaled, rotated and shifted in 3D to fit patient's anatomy.

Topographic Modelling

The information on the shape of mucous soft tissue is added to the graphical scene after laser scanning the gips model or other negative impression taken from the mouth. The mesh surface of gips model is registered to CT diagnostic data and visualized with or without the bone surface. Important element of the topographic modelling is the clipping and contur tracing algorithms together with an appropriate texture mapping onto planes or surface meshes. The effective use of these new methods needs special programming technique based on OpenGL (OpenGL 2.1: www.opengl.org/documentation/) or DirectX (The DirectX SDK: http://msdn.microsoft.com) graphical libraries and suitable hardware support. The conventional, CPU based programming can slow down the output causing large delay in visualization that hinders these new methods from surgical planning.

The bone surface is first reconstructed by segmentation and marching cubes algorithms which are available in several third party applications (Osirix Mac OSX version is used in this article). After it the exported model of bone surface, which is automatically aligned with CT data, can be included in modelling. The 3D scene now contains several graphical elements, such as

Figure 2. Modelling centric occlusion in diagnostic environment. The 3D volumetric resampling is performed separately for the upper and lower subvolumes (maxilla and mandible) above the upper triangle and under the lower triangle, respectively.

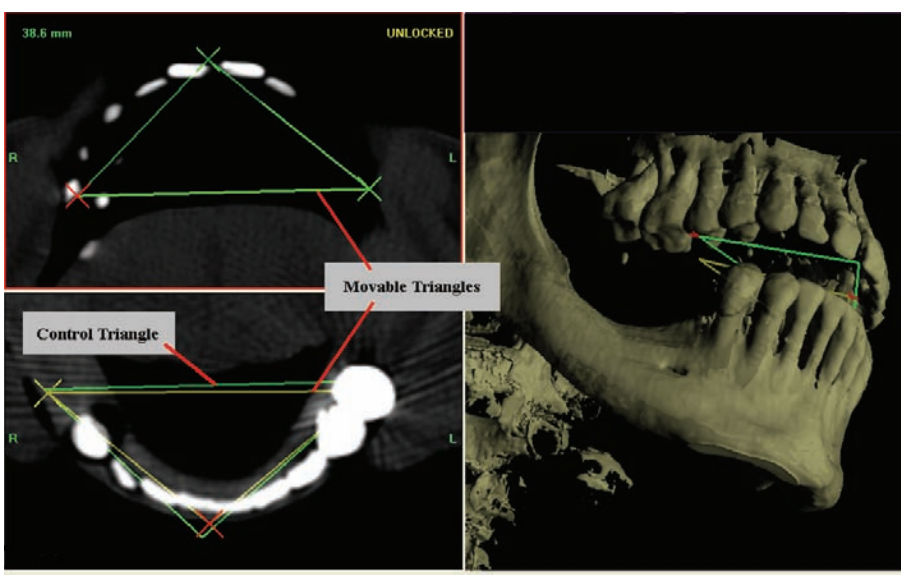

Figure 3. Modelling local interocclusal contacts in resampled volume (a and b: transversal and tangential planes). Implant planning has been made in parallel with dentition planning. The surface model (c and d) is given according to the original volume sampling in CT and shows the final results of planning.

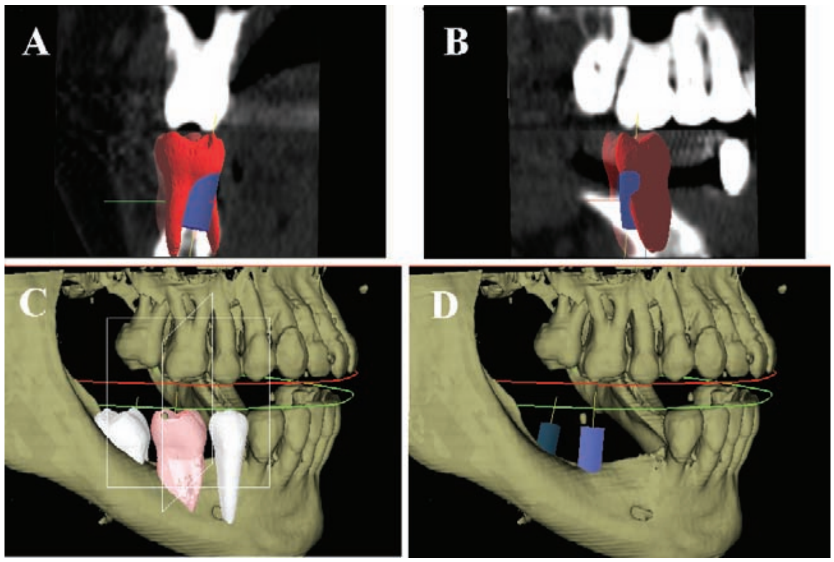

surface mesh of the gips model for soft tissue representation, bone surface, CT volumetric model, implants, virtual hand piece for active navigation and clipping planes for interactive visualization of internal structures.

Following figures show samples of texture mapping onto the clipping plane defined on the registered model of soft tissue (Figure 4a). The critical procedure for implant localization can be greatly simplified. The optimum software implementation of previous calculation utilizes the power of 3D texture programming and graphics accelerator card. The real-time calculation and visualization of resampled CT images give a chance for fast, convenient diagnostic analysis.

Bone Clipping

The reconstruction of bone surface of the maxillofacial area is usually difficult because of frequent artifacts seen in CT images. The marching cubes algorithm (Lorensen and Cline, 1987) generates noisy surface with abundant components in mesh. Several approaches are known to decrease artifacts and improve surface reconstruction (Bazalova et al, 2007, Krsek et al, 2007, Yongbin et al, 2007, Beaulieu and Yazdi, 2006). The visibility of complex region at tooth-jaw bone transitions can be greatly enhanced by clipping at critical locations. The relationship between the topographic and bone surfaces can be analysed and small details visualized by plane and volume clippings. This procedure enhances the visibility of critical layer between the bone surface and the surface of mucous soft tissue. The clipping can be performed in real time synchronized or unsynchronized to the implant alignment procedure. The unclipped surface models of bone and soft tissue are usually displayed in noisy 3D scene with disturbing metal artifacts. The hidden elements of the implant base and abutment tool can be made visible with clipping planes. Figures 4B and C illustrate the results after clipping with transversal and horizontal planes. Both clipping interactions are locked to the actual position and orientation of implant. Further clipping is possible by volumes

Figure 4. (a) Topographic modelling with vertical and horizontal clipping planes, contur detection with soft tissue surface and CT texture mapping (both clipping planes are locked to implant and can be moved in real-time). (b) and (c): Clipping with transversal and horizontal planes. The clipping is applied for registered models of bone (white) and surface of soft tissue (green). Distance analysis between the bone surface and soft tissue is possible by appropriate compression and expansion algorithms applied to the surface representing soft tissue.

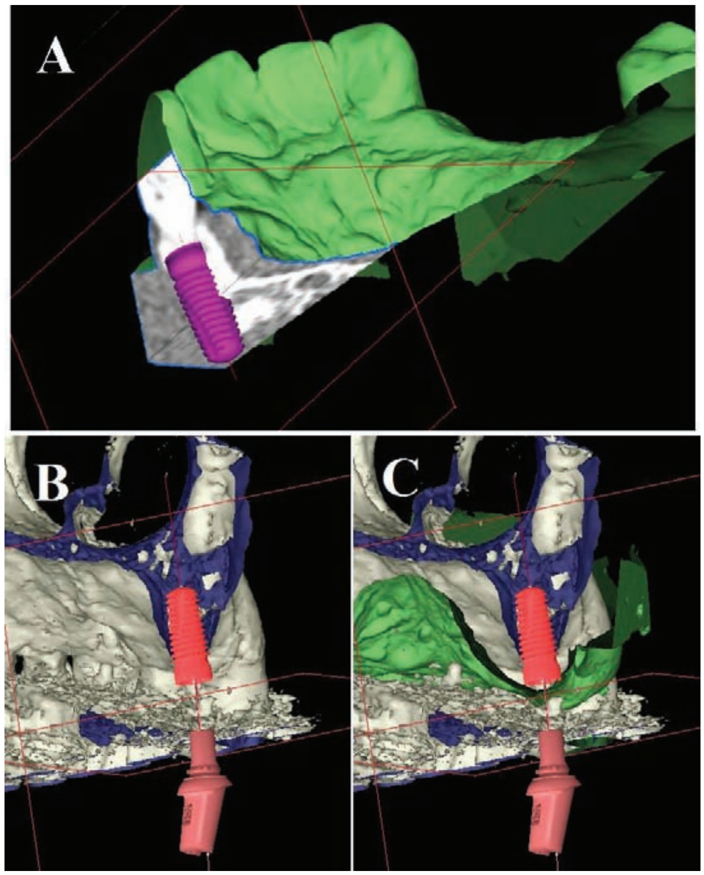

with resizable edges. Graphical manipulations (clipping plane rotation around the implant axis, resizing of volume clip edges near the implant) help in detailed visualization. Surface expansion and compression tools can be easily implemented in this environment to support distance analysis between the bone surface and soft tissue. This analysis can give valuable information for surgery. At this time the real-time clipping technique is more acceptable in practical applications than any filtering or image pre-processing method.

HAND PIECE NAVIGATION CONTROL

Previous results of graphical modelling and visualization can be validated in active navigation after the registration of surgical space and drill calibrations have been done. The registration to the CT volume can be performed with the help of surface fiducials located on the template (Figure 5a). The registration should be handled as SVD ("singular value decomposition") problem and this way, even with ill-defined marker positions, a least-square estimate always can be found for the registration matrix (Arun et al, 1987, Press et al, 1992).

The hand piece calibration has three steps (using optical tracking with passive sensors):

1. Tip offset vector calculation is based on the known pivoting procedure (Bardosi and Pongracz, 2007, Pongracz et al, 2007) and gives back results with accuracy under 0.2 mm (mean sqrt variation from pivoting, 50-100 samples);
2. Drill axis direction was estimated by surface scanning (50-200 samples) with the pointer; the estimated projection error remained in the range of 0.15-0.2 mm;
3. Final orientation of tool's space is aligned to the tool's geometry (handle position) by the pointer of the tracking system.

This procedure is flexible and accurate enough to use for small dental hand piece and also usable in many cases during research and development period of navigation systems.

Tip offset vector calculation. The drill calibration (both for template drilling and active navigation) is based on the known pivoting procedure (tip offset vector calculation) (Figure 5b).

Tip offset calculation steps:

- Sampling data by rotating the tool around the tip;
- All points lie on a tip-centered sphere;
- Task: find the center point (tip offset) (**t**);

$$\mathbf{A} = \begin{bmatrix} x_2 - x_1 & \cdots & x_n - x_{n-1} \\ y_2 - y_1 & \ddots & y_n - y_{n-1} \\ z_2 - z_1 & \cdots & z_n - z_{n-1} \end{bmatrix}$$

$$B = \frac{1}{2}\begin{bmatrix} x_1^2 + y_1^2 + z_1^2 \\ \vdots \\ x_n^2 + y_n^2 + z_n^2 \end{bmatrix}$$

$$\min_x \|\mathbf{At} - \mathbf{B}\|$$

- SVD problem

Drill axis calculation. The second phase of the calibration (axis direction) starts with data capture on that part of device which has a cylinder shape with an axis identical with the tip direction. An optimization algorithm (Levenberg-Marquardt method; Press et al., 1992) was implemented which uses the output of data capture made by the random move of the pointer on the tool cylinder (Figures 5c and d). This optimization procedure projects first the random surface points onto the plane centered by the tip offset vector which was determined during the pivoting phase. The 3D projection transform for the actual axis direction is calculated from two orientation angles. These angles are the parameters to be optimized. On output the axis calibration procedure gives back the orientation angles for the tip axis, the cost value at optimum and the estimated diameter of the fitted cylinder.

Tool axis calibration algorithm:

- 2 rotation angles used to define „projection plane", relevant to the problem (Φ, Ψ);
- Center the data origin to the tip offset (preset during tip offset pivoting);
- Cost function is the empirical variance of the distances of the projected points from the origin, as related to the rotation angles:

$$C(\varphi, \Psi) = \frac{1}{N}\sum_{i=1}^{N}\left[\mu\,(R_{\varphi,\Psi}\,p) - R_{\varphi\Psi}\,p^i\right]^2$$

$$\mu(R_{\varphi,\Psi}\,p) = \text{tip offset} \qquad (\varphi, \Psi) \in \left[-\frac{\pi}{2}; \frac{\pi}{2}\right]^2$$

where $R_{\varphi,\Psi}$ is the rotation/projection matrix.

The final orientation of tool's space can be aligned to the tool's geometry (handle position) by an up-vector defined by the pointer.

Figure 5. Registration and drill calibration controls in the navigation panel of dental planning and navigation program. (a) Typical arrangement of registration panel. The registration procedure is marker-based with accuracy in the range of 0.3 to 0.6 mm. The patient is scanned in CT lab with a template containing four fiducials. (b) Tip offset calibration for navigated drill. The offset vector points from the sensor's space origin to the drill tip. (c) and (d): Axis vector calibration of small dental hand piece. The system reads in location and orientation values for tool sensor and pointer sensor during the random move of the pointer on drill head.

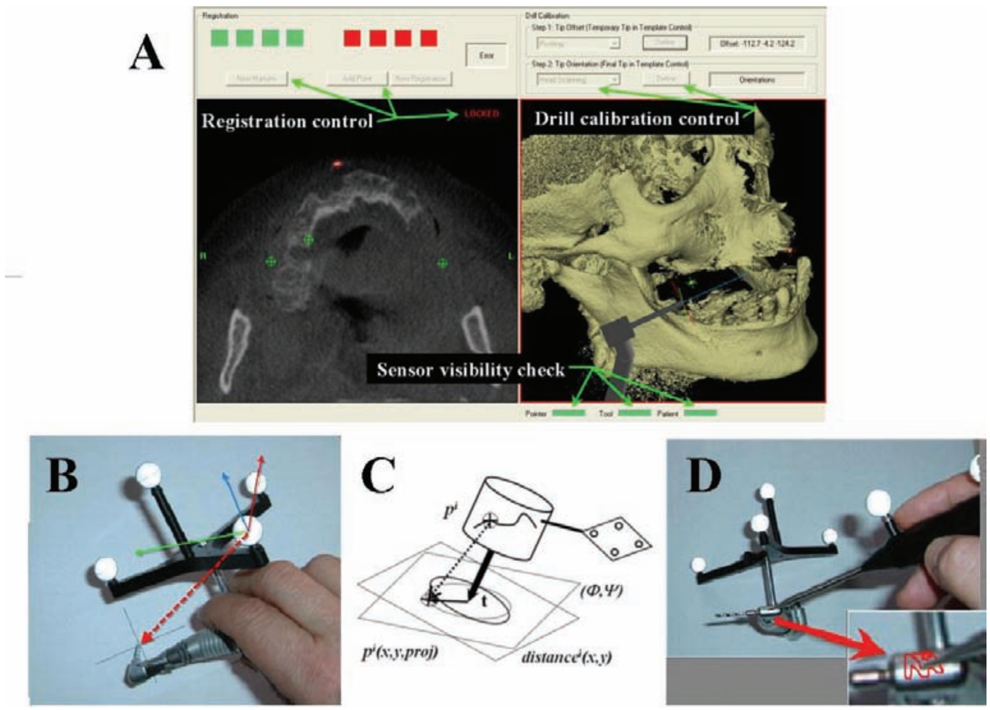

SYSTEM DESIGN FOR ACTIVE NAVIGATION

The architecture of the software implementation can follow different principles: 1/ modular design with panels reflecting well distinguished steps in surgical workflow; 2/ highly simplified view integrating several steps in workflow. The latest development in computer hardware offers powerful support for real-time graphical programming (Burdea and Coiffet, 2003). The improved quality and fast, direct visualization of anatomy during surgery revives wider use of active navigation. Modern programming techniques with hardware accelerators help to improve applications for surgical planning. Large volumetric or surface models can be moved, clipped or resampled (recalculated according to non-standard sampling directions) in real time. The interaction of different diagnostic models can be visualized with fine details. Communication with new peripherals like 3D mouse can make the graphical manipulation of virtual scenes more and more acceptable for medical personnel and will have an increasing impact on dentistry in the future (Huff et al, 2006).

The inadequate drill calibration methods can influence the accuracy of active navigation of small dental hand piece. Therefore, generally usable calibration procedure is needed, which, by means of the methods known in reverse engineering, accurately estimates the tip offset and axis direction of navigated device relative to the space of an attached motion sensor. An implementation of modular calibration for improved accuracy control has been described in this article. This method gives stable output without the use of prefabricated adapter clamps known in commercial systems.

CONCLUSION

Novel visualization and modelling techniques have been summarized for use in field of dental implantology. New graphical tools have been presented for functional modelling. Latest modelling incorporates inter-occlusal analysis of teeth contacts and simulation of dentition together with virtual implant positioning. The critical relationship between the jaw bone surfaces and the mucous soft tissue can be visualized. An implant planning and navigation system has been developed which implements the new features presented in this article.

ACKNOWLEDGMENT

The author thanks to Dr. M. Truppe (Karl Landsteiner Institute, Vienna) for medical advices, Zoltán Bárdosi (Eötvös Lóránd University, Budapest) for help in software development and Northern Digital Europe GmbH (Radolfzell, Germany) for supplying us with the Polaris system. This work was supported in part by the Bureau of National Research and Development in Hungary under the combined EU/hungarian grant GVOP-3.3.3-05/1.-2005-0002/3.0.

REFERENCES

Arun, K. S., Huang, T. S., & Blostein, S. D. (1987). Least square fitting of two 3-D point sets. *IEEE Trans Patt Anal Machine Intell (PAMI), 9*, 698-700.

Bardosi, Z., & Pongracz, F. (2007). Flexible drill/endoscope calibration method for navigation. *Proc.of 4th International Conference on Computer Aided Surgery Around the Head*, Innsbruck, (pp. 11-13).

Bazalova, M., Beaulieu, L., Palefsky, S., & Verhaegena, F. (2007). Correction of CT artifacts and its influence on Monte Carlo dose calculation. *Medical Physics*, *34*(6), 2119-32.

Beaulieu, L, & Yazdi, M. (2006). Method and apparatus for metal artifact reduction in computed tomography. *Patent Pub. No.: WO/2006/039809 (US), PCT/CA2005/001582 (Int.)*

Burdea, G. C., & Coiffet, P. (2003). *Virtual reality technology, (2nd Ed.) with CD-ROM.* New York: Wiley.

Ewers, R., Schicho, K., Undt, G., Wanschitz, F., Truppe, M., Seemann, R., & Wagner, A. (2005). Basic research and 12 years of clinical experience in computer-assisted navigation technology: a review. *International Journal of Oral and Maxillofacial Surgery, 34*, 1-8.

Hassan, H. et al. (2005) A volumetric 3D model of the human jaw. *Proceedings of 19th International Congress and Exhibition of CARS2005, Berlin, Germany, Elsevier ICS 1281,* 1244-49.

Huff, R., Dietrich, C. A., Nedel, L. P., Freitas, C., Comba, L. D., Olabarriaga, S. D. (2006). Erasing, digging and clipping in volumetric datasets with one or two hands. *VRCIA'06 Proceedings of the 2006 ACM int. conf. on Virtual reality continuum and its application, Hong Kong,* 271-278.

Humphries, S., Christensen, A., & Bradrick, J. (2006). Cone beam versus conventional computed tomography: comparative analysis of image data and segmented surface models. *International Journal of CARS (Computer Assisted Radiology and Surgery), Suppl. 1,* 398-400.

Katsumata, A., Hirukawa, A., Okumura, S., Naitoh, M., Fujishita, M., Ariji, E., & Langlais,R. P. (2007). Effects of image artifacts on gray-value density in limited-volume cone-beam computerized tomography. *Oral Surg Oral Med Oral Pathol Oral Radiol Endod*, *104*, 829-36.

Krsek, P., Spanel, M., Krupa, P., Marek, I., & Cernochov, P. (2007). Teeth and Jaw 3D Reconstruction in Stomatology. *Medical Information Visualisation – BioMedical Visualisation, MediVis 2007,* 23-28.

Lorensen, W. E., & Cline, H. E. (1987). Marching cubes: A high resolution 3D surface construction algorithm. *Computer Graphics (SIGGRAPH '87 Proceedings), 21,* 163-169.

Massler, M. & Schour, I. (1958). *Atlas of the Mouth*. Chicago: American Dental Association.

Pongracz, F., Bardosi, Z., & Szabo, L. (2005). Dentition planning for image-guided implantology. In *Proc. of CARS (Computer Assisted Radiology and Surgery), International Congress Series, Chicago, 1268*, (pp. 1168-1173).

Pongracz, F., & Bardosi, Z. (2006). Dentition planning with image-based occlusion analysis, *International Journal of CARS (Computer Assisted Radiology and Surgery)*, *1*(3), 149-156.

Pongracz, F., & Bardosi, Z. (2007). Navigated drilling for dental implants based on virtual occlusion analysis: presentation of a new approach. *Proc.of 4th International Conference on Computer Aided Surgery Around the Head*, Innsbruck, (pp. 125-127).

Pongracz, F., Szabo, L., & Bardosi, Z. (2007). Planning and navigation tools for dental implantology. *Proc.of Automatisierungstechnische Verfahren für die Medizin Nr.267,* München, (pp. 41-42).

Press, W. H., Teukolsky, S. A., Vetterling, W. T., & Flannery, B. P. (1992). *Numerical Recipes in C. The Art of Scientific Computing.* Cambridge: Cambridge University Press.

Siessegger, M., Schneider, B. T., Mischkowski, R. A., Lazar, F., Krug, B., & Klesper, B. (2001). Use of an image-guided navigation system in dental implant surgery in anatomically complex operation sites. *J Craniomaxillofac Surg, 29,* 276-81.

Yongbin, Z., Lifei, Z., Zhu, X. R., Lee, A. K., Chambers, M., & Lei, D. (2007). Reducing metal artifacts in cone-beam CT images by preprocessing projection data. *Int. J. Radiation Oncology, Biology, Physics. 67,* 924-932.

KEY TERMS

Active Navigation: The type of surgical interaction where the surgical tool is moved under continuous 3D motion tracking on a motion path which is selected freely by the surgeon.

Centric Occlusion: The ideal, closed position of upper and lower jaws. The teeth contacts in this case represent the ideal relationships in the mouth.

Hardware Accelerator: The name of an internal element of computer hardware which supports the visualization of complicated 3D graphics.

Maxilla and Mandible: Upper and lower jaws, respectively.

Open GL: The name of a graphical library which is frequently used during software development with complex 3D visualizations.

Optical Tracking: It is a procedure where the motion of a rigid object is continuously followed by cameras through sensors attached rigidly to the object.

Surface Model: Mathematical representation of surfaces. Ordered sequence of large number of small polygons (usually triangles) which can be placed in 3D graphical scene created by programming.

Surgical Template: Supporting tool or guide to help surgical interaction by guiding tools into the target position. Computerized dental implantology uses frequently this approach to prepare implant placement into jaw.

Tip Offset in Navigation: The 3D vector representing the offset from the origo of an attached motion sensor to the tip of the navigated drill. The tip offset vector is defined in the local coordinate space of the attached sensor.

Tip Direction in Navigation: The 3D axis vector representing the direction of the drill axis within the coordinate space of the attached motion sensor.

Topographic Surface: The surface which represents 3D variability of shape of an object. Laser topography can be created by laser scanning of the visible surface of an object made from hard material.

Volumetric Model: Mathematical representation of 3D grid consisting of voxels (3D equivalents of pixels) in vertices. The model can be filled up by reading in the sequence of grayscale medical images.

Chapter XII
Finite Element Analysis and its Application in Dental Implant Research

Antonios Zampelis
School of Applied Mathematics and Physical Sciences, Greece

George Tsamasphyros
School of Applied Mathematics and Physical Sciences, Greece

ABSTRACT

Biomechanical research has gained recognition in medical sciences. Osseointegrated dental implants, being medical devices functioning under constant load, are one of the focal points of such research. One of the most powerful tools for biomechanical research on dental implants is finite element analysis (FEA). This chapter will cope with basic elements of FEA research, the mechanical properties of bone and the various parts of dental implants, as well as delve into published literature on the subject.

INTRODUCTION

Finite element analysis (FEA) is a computer simulation technique used in engineering analysis. It uses a numerical technique called the finite element method (FEM). There are many finite element software packages available, both free and proprietary. The sophistication of this technique has rendered it an invaluable tool in biomechanical research.

The finite element analysis was first developed in 1943 by Richard Courant, who used the Ritz method of numerical analysis and minimization of variational calculus to obtain approximate solutions to vibration systems. Shortly thereafter, the work of M.J.Turner, R.W.Clough, H.C.Martin and L.J.Topp in 1956 established a broader definition of numerical analysis. The researchers centered on the "stiffness and deflection of complex structures". Development of the finite element method in structural mechanics is usually based on an energy principle such as the virtual work principle or the minimum total potential energy principle.

Figure 1. Close up of an implant cervix (right) and bone (left). The finite elements are depicted as the ares marked by white lines. Each quadrilateral element consists of four nodes. The different colors depict iso-stress areas

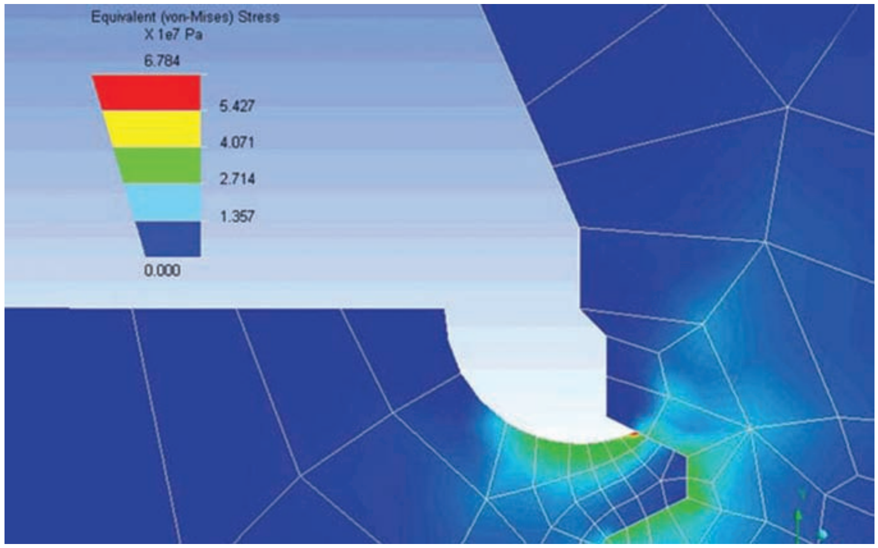

In its applications, the object or system is represented by a geometrically similar model consisting of multiple, linked, simplified representations of discrete regions-i.e. finite elements on an unstructured grid. Equations of equilibrium, in conjunction with applicable physical considerations, such as compatibility and constitutive relations, are applied to each element and a system of simultaneous equations is constructed. The system of partial differential equations is solved for unknown values using the techniques of linear algebra or nonlinear numerical schemes, as appropriate.

In lay terms, the mathematical model is represented by a mesh geometrically identical to the object being studied. The mesh is broken down to elements. There is a set number of elements for a distinct mesh, hence the term finite element analysis. Each element is defined by points called nodes. Depending on the type of analysis, a wide variety of elements can be used, such as one-dimensional (straight or curved), two-dimensional (triangles or quadrilaterals), torus-shaped and three-dimensional (such as tetrahedrals and hexahedrals). As a force is applied, these interconnected elements start to move. Movement is defined by means of displacement of their nodes. This displacement is transformed, through the calculations, to stress and strain values (Figure 1). While being an approximate method, the accuracy of the FEA method can be improved by refining the mesh in the model using more elements and nodes.

A common use of FEA is for the determination of stresses and displacements in mechanical objects and systems. However, it is also routinely used in the analysis of many other types of problems, including those in heat transfer, fluid dynamics and electromagnetism. FEA is able to handle complex systems that defy closed-form analytical solutions.

Finite element analysis is also frequently used in biological systems, for example in orthopedics, but also for dental implants. In fact, realization of the importance of biomechanical aspects in implant dentistry have rendered FEA an essential tool in dental implant research.

Among the subjects investigated in dental implantology are both material properties and biomechanical performance of implants and their components. The behavior of titanium parts, such as abutments and screws, has been put under scrutiny to determine their function under load and the possibility of failure due to fatigue. From a mechanical point of view, such studies are trivial.

On the other hand, the biological behavior of implants integrated in bone is a more complicated matter. A number of studies have investigated the effect of implant length, diameter, shape, as well as different placement configurations and the resulting stresses transmitted to the bone. Often, the effect of prosthetic material and shape of construction, such as the inclusion of cantilevers, is taken into consideration.

The main concern with the application of FEA in implant research is to which extent a mathematical model can represent a biological system. Published studies show a notable trend towards optimization of mathematical models. Improved software and a dramatic increase in easily available computational power have assisted in this trend.

MATERIAL PROPERTIES

In order to understand the structure, material and results of any FEA study, a basic understanding of certain terms is required. The intricate mechanics of bone will also be discussed in this section.

Young's Modulus

Young's modulus, also known as elastic or tensile modulus, is a measure of the stiffness of a material. It is one of several elastic moduli and widely used in FEA. It is named after Thomas Young, an 18^{th} century British scientist.

Young's modulus is defined as the ratio of stress over strain in a region in which Hooke's Law is obeyed for the material (Anonymous, 2008b) In lay terms, it represents the relative stiffness within the elastic range (the range of deformation in which the material can revert completely to its undeformed state). The elastic modulus can be determined from a stress-strain curve by calculating the ratio of stress to strain (Figure 2). A ratio of stress, which has units of pressure, to strain, which is dimensionless, results in Young's modulus being measured in units of

Figure 2. Young's modulus as a stress-strain curve. Strain is in the x-axis, stress is in the y-axis. (a) Elastic limit, (b) upper yield strength, (c) lower yield strength, (d) ultimate stress, (e) breaking stress

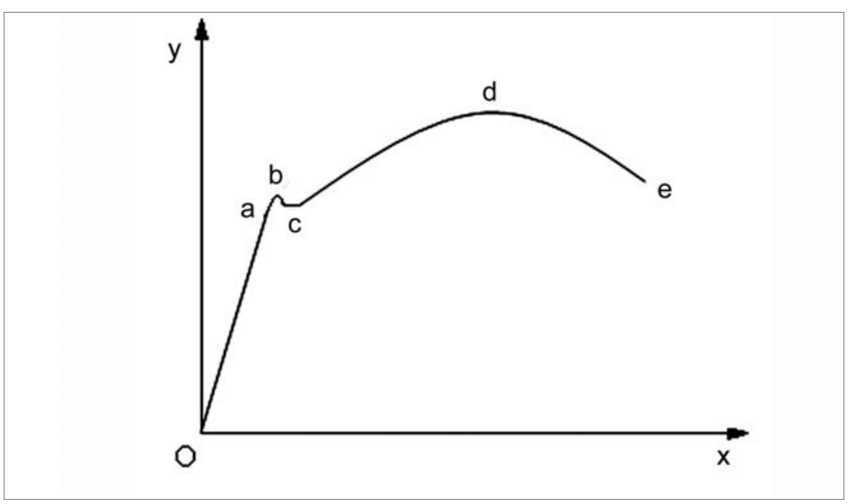

Figure 3. The green area depicts the bar cross-section. The schematic shows the bar profile before (solid line) and after elongation (dotted line)

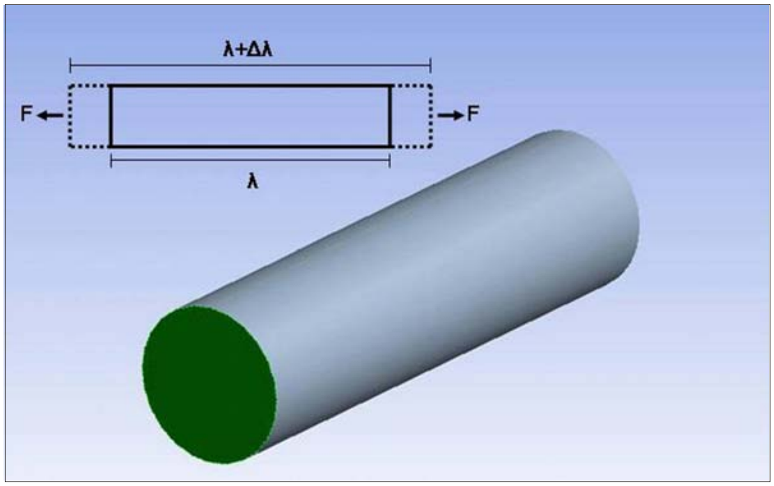

pressure. The SI (International System) unit of modulus of elasticity (E) is the pascal (N/m^2). Practical units include the megapascal (MPa) and gigapascal (GPa or kN/mm^2).

Materials that obey to Hooke's Law show a constant Young's modulus over a range of strains. Such materials, including steel, carbon fiber and glass, are called linear. Rubber and soils are considered non-linear materials (except at very small strains). An important distinction is between isotropic and anisotropic materials. Most metals and ceramics are isotropic, meaning that their mechanical properties are the same in all directions. Wood, on the other hand, is anisotropic. Isotropic materials can be treated in certain ways to make them anisotropic, thus giving them different mechanical properties when load is applied in different directions. In such materials, Young's modulus varies depending on the direction of the load applied. A typical example is carbon fibre, which is much stiffer when a load is applied parallel to its fibers.

If we apply a tensile force of 100N on a bar along its longitudinal axis, the stress can be calculated as:

$$\sigma=F/A$$

where F is the force applied and A the cross-section surface of the bar (Figure 3). If λ is the total initial length of the bar, after force application the bar will be elongated by Δλ. Therefore, strain, which is the deformation of our object, will be calculated as:

$$\varepsilon=\Delta\lambda/\lambda$$

It is easy to deduct that strain is a percentile showing the amount of deformation. Finally, Young's modulus is represented by the following formula:

$$E=\sigma/\varepsilon$$

Poisson's Ratio

Poisson's ratio, named after Simeon Poisson, is the ratio of relative contraction strain, or transverse strain (normal to the applied load), divided by the relative extension strain, or axial strain (in the direction of the applied load) (Anonymous, 2008a).

Figure 4. Poisson's ratio. As the cube is compressed in the vertical direction, it stretches laterally

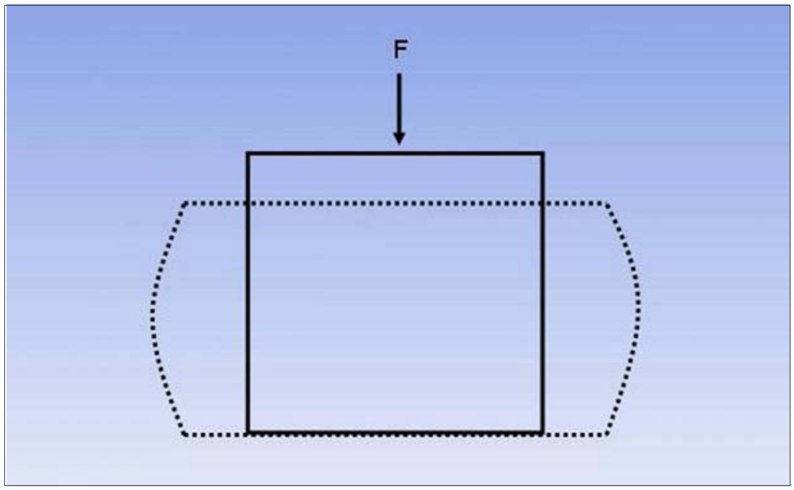

Table 1.

Material	Young's Modulus (in GPa)	Poisson's ratio
Composite resin	9-21	0,24
Porcelain	68-107	0,19
Titanium	105-120	0,33
Gold Alloy	77-100	0,33
Tooth Enamel	70-80	0,33
Cortical Bone	117	0,3
Trabecular Bone	1,37	0,3

When a sample is stretched in one direction, it tends to contract in the other two directions. Conversely, when the sample is compressed in one direction, it tends to expand in the other two (Figure 4). Poisson's ratio (v) is a measure of this tendency. For stable materials, the Poisson's ratio cannot be less than -1 nor greater than 0.5. Most materials have a ratio between 0 and 0.5. For example, cork is close to 0, most steels are around 0.3 and rubber is almost 0.5. A negative Poisson's ratio is found in some materials, mostly polymer foams. These materials are called auxetic (from the greek word αυξητικό=increasing) and, when stretched in one direction, become thicker in perpendicular directions.

If the material is compressed along its axial direction:

$$v=-\varepsilon_{trans}/\varepsilon_{axial}$$

where v is the resulting Poisson's ratio, ε_{trans} is transverse strain and ε_{axial} is axial strain.

The values of Young's modulus and Poisson's ratio for some common materials are presented in Table 1.

Bone Properties

In contrast to engineering research, where it is a norm to study materials with well defined properties, biomechanical research must deal with complex, living structures such as bone. From a mechanical point of view, bone is an anisotropic material. Furthermore, it has the potential to self repair when it is submitted to severe stress.

Bone is a hard, lightweight matter, formed mostly of calcium phosphate and incorporating basic characteristics of a composite material. It has high compressive strength but poor tensile strength, therefore resisting pushing forces well, but not pulling forces. Bone is brittle, but has a high degree of elasticity, due to its high concentration in collagen. In the human skeleton, we can distinguish two main categories, long bones (eg the tibia) and flat bones (eg most bones of the scull), followed by smaller categories such as short, irregular and sesamoid bones.

Despite the different shapes and function of various bone groups, all bones share similar characteristics. Bone comprises of two distinct layers, the outer being called compact, also dense or cortical, and the inner layer called trabecular, also cancellous or spongy, bone. Compact bone is hard and incorporates very few gaps, accounting for 80% of the total mass of an adult skeleton. In compact bone we can find a series of tubes around narrow channels, called Haversian canals. These canals surround blood vessels and nerves. Such an arrangement is conducive to mineral deposit and gives bone its strength. Trabecular bone, on the other hand, is composed of a network of rod- and plate-like elements, making it lighter and allowing room for blood vessels and marrow. It is apparent that bone is a complex structure, with inherent difficulties to determine its mechanical properties.

The elastic modulus of bone has been investigated in experimental trials (Mente & Lewis, 1989). The authors of this study developed a procedure to measure the elastic modulus of small specimens by direct testing of cantilever-type specimens. The samples of trabecular bone were compared to machined aluminium and cortical bone, in order to test the accuracy and reproducibility of the method. The results were entered into a finite element modeling software and a combination of the experimental and calculated displacement was used to determine the actual elastic modulus of trabecular bone. The authors concluded that the calculated elastic modulus was significantly lower than values reported in the literature.

In another study (Katsamanis & Raftopoulos, 1990), the Hopkinson bar stress technique and a universal testing machine were used to investigate dynamic and static mechanical properties of cortical bone taken from the femur of fresh cadavers. This study reported a Young's modulus, Poisson's ratio and viscosity of cortical bone consistent with values found in the literature. Bending tests are common when investigating bone mechanical properties (Hara, Takizawa, Sato, & Ide, 1998; Lotz, Gerhart, & Hayes, 1991; Spatz, O'Leary, & Vincent, 1996). Other techniques, such as measurement of nano-indentation of bone tissue and subsequent calculation of the elastic modulus, have been employed, only to verify that there is a wide variation of elastic properties in the bone of different individuals (Zysset, Guo, Hoffler, Moore, & Goldstein, 1999).

More modern approaches to determining bone properties include the evaluation of imaging techniques (van Lenthe, van den Bergh, Hermus, & Huiskes, 2001). The researchers in this study investigated the feasibility of deriving the elastic modulus of trabecular bone from microfinite element analysis in combination with ultrasound and bone mineral density measurements. The trabecular morphology was constructed based on microcomputed tomography. The authors concluded that ultrasound, as well as computed tomography or magnetic resonance imaging, can be used to estimate bone stiffness. Magnetic resonance imaging (MRI) is supported by fur-

Figure 5. Screw-type implant, abutment and screw

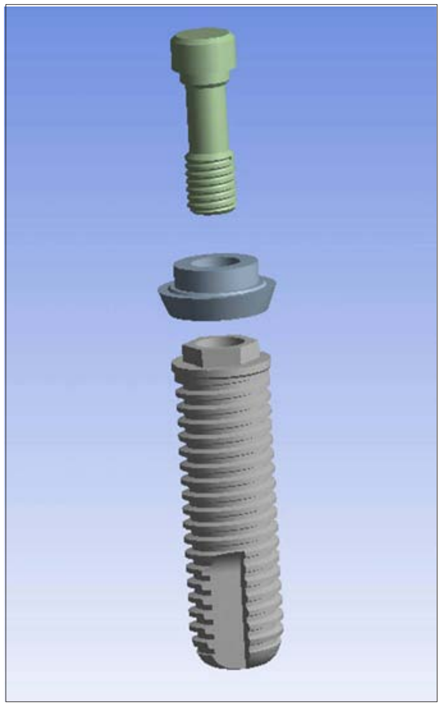

ther studies as a good tool for investigating bone properties (Mehta, Rajani, & Sinha, 1997; van Rietbergen, Majumdar, Newitt, & MacDonald, 2002), as well as computed tomography (Van Oossterwyck et al., 2000).

It is obvious that detailed parameters of bone anatomy and mechanical properties must be taken into account in biomechanical research. Simplified representations of bone as a uniform material are not encouraged, nor vaguely determined mechanical properties. This is further accentuated by studies on stress distribution around oral implants, where it is shown that bone-implant interface, bone elastic properties and bone anatomy greatly influence loading patterns (Van Oosterwyck et al., 1998).

Mechanical Behavior of Titanium Implant Components

The mechanical behavior of titanium implant parts has yielded a significant amount of research. The implant complex consists of the implant, abutment and abutment screw (Figure 5). The implant is embedded in bone, while the abutment serves as an extension penetrating the oral mucosa, on which the prosthetic reconstruction is anchored. The abutment is fixated on the implant with an abutment screw tightened by a specific torque. The friction coefficient between these titanium parts seems to affect the amount of preload inherent in such a complex after tightening the screw with a given torque (Lang, Kang, Wang, & Lang, 2003).

Implant Properties

During chewing or clenching, the masticatory forces are transferred from the prosthesis to the implants. This leads to implant bending (Glantz et al., 1993). Bending overload has been implicated as a major risk factor for implant fracture (Rangert, Krogh, Langer, & Van Roekel, 1995). These bending moments have been verified by use of load cells in vivo (Richter, 1998).

Stress on the implant and the alveolar bone have been investigated from the early years of implantology (Atmaram, Mohammed, & Schoen, 1979). In fact, finite element analysis has been proposed as a useful research tool for designing implants 30 years ago (Weinstein, Klawitter, & Cook, 1979).

Early studies on blade-type implants demonstrated that the material and, consequently, the elastic modulus of an implant can affect stress distribution in the supporting bone (Cook, Klawitter, & Weinstein, 1981). Since then, screw shaped titanium implants have dominated the dental market. The incorporation of stress absorbing elements in titanium implants does not affect stress transfer to the bone (van Rossen, Braak, de Putter, & de Groot, 1990).

The use of finite element analysis to investigate the mechanical properties of dental implants and stress distribution in the implants and surrounding bone has been compared to in vitro strain gauge measurements (Akca, Cehreli, & Iplikcioglu, 2002; Iplikcioglu, Akca, Cehreli, & Sahin, 2003). This research group worked on validating FEA through comparison with in vitro strain gauge measurements of implants embedded in methyl methacrylate. The strain gauges were bonded to the cervical part of the implants, while computer generated identical models were constructed. The researchers found differences between the strains measured and those calculated by FEA. In particular, strains obtained from strain gauge analysis were greater than those for three-dimensional finite element analysis. However, the pattern of strain distribution was similar for both methods.

Published research on the importance of implant shape, length etc will be covered in a separate section.

Abutment Properties

The abutment is an integral part of the dental implant, as it is the means by which the restoration is anchored on the implant. A number of studies utilizing finite element analysis have been published on the properties of different abutments. As in all FEA studies, optimization and refinement of the mesh is important in order to obtain accurate results (Holmes, Haganman, Aquilino, Diaz-Arnold, & Stanford, 1997).

When abutments are tightened to the implants by means of screws, a preload is developed. The amount of preload generated is dependent on the tightening torque applied, which, in turn, is affected by the inter-component friction. It has been shown by means of FEA that, when the friction coefficient of implant components varies, it affects the tightening torque required to achieve a certain amount of preload (Lang, Kang, Wang, & Lang, 2003). In this study, it was demonstrated that a lower friction coefficient between components allowed to reach the desired amount of preload in the implant-abutment complex with a lower tightening torque. Different materials for the abutment may also affect how stress is transferred to the implant (Lewis, 1994). This finding, however, was produced by means of two-dimensional FE models and is in contrast with findings from an in vitro study on dynamic loading of abutments with different mechanical properties, where abutment material failed to influence strain transfer from the abutment to the implant and bone (Morton, Stanford, & Aquilino, 1998).

The dimensions and particular shape of an abutment have been investigated in several studies. Implants are available in different diameters, ranging, in average, from 3 to 6mm. Implants and

Figure 6. Implant with external connection hexagon (left) and internal connection (right)

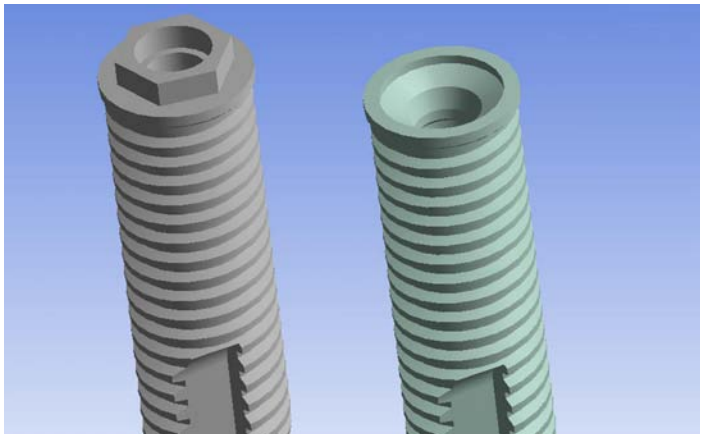

abutments of large diameter are believed to lower the transferred stress from the implant complex to the bone (Tuncelli, Poyrazoglu, Koyluoglu, & Tezcan, 1997), presumably due to the increased interface surface.

Implant diameter alone cannot solve all placement problems. When there is limited bone availability, the implant may have to be placed at an angle to the occlusal plane. In such cases, an angulated abutment must be used. Care must be taken when evaluating FEA studies on angulated abutments and stress transfer. Studies evaluating a single implant and abutment tend to show higher stress generation (Clelland, Lee, Bimbenet, & Brantley, 1995). This is easily explained by the application of forces at an angle to the long axis of the implant and parallel to the abutment axis, which produce a bending moment (Clelland, Lee, Bimbenet, & Brantley, 1995; Papavasiliou, Kamposiora, Bayne, & Felton, 1996). In contrast, stress in the bone around implants splinted with a fixed bridge is not affected by the geometry of the abutment (Zampelis, Rangert, & Heijl, 2007).

The first well documented implants belonged to the Brånemark System (Nobel Biocare AB, Sweden). These implants, which are still available, had an external connection. This connection consisted of a hexagon on top of the implant. The respective abutment had a hexagon cavity that fit on the implant hex. Nowadays, most implant companies opt for an internal connection, where the abutment is inserted into the implant (Figure 6). The reason behind this shift was mainly soft tissue problems associated with a poorer fit of external connection components, resulting in bacterial ingrowth between the implant and abutment (Persson, Lekholm, Leonhardt, Dahlen, & Lindhe, 1996). A popular design for such internal connection abutments is one where the lower section of the abutment has a morse taper (Merz, Hunenbart, & Belser, 2000). Finite element analysis has demonstrated that a conical connection results in lower and more evenly distributed stress compared to a conventional, flat top connection (Hansson, 2000). The same author demonstrated that, if the conical connection is placed higher than the bone level, this advantage disappears (Hansson, 2003). The morse taper connection is discussed in yet another study, where an important problem of FEA is presented (Perriard et al., 2002). The results from the analysis indicate that areas of high peak stress may, indeed, be geometry dependant computational artifacts. Further discussion on the importance of geometry in FE models will follow in another section of this chapter.

The introduction of esthetic materials such as zirconium in the fabrication of implant abutments has further accentuated material oriented research. Zirconium is considered a good material for abutments, having a satisfactory fracture strength and good fit with minimal deformation after repeated high loading (Gehrke et al., 2006).

Mechanical Behavior of Prosthetic Reconstructions

Prosthetic reconstructions are divided into two main categories, fixed and removable. Fixed restorations are further distinguished as screw retained or cemented. Such restorations may consist of a metal frame dressed with acrylic or porcelain, only acrylic or only porcelain. Choice material is based on cost, ease of construction, expected functional burden and esthetics.

The geometry of a prosthesis can also vary considerably. In a severely resorbed jaw, the distance from the implant to the occlusal plane is increased, resulting in a higher prosthesis. In a patient with large teeth, the width of the prosthesis may also have to larger. Finally, anatomical reasons may prohibit implant placement in the posterior parts of the jaw. In such cases, if we want to incorporate molar teeth in our reconstruction, we have to resort to the use of cantilever extensions.

Prosthesis Geometry

The physics of cantilever units clearly indicate that bending moments result in increased stresses. The bending moment is proportional to the magnitude of the force applied and the length of the lever arm:

$$T = F \times \lambda$$

where T is the bending moment, F the applied force and λ the length of the lever arm. Finite element studies clearly agree that the incorporation of a cantilever unit in an implant supported prosthesis results in increased stress around the implant adjacent to the cantilever (Stegaroiu, Sato, Kusakari, & Miyakawa, 1998; van Zyl, Grundling, Jooste, & Terblanche, 1995; Williams et al., 1990; Zampelis, Rangert, & Heijl, 2007).

As stated above, increasing the length of the cantilever results in a proportional increase in bending moment and stress. Using longer implants does not have an effect on stress transferred to the bone (Sertgoz & Guvener, 1996). To minimize the possibility of plastic deformation and fracture, cantilever beams must be constructed with a favorable cross-section (Young, Williams, Draughn, & Strohaver, 1998).

Figure 7. Bending moment with cantilevers of high (continuous line) and low stiffness (dotted line). T) bending moment, F) force, λ) lever arm length

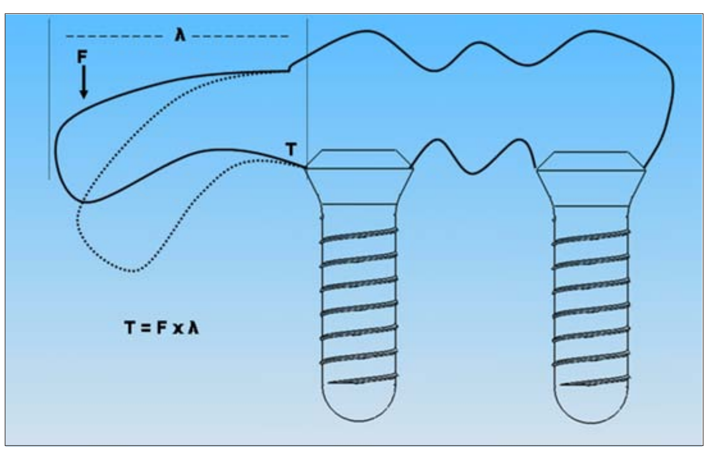

Another way to minimize the effect of cantilever arms is to design the prosthesis so that the cantilever arm is flexible and infraoccluding (Laurell, Lundgren, Falk, & Hugoson, 1991). However, it is important to stress that, when chewing, the interfering food particles transfer a constant force on the cantilever extension and, irrespective of the amount of deflection, the bending moment is the same (Figure 7).

Prosthesis Materials

The prosthesis materials can be chosen based on several criteria. These materials are believed to affect the mechanical behavior of the reconstruction. FE studies sometimes argue for the protective role of acrylic restorations (Ciftci & Canay, 2000), while in vivo studies tend to demonstrate minimal or no influence of the prosthesis material on the loading of implants (Duyck et al., 2000).

Once more, it is important to always bear in mind the methodology of each study and the model proposed. In a FE study on the effect of various veneering materials on stress distribution in the bone surrounding an implant, it was shown that, in the models with acrylic and composite as veneer material, stress in the bone was lower (Ciftci & Canay, 2000). In contrast, studies where multiple implants are splinted with the prosthesis show that the veneering material has no (Papavasiliou, Kamposiora, Bayne, & Felton, 1996) or little influence on stress distribution in the surrounding bone (Sertgoz, 1997).

It is not the objective of this chapter to investigate clinical evidence on the effect of prosthesis material on stress distribution in the supporting implants and bone. In light of the conflicting evidence it is, however, useful to bear in mind that most published studies propose dissimilar FE models that can produce conflicting results.

IMPLANT SHAPE

Today there are literally hundreds of commercially available implant systems. Most, if not all, are screw-shaped. Each system offers implants at varying diameters and lengths. Some systems have a research background behind their proposed products, while other implants are designed based on anecdotal evidence.

Two main areas of interest in biomechanical implant research are the dimensions and specific design of different implant systems. These will be covered in the following sections.

Implant Length and Diameter

Implant dimensions are defined by an implant's length and outer diameter. Both affect the total surface of the implant available for osseointegration. It is believed that a larger surface will lead to greater implant stability. This leads numerous clinicians to choose longer implants for the rehabilitation of edentulous patients, often based on reviews and opinion articles (Misch, 1999). While there is nothing inherently wrong with placing a long implant instead of a short one, provided that there is enough available bone to receive the implant, the objective of scientific research should be to investigate the minimum surface required to achieve a stable result in cases where, in fact, placement of a long implant is not possible.

The irrelevance of implant length on the stress transferred to the bone has been shown by means of 3-dimensional finite element analysis (Sertgoz & Guvener, 1996). The authors concluded that, in the case of a fixed denture supported by six implants, implant length did not affect stress in the bone. This is in accordance with other studies on the subject. In a study on single implants loaded obliquely, it was shown that bone stress was not affected by implant length, while bicortical anchorage tended to increase stress on the implant

(Pierrisnard, Renouard, Renault, & Barquins, 2003). Two dimensional FE analysis of splinted implants produces identical results (Zampelis, Rangert, & Heijl, 2007).

The importance of short implants is illustrated in a study comparing the usage of short implants in cases of posterior edentulism to the incorporation of cantilever extensions. It is obvious from the results that short implants were associated with far lower stress compared to cantilevers, creating a biomechanically more favorable situation (Akca & Iplikcioglu, 2002).

Some studies, nevertheless, tend to disprove the above findings. A 3-D FE study evaluating implant type (screw vs cylinder), implant length and bone quality concluded that longer implants were associated with lower stress in the bone (Tada, Stegaroiu, Kitamura, Miyakawa, & Kusakari, 2003). The main factor of influence, however, was bone quality and not implant length. Another study on implant diameter, length and taper produced similar results, although the reported results included bone strain and not stress (Petrie & Williams, 2005).

Of the above studies, the work of Pierrisnard and coworkers (2003) offers some valuable insight into the biomechanics of dental implants. The authors show beyond any doubt that the cortical layer of the bone and more specifically its most coronal part, carries the major part of the load applied. Compared to the cortex, only a small amount of stress is transferred to the trabecular bone. Thus, the biggest part of the implant, which is embedded in trabecular bone, contributes ever so slightly to the total stability of the implant.

In a following section, the influence of the bone-implant interface and its accurate modeling will be discussed. It must be born in mind that computational artifacts may be associated with peak stress values that are excessively high. Therefore, it is useful for publishing authors to include the distribution of stress values in their reports and not just the maximum values.

Implant Design

The importance of implant shape on bone stress has been discussed since the era of blade implants (Cook, Klawitter, & Weinstein, 1982b). More recent studies comparing implants with a stepped vs straight cylinder shape (Holmgren, Seckinger, Kilgren, & Mante, 1998) or a cylinder vs screw shape (Tada, Stegaroiu, Kitamura, Miyakawa, & Kusakari, 2003) argue against the use of straight cylinders. From a clinical point of view, straight cylinder implants are no longer commercially available, nonetheless because those marketed in the nineties incorporated a very rough surface, frequently associated with pronounced periimplantitis (Albrektsson, Sennerby, & Wennerberg, 2008).

Attempts to compare several shapes of commercially available or experimental implants have shown that stress distribution in the surrounding bone may vary significantly (Joos, Vollmer, & Kleinheinz, 2000; Rieger, Adams, & Kinzel, 1990; Rieger, Mayberry, & Brose, 1990). The patterns of stress distribution observed with certain designs of implants have led researchers to investigate the possibility of developing implants with a high initial stability and favorable stress dispersion, suitable for immediate loading (Pierrisnard, Hure, Barquins, & Chappard, 2002).

What remains to be proven is to what extent the differences observed are of clinical relevance. It is undeniable that different implant shapes may carry load to the supporting bone in different magnitudes, but there is still no solid proof of a load “threshold”, above which implant failure may be observed.

BONE-TO-IMPLANT INTERFACE

The interface between implants and bone is an area of great interest. The intricate details of this interface make dental implants such interesting research objectives. There are two main areas of distinction. One is the microscopical level of the interface, relating to the surface structure of the implant. The surface roughness of an implant can affect its initial stability, facilitating and accelerating osseointegration (Albrektsson, Sennerby, & Wennerberg, 2008). The second area of interest is the macroscopical contact area of implant and bone. This contact surface causes many problems as to how it can be accurately modeled in a FE environment. It is not uncommon to see peak stress artifacts in implant FE studies at the bone-implant interface and, more particularly, at its most coronal part.

The effect of tissue ingrowth into the porous surface of a cylindrical implant was assessed in a 3-D FE environment (Cook, Klawitter, & Weinstein, 1982a). Two models were constructed. In the first model, bone ingrowth into the implants rough surface was simulated. In the second model, direct bone-to-implant contact was assumed. The results from the FE analysis were compared to results from mechanical testing on implants inserted in canine jaws. The model simulating tissue ingrowth was found to be in better accordance with the experimental data.

Porous implant surface has also been compared to plasma sprayed surface, an older surface modification technique (Simmons, Meguid, & Pilliar, 2001). The finite element models demonstrated that the porous surface was, indeed, beneficial in terms of a more favorable strain distribution.

Considering bone and implant as bonded bodies has been shown to be of lesser importance (Rieger, Adams, Kinzel, & Brose, 1989), meaning that, although close adaptation is desirable, a bonded interface does not alter stress distribution in the bone. In contrast, the amount of adaptation, or osseointegration, has a profound effect on the pattern of stress distribution (Lai, Zhang, Zhang, Yang, & Xue, 1998). At the early stages of integration, very high stresses are located in the crestal bone region, while development of integration reduces severe stress peaks and ingrowth of tissue almost eliminates them (Borchers & Reichart, 1983).

One group of researchers proposed the use of large sliding contact elements to simulate bone-implant micromotion and test if it is feasible to predict implant micromotion as a risk factor for osseointegration (Viceconti, Muccini, Bernakiewicz, Baleani, & Cristofolini, 2000). The authors concluded that their proposed technique was the only one that did not exceed their accuracy threshold.

Figure 8. Modeled bone crater to assure identical bone-to-implant anatomy regardless of inclination. Cervix of the perpendicular (left) and 45 degree tilted implant (right)

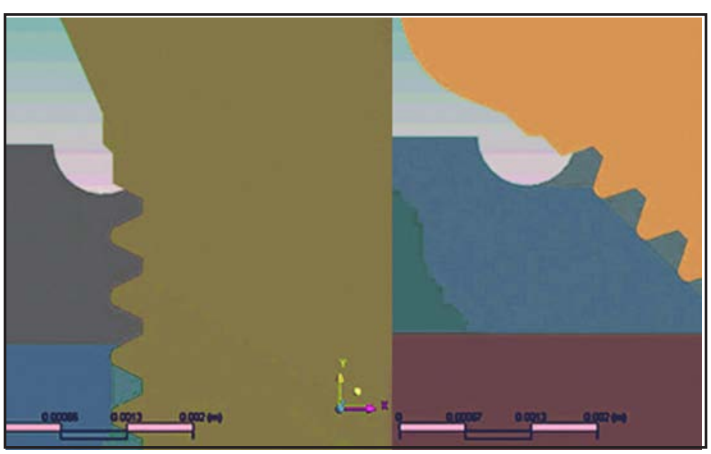

Macroscopic modeling of the bone-implant interface is also important. The first obvious step in FE analysis is to optimize the mesh in this area. This is commonly done by element downsizing (Sato, Wadamoto, Tsuga, & Teixeira, 1999). Smaller and more elements produce a more detailed mesh. Element downsizing is continued until the differences between models are negligible. Many times, however, compromises must be made, since extremely fine meshes demand large computational power.

Probably the most problematic area for modeling is the most coronal bone-to-implant contact. One research group compared FEA to in vitro strain gauge measurements on a Morse taper implant (Iplikcioglu, Akca, Cehreli, & Sahin, 2003). The researchers found some differences in the results of the two methods in the coronal part of the interface.

Another research group investigated the effect of marginal bone resorption on bone stress (Kitamura, Stegaroiu, Nomura, & Miyakawa, 2004, 2005). The researchers created FE models of osseointegrated implants with normal bone and horizontal, vertical or angular bone resorption. While normal bone and horizontal resorption produced similar results, angular resorption was associated with lower stress. The authors speculated that bone resorption might be a protective mechanism, in order for the bone to reach a stable state. It is more probable, however, that the angular resorption produced a more asymptotic bone-to-implant contact, avoiding acute angles of contact and peak stresses.

A similar experimentation has been published in another study (Zampelis, Rangert, & Heijl, 2007). A microscopic crater was created at the distal surface of the experimental implants, to ascertain an identical bone-to-implant interface anatomy regardless of how the implants were inserted in the bone (Figure 8). This method proved reliable and succesful in avoiding peak stresses.

IMPLANT PLACEMENT CONFIGURATIONS

Various components of implant therapy and their biomechanical characteristics have been presented. However, these biomechanical aspects intertwine to form the biomechanical complex of dental implants. This refers not only to the separate parts of an implant reconstruction, but how they are put together. Designing the placement of implants is equally important as how the prosthesis will be fabricated (Rangert, Sennerby, Meredith, & Brunski, 1997).

In order to minimize the bending effect of oblique forces, placing several implants in a staggered (offset) series has been proposed. FE studies have disproved this theory by showing that offset placement of implants does not result in lower stresses (Akca & Iplikcioglu, 2001; Sato, Shindoi, Hosokawa, Tsuga, & Akagawa, 2000).

Bicortical anchorage is sometimes used to improve initial stability of implants. The work of Pierrisnard and coworkers (2003) mentioned above showed that not only did bicortical anchorage have little effect on bone stress, it did, in fact, result in higher implant stress.

Lack of bone availability in the posterior segments of the upper and lower jaw, along with the presence of anatomical landmarks such as the maxillary sinus and the mandibular nerve, have led to the development of a technique incorporating inclined (tilted) implants. Although clinical data exist to support this technique (Krekmanov, Kahn, Rangert, & Lindstrom, 2000; Malo, Rangert, & Nobre, 2003), FE data are few. Published studies are actually investigating related topics, like placing a cylinder implant perpendicular to the Spee curve (Satoh, Maeda, & Komiyama, 2005), or placing a single implant in a resorbed jaw and loading it with an oblique force (Watanabe, Hata, Komatsu, Ramos, & Fukuda, 2003).

One of the first published FE studies on the subject of tilted implants utilized a simplified, well defined 2-D finite element model where distally tilted implants were evaluated as an alternative to cantilever extensions (Zampelis, Rangert, & Heijl, 2007). The authors concluded that bone stress around tilted implants was identical to that around non-tilted implants. This stress was significantly lower than that around implants supporting cantilever extensions.

DISCUSSION

The results from biomechanical research are frequently misinterpreted, even by the very authors of relevant studies. It must be realized that FEA, albeit a powerful engineering tool, cannot, yet, fully and reliably simulate a biological system as complicated as the human body.

A frequent observation that bears questioning is for bone stress values to be treated as absolute numbers. When the properties of a prosthesis are investigated, it is quite easy to determine if plastic deformation, fatigue or fracture will occur, since the materials are well defined and easy to simulate. Bone, on the other hand, is a very complex structure. Despite its anisotropic anatomy, bone is often considered isotropic to facilitate modeling, its elastic properties being approximated. This simplification is not necessarily poor practice, as it makes construction of basic models less complicated. Nevertheless, we cannot draw absolute conclusions on the nature and behavior of bone in a FE environment if we fail to simulate it properly.

It is obvious that a stress value alone does not offer much insight. The stress/strain threshold for bone injury is still unclear in the literature, while, in clinical practice, there is no proof of acute bone fracture due to implant overload. A number of FE studies speculate on possible prediction of bone loss around implants due to overload, but we must bear in mind that overload is a vaguely supported concept. More important is the fact that bone resorption is a dynamic process that is biologically driven. There is absolutely no comparison between material fatigue and bone loss, since bone responds to stimuli by remodeling, something simple materials cannot do. Getting into details concerning inflammation driven bone resorption in the form of periimplantitis exceeds the scope of this chapter and will not be commented upon.

Far more meaningful is the use of FEA as a comparison tool. In the study of Zampelis and coworkers (2007), simple models are constructed to test different implant placements and their effect on bone stress. The results from this study confirm, in statistical terms, the null hypothesis of no difference between implant placements. Pierrisnard and coworkers (2003) used a similar approach to compare implants of varying length. It is stressed, once more, that, if a difference in stress levels was found in these studies, it would be extremely difficult to speculate whether a particular value would be considered pathological.

Studies that do not adopt a precise, consistent approach towards proper modeling should be evaluated with scepticism. Yet, there are published studies where copious algorithms are described and analytical methods developed, only to use a simplistic model of cylinders embedded in a uniform matter considered jawbone. Simple models, allowing focus on specific parameters, are very useful, but we must be able to understand their limitations.

Future research must focus on optimization and validation of bone modeling. Once the complexities of this live tissue can be simulated in a mathematical model, new research horizons will extend. At the same time, ongoing research must make the most of available computational power to produce interesting, educational experimental data that will broaden our knowledge on the biomechanics of dental implants.

Another use of FEA will be to test original hypotheses which can, consecutively, be tested in vivo. In this way, differences found in FEA can be further investigated for clinical significance.

ACKNOWLEDGMENT

This chapter is dedicated to the memory of Bo Rangert.

REFERENCES

Akca, K., Cehreli, M. C., & Iplikcioglu, H. (2002). A comparison of three-dimensional finite element stress analysis with in vitro strain gauge measurements on dental implants. *Int J Prosthodont, 15*(2), 115-121.

Akca, K., & Iplikcioglu, H. (2001). Finite element stress analysis of the influence of staggered versus straight placement of dental implants. *Int J Oral Maxillofac Implants*, *16*(5), 722-730.

Akca, K., & Iplikcioglu, H. (2002). Finite element stress analysis of the effect of short implant usage in place of cantilever extensions in mandibular posterior edentulism. *J Oral Rehabil, 29*(4), 350-356.

Albrektsson, T., Sennerby, L., & Wennerberg, A. (2008). State of the art of oral implants. *Periodontol 2000*, *47*, 15-26.

Anonymous. (2008a). *Poisson's ratio*. Retrieved July 18th, 2008 from the OLPC Wiki: http://en.wikipedia.org/wiki/Poisson_ratio

Anonymous. (2008b). *Young's modulus*. Retrieved July 18th, 2008 from the OLPC Wiki: http://en.wikipedia.org/wiki/Young_modulus

Atmaram, G. H., Mohammed, H., & Schoen, F. J. (1979). Stress analysis of single-tooth implants. I. Effect of elastic parameters and geometry of implant. *Biomater Med Devices Artif Organs, 7*(1), 99-104.

Borchers, L., & Reichart, P. (1983). Three-dimensional stress distribution around a dental implant at different stages of interface development. *J Dent Res, 62*(2), 155-159.

Ciftci, Y., & Canay, S. (2000). The effect of veneering materials on stress distribution in implant-supported fixed prosthetic restorations. *Int J Oral Maxillofac Implants, 15*(4), 571-582.

Clelland, N. L., Lee, J. K., Bimbenet, O. C., & Brantley, W. A. (1995). A three-dimensional finite element stress analysis of angled abutments for an implant placed in the anterior maxilla. *J Prosthodont, 4*(2), 95-100.

Cook, S. D., Klawitter, J. J., & Weinstein, A. M. (1981). The influence of implant elastic modulus on the stress distribution around LTI carbon and aluminum oxide dental implants. *J Biomed Mater Res*, *15*(6), 879-887.

Cook, S. D., Klawitter, J. J., & Weinstein, A. M. (1982a). A model for the implant-bone interface characteristics of porous dental implants. *J Dent Res*, *61*(8), 1006-1009.

Cook, S. D., Klawitter, J. J., & Weinstein, A. M. (1982b). The influence of implant geometry on the stress distribution around dental implants. *J Biomed Mater Res, 16*(4), 369-379.

Duyck, J., Van Oosterwyck, H., Vander Sloten, J., De Cooman, M., Puers, R., & Naert, I. (2000). Influence of prosthesis material on the loading of implants that support a fixed partial prosthesis: in vivo study. *Clin Implant Dent Relat Res, 2*(2), 100-109.

Gehrke, P., Dhom, G., Brunner, J., Wolf, D., Degidi, M., & Piattelli, A. (2006). Zirconium implant abutments: fracture strength and influence of cyclic loading on retaining-screw loosening. *Quintessence Int*, *37*(1), 19-26.

Glantz, P. O., Rangert, B., Svensson, A., Stafford, G. D., Arnvidarson, B., Randow, K., et al. (1993). On clinical loading of osseointegrated implants. A methodological and clinical study. *Clin Oral Implants Res, 4*(2), 99-105.

Hansson, S. (2000). Implant-abutment interface: biomechanical study of flat top versus conical. *Clin Implant Dent Relat Res, 2*(1), 33-41.

Hansson, S. (2003). A conical implant-abutment interface at the level of the marginal bone improves the distribution of stresses in the supporting bone. An axisymmetric finite element analysis. *Clin Oral Implants Res, 14*(3), 286-293.

Hara, T., Takizawa, M., Sato, T., & Ide, Y. (1998). Mechanical properties of buccal compact bone of the mandibular ramus in human adults and children: relationship of the elastic modulus to the direction of the osteon and the porosity ratio. *Bull Tokyo Dent Coll, 39*(1), 47-55.

Holmes, D. C., Haganman, C. R., Aquilino, S. A., Diaz-Arnold, A. M., & Stanford, C. M. (1997). Finite element stress analysis of IMZ abutment designs: development of a model. *J Prosthodont, 6*(1), 31-36.

Holmgren, E. P., Seckinger, R. J., Kilgren, L. M., & Mante, F. (1998). Evaluating parameters of osseointegrated dental implants using finite element analysis--a two-dimensional comparative study examining the effects of implant diameter, implant shape, and load direction. *J Oral Implantol, 24*(2), 80-88.

Iplikcioglu, H., Akca, K., Cehreli, M. C., & Sahin, S. (2003). Comparison of non-linear finite element stress analysis with in vitro strain gauge measurements on a Morse taper implant. *Int J Oral Maxillofac Implants, 18*(2), 258-265.

Joos, U., Vollmer, D., & Kleinheinz, J. (2000). [Effect of implant geometry on strain distribution in peri-implant bone]. *Mund Kiefer Gesichtschir, 4*(3), 143-147.

Katsamanis, F., & Raftopoulos, D. D. (1990). Determination of mechanical properties of human femoral cortical bone by the Hopkinson bar stress technique. *J Biomech, 23*(11), 1173-1184.

Kitamura, E., Stegaroiu, R., Nomura, S., & Miyakawa, O. (2004). Biomechanical aspects of marginal bone resorption around osseointegrated implants: considerations based on a three-dimensional finite element analysis. *Clin Oral Implants Res, 15*(4), 401-412.

Kitamura, E., Stegaroiu, R., Nomura, S., & Miyakawa, O. (2005). Influence of marginal bone resorption on stress around an implant--a three-dimensional finite element analysis. *J Oral Rehabil, 32*(4), 279-286.

Krekmanov, L., Kahn, M., Rangert, B., & Lindstrom, H. (2000). Tilting of posterior mandibular and maxillary implants for improved prosthesis support. *Int J Oral Maxillofac Implants, 15*(3), 405-414.

Lai, H., Zhang, F., Zhang, B., Yang, C., & Xue, M. (1998). Influence of percentage of osseointegration on stress distribution around dental implants. *Chin J Dent Res, 1*(3), 7-11.

Lang, L. A., Kang, B., Wang, R. F., & Lang, B. R. (2003). Finite element analysis to determine implant preload. *J Prosthet Dent, 90*(6), 539-546.

Laurell, L., Lundgren, D., Falk, H., & Hugoson, A. (1991). Long-term prognosis of extensive polyunit cantilevered fixed partial dentures. *J Prosthet Dent, 66*(4), 545-552.

Lewis, G. (1994). A parametric finite element analysis study of the stresses in an endosseous implant. *Biomed Mater Eng, 4*(7), 495-502.

Lotz, J. C., Gerhart, T. N., & Hayes, W. C. (1991). Mechanical properties of metaphyseal bone in the proximal femur. *J Biomech, 24*(5), 317-329.

Malo, P., Rangert, B., & Nobre, M. (2003). "All-on-Four" immediate-function concept with Branemark System implants for completely edentulous mandibles: a retrospective clinical study. *Clin Implant Dent Relat Res, 5 Suppl 1,* 2-9.

Mehta, B. V., Rajani, S., & Sinha, G. (1997). Comparison of Figure processing techniques (magnetic resonance imaging, computed tomography scan and ultrasound) for 3D modeling and analysis of the human bones. *J Digit Imaging, 10*(3 Suppl 1), 203-206.

Mente, P. L., & Lewis, J. L. (1989). Experimental method for the measurement of the elastic modulus of trabecular bone tissue. *J Orthop Res, 7*(3), 456-461.

Merz, B. R., Hunenbart, S., & Belser, U. C. (2000). Mechanics of the implant-abutment connection: an 8-degree taper compared to a butt joint connection. *Int J Oral Maxillofac Implants, 15*(4), 519-526.

Misch, C. E. (1999). Implant design considerations for the posterior regions of the mouth. *Implant Dent, 8*(4), 376-386.

Morton, D., Stanford, C. M., & Aquilino, S. A. (1998). Evaluation of resilient abutment components on measured strain using dynamic loading conditions. *J Prosthet Dent, 80*(1), 46-51.

Papavasiliou, G., Kamposiora, P., Bayne, S. C., & Felton, D. A. (1996). Three-dimensional finite element analysis of stress-distribution around single tooth implants as a function of bony support, prosthesis type, and loading during function. *J Prosthet Dent, 76*(6), 633-640.

Perriard, J., Wiskott, W. A., Mellal, A., Scherrer, S. S., Botsis, J., & Belser, U. C. (2002). Fatigue resistance of ITI implant-abutment connectors: A comparison of the standard cone with a novel internally keyed design. *Clin Oral Implants Res, 13*(5), 542-549.

Persson, L. G., Lekholm, U., Leonhardt, A., Dahlen, G., & Lindhe, J. (1996). Bacterial colonization on internal surfaces of Branemark system implant components. *Clin Oral Implants Res, 7*(2), 90-95.

Petrie, C. S., & Williams, J. L. (2005). Comparative evaluation of implant designs: influence of diameter, length, and taper on strains in the alveolar crest. A three-dimensional finite-element analysis. *Clin Oral Implants Res, 16*(4), 486-494.

Pierrisnard, L., Hure, G., Barquins, M., & Chappard, D. (2002). Two dental implants designed for immediate loading: a finite element analysis. *Int J Oral Maxillofac Implants, 17*(3), 353-362.

Pierrisnard, L., Renouard, F., Renault, P., & Barquins, M. (2003). Influence of implant length and bicortical anchorage on implant stress distribution. *Clin Implant Dent Relat Res, 5*(4), 254-262.

Rangert, B., Krogh, P. H., Langer, B., & Van Roekel, N. (1995). Bending overload and implant fracture: a retrospective clinical analysis. *Int J Oral Maxillofac Implants, 10*(3), 326-334.

Rangert, B., Sennerby, L., Meredith, N., & Brunski, J. (1997). Design, maintenance and biomechanical considerations in implant placement. *Dent Update, 24*(10), 416-420.

Richter, E. J. (1998). In vivo horizontal bending moments on implants. *Int J Oral Maxillofac Implants, 13*(2), 232-244.

Rieger, M. R., Adams, W. K., & Kinzel, G. L. (1990). A finite element survey of eleven endosseous implants. *J Prosthet Dent, 63*(4), 457-465.

Rieger, M. R., Adams, W. K., Kinzel, G. L., & Brose, M. O. (1989). Finite element analysis of bone-adapted and bone-bonded endosseous implants. *J Prosthet Dent, 62*(4), 436-440.

Rieger, M. R., Mayberry, M., & Brose, M. O. (1990). Finite element analysis of six endosseous implants. *J Prosthet Dent, 63*(6), 671-676.

Sato, Y., Shindoi, N., Hosokawa, R., Tsuga, K., & Akagawa, Y. (2000). A biomechanical effect of wide implant placement and offset placement of three implants in the posterior partially edentulous region. *J Oral Rehabil, 27*(1), 15-21.

Sato, Y., Wadamoto, M., Tsuga, K., & Teixeira, E. R. (1999). The effectiveness of element downsizing on a three-dimensional finite element model of bone trabeculae in implant biomechanics. *J Oral Rehabil, 26*(4), 288-291.

Satoh, T., Maeda, Y., & Komiyama, Y. (2005). Biomechanical rationale for intentionally inclined implants in the posterior mandible using 3D finite element analysis. *Int J Oral Maxillofac Implants, 20*(4), 533-539.

Sertgoz, A. (1997). Finite element analysis study of the effect of superstructure material on stress distribution in an implant-supported fixed prosthesis. *Int J Prosthodont, 10*(1), 19-27.

Sertgoz, A., & Guvener, S. (1996). Finite element analysis of the effect of cantilever and implant length on stress distribution in an implant-supported fixed prosthesis. *J Prosthet Dent, 76*(2), 165-169.

Simmons, C. A., Meguid, S. A., & Pilliar, R. M. (2001). Differences in osseointegration rate due to implant surface geometry can be explained by local tissue strains. *J Orthop Res, 19*(2), 187-194.

Spatz, H. C., O'Leary, E. J., & Vincent, J. F. (1996). Young's moduli and shear moduli in cortical bone. *Proc Biol Sci, 263*(1368), 287-294.

Stegaroiu, R., Sato, T., Kusakari, H., & Miyakawa, O. (1998). Influence of restoration type on stress distribution in bone around implants: a three-dimensional finite element analysis. *Int J Oral Maxillofac Implants, 13*(1), 82-90.

Tada, S., Stegaroiu, R., Kitamura, E., Miyakawa, O., & Kusakari, H. (2003). Influence of implant design and bone quality on stress/strain distribution in bone around implants: a 3-dimensional finite element analysis. *Int J Oral Maxillofac Implants, 18*(3), 357-368.

Tuncelli, B., Poyrazoglu, E., Koyluoglu, A. M., & Tezcan, S. (1997). Comparison of load transfer by implant abutments of various diameters. *Eur J Prosthodont Restor Dent, 5*(2), 79-83.

van Lenthe, G. H., van den Bergh, J. P., Hermus, A. R., & Huiskes, R. (2001). The prospects of estimating trabecular bone tissue properties from the combination of ultrasound, dual-energy X-ray absorptiometry, microcomputed tomography, and microfinite element analysis. *J Bone Miner Res, 16*(3), 550-555.

Van Oossterwyck, H., Duyck, J., Vander Sloten, J., Van der Perre, G., Jansen, J., Wevers, M., et al. (2000). Use of microfocus computerized tomography as a new technique for characterizing bone tissue around oral implants. *J Oral Implantol, 26*(1), 5-12.

Van Oosterwyck, H., Duyck, J., Vander Sloten, J., Van der Perre, G., De Cooman, M., Lievens, S., et al. (1998). The influence of bone mechanical properties and implant fixation upon bone loading around oral implants. *Clin Oral Implants Res, 9*(6), 407-418.

van Rietbergen, B., Majumdar, S., Newitt, D., & MacDonald, B. (2002). High-resolution MRI and micro-FE for the evaluation of changes in bone mechanical properties during longitudinal clinical trials: application to calcaneal bone in postmenopausal women after one year of idoxifene treatment. *Clin Biomech (Bristol, Avon), 17*(2), 81-88.

van Rossen, I. P., Braak, L. H., de Putter, C., & de Groot, K. (1990). Stress-absorbing elements in dental implants. *J Prosthet Dent, 64*(2), 198-205.

van Zyl, P. P., Grundling, N. L., Jooste, C. H., & Terblanche, E. (1995). Three-dimensional finite element model of a human mandible incorporating six osseointegrated implants for stress analysis of mandibular cantilever prostheses. *Int J Oral Maxillofac Implants, 10*(1), 51-57.

Viceconti, M., Muccini, R., Bernakiewicz, M., Baleani, M., & Cristofolini, L. (2000). Large-sliding contact elements accurately predict levels of bone-implant micromotion relevant to osseointegration. *J Biomech, 33*(12), 1611-1618.

Watanabe, F., Hata, Y., Komatsu, S., Ramos, T. C., & Fukuda, H. (2003). Finite element analysis of the influence of implant inclination, loading position, and load direction on stress distribution. *Odontology, 91*(1), 31-36.

Weinstein, A. M., Klawitter, J. J., & Cook, S. D. (1979). Finite element analysis as an aid to implant design. *Biomater Med Devices Artif Organs, 7*(1), 169-175.

Williams, K. R., Watson, C. J., Murphy, W. M., Scott, J., Gregory, M., & Sinobad, D. (1990). Finite element analysis of fixed prostheses attached to osseointegrated implants. *Quintessence Int, 21*(7), 563-570.

Young, F. A., Williams, K. R., Draughn, R., & Strohaver, R. (1998). Design of prosthetic cantilever bridgework supported by osseointegrated implants using the finite element method. *Dent Mater, 14*(1), 37-43.

Zampelis, A., Rangert, B., & Heijl, L. (2007). Tilting of splinted implants for improved prosthodontic support: a two-dimensional finite element analysis. *J Prosthet Dent, 97*(6 Suppl), S35-43.

Zysset, P. K., Guo, X. E., Hoffler, C. E., Moore, K. E., & Goldstein, S. A. (1999). Elastic modulus and hardness of cortical and trabecular bone lamellae measured by nanoindentation in the human femur. *J Biomech, 32*(10), 1005-1012.

KEY TERMS

Biomechanics: Research field involved in the structural and mechanical behavior of biological systems

Elastic Properties: The properties of a material which define how the material deforms in reaction to force application

Finite Element Analysis: Mathematical method for solving engineering problems

Implant: A device implanted in the human body - in the present context a dental implant inserted in the human jaw to replace one or more missing teeth

Osseointegration: The biological process during which a foreign body is rigidly anchored in the host tissues (bone) and maintains this anchorage under functional loading

Section V

Software Support in Clinical Dental Management and Education

Chapter XIII
Electronic Oral Health Records in Practice and Research

Amit Chattopadhyay
University of Kentucky, USA

Tiago Coelho de Souza
University of Kentucky, USA

Oscar Arevalo
University of Kentucky, USA

ABSTRACT

Electronic Oral Health Records (EOHRs) contains all personal health information belonging to an individual and is entered and accessed electronically by healthcare providers over the person's lifetime. This chapter presents a systematic review about EOHRs, describes the current status of availability of EOHR systems, benefits and barriers for implementation and EOHR usage in clinical, public health and research settings to pave the way for their rapid deployment. The chapter draws the scenario of how a fully integrated EOHR system would work and discuss the requirements for computer resources, connectivity issues, data security, legal framework within which a fully integrated EOHR may be accessed for real time data retrieval in service of good patient care practices. This chapter also describes the need for defining required criteria to establish research and routine clinical EOHR and how their differences may impact utilization and research opportunities to establish practice-based research networks.

INTRODUCTION

In 2003, Sittig, Kirshner and Maupomé (Sittig et al.2003) described an informatics-oriented, future-patient care scenario and identified key functions, applications, or technologies in the field of dental informatics. The scenario envisioned a completely paper-less series of interaction between a patient, his/her dentist, and several specialists starting from her initial presentation to completion of a series of procedures and scheduling periodic recall leading to an "ideal" treatment experience. It would be naive to think that such a system will not happen – its fundamentals are already in place. Such a system does not require technological marvels, but only needs proper integration of technologies that are in existence for some time. Central to this variety of tasks and sub-tasks in the oral health care system is the patient's health record.

Traditionally, patient information ranging from clinical history to research results has been stored in hard copy format all around the world. Such a storage system demands ever increasing space and is prone to easy destruction requiring great security systems for its physical existence and control of privacy of the information. Such a system also poses difficulty in duplication of data when needed, availability of real-time up-dated patient information over space and time, and poses even greater difficulty in organizing and aggregating the data for analyses. With the advent of computerized information processing and ever increasing cheap computer disk space and memory, it has become imperative to use this easily available resource to organize health records of patients in an easily retrievable manner in digitized format called electronic health records (EHRs).

EHRs digitize the contained information becoming a database that allows easy access to the information from individual EHRs, or in an aggregated manner. Development of electronic records for oral health requires substantial departures from standard EHRs because several specialty-specific nuances need to be incorporated to appropriately address the needs and maximize the benefits for patients, researchers, practitioners and academicians. Although EHRs have come into existence in routine medical care facilities, their adoption has been slow for a variety of reasons. Similarly, although development and incorporation of electronic oral health records (EOHRs) in day to day clinical practice has been anticipated, forecast and urged for long (Green 1996, Greenwood 1997, Miller 1995, Rada 1995, Schleyer 1995, Schleyer et al. 2001, 2003, Snyder 1995, Walther 1998), their adoption has been still slower. To respond proactively to the digital transformation of oral health care, dentists must become familiar with technologies and concepts (Umar 2002a, 2002b). They must learn what new information technology can do for them and their patients and then develop creative applications that promote the profession and their approaches to care (Bauer & Brown 2001).

WHAT IS EOHR?

Terminology of EHRs have undergone several changes and currently several terms are still used to represent EHRs. Terms such as: automated medical record (AMR), clinical data repository (CDR), computerized medical record (CMR), computerized patient record (CPR), computer-based patient record system (CPRS), electronic health record (EHR), electronic medical record (EMR), electronic patient record (EPR), lifetime data repository (LDR), virtual health record (VHR), virtual patient record (VPR) are some of the terms that have used interchangeably for EHRs. In dentistry, these systems have been variously referred to as: "electronic dental records", "dental electronic records", "electronic dental patient records", "electronic patient record system", "computer-based patient record", and "dental EHR". However, the term EOHR is more comprehensive compared to and is frequently being used universally – therefore, we resolved to use this term.

In general, EOHR is an electronic repository of patients oral health related information in form of a database at the back-end. Therefore EOHR contains a wide array of information (Heid et al.2002) including:

- Patient demographics
- Practitioner characterization
- Immunizations
- Health history

- Health conditions/ problems
- Examinations and findings
- Treatment plans/ clinical orders
- Diagnostic observations
- Radiographs, laboratory data and other investigation reports
- Prescribed medications
- All therapeutic interventions
- Hospital admissions and attendances
- Scheduled events
- Patient encounters

EOHR, therefore "contains all personal health information belonging to an individual and is entered and accessed electronically by healthcare providers over the person's lifetime. EOHR extends beyond acute inpatient situations including all ambulatory care settings at which the patient receives care. Ideally it should reflect the entire health history of an individual across his or her lifetime including data from multiple providers from a variety of healthcare settings, primarily to support continuing, efficient, and quality healthcare." (WHO, 2006) EOHRs must also continue to meet legal, confidentiality, and retention requirements of the patient, the attending health professional and the healthcare institution/ country

The Status of EOHRs

Currently, the use of EHRs and EOHRs and their outcomes are still considered as scientifically reportable events and clear quality assurance guidelines are derived from the HIPAA in the US.

EOHRs are slowly being recognized as the cornerstone of data storing and management on clinical, public health and research settings all over the world although the main thrust of evolving workable EOHRs has remained in the developing world, especially Canada, the United States, United Kingdom, Germany, Australia and New Zealand. EOHR development and adoption are also being reported from the developing countries such as Argentina, Brazil, China, Hong Kong, India, Indonesia, Korea, Malaysia, Singapore, Taiwan, and Thailand. In general, the world over, the introduction of EHR "seems overwhelming and almost out of reach to many healthcare providers and administrators as well as medical record/health information managers" (WHO, 2006).

The US Department of Health and Human Services (DHHS) took the lead in developing a National Health Information Infrastructure (NHII) which is a voluntary initiative aiming at improving "the effectiveness, efficiency and overall quality of health and health care in the United States". This infrastructure has been conceived as "a comprehensive knowledge-based network of interoperable systems of clinical, public health, and personal health information that would improve decision-making by making health information available when and where it is needed" (DHHS 2004) NHII integrates various aspects of individual health, health care, and public health such as: technologies, standards, applications, systems, values, and laws. The central focus of NHII is to implement computer-based patient records for most Americans, connect personal health information with other clinical and public health information, and enable different types of care providers to access computer-based patient records.

USDHHS pointed out categorically that the NHII is not a centralized database of medical records or a government regulation. The NHII integrates the "'lessons-learned' from other National systems (Canada, United Kingdom, and Australia) and ongoing projects". The NHII has three defined stages with outlined timelines: 1) development of leadership (2-years); 2) building collaboration between stake holders (5-years); and 3) Developing and implementing the infrastructure in all relevant public and private sectors (10-years – final target year: 2014) (USDHHS 2004).

Development of the NHII begot the question: Should dentistry be part of the National Health Information Infrastructure? (Schleyer et al. 2004b). The authors pointed out that the advantages of NNHII including "transparency of health information across health care providers, potentially increased involvement of patients in their care, better clinical decision making through connecting patient-specific information with the best clinical evidence, increased efficiency, enhanced bioterrorism defense and potential cost savings" and argued for integration of Dentistry into the NHII (Schleyer et al. 2004b).

EOHR: BENEFITS

EOHRs provide immense benefits in storage, retrieval, and utilization of data and are a key component of establishing efficient and effective evidence based clinical practices. EOHR help to save time and money by reducing paper work, duplicate laboratory and radiologic testing and eliminating the need for dictating services, reducing transcribing errors. In general, EOHRs:

- Improve the accuracy, precision and quality of data recorded in a health record and reduce errors in data recording
- Enhance access to patients' healthcare information by clinicians, researchers and public health authorities and increasing the ability to share data and facilitating continuity of care.
- Improve the quality of care as a result of having health information immediately available at all times facilitating inter-consulting among health care providers.
- Improve the efficiency of the health care delivery system.
- Contain healthcare costs

Access to Clinical Data, Medical Information and Population Data

Without an up-to-date record, it often becomes difficult to provide time high-quality care. Clinical dentistry has a need for complete current data on patients including medical history, radiological, laboratory, patient's drug sensitivity, resistances and allergies. Often such data may be present in different physical locations across clinics and centers which make difficult to procure and may lead to repeated procedures and testing. EOHRs allow available data to be accessed easily, even from distant locations in a comprehensive manner at any time of the day. This increases the efficiency of medical care and also allows speedy resolution to several issues by bypassing logistic problems related to manual chart retrieval and storage problems. Because EOHRs can be easily duplicated, it is also possible for more than one clinician to access the records at different places simultaneously. At the same time, integrating technological advances such as tele-dentistry into the system allows for quick conferences between multiple clinicians, laboratory staff, administrators and healthcare/ insurance managers.

Evidence based practice demands ready knowledge about recent advances. EOHRs address this issue by allowing the presentation of current medical findings which can be incorporated both actively and passively. Using EOHRs, practitioners can easily integrate references and cross-checks by incorporating guidelines, protocols, recommendations, clinical notes, directions at the point of care efficiently and effectively. EOHRs may also incorporate "built-in rules, alerts, or reminders that act to remind clinicians about care that is due for patients, both for preventive care and for chronic disease management. In more advanced systems, these reminders may allow for resolution of the issue at the point of care, allowing a clinician to resolve the issue from within the alert itself." (Cusack, 2008)

EOHRs can add functionality to track population data and parameters, incorporate flags to schedule and recall patients for preventive care, follow-up patients with a set of risk factors. The clinician can easily not just track laboratory, pathology, radiologic tests, but can also incorporate automatic flagging and alerts for abnormal results. Use of EOHRs eliminates the need for dictation and use of transcribing services. This eliminates a source of errors resulting from medical transcription errors.

Improvement in Patient Safety and Quality of Care

The Institute of Medicine's (IOM) report *To Err is Human* (IOM 2000) estimated that up to 98,000 patients were dying each year in the United States because of medical errors. A subsequent report suggested that the IOM's figure be an underestimate and the true number may be as high as 225,000 a year (Healthgrades 2004). Medical errors have been reported in dentistry resulting from procedural, diagnostic, dispensing, prescription and other processes (Pontes et al.2008, Ogunbodede et al.2005, Kim 2004, Bergenholtz et al.2004, Kim 2004, Krol et al.2002, Vaubert et al.1999, Oakley & Brunette 2002).

EOHRs with inbuilt rules, alerts, stops, range checks can go a long way in preventing a large proportion of these errors and maximize patient safety. It has been reported that even achieving a 10% improvement in quality care measures for the population served by small offices could have a substantial effect on public health (Baron, 2007) and EHRs contribute substantially to this improvement.

For example, in a pilot study at the University of Washington, a diabetes care module was developed, and the feasibility of allowing patients with type 2 diabetes to co-manage their disease from home using institutional EHR and web access by the patients in which one newly diagnosed patient was started on an oral hypoglycemic, underwent two upward dose adjustments, and achieved control by reducing HbA1c from 8.0% to 6.1% (Goldberg et al.2003). Similarly, several recent studies have reported the use of EOHRs to successfully assess health risk and improve oral health care quality and dental education. (Atkinson 2002, Delany 2004, Delrose 2000, Finkeissen et al.2002, Fouad & Burleson 2003, Freydberg 2001, Reis-Schmidt 2000)

Clinical Quality Assurance and Education Improvement

EOHRs play a major role in dental educational institutions in terms of improving student and patient experience, quality assurance, improving quality of education, and inculcating principles of evidence based practices among dental students and residents.

The international development and deployment of an electronic modularized dental curriculum is central to the development of an electronic engine to be used for the effective management of dental education. This will ensure continuity in high quality of care across all boundaries, through the continuous updating of its content and linkages to contemporary resources and databases. An electronic engine to be used for the effective management of dental education in a comprehensive dental school/hospital setting is at the core of an international 'virtual' dental education institution. The issue of policy development necessary to ensure consistency, quality and management for an electronic engine is at the very centre of: a) systems management and system databases; b) records of students, patients and personnel; and c) financial records.(Eplee et al.2002)

For example, in a recent study, Shelly et al.(2007) evaluated the use of an EOHR system to assess quality of care in an academic dental institution. Their primary outcome of interest was the timeliness and completeness of restorative care following completion of nonsurgical root canal therapy. They were quickly able to query the system and develop a report assessing permanent restoration, teeth build-ups, complete coverage restorations and were able to assess if patients were receiving recommended treatment. They were able to use EOHR "to objectively and efficiently assess one aspect of quality of care in a dental school environment" and found the use of EOHR to help in clinical assessment and quality assurance.

Minimizing Medication Errors

The Agency for Healthcare Research and Quality (AHRQ) in the United States has defined error as an act of commission (doing something wrong) or omission (failing to do the right thing) that leads to an undesirable outcome or significant potential for such an outcome. Medication errors may or may not cause harm to the patient. Such errors include any errors in dose, route, frequency, and drug choice (IOM 2000, Cusack 2008) that may due to prescribing multiple drugs of similar class, or due to drug-drug, and other possible interactions. Adverse drug events (ADE) may or may not involve medication errors, but may be avoidable if a patient has previous history of similar or related events. ADEs need to be tracked irrespective of whether they occur due to medication error or not.

EOHRs, when linked to electronic prescription systems and drug checking software, can reduce ADE and medication errors by alerting the clinician of such possibilities (for example through a pop-up message about ADE's and drug interactions, related to medications being prescribed, and by cross checking prescriptions against patient history, laboratory test results and other prescribed medications). One study found that some 21% of the prescriptions had errors (Shaughnessy & Nickel 1989). EOHRs also minimize errors resulting from legibility of prescriptions and prevent difficulties resulting from lost/ mutilated/ forgotten prescriptions and fraudulently prepared prescriptions. Drug dosing calculations based on patient's age and weight linked with updated information on liver, renal and other patho-physiological conditions can reduce dosing errors by calculating correct dosages, and modifying those in real-time on an as per need basis.

ADOPTION OF EOHRS IN CLINICAL SETTINGS

The fact that electronic systems, especially computers in dental clinical offices could revolutionize clinical management and practice was recognized very early. The earliest article we found that dealt with electronic data processing in the storage and retrieval of dental patient file information was published in 1967. (MacGregor & Halabisky 1967) With the advent of personal computers, their role in clinical dentistry was envisioned quickly and several articles predicted various scenarios of automated clinical practice. (Green 1996, Greenwood et al. 1997. Miller 1995)

A British study noted that despite the advantages of using computerized systems, many dental practices were only using them to a limited extent. (John et al. 2003) In a study about the adoption, utilization and attitudes toward clinical computing Schleyer et al.(2006) surveyed 256 randomly selected general dentists in the US using a 39-item interview questionnaire. These dentists were selected from among 1159 because they met the eligibility criteria of having computers at chairside. Among these, only 102 (39.8%) could be interviewed. The authors found that 1.8% of the dentists were working in a completely paperless environment. "Auxiliary personnel, such as dental assistants and hygienists, entered most data. Respondents adopted clinical computing to improve office efficiency and operations, support diagnosis and treatment, and enhance patient communication and perception. Barriers included insufficient operational reliability, program limitations, a steep learning curve, cost, and infection control issues." (Schleyer et al.2006)

… general dentistry has become increasingly computerized in the past 20 years…the proportion of all dental offices (generalists and specialists) with computers has increased from 11% in 1984 to over 85% in 2000. According to data from the Dental Products Report (DPR), a dental trade publication, the adoption of computers in treatment rooms follows a similar curve with a time lag of approximately 13 to 15 years. The 2004 Survey on computer/ internet usage by the DPR found that 30% of all general dentists used computers in the operatory [an operatory is a treatment room or bay equipped with a dental chair] (Goff 2004). Respondents' primary uses for computers at chairside included scheduling (77.9%), treatment planning (63.9%), patient education (60.7%), hard tissue charting (58.2%), and periodontal charting (54.1%). (Schleyer et al.2006)

Implementing clinical computing in a dental office is a difficult undertaking for a number of reasons. Most dental offices are small (75.3% of all dentists work in a solo practice) (ADA 2003) and thus cannot spend large amounts of capital on information technology (IT). Limited personnel resources require that most dentists outsource the installation and maintenance of the IT infrastructure to a vendor or consultant. Dental computer applications are complex because they must integrate and maintain structured data (such as intraoral findings, treatment plans, and the medical/dental history), free text (such as progress notes), images (such as radiographs and photographs), and three-dimensional models. (Eisner et al.1993) On a small scale, these systems integrate the functions that are typically found in medical software applications for registration, admission, discharge, and transfer; laboratory results; picture archiving and communications; computer-based patient records (CPRs); and billing and insurance processing. Currently, different companies supply the necessary software and hardware components, which makes integration a significant challenge for end users (Schleyler 2004a) … future research must address usefulness and ease of use, workflow support, infection control, integration, and implementation issues." (Schleyer et al.2006)

A study conducted by Flores-Mir reported on the perceptions of Canadian dentists. Using an anonymous self-administered survey by mail to a stratified random sample of 1,096 Canadian dentists (283 were finally available for analysis), the study found: the "usefulness of digital technologies in improving dental practice and resolving practice issues; to determine dentists' willingness to use digital and electronic technologies; to determine perceived obstacles to the use of digital and electronic technologies in dental offices; and to determine dentists' attitudes toward Internet privacy issues." (Flores-Mir et al. 2006)

Diffusion of innovation is the process by which an innovation is communicated through certain channels over time among the members of a social system (Rogers 2003). Depending upon whether people innovate or adopt innovation, they can be divided into: innovators, early adopters, secondary adopters, tertiary adopters, quaternary adopters, and laggards. Innovators are very few and only a small number of people are early adopters. Most people fall under "secondary, tertiary and quaternary adopters" depending upon how quickly they adopt the innovation. Laggards are the most skeptical people who are the last to adopt the innovation. In relation to EOHRs, at this time, it seems that in the US, early adopters have appeared and are incorporating EOHRs in their dental clinical environment.

EOHRs have started to make inroads into dental clinics and institutions slowly – though EOHRs are being increasingly adopted by dental professionals, the adoption rate is slow as is evident from the findings of the studies described above.

EOHRs may be viewed as innovations and adoption of innovations takes time because adoption of EOHRs requires behavioral modification on part of dental professionals. Behavior changes are slow and acceptance and adoption of innovations occur through processes known as “diffusion of innovation”. In relation to EOHRs, at this time, it seems that in the US, early adopters have appeared and are incorporating EOHRs in their dental clinical environment.

Commercial EOHR systems are critical to universal adoption of EOHRs across the world because the development of these systems represent good business opportunities for private investors. Larger scale adoption of EOHRs will require settling of the commercial EOHR offerings. Currently there are several major technical problems facing the developers of EOHR programs which may prevent quick adoption of EOHR by most of the dental community.

EOHR: PROBLEMS, PITFALLS AND BARRIERS

The interest in implementing EHR is similar in developing and developed countries as are the key issues, challenges and barriers (WHO 2006). Different countries and Institutions within countries are at different stages of implementation of EOHRs. While some countries are in the planning stage, others have implemented pilot projects, and some have implemented functional systems and are progressing to large-scale deployment and development of nationally integrated systems. Slow adoption of EOHRs has been attributed to several factors such as: clinician resistance, high costs, skepticism about return on investment, misaligned incentives, and technical issues related to their compatibility with query systems and larger back-end database systems. Anecdotal evidence suggests that EOHRs do not represent clinical information with the same degree of completeness and fidelity as paper records. These issues, challenges and barriers may be summarized into the following points.

- Resistance to change on part of healthcare providers
- Lack of standard terminology
- Issues related to clinical data entry
- Data coding issues and lack of skill in using disease classification systems
- Concerns about the correct software choice
- Issues related to integration of EOHR software with existing database systems
- High costs of hardware and software
- Data security, privacy and confidentiality issues
- Resistance to computer technology
- Lack of computer literacy and need for relearning and updating skills
- Concern about availability/ retrieval and accuracy of information in a timely manner
- Quality of electronic healthcare information and accuracy of data entries
- Issues related to space requirement and other associated logistics
- Involvement of clinicians and hospital administrators

Dealing barriers in implementing EOHRs require deft management of all or some of the points mentioned above. We approached a clinic manager of an academic institution in the US who described his experience in implementing EOHRs in an academic institution. He responded:

The initial function of the clinical management system (CMS) was for keeping accurate track of patients, procedures and billing. The CMS had 7 or 8 components, one of which was the EOHR. To make use of the EOHR it was necessary to implement the major pieces of the CMS which feed into the EOHR. A major concern for implementation was the significant dollar investment. The initial investment can be hundreds of thousands *of dollars and then the yearly maintenance fees in addition to licensing for users although some software is based on having blocks like 1-25, 25-50, 100+, etc. Although there is basic software that works well in private practice, in that particular academic institution we were charged to implement an enterprise CMS for the network offices that would eventually go into the dental school.* (Sullivan 2008).

Data Related Barriers

Lack of uniform standard data format and record content across clinical facilities is a major limitation for implementation of EOHR. Practitioners use different record formats, and even those using the same format may not collect data uniformly. This factor limits the integration of data among clinical facilities and health care organizations. This issue is compounded because different commercial EOHR systems use different formats and different technical specifications for the data. Technical data related barriers include:

- Different data formats and specifications used by different EOHRs.
- Lack of diagnostic codes impedes linking of diagnostic, treatment and claims data sets
- Adoption of ICD systems or procedure codes is not uniform and a variety of terminology exists to describe diagnoses, treatment and procedures
- Lack of universal identifiers (in several settings).

The dental profession should develop a more common record with standard diagnostic codes and clinical outcome measures to make the EOHR more useful for clinical research and improve the quality of care (Atkinson et al.2002). Bailit (2003) has pointed out the problem of inaccurate and non-specific diagnoses found in dental charts:

… the nomenclature used to describe dental diseases and treatments. For example, stating that the patient has periodontal disease means little, since this is a very broad term and does not describe the location, severity, or type of periodontal disease. Further, there is considerable subjectivity in how different dentists use this term. This means that periodontal disease may mean one thing in one practice but something different in another practice. Of course, this problem is not unique to dentistry, but it is a problem for researchers trying to use record data to understand why some patients are receiving certain services.

Data charting: Charting of dental data is a tedious and time consuming process. Therefore for those who are used to manual charting, the transition to electronic format involves re-learning the entire process and re-orienting to a new process. Flipping through paper is different from clicking through tabs. Similarly, the orientation of data fields in paper formats and EOHR are substantially different in structure.

A typical scenario leading to frustration out of technical issues not easily resolvable by the data entry operator or similar end user that occurs with EHR was recently reported by Baron (2007):

Unfortunately, our electronic signature did not transfer the contents of that document to the chart as data that a computer could conveniently manipulate. For that to happen, data must be entered into the chart in a structured format… An EHR is a large, highly structured database. Because patients do not usually present themselves or their histories in a structured data format, EHR users must translate what they hear or read into a format that the computer can use... Although much information can be readily translated (for example, medication data), some of it cannot (for example, recording for preserving the patient's voice). Electronic interfaces can automatically *import certain data, such as quantitative laboratory results, into the chart in a structured format. However, interfaces may not be reliably available for many clinical data."*

However, data retrieved from EOHRs although present in electronic form, give rise to several issues. Most EOHRs export data elements in Excel format. This limits the analytical functionality of the data to those functions that may be easily performed in Excel. However to maximize analytical yield, specialized statistical software need to be used. Transferring data from Excel to formats suitable for statistical software requires thorough checking of the Excel spreadsheets for appropriate marking of missing data, correct formatting of date and data fields etc., a process generally called as "data cleanup". Data clean up preparation of data elements and formats for proper use in statistical analytical software consumes a large amount of data analyst's time, apart from being a tedious process. Most of the times, analysts involved in cleaning of such data annotate their data clean-up outputs with a "the best that I could do". Anecdotal data suggests that in a study, some 90-95% of the total time is taken up in data cleaning whereas the actual analysis takes only 5% of the time. Our experience at the University of Kentucky has also been along similar lines. Furthermore, the data cleanup process cannot be automated because of non-standard terminology, data fields, varying formats and filters and variables across different EOHR programs. If multiple formats are to be accommodated in an analysis of data aggregated from different sources, the enormous data cleanup time required may even prohibit the conduct of the analysis.

In order to obtain greater harmony across EOHRs and make these systems better than paper records, the question to be asked is: what information should be contained in EOHRs, and in what format should those be inputted, retained and exported? A recent qualitative study reported an attempt to develop a basic content model for clinical information in paper-based records and examine its degree of coverage by commercially available EOHRs. (Schleyer et al.2007) The general conclusions from the study were revealing:

- Although dental records contain a relatively large number of fields, there is little agreement on what those fields should be.
- A complied list of dental record elements aggregated across different paper record formats contained more data elements than any EOHR system (70% of the elements were present in EOHR).
- Dental schools' records covered slightly more categories dentists' and vendors' records.
- Dental schools use more comprehensive medical history forms.
- There was a relatively high level of agreement on categories among paper-based and computer-based record formats.
- This agreement did not extend to data fields – only 57% of the data fields occurring in five or more paper records were contained in more than two EOHRs.
- Limitations in information representation in EOHRs were evident in charting hard tissue and periodontal findings, and procedures.
- Dedicated fields associated with developing problem lists or making diagnoses were absent in EOHRs
- Information coverage in EOHRs were more limited that paper formats

EOHRs contain lesser information and provide limited scope for covering clinical information that clinicians' may wish to add. Furthermore, data fields/ elements in EOHRs are grouped differently than paper formats which may lead to clinician's resistance in using EOHRs. Extensive navigation requirements in EOHRs through routines that may be perceived as counterintuitive may also be a limiting factor in clinician's resistance in using EOHRs. This suggests that the front-end interface of EOHR may need major modifications and re-designing to improve clinician compliance with using EOHRs on regular basis.

Data Entry Issues

Anecdotal data suggests some uneasiness in using a chair side computer for clinical data entry as it leads to breaks in the "rhythm" of clinical work. Infection control issues have also been raised by some clinicians. One alternative could be to record the data in paper and then input it into the EOHR. However, such a mechanism leads to repetitive work, increases costs and is time consuming. An alternative to have dedicated personnel for direct data entry as the clinician dictates is expensive and has the potential for transcription entry errors. As an alternative to these methods, voice activated direct data entry systems have drawn considerable attention as an ideal mechanism for data entry. Therefore, the possibility of a voice activated data entry system integrated with an EOHR system could be a perfect solution to popularize adoption of EOHRs.

Speech recognition in voice activated systems allows clinicians a hands-free option for interacting with computers, which is important for dentists who have difficulty using a keyboard and a mouse while working with patients. While roughly 13% of all general dentists with computers at chairside use speech recognition for data entry, 16% have tried and discontinued using this technology. (Yuhaniak et al.2007) Voice-activated modules are available for most leading EOHRs. "Improvements in speech recognition and microphone technology have helped voice-activated charting and clinical note dictation become more accurate, faster and easier to carry out than previously possible." (Drevenstedt et al.2005).

It has been suggested that with improvement of technology, voice activation will become a mainstream part of dental computer technology. Currently speech functionality faces several hurdles. It has been suggested that instead of being intuitive, speech functionality is directly comparable to using a mouse and the available systems require memorizing an enormous amount of specific terminology opposed to using natural language. "Overall, limited speech functionality reduces the ability of clinicians to interact directly with the computer during clinical care. This can hinder the benefits of electronic patient records and clinical decision support systems." (Yuhaniak et al.2007)

In an attempt to solve these issues, a recent study reported the analysis of structured data entry for dentistry using an interactive dental cross (DentCross component). This component is a graphic part of dental documentation connected to an EOHR. In conjunction with an automatic speech recognition system, based on a statistical approach, the speaker-independent (DentVoice component) made the data entry easier and faster. The study showed the practical ability of the DentCross component to deliver a real service to dental care and the ability to support the identification of a person in forensic dentistry. (Zvarova 2008)

Another recent study from the European Center for Medical Informatics, Statistics and Epidemiology at Prague in the Czech Republic (EuroMISE Centre) also reported encouraging results in voice activated EOHR technology using DentCross and DentVoice components (Nagy 2008). This study reported that "the junction of voice control and graphical representation of dental arch makes hand-busy activities in dental praxis easier, quicker and more comfortable." It is anticipated that these advancements will lead to better quality of the data stored in a structured form in dental EOHRs.

Security Issues and Health Information Protection

Security of data, when in storage or when transported/ transmitted via electronic medium, has been a major concern with patients, administrators, and governments. Personal information privacy issues have been regulated strongly in developed countries. The European Commission (1995) through the Directive 95/46/EC protected right to privacy of individuals with regard to the processing of personal data and transfer of data. Protection of electronic storage of clinical records was mandated in Japan through the directive number HPB No. 517 (Director-General HPB Japan 1999). Although the HPB No. 57 regulated data storage, these directives fell short of complete privacy of data:

These criteria must be followed when storing clinical records in electronic form, but do not need to be followed when using the information from the clinical records. However, an individual medical facility must pay attention to ensure the proper utilization of information from clinical records stored in various systems (i.e. source-input system, new and old systems). (Director-General HPB Japan 1999)

Because EOHRs deal with personally identifiable information and the nature of information is personal and private for the patient, the importance of maintaining privacy, security and confidentiality is paramount. To protect personal health information (PHI), measures are being taken at different level of social organization dealing with PHI – policy, judicial-legal, administrative, personnel and software levels. This issue has become more important due to the potential security breaches in databases that are reported in the media regularly and frequently. Data security is a major concern because of the potential for great harm that stolen data may cause in the hands of unscrupulous elements.

Computer-based, electronic dental record keeping involves complex issues of patient privacy and the dental practitioner's ethical duty of confidentiality… Authenticating the electronic record in terms of ensuring its reliability and accuracy is essential in order to protect its admissibility as evidence in legal actions. Security systems must be carefully planned to limit access and provide for back-up and storage of dental records. Carefully planned security systems protect the patient from disclosure without the patient's consent and also protect the practitioner from the liability that would arise from such disclosure. Human errors account for the majority of data security problems. Personnel security is assured through pre-employment screening, employment contracts, policies, and staff education. Contracts for health information systems should include provisions for indemnification and ensure the confidentiality of the system by the vendor. (Szekely 1996)

The lead in assuring security of PHI was taken by the US with the enactment of the Health Insurance Portability and Accountability Act (HIPAA) that was enacted by the U.S. Congress in 1996 under the Clinton Administration. It is also known as the Kennedy-Kassebaum Act. Title I of HIPAA protects health insurance coverage for workers and their families when they change or lose their jobs. Title II of HIPAA, known as the Administrative Simplification provisions, requires the establishment of national standards for electronic health care transactions and national identifiers for providers, health insurance plans, and employers. (USDHHS 2008, ADA 2005) HIPAA requires PHI to have administrative, physical and technical safeguards. A primary goal of HIPAA is to maintain confidentiality of an individual's identifiable health information if it is transmitted by electronic means for administrative purposes. (USDHHS 2001, Pai & Zimmerman 2002) The phrase, "identifiable health information," means the information itself can be directly or indirectly linked to a person. Another goal of HIPAA is the establishment of commonality of the format used for administrative "transactions."(Chasteen et al.2003a, 2003b)

The HIPAA privacy rule is designed to protect a patient's personal health information from being accessed by an unauthorized person. It mandates the creation of a format to be used by healthcare entities such as a dental clinic/ office/ hospital which transmit health information electronically to protect the confidentiality and security of health information by setting and enforcing standards. (Walker 2002) "The security regulations contain standards with both 'required' implementation specifications and 'addressable' implementation specifications. The security regulations require covered entities to adopt administrative, physical and technical safeguards to protect electronic protected health information." (Sfikas 2003) Some functions covered under HIPAA include: enrolment, claims (encounters, status, payments, and attachments), referrals, eligibility verification, premium billing, and first report of injury or compensation. All EOHR systems therefore are required to confirm to HIPAA mandates, and to modifications of regulations specific to the countries where those are used. (Day 2000, 2001) It is expected that other countries will develop their own regulations by adapting existing regulations from European Union, Japan and USA.

Impact on Workflow

Impact of EHR on workflow in terms of slowing down clinical work has been known to contribute to clinician resistance in using EHRs (Dansky et al.1999). Clinicians were concerned that a negative impact on workflow would reduce productivity. However, EHRs require re-learning and adapting to a new paradigm of data entry, and the learning-curve integrated in this need to re-learn may be the bottleneck for the workflow impact. It has been shown that once clinicians learn the EHR processes, their workflow and productivity return to normal in 30 days (Krall 1995).

It has been suggested that the possible slow-down in workflow with an EHR may be mitigated by using templates and forms. However, prior to implementing an EHR, paper templates should be created around all commonly seen diagnoses follow-up (Cusack 2008) and electronic templates should be adequately tested against those as has been reported by Schleyer et al.(2007). Thereafter, the electronic templates should be modified for comprehensive coverage, smooth navigation and ease of use in a busy clinical facility.

ESTABLISHING EOHR AND TRANSFORMING FROM PAPER RECORDS TO ELECTRONIC RECORDS

With the massive growth in computer technology and exponentially reducing digital storage space costs, implementing EOHRs is not really a choice anymore, but a necessity. An EOHR has become a priority in many countries, including the UK (Reynolds et al. 2008).

In the last several years, dentistry has crossed over into the new frontier of electronic dentistry. It has embraced such developments as computer programs for producing digital radiographs and photographs, as well as digital programs that enhance these images, store and organize them into a retrievable "chart-like" fashion, and transmit them via the Internet. In Europe, I saw patients with an electronic "health card." This credit card-sized CD can carry all the information on a patient's written charts, results of laboratory tests, radiographic/imaging information and more. It is expected that the mobile phone will be an alternate vehicle for patient records, and that these records will be accessed with a password security system. This will allow patients to carry their records from location to location. Certainly, the dental implications of such seemingly advanced processes are evident. The expression, 'The future is now,' was never truer. (Schutze 2001)

One of the key problems faced by any institution or clinical facility when converting from a paper-based/ manual health record system to EOHR is the planning of such a transition because the change reflects a paradigm shift in the way daily work is done. When instituting any major large-scale change, it is generally necessary to establish an Executive committee or hire a consultant knowledgeable in EOHR. These individuals must be integrated from the first day of planning and retained until the transition is completed.

WHO has developed a step-by-step manual to guide implementation of EHRs in developing countries (WHO 2006). The WHO guide reviews current health record systems and policies related to medical records practice. Thereafter it provides a sequential guidance to every aspect of setting up EHRs: planning for the introduction of an EHR; developing an implementation plan; factors to be considered when developing an EHR implementation plan; and finally points out the issues and challenges, providing reasonable solutions. This document is downloadable freely from WHO web site [http://www.wpro.who.int/publications/PUB_9290612177.htm] and is a very useful guide to anyone anywhere wanting to set up an EOHR system.

In order to implement electronic technology dependent methods, some key safeguards are necessary to ensure proper functioning. The basic general needed safeguards for EOHRs include existence of:

- Regular, reliable and efficient back-up system and protocol
- Electrical system emergency preparedness protocol and disaster-recovery protocol for EOHR
- Efficient, practical and easy to use security for work stations and servers and data
- Control over who is able to access the data and a system for data de-identification of data when accessed by individuals who do not need to know the patients' identity
- Mechanism to identify who accesses and/or modifies the data.

In the early 1990's the American Dental Association (ADA) published the monograph "The Computer-based Oral Health Record," to describe a specific EOHR that complements the EHR used for general healthcare. Subsequently, the ADA established a Standards Committee for Dental Informatics (SCDI) that promoted the application of information and various computerized technology. (Heid et al.2002) In 2001, the SCDI developed American National Standards Institute/ADA Specification 1000: Standard Clinical Data Architecture (ADA 2006) outlining the Structure and Content of an Electronic Health Record and is the first ANSI standard that defines the fundamental data structures used to create patient health records. The standard promotes the sharing of like data between dentists, physicians, and hospitals (Harrell et al. 2005). "This is a blueprint from which commercial vendors are encouraged to build uniform health records in interoperable practice management systems to prevent incompatibility problems between vendor systems. The SCDI is preparing an informational report called "Practitioner's Guide to Electronic Dental Records" to specify the capabilities of computer-based dental record systems." (Hamilton 2005) The ADA Technical Report No. 1004 provides a checklist of features and functions helps the dentist determine specific requirements and their priorities. "Characteristics of specific systems are then compared to these specific needs to rank the available choices. The report has also been updated to reflect increasing sophistication in the industry such as the charting interface of the clinical workstation. This specification will also be updated to reflect the growth of web-based systems and dental specialty requirements." (ADA 2004)

Supported by the ADA, orthodontic oriented solutions are being developed to send patient information to colleagues allowing practitioners to share the same patient record across different software programs by solving technical incompatibilities. (Magni et al. 2007) These orthodontic EOHRs aim to establish a seamless interchange of data between software programs and to create a standard for electronic orthodontic patient records.

EOHR SYSTEMS IN THE MARKET

Several EOHR systems are available in the market around the world, but most developers are in the US – most systems are commercial although few are freeware. Several notable systems are being developed by firms based in Canada, France, Germany, New Zealand, and elsewhere. Table 1 provides a list of commercially available and freeware EOHR systems along with the web addresses of the firms that are involved in developing those programs. Different EOHR programs work differently and comparative studies are rare. Only one comparative analysis has been published so far which found that commonly mentioned strengths of the software applications included easy to use/learn, scheduling, integration and flexibility, whereas common weaknesses included complexity, and integration issues. (Schleyer et al.2006)

The market-share of different programs varies. A study published in the United States found that the top five systems in terms of market share were Dentrix (26.2%) and Easy Dental (9.8%) (both from Dentrix Dental Systems, American Fork, UT), SoftDent (15.0%) and PracticeWorks (7.9%) (both from Kodak Corp., Rochester, NY), and EagleSoft (11.0%) (Patterson Dental, St. Paul, MN). (Clinical Research Associates, 2003 cited in Schleyer et al.2006) Anecdotal data suggests that in the US dental schools, AxiUm is commonly used system with EOHR software.

The main features included in the EOHR systems available in the market are : (a) appointment management, (b) clinical charting, (c) employees management, (d) financial management,(e) generation of presentations, (f) image interface, (g) insurance management, (h) laboratory tracking, (i) marketing management, (j) patient & family information, k) practice paperless, (l) prescription writing, m) reports tool, n) software integration, (o) touch screen, (p) treatment plan, and (q) 3D feature. Pricing of different commercial software vary substantially. Some have no up-front cost where one does not have to purchase the software *per se* but has to pay a monthly or annual fee for use the product (license). Others use a more traditional mechanism which one purchases at a one-time cost. Still others ask for payments of different services, such as support, maintenance or updates.

Table 1. Comprehensive list of EOHRs available in the market (in alphabetical order)

No.	Software name	Company	Country	Website
1	ABELDent	ABELSoft Corporation	Canada	www.abeldent.com
2	ACE Dental	American Computer Exchange	USA	www.ace-dental.com
3	AD2000	CLG	Canada	www.ad2000.info
4	Ad.I.C.O	Software Odontólogo	Argentina	www.software-odontologo.com.ar
5	ADSTRA Management	ADSTRA Systems Inc.	Canada	www.adstra.com
6	AlphaDent	AlphaDent	USA	www.alphadent.com
7	AltaPoint Dental	AltaPoint Data Systems, LLC	USA	www.altapoint.com
8	Apollonia	Procedia GmbH	Germany	www.procedia.de
9	AxiUm	Exan Enterprise	Canada	www.exanacademic.com

continued on the following page

Table 1. continued

No.	Software name	Company	Country	Website
10	BioDente	BioManager	Brazil	www.biomanager.com.br
11	Bridge-IT	Fusion Software Ltd.	United Kingdom	www.fusionsoftwareuk.co.uk
12	CDM	CamSight Co., Inc.	USA	www.camsight.com
13	Ciraden	Ciraden, Inc.	USA	www.ciraden.com
14	ClearDent	Prococious Technology Inc.	Canada	www.cleardent.com
15	Curve DMS	Curve Dental	Canada	www.curvedental.com
16	DAISY	Dentist Management Corp.	USA	www.daisydental.com
17	Data Team DDS	Data Team Corporation	USA	www.datateamdds.com
18	Datacon	Datacon Dental Systems	USA	www.datacondental.com
19	DDS Works	DDS Works	USA	www.ddsworks.com
20	DentaGrama	DentaGrama	Colombia	www.dentagrama.com
21	Dental 2000	Complete Systems, Inc.	USA	www.completesys.com
22	Dental Business	BioManager	Brazil	www.biomanager.com.br
23	Dental Clinic	Codegroup	Serbia & Montenegro	www.codegroup.co.yu
24	Dental Clinic	Dental Clinic	Brazil	www.dentalclinic.com.br
25	Dental-Exec	DSN Software, Inc.	USA	www.dentalexec.com
26	Dental 4 Windows	Centaur Software Development	Australia	www.centaursoftware.com.au
27	Dentalis	Dentalis Software	Brazil	www.dentalis.com.br
28	DentalManager	Larix Dental Concepts	Netherland	www.larixtechnology.nl
29	DentalMate	MDC Services, Inc.	USA	www.dentalmate.com
30	Dental Office	Rh ! Software Ltda.	Brazil	www.dentaloffice.com.br
31	Dental Office Manager Studio	Applied Computer Concepts	USA	www.dom2.com
32	DentalPro	Random Information Systems	USA	www.dentalprosoftware.com
33	Dentalpro	Prodoctor Software Ltda.	Brazil	www.dentalpro.com.br
34	Dental System	Dialog Medical Systems, Inc.	Canada	www.dialogmedsys.com
35	DentalVision	Henry Schein, Inc.	USA	www.discusdentalsoftware.com
36	DentalVox Plus	Softart	Colombia	www.dentalvox.org
37	DentalWare	OptiMicro Technologies, Inc.	Canada	www.dentalware.com
38	DentalWriter	Nierman Practice Management	USA	www.dentalwriter.com
39	Dentech	Softech, Inc.	USA	www.dentech.com
40	Denticon	Planet DDS, Inc.	USA	www.planetdds.com
41	DentiLogic	DentiLogic	Argentina	www.dentilogic.com
42	DentiMax	DentiMax	USA	www.dentimax.com
43	Dentisoft Office	Dentisoft Technologies, Inc.	USA	www.dentisoft.com
44	Dentista Pro	Logicroutes, Inc.	Philippines	www.logicroutes.com
45	Dentitek	Progitek dev, Inc.	Canada	www.progitek.ca
46	DentoNovo	NovoLogik, Inc.	Canada	www.novologik.com

continued on the following page

Table 1. continued

No.	Software name	Company	Country	Website
47	Dent-O-Soft	B-tech	Greece	www.dentist.gr
48	Denturist Office Manager	Specialized Office Systems	Canada	www.denturistsoftware.com
49	Denturotek	Progitek dev, Inc.	Canada	www.progitek.ca
50	Dentrix	Henry Schein, Inc.	USA	www.dentrix.com
51	Diamond Dental Software	Diamond Dental Software	USA	www.diamonddentalsoftware.com
52	Didimo	Galeon Technology Solutions	Costa Rica	www.gtscr.com
53	DOM for Windows	BRS Systems LLC	USA	www.brscomputing.com
54	EagleSoft	Patterson Dental Supply, Inc.	USA	www.eaglesoft.net
55	EasyDent	Data Tec, Inc.	USA	www.ezdent.com
56	EasyDental	Easy Software	Brazil	www.easysoft.com.br
57	Easy Dental	Henry Schein, Inc.	USA	www.easydental.com
58	EdgeDMS	Edge Health Solutions, Inc.	Canada	www.edgehealthsolutions.com
59	Efficient	Efficient System	Brazil	www.efficientsystem.com.br
60	EndoVision	Henry Schein, Inc.	USA	www.discusdental.com
61	Eurodent 2000	Inforabaco, S.L.	Spain	www.inforabaco.com
62	EZ 2000	EZ 2000, Inc.	USA	www.ez2000dental.com
63	EXact	Software of Excellence	New Zealand	www.soeidental.com
64	ExcelDent	ExcelDent	Canada	www.exceldent.ca
65	EXDental	EXDental	Brazil	www.exdental.com.br
66	Foxteeth	Foxteeth Software, LLC	USA	www.foxteeth.com
67	Galeno Dental 2000	Galeno Software	Mexico	www.galeno.com.mx
68	GCS DentOffice	Glendale Computer Services	USA	www.gcshealth.com
69	Genesis	Genesis Software	USA	www.genesissoftware.com
70	Gesden	Infomed	Spain	www.infomed.es
71	Gold Dental Management	Gold Dental Management Systems	Canada	www.gold-dent.com
72	Grin Dental Software	Environmental Design, Inc.	USA	www.edvan.com
73	GSD academic	General Systems Design, Inc.	USA	www.gsdgi.com
74	GSD groups	General Systems Design, Inc.	USA	www.gsdgi.com
75	iDental	HealthWare Corporation	USA	www.hwdental.com
76	impDAT	Kea Software GmbH	Germany	www.impdat.com
77	LiveDDM	Doctor Company, Inc.	Canada	www.liveddm.com
78	MacDent Pro	DDSMac, LLC	USA	www.macdentpro.com
79	MacPractice DDS	MacPractice, Inc.	USA	www.macpractice.com
80	Maxident	Maxim Software Systems	Canada	www.maximsoftware.com
81	MediaDent SQL	MultiMedia Dental Systems, Inc.	USA	www.mediadentusa.com

continued on the following page

Table 1. continued

No.	Software name	Company	Country	Website
82	MLS	Marcelo Liberati Sistemas	Argentina	www.marceloliberati.com.ar
83	MOGO	MOGO, Inc.	USA	www.mogo.com
84	Oasis	Software of Excellence International Ltd.	Australia	www.oasis-software.com.au
85	OdontoDop	Doper Tecnologia e Sistemas Ltda.	Brazil	www.doper.com.br
86	Odontológico	The Best Media Software Ltda.	Brazil	www.bestsoftware.com.br
87	Odontology	Avansys	Colombia	www.avansys.com.co
88	OdontoPlus	CarSan Software	Colombia	www.freewebs.com/odontoplus
89	OdontoSoft Millennium	GB Systems	Argentina	www.odontosoft.com
90	OdontoSys	IAQ Software	Uruguay	www.odontosys.com
91	OdontoWay	LS-Sistemas Ltda.	Brazil	www.lssistemas.com
92	Odisea	Aura	Colombia	www.aura.com.co
93	Office-Partner	Office Computer Systems, Inc.	USA	www.ocsdental.com
94	OmegaPrax Dental	Damar Software	USA	www.damarsoftware.com
95	OMSVision	Henry Schein, Inc.	USA	www.discusdentalsoftware.com
96	Open Dental	Open Dental	USA	www.open-dent.com
97	OPMS	Kodak Corp.	USA	www.kodakdental.com
98	Oral Surgery-Exec	DSN Software, Inc.	USA	www.oralsurgeryexec.com
99	Ortho Easy	Dental Soft.	Brazil	www.dentalsoft.com.br
100	OrthoFast	UpSide	France	www.upside.fr
101	OrthoNovo	NovoLogik, Inc.	Canada	www.novologik.com
102	Orthotek	Progitek dev, Inc.	Canada	www.progitek.ca
103	Orthotrac	Kodak Corp.	USA	www.kodakdental.com
104	Orthoware	Kodak Corp.	USA	www.kodakdental.com
105	Ortomed	Infomed	Spain	www.infomed.es
106	Pappyjoe	DR Toms International	India	www.pappyjoe.com
107	Paradigm Office Suite	Logic Tech Corporation	Canada	www.ltonline.com
108	PBS Endo	ProBusiness Systems, Inc.	USA	www.pbsendo.com
109	PeakDent	iDenex company	USA	www.peakdent.com
110	Perio-Exec	DSN Software, Inc.	USA	www.perioexec.com
111	PerioVision	Henry Schein, Inc.	USA	www.discusdentalsoftware.com
112	PerfectByte Dental	PerfectByte	USA	www.perfectbyte.net
113	PerfectByte Ortho	PerfectByte	USA	www.perfectbyte.net
114	Practice-Web	Practice-Web, Inc.	USA	www.practice-web.com
115	PracticeWorks	Kodak Corp.	USA	www.kodakdental.com
116	PracticeX	Exan Mercedes Software, Inc.	Canada	www.exanmercedes.com
117	Prime Dental	Prime Dental Software	USA	www.primedentalsoftware.com
118	ProDent	HartSystem Informática	Brazil	www.hartsystem.com.br
119	ProPráctica	ProPráctica Dental Software	Colombia	http://propractica.tripod.com

continued on the following page

Table 1. continued

120	Salud	Two-Ten Health Ltd.	Ireland	www.twotenhealth.com
121	SAM Odontologia	Nadoza S.R.L.	Argentina	www.nadoza.com.ar
122	SaralDent	SARAL Solutions	India	www.sarals.com
123	Sigosoft	BIMS of Perú	Peru	www.bimsac.com
124	Soel Health	Sofftware of Excellence	New Zealand	www.soeidental.com
125	Softdent	Kodak Corp.	USA	www.kodakdental.com
126	Star Byte Dental	Star Byte Systems, Inc.	USA	www.starbytesystems.com
127	SuzyDental	Suzy Systems, Inc.	USA	www.suzy.com
128	TalkTeeth	TalkTeeth	Egypt	www.talkteeth.com
129	The Complete Practitioner	Teleo Practice Services, Inc.	USA	www.teleoservices.com
130	TheSpecialist	Zalik Software Development	Canada	www.zaliksoft.com
131	Tiradentes	BioManager	Brazil	www.biomanager.com.br
132	ToothPics	ToothPics Company	USA	www.toothpicscompany.com
133	Tops	Cogent Design, Inc.	USA	www.iwanttops.com
134	ViewPoint	Ortho Computer Systems, Inc.	USA	www.orthoii.com
135	VisualDent	Innova Soluciones Tecnológicas	Chile	www.visualdent.com
136	Windent EE	HealthSoft, Inc.	USA	www.windent.com
137	Windent SQL	HealthSoft, Inc.	USA	www.windent.com
138	Windent OMS	HealthSoft, Inc.	USA	www.windent.com
139	W-Odonto	WAKO Software	Bolivia	www.wakosoft.com
140	XLDent	PEB of America, Inc.	USA	www.xldent.com

EOHRS IN RESEARCH AND PUBLIC HEALTH

EOHRs in Practice Based Research

Practice Based Research Networks (PBRNs) are teams of practicing dentists who investigate "everyday" issues in the delivery of oral healthcare with greater scientific rigor (NIDCR 2008).

In March of 2005, the US National Institute of Dental and Craniofacial Research (NIDCR) announced it has awarded three grants, totaling $75 million that establish regional "practice-based" research networks (PBRN) to investigate with greater scientific rigor "everyday" issues in the delivery of oral healthcare. (NIDCR 2008) The goal of PBRNs is to encourage practicing dentists and hygienists to propose and conduct each clinical study in close collaboration with their network colleagues. The general idea of developing the PBRNs is to address practical, real-world issues and generate data that will be of immediate interest to practitioners and their patients. (NIDCR 2008) Recently, a group of dental practitioners participating in the PBRN effort wrote about their perspective calling the effort to be a "win-win for private-practice dentists and the future of dentistry". (Veitz-Keenan 2007) Although not enough data is available at *this moment about success or utility of PBRNs in dentistry, such networks have been in existence in medical research for over two decades; they have generally been successful (Moskowitz 2007) and have resulted in significant clinical protocol changes.* (Chattopadhyay et al. 2008)

Successful PBRN activity requires that the PBRNs are linked group of clinical practices that can pool their data and resources to conduct research. Such data sharing will be possible only through coordinated use of compatible and standardized EOHR systems that allow data sharing and analyses. Similarly, administrative databases are also reservoirs of wealth of information that contribute greatly to develop workable health improvement policies. Several studies demonstrated the benefit of linking the service data to patient or provider characteristic through EOHRs. (Leake, Werneck 2005) The success of PBRNs depends upon active participation of dental practitioners who must use computers and EOHRs. As noted earlier, adoption of computerization among dentists have been slow. Training and follow-up support may encourage dental practice teams to develop more positive attitudes towards computerization and encourage them to use computers more extensively in clinical practice. (John et al. 2003)

EOHRs in Dental Public Health

Public health policies are usually based on analyses of data collected over a long period of time which also requires time for analyses. This creates a large time lag between the origin of the data and development and enactment of policies by when the nature of oral health realities may have changed. Use of EOHRs in PBRNs, public health settings and in other relevant clinical examination based surveys can help speed up the process and reduce the time between data collection and publication of analytical results from the survey thereby making policy making in "real time" possible - use of EOHRs can help

A recent report discussed and identified important design, implementation, and methodological issues with current EHR systems and their role in public health (Kukafka et al.2007). The authors suggested that "in order to support public health's traditional focus on preventive health and socio-behavioral factors, EHR data models would need to be expanded to incorporate environmental, psychosocial, and other non-medical data elements, and workflow would have to be examined to determine the optimal way of collecting these data." They also argue that redesigning EHR systems to support public health offers benefits not only to the public health system but also to consumers, health-care institutions, and individual providers. Although the need of immediate real time data in oral health surveillance is not as urgent as in surveillance for bioterrorism (biosurveillance), the characteristics and issues involved in data transmission from EOHRs in remote areas are the same as for biosurveillance.

Biosurveillance requires near-real-time event monitoring to enable early event detection and rapid response (Ventres et al.2000). The US Healthcare Information Technology Standards Panel's Biosurveillance Technical Committee has done extensive work on standards and interoperability issues for biosurveillance, employing a use case that involves transmitting ambulatory care, emergency department visit, utilization, and lab results data in standardized and anonymized format to public health agencies within one day. Steps in biosurveillance data transfer will include identifying relevant information, aggregating data, and anonymizing it, formatting it to public health specifications, identifying the relevant public health agencies, transmitting the data to them, and logging all transactions. Data could be sent data directly from individual health-care organizations, through some intermediary net-

worked organization, or through a combination of models. Importantly, this standards project is being harmonized with that of the EHR. The Biosurveillance Technical Committee has published extensive reports (BTC 2006a, 2006b) on standards needed to support this goal, as well as on remaining interoperability issues. (Kukafka et al.2007).

It has been suggested that guidance on what data elements to include may be gleaned from the Chronic Care Model (Wagner 1998) developed to reformulate healthcare from an acute care model in managing chronic diseases into a public health model.

One idea for use of EOHRs in public health setting is to use them in mobile devices so that data collection and transfer can be speeded up from remote areas. “No ideal customisable mobile digital solution currently exists but evidence from general healthcare use suggests that there are valuable features that can aid the general dental practitioners such as personal management and point of source assistance” (Reynolds et al.2008). Wireless personal digital assistants (PDA) together with data secure transmission of digital clinical information could be used in order to assist in disaster victim identification in areas where GSM cellular networks are available (Salo et al.2007). An experiment in the state of New York used PDAs for data collection in remote areas, but the program witnessed several transmission and integration problems inhibiting effective use of PDAs for such activities in oral health surveillance (Kumar 2008).

However, wireless transmission of records has recently been successfully adopted in orthodontic clinics.

Wireless cellular broadband technology currently transmits data at speeds that only wired broadband connections were capable of until now. By using high-speed data access protocols such as evolution data optimized (EV-DO) or enhanced data rate for global system for mobile communications evolution (EDGE), gaining access to patient data in an orthodontic office remotely has become a relatively simple task. Affordable and convenient cellular broadband networks allow the orthodontist to remotely access schedules, and update, review, add, or modify data virtually from anywhere. Newer generation wireless broadband technologies have made the virtual office a reality. (Mupparapu 2007)

Further enhancement of use of technological advancements will make it possible to use remote area data collection and their real time availability in analytical centers possible through the use of EOHRs that are adaptable to mobile data collection instruments such as PDAs and other hand held devices.

EOHR Input in Research Data

Data needs for oral health related clinical and public health research, especially when integrated with etiological research and basic science information are special. For example, the scientific methods require minimizing within- and between-examiner variability, highly accurate, and precise, regular periodic unbiased measurements and a battery of biologic measurements along with detailed disease and exposure measurements that may be out of scope of routine clinical EOHRs. However, clinicians involved in PBRNs would need to have access to such detailed parts of EOHRs for the purpose of research.

A general understanding of the measurement of dental diseases can help practitioners in the process of assessing the patient’s future risk of disease. More importantly, as clinical studies shift from the traditional academic setting to practice-based networks, practitioners might play a more significant role in research. An important issue in oral health disease management in the future *will be the standardization of clinical criteria and the development of alternative mechanisms of data collection for epidemiologic purposes.* (Chattopadhyay et al.2008)

To incorporate such standardization requirements may need substantial expansion of EOHRs which might make them prohibitively expensive or difficult to deploy in clinical settings. "It is not possible to extend the EHR data model to capture the entire host of factors, but an EHR's data model should represent those data elements that are known to contribute to the disease process in order to provide decision support and/or data transfer" to research centers on an as-per-need basis (Kukafka et al.2007).

It is however possible to develop modular EOHRs where clinical, practice, public health and research needs could be addressed by designing separate modules that can be appended to a core EOHR leading to an integrated database that can be as comprehensive as the need be, and yet deployed in smaller modules. Such a modular system can also be integrated with a clinical decision support system. (Benn et al.2000) A modular approach would enhance the scope of using EOHR system for a variety of activities beyond routine clinical work. For example, a public health EOHR modules would allow "high-quality population-level research by improving data quality, pooling it, and making it available for analysis through traditional epidemiological or data-mining methods' (Kukafka et al.2007); allow modification and redesign large surveys; expand scope of the type and depth of data collected from individuals; improve recruitment for clinical trials.

ESTABLISHING A PAPERLESS DENTAL OFFICE

The vision of a completely paperless office has the EOHR at its center, and needs several technologies to be integrated into a seamless working whole from which all benefits of EOHR can be utilized to maximum by clinicians, researchers, academicians and public health professionals and policy makers. Apparently there is a gap in the direction of research and implementation of an obviously needed system that would be conducive for modern methods of health information storage, retrieval and usage. Furthermore, implementation of EOHR is lagging way behind the available hardware and software resources for implementing EOHR. At the same time, it seems that the need for dental research databases and routine clinical use databases will have different sets of requirements to maximize analytical outputs from EOHR.

To make paperless offices possible will require researchers and dental professionals to address multiple grand challenges… The following applications, processes, and technologies would need to be designed, developed, and implemented:

1. *A system could profile patient risk for specific chronic oral disease status*
2. *A population-based system could assess the likelihood of successful outcomes for dental treatments such as implants, periodontal surgery, prostheses, amalgam, plastic, cast, and ceramic restorations.*
3. *3-D image manipulation and simulation systems could illustrate the effect on the current patient's appearance of specific proposed procedures,*
4. *An automated treatment planning system for all dental diagnoses could be used by clinicians (evidence-based guidelines for dental diseases and conditions, multiple semi-edentulous conditions, and malocclusions).*
5. *A decision aid for patients would help them learn about all personally relevant and applicable dental treatment options. Such a support system would also help patients in a decision making process that would lead*

to a value-based choice among the various alternatives.

6. *Procedures and processes would be needed to capture and analyze digital images progressively over time to track hard-tissue changes.*
7. *Nano-robots would be used intra-orally to monitor and transmit information on various markers of oral health status, such as salivary pH fluctuations and long-term trends, degree of mineralization shifts at certain index tooth surfaces, salivary enzyme and bacteriologic make-up changes over time, and information about crevicular fluid flow and composition.*
8. *Computer-based simulations could incorporate haptic feedback and thus allow students to develop and enhance their fine motor skills.* (Sittig et al.2003)

To attain this scenario, the following challenges that must be addressed:

1. *To develop a knowledge-based ontology of dental concepts from which one could extract a standardized controlled clinical terminology to describe dental signs, symptoms, conditions, diseases, and treatments (i.e., procedures, methods, techniques, materials, and devices).*
2. *To develop an evidence base of etiology, diagnosis, prevention, treatment, and treatment outcomes (including materials, methods, techniques, and usage) for a large proportion of dental patients and dental practices.*
3. *To develop a comprehensive electronic oral health record that is seamlessly integrated into the automated medical record. Such*
4. *To develop a nationwide oral health database that contains basic patient-level diagnostic, treatment, and outcome data linked to a nationwide medical database*
5. *To automate data capture, integration, and synthesis to create real-time, knowledge-based, clinical monitoring systems based on both continuously and intermittently available analog and digital data.*
6. *To develop learner-centered educational systems that select a learning goal, evaluate the student's abilities, and determine the individual learning style* (Sittig et al.2003)

CONCLUSION

Adoption of EOHR offers multiple benefits for clinical practitioners, academicians and researchers including ready access to patients' information, decreased medical errors, ability to share information with providers and health care organizations, collection of data for research purposes, etc. EOHRs must also balance the need to be integrated with EHRs although any EOHR system cannot be subordinate to, or a subset of, an EHR. From a public perspective, EOHR could result in improved oral health outcomes and reduced health care expenditures. While much progress has been made several challenges remain to be overcome. Integration of EOHR has been slow because it represents re-engineering current practices and processes, dealing with technical difficulties and data safety issues, which many perceive outweigh the benefits. However, as government and health care systems strive for improved efficiency and quality, the refinement of EOHR and wide adoption in dentistry seems to be where the future lies.

REFERENCES

ADA (2003). American Dental Association Survey Center. *Survey of dental practice.* Chicago: American Dental Association.

ADA (2004). *ADA Specification 1004 Computer Software Performance for Dental Practice Soft-*

ware. [www page]. URL http://www.ada.org/prof/resources/standards/informatics_reports.asp

ADA (2005). *Health Insurance Portability and Accountability Act (HIPAA) [www page]*. URL http://www.ada.org/prof/resources/topics/hipaa/index.asp

ADA (2006). *ADA Specification 1000: Standard Clinical Architecture for the Structure and Content for the Electronic Health Record*. [www page]. URL http://www.ada.org/prof/resources/standards/informatics_reports.asp

Atkinson, J. C., Zelle, G. G., & Shah, C. (2002) Electronic patient records for dental school clinics: More than paperless systems. *Journal of Dental Education*, *66*, 634-642.

Bailit, H. L. (2003). Health services research. *Adv Dent Res, 17*, 82-85.

Baron, R. J. (2007). Quality improvement with an electronic health record: Achievable, but not automatic. *Ann Intern Med, 147*, 549-552.

Bauer, J. C., & Brown, W. T. (2001). The digital transformation of oral health care: Teledentistry and electronic commerce. *J Am Dent Assoc, 32*, 204-209.

Benn, D. K., Kostewicz, S. H., Dankel, D. D., Segal, R., Schmidt, S. O., & Chardon, Z. (2000). Designing an electronic patient record with multiple real time decision support modules for managing diseases. *Proc AMIA Symp, 1168*.

Bergenholtz, G., & Spångberg, L. (2004). Controversies in endodontics. *Crit Rev Oral Biol Med, 1, 15*(2), 99-114.

Biosurveillance Technical Committee (BTC) (2006a). *Standards gap and overlap analysis biosurveillance use case: visit, utilization, and lab results data*. In: Office of the National Health Information Technology Coordinator, (Ed.), Evaluation of Standards Harmonization Process for HIT: Healthcare Information Technology Standards Panel.

Biosurveillance Technical Committee (BTC) (2006b). *Selected standards*. In: Office of the National Health Information Technology Coordinator, editor. Evaluation of Standards Harmonization Process for HIT: Healthcare Information Technology Standards Panel.

Chasteen, J. E., Murphy, G., Forrey, A., & Heid, D. (2003). The Health Insurance Portability & Accountability Act and the practice of dentistry in the United States: Electronic transactions. *J Contemp Dent Pract , 4*(4), 108-120.

Chattopadhyay, A., Arevalo, O., & Sohn, W. (2008). Understanding measurement of dental diseases and research participation in practice set-up. *Dent Clin North Am*, *52*(2), 367-86.

Cusack, C. M. (2008). Electronic health records and electronic prescribing: Promise and pitfalls. *Obstet Gynecol Clin N Am*, *35*(1) 63–79, ix.

Dansky, K. H., Gamm, L. D., Vasey, J. J., & Barsukiewicz, C. K. (1999). Electronic medical records: Are physicians ready? *J Healthc Manag*, *44*, 440–54 [discussion: 454–5].

Day, J. (2000) Cyberinfo: Privacy and personal health data in cyberspace. *J Contemp Dent Pract*, *1,* 1-6.

Day, J. (2001) Privacy and personal health data in cyberspace: The role and responsibility of healthcare professionals. *J Contemp Dent Pract*, *1*(2), 02-06.

Delany, J. (2004). Riding the wave of the future. Electronic patient charting debuts in student clinic. *Penn Dent J*, (pp. 2-5).

Delrose, D. E., & Steinberg, R. W. (2000). The clinical significance of the digital patient record. *J Am Dent Assoc*, *131*, 57S -60S.

DHHS. (U.S. Department of Health and Human Services) (2001). *HIPAA Administrative Simplification, Proposed Security Rule*. [www page]. URL http://aspe.os.dhhs.gov/admnsimp/bannerps.htm#security

DHHS (U.S. Department of Health & Human Services) (2004). The National Health Information Infrastructure (NHII 2002-2004) [WWW page]. URL. http://aspe.hhs.gov/sp/NHII/index.html

DHHS (2008). Medical Privacy - National Standards to Protect the Privacy of Personal Health Information. [WWW page]. URL http://www.hhs.gov/ocr/hipaa/

Director-General, Health Policy Bureau of Japan (1999). The Electronic Storage of Clinical Records. [www page]. URL http://www.medis.or.jp/2_kaihatu/denshi/file/e_notification990422.pdf

Drevenstedt, G. L., McDonald, J. C., & Drevenstedt, L. W. (2005). The role of voice activated technology in today's dental practice. *J Am Dent Assoc*, *136*, 157-161

Eisner, J., Chasteen, J., Schleyer, T., & Feldman, C. (1993). *The computer based oral health record: a new foundation for oral health information systems*. Chicago: American Fund for Dental Health.

Eplee, H., Murray, B., Revere, J. H., Bollmann, F., Haddad, G., Klimek, J., Barna, S., Rhodes, G., Looki, T., Malone, A., Molvar, M., Pienkowski, B., Schoonheim, M., & Teravainen J. (2002). Electronic management systems. *Eur J Dent Educ*, *6*(Suppl. 3), 152-160 File 16.

European Commission. (1995). Directive 95/46/EC. [www page]. URL www.cdt.org/privacy/eudirective/EU_Directive_.html

Finkeissen, E., Weber, R., Haßfeld, S., Koke, U., & Wetter, T. (2002). AIDA - Experiences in compensating the mutual weaknesses of knowledge-based and object-oriented development in a complex dental planning domain. *Methods of Information in Medicine*, *41*(2), 168-176.

Flores-Mir, C., Palmer, N. G,, Northcott, H. C., Khurshed, F., & Major, P. W. (2006). Perceptions and attitudes of Canadian dentists toward digital and electronic technologies. *J Can Dent Assoc*, *72*(3), 243.

Fouad, A. F., & Burleson, J. (2003). The effect of diabetes mellitus on endodontic treatment outcome Data from an electronic patient record. *J Am Dent Assoc*, *134*, 43-51

Freydberg, B. K. (2001). Connecting to success: Practice management on the Net. *J Contemp Dent Pract*, *3*(2), 050-061.

Goff, S. (2004). The Computerized operatory. *Dental products report* [WWW page]. URL: http://www.dentalproducts.net

Goldberg, H. I., Ralston, J. D., Hirsch, I. B., Hoath, J. I., & Ahmed, K. I. (2003). Using an Internet comanagement module to improve the quality of chronic disease care. *Jt Comm J Qual Saf.*, *29*(9), 443-51.

Green, S. R. (1996). Electronic vs. traditional recordkeeping. *Dent Econ*, *86*(8), 60-5.

Greenwood, S. R., Grigg, P. A., Vowles, R. V., & Stephens, C. D. (1997). Clinical informatics and the dental curriculum. A review of the impact of informatics in dental care, its implications for dental education. *Eur J Dent Educ*, *1*(4), 153-61.

Hamilton, J. (2005). Is the paperless practice possible?: A look at the ADA's electronic health record initiatives. *J Am Dent Assoc*, *136*, 161-162.

Harrell Jr., W. E., Stanford, S., & Bralower, P. (2005). ADA initiates development of orthodontic informatics standards. *Am J Orthod Dentofacial Orthop*, *128*(2), 153-6.

HealthGrades (2004). *Patient safety in American hospitals* [WWW page] URL http://www.healthgrades.com/media/english/pdf/HG_Patient_Safety_Study_Final.pdf

Heid, D. W., Chasteen, J.,& Forrey, A. W. (2002) The electronic oral health record. *J Contemp Dent Pract.*, *15, 3*(1), 43-54.

Institute of Medicine (IOM) (2000). *To err is human: Building a safer health system*. Washington DC: National Academy Press.

John, J. H., Thomas, D., & Richards, D. (2003). Questionnaire survey on the use of computerisation in dental practices across the Thames Valley region. *British Dental Journal, 195,* 585-590.

Kim, S. (2004). Modern endodontic practice: Instruments and techniques. *Dent Clin North Am*, *48*(1):1-9.

Krall, M. (1995). Acceptance and performance by clinicians using an ambulatory electronic medical record in an HMO. *Proc Annu Symp Comput Appl Med Care*, (pp. 708–11).

Krol, D. M., Stump, L., Collins, D., Roumanis, S. A., & Radford, M. J. (2002). A qualitative analysis of medication use variance reports. *Jt Comm J Qual Improv., 28*(6), 316-23.

Kukafka, R., Ancker, J. S., Chan, C., Chelico, J., Khan, S., Mortoti, S., Natarajan, K., Presley, K., & Stephens, K. (2007). Redesigning electronic health record systems to support public health. *J Biomed Inform., 40*(4), 398-409.

Kumar, J. V. (2008). *Problems with use of PDA in oral health surveillance in New York State*. Unpublished personal communication.

Leake, J. L., & Werneck, R. I. (2005). The use of administrative databases to assess oral health care. *J Public Health Dent, 65*(1), 21-35.

MacGregor, D. G., & Halabisky, W. A. (1967). Electronic data processing in the storage and retrieval of dental patient file information. *J Dent Educ*, *31*(4), 499-507.

Magni, A., de Oliveira Albuquerque, R., de Sousa, R. T., Hans, M. G., & Magnid, F. G. (2007). Solving incompatibilities between electronic records for orthodontic patients. *Am J Orthod Dentofacial Orthop*, *32,* 116-21

Miller, M. C. Expanding dental practices with computer technology. *Dent Today*. 1995 Sep *14*(9), 72-81.

Monteith, B. D. (1991). The electronic patient record and second generation clinical databases: problems of standards and nomenclature. *J Dent Educ, 55*(4), 246-52.

Moskowitz, E. (2007). *Clinical Research in Dentistry*. N Y State Dent J, *73*(3), 4.

Mupparapu, M. (2007). Remote access of electronic patient data with cellular wireless broadband technology. *Am J Orthod Dentofacial Orthop*, *132*, 260-5

Nagy, M., Hanzlicek, P., Zvarova, J., Dostalova, T., Seydlova, M., Hippman, R., Smidl, L., Trmal, J., & Psutka, J. (2008). Voice-controlled data entry in dental electronic health record. *Stud Health Technol Inform, 136,* 529-34.

NIDCR. (2008). NIDCR Awards Grants for New Practice-Based Initiative.) [WWW page]. URL http://www.nidcr.nih.gov/Research/ResearchResults/ScienceBriefs/CurrentSNIB/PBRNOverviewClinicalResearch.htm

Oakley, C., & Brunette, D. M. (2002). The use of diagnostic data in clinical dental practice. *Dent Clin North Am*, *46*(1), 87-115.

Ogunbodede, E. O., Fatusi, O. A., Folayan, M. O., & Olayiwola, G. (2005). Retrospective survey of antibiotic prescriptions in dentistry. *J Contemp Dent Pract. 15*, *6*(2):64-71.

Pai, S. S., & Zimmerman, J. L. (2002). Health Insurance Portability and Accountability Act (HIPAA). Implications for dental practice. *Dent Today. 21*(10), 106-11

Pontes, F., Pontes, H., Adachi, P., Rodini, C., Almeida, D., Pinto, D. Jr. (2008). Gingival and bone necrosis caused by accidental sodium hypochlorite injection instead of anaesthetic solution. *Int Endod J, 41*(3), 267-70.

Rada, R. E. (1995). Document imaging and the patient chart: Envisioning the future for your practice. Ill *Dent J*, *64*(3), 127-32.

Reis-Schmidt, T. (2000). Clinical software & electronic charting--Essential tools. *Compend Contin Educ Dent*, *21*(5), 416-21.

Reynolds, P. A., Harper, J., & Dunne, S. (2008). Better informed in clinical practice - A brief overview of dental informatics. *British Dental Journal*, *204*, 313-317.

Rogers, E. M. (2003). *Diffusion of innovations*, Fifth Edition. New York: Free Press.

Roy, M. (2008). Your data breach was probably avoidable. *eWeek*, *25*(19):24.

Salo, S., Salo, H., Liisanantti, A., & Reponen, J. (2007). Data transmission in dental identification of mass disaster victims. *J Forensic Odontostomatol.*, *25*(1), 17-22.

Schleyer, T. (1995). *TEPR95 Proceedings*, (pp. 299-306). Newton, MA: Medical Record Institute.

Schleyer, T., Spallek, H., & Hernandez, P. (2007). A qualitative investigation of the content of dental paper-based and computer-based patient record formats. *J Am Med Inform Assoc, 14*, 515-526.

Schleyer, T., & Spallek, H. (2001). Dental informatics. A cornerstone of dental practice. *J Am Dent Assoc, 132*(5), 605-13.

Schleyer, T., Speller, H., Battling, W. C., & Corby, P. (2003). The technologically well-equipped dental office. *J Am Dent Assoc*, *134* 30-41.

Schleyer, T. K. (2004a). Why integration is key for dental office technology. *J Am Dent Assoc*, *135*(Suppl), 4S-9S.

Schleyer, T. K. (2004b). Should dentistry be part of the National Health Information infrastructure?. *J Am Dent Assoc*, *135*(12), 1687-95.

Schleyer, T. K., Thyvalikakath, T. P., Spallek, H., Torres-Urquidy, M. H., Hernandez, P., & Yuhaniak, J. (2006). Clinical computing in general dentistry. *J Am Med Inform Assoc*, *13*, 344-52.

Schutze, H. J. (2001). Walk with a pen, or fly with a computer. Can electronic dentistry work for you? *N Y State Dent J*, *67*(10), 24-9.

Sfikas, P. M. (2003). HIPAA security regulations. Protecting patients' electronic health information. *J Am Dent Assoc*, *134*, 640-643.

Shaughnessy, A. F., & Nickel, R. O. (1989). Prescription-writing patterns and errors in a family medicine residency program. *J Fam Pract*, *29*, 290–5.

Shelley, P. Q., Johnson, B. R., & BeGole, E. A. (2007). Use of an electronic patient record system to evaluate restorative treatment following root canal therapy. *Journal of Dental Education*, *71*, 1333-1339.

Sittig, D. F., Kirshner, M., & Maupomé, G. (2003). Grand challenges in dental informatics. *Adv Dent Res*, *17*, 16-19.

Snyder, T. L. (1995). Integrating technology into dental practices. *J Am Dent Assoc.*, *126*, 171-178.

Sullivan, D. (2008). [Dental record systems]. Unpublished personal communication.

Szekely, D. G., Milam, S., et al. (1996). Legal issues of the electronic dental record: security and confidentiality. *J Dent Educ*, *60*(1), 19-23.

Umar, H. (2002a). Capabilities of computerized clinical decision support systems: The implications for the practicing dental professional. *J Contemp Dent Pract*, 1(3), 027-042.

Umar, H. (2002b). Clinical decision-making using computers: Opportunities and limitations. *Dent Clin North Am*, *46*(3), 521-38.

Vaubert, V. M., Moon, P. C., & Love, B. J. (1999). Extractable free monomers from self-cured dental sealants resulting from dispensing errors. *J Biomed Mater Res, 48*(1), 5-8.

Veitz-Keenan, A., Berkowitz, G. S., Brandes, I., Goldberg, K. L., Hamlin, D. A., Margolin, R., & Oen, K. (2007). Practice-based research networks. *N Y State Dent J, 73*(3), 14-15.

Ventres, W., Kooienga, S., Vuckovic, N., Marlin, R., Nygren, P., & Stewart, V. (2006). Physicians, patients, and the electronic health record: An ethnographic analysis. *Ann Fam Med, 4*(2), 124–131.

Wagner, E. H. (1998). Chronic disease management: what will it take to improve care for chronic illness? *Eff Clin Pract., 1*(1), 2-4.

Walker, R. J. (2002). HIPAA strategy for dental Schools. *J Dent Educ., 66*(5), 624-33.

Walther, W. (1998). Knowledge through documentation: From patients' data records to the basis of knowledge." *Int J Comput Dent, 1*(1), 18-28.

WHO. (2006). *Electronic health records: Manual for developing countries.* WHO, Manila, Philippines.

Yuhaniak, I. J., Fernando, S., Schleyer, T., & Spallek, H. (2007). Speech recognition in dental software systems: Features and functionality. *Stud Health Technol Inform, 129*(Pt 2), 1127-31.

Zvárová, J., Dostálová, T., Hanzlícek, P., Teuberová, Z., Nagy, M., Pies, M., Seydlová, M., Eliásová, H., & Simková, H. (2008). Electronic health record for forensic dentistry. *Methods Inf Med, 47*(1), 8-13.

KEY TERMS

Electronic Oral Health Record: An electronic repository of patients oral health related information that contains all personal health information belonging to an individual and is entered and accessed electronically by healthcare providers over the person's lifetime

HIPAA: Health Insurance Portability and Accountability Act (USA), enacted in 1996; protects health insurance coverage for workers and their families when they change or lose their jobs; Provides for maintaining confidentiality of an individual's identifiable health information if it is transmitted by electronic means.

Clinical Decision Systems: Systems representing a conglomeration of clinical knowledge management technologies that support the clinical process to help with differential diagnosis, final diagnosis, investigations, treatment selection and follow up care.

Practice Based Research Network: Teams of practicing dentists who investigate "everyday" issues in the delivery of oral healthcare with greater scientific rigor

Practice Management Software: Software that allows management of all aspects of a clinical practice including patient history, health records, billing etc.

Paperless Dental Office: A dental office where use of paper for record keeping, billing and other official work is eliminated unless absolutely necessary. Such an office keeps all records in electronic format, and also interacts with patients, insurance, specialist and other officials electronically.

Chapter XIV
Haptic-Based Virtual Reality Dental Simulator as an Educational Tool

Maxim Kolesnikov
University of Illinois at Chicago, USA

Arnold D. Steinberg
University of Illinois at Chicago, USA

Miloš Žefran
University of Illinois at Chicago, USA

ABSTRACT

This chapter describes the haptic dental simulator developed at the University of Illinois at Chicago. It explores its use and advantages as an educational tool in dentistry and examines the structure of the simulator, its hardware and software components, the simulator's functionality, reality assessment, and the users' experiences with this technology. The authors hope that the dental haptic simulation program should provide significant benefits over traditional dental training techniques. It should facilitate students' development of necessary tactile skills, provide unlimited practice time and require less student/instructor interaction while helping students learn basic clinical skills more quickly and effectively.

INTRODUCTION

In a comprehensive virtual reality (VR) simulator there are two important aspects that ultimately impact the way users interact with virtual objects: the visual impression of an object and touch-enabled interaction with it. While touch is one of the most fundamental ways for people to perceive physical objects (Gardner, 1983), until recently VR simulators focused primarily on the audio and visual aspects of simulation (Laycock & Day, 2003). However, to explore an object of interest we would like to be able to sense its physical properties by applying forces to it (Van Shaik et al., 2004; Broeren et al., 2007; Bird & Gill, 1987). This is possible by using special mechanical tools, called haptic devices, that enable the user to feel the feedback forces (Thurfjell et al., 2002). Recent technological advances have resulted in the production of a variety of affordable haptic devices, such as PHANToM™ Desktop (Massie & Sallisbury, 1994), providing possibilities for creating sophisticated simulation systems with vastly improved touch-based human-machine interfaces. Haptics allows the user to feel, manipulate and interact with the object displayed on the PC monitor. The user can touch, move and feel an existing distant object indirectly through a robotic arm. Furthermore, haptics provide force feedback to humans interacting with virtual or remote environments since the robotic arm is able to provide preprogrammed guidance.

This chapter is dedicated to exploring the uses and advantages of haptics-based simulators as an educational tool in dentistry. Tactile skills training, so necessary in dentistry, is very time-consuming, and requires extensive one-on-one instructor-student interaction. Traditionally trained students do not feel what the instructor feels nor can they be physically guided by the instructor performing a procedure. At the same time, high visual acuity is required from the student.

To aid in solving many of these problems, a prototype haptics-based VR dental simulator for training first-year dental and hygiene students to do periodontal probing and detect caries active and non-caries active white spot lesions (PerioSim©) has been developed at the University of Illinois at Chicago (UIC) through joint efforts of the College of Dentistry and College of Engineering. The addition of haptics allows the trainee to feel and interact with onscreen objects. The device is designed for training and evaluation of performance in periodontal probing and white spot caries activity by dental students, hygiene students and practicing professionals. These technological tools being developed at UIC should aid in solving some of the pressing problems faced by dental schools, such as the decreasing pool of dental school instructors, the reduction in time instructors interact with students, and the limited time available to practice various dental procedures. Furthermore, computer technology can dramatically reduce the need for students to practice on patients.

SIMULATOR COMPONENTS

The simulator system consists of a high-end computer workstation with appropriate software (listed below), a haptic device, and a stereoscopic computer monitor with stereo glasses. The computer renders three-dimensional (3D) graphics that can be viewed with the stereo glasses, and operates the haptic device that provides a realistic tactile sensation. Onscreen VR instruments can be manipulated on this monitor by operating the haptic device stylus for sensing life-like contact and interaction with teeth and associated periodontal structures.

The haptic device utilized in the system is PHANToM™ Desktop (SensAble Technologies, Woburn, MA, USA). It provides a range of motion approximating hand movement pivoting at the wrist. The device includes a passive stylus and provides 6-degree-of-freedom (6-DOF) positional sensing and 3-DOF force feedback. The PHANToM™ haptic device connects to the PC via a parallel port (EPP) interface. The device allows the user of the simulator to move freely and explore the virtual environment with the stylus without feeling any unnecessary or unnatural forces. The tactile sensation is created by the actuators and breaks which are, in turn, controlled by the simulator software. There exists another variation of the PHANToM™ haptic device that can provide 6-DOF force feedback but this is extremely costly. The less expensive 3-DOF force feedback haptic device is used in this project. As such, only forces (and not torques) can be displayed by the device and the haptic interaction is effectively limited to single-point contacts. The default haptic update rate provided by the PHANToM™ is 1 kHz. A parallel port interface connects the haptic device with a Dell Xeon 530 Workstation (Dell, Austin, TX, USA) equipped with 3.0 GHz dual CPU, 2 GB RAM, and 256 MB nVidia Quadro FX 3400 Graphics Card (nVidia, Santa Clara, CA, USA). A high quality Crystal Eyes™ monitor with Crystal Eyes™ stereo glasses (Stereo Graphics Corp., San Rafael, CA, USA) is used to view 3D graphic images generated on the workstation. A PowerPoint™ (Microsoft Corp., Redmond, WA, USA) presentation on a second monitor (flat panel Dell LCD) provides basic procedure information and instructions (Figure 1).

The simulator software (PerioSim©) is developed in C++ programming language using several specialized libraries.

General Haptic Open Software Toolkit (GHOST™, SensAble Technologies, Woburn, MA, USA) (Thurfjell et al., 2002) is employed in order to use the PHANToM™ haptic device in the simulator. This general cross-platform haptic application programming interface (API) processes the interaction with the haptic device by constantly monitoring for collisions between the stylus, representing a dental instrument on the screen, and the objects in the virtual environment (collision detection), and computes the force to be conveyed to the user through the haptic device when a collision occurs (haptic rendering). The illusion of touching the onscreen object is created in this way. The API allows developers to control various physical properties of virtual objects such as location, mass, friction and stiffness.

For the graphical display of the objects on the screen, the Coin3D™ (Systems in Motion AS, Oslo, Norway) library is used. This is a special API for rendering 3D graphics. It is important to have the two API data structures (GHOST™ and Coin3D™) synchronized, so that visual and haptic data refer to the same virtual scene and are therefore consistent. For the various elements of

Figure 1. Simulator setup: the operator wearing 3D glasses, 3D visualization monitor, haptic device and LCD flat panel monitor.

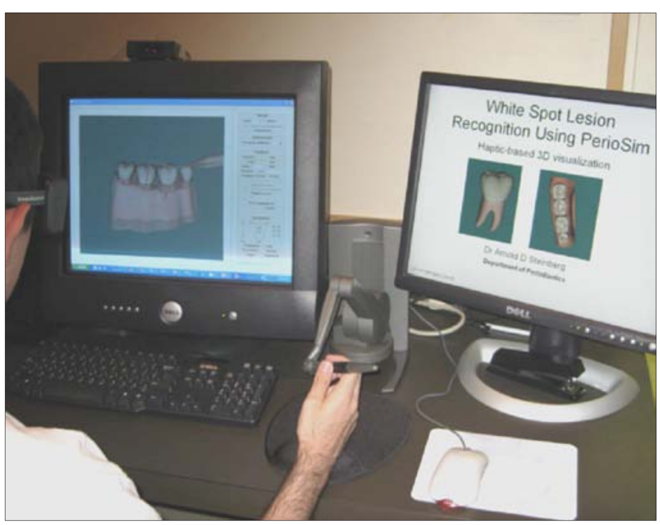

common graphical user interface (GUI) Fast Light Tool Kit (FLTK™) (Digital Domain, Venice, CA, USA) is used. Such elements include buttons, menus, dials and various selectors.

The simulator provides both visual and haptic feedback, therefore the simulator software must update both haptic and visual data without any noticeable delay between the two. The haptics update routine runs strictly at 1 kHz and is maintained by the API library and the PHANToM™ hardware. This refresh rate is high enough to simulate realistically a wide variety of materials, including the tissues that are present in a human mouth, even some very stiff materials such as a tooth surface. When performing the rendering of stiff materials special care needs to be taken to maintain the stability of the system. The system must have sufficiently high haptic refresh rate. The provided rate of 1 kHz is high enough for all practical purposes, but if the rate drops below this value (e.g. the hardware is too slow), an appropriate error message is displayed to the user. The graphics update routine runs at about 30 Hz on this system. It is maintained by the Coin3D™ graphics library and its refresh rate depends on the CPU speed. This refresh rate is sufficient for visualization purposes, so there are no noticeable latencies. If slower hardware is used, the graphics refresh rate is automatically reduced and delays in displaying the graphics may be introduced. For realistic simulation the graphics refresh rate should be at least 25 Hz.

A realistic, finely detailed model of a four-tooth mouth segment (lower right 2nd bicuspid through lower right 3rd molar) was developed by Illumen Group, Evanston, IL, USA for use in PerioSim©. The model contains gingiva, bone, connective tissue attachment, junctional epithelium and teeth depicted in Virtual Reality Modeling Language (VRML). VRML is an open standard for representing 3D interactive vector graphics. With this model periodontal structures can be observed in both normal and pathological states allowing students to view, feel and study differences between these states in a 3D environment while having unlimited time to practice on the simulator (Figure 2).

Additionally, a depiction of caries active and caries inactive lesions (white spot lesions) are shown on various surfaces of the 1st and 2nd molars, permitting students to differentiate these conditions (Figure 3). The trainee has unlimited practice time to become familiar with the visual as well as tactile aspects of early dental caries (white spot lesions). Since the anatomical models have been developed in the VRML format, they are easy to reuse in other applications and can be shared over the Internet. This format also al-

Figure 2. Various individual periodontal structures can be seen in healthy and diseased areas. Also shown are two white spot lesions with the one on the left being felt as caries active.

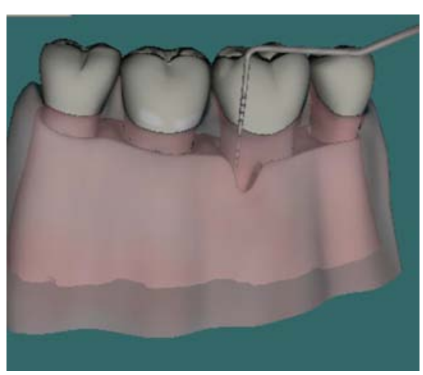

Figure 3. Shepherd's hook explorer evaluating possible carious white spot lesions on the occlusal of the model.

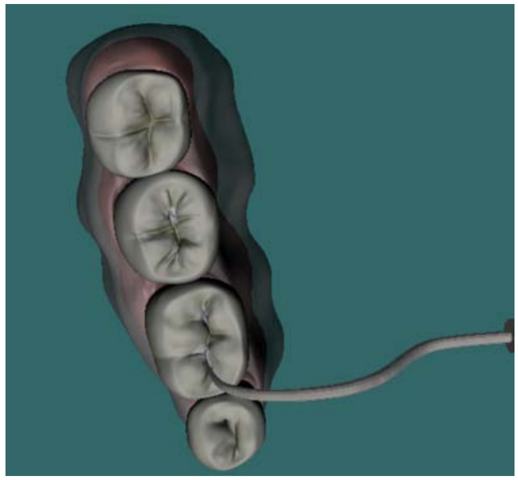

lows for easy modifications of the models in the future. Additional features such as normal and periodontal disease induced bone pathologies, gingival pathologies and calculus, have been modeled in VRML format, and overlaid within the main model. Two-dimensional (2D) models are being used as a reference in developing the 3D models that will depict both a healthy and diseased periodontium.

Interestingly, such demanding graphics applications were formerly run on expensive graphics supercomputers, however now comparatively low cost equipment can provide enough computational power to run the simulator software. The current system can now be run easily on a dual core desktop PC. A completely portable version of the simulator has been developed using a dual core laptop PC with a parallel port adaptor for attaching the haptic device. Reduced cost and compact size of such systems are important assets that allow haptics-based virtual reality technology to be widely used in a broad range of applications including dental education.

SIMULATOR FUNCTIONALITY

The simulator consists of several functional blocks realized in its software. These include model selection, graphics and haptics control as well as record and replay functionality.

Model Selection

Currently there are over 10 dental instruments which may be chosen for haptic use, including Williams, UNC15 and CP12 periodontal probes, Shepherd's hook, periodontal explorer, and Gracey scaler. New instruments, gingiva, teeth, bone and other components for the 3D VRML models can be added easily when desired. These 3D models are geometrically and anatomically accurate and constructed to our specifications by a commercial graphics company (Illumen Group, Evanston, IL, USA). Once 3D VRML models are constructed they can be configured for use through a special configuration file, and observed and felt in the PerioSim© program through a haptic device. This functionality was incorporated in the latest version of the software in order to make it more versatile and allow the user to handle most routine adjustments to the simulator without any need for a programmer. This was also done to allow the simulator to be used for any training system, be it medical or non-medical: requiring only the specific 3D instrument models and/or the 3D model of the system. Thus, PerioSim© can be used for a variety of applications.

3D movements of any of the selected instruments are through the use of the stylus attached to the haptic device. The user can also rotate the model in one of the three planes (*XY*, *YZ*, *XZ*) and move the model along one of the three axes (*X*, *Y*, *Z*) using the navigation control block.

Graphics Control

In the main window of the simulator the user can see the full-screen 3D model of a lower right quadrant of a dental arch along with the main control panel. The main control panel (Figure 4) can be hidden and reactivated by using pre-assigned function keys. The main control panel contains a variety of controls for navigation which include options to select and manipulate gingiva, teeth, bone and any other model objects. The trainee can induce varying degrees of transparency of the selected objects using a slider bar.

Another available feature is the ability to turn on or off groups of objects. Initially, two groups are formed: gingiva and bone in one group and teeth in the other. The groups may be reconfigured by the user in the configuration file. Special buttons allow users to switch immediately to buccal, occlusal or lingual views of the model. For other applications (e.g. non-dental) these views may be redefined in the configuration file as well. Also available is the positioning aid tool that allows the trainee to observe for 2 seconds the occlusal

Figure 4. Main control panel

view of the entire scene, which includes the dental instrument. In many cases this aids the user, especially a novice, to achieve the proper alignment of the instrument for a specific procedure.

Haptics Control

In the main window of the simulator the user can control the haptic properties of the simulation process. This includes the basic ability to turn haptics on or off for each selected object.

A force magnitude indicator (in vertical grams-force being applied) allows the student to feel the small amount of force used for periodontal probing. It is well documented that the force of around 20 gf (0.196 N) is all that is required for periodontal probing (Magnusson et al., 1988; Van Der Velden, 1979). However, it is difficult, if not impossible, to describe to a student how much force this is. With the use of a haptic device, the exact force reading can be viewed and felt by instructor and student, thus greatly enhancing the learning experience. Once the required force of 20 gf (0.196 N) is reached, the force magnitude indicator changes color from white to red. This sends a visual cue to the student to reinforce the experience.

The additional haptic parameter panel can be viewed by using one of the function keys. It contains the four sliders controlling several haptic parameters for teeth, gingiva or bone (Figure 5).

The haptic parameter panel controls the following parameters:

- **Viscosity:** The resistance that a material offers to flow when it is subjected to a shear stress (Parker, 1984).
- **Stiffness:** The ratio of a steady force acting on a deformable elastic medium to the resulting displacement (Parker, 1984).
- **Static friction:** The force necessary to start one solid surface just sliding over another horizontal surface (Lord, 1986).
- **Dynamic friction:** The force necessary to keep one solid surface just sliding over another horizontal surface (Lord, 1986).

These haptic parameters can be altered separately for each object.

Record and Replay Functionality

An important functionality implemented in the simulator is 3D haptic recording and playback capability allowing the user to record the motion of an instrument for up to 5 minutes. This allows an instructor to create short scenarios of

Figure 5. Haptics control panel

procedures, such as periodontal probing, which can be stored and played back on the computer by the student at any future time, either from storage media or over the Internet.

A recorded 3D motion can be filtered to eliminate or decrease any extraneous movements using a built-in 3rd order Butterworth filter (Butterworth, 1930) with an adjustable cut-off frequency (f_c). In this application, the value of the cut-off frequency that was suitable for the removal of unintentional hand shaking or tremor was experimentally found to be $f_c = 1.5\,\text{Hz}$. The recorded motion can be saved in a specified file, and then exported and viewed on any other PC using the developed viewer application. The viewer is essentially a much-simplified version of the simulator with all the haptic features removed. The recorded 3D motion can be played back in one of the three modes:

1. **Observation mode:** During playback a trainee can cradle the stylus, observe a "ghost" (green transparent) image of the original instrument and view the on-screen instrument movement. A recorded procedure can be paused and the 3D viewing component of the program permits playback from any angle, so that the user can observe various views of an instrument, teeth, and any other periodontal structures, both healthy and diseased. Various degrees of transparency can be applied to this model.
2. **Learning mode:** A trainee holds the haptic stylus and actually physically feels it guiding his/her hands through exactly the same movements felt by an instructor while encountering the same tactile feedback. This hands-on nature of the procedure is a major benefit of the robotic properties of PerioSim© , making the process more enticing for most students.

In this mode, the recorded graphics data is displayed as in the observation mode and a haptically-rendered guiding force is applied that drags the user-controlled instrument to the desired recorded position. This guiding force is calculated according to the following algorithm. First, the difference vector, Δp, between the desired position of the tip of the instrument, p_{goal}, and its actual position, p_{act}, is calculated as

$$\Delta p = p_{goal} - p_{act} \tag{1}$$

Then, the guiding force F is calculated as a function of this difference vector according to the expression

$$F = \begin{cases} \dfrac{k\|\Delta p\|_2^2}{\varepsilon_1}, & \|\Delta p\|_2 < \varepsilon_1 \\ k\|\Delta p\|_2, & \varepsilon_1 \le \|\Delta p\|_2 \le \varepsilon_2 \\ 0, & \|\Delta p\|_2 > \varepsilon_2 \end{cases} \tag{2}$$

where k (the proportional coefficient), ε_1 and ε_2 are some parameters. In Eq. (2) the guiding force F is proportional to the distance between the desired and actual position of the tip of the instrument if the distance is between ε_1 and ε_2 units. If the distance is greater the guiding force is turned off completely being set to zero. It is assumed that in this case the user has decided to abandon the learning mode. As the actual position of the tip gets closer than ε_1 units to the target position, the value of the force is determined using a quadratic function. This is done to insure that the absolute value of the guiding force is sufficiently low at the points where $p_{goal} \approx p_{act}$, so that the user does not feel these sudden force "jumps", particularly when the value of the proportional coefficient k is high. Computed value of the guiding force F is passed through the limiter

$$F_0 = \begin{cases} F, & \|F\| \le F_{\max} \\ F_{\max}\,\mathrm{sgn}(F), & \|F\| > F_{\max} \end{cases} \quad (3)$$

where we make sure that the displayed force F_0 is not greater than $F_{\max}$, the maximum possible value that can be displayed through the system. This parameter is based on the specifications of the haptic device as well as safety concerns. Generally, parameters k, ε_1 and ε_2 are determined experimentally. In the current system $k = 0.1$, $\varepsilon_1 = 10\,\mathrm{mm}$ and $\varepsilon_2 = 60\,\mathrm{mm}$. A limiting constraint $F_{\max} = 0.5\,\mathrm{N}$ on the rendered force was also set, but in principle greater forces can be displayed.

To take into account not only position but also orientation information, the difference vector $\Delta\alpha$ between the desired orientation of the instrument α_{goal} and its actual orientation α_{act} is also calculated in the program loop as

$$\Delta\alpha = \alpha_{goal} - \alpha_{act}, \quad (4)$$

where the quantities α_{goal} and α_{act} are expressed using Euler angles.

Two different techniques can be used to teach the correct orientation of the instrument. The most obvious teaching method would be to calculate a guiding torque and exert it through the haptic device. This approach is essentially the same as that applied to teach the correct position of the instrument. In this case, however, a very expensive 6-DOF haptic device is required. Another approach can be used with more affordable 3-DOF haptic devices. To draw the user's attention to the wrong orientation of the instrument, a clue can be given using modalities other than haptics, e.g. a visual clue and/or a sound. In our system both are used. Visual cues are the most important since such cues are the usual way by which most learning occurs. In the visual clue method, sight is used to observe the instrument stereoscopic position and its proper 3D alignment in relationship to both the gingiva and the tooth surface. Instrument, gingiva and tooth alignment can be further modified by viewing these relationships from different views (e.g. buccal, lingual, occlusal and angled views). By using these viewpoints, the observation of an instrument going improperly into the structure of the tooth or gingiva can be quickly compensated for and corrected by the user. An alarm that is controlled by the logic is used to enhance the visual cues:

$$\mathrm{ALARM} = \begin{cases} \mathrm{ON}, & \|\Delta\alpha\|_2 > \gamma \\ \mathrm{OFF}, & \|\Delta\alpha\|_2 \le \gamma \end{cases} \quad (5)$$

where γ is an experimentally determined threshold parameter. In our system, $\gamma = 0.5$ rad. Expression (5) is continuously re-evaluated in the main loop of the program.

It is important to note that when a user follows the prerecorded trajectory perfectly, he/she feels the same tactile feedback that was felt by the instructor. This means that in the case of perfect trajectory tracking an ideal haptic playback can occur, i.e. the student will both follow the recorded trajectory and feel the forces that were felt by the expert when the recording was made (Williams et al., 2004).

3. **Testing mode:** This mode is designed for testing the ability to repeat a recorded procedure; e.g. periodontal probing or initial caries evaluation. No recorded graphics or haptics data are displayed (although either or both of these capabilities could be turned on if needed). The trainee can perform the same procedure recorded by the instructor and receive instant grading of how well the procedure was performed. An aggregate score G is determined as:

$$G = 100 - \frac{r_1}{N}\sum_{i=1}^{N}\left(\|\Delta p_i\|_2 + r_2\|\Delta\alpha_i\|_2\right), \quad (6)$$

where Δp_i and $\Delta\alpha_i$ are vectors of differences in position and orientation calculated on the ith frame according to Eqs. (1) and (4), N

is the total number of frames in the testing sequence, r_1 and r_2 are experimentally determined parameters. We used $r_1 = r_2 = 5$. From Eq. (6) it can be seen that the score reaches its maximum of 100 when $\Delta p_i = 0$ and $\Delta\alpha_i = 0$ for all values of i ranging from 1 to N. Since it is convenient to give the score on a standard scale between 0 and 100 points, the displayed grade G_0 needs to be limited to non-negative values according to

$$G_0 = \begin{cases} G, & G \geq 0 \\ 0, & G < 0. \end{cases} \quad (7)$$

It may be desirable to slow down the playback in the observation and learning modes or even stop it completely, so that a student can absorb the unfamiliar technique better. Then, if desired, he or she can rotate the model and take a look at the position of the instrument from various angles. In the simulator it is possible to adjust the speed of the playback by using the *Playback speed* slider.

Furthermore, an overall score can be provided, or an evaluation of the various components of the test can be procured. This includes: speed of test performance, accuracy of following instructor's instrument path, accuracy of instrument to gingiva/tooth stereoscopic placement, similarity of student instrument pressure to that of instructor, accuracy of probe reading and gingiva to tooth attachment loss.

Learning to perform specific translational movement patterns using haptic guidance can improve short-term performance, but appears to result in slow learning and rapid forgetting in a rehabilitation process (Liu et al., 2005). However, it appears that limited knowledge is available in this complex process and that further studies in training human subjects are required.

REALITY ASSESSMENT

Interaction with a few of the dental teaching faculty was needed on a regular basis during the development of the PerioSim© to identify the strengths and weaknesses of the simulator from a clinician's point of view. Thirty experienced dental and hygiene instructors from a variety of clinical areas were then used to assess the realism of this system and determine which components required further development (Steinberg et al., 2006; Steinberg et al., 2007). Faculty/practitioners found the images very realistic for teeth and instruments, but less so for gingiva. Tactile sensation was realistic for teeth but not so for gingiva. The probing instruments were realistic and the millimeter markings easy to read. Faculty believed the simulator had a high training potential, were enthusiastic about its potential for evaluating students' basic procedural skills and anticipated incorporating this device into teaching. The study suggested that the self-contained teaching and training program in periodontal probing should aid students in the development of tactile skills necessary in dentistry.

SUPPLEMENTING THE SIMULATOR WITH A TRAINING CD

A self-training, instructional CD was developed to introduce students to the PerioSim© and the basic techniques they would practice later on the simulator (Steinberg et al., 2008). This CD enabled students to:

- Differentiate between a healthy sulcus and a pathological gingival sulcus (pocket).
- Understand proper instrument positioning, angulation, and location during periodontal probing.
- Practice reading the probing depths of healthy sulcus and pathological gingival

sulcus (pocket) and self-test the accuracy of these readings.

- Become familiar with probing procedures so he/she can visualize the relationships between a probe and the teeth and other periodontal supportive structures s from any angle
- Have unlimited practice time to hone the above skills.

REACTIONS TO USING THE PERIOSIM©

Much has been learned by observing clinical instructors and students using PerioSim© technology as it has been developing over the past five years. Students have been able to learn to use the PerioSim© much more rapidly than the instructors have. The students' shorter learning curve was probably due to their lifelong familiarity with computers. Nevertheless, both students and instructors were able to use the device within approximately 5 minutes. This is an important factor in today's learning environment where time limitations are an important factor. It is well known that the cost of technology decreases as availability increases, so computer simulations such as this one will decrease in cost over time. Another benefit of simulations over traditional models is that the simulations do not wear out as do the models.

A class of 30 postgraduate students first used PerioSim© in Fall 2007 and learned to use it to determine pocket depths and inspect initial white spot lesions for activity. These students then answered a short questionnaire where they were asked to compare the simulator to their real-life experiences. These dentists reported that PerioSim© was easy to learn and effectively mirrored real oral conditions. These training sessions are to be repeated in the Fall semester of 2008 with a similar group of postgraduate students. In the Fall semester of 2008 first-year dental students and hygienists will use PerioSim© to practice differentiating between active and inactive white spot lesions. When using a simulator there will be no damage to tooth enamel, as would be the case if a student applied too much force to defects in actual teeth. They will be warned when too much pressure is applied, alerting them to the very small force required to identify carious lesions.

We found it interesting that users reported that although their hand was on the off-screen stylus, their brain appeared to react to the 3D model on screen as if they were manipulating the instrument itself, not its virtual image. This reaction have been most likely due to the simulator's tactile feedback causing users to react as though movements and sensations involved when manipulating the onscreen instruments were real.

It was noted that using a 3D VR display monitor, along with the stereo glasses, did create a feeling of depth in the display. This was especially useful to novice users unfamiliar with the simulator system. However, as users became proficient at using the simulator setup, they were able to use the system with only the flat-panel LCD display monitor with satisfactory results.

If one has a computer equipped with an appropriate haptic interface and is able to download the software needed to render the haptic texture, one can use PerioSim© anywhere. Then a user, who has both the hardware and necessary software, will have the sensation of touching an object, moving it, rotating it into any position, and feeling its contours as it appears on their computer screen.

CONCLUSION

Over the last decade there has been a marked increase in the use of technology in medical education. Concomitantly, dental education has also seen an increased use of technology in both learning and training. The growing use of computers, networking, the Internet, multimedia programs, use of 3D, VR simulators, and finally haptics have contributed to the enhancement of medical and dental education. The vast amount of publications and conferences dealing with educational technology supports these observations. PerioSim© provides realistic 3D models with haptic sensing, replay and recording ability, unlimited practice time, and the ability to share recordings of the procedures online. These features combine to make it an ideal supplement to traditional teaching methods.

REFERENCES

Bird, M., & Gill, G. (1987). Individual differences and technology attributes: An examination of educational technology considerations related to trade and industry training. *Australian Journal of Educational Technology, 3*(2), 108–118.

Broeren, J., Sunnerhagen, K., & Rydmar M. (2007). A kinematic analysis of a haptic handheld stylus in a virtual environment: A study in healthy subjects. *Journal of NeuroEngineering and Rehabilitation, 4*(13).

Butterworth, S. (1930). On the theory of filter amplifiers. *Wireless Engineer, 7*, 536–541.

Gardner, H. (1983). *Frames of mind: the theory of multiple intelligences.* New York: Basic Books.

Laycock, S., & Day, A. (2003). Recent developments and applications of haptic devices. *Computer Graphics Forum, 22*(2), 117–132.

Liu, J., Emken, J. L., Cramer, S. C., & Reinkensmeyer, D. J. (2005). Learning to perform a novel movement pattern using haptic guidance: slow learning, rapid forgetting, and attractor paths. In *Proc. of the 9th International Conference on Rehabilitation Robotics*, (pp. 37-40).

Lord, M. P. (1986). *Macmillan dictionary of physics.* London: The Macmillan Press Ltd.

Magnusson, I., Clark, W. B., Marks, R. G., Gibbs, C. H., Manouchehr-Pour, M., & Low, S. B. (1988). Attachment level measurements with a constant force electronic probe. *Journal of Clinical Periodontology, 15*(3), 185-188.

Massie, T. H., & Salisbury, J. K. (1994). The PHANToM haptic device: A device for probing virtual objects. In *Proc. of ASME Winter Annual Meeting, Symposium on Haptic Interfaces for Virtual Environment and Teleoperator Systems*, (pp. 295-300).

Parker, S. P. (Ed.). (1984). *McGraw-Hill dictionary of physics.* New York: McGraw-Hill Book Company.

Steinberg, A. D., Ashrafi, S., Žefran, M., & Kolesnikov, M. (2008). Facilitate learning periodontal probing skills by using a CD with 3D video recordings. *ADEA 85th Annual Session and Exhibition*.

Steinberg, A. D., Bashook, P. G., Drummond, J. L., Ashrafi, S., & Žefran, M. (2007). Assessment of faculty perception of content validity of PerioSim, a haptic-3D virtual reality dental training simulator. *Journal of Dental Education, 17*, 1574–1582.

Steinberg, A. D., Drummond, J. L., Bashook, P. G., Žefran, M., & Ashrafi S. (2006). Haptic 3D virtual reality dental training simulator reality validation. *Journal of Dental Research, 85*(A), 1264.

Thurfjell, L., McLaughlin, J., Mattsson, J., & Lammertse, P. (2002). Haptic interaction with virtual objects: the technology and some applications. *Industrial Robot: An International Journal, 29*(3), 210-215.

Van Der Velden, U. (1979). Probing force and the relationship of the probe tip to the periodontal tissues. *Journal of Clinical Periodontology, 6*(2), 106–114.

Van Schaik, P., Turnbull, T., Van Wersch, A., & Drummond, S. (2004). Presence within a mixed reality environment. *CyberPsychology & Behavior, 7*(5), 540–552.

Williams, R. L., Srivastava, M., Conaster, R., & Howell, J. N. Implementation and evaluation of a haptic playback system. *Haptics-e, 3*(3).

KEY TERMS

Collision Detection: The process of determining if two or more virtual objects are intersecting.

Dental Simulator: An interactive computer simulator of a patient's mouth which includes the teeth, gingiva, bone, connective tissue and is capable of simulating normal and certain pathological states.

Guiding Force: An artificial force created in the simulator to drag the user-controlled instrument to the desired position.

Haptic Device: Robotic input/output device with force feedback capabilities that enables the user to get the impression of touching virtual objects.

Haptic Recording and Playback: The process of recording the haptic data (usually, along with the graphics data) during the simulation, and its subsequent playback. This allows the user to not only perceive the visual information from the recorded clip, but also feel the corresponding tactile sensations.

Haptic Rendering: The computation of the force to be conveyed to the user through the haptic device when a collision occurs. After the amount of force and its direction are determined, this information is sent to the haptic device for execution.

Haptics: The area of robotics dealing with devices designed to simulate pressure, texture, vibration and other sensations related to touch.

Refresh Rate: The speed at which the visual or haptic information displayed to the user is updated. For realistic simulations the graphics refresh rate should be no less than 25 Hz, while the haptics refresh rate should be at least 1 kHz.

Virtual Reality: An immersive and interactive simulation of either reality-based or imaginary images and scenes.

Chapter XV
Digital Library for Dental Biomaterials

Anka Letic-Gavrilovic
International Clinic for Neo-Organs – ICNO, Italy

ABSTRACT

In this chapter, the author will demonstrate and describe a project to develop a unique database with multilingual information and knowledge resource for biomedical dental materials and their properties. The database will be populated with high-quality, peer-reviewed information, equipped with an original search engine which would include all necessary information to (1) do standardization of therapeutic treatments (2) understand, the tissue response to biomaterials; (3) identify biomaterials and tissue matrix environment, to allow deeper understanding of the underlying relationship which allow more effective device design and engineering; (4) develop enabling tools by improvements in high-throughput assay and instrumentation, imaging, modalities, fabrication technologies, computational modelling and bio-informatics;(5) promote scale up, translation and commercialisation.

INTRODUCTION

The digital revolution affects our lives daily. The introduction of computer technology has greatly affected the way the restorative dentist practices, and the evolution of cyber technologies in dentistry are no longer a fantasy. Adhesive dentistry has replaced the manner in which we prepare, restore, and bond restorations to teeth. The entire field of ceramics and methods of fabricating aesthetic restorations are entering a new era. The exceptional prognosis of various implant systems has changed the way we think about maintaining hopeless teeth. Through tissue engineering

(TE), the 21st century may be revolutionary in the way we replace missing teeth and lost tooth structure.

Further on, in today's globalized world, scientific discoveries are introduced and swiftly absorbed into clinical practice. In dentistry, new products are launched daily, most of which are used in oral and dental surgery. When these products or biomaterials, are used, they come into direct contact with living tissues, such as dentin, pulp, the alveolar bone and periodontal tissue, and sometimes stay in contact for prolonged periods (Figure 2a).

In order to gather together huge knowledge from this interdisciplinary field, we will try to help in this work, organizing **digital library for dental biomaterials,** its long-term preservation, accessibility and usability. Consequently, our tem plan to create new digital library which will be designed to cover the following aims, as presented in Road map at Figure 1.

- Allowing content and knowledge to be produced, stored, managed, personalized, transmitted, preserved and used reliably, efficiently and at low cost;
- Allowing making the management and production tools for digital resources easier and more cost- effective, to create and reuse;
- Allowing more creative approaches to content and knowledge, enabling creators to design more participative and communica-

Figure 1. System architecture of digital library for dental biomaterials

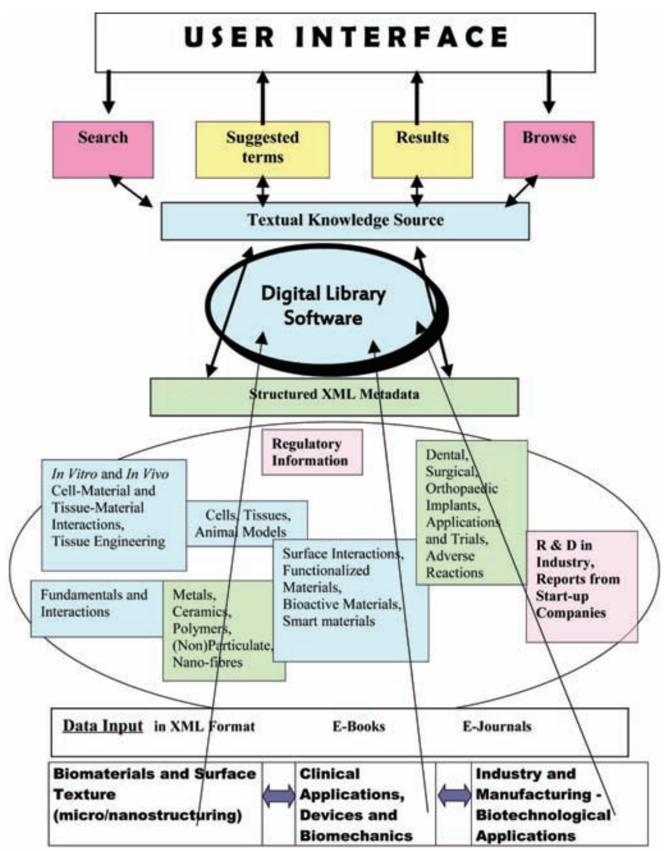

tive media and increase the productivity of publishers;

- Enabling the mass-individualization of learning experiences, through systems allowing faster acquisition of competences and skills, increased knowledge worker productivity, and more efficient organizational future learning processes.

Biomaterial is defined, in the broader sense, as any pharmacologically inert material that is capable of interacting with a living organism without causing adverse reactions either at the site of the implant or across the whole organism (Agrawal,1998). The treatment with dental biomaterials of gum, mucosal and hard tissues, represents a therapeutic risk that can only be contained if the dental professional has knowledge of the qualities, strengths and properties of the products (Table 7). The use of biomaterials without any recognized criteria for bio-safety not only causes clinical problems such as therapeutic failure, but also gives rise to ethically conflicting situations (Table 12). This is because the patient may undergo treatment without knowing about the subsequent risks, either to himself or to the dental professional.

Because of that, we need to open up new ways to use masses of data resulting from experiments and observations in the scientific process (Figure 2a) and to extract meaning from this data stored in repositories in combination with other scientific information resources. We need more effective technologies for intelligent content creation and management (The Global Technology Revolution, 2001), and for supporting the capture of knowledge and its sharing and reuse. Examples of few digital libraries are shown in Figure 2b.

Figure 2. (a) Examples of application of few biomaterials in Maxillo-facial and oral surgery reconstructions; (b) List of few digital libraries existing on WEB where biomaterial's characteristics could be found.

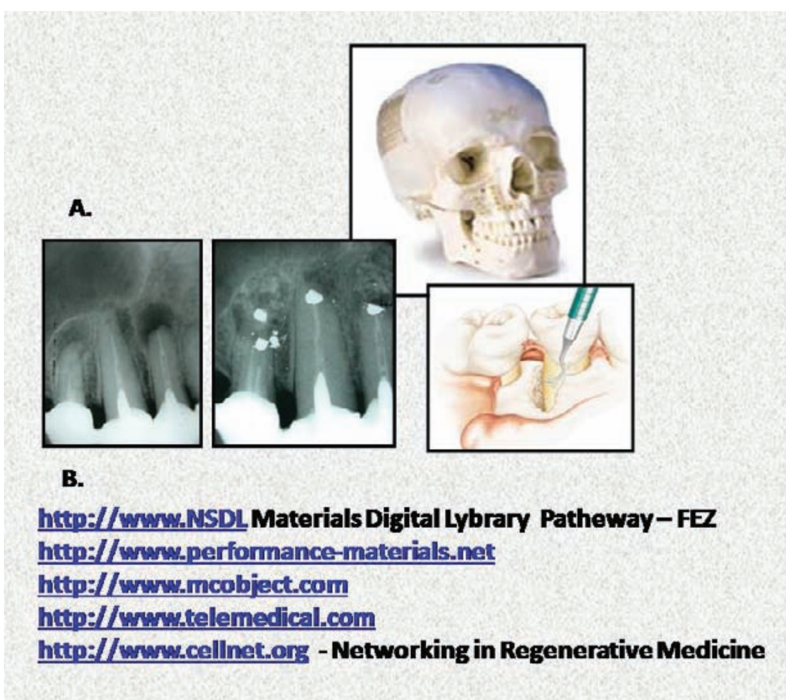

STATE OF THE ART OF THE DIGITAL RESEARCH AREA

Everything started and came from the projects **DELOS** and **ERPANET.** DELOS, a thematic network on digital libraries, co-organized a joint workshop with the National Science Foundation in 2003, which gave rise to the report "Invest to Save". This report identified the main problems faced by libraries in particular and organizations in general with the transition from the analogue to the digital world in terms of long-term archiving and preservation. The associated research agenda identified a number of priorities later reflected in calls for proposals under FP6-IST of Euporean Commision (EU) and in the activities of the **NDIIPP (National Digital Information Infrastructure and Preservation Program**) in the United States. The ERPANET project was an accompanying measure whose main objective was to raise awareness of digital preservation among the organizations concerned: memory institutions (museums, libraries and archives), the ICT and software industry, research institutions, government bodies, entertainment and creative industries, and commercial sectors (including for example pharmaceuticals, petro-chemicals and finance). This included the creation of a knowledge base on state-of-the-art developments in digital preservation and the transfer of that expertise among individuals and institutions. ERPANET organized, between 2003 and 2004, more than 20 workshops bringing together several hundred experts and practitioners in digital preservation across Europe (Third European Report on Science & Technological Indicators, 2003; University Of Glasgow, 2008). The project **PLANETS** brings together the national libraries and archives of several European countries (UK, NL, DK, CH, DE, AT) and focuses on the preservation of the assets held by these institutions. The goal is to develop a coherent methodological approach and a set of technological tools that can be adopted by similar organisations across Europe. The project **CASPAR95** involves major research organisations in Europe (CCLRC (UK), CNRS (FR), CNR (IT), European Space Agency) and broadens the scope of work to also cover the preservation of scientific data, audiovisual content and digitised cultural heritage. The research agenda of these projects includes the discussion and development of relevant technical standards, their adoption by standards bodies and their promotion among the industry and users. Both projects adopt the OAIS model as the main architectural reference for their implementation of digital preservation systems. These developments are expected to offer a solution to the immediate problems faced by organisations having to deal with the long-term preservation of their digital resources. Despite the high expectations placed in PLANETS and CASPAR, the magnitude of the problem faced requires further research work. In order to prepare more extensively for future work in this area, the Commission is also funding the coordination action **DPE (Digital Preservation Europe)** (Preservation, 2000;) whose remit includes updating the research agenda of DELOS, reflecting the new challenges resulting from the evolution of the internet and Web-publishing technologies and the wide adoption of ICT by the research community. The work being carried out by DPE is already visible in the preparation of FP7-IST (Papers from the Preservation Conference (2000). The work programme 2007-2008 in challenge 4 – "Digital Libraries and Content" establishes digital preservation as a priority and calls for research on "radically new approaches to digital preservation", capable of addressing critical issues of high volume, dynamic and volatile Web content, the evolving meaning and usage context of digital content and the need to safeguard integrity, authenticity and accessibility over time (Project PRISM). Other relevant projects are **DILIGENT, DRIVER** and **EURO-VO-DCA** launched in FP6 EU funding projects. The DILIGENT project aims to build a knowledge layer on top of the existing **GEANT** and middleware layers. DILIGENT deals with many issues relevant for digital repositories (i.e. data management, common approach to standards, protocols and interfaces, interaction between national and international repositories, handling complex objects).

One of the main objectives for the achievement of the **Lisbon Agenda** is the investment of three percent of GDP in research and development by EU Member States by 2010 (The Global Technology Revolution, 2001). In connection with the fact that all research builds on earlier work, and depends on scientists' possibilities to share and access scientific publications and research data, the efficiency of the system for dissemination of and access to research results and data significantly contributes to overall technological advance, and is essential for innovation and economic performance.

The environment in which research is conducted and disseminated is undergoing profound change, with new technologies offering new opportunities and changing research practices demanding new capabilities. New opportunities and new models could enhance the dissemination of research findings and maximize the returns on investment in R&D. The potential benefits of better and quicker access to scientific information for the efficiency of research include:

- Acceleration of the research and discovery process, leading to increased returns on R&D investment;
- Avoidance of duplicative research efforts, leading to savings in R&D expenditure;
- Enhanced opportunities for multi-disciplinary research, as well as inter-institutional and inter-sectional collaborations.

Another important benefits of digital library is **data mining** (Biomaterials Research, 1999). New information services could emerging that build on the results of individual research projects, gathering scientific literature and data, and using data mining techniques. More and more examples of the use of text mining technology in the academic field and in the commercial sector demonstrate the value of this technology for such diverse applications as content production for bio-databases, mining of electronic health records and mining the abstracts of journal articles. Peer-reviewed journals play a critical role in the selection of relevant raw material and are frequently the starting point for the development of new information resources. An interesting example is the **Cochrane Library**. The Cochrane Library is a growing source of reliable evidence about the effects of health care. Evidence-based results from among the major bibliographic databases are collected and evidence is put together for and against the effectiveness and appropriateness of treatments (medications, surgery, education, etc.) in specific circumstances.

Patents are also an important scientific and technical information resource with great potential. Given their public domain nature, facilitating its digitization and online access will also contribute to enhancing access to and preservation of scientific information. Some initiatives have been taken to this end by both institutional and private entities. The European Patent Office—a major player in the digital patent databases and related services—has set up **espace@net.**

More recently, Google has launched a service that aims at enabling the wider public to access patent information in a structured and user-friendly way.

In the domain of Biomaterials Engineering, the ***Materials for Medical Devices Database®***, **ASM International** is the first and only comprehensive database created specifically to support medical device design (Figure 2, ex.2); fully relational and modular, featuring both materials properties and biological response data for medical device designers. The ***Materials for Medical*** **Devices Database** provides designers of medical devices with a comprehensive and authoritative source of mechanical, physical, biological response and drug compatibility properties for the materials and coatings used in cardiovascular devices. **Researchers**

and designers of medical devices get access to authoritative information and knowledge from thousands of citations to published literature, **FDA device approval information**, and manufacturers' datasheets and websites (FDA Dental Devices, WEB site) (Table 2). It is useful for the identification, screening and selection of material grades, manufacturing processes and suppliers appropriate for orthopedic and cardiovascular applications In-house installations can be extended to include someone's own proprietary data to provide organization a complete materials information management solution. The main imperfection of the ***Materials for Medical Devices Database®*, ASM International** is in absence of relevant legal and regulatory information within the EU related to biomaterial manufacturers, final products and medical devices (Web Site Profiler).

AIM

Our project aims to develop a unique, multilingual information and knowledge resource for dental materials and their properties, populated with high-quality, peer-reviewed information, equipped with an original search engine which will include biocompatibility criteria, and readily available as a Web service. Detailed schematic presentation in Figure 1. Since this is one of the first project or research in this domain, our starting point in research and development will be the key results available in the literature.

Objectives of this proposal are as follows:

- Development of new techniques for biomaterials data collection and classification
- Development of a new design methodology for overlapping decentralized algorithms
- Design of the knowledge-based expert system for data classification (Defining system architecture and developing heuristics and methodology for data classification)
- Software development - Design of computer architecture for implementation and interaction
- Implementation of the digital library, databases, search engines and software modules
- Setting up a strategy for transfer of the developed project onto the users level
- Specific training activities for end-user partners.

The work will strengthen the link between content, knowledge and permanent learning processes. The work carried out under this project will contribute to the implementation of the **"i2010: Digital Libraries"** initiative (Web Site Profiler).

Our project objectives are also in accordance with **the European Council Conclusions on scientific information in the digital age*: access, dissemination and preservation 2832nd COMPETITIVENESS (Internal market, Industry and Research) Council meeting Brussels, 22 and 23 November 2007*** (Lupovici, 2000; Metadata Engine Project, PANDORA project)***:***

1. Access to and dissemination of scientific information—publications and data—are crucial for the development of the European Research Area, and can help accelerate innovation;
2. The Internet has created unprecedented possibilities to disseminate, share and build on the outcome of research efforts;
3. Information and communication technologies revolutionize the way scientists communicate, perform research and produce knowledge;
4. In an era of high speed connectivity and high performance computing, data emerges as key for modern science;
5. The systems by which scientific information is published are pivotal for its dissemination and quality control, in particular through

Table 1. Basics standards for creating digital libraries: Implementing standards, metadata, interoperability and preservation

How do these standards work together for digital libraries?

A container format such as METS allows for packaging together forms of metadata with objects or pointers to object

METS records the (possibly hierarchical) structure of digital objects, the names and locations of the files that comprise those objects, and the associated metadata

A container for metadata and file pointers

A METS document may be a unit of storage or a transmission format

METS is extensible and modular, using "wrappers" or "sockets" where elements from other schemas can be plugged in.

METS uses the XML Schema facility for combining vocabularies from different Namespaces

Using METS, MODS, PREMIS and MIX: http://www.loc.gov/premis/louis.xml

PREMIS is:

- A data dictionary for metadata to support the long-term preservation of digital objects
- A piece of the necessary infrastructure for implementing reliable, sustainable preservation programs
- A supporting set of XML schema for implementation in a variety of contexts
- A maintenance activity hosted at LC including an Implementers' Group and Editorial Committee

A quality Website must:

• be transparent, clearly stating the identity and purpose of the Website, as well as the organization responsible for its management;

• select, digitize, author, present and validate content to create an effective Website for users;
• implement quality of service policy guidelines to ensure that the Website is maintained and updated at an appropriate level;

• be accessible to all users, irrespective of the technology they use or their disabilities, includingnavigation, content, and interactive elements;

• be user-centered, taking into account the needs of users, ensuring relevance and ease of use through responding to evaluation and feedback;

• be responsive, enabling users to contact the site and receive an appropriate reply. Where appropriate, encourage questions, information sharing and discussions with and between users

• be aware of the importance of multi-linguality by providing a minimum level of access in more than one language;

• be committed to being interoperable within cultural networks to enable users to easily locate the content and services that meet their needs;

• be managed to respect legal issues such as IPR and privacy and clearly state the terms and conditions on which the Website and its contents may be used;

• adopt strategies and standards to ensure that the Website and its content
can be preserved for the long time

peer review, and thus have a major impact on research funding policies and on the excellence of European research;

6. Universities, libraries, research performing and research funding organizations, scientific publishers and other stakeholders have in recent years made considerable investments in information technologies for online accessibility;

7. Effective and long-lasting digital preservation of scientific information is fundamental for the current and future development of European research.

DIGITAL COLLECTION STRATEGIC PLAN

One of the main problems faced by scientists today is that they are overwhelmed with data. As scientific problems become more complicated, the models and instruments they use to study them become more complex, so the amount of data is increasing rapidly. This explosion in scientific data creates new challenges in how the data is stored, retrieved, analyzed and manipulated.

This is not just a problem for the scientists. Given the importance of research in science and engineering for innovation, our ability to find answers to these questions will directly affect Europe's competitiveness. Europe has the opportunity to be in the front line of international developments in this field. The digital libraries initiative aims at making European information resources easier and more interesting to use in an online environment. Technological progress can greatly contribute to the accessibility and use of scientific information. For example, better search tools can help researchers find information and progress in new areas and collaborative tools can enhance the way in which researchers share information.

High-speed communication networks, distributed storage, and sharing of computational resources and data processing allow scientists to tackle the full scientific process in an innovative and more effective way. What is missing, however, is effective ways of sharing and transferring knowledge.

The scope of our project is to include information on biomaterials (including ethical questions) for application in various Specialties of Dentistry, such as: Dental Public Health , Endontics, Oral and Maxillofacial Radiology, Oral and Maxillofacial Surgery, Orthodontics, Pedodontics, Periodontics, Prosthodontics, as well as for legislative and regulatory authorities (Figure 1).

- Several online search algorithms will be developed and made accessible through the Web site:
- Classic search engine for the database, which will enable simple, flexible and high-performance search.
- Google search engine, for fast, unstructured search.
- Special algorithms based on artificial intelligence and fuzzy search that will resolve *two issues*:
- Cross-referencing of biomaterials, with the opportunity to propose equivalents and »close matches« when there are no official recommendations by standards and manufacturers. Normally, recommendations that consider biocompatibility are very rare if not nonexistent, and the newly developed algorithm will use biocompatibility as a criterion as well.
- Identification of biomaterials, based on their chemical composition. Similarity of biomaterials will be calculated by considering biocompatibility.

Development of marketing strategy will be based on extensive analyses of international marketing environments, researching foreign markets, especially views about the dimensions, from creators of each market environment separately, analyses and comparisons of the competitive marketing strategies. Market opportunities, weaknesses, risk, priorities for the proposed Biomaterials digital library on each specific market, separately (for EU and other world markets) will be determined, as well as optimal marketing communication according to the needs of the end-users of digital library (with the well-known methods). Our multidisciplinary research aim will:

Set up a strategy for transfer of the developed digital library for dental materials onto the users level;

- Provide distribution of such digital library;
- Transfer knowledge of marketing strategy for the emergence of our digital library onto a specific market for industrial products;
- Provide development of own international marketing programme for use in the future;
- Provide marketing communication between the manufacturer and end-user in the field of dental biomaterials;
- Develop a marketing model as an efficient response to digital library end-users
- Provide an international recognition of the proposed digital library in the targeted markets.

The result of this project will be translation of the multidisciplinary research on biomedical materials and devices data and processes to wide range of biomedical materials digital library users, optimizing the delivery of information to healthcare professionals, biotechnology engineers, graduate and postgraduate students, biomedical materials manufacturers, medical device manufactures, etc. Strong EU-based biomedical research will enhance competitiveness of the European pharmaceutical and healthcare industries. It is therefore imperative that the EU creates an environment conductive to innovation in the public and private sectors.

Additionally innovative aspects of the project:

- Highly configurable and customizable collaboration environment supporting the creation of close virtual communities, providing services like Members Management, Email/Sms, Calendar with Chat and Whiteboard functionalities, Forum, Workflow, Web Content Management, Advanced Search, etc (Web Site Profiler);
- Powerful workflow engine able to simulate and orchestrate the execution of any collaboration process;
- Knowledge Management module for annotating the material stored in the Digital Library based on a pre-defined ontology for later semantic information and knowledge extraction;
- Semantically enhanced search engine, able to retrieve information based on knowledge base entities patterns search;
- Semantic annotation, discovery and invocation of Web services based on the WSMO initiative;
- Advanced security methods for authentication, authorization, access control and non-repudiation (Certificates, Smart cards, Time Stamping, Biometric Authentication, RBAC)

Estimated global market size of electronic data libraries for biomaterials on mid- to long-term (5 to 7 years) is 20 million Euros. Even at that point, market will be far from being mature. Our project will provide reliable digital library, technology-enhanced learning concept and appropriate algorithms to be used in different fields of biomaterials research and processing. These results will support the work programme's goal, **Digital libraries** and technology-enhanced learning". Developed algorithms will, with minor modifications, be suitable to monitor and identify the faults and range of irregularities in vehicles, increasing their safety, with significant socio-economic implications for the society. Furthermore, the growing use of life sciences and biotechnology, for the development of drugs, vaccines and innovative therapies, as well as the applications of "nanomedicine" and "nanobiomaterials", represent huge potential for innovation and growth. The health sector must take advantage of innovation and technology where this will lead to greater efficiency and health improvements.

Defining Digital Library Architecture and Developing Heuristics and Methodology for Data Classification

Firstly, characterization methodologies, process modeling, functional tests and specifications of biomedical constructs and devices will be defined. Based on the review of resources, distribution and limitations, we will select the best way to classify biomaterials associated to the medical devices, TE and regenerative medicine. After analyzing, compiling and peer reviewing of the information sources and industrial needs, details of the system architecture of the digital library will be defined. The basic building blocks of the architecture will be: (1) central database, (2) data input databases and workflow, (3) content management system, and (4) online search engines.

Our **Dental biomaterials digital library**, after analyzing, compiling and peer reviewing of the information sources and industrial needs, details of the system architecture of the digital library will be defined. The basic building blocks of the architecture will be: (1) central database, (2) data input databases and workflow, (3) content management system, and (4) online search engines

A large relational database as a unique, consistent data infrastructure for including all the compiled information will be in the core of the system. This central database will synthetize and include comprehensive biomaterial information, such as biomaterials classification and composition, physical and mechanical properties, special properties, biological behavior and biocompatibility, application guidelines, cross-referencing etc. Figure 1 and Tables 4, 5, 6, 7, 8, 9, 10, 11, 12, and 13. The central database will be structured to provide flexibility, extensibility and high search performance, and will consequently have data warehouse architecture. In order to populate central database, production databases for data entry will be defined. The data entry process needs to follow clear editorial and quality assurance guidelines, which will be defined using a workflow, which will then be implemented in data input applications. In order to provide access to all the information to as broad audience as possible, the system will be intristically multilingual. Starting with major European languages like English, German, and Italian, the system will be extensible to other European languages. To manage large amounts of multilingual system and content, a dedicated content management system (CMS) will be designed. Beside managing content and editorial workflow, the CMS will include the complete humane-machine interface of the system, thus making it easily expandable to new languages.

A hybrid Web-based search engine will be defined atop of the central database in this step, with the objective to achieve robustness, superior search performance, and multiplicity of search modes. Classic search strategies will be combined with Google search engine and special algorithms based on artificial intelligence and fuzzy search for material identification and cross-referencing.

Implementation of the Digital Library, Databases, Search Engines and Software Modules

The system will be implemented as a versatile, easy-to-use and multilingual online service, readily available for medical devices manufacturers, medical and dentistry practitioners, material professionals, regulatory bodies, scientific community, and other interested parties (Table1).

Implementation includes central database creation, implementation and deployment of production databases, data entry workflow, content management system and Web-based programs for peer-to-peer knowledge exchange, and entering compiled data information into the production databases. In parallel, Web site interface and search engines will be implemented. (Table 1).

After relevant amount of information and content is added, it will be propagated to the central database and functional prototype will be launched to the Web for testing by selected groups of users from industry and academia.

System Deployment

The goal of this activity is to form a large network of participants for information and knowledge exchange and leverage. Special opportunities will be offered to universities and scientific community: they can enter into collaboration by contributing to the digital library and in return access will be granted for educational and research purposes, thus stimulating knowledge and information exchange. In the future, similar benefits may be mutually exchanged with regulatory bodies and Standards Development Organizations (SDOs).

Together with special courses and training workshops that will be organized predominantly for academic users, beta testing and refinement of the system will be organized.

Our work plan directly covers most of the objectives, including the following advances:

Standards, Metadata, Interoperability and Preservation

Standards are a part of every day life whether we realize it or not.Metadata is used to facilitate the understanding, characteristics, and management usage of data (Table 1). The metadata required for effective data management varies with the type of data and context of use (Metadata Engine Project). In a library, where the data is the content of the titles stocked, metadata about a title would typically include a description of the content. Standards particularly relevant to the development of digital asset management in Further Education are: METS Metadata Encoding and Transmission Standards. METS is a developing standard for the sharing of assets and related metadata and it can reasonably be expected to establish a 'market' presence as an exchange standard. The potential of METS to digital asset management systems is that it is capable of storing and exchanging metadata from a number of standards at once. It can also bundle this data with the object. This will allow the developed system to exchange the wider range of metadata formats that it has created in a single transaction. Standards are essential for interoperability between systems.

Interoperability refers to the ability of a system to interact and exchange data with one or more other systems. This can be in the form of direct data exchange or the exporting, transformation and importing of records. Interoperability is not just about being able to get multiple services to present their data coherently in the same place - it is also about the data making sense in that other context.

When data moves between systems the differences between the internal requirements of the systems creates an "interoperability boundary" that has to be crossed. The changes to the metadata that are required to cross this interoperability boundary may be structural, semantic, or syntactical.

Another reason for supporting the use of a standards in a system is the potential to migrate to future systems. Further, standards are essential to support preservation forever (Table 1).

Long-term preservation of assets is an important aspect of digital asset management within the wider information environment. It is particularly important in ensuring that future users have access to original information, so that knowledge may be built upon. In traditional knowledge repositories this has been recognized since the earliest libraries; in modern society this has tended to be catered for by national and university libraries maintaining copies of works. Preservation in the academic world is particularly important for historical, cultural, and scientific research; it should be noted however, that the usefulness of an information asset in the future cannot be completely predicted in the present.

In many ways, preservation of paper-based assets is a simple matter assuming that storage and curation costs can be borne. Digital assets offer opportunities of much lower cost storage but also raise new problems relating to the formats in which assets are stored and ability to retrieve them in the context of new technologies. In considering the development of a strategy for digital asset management it might be useful to consider the **OAIS** model of preservation (Consultative Committee for Space Data Systems, 1999; Preservation, 2000).

Intellectual Property Rights IPR to be Implemented in our Project Are:

- Defining architecture of the digital library, databases, search engines and software modules (COPYRIGHT)
- Developing methodology for classifying biomaterials properties and the structure of the central database (COPYRIGHT)
- Defining production databases, data entry workflow, editorial process and content management (COPYRIGHT)
- Developing search engine and artificial intelligence based algorithms for biomaterials search, comparison and cross-referencing (COPYRIGHT and possibly PATENT)
- Implementation of operational and production databases (COPYRIGHT)
- Implementation of developed algorithms, their interdependences and integration (COPYRIGHT)
- Design and implementation of online, multilingual HMI (Human Machine Interface) in user-friendly programme environment adapted for application in biomaterials industry (COPYRIGHT)
- Systems, algorithms and programmes which will be subject of intellectual property protection are related to:
  - New biomaterial classification methods
  - New AI-based search algorithms
  - System design and implementation

DENTAL BIOMATERIALS: DIVERSITY AND COMPLEXITY

Research from Concept to Clinic

The subject of **biomaterials** resides at a multidimensional interface between chemistry, chemical engineering, materials science, mechanics, surface science, bioengineering, biology, and medicine, with considerable input from ethicists, government-regulated standards organizations, and entrepreneurs. The field has seen consistent growth since its inception and a steady introduction of new ideas and productive branches. Some examples of these outgrowths from biomaterials that have evolved into identifiable fields of their own include controlled release, diagnostic arrays, and tissue engineering TE.

Although medical implant materials have been used for at least 2000 years (some historians trace sutures back 32,000 years), most early medical implants were doomed to failure because important concepts relating to infection, materials, and the biological reaction to materials were not yet established.

A Little History on Biomaterials indicates the **socio-cultural importance** of digital library developments as shown in Exhibit 1.

On the other hand, the history of implants development confirms the permanent evolution of biomaterials:

The first generation of biomaterials: (1) "ad hoc" implants, (2) specified by physicians using common and borrowed materials, (3) most successes were accidental rather than by design (Galletti,1988).

Examples of first generation implants: (i) gold fillings, wooden teeth, PMMA dental prosthesis, (ii) steel, gold, ivory, etc., bone

Table 2. Food and Drug Administration – Department of Health and Human Services- Listing of Dental Devices (Changed and adapted)

DIAGNOSTIC DEVICES

-Gingival fluid measurer.
- Pulp tester.
- Electrode gel for pulp testers.
- Caries detection device.
- Laser fluorescence caries detection device.
- Extraoral source x-ray system.
- Intraoral source x-ray system.
- Dental x-ray exposure alignment device.
- Cephalometer.
- Dental x-ray position indicating device.
- Lead-lined position indicator.
- Sulfide detection device.
- Dental x-ray film holder.
- Dental sonography device.
- Jaw tracking device.

SURGICAL AND MISCELLANEOUS DEVICES

- Bone cutting instrument and accessories.
- Intraoral dental drill.
- Dental handpiece and accessories.
- Gas-powered jet injector.
- Spring-powered jet injector.
- Dental diamond instrument.
- Dental hand instrument.
- Intraoral ligature and wire lock.
- Fiber optic dental light.
- Dental operating light.
- Dental injecting needle.
- Bone plate.
- Rotary scaler.
- Ultrasonic scaler.
- Intraosseous fixation screw or wire.
- Dental electrosurgical unit and accessories.

THERAPEUTIC DEVICES
ORTHODONTIC APPLIANCES AND ACCESSORIES

- Orthodontic plastic bracket.
- Extraoral orthodontic headgear.
- Preformed tooth positioner.
- Teething ring.
- Intraoral devices for snoring and intraoral devices for snoring and obstructive sleep apnea.
- Oral rinse to reduce the adhesion of dental plaque.
- Abrasive device and accessories.
- Oral cavity abrasive polishing agent.
- Saliva absorber.
- Ultraviolet activator for polymerization.
- Airbrush.
- Anesthetic warmer.
- Articulation paper.
- Base plate shellac.
- Dental chair and accessories.
- Prophylaxis cup.
- Rubber dam and accessories.
- Ultraviolet detector.
- Dental floss.

PROSTHETIC DEVICES AND MATERIALS

- Amalgam alloy.
- Noble metal alloy.
- Mercury and alloy dispenser.
- Dental amalgamator.
- Dental amalgam capsule.
- Preformed anchor.
- Resin applicator.
- Articulator.
- Precision attachment.
- Resin tooth bonding agent.
- Facebow.
- Dental bur.
- Calcium hydroxide cavity liner.
- Cavity varnish.
- Dental cement.
- Preformed clasp.
- Hydrophilic resin coating for dentures.
- Coating material for resin fillings.
- Preformed crown.
- Gold or stainless steel cusp.
- Preformed cusp.
- Karaya and sodium borate with or without acacia denture adhesive.
- Ethylene oxide homopolymer and/or carboxymethylcellulose sodium denture adhesive.
- Carboxymethylcellulose sodium and cationic polyacrylamide polymer denture adhesive.
- Ethylene oxide homopolymer and/or karaya denture adhesive.
- Polyacrylamide polymer (modified cationic) denture adhesive.
- Carboxymethylcellulose sodium and/or polyvinylmethylether maleic acid calcium-sodium double salt denture adhesive.
- Polyvinylmethylether maleic anhydride (PVM-MA), acid co-polymer, and carboxymethylcellulose sodium (NACMC) denture adhesive.
- OTC denture cleanser.
- Mechanical denture cleaner.
- OTC denture cushion or pad.
- OTC denture reliner.
- OTC denture repair kit.
- Preformed gold denture tooth.
- Preformed plastic denture tooth.
- Partially fabricated denture kit.
- Endosseous dental implant abutment
- Endosseous dental implants
- Subperiosteal implant material.
- Impression material.
- Optical Impression Systems for CAD/CAM.
- Resin impression tray material.
- Polytetrafluoroethylene (PTFE) vitreous carbon materials.
- Tooth shade resin material.
- Dental mercury.
- Base metal alloy.
- Pantograph.
- Retentive and splinting pin.
- Bracket adhesive resin and tooth conditioner.
- Denture relining, repairing, or rebasing resin.
- Pit and fissure sealant and conditioner.
- Temporary crown and bridge resin.
- Root canal post.

continued on following page

Table 2. continued

THERAPEUTIC DEVICES ORTHODONTIC APPLIANCES AND ACCESSORIES	PROSTHETIC DEVICES AND MATERIALS
- Heat source for bleaching teeth. - Oral irrigation unit. - Impression tube. - Dental operative unit and accessories. - Massaging pick or tip for oral hygiene. - Porcelain powder for clinical use. - Silicate protector. - Boiling water sterilizer. - Endodontic dry heat sterilizer. - Cartridge syringe. - Manual toothbrush. - Powered toothbrush. - Disposable flouride tray. - Preformed impression tray. - Intraoral dental wax.	- Root canal filling resin. - Endodontic paper point. - Endodontic silver point. - Gutta percha. - Endodontic stabilizing splint. - Posterior artificial tooth with a metal insert. - Backing and facing for an artificial tooth. - Porcelain tooth. - Bone grafting material. - Total temporomandibular joint prosthesis. - Glenoid fossa prosthesis. - Mandibular condyle prosthesis. - Interarticular disc prosthesis (interpositional implant). - Endosseous dental implant accessories.

Exhibit 1.

The Romans, Chinese, and Aztecs used gold in dentistry over 2000 years ago. Ivory & wood teeth. Aseptic surgery 1860 (Lister). Bone plates 1900, joints 1930. Turn of the century, synthetic plastics came into use - WWII, shards of PMMA unintentionally got lodged into eyes of aviators - Parachute cloth used for vascular prosthesis. 1960 - Polyethylene and stainless steel being used for hip implants.

plates, (iii) glass eyes and other body parts (iv) dacron and parachute cloth vascular implants.

The second generation of biomaterials: (1) engineered implants using common and borrowed materials (2) developed through collaborations of physicians and engineers, (3) built on first generation experiences, (4) used advances in materials science.

Examples of second generation implants: (i) titanium alloy dental and orthopedic implants, (ii) cobalt-chromium-molybdenum orthopedic implants, (iii) UHMW polyethylene bearing surfaces for total joint replacements and (iv) heart valves and pacemakers

The third generation of biomaterials: (1) bioengineered implants using bioengineered materials, (2) few examples on the market, (3) some modified and new polymeric devices and (4) many under development.

Examples of third generation implants: (i) tissue engineered implants designed to regrow rather than replace tissues (Letic et al.,2005), (ii) Integra Life Sciences artificial skin.

Biomaterials (Table 2, 3, 5, and 6) are used in the oral cavity either to restore function, comfort, or aesthetics caused by developmental disorders, disease, or trauma. More elective procedures are being requested and performed purely for aesthetic purposes as the incidence of caries has dropped in certain population groups and as patients have

Table 3. Dental materials

RESTORATIVE MATERIALS	**GYPSUM PRODUCTS**
Dental Amalgam	General – Gypsum
Zinc Phosphate Cement	Plaster of Paris
Polycarboxylate Cement	Artificial Stone
Glass Ionomer Cement	
Zinc Oxide And Eugenol	**DENTAL WAXES**
DENTAL RESINS FOR RESTORATIVE DENTISTRY	General – Waxes
	Inlay Wax
Acrylic Resins	Baseplate Wax
Composite Resins	Sticky Wax
Acid Etch Technique	Utility Wax
Pit and Fissure Sealants	Disclosing Wax
Intermediate Restorative Material	Boxing Wax
	Low-fusing Impression Wax
MISCELLANEOUS DENTAL MATERIALS	
	IMPRESSION MATERIALS
Calcium Hydroxide	
Root Canal Filling Materials	Agar-Type Hydrocolloid
Gutta-Percha Points	Alginate-Type Hydrocolloid
Silver Root Canal Points	Synthetic Rubber Base Impression Materials
Cavity Lining Varnish	
Dental Porcelain	
Polishing Materials	
DENTAL GOLD AND GOLD ALLOYS	
Gold Foil	
Casting Gold Alloy	
Gold Alloy Solder	
Wrought Gold	
Gold Plate	
Non Precious Alloys	

become more aware of various restorative or cosmetic options. However, the replacement of diseased tooth structure or missing teeth accounts for the bulk of work in restorative dentistry. The instruments and materials used in the surgical aspects of oral, maxillofacial and periodontal surgery have much in common with medicine (Table 4). Laboratory-based biomaterials (Table 3) research is essential to the genesis and development of new and improved biomaterials for dentistry and orthopaedics. The number and complexity of questions requiring resolution far exceeds the worldwide resources available for Randomized Clinical Trials. Hence, careful and appropriate laboratory modeling is also needed to replicate key features of the oral environment, including its biomechanical, thermal, optical, chemical, biochemical and cellular aspects. Our digital library will address all of these dimensions of research, and contribute to an enhanced mechanistic understanding of biomaterial behavior in vivo. Our rresearch interest involves the whole field of dental and orthopaedic biomaterials, but especially in metals, ceramics, polymer systems, composites/ adhesives, smart and nanomaterials (Tab. 2, 3, 5, 10,11,). Biomaterials for dental operative use entail special ‘boundary conditions’ on account especially of: (1)micro-engineered small quantities; (2) constrained cavity-filling placement; (3) alveolar bone grafting within GTR (guided tissue regeneration) and GBR (guided bone regeneration); (4) in situ composites solidification.

The following specific topics are illustrative of diversity and complexity of biomaterials used in dental daily practice. The digital library could greatly facilitate understanding of their use:

- The stability of interfaces between host tissues and restorative biomaterials is crucial (Table 5) Substantial advances have been made in understanding the interface of hard substrates such as dentine and bone, but these hybrid bonding zones are challenged clinically by the rapid development of intra-coronal stress arising from molecular setting processes. Are to be studied polymerization-shrinkage phenomena, especially in the dynamics of photo-polymerization. Photo-activation methods, based on LED light sources, have now been deployed and these are being carefully evaluated, along with composite biomaterials based around novel chemistry and systematically-varied formulations.
- Metal-free biomaterials - required to withstand functional stresses - are usually designed around composite structures and/or high performance ceramics. These cannot be dissolved so as to apply classical analytical methods. Investigation of their behavior and internal microstructures, down to the molecular and nano-scales requires development of appropriate spectroscopic, viscoelastic and image-analysis techniques. There are much more experimental methods, including Photo-DSC, FTIR, Rheology, X-Ray 3-D micro-tomography and Fracture-Mechanics, for this purpose.
- Natural bio-composites utilize fibers as well as particulate ceramics for reinforcement. Are to be develop user-friendly, economical and strong fiber-reinforced biomaterials for applications in endodontics, temporary restoratives and fixed and removable prosthodontics.
- Clinical placement of biomaterials is greatly affected by their perceived ease of handling and manipulation in vivo. However, these clinical impressions are frequently highly subjective and non-transferable.
- Aesthetic dentistry relates to the optical properties of biomaterials, and this also depends on their surface morphology as well as their internal microstructure.

The success of biomaterials is seen in the importance to modern medical therapies, in the **economic potential** of the market, and the steady growth of the field over more than 50 years.

The next several years will be critical for the maturation of biomaterials for TE science and its role in clinical medicine. Elucidation of the fundamental structure-function relationships in normal and diseased or damaged tissue through sound basic research will continue to be a prerequisite. In addition, consideration of the different elements in the product development continuum from inspiration, product design and bench studies, to the clinic are vital. Because of the limited availability of organs and the increasing demand of such, new research has been initiated some years ago to develop biological, in vitro engineered transplants.

Although great progress has been made in field, still remains some serious problems in biomaterials and TE science, such as: defining, researching and/or selecting the appropriate biomaterial's physical/chemical and other weakness in relation to host (Table 5) and the problems and challenges in the field of biocompatibility. These problems need to be understood and specifically address the general lack of knowledge relating to:

- The rapid development of **regulations and standards** over recent years in the biomedical field;
- The principles behind the correct interpretation and use of such regulations and stan-

Table 4. Various metal and non metal materials are used to fabricate Instruments for dental use and in the high level dental technologies

TYPICAL INSTRUMENTS SETUPS
Basic Examination Setup
Anesthetic Setup
Rubber Dam Instrument Setup
Restorative Setups
Surgical Setups
Routine tooth Extraction Setup
Endodontic Instrument Setups

LIST OF INSTRUMENTS USED IN RESTORATIVE PROCEDURES
Removing Decay
Finishing The Cavity Preparation
Preparing and Placing the Base Material
Confining the Restorative material in Cavity Preparation
Preparing and Placing of the Restorative Material
Finishing the Restorative Material

DENTAL TECHNOLOGIES
Air-Abrasion,
Bone Replacement,
CAD/CAM,
Caries Detection Solution,
CAT Scans,
Composite Materials,
Diagnodent,
Dental Implants,
Desensitizers,
Digital X-rays,
Electric Hand Pieces,
Internet,
Intra-Oral Camera,
Lasers,
Optical Scanners,
Microscope,
NTI Splint,
Periodontal Antibiotics,
VELscope,
ViziLite,
Periometer,
The Wand,
Pedodontics,
Periodontics,
Prosthodontics,

dards, the best methods necessary as part of the evaluation of **safety of biomedical materials and devices**;

- The importance of issues relating to **standardization and quality of testing**;
- The forthcoming role that **risk analysis** will play in evaluating biological safety;
- The structure of standardisation and the function of the standards within the framework of the European and US legislation and the moves towards **global harmonisation**.

In order to approach resolutions of aforementioned problems, our digital library project will be focused on (Road map schematised in Figure1):

1. Selecting and collecting data from literature, experimental results (*in vitro*, *in vivo*, etc.), standards, manufacturing specifications, scientific papers and other equivalent data sources related to biomedical materials from all over the world.
2. Analyzing, compiling and peer reviewing all these data and information sources prior to Web publication.
3. Structuring large relational database as a unique, consistent data infrastructure for including all the compiled information. Besides that, the database will be structured to provide flexibility, extensibility and high search performance.
4. Entering the compiled information into the database. As a part of this process, data structures and Web-based programs for the database updating will be created, as well as Web-based program for peer-to-peer knowledge exchange.
5. Publishing the content via the specialized Web site to professionals worldwide, with

Table 5. Example of dental and medical materials and their applications

MATERIALS	PRINCIPAL APPLICATIONS
A. Metals and Alloys	
316 Stainless Steel-CP-Ti,	Fracture fixation, stents, surgical instruments, bone and joint replacement,
Ti-Al-V, Ti-Al-Nb,	fracture fixation, dental implants, pacemaker, encapsulation
Ti-13Nb-13Zr, Ti-Mo-Zr-Fe	Bone and joint replacement, dental implants, dental
	Bone plates, stents, orthodontic wires
Co-Cr-Mo, Cr-Ni-Cr-Mo	Dental restoration
Ni-Ti	Antibacterial agents
	Electrodes
Gold Alloys	Dental restorations
Silver products	
Platinum and Pt-Ir	
Hg-Ag-Sn amalgam	
B. Ceramics and Glasses	
Alumina	Joint replacement, dental implants, dental
Zirconia	Various parts of dental replacement
Calcium Phosphates	Bone repair and augmentation, surface coatings on metals
	Bone replacement
Bioactive glasses	Dental restorations
Porcelain	Heart valves, percutaneous devices, dental implants
Carbons	
C. Polymers	
Polyethylene	Joint replacement
Polypropylene	Sutures
PET	Sutures, vascular prosthesis
Polyamides	Sutures
PTFE	Soft-tissue augmentation, vascular prosthesis
Polyesters	Vascular prosthesis, drug-delivery system
PVC	Tubing
PMMA	Dental restorations, intraocular lenses, joint replacement (bone cements)
	Soft tissue replacement.
Silicones	Drug-delivery systems
Hydrogels	
D. Composites	
BIS-GMA-quartz/silica filler	Dental restorations.
PMMA-glass filler	Dental restorations (dental cements).
PLLA/beta-TCP	Bone replacement

a flexible multi-layer access system, thus providing a quick, easy online access via a single portal to consistent and relevant materials information.

6. Developing Web-based search engine that will combine robustness, superior search performance, and multiplicity of search modes, and will be combined with additional special software modules for material cross-referencing and identification.
7. Deploying multilingual system and content, in order to provide access to all the information to as broad audience as possible. Starting with major European languages like English,

Table 6. The effect of the various environmental factors on materials/device/tissue - relationship (Adapted from Gautam P. et Valiathan, 2008)

Manufacturing
1. Fabrication methods 2. Consistency and conformity to all requirements 3. Quality of row materials 4. Superior techniques to obtain excellent surface finishing or texture 5. Capability of material to get safe and efficient sterilization 6. Cost of product
***In vivo* interface device/tissue depends on**
1. Type of material – change in properties: Mechanical, Physical, Chemical 2. Static/dynamic stresses 3. Projected device life 4. Interactions with other device components
Mechanism of material degradation *in situ*
1. Local deleterious changes corrosion dissolution chemical modification ·swelling ·leaching wear **2. Harmful systemic effects**
Material properties adversely affected
1. strength 2. fatigue strength 3. fracture toughness 4. stiffness (elastic modulus) 5. surface roughness 6. wear resistance 7. chemical stability 8. time dependent deformation

German, French, Spanish, and Italian, the system will be extensible to other European languages, as well as to Chinese, Japanese, Arabic, etc.

Having all this in mind our project will provide comprehensive **Digital library** which will synthesizes and include the following data and information (Figure 1):

- Biomaterials classification and composition with Relevant references (Tables 3, 5);
- Standards and best practices for determining properties and biocompatibility; Physical properties, such as density, conductivity, melting ranges, solubility in water, surface tension, viscosity, biomaterials performances for application in biomedical environments, resorbability, etc. surface

characterization (Tables 6, 7, 8, 9, 10, 11)

- Mechanical properties, such as tensile stress, compressive stress, hardness, impact strength etc (Tables 5 and 7).
- Special properties, applicable for some groups of materials, such as colours of dental shade guides, creep of amalgam, etc.
- Biological behaviour in the human body (Table 6).
- Biocompatibility, such as corrosion properties, toxicity (systemic and local), allergic potential, mutangenicity and carcinogenicity, biocompatibility test methods and test results (when available and applicable), affinity and strength among inorganic and organic phases as interface phenomena (Table 6)
- Guidelines for the biomaterials applications (Table 5);
- Cross-reference tables of equivalent materials;
- Technologies of application and processing Biomaterial manufacturers; (Tables 2, 3, 9).
- Relevant legal and regulatory information both from within and outside of the EU
- Biomaterial manufacturers;
- Final products and medical devices (Table 2).

CLASSES OF DENTAL BIOMATERIALS

Dental materials for restorative dentistry include (Tables 3 and 5): Metals, such as Amalgam alloys for direct fillings; Noble metals and alloys for direct fillings, crowns and bridges, and porcelain fused to metal restorations (Letic et al., 2000;2000a).

Base metals and alloys for partial-denture framework, porcelain-metal restorations, crowns and bridges, orthodontic wires and brackets, and implants; Ceramics for implants, porcelain-metal restorations, crowns, inlays, and veneers, cements, and denture teeth; Composites for replacing missing tooth structure and modifying tooth colour and contour; Polymers for denture bases, plastic teeth, cements, and other applications. These materials must withstand forces during either fabrication or mastication, retain their strength and toughness, and be resistant to corrosion, friction, and wear. Similar to implantable devices for non dental applications, they must also be biocompatible (Craig et al.,2002).

METALS: DATA COLLECTION AND SELECTION

Metals are probably the oldest form of materials used for dental implants and the most common type of materials used so far.

Metals are widely used as biomaterials due to their properties, such as strength and toughness (Table 7). For instance, some of the most common orthopaedic surgeries involve the implantation of metallic implants. In addition to orthopaedics, metallic implants are used in maxillofacial and oral surgery. Although many metals and alloys are used for medical device applications, the most commonly employed are stainless steels, commercially pure titanium and titanium alloys, and cobalt-base alloys.

Shape Memory Alloys, patented as Nitinol (nickel-titanium alloy), have very wide use because of their exceptional elasticity, their shape memory, their good resistance to fatigue and wear, and their relatively good biocompatibility.

Shape memory alloys are characterized by their ability to return to their original shape after heating to their transformation temperature after having been deformed. This is known as the shape memory effect and is caused by a change in the crystalline structure during the transition from the martensitic phase to the austenitic phase. It gives these materials attractive actuation capabilities.Shape memory alloys have a high power to weight ratio (up to ten times that of conventional actuation systems) and in the martensitic phase they can withstand large amounts of recoverable strain (up to 8%). When heated to above their transition temperature they can exert high recovery stresses of up to 700MPa which can be used to perform work. On the downside, they are relatively inefficient (less than 10%), having a slow response speed (predominantly dictated by the need for cooling) and are relatively complex to control due to inherent non-linearities and hysteresis in the shape memory effect. The most common shape memory alloy is Nitinol and alloy of nickel and titanium.

Amalgam remains the hardest and strongest material available today for direct placement restorations. It is easy to use, helps maintain a seal against leakage by developing corrosion at the amalgam-tooth interface (although modern amalgams do this much less effectively), and has withstood the test of time. Use of amalgam in humans has become controversial due to concerns regarding its mercury content and resultant potential health hazard. As in many controversies, opposing views vary widely and are argued passionately by their proponents. A poor aesthetic result is another reason for a decline in amalgam use since it does not match natural tooth structure and darkens over time.

Gold-based alloys were the first alloys to be used for implants, probably because these alloys were available in dentistry, but they promoted the fibrous interface with a bone, i. e. a distant osteogenesis with a short lifespan. **Cobalt-chromium** alloys were also developed and used as endosseous implants and in prosthodontics. However, the fundamental problem with these metals and alloys was the fibrous response which they promoted with the bone. By today's standards, none of these materials are biocompatible, probably because of their corrosion effected by the living tissue and the release of elements into the tissue. Today, these metals have largely been replaced by titanium and titanium alloys (Tables 5, 8, 19).

Titanium, Titanium Alloys and Modifications of Implant Devices

Titanium is used in stomatology, particularly in implantology because its chemical, physical and biological properties provide good biocompatibility. As titanium has a unique combination of properties (light weight, high strength to weight ratio, low modulus of elasticity, and excellent corrosion resistance), titanium and some of its alloys are important materials in medicine.

Superior fracture and fatigue resistance caused them to become the materials of choice in traditional load-bearing applications. Friction and wear are important properties of materials (Table 7) and represent the response of a material pair in a certain environment to imposed forces, the characteristics of the relative motion, the contact pressure between the surfaces, the temperature, the stiffness and vibration properties of the supporting structures, and lubrication (the presence of a lubricating film, such as saliva, separates surfaces during relative motion and reduces frictional forces and wear). Nowadays, titanium and its alloys, with additional advantages (excellent biocompatibility, good local spot wettability, and easy shaping, weldability and finishing via a number of mechanical and electrochemical processes) have become important material in dentistry. Although more research is needed in such areas as development of optimum casting investments, device design and control of biological responses, the future holds bright prospects of use of titanium as biomaterial.

Cp Ti (Tab. 8A) and titanium alloys, such as Ti-6Al-4V or as NiTi or TiNbZr, Ti-6Al-7Nb and others (Tab. 8B), have been used for manufacturing implants for the last 25 years. However, in spite of their excellent mechanical and physical properties, the worldwide medical use was hindered by their alleged toxicity, carcinogenicity or genotoxicity, hard metal disease by TiN and TiC fibroblast-mediated osteolysis or merely by their highly questionable longevity in vivo. An extensive and excellent metanalytic review on biological factors contributing to failures of osseointegrated oral implants of Branemark type was published by Esposito, 1998. Comparative investigation found that Ti implant system, apposes more bone than ceramic systems, although alternatives concerning the type of Ti alloy and bioactive surface layer engineering, generate extremely diverse results in osseointegration

From the biocompatibility point of view, the two critical success factors for inductive osteogenesis i.e. osteoinduction that we expect from titanium or other implants, are: (i) chemical composition and reactivity of bioactive surface layer; and (ii) topography i.e. roughness of the surface in contact with the bone.

Ti implant surface has been the focus of multi technical approaches and manipulations (both mechanical and physico-chemical), which were targeted to enhance the responsiveness of the host tissue to the implant, to promote in situ osteoinduction and thus to prolong the longevity of the implant (Tables 5,8). Pure titanium (cpTi) is available in four grades: 1-4. Ti contains dissolved oxygen, N, H, C and Fe in various amounts and forms a strong and tightly-bound oxide over the surface (TiO2). This oxide forms instantaneously and spontaneously at all temperature. Its thickness is 5-10 nm, with tendency to grow up to 200 nm. This layer, described as passive, is capable of withstanding a saline, physiological environment without disintegrating, and is believed to give Ti its biocompatibility. This oxide layer (TiO2) makes Ti casting difficult, largely is responsible for the outstanding corrosion resistance of cpTi and Ti alloys of any known implant material.

Recently, many biotechnological improvements were made to the surface layer of Ti (Tables 6 and 8). The question which arises is whether the efforts that scientist have undertaken thus far, for upgrading both the quality of the composition of the implant and the quality of its bioactive surface layer, are sufficient to achieve a desirable control of tissue response, i..e. to have a better osteogenesis. Combination of chemical and mechanical manipulations were reported to improve the surface layer. For instance: polished cpTi was acid-etched in two ways: (i) the natural

Table 7. Physical-chemical properties of metallic and non-metallic materials used in dentistry

Coefficient of Friction	Permanent Deformation
Coefficient of Thermal Expansion (Linear)	Poisson’s Ratio
Color Range of Natural Teeth	Proportional Limit
Colors of Dental Shade Guides	Shear Strength
Surface Free Energy	Solubility and Disintegration in Water
Surface Tension	Specific Heat
Tear Energy	Heat of Fusion
Tear Strength	Heat of Reaction
Bond Strength (Between Restorative Materials and Tooth Structures)	Strain in Compression
	Thermal Conductivity
Hardness Number (Mohs’ Hardness)	Thermal Diffusivity
Transverse Strength	Duration
Contact Angle	Compressive strength
Creep of Amalgam	Tensile Strength
Density	Vickers Hardness
Flow	Creep of Amalgam
Impact Strength	Critical Surface Tension
Index of Refraction	Density
Melting Temperatures	Elastic Modulus
Penetration Coefficient	Viscosity
Percent Elongation	Lied Strength
Dynamic Modulus	Zeta Potential

oxide was dissolved with hydrofluoric acid and a new oxide layer was grown by oxidation in nitric acid (HF/HNO3); or (ii) Ti was pre-treated with HF/HNO3 and then machined, HF/HNO3 etched, fine or coarse sand-blasted and then HCl/H2SO4 etched, HF/HNO3 etched and electropolished and HF/HNO3 etched and Ti plasma-sprayed. The different chemical treatments resulted in distinct differences in surface roughness when examined by light microscopy, i.e., roughness was changed from the smoothest to the roughest. Subsequently, the effects of surface roughness on the function of osteoblast-like cells were measured. Acid-etching pre-treatment were used for covalent attachment of selected biological molecules as alkaline phosphatase and albumin. These developments generated different kinds of interfaces between Ti and bone tissue, as described later. Subsequent chemical procedures on Ti were: deposition of thin polymeric film from ethylene plasma, alkali- and heat-treated Ti, biomimetic method for apatite nucleation for bone-like apatite-formed Ti or electrochemical apatite deposition. These chemical manipulations have two key results in common: changes on TiO2 layer reactivity and surface fine topography.

The implant surface roughness is essential for interfacial interaction with local tissue around implant, particularly for osteoblast. Osteoblasts, osteoblast-like osteosarcoma cells, macrophages, fibroblasts, bone marrow cells, nicely grow on polished Ti surfaces. However, they need not only excellent chemical conditions, but also particular topographic conditions of the surface layer to create an environment conducive to optimum cell morphology and activity. Optimum roughness of Ti implants (e.g., 4000-4500 nm, or 600 grit, or 300 A) was shown to significantly affect osteoblast cell response. For instance, it can decrease the cell number, but increase the expression of more mature cellular phenotype such as: alkaline phosphatase (ALP), osteocalcin (OC), transforming growth factor β and prostanglandin E2 and the response of MG63 osteoblast-like cells to 1,25-(OH)2D3. An example of such a coating material is the commercially available composite materials, such as "Bonelike" which is a synthetic bone material, hydroxyapatite reinforced with tiny glass particles. This material can be used to provide a layer on the surface of pure titanium that its developers hoped will lead to better incorporation of any implant.

Surface roughness modulates the local production of growth factors and cytokines such as prostanglandin (PGE2) and transforming growth factor β 1 (TGF-β 1) by osteoblast-like MG-63 cells. Significant high levels of cellular attachment were observed when using rough, sand-blasted surfaces with irregular morphologies.

Coatings on Implant Devices

Bone formation on the bioactive surface layer of the implant may be directly influenced by effects of the quality of the surface layer on osteogenic cells behaviour (Tables 5 and 9). From the character and amount of bone formation around different implants, it can be concluded whether the used materials are biocompatibile. This is why we should fully understand the process of bone growth around implants, as well as the reaction of the bone to trauma or to various properties of the implant surface layer.

The classical protocol of osseointegration was based on the success of the uncoated cpTi, treaded root-form implant. Long-term clinical data support the use of this material as an ideal dental implant. Basically, Ti is osteoinductive and it may create physico-chemical bonds with the bone. However, current data substantiate the use of a variety of implant surface biomodifications, coatings, as well as geometries to attain osseointegration.

Therefore, the next step in the upgrading of the quality of implant surfaces was the addition of coatings onto the implant in the following ways (Table 8) : (a) metal to metal; (b) ceramic to metal; and (c) biological active molecules on metal on

Table 8. Types of titanium and titanium alloys used for dental devices and implants (Letic-Gavrilovic et al.,2000)

Type of Alloys	**Technological Improvements of Ti surfaces (C)**	**Relationship of various alloys with host tissues (D)**
A) Pure Ti (cpTi, grade 1-4)	**1. Physical manipulations:** a) mechanical working - machining - polishing) - grooved surface (V shaped) - smooth polished - surface blasted b) plastic forming - hydrothermal method for coating HA - sol-gel prepared sintered titanium - shape memory c) plasma treatment - argon plasma cleaning and etching treatment d) ion implantation (N, C, B)	**BIOTOLERANT** - distant contact with connective tissue capsulae: Eg: Co, Cr, Mo, Au, Polymers **BIOINERT** - direct contact : Eg: Ti, Al, Ta, Ceramics **BIOACTIVE** - chemical bonding - osteogenesis: Eg: Ca-HA, CaP **OSTEOINDUCTIVE** - physico-chemical bonds, new bone: Eg: Ti alloys with coatings
B) Alloys with various metals 1.Ti90-6AL-4V (Ti6A14V) 2.NiTi (Ni90Ti10; Ti50Ni50; Ti70Ni30) 3.Ti-6AL-7Nb 4. TiNbZr 5. Titanium beta 3 (Ti77.5/Mo12/Zr6/Sn4.5)	**Chemical manipulations:** a. ACID-ETCHED - pretreated with: -hydrofluoric/ nitric acid (HF/HNO3) -HF/HNO3 and machined -HF/HNO3 and sand-blasted and HCl/ H2SO4 acids -HF/HNO3 and electropolished -HF/HNO3 and Ti plasma-sprayed b. chemically treated with Ca-P c. alkali- and heat- treated d. covalent immobilization of bioactive organic molecules e. ethylene plasma polymeric film coating f. electropolished g. biomimetic method	

ceramics or diverse functional carriers. Ti has been used to date as a biological substrate of many osteoconductive and osteoinductive, inorganic or organic coatings, such as ceramics of different kind, glass, adhesion proteins, extracellular bone matrix proteins, growth factors and cytokines. The primary goal of coated implants was to combine the benefit of a bioactive surface layer with the properties of the substrate i.e., the strength of the underlining metal. The application of different types of ceramics onto titanium surface, was aimed at gaining two advantages: bonding osteogenesis and connective tissue osteogenesis. Ceramic coatings on titanium-based implants combine osteoconductivity and osteoinductivity, and additionally improve the strength of chemical bonds of the implant-bone interface.

Various Ti implant coating methods were developed: plasma spraying, chemical vapour deposition process (CVD) and physical vapour deposition process (PVD), slip casting/sintering, electrophoretic deposition/sintering, electrochemical deposition, and sputter coating, but plasma spraying is most commonly used one. Chemical vapour deposition (CVD) process with high temperature (500-1000°C) of the substrate is not very suitable for dental alloys. In dentistry, the more recent physical vapour deposition (PVD) process may be used. For example, under vacuum conditions, evaporated Ti is applied on thoroughly-cleaned metal surfaces, while feeding nitric or carbon gas in order to produce TiN or TiC.

Coatings have a paramount clinical importance in the following cases: (a) big defects and poorly supportive bone; (b) when a very small or very big implant should be applied; (c) repeated surgical procedure or re-implantation; (d) type III and IV bone ; and (e) in fresh extraction site. In each of this cases, given the adverse local conditions, the use of an implant with a coating or a sol-coated biomaterial, as a carrier of biologically active molecules, is recommended.

CERAMICS: DATA COLLECTION AND SELECTION

Traditionally, ceramics have seen wide scale use as restorative materials in dentistry. (Tables 2,3,5,9) These include materials for crowns, cements, and dentures. Some ceramic materials are used for bone repair and augmentation.

Ceramics are stiff, hard and chemically stable and are often used when wear resistance is vital. Of the large number of ceramics known, only a few are suitably biocompatible. The main problem with ceramic components is that they are brittle and relatively difficult to process.

Bioceramics can have structural functions as tissue replacements, can be used as coatings to improve the biocompatibility of metal implants, and can function as resorbable lattices, which provide temporary structures and a framework that is dissolved, replaced as the body rebuilds tissue. The thermal and chemical stability of ceramics, their high strength, wear resistance and durability all contribute to making ceramics good candidate materials for surgical implants. Some ceramics even feature drug-delivery capability. Smart Ceramics (Cercon) was invented in 1995 as “all ceramic teeth bridge” enabling the direct machining without stainless steel or other metals. The overall product is metal-free, biocompatible and crack resisting formation.

Gadgets for Dental Applications

Ceramics play a vital role in the manufacture and function of various gadgets used in dental science (Table 4). Various recently introduced diagnostic and working tools of which ceramics play an integral part include: Radio Visio Graphy (RVG), Pulp tester Apex locators 1st generation

Table 9. Application of different coatings on Implantable dental device in order to improve biological response (Letic-Gavrilovic et al.,2000)

COATINGS
A. metal on metal
B. ceramic on metal
C. Functional coatings- biologically active molecules on metal/ceramic
A. Methods for coatings on METAL

continued on following page

Table 9. continued

Arc plasma spraying CVD - chemical vapor deposition process The CVD process is defined as the deposition of a thin solid film from a chemical reaction involving gas species at a heated substrate Nanocrystalline Diamond - NCD), PVD - physical vapor deposition process - ion planting. The surface to be coated is in contact with a plasma- high vacuum thermal evaporation- RF magnetron sputtered
B. Ceramic coatings (osteoconductive)
1. nonapatite calcium phosphat, 2. apatite CaP (principally HA) 3. glass ceramic, bioactive glass 4. titanium nitride (TiN) 5. titanium carbide (TiC) 6. diamond-like carbon (DLC) 7. silicon carbide (SiC) AlCaP 8. HA ceramic 9. bioactive glass membrane 10. TCP beta 11. bone ceramic (TBC) 12. coraline 13. Titanium 14. 3-dimensional carbon/carbon composite (3D C/C)
C. Functional coatings as carriers for different growth factors ***Natural and synthetic biomaterials***
Allogeneic demineralized bone matrix (DBM) Collagen - fibrous collagen membrane, type I collagen, type IV collagen Bovine matrix non-collagen protein Cartilage strips Resorbable and nonresorbable membranes for Guided Bone Regeneration a) basement membrane matrix (Matrigel) b) expanded polytetraflouroethylene (ePTFE) membrane Fibrin Biodegradable synthetic polymers of polylactic acid (PLA),(PLA-PEG; PLGA

- resistance based, 2nd generation - impedance based, 3rd generation - frequency based.

Piezo Ceramics

Piezoelectricity can be defined as pressure electricity which is a property of certain classes of crystalline materials including natural crystals of Quartz, Rochelle salt and Tourmaline plus manufactured ceramics such as Barium Titanate and Lead Zirconate Titanates (PZT). When mechanical pressure is applied to one of these materials, the crystalline structure produces a voltage proportional to the pressure. Conversely, when an electric field is applied, the structure changes shape producing dimensional changes in the material.

The piezoelectric materials use polycrystalline ceramics instead of natural piezoelectric crystals. They are more versatile with physical, chemical and piezoelectric characteristics able to be tailored to specific applications. The hard, dense ceramics can be manufactured in almost any given shape or size, which are chemically inert and immune to moisture and other atmospheric conditions.

Therapeutic Ceramics

Silicate Cement

Silicates constitute the first dental cement to use glass as its component. The cement powder is a glass consisting silica, alumina and fluoride compounds. The liquid, on the other hand, is an aqueous solution of phosphoric acid with buffer salts. The cement powder and liquid are mixed together resulting in an acid-base reaction. Fluoride ions are leached out from the set cement, which is responsible for the anti-cariogenic property exhibited.

Glass Ionomer Cement (GIC)

Glass ionomer cement represents a logical step in the evolution of therapeutic cements. GIC's are composed of glass powder and a polycarboxylic acid. They constitute an improved version of the silicate cement, in which the liquid is replaced by carboxylic acids with glass remaining as the powder. It is the most popular dental cement that is used in various aspects. The highlight of this material is demonstrated by its superior biocompatibility and anti-cariogenic property. Modifications of glass ionomer cement include the high density Glass ionomers, packable ionomers for use in Atraumatic Restorative Treatment (ART). Resin modified GIC incorporate resins in their powder component for better strength. When mixed wet, protons from the polymeric acid exchange with calcium and aluminium cations in the surface of the glass particles. The cations then form electrostatic bonds with carboxylate groups in the polymer chains, effectively cross-linking them to form a gel that sets the cement.

Bioceramics

Bioceramics are a group of ceramics, which are biologically active materials rich in calcium and phosphate. Hydroxyapatite and tricalcium phosphate are similar in composition to bone and teeth and can be used for augmentation of alveolar ridges and filling bony defects. They are manufactured and are available in block, granular and injectable forms. These bioactive materials are packed in the required site providing a scaffold for new bone growth and are osseoinductive in nature. The various forms of bioceramics are Single crystals (Sapphire), Polycrystalline (Hydroxyapatite) Glass (Bioactive glass) Glass ceramics (Ceravital) Composites (Stainless steel reinforced Bioglass). There are about four types of bioceramics:

- **Inert:** Attached by compact morphological fixation. e.g, Alumina, Carbon
- **Porous:** Attached by vascularization through pores. e.g, Porous Alumina.
- **Surface active:** Directly attach by chemical bonding with bone.e.g, Bioglass, Hydroxyapatite
- **Resorbable:** Designed to be slowly replaced by bone. e.g, Tricalcium Phosphate (TCP).

Ceramic coatings on dental implants, such as Calcium phosphates (hydroxyapatite- HA) appear to have better biological response than cpTi or Ti alloy alone, even if their clinical predictability remains controversial. Coatings seem to promote faster bone adaptation, higher bone implant strength, better osteoblast precursor activity, bone growth around dental implants and thus bonding of the bone to the implants, i.e. osseointegration.

HA coatings were highly considered because they enhance osseointegration, and they lead to the formation of more mineralised extracellular matrix (ECM) and to faster bone formation with respect to Ti substrates alone. The philosophy was that HA has an advantage over smooth Ti surfaces having: (1) bioactive surface versus an inert Ti surface; (2) higher bond strength of the bone to the implant; and (3) increased bone-to-implant contact. In spite of reports about overstressing, rapid, bone-resorption adjacent to HA-coated implants, short-term survival rates (from 6 months to 6 years), or other causes of failures, there are still evidence of positive effects of HA coatings on osseointegration.

Recently, other ceramic coatings, such as titanium nitride (TiN) and titanium carbide (TiC**),** have been proposed for implantology (Tab.6 and 19). In general, biocompatibility of TiN in cell culture and animal tests was evaluated positively. Aesthetic appearance (gold-coloured layer) is questionable and probably culture dependent. However, longitudinal clinical studies have been scarce so far. In total joint arthroplasty, a diamond-like carbon (DLC) coating was applied onto Ti. TiC coatings were developed to fit straight stems and cementless accetabular implants. Subsequent studies questioned the biocompatibility of TiC on grounds of toxicity or hard metal disease. Also vitreous carbon, pyrolytic carbon, pyrolytic graphite/silicon-carbide were occasionally used as Ti coating on implants.

BIOCOMPOSITES: DATA COLLECTION AND SELECTION

The most successful composite biomaterials (biocomposites) are used in the field of dentistry as restorative materials or dental cements (Table 5). Although carbon-carbon and carbon reinforced polymer composites are of great interest for bone repair and joint replacement because of their low elastic modulus levels, these materials have not displayed a combination of mechanical and biological properties appropriate to these applications. Composite materials are, however, used extensively for prosthetic limbs, where their combination of low density/weight and high strength make them ideal materials for such applications. Smart composites containing ACP (amorphous calcium phosphate) is one of the most soluble of the biologically important calcium phosphates, exhibiting the most rapid conversion to crystalline hydroxyappatite (HAP) (Letic et al.,2004). ACP, when incorporated in specially designed and formulated resins to make a composite material, will have an extended time-release nature to act as a source for calcium and phosphate, useful for preventing caries. Biodegradable bone cements are highly desirable because they can provide for immediate structural support and, as they degrade from the site of application, they allow the ingrowth of new bone for complete healing of the bone fracture.

Although improvement has occurred in the field of dental adhesives and composites, problems with composite restorations still exist. The most serious problem is polymerization shrinkage, which causes gap formation and cusp deflection. Both of these problems show clinically as postoperative sensitivity and pain. Based on the review of available articles, it appears that the use of liners is still desirable because liners may help overcome these problems. Both flowable resin composites and resin-modified glass ionomers (RMGIs) have a lower modulus of elasticity than restorative composites, which may counteract some of the polymerization shrinkage of the restorative composites. Because of the low viscosity of RMGIs and flowable resin composites, they can wet the tooth better than restorative composites and decrease the chances of gaps. RMGI liners appear to perform better than flowable resin composites because of their physical properties. Additionally, placing the self-adhesive RMGI liner on the areas of deep dentin can protect this sensitive dentin from the strong conditioners needed for the subsequent bonding procedure. From the clinician's standpoint, overcoming these problems translates into less postoperative sensitivity.

BIOPOLYMERS: DATA COLLECTION AND SELECTION

A wide variety of polymers are used in medicine as biomaterials. Their applications range from facial prostheses to tracheal tubes, from kidney and liver parts to heart components, and from dentures to hip and knee joints (Tables 5 and 10). Polymeric materials are also used for medical adhesives and sealants and for coatings that serve a variety of functions. They are widely used as implant materials as they have physical properties that are most similar to the natural tissues. Use of polymers includes wound dressings, tendon replacements, intraocular lens replacement and joint linings. The polymers that are widely used include polyethylene, PET, PTFE and polyurethane and themselves are well tolerated in the human body. However, additives and molecules released from polymer breakdown can lead to allergic and inflammatory responses.

The use of polymers as biomaterials started over 2500 years ago with collagen (found in animal tissue) used as a surgeons thread. In the 1970's the polymer polyglycolic acid (PGA) was developed as synthetic degradable sutures.

PGA was further developed over the next few decades and was used in implants that would slowly release desired chemicals into the body and scaffolding on which replacement organs could be grown, for TE (Letic-Gavrilovic et al.,2004; 2005). Over 25 different types of cells have been grown on the polymer scaffolds, and skin grown on these scaffolds has been successfully transplanted to heal diabetic skin ulcers. It is hoped that in the future these scaffolds will be used to grow nerve cells for use in spinal cord repairs, bone or cartilage cells for joint repairs, pancreatic cells to make insulin for diabetics, and liver cells to make livers for transplantation Advances in the design of stimuli-responsive polymers have created opportunities for novel biomedical applications. Changes in shape, surface characteristics, solubility, formation of an intricate molecular self-assembly and a sol-gel transition enabled several novel applications in the delivery of therapeutics, tissue engineering, cell culture, bio separations, bio mimetic actuators, immobilized bio catalysts, drug delivery and thermo responsive surfaces. One area of intense research activity has been the use of biocompatible polymers for controlled drug delivery. It has evolved from the need for prolonged and better control of drug administration. The goal of the controlled release devices is to maintain the drug in the desired therapeutic range with just a single dose.

The list of new polymers developed specifically for medical applications is far too long to describe here. We have chosen to focus on two types of synthetic biomaterials: (a) hydrogels and hybrid polymer systems, which are attractive owing to their high water content and tissue-like properties, and (b) smart materials, which can rapidly respond to changes in the in vivo environment.

Hydrogels are crosslinked polymer networks that are insoluble but swellable in aqueous medium. These materials offer an environment that resembles the highly hydrated state of natural tissues, making them excellent candidates for tissue engineering and drug delivery. Hydrogels and bone cements, can, for instance, be used as an interface between bone and an implant with the aim of providing a mechanism for fixing a prosthesis in the intramedullary cavity. The bone cements would, in principle, dilate in a controlled manner by absorption of body fluids and achieve fixation by an expansion mechanism. The physical properties of hydrogels make them also very useful for controlled-release applications, such as the delivery of contraceptives, opthalmic, antiarhythmics, hormones, enzymes, anticancer agents, anticoagulants, antibodies. Biodegradable polymers like poly(lactic acid) (PLA), poly(glycolic acid) (PGA) and their copolymers, have recently found numerous applications in a variety of drug-delivery systems (Letic et al., 2001;2003). A potential alternative, for the currently used materials, is starch-based polymer which are well-known biodegradable materials.Hydrogels are three-dimensional polymeric networks held together by cross-linked covalent bonds and weak cohesive forces in the form of either hydrogen bonds or ionic bonds. These mechanisms include ionic (e.g., alginate), physical (e.g., pluronics and peptide self-assembling gels), and chemical bonds (e.g., fibrin glue and multivinyl methacrylate and acrylate derivatives). Hydrogels are, by definition, a broad class of hydrophilic polymeric materials which have the inherent ability to swell in water and other suitable solvents, capable of imbibing and retaining more than 10% of their weight in water within the gel structure. Attributes such as permeability to small molecules (such as tissue metabolites), a soft consistency, and a low interfacial tension between the gel and an aqueous solution are some of the important properties which have helped to generate interest in hydrogels as useful biomaterials. Additionally, the facility of purification, a high equilibrium water content (advantageous for the permeability and biocompatibility of these materials), along with their sterilizability makes them extremely versatile. The utility of hydrogels as biomaterials lies also in the similarity of their physical properties with those of living tissues.

There has been great interest in implantable biomaterials that are *injectable* as well as biodegradable. The development of hybrid polymer systems (copolymers, complexes, hydrogels, blends, etc.) based on natural and synthetic macromolecules and their open wide spectrum of applications in the biomaterials science has received tremendous attention. Natural and synthetic biodegradable polymers hold great promise for use as scafolds in TE. Main advantage of polymers are theirs properties which can be engineered for a wide range of medical applications (Letic et al., 2002;2002a). Of particular interest to oral-maxillofacial applications are injectable, in situ polymerizable, biodegradable polymer scafolds for filling irregularly shaped bone defects with minimal surgical intervention. A biodegradable support material would be ideal, as it would eliminate the need for a second surgery to remove the fixation device. Furtheron, in order to avoid the inconvenient surgical insertion of large implants, injectable biodegradable and biocompatible polymeric particles (microspheres, microcapsules, nanocapsules, nanospheres) could be employed. Since the range of potential TE applications is broad, there is a continuous ongoing search for materials which either possess particularly desirable tissue-specific properties, or which may have

Table 10. Synthetic polymers – Selected examples

Non-Degradable		**Biodegradable**	
Materials	**Principal applications**	**Materials**	**Principal applications**
	sutures		suture
Polyamides	device housings vascular grafts	Poly-lactic/glycolic acid	bone plates, bone pins
Polycarbonates	tubing, blood bags	Poly-orthoesters	wound closure
Polyesters	tubing, coatings		alveolar bone, tendon
PVC	tubing, soft tissue	Cyanoacrylates	repair
Polyurethanes	hip & knee bearing	Polylactic acid	
Silicones			
UHMWPE			

broad applicability and can be tailored to several tissue systems. Naturally derived materials biodegradable polymers show great promise, for TE applications. Natural biopolymers are composed of extracellular matrix (ECM) glycoproteins that are conserved among different species and that can serve as intrinsic templates for cell attachment and growth. Contrary to the synthetic, natural polymers are more easy for processing, degradability, biocompatibility, exhibition of bone-analogous properties, bone bonding, and ability to be surface engineered to produce desired mechanical and biological behaviours. In addition, and not less important, polisaccharide-based natural polymers are significantly less expensive than most commercial synthetics. Bio-polymers could be used as filling elements of irrregular defects for orthopaedic and maxillo-facial surgery, as bone cements, and drug delivery carriers. Other proposed natural polymers could be used for preparation of biodegradable and resorbable (Table 10) bio-membranes for epidermis protection, with special relevance in the field of burning, separation membranes to avoid adherences between different tissues in postoperative process, dental filling composites, membranes and supports for jaw regeneration, etc.

From the practical point of view, we expect that this new biomaterials will promote biological response of the treated tissue giving the following results:

- Plastic, multy-functional device, which dramatically help surgeons to fill irregularly shaped defects with minimal intervention;
- To enormously faster osseointegration (not less than 50% reduction of ossification time);
- To eliminate second surgery step, and therefore prolongs life of implanted prosthesis and reduce number of post-surgery complications:
- Drug delivery device for long controlled drug release will enormously help chronic patients eliminating multy interventions and reducing more than 50% costs of their treatments.

Resorbable and Non Resorbable Membranes for GTR and GBR

Guided Tissue Regeneration (GTR) is a surgical procedure that specifically aims to regenerate the periodontal tissues when the disease is advanced and could overcome some of the limitations of conventional therapy. GTR is a procedure that enables bone and tissue to re-grow around an endangered tooth or if the tooth is lost to increase the amount of bone for implant placement

Guided Bone Regeneration (GBR) is a current treatment for periodontal bone defects. In the GBR technique, a barrier membrane (Table 8) is placed over the periodontal defect to prevent the in-growth of cells from the gingival connective tissue, epithelium, and the periodontal ligament.

GBR membrane materials must maintain their barrier function long enough to allow osteoblasts to migrate into the wound.The distance to be spanned determines the time the membrane must function properly. Resorbable and non-resorbable membranes have been used as a GBR barrier. However, non-resorbable membranes must be surgically removed after the healing period. A resorbable membrane that can transmit tissue fluid, but excludes undesired cells from the clot, would have the advantage of not requiring surgical removal. Recent studies have reported the successful use of resorbable membranes in GBR (Letic et al.,2002;2002a;2005)

1. Osteopromotive membranes of expanded polytetrafluoroethylene (ePTFE; GORE-TEX) facilitate guided bone regeneration, are **not resorbable** and require a second procedure to be removed. The combination of membrane placement with rhBMP-2 may be of value in the clinical applications for bone regeneration purposes. This finding is

also valuable for choosing carrier materials for delivery of other growth-stimulatory substances, in combination with membranes. ePTFE membrane plus BMP can be combined with Ti implants, demineralized freeze-dried bone (DFDB), and with the growth factors PDGF-BB, PDGF/IGF-I or rhBMP (Table 9). Clinical results, demonstrated that ePTFE membranes plus PDGF/IGF-I, had the -highest bone density compared with controls receiving membranes alone and they also allow the bone to grow directly around the implant.

2. Basically there are two types of biologically **resorbable** biomaterials: (a) synthetic polymers of lactide-/glycolide- and polylactic acid; and (b) collagen. Collagen plays an important role in wound healing since it is present in connective tissue capsules which lie around implanted materials. The influence of collagens, including collagen I, III and IV on in vitro cell proliferation greatly depends on the cell cultures. Collagen membranes are used in clinical applications because their compact layer protects against soft tissue invasion and their porous texture enables the integration of newly formed bone tissue. The amount of collagen type I and III during soft tissue capsule formation varies, depending on the type of metal implants. The properties of collagen favour cell attachment. Collagen I was reported to inhibit cell proliferation, whereas collagen IV had no effect. It can be used independently or in association with various biomaterials, such as polystyrene, low and high crystallinity HA and rough Ti.

Osteopromotive Growth Factors on Implant Devices

Polypeptide growth factors are a class of natural biological bone mediators regulating the critical cellular events which are involved in wound healing: cell proliferation, chemotaxis, differentiation, and matrix synthesis. Growth factors elicit their effects by binding to specific cell surface receptors, which transduce signals to the nucleus via complex signal transduction pathways. Examples of growth factors found in bone, cementum and healing tissues include platelet-derived growth factor (PDGF), transforming growth factor β (TGF-β), acidic and basic fibroblast growth factors (a- and b-FGF), insulin-like growth factors (IGF-I and II), cementum-derived growth factor (CGF) and the bone morphogenetic proteins (BMPs). The in situ factors which induce osseointegration of the implant material are not fully understood, but most researchers agree that the contact between the bioactive surface layer of the implant and the bone is not static but dynamic (Letic et al.,2001;2003).

SMART BIOMATERIALS: DATA COLLECTION AND SELECTION

The use of biocompatible smart materials has revolutionized many areas in regenerative medicine (Gautam, 2008). The term "smart materials" refers to a class of materials that are highly responsive and have the inherent capability to sense and react according to changes in the environment. Biomedical applications of smart materials involve their use in tissue engineering, cell culture, bioseparations, biomimetic actuators, immobilized biocatalysts, drug delivery and thermoresponsive surfaces. Applications of stimuli-responsive, or "smart", polymers in areas like dentistry, biomedical engineering, delivering of therapeutics, tissue engineering, bio separations are an indicator of the potential and rapid progress in this area.

Smart Biomaterials can senses and reacts according to changes in the environment. For that reason they are often also called "responsive materials". Early smart material applications started with magnetostrictive technologies. These involved the use of nickel as a sonar source during WW1. Smart materials can be classified as: (1) passive smart materials that respond to external change without external control; (2) active smart materials that utilize a feedback loop to enable them to function like a cognitive response trough an actuator circuit; (3) very smart materials that sense a change in the environment and respond (e.g., by altering one or more of their property coefficients, tuning their sensing or actuation capabilities); and (4) intelligent materials that integrate the sensing and actuation functions with a control system. When smart biomaterials respond i*n vivo*, it can be exploited to control parameters such as drug release, cell adhesiveness, mechanical properties, or permeability. Several approaches have been examined for stimulants such as pH , temperature, and light.

The body employs changes in pH to facilitate a range of different processes.

For example, drug delivery by oral administration is attractive to many patients who require routine, periodic delivery of drugs. However, for the drug to remain effective, it must survive the acidic pH of the stomach.

BIOLOGICALLY INSPIRED MATERIALS

In an effort to design materials that will perform their intended functions in the presence of cells and/or in vivo, we as engineers and scientists can look to biology and take advantage of biological processes that have evolved over thousands of years.

Self-Assembled Biomaterials

One of the many fascinating aspects of biology is the self-organization of molecules into hierarchal structures that perform a specific task. This self-organization or self-assembly is based on the formation of weak noncovalent bonds, typically hydrogen, ionic, or van der Waals bonds or hydrophobic interactions. For example, amphiphilic molecules have hydrophobic and hydrophilic segments that self-assemble into distinct structures, such as micelles, vesicles, and tubules that are nanometers in length. When dispersed in an aqueous solvent, the hydrophobic segments in the amphiphilic molecules agglomerate, driving out water and, as a result, producing a well-ordered structure that can be useful in a number of different biomedical applications. A naturally occurring amphiphilic molecule is a phospholipid, which largely composes the cell membrane. Alternatively, a polymer (or oligomer) of amino acids can be synthesized to contain a number of different regions (hydrophobic, hydrophilic, charged, etc.) that under certain conditions will self-assemble into a macroscopic hydrogel. In general, the final three dimensional structure of the self-assembled material is dependent on the molecule's length and composition . Thus, by systematically synthesizing a molecule, a desired 3-D structure can be produced. These self-assembled biomaterials are promising new materials that can be engineered for applications in nanotechnology and in tissue engineering for drug and cell carriers. These materials may be particularly beneficial because the engineered peptides will take on a 3-D shape that may be recognized by the in vivo environment, more so than a conventionally synthesized material, and furthermore will breakdown into amino acids that the body is well equipped to deal with.

Biomimetic Biomaterials

Direct mimicry of biological processes represents an important strategy in modern biomaterials. Hydroxyapatite is the natural mineral in bone. There is now a huge amount of literature describing the use of hydroxyapatite and other forms of calcium phosphate coupled with synthetic and other natural biomaterials to induce bone formation. Nacre, the aragonite-rich lining of many seashells, also induces rapid bone formation. Nacre contains about 5% protein that serves as a "mortar" to bind together a brick-like mineral structure. A biomimetic approach to creating synthetic nacre-like structures has been published. Normal tissues have a complex 3-D architecture important for the mechanics and functionality of the biological organism. Biomimetically, we might emulate such structures with synthetic biomaterials. Synthetic materials offer the ability to generate many different kinds of 3-D structures with precise control over the final macroscopic properties and degradation profiles by varying the chemistry and processing techniques. However, synthetic materials provide little control over cell behavior and tissue response in vivo. Thus, to generate a biomaterial for a specific cell type and/or tissue, efforts have focused on adding biological cues to synthetic materials in an attempt to mimic the native tissue while simultaneously maintaining control over the material properties.

Biomimetic Nano-Scaffolds

Repair of tooth-supporting structures destroyed by the chronic inflammatory disease-peridontitis is a major goal of oral reconstructive therapy. It was proposed developing a novel scaffolding system that can also deliver regenerative agents to periodontal defects. This system consists of a nano-fibrous polymer scaffold modified with bone mineral- mimicking apatite that contains microspheres for delivery of bioactive molecules such as bone morphogenetic protein- 7 (BMP- 7), to periodontal defects. It is expected that this scaffolding/factor delivery system will promote periodontal regeneration at the defect site by providing an environment for enhancing adhesion and migration of putative cells such as osteoblasts, cementoblasts, and periodontal ligament (PDL) fibroblasts as well as promoting differentiation of their progenitor cells. Moreover, this scaffolding delivery system will allow for permeation of nutrients, metabolites, and signaling molecules required for cell proliferation, differentiation and 3D tissue formation.

Periodontal Engineering Using Biomimetic Nano-Scaffolds

Periodontal diseases result in loss of supporting tissues including bone, cementum, and periodontal ligament (PDL), ultimately leading to tooth loss if left untreated. Unfortunately, dental tissue loss has the second largest patient population next to blood transfusion. The restorative results of the current therapies are often disappointing and unpredictable. It was proposed a novel biomimetic/tissue engineering approach. In this approach an unique nano-fibrous polymer scaffolding (mimicking collagen architecture), modified with apatite (mimicking bone mineral), and containing microspheres for delivery of bioactive factors (mimicking development and reparative signaling cascades) will be used in periodontal osseous defects to: promote activities of cells at the healing site, e.g., osteoblasts, cementoblasts, and PDL fibroblasts (and their progenitor cells), allow for nutrients, metabolites, and signal molecules to permeate, and guide cell proliferation, differentiation and tissue neogenesis in 3D. The specific aim of this project would be:

- To test whether polymer scaffolds with nano-fibrous pore walls are superior to scaffolds with "solid" pore walls, and whether bone mineral-mimic apatite promotes calcified tissue formation, in vitro.
- To develop a combined nano-fibrous scaffold/biodegradable microsphere delivery system that allows for controlled release and improve bioavailability of putative periodontal regenerative factors and to evaluate their regenerative function, in vitro.
- To confirm that the microsphere/scaffold systems selected based on the results from studies under aims 1 and 2, provide a superior environment for regeneration of periodontal

tissues, in vivo.By accomplishing these specific aims, results will be significantly advanced, in new and improved periodontal regenerative therapies. Furthermore, the ability to manipulate the scaffolding structure and control the rate and types of factors delivered, this system can be utilized to answer many fundamental questions in regenerative biology, including other tissue engineering applications.

NANOBIOMATERIALS

Nano-Features and Nano-Particles in Restorative Dentistry

The word "nano" in Greek actually means "extremely small" or one billionth. The actual size of the calcium deposits on the NanoTite Implant (3i) are as small as 20 nanometers and can best be seen at 20,000X magnification. Nanotechnology is technology done on a nanometer scale. In the physical world we have all been familiar with the three states of matter, solid, liquid and gas. There is one more, the interfacial or surface state. The physical world becomes very different at the surface of materials, and some very interesting physical properties come with materials in this"surface" state. When materials are at the nanometer scale, they are in many ways in the surface state of matter. We can also manipulate down to individual molecules or groups of atoms to make useful materials and devices (Table 10). Nanomaterials, sometimes called nanopowders when notcompressed, have grain sizes in the order of 1-100 nm in at least one coordinate and normally in three.

Patient applications and benefits of the NanoTite Implant include use to replace single or multiple missing teeth due to cavities, decay, trauma or disease. The NanoTite Implant (3i) , like all dental implants, is designed to help preserve bone structure and natural facial contours. Additionally, the NanoTite Implant may help patients increase overall confidence due to a brand new smile! "I think It's One Nano Step For Man, One Giant Leap For Implant Dentistry!" adds Dr. Meltzer.

Hybrid Plastics Inc. (USA) received a $750,000 grant from the National Institutes of Health to develop nanocomposite-based dental materials. This grant will allow the company to develop a prototype adhesive and restorative system for bonding, shrinkage control and corrosion resistance. The materials will be based on Hybrid's "POSS Nanostructured" building blocks. Hybrid is working on the project with Ohio State University's College of Dentistry (USA) and dental supply firm Pentron Corp. Another company Hybrid and Pentron developed Nano-Bond, dental bonding agents commercially launched 2003 year. Two technologies are currently under investigation, nano-fibre coatings to encourage linear cellular growth and mineral nano-particles in a colloidal suspension to interact with the damaged tooth.

Nano-Fibre Coatings

The investigation of the biological effect of nano-fibre coatings on the trans-mucosal element of the endosseous dental implants. Human gingival fibroblast cells have demonstrated the ability to align, proliferate and secrete collagen in the direction of the nano fibres in preference to other topographies. It was hypothesised that if this topography is applied in a circumferential dierection around the implant abutment, gingival fibroblasts will align to this surface nanotopography, leading to the secretion of collagen fibres circumferentially around the implant, forming a tight fibrous collar This fibrous soft tissue attachment will protect the underlying osseous attachment from bacterial attack and breakdown.

Mineral Nano-Particles

The investigation of the ability of colloidal nano-particles (Hydroxy-apatite, silica, an analogue of silica or a calcium compound) to infiltrate demineralised (carious) dentine and act as a "seed" for further remineralisation. It is hypothesis that the application of an appropriate formulation of colloidal nano-particle to a carious lesion may prevent further demineralisation and given the right environment it may encourage remineralisation.

SAFETY OF DENTAL DEVICES AND BIOMATERIALS

Biological Response to Dental Device Materials

All materials intended for application in humans as biomaterials, medical devices, or prostheses undergo tissue responses when implanted into living tissue (biocompatibility) (Anderson, 2001). Alloys must demonstrate biocompatibility by conducting toxicity testing according to ANSI/ADA (USA) document, which describes recommended standard practices for biological evaluation of dental materials. This testing requirements include cytotoxicity testing that evaluates cell death in L929 or HeLa cell cultures exposed to the alloy, hemolysis testing in rabbit blood and mutagenicity testing conducted according to the Ames test. Corrosion testing must be completed for new alloys by comparing their performance to alloys that have been in use successfully for at least five years.

In order to avoid undesirable problems with Biomaterials and/or Devices, we suggest to follow the materials safety procedures as shown in Table 11. Any material implanted into the body evokes a biological response which could be dangerous. Some responses are simply fibrous capsule formation protecting both the implant and the host. However some responses develop into chronic inflammatory responses with macrophage accumulation and development of giant cells. The in vitro studies are being developed, and so far there is much data accumulated on PMMA (polymethyl-methacrylate: bone cement), HA (hydroxyapatite, a calcium phosphate ceramic used to coat dental and orthopedic implants), and the oxides of titanium and cadmium which would be the surface of implants made of these metals. The production of biologically active substances such as nitric oxide and tumour necrosis factor TNF alpha (which are important substances in inflammatory responses and the production of cytokines such as Il-6, Il-4, and Il-10) involved in the immune responses are being assessed. Lipopolysaccharide (LPS), which is a component of the cell wall of Gram negative bacteria and a known stimulant of cells, is added to macrophage cultures in the presence and absence of the particles. It is evident to date that there is strong production of the biologically active substances by the LPS alone. The addition of HA or PMMA, with the LPS to the macrophage cultures, markedly potentiates the production of these substances. Whether it is additive or synergistic is still being assessed.

Table 11. The applications in surface coating of selected nanomaterials

NANOMATERIALS	APPLICATIONS
Metal oxides such as Ceria, Zinc oxide, Aluymina, Zirconia	Coating on dental implants, Car catalysts, fuel cells, transparent UV, absorbers, antibacterial functions, structural ceramics, Sunscreens.
Carbon	Electrical and thermal conductors Coating on dental implants
Aluminosilicate (imogolite)	Catalyst support, ceramics filter, and humidity controlling building materials
Calcium phosphates (hydroxyapatite)	Bone grafts in periodontology, Coatings on dental Implants

Table 12. Dental devices safety data sheet

Product and Company Identification
Composition and Information of Ingredients
Hazards Identification
First aid Measures
Fire Fighting
Accidental Release Measures
Handling and Storage
Exposure Controls/Personal Protection
Physical/Chemical Characteristics
Stability and Reactivity
Toxicological Information
Ecological Information
Disposal Consideration
Transport Information
Regulatory Information

On the other hand, the presence of the metallic oxides depresses the response to LPS.

The in vivo data have indicated the formation of a capsule composed of fibroblasts and macrophages when the material is placed into the peritoneal cavity for several days. These cells can then be grown in culture and their activity assessed. The production of the biologically active substances by these peritoneal cells in the absence of LPS is very low. The addition of LPS stimulates the active response. The in vitro data and the in vivo data seem to be in agreement and giving correlative studies.

These findings on the different responses to the different particles and materials will help delineate the differences in biological reaction. Natural latex in medical devices can cause life-threatening Type 1 allergic reactions in individuals sensitized to latex proteins. HSB latex research project was initiated to solve the problem of severe allergic reactions. It included efforts to provide basic data on the nature of allergens and to develop methodology for evaluating the allergenic potential of latex products. The studies are focused on the identification of allergenic proteins in latex in order to reduce or eliminate them from finished latex products.

Risk Associated with Metals in Dental Prostheses

Development of tumours near medical implants raises concerns regarding the safety of certain implant materials. Metal prostheses consist mainly of iron in titanium and cobalt alloys**.** Copper is the main component of dental casting alloys and amalgams. All implanted metallic materials corrode and release ions or particulate matter into the surrounding tissue (Esposito et al.,1998). It has been suggested that long-term use of medical implants, made from either metallic or synthetic materials, may cause mutations or be carcinogenic. Better understanding of the processes and interactions between materials and the biological environment is needed for assessing the risk of a variety of metal-containing dental devices. Studies are being conducted in order to evaluate the effects of mercury vapour on gene expression in rat brain.

Mercury constitutes 50% of dental amalgam, and amalgam restorations release small amounts of mercury vapour (elemental mercury). This vapour is absorbed and distributed throughout the body, localizing in the kidney and brain. Dental practitioners who use mercury have elevated urinary mercury levels, and in persons who have amalgam restorations, the number of amalgams is directly proportional to the urinary mercury concentration. Since mercury is a known neurotoxicant, exposure to mercury vapour during pregnancy may interfere with brain development. In contrast to animal studies, reports of human reproductive and developmental effects due to occupational vapour exposure have been inconclusive.

CONCLUSION

The Dental Biomaterials Digital Library will be structured as a unique, consistent data infrastructure including all the compiled information, and it will provide flexibility, extensibility and high search performance. The compiled information will be entered into the database, data structures and Web-based programs for the database. Updating will be created, as well as Web-based program for peer-to-peer knowledge exchange.

The content will be published via the specialized Web site to professionals worldwide, with a flexible multi-layer access system, to provide a quick, easy online access via a single portal to consistent and relevant materials information. Web-based search engine with superior search performance, and multiplicity of search modes will be developed, combined with additional special software modules for material cross-referencing and identification. Multilingual system and content will be deployed, in order to provide access to all the information to as broad audience as possible.

Expected Benefits of Digital Library

The expected results are to:

1. Research, structure, review and harmonize various data and information sources for Dental Biomaterials worldwide.
2. Develop and deploy digital library for dental biomaterials, as the world's most comprehensive information resource for biomaterial properties, applied in dentistry, and other fields.
3. Develop innovative ways and search mechanisms for finding information from the database.Create necessary know-how, human and equipment infrastructure to continue with permanently updating and upgrading the database and the complete system.
4. Form a large network of participants for information and knowledge exchange and leverage.

Market segments will include:

- Dental device manufacturers
- Dentistry practitioners
- Material specialists
- Regulatory bodies (Institutes on Standards and Technology, Institutes of health, etc.)
- Research and scientific community (Universities, Research institutes and centres, University hospitals, Pharmaceutical companies, Biomedical engineering students, etc.).

The obtained results will gain a broader understanding of the work being performed globally by identifying, visiting and assessing work being done at key research centres for Dental Biomaterials. Examining new cross-disciplinary strategies will help to identify "knowledge gaps" in critical areas of material and clinical science and engineering that need to be filled in order for the potential of biomaterials engineering to be realized by end users of Dental Biomaterials Digital Library.

ACKNOWLEDGMENT

This chapter is based in part of the Proposal project for RTD European Commission-VII Framework. The author gratefully thank to the colleagues for their help.

REFERENCES

Agrawal. (1998). Reconstructing the human body using biomaterials. *J Met*, 50(No. 1), 31.

Anderson, J.M. (2001). Biological responses to materials. *Annu Rev Mater Res*, *31*, 81–110.

Biomaterials Properties Database (1996). University of Michigan, Copyright © Quintessence Publishing. http://www.lib.umich.edu/dentlib/Dental_tables/toc.html

Biomaterials Research http://www.biomaterials.group.shef.ac.uk/biomaterials/index.php

Consultative Committee for Space Data Systems. (1999). *Reference model for an Open Archival Information System (OAIS)*, Red Book, Issue 1. CCSDS 650.0-R-1. Washington, D.C.: National Aeronautics and Space Administration. http://ssdoo.gsfc.nasa.gov/nost/isoas/ref_model.html

Craig, R.G., & Powers, J. M.(2002). *Restorative dental materials*, 11th ed.,Ed., Mosby, Inc., An Affiliate of Elsevier Science.

Esposito, M., Hirsch, J-M., Lekholm, U., & Thomsen, P. (1998). Biological factors contributing to failures of osseointegrated oral implants. *Eur J Oral Sci*, *106*(1), 527-52.

FDA dental devices aproval Web site http://www.fda.gov/cdrh/index.html

Galletti.(1998). Artificial organs: Learning to live with risk. *Tech. Rev*, (pp. 34–40).

Gautam, P., & Valiathan, A. (2008). Bio-smart dentistry: Stepping into the future! *Trends Biomater. Artif Organs*, *21*(2), 94-97.

Letic, A., Crudo, V., & Abe, K. (2002).Tooth-germ morphogenesis signals for 3D tissue engineering scaffolds in oral reconstructions. *Tissue Engineering*, *8*(6) Abs. O-118, 1165.

Letic, A., Crudo, V., & Abe, K. (2002a). Microspheres-based tissue engineering product for craniofacial bone reconstruction. *Tissue Engineering, 8*(6) Abs. PP-169, 1234.

Letic-Gavrilovic, A., & Bakos, D. (2005). Membranes and bone substitutes in reconstructive surgery. Nova Science Publishers,Inc. USA. ISBN 1-59454-368-2, In B.M.Caruta, (Ed.), *Polymeric materials: New research*, (pp. 107-139).

Letic-Gavrilovic, A., Fini, M., Giavaresi, G., Giardino, R.,& Abe, K. (2001). Evaluation of composite collagen/hydroxy-apatite implantation and nerve growth factor (NGF) delivery on new bone ingrowth, *Acta Veterinaria*, *51*(5-6), 299-310.

Letic-Gavrilovic, A., Todorovic, L. J., & Abe, K. (2004). Oral tissue engineering of complex tooth structure on biodegradable DLPLG/beta-TCP scaffolds. In N. Hasirci & V, Hasirci (Eds.), *Biomaterials: From molecules to engineered tissue*, (pp. 267-281). Kluwer Academic/Plenum Publishers, USA, .

Letic-Gavrilovic, A., Piattelly, A., & Abe, K. (2000). Nerve growth factor beta (NGF beta) delivery via collagen/hydroxyapatite composite and new bone ingrowth. *J Mat Sci: Mat Med*, *14*, 1-8.

Letic-Gavrilovic, A., Scandurra, R., & Abe, K. (2000). Genetic potential of interfacial guided osteogenesis in implant devices *Dent Mater J*, *19*(2), 99-132.

Lupovici, C., & Masanès, J. (2000). *Metadata for Long Term Preservation*. NEDLIB report series, 2. The Hague: Koninklijke Bibliotheek.. http://www.kb.nl/coop/nedlib/results/D4.2/D4.2.htm

Metadata Engine Project: http://meta-e.uibk.ac.at/

PANDORA project: http://pandora.nla.gov.au/pandora/

Papers from the Preservation (2000) conference and presentations from the Information Infrastructures for Digital Preservation workshop are available on the RLG Web site: http://www.rlg.org/events/pres-2000/

Preservation 2000: an International Conference on the Preservation and Long Term Accessibility of Digital Materials: http://www.ukoln.ac.uk/events/cedars-2000/

Project Prism: http://www.prism.cornell.edu/main.htm

The Global Technology Revolution: Bio/Nano/Materials Trends and Their Synergies with Information Technology by 2015. (2001), RAND.

Third European Report on Science & Technology Indicators (2003) - Towards acknowledge-based economy. European Commission (EC).

University of Glasgow, Humanities Advanced Technology and Information Institute, MPhil in Digital Management and Preservation. http://www.hatii.arts.gla.ac.uk/Courses/DigitalMPhil/

Web Site Profiler: http://www.cs.cornell.edu/Courses/cs501/2000fa/project-folder/profiler.htmli2010: Digital Libraries Initiative http://ec.europa.eu/information_society/activities/digital_libraries/index_en.htm

KEY TERMS

Biocompatibility: Tissue responces to the biomaterials without pathological reactions. Recent advances in the design and composition of bioactive surface layers of implants and to improve osseointegration and durability properties, which are required for long-term implantation in the living body.

Calcium Phosphates (hydroxyapatite-HA): Bioceramics of crystalline structure very similar to the human bone structure. Calcium phosphate ceramics (HA and β-TCP) are considered as the most biocompatible synthetic substance which are known to be used in hard tissue implantation. These biomaterials are not osteogenic per se, in that they do not induce ectopic bone formation. However, they provide a physical matrix suitable for deposition of new bone and display growth-guiding properties causing the bone to extend into otherwise non-occupied spaces.

Dental Biomaterials: Biomaterials or any pharmacologically inert material that is capable of interacting with a living organism. It represents various Dental implants for jaws and facial hard tissues, gums or teeth, to be used with recognized criteria. They are used in the oral cavity either to restore function, comfort, or aesthetics caused by developmental disorders, disease, or trauma. More elective procedures are being requested and performed purely for aesthetic purposes as the incidence of caries has dropped in certain population groups and as patients have become more aware of various restorative or cosmetic options. However, the replacement of diseased tooth structure or missing teeth accounts for the bulk of work in restorative dentistry.

Digital Library: Database of masses of data resulting from experiments and observations in the scientific processes. Digital libraries are readily available as an online service for medical devices manufacturers, medical and dentistry practitioners, material professionals, regulatory bodies, scientific communities, and other interested parties through single- and multi-user licensing. If it proves useful and requested by the market, CD editions could be derived from the main digital library.

Material Properties: Multidimensional interface between chemistry, chemical engineering, material science, mechanics, surface science, bioengineering, biology and medicine.

Periodontal Tissue: Supporting teeth tissues including bone, cementum, periodontal ligament and gums.

Search Engines: Digitalized process of data mining based on simple, flexible, structured or unstructured performances of artificial intelligence. For Dental Biomaterials Library a hybrid Web-based search engine will be defined atop of the central database in this step, with the objective to achieve robustness, superior search performance, and multiplicity of search modes. Classic search strategies will be combined with Google search engine and special algorithms based on artificial intelligence and fuzzy search for material identification and cross-referencing.

Smart Biomaterials: Refers to a class of materials that are highly responsive and have the inherent capability to sense and react according to changes in the environment.

Titanium (Ti): Ti is a transition metal with Atomic Number 22, Atomic mass 47.88. Since it is strong and resists acids it is used in many alloys. TiO_2, white pigment that covers surfaces very well, is used in paint, rubber, paper and many others industries. Ti is used in implantology, because its chemical, physical and biological properties provide very good biocompatibility.

Chapter XVI
Rapid Prototyping and Dental Applications

Petros Koidis
Aristotle University of Thessaloniki, Greece

Marianthi Manda
Aristotle University of Thessaloniki, Greece

ABSTRACT

The present chapter deals with the introduction and implementation of rapid prototyping technologies in medical and dental field. Its purpose is to overview the advantages and limitations derived, to discuss the current status and to present the future directions, especially in dental sector. Furthermore, a flowchart is outlined describing the procedure from the patient to the final 3-D object, presenting the possible alternatives in the process. Finally, an example is presented, decribing the process of the construction of high accurate surgical guided templates in dental implantology, through rapid prototyping.

INTRODUCTION

Computational modeling represents the simulation of real-world scenarios in a virtual environment throught the transformation of physical structures into numerical models. It has revolutionized the engineering and science over the last 30 years, by integrating itself into many aspects of the modern life from entertainment through medicine. The framework of operating in an in-silico field allows the practitioner to handle and analyze numerical models of great complexity and under convoluted conditions, with relative ease and mainly safety.

The last years, the computer modeling is experiencing increasing application and extending deeper in the fields of biology and medicine, across a vast range of scale, from the individual molecules and cells of the micro-world, through the varieties of tissue and interstitial interfaces, to complete organs, organ systems and body parts of the macro-world (Robb RA, 1999).

The framework of bio-tissue informatics includes a variety of scientific and engineering disciplines, according which the computational simulation of internal and external configuration of biological structures is conducted, often providing information about biological, biophysical and biochemical properties. It is a matter of multidisciplinary procedure, expressed as bio- or biomimetic modeling. Formerly, biomodeling was used to express a generic term, defining the process during which a biological structure could be transformed into a solid substance (D' Urso, 1998). Though, currently, after the advances and the vast implementation of the computed technology innovations, the definition of biomodeling can be extented in order to include the fidel replication of a biological structure in terms of geometry or morphology both in a computer-based or a solid physical form. Based on the latter definition of biomodeling, the resulted output-forms (biomodels) can be classified into: a) computed-based and b) physical biomodels. The formers can be further divided into virtual and computational biomodels. Physical models constitute the physical production in an actual or scaled size of a computer-based, virtual, usually, models by engineering technologies (Lohfeld S, 2005).

Each kind of computer-based model constitutes an *object system* (such an anatomical organ), which may undergoes specific object –operations, the results of which provide information of qualitative and / or quantitative nature. These operations are highly independed and may be distinguished in: a) visualization, b) manipulation and, finally, c) analysis. More specific, visualization serves the viewing and comprehending the structures and the dynamics of the object system. Manipulation aims at the altering of the object system either by changing the relationship among the consisted objects or by altering the objects themselves. On the other hand, analysis aims at the extraction of quantitative measures of certain parameters, which are related to the functionality of the object system (Sun W, Lecturer Topic Sp.AYO1O2). Virtual biomodels are directed to suit the purpose of visualization and manipulation, while computational models are suited for the purpose of the analysis and, specifically, of the biomechanical analysis, exhibiting stress and strain distributions (Udupa JK, 1999).

The increasing potentiality of the computed-aided technology, through its provided operations, has been and it is expected further to be the vehicle to the accomplishment of several clinical objectives, both in medical and dental field. Specifically, its major so far contribution has been scored for the tissue engineering field, where new disciplines have been raised, by developing the computer-aided tissue engineering (CATE). Tissue engineering had been developed as an attempt to resolve the shortage in tissue and organs for translaplantation therapy, by developing tools for patient-specific biological substitutes, in order to restore, mentain and improve tissue function. Though, today, CATE has branch out into four major categorizes, which are the (a) computer-aided tissue anatomical modeling, (b) computer-aided tissue classification, (c) computer-aided tissue implantation and (d) computer-assisted surgery (Sun W, 2002).

Explicitly, computer-aided anatomic modeling constitutes the realization in form of 3d-representation of tissue anatomy, originated form non-invasive data acquisition, usually computed tomography (CT) and magnetic resonance image (MRI). The biomodels derived are able to be submitted, through certain format files, in rapid prototyping (reverse engineering), in computed-aided based environment and biomechanical analysis. A number of proceedings control the development of the anatomic model according to its final destination (Sun W, 2005).

As far as concern the computer-aided tissue classification, this is mainly made for the hard and soft tissues, which is used for the deformable modeling in surgical simulation. This is occurred via virtual reality deformable models (single animation of tissue deformation) or mathematical deformable models (simulation of the exact physical behavior) (Terzopoulos D, 1990, Chen DT, 1992). Another advantage of tissue classification is the identification of trauma and its contribution in tumor diagnosis.

Computer-aided tissue implantation includes scaffold guided tissue engineering or else named computer-aided system for tissue scaffolds (CASTS). This technique eliminates the reliance of the results on users' skills, which is prerequisite in the convectional techniques. Though, there is criticism about the model validation and, especially, the limitation about the internal architecture built (Leong KF, 2002). Furthermore, the computer-aided tissue implantation involves the tissue replacement with artificial organs (total knee and hip replacement as well as total implantable artificial heart).

The application of computer-aided technologies in surgical procedures covers the preoperative diagnosis and the planning of surgical procedures. It also contributes in the training of both patient and less experienced surgeons as well as in the communication between the operative team.

The applications of computer-aided biomodeling can be further classified into those whose functions are limited inside the computational environment and to those that they use the computational environment as the mean in order to design the original desired parameters of the products that are going to become solid physical structures, suited for biological substitutes. The key for the accomplishment of this goal are several manufacturing techniques, based on which the information derived from the in-silico environment may become an accurate reality of the computational prototype. These techniques are included in the domain of reverse engineering and they can be classified into two major divisions: (a) the substractive and (b) the additive ones. The substractive ones include the—earlier—numerically controlled machining, according which the physical model is fabricated through beeing carved away from a solid block of the desired material (Petzold R, 1999). The additive ones include the—newer—rapid prototyping, usually referred as solid freeform fabrication or sometimes as rapid manufacturing, layered manufacturing, additive fabrication and, colloquially, art-to-part technology (Pham DT, 1998). Through this process, physical models are produced in a gradual, controlled way, by selectively solidifying one horizontal layer (each layer represents the shape of the cross-section of the model at specific model) at a time (layer-by-layer) with stepwise submergence along the vertical axis, until the part is completed. The limitations of the former are referred to the machine restriction, the material employed, the inability of creation models with complex internal morphology, the lower accuracy of the final product to the length of the process as well as the cost (Klein HM, 1992).

RAPID PROTOTYPING

Rapid prototyping technologies were firstly introduced in the early 1980s, in the mechanical engineering field, in order to evaluate the ease of assembly and manufacture of designed products ahead of actual production. Ever since, pervading in, almost, every scientific sector, more than twenty rapid prototyping systems have been developed and commercialized, with the advent of stereolithography in 1986. Though, not untill 1990s, these technologies started to officiate in the medical and biomedical field, establishing the medical rapid prototyping as the tool of human anatomy's recreation (Webb PA, 2000). So, medical rapid prototyping is used to describe the process of using radiant energy to capture morphological data on a biological structure and the procesing of such data on a computer, to generate the code required to manufacture the structure, by a rapid prototyping apparatus.

Medical Applications

Anatomical and Physical Modeling in Treatment Planning

When considering reconstructive surgery, it is often difficult to ascertain the exact nature of affected internal anatomy. Although advances in computed tomography (CT) and magnetic resonance imaging (MRI) have enabled the generation of 3D reconstructions of internal anatomy, they are often only available as fixed 2D images. These may obscure important details or prove ambiguous depending upon the angle of view (Bibb 2000).

Rapid prototyping is impacting medicine in several important ways (Giannatsis 2007). Its beneficial utility has been reported through clinical prospective studies and case reports, facilitating the explanation, planning and execution of the surgical phase by the practitioner in certain medical specialities such as oral and cranio-maxillo-facial surgery, neurosurgery, orthopeadics and cerebrovascular surgery (da Rosa 2004). Syndroms (Crouzon's disease, Aperts's syndrome), tumors (meningioma, C2 osteoblastoma), congenital and development abnormalities (craniosynosteosis, encephalocoeles, facial clefts, hypertelorism, hemifacial microsomia, congenital kyphoscoliosis, congenital idiopathic juvenil thoracolumbar scoliosis), post-traumatic deformities are some of the plethora of pathological cases, where biomodeling and rapid prototyping were used as part of a sucessfull treatment (Izatt 2007). However, the use of rapid prototyping in the medical treatment was more frequent for the dentofacial anomalies (28.9%), followed by the congenital diseases (20%), neoplasms (19.2%) and the trauma (15%) (Winder 2005).

The incorporation of rapid prototyping in the treatment planning seems to improve the surgical planning (especially the complex ones), by enhancing the diagnostic quality, enabling the surgical phase to be simulated prior to the actual surgery and by setting a visualized end-point of the optimized surgical outcome (Petzold 1999, Singare 2008). During this conditional surgery process, the surgeon has the opportunity to directly estimate, study, measure and manipulate the region of interest and the surrounding tissues, to design and prefabricate custom-made implants, control their adaptation within the deformity and analyze their biomechanical behavior, so as to investigate the tissue mechanics in cases that ethics do not allow the in vivo experiments (Heckmann 2001, Adam 2002). Though, the greater advantage according to most of the surgeons is the ability of preparation of templates for intra-operatively guiding and positioning of screws, plates and implants during surgery, for executing other surgical techniques (resections and osteotomies) and for shaping bone grafts (D' Urso 1998, Brown 2002, Lal 2006, Milovanovic 2007). Finally, rapid prototyping models may be great communication tools for teaching and explaining purposes either between surgeon and patient or among the members of surgical team (Milovanovic 2007). Consequently, rapid prototyping constitutes an important adjunct for intra-operative navigation which results in less extensive instrumentation, increasing surgical confidence, securing safer intra-operative procedure with lower complications and risks, better fitting of the artificial body parts, saving time and cost and, finally, ensuring more accurate predictability of the final surgical outcomes (Erickson 1999, D' Urso 2000, Muller 2003). It is amazing the fact of reported surgery's cancellation after the diagnosis through physical model that the abnormality would not further developed. The diagnosis was confirmed with the followed good clinical outcome.

Rating the impact of rapid prototyping in the surgical procedures as highly beneficial, in a post-operative survey conducted by the D'Urso team, it has been concluded that the rapid prototyping combined with the conventional image modalities not only improves the vast majority of theurapeutic results, but, for some clinical cases, it was the prerequisite in order for the desired results to be achieved (Izatt 2007). That is the reason why rapid prototyping applications in certain clinical cases are increasing in both scope and frequency.

Anatomical and Physical Modeling in Reconstructive and Regenerative Medicine

Beyond the diagnostic and training / educating performance that the physical models have, rapid prototyping play a more assertive role in the treatment arena of reconstructive / plastic and regenerative medicine, through the development of computer-aided manufacturing of prosthetic devices (implants) and scaffolds, respectively. (Bill 2004, Hutmacher 2007).

A rough outline of the prosthetic materials used in reconstructive surgery includes the autologous or homologous bone grafts, allografts and bone cements mainly based on poly (methyl methacrylate) (PMMA), ceramic and metals, either alone or in combination (Vail 1999). Though, ceramics and metals in a customized form have the edge on the other materials, since their use is not restricted from the donor site morbidity, the material supply, the stress-shielding effect and the pathogen transfer (Vail 1999). Their major advantage is the potentiality of customization either during the surgical phase or prior to.

The pre-fabrication of individual implants derived from patient-specific computational data source is often preferred over the customization techniques on actual surgical site or prefabricated standard sized replacement parts selected from a range provided by manufacturers based on anthropomorphic data. The prosthetic treatment modality of the osseous deficiencies through intra-operatively (direct) modeling of the implanted devices may compromise the final surgical outcome as far as conecrn the easthetics and the functionality. The restriction of the selected materials and the implant shaping may result in stress experienced by the patient (Wurm 2004). Moreover, the use of alloplastic decreases the long-term maintenance, combined with a prolonged surgical procedure time and increased materials for intra-operative modeling may result in an inflammatory tissue response (Vale 1997).

Furthermore, the prefabricated standard implants constitute “ideal” objects that work satisfactorily in a range of sizes and for some types of procedures. Though, there are always patients outside the standard range, between sizes, or with special requirements caused by diseases or genetics. Craniofacial surgeons do not routinely recommend prefabricated implants to their patients with large cranial defects. For these cases, a custom– made prosthesis, which will precisely “fit, fill and function” in the deficient anatomy is required (Adam 2002, Dean 2003).

The challenge in the indirect fabrication of individual models is the extraction or creation of accurate contours from the virtual 3d-reconstructed patient’s anatomy, based on which the implant modeling will be directed. The method of designing and constructing implants through rapid prototyping is based on two philisophies: a) the morror-image production and b) the CAD-based contour generation (Hieu 2003).

During the mirror-image production, the healthy side of patient’s anatomy in form of virtual model is required in order to be mirrored at the contra-lateral side, where the osseous deformity exists. A substracting and merging procedure is followed based on sophisticated algorithms, according which the mirrored surface will be matched with the contours at the defect edge. The method is quite simple and predictable, except from the cases of excisting asymmetrical anatomies, which must be a priori diagnosed, so as to be included in the procedure either through practitioner’s intervation or by proceeding in a CAD environment (Bruant 1988, Connell 1999, Hieu 2002, Metzger 2007).

The CAD-based contour generation is based on the transformation of the patient’s related imaging data in a CAD system, where the excisted contours are used for defining the borders of individual implant's shape, so as the implant's edges closely fit the defect edges. The desining of the implant is accomplished by using the non-uniform rational b-splines and the freeform surfaces are generated by extrapolation of the surface contours of the defects, surrounding bone (Winder 2006) (Figure 1).

Despite the wide implementation of rapid prototyping in reconstructive medicine, its applicability is not empty of errors, while several studies have attempted to investigate the accuracy of rapid prototyping implants. Ranking the validation of the computer-aided generated implants, it seems that they are clinically acceptable. Choi (2000) presenting an analysis study of the errors in medical physical models, resulted that the deviation compared to the original surface approximated 0.62+/- 0.35mm (Choi, 2000). Though, other studies present higher or lower deviations within a range of 0-2mm (Nizam 2006; Winder 2006). This may give a prospect for greatly improved health, while the conquest of mortality is visible on a distant horizon.

Despite the admitted effect of computer-aided implantology in the reconstructive medicine, the ultimate goal of the prosthetic treatment is tissue regeneration. In order to overcome the limitations (immunological intolerance) of biomaterial implantation and organ transplantation, scaffold-based tissue engineering was developed, where *in vivo* tissue regeneration is promoted through guided wound healing as part of normal tissue repair process; and /or bioartificial organs in vitro

Figure 1. A helical 3D CT data set of the patient's skull (a) is acquired. A wax template is used for fabrication of the CFRP implant (b), which exactly fits into the defect of the biomodel (c) as well as into the actual patient's defect during surgery (d). Wurm G, Tomancok B, Holl K, Trenkler J. Surg Neurol : 2004;62:510–21

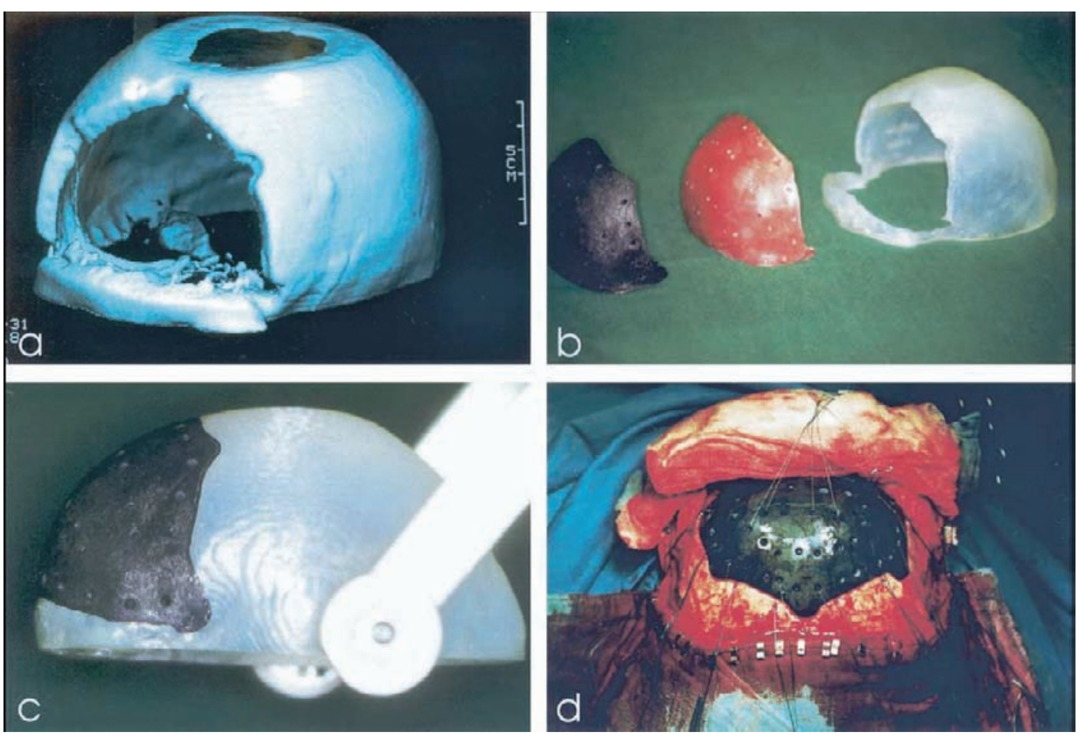

are created (Langer 1993; Sun_2004d; Vacanti, 2006). Solid freeform fabrication systems have the potential to optimise these scaffolds and achieve not only the desired level of geometrical complexity into the scaffold, but also may attain reproducability, reliability, and high customization (Stevens 2008).

The role of computer-aided systems for tissue scaffolds is: (a) to delimit the macro-environment in shape and in volume inside which the tissue will be regenerated, (b) to perform the optimum functionality as long as the healing process is taking place and (c) to create the biochemical and genetic substratum in order for the tissue regeneration to be enhanced and accelerated (Hollister 2002). In order for these goals to be achieved, certain criteria must be fullfiled, even if it is admitted that: (a) the combination of some of those requirements is competing (Hollister 2005), (b) the "ideal" term for scaffolds is subjective, depending on the tissuue to be repaired (Hutmcher 2004), (c) there is no much of experimental data about which requirement is most effective in the healing process (Hollister 2002). The aforementioned make the construction of an ideal *per se* scaffold difficult and render their further optimization and testing imperative (Hutcmaher 2000, 2004). So, the minimum set of criteria required, so as the basic principles to be accomplished are:(a) the modulation of the morphological properties (pore architecture, size and interconnectivity) which facilitate the tissue integration, the vasculirization and the diakinesis of biological components, nutrients and metabolites, (b) the selection of biocompatible materials which determine the equilibrum between the tissue regeneration and scaffold degradation, through controlled biodegradability or biosorbability patterns, (c) the selection of surface chemistry to favour cellular attachment, differentiation, proliferation and *ne novo* production of extra-cellular matrix and, finally, (d) the determination of the mechanical performance so as the mechanical changes occured during the healing phase to be compensated in favour of tissue regeneration (Hutmacher, 2000).

So, scaffolds' computational designing and simulating based on the above principles constitutes a critical issue, coupled with their clinical performance and reliability. The framework of scaffolds' computational designing and simulation prior to rapid prototyping fabrication comprises: (a) the representation of scaffold topology, (b) the attribution of initial scaffold characteristics and (c) the definition of time-dependent scaffold performance (Hollister, 2008). (Figure 2)

The representation of scaffolds topology may be developed either in a vector-based modeling environment, using computer- aided design techniques or may be rely on specific-patient data obtained from image modalities, using image-based design techniques (IBD) (Sun 2004e; Hollister, 2004). The construction of scafforlds and the attribution of their inital characteristics is a combinative two-phase solid-void design problem which must be coupled with the identification of their maximum effective mass transport (permeability and diffusion), electrical (conductivity) and mechanical properties (steffiness), according to the objective functions (Guest, 2006). The difficulty derived is the competing behaviour of some properties towards the morphological characteristics of the scaffolds and the limitation of the methods used in the optimization of a single property (Sigmund, 1997). The problem has been faced through homogenization theory, which projects the microstructural behaviour of the material to the macroscopic properties and the relative new topology optimization theory which investigates the optimal distribution material phases in a given design domain (Hollister SJ, 2005; Lin 2004a, 2004b).

Finally, one of the most significant as well as dufficult issues in scaffold fabrication process is the ability for the tissue regeneration and scaffold degradation to be simulated. Both are dynamic and time-dependend biological procedures, which

Figure 2. (a) Part fabricated from Solidscape ModelMaker 2, (b) mold made by dewaxing fabricated part, (c) final sintered HA scaffold made by casting. Sintering causes a 27% reduction in linear dimension that is accounted for by enlarging the mold design by 27%. Hollister SJ, Maddoxa RJ, Taboas JM. Biomaterials: 23 (2002) 4095–4103

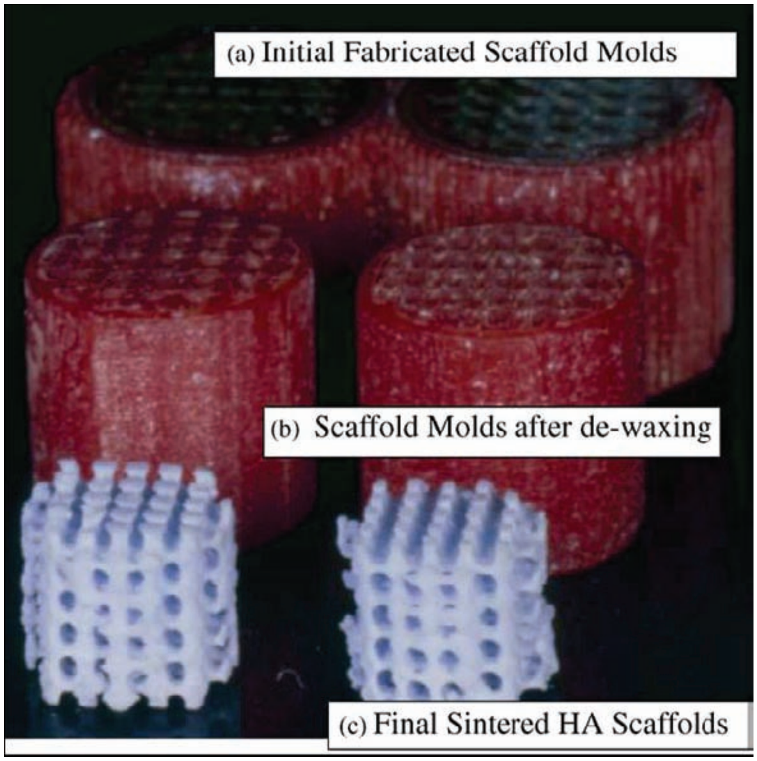

are controlled by the interaction of mechanical, chemical, cellular and extracellular factors, rendering the predictability of the clinical scaffolds performance unforeseen. In the literature, there are several mathematical models, trying to simulate the bilogical chain in tissue regeneration, though the optimization and predictability of the process demands further investigation (Hollister, 2008).

There is a vast availability of conventional fabrication methods (solvent-casting, gas foaming, melt moulding, freeze drying etc) for the construction os scaffolds (Sachlos, 2003; Stevens, 2008). Though, the long-term use has revealed several disadvantages related with the inadequate control of scaffolds' morphological features (Yeong, 2004), the lack of consistency and reproducability (Tan 2005a, 2005b), the inapropriate microenvironment due to the production and insufficeint removal of undesired metabolites (Kohn, 2002) and, finally, with the limited tissue growth due to the diffusion of constraints in the foam-based structures (Freed, 1998). Rapid protototyping technology provide a solution to this problem, while and many adoptations have beem made to successfully overcome other dreawbacks that have been developed related with the fabrication conditions compromising the biomechanical peformance of scaffold such as the difficulty in support powder removal, the presence of toxic organic binders and the high temperature processing. The alternative of indirect rapid prototyping through the creation of sicrifacial moulds to be invested may combine the safety of process issue with the maintainance of the scaffolds' optimized biomechanical cues (Sachlos, 2003)

The success of tissue engineering is absolutely related to the optimising the scaffold and solid freeform fabrication has the potential to do so.

Rapid Prototyping in Dentistry

Dental Applications

CAD/CAM technologies have been successfully introduced in the field of dentistry over a number of years. In 1971, Francois Duret introduced the CAD/CAM process to restorative dentistry, while, in 1983, he produced the first CAD/CAM dental restoration (Duret 1988). Dental applications of CAD/CAM technology in dentistry remained restricted to finished ceramic restorations, such as inlays and crowns, for nearly two decades. Beginning in the 1990s, its applicability expanded into restorative aspects of dentistry. Though, these techniques were based on milling, which is a substractive way of fabrication of solid block, followed by the aforementioned shortcomings. The need of facing the geometrical complexity and the expense, that milling could not, let rapid prototyping to be introduced into dental field. The latter has the potential to become the next generation in fabrication methods in dentustry, even if now its application is not an ordinairy feature in the clinical routine (Liu, 2006).

Beyond its known contribution related with the diagnosis, education and surgical planning, the main dental areas that rapid prototyping have been or can be implemented are: (a) restorative dentistry, (b) dental implantology, (c) orthodontics (Chan, 2003).

Restorative Dentistry

The emergence of the rapid prototyping technology has innovated the clinical and laboratory procedures followed, during the fabrication of dental prostheses, by eliminating or abolishing some intermediate stages and independing the quality of the outcomes from the practitioners' skills (Harris, 2002). Rapid prototyping –directly or not- expands in both fixed and removable prosthodontics (Bibb, 2006; Strub, 2006; Williams, 2006; Sun, 2007). Latest years, its major impact is on investment casting of the metal framework (copings, crowns, fixed partial dentures, removable partial dentures or other castable prosthetic features) (Wu, 2001; Williams, 2004, 2006). The wax patterns of the metal framework are built from CAD models which are created based on the laser digitized geometrical data. With the "computer-printed" wax patterns, the metal prostheses can be cast following the rest of the investment casting procedure (Eggbeer, 2005). This indicates the potential of the new method, which is capable of replacing the traditional "impression taking and waxing" procedure. Furthermore, if the thermal expansion of the casting mold (investment) is known, the rapid prototyping patterns can be designed to the equired size by scaling the CAD model thereby offsetting the casting shrinkage. So, through iterative improvement of the runner and gating system and the casting parameters by means of numerical simulations, the risk of the shrinkage and gas pores is avoided or minimized (Williams, 2004).

In addition, CAD/CAM / rapid prototyping gains increasingly importance in prosthetic dentistry using nonmetallic aesthetic materials. Several follow-up studies have been conducted, examining the performance of ceramic crowns, inlays and onlays, constructed by these technologies. The main problem derived from theses constructions are the inacurracies resulting from scanning process, software design, fabrication process and shrinkage effects, related to the poor restoration fit. In vitro studies have revealed mean marginal gaps of 64-83μm, while few metric data on clinical fit of all-ceramic single-tooth restorations are available. Within the limits of the reported studies, the results suggest that the accuracy of CAD / CAM generated all-ceramic fixed partial dentures is satisfactory for clinical use. (Reich, 2005). In a ten-year prospective clinical study CAD/CAM inlays and onlays, the authors reported very high patient satisfaction after a decade of clinical service. They concluded that CAD/CAM restorations made of feldspathic ceramic appear to be acceptable in private practice (Otto 2002). In a seventeen-year study of case series, the same researchal group concluded that that the survival propability of CAD / CAM inlays and onlays is 88.7%, which is a very respectable clinical outcome (Otto, 2008)

Implant Dentistry

Nowdays, the treatment modality of dental implants has proven to be a predictable prosthetic option, with minimum risks and complications when certain prerequisites are taken into consideration into the treatment planning. One of the major factors contributing in treatment's reliability is the proper implant placement, impacting in aesthetics (Kopp, 2003). and functionality (Rangert, 1995). Untill recently, implant placement was secured by the conventional fabrication of surgical guiding templates, though not providing the desired accuracy. This limitation is overcomed through interactive computer and rapid prototyping technologies, through which precise planning of dental implant placement and construction of accurate guide splints is performed (Azari, 2008; Jabero, 2006).

Inside a 3-D computentional environment and based on patient-specific data derived form computerized tomography combined with the ultimate outline of prosthetic restoration and the patient's anatomy, the desired implants may be selected in terms of lenght, diameter and compagny; and placed in terms of thesis or buccolingual / mesiodistal tilting in patients' jaw, by translating or changing the angulation of implants. Furthermore, selection of abutment in different angulations and abutment collars are available in a database of commercial prosthetic features, in order to compensate the derived problems and otpimize the aeshetic and biomechanical result. The precision of this technology further allows a final prosthesis to be fabricated before implant placement that can then be delivered at the completion of the implantation procedure (Lal, 2004; Parel, 2004). Precision of CAD/RP technologies ahs been evaluated preclinically and clinically, suggestin that the rapid prototyping tampletes have the potential to improve accuracy (Sarment 2003; Do Giacomo, 2005). Finally, RP techniques in dental implantology result in minimization of intraoperative radiographs, the simplification of drilling sequence result in a reduction of chairtime and osseous exposure, which may decrease overall implant morbidity and postoperative complications (Wong, 2007).

Another contribution of rapid prototyping in dental implantology is the ability to design customized implants and fixtures as well as the pontentiality to create biologically active implants. Using rapid prototyping to make patient-specific dental implants is a potential alternative to standard implants, for patients who may be outside the standard range or demand special requirements due to diseases or genetics. The manufacture of biologically active implants is a new area for rapid prototyping application. Many investigations have been performed recently, but it will take years for this technique to be widely employed in practise (Liu, 2006).

Finally, rapid prototyping has been used in clinical cases as part of the protocol for tooth autotransplantation, in cases of treatment of missing teeth or replacement of avulsed or traumatized teeth, when there is a donor tooth available. Specifically, rapid prototyping was used in order to create physical models of the recipient's jaw and donors tooth, in order for the donor's tooth adaptability to be examined with the highest desired accuracy (Lee, 2001).

Orthodontics

Another field of dentistry which has been revolutionized by CAD/RP technologies is orthodontics. The computerized patients' data acquisition through the 3D-representation of patients' anatomy constitutes a complementary process to the traditional one and in combination with the 2-D imaging (cephalometric radiography) and the 3-D diagnostic casts, improves the traditional way of orthodontic diagnosis, treatment planning and treatment's efficiency (Müller-Hartwich, 2007). While conventional model analysis is performed manually with a number of limitations in terms of accuracy and measuring ability and despite the efforts (photography, holographic technology, 3-D co-ordinate measuring technique) made to resolve this problem (Cha, 2007), only CAD/RP process manage to provide high accuracy in the multifactorial process of the treatment's outcome, by controlling and eliminating errors related with factors such as the proper bracket placement, wire bending, wire selection, variation in adhesive thickness, manufacturer's tolerance, operator's acuity and fatigue, not to mention misdiagnosis and malpractise (Mah, 2001).

Thanks to the aforementioned technological advances of CAD/RP techniques, new systems have been developed in the manufacturing area of bracket-archwire system, by replacing mass-produced prefabricated appliances with fully customized brackets and archwires (Wiechmann, 2003). (Figure 3)

More specific, undesirable tooth movement because of bracket placement errors and arch-wire errors may be significantly reduced, thereby improving precision and predictability of tooth movement. Especially in lingual ortodontics, three of the most frequently cited drawbacks of lingual appiances have been solved such as the difficult bonding and rebonding procedures, the more frequent accidental debonding, the problematic finishing processes and the patient discomfort (Mujagic, 2005). Furthermore, new treatment

Figure 3. (a) In rapid prototyping, brackets are first produced in wax, applied in 0.02 mm layers. Red support wax required for 3D production is removed thermally. (b) Wax lingual brackets before casting. (c) Gold lingual brackets after casting. Wiechmann (d), Rummel al V, Thalheim A, Simon JS, Wiechmann L. Am J Orthod Dentofacial Orthop 2003;124:593-9.

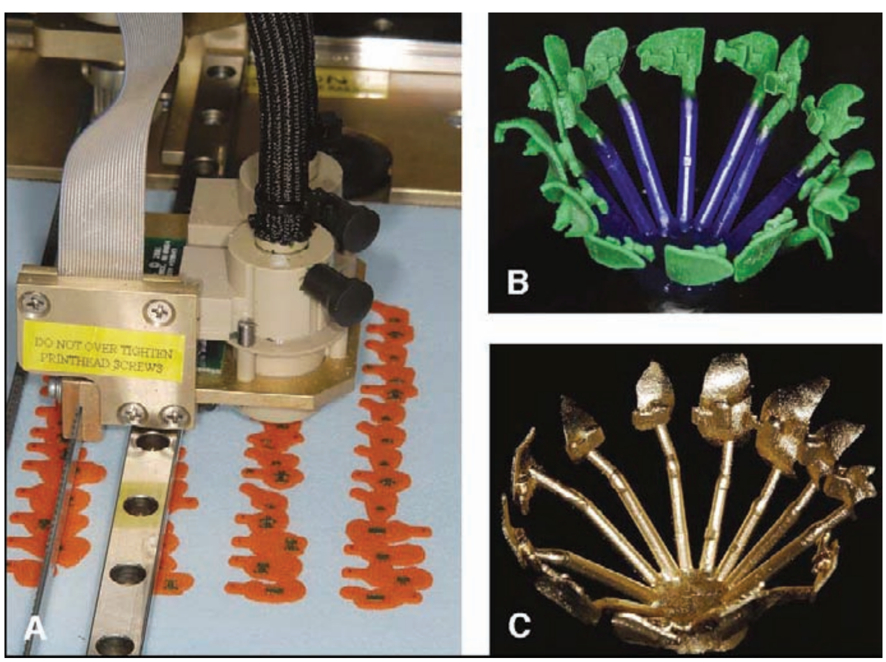

modalitites that utilize computer-based virtual orthodontic models have been developed in order to produce series of clear removable aesthetic appliance.

So, rapid prototyping is used to design orthodontic devices with the specific patient's tooth alignment. The specific tooth aligment characteristics for an individual are included in the prototype, allowing for development of a biomechanically correct geometry that improves the fit, comfort and stability. Through this process, the number of times that orthodontics have to refitted is decreased, thus cutting down the overall cost (Faber, 2006).

Models Fabrication Procedure

The basic process, according which the physical anatomical model or device is fabricated, is describe through the following steps (Chua, 2003) (Figures 3a and b):

- CT / MRI imaging
- 3-D object reconstruction through image processing
- Data conversion into STL format and transmission
- Model slicing into cross-sectional layers
- Model fabrication in a stratificated way
- Postprocessing (Clean an finish of the model)

Non-Invasive Data Acquisition

Three-dimensional (3D) imaging was developed to provide both qualitative and quantitative information about an object or object system, derived from non-invasive imaging data acquisition, like obtained with multiple image modalities including digital radiography, magnetic resonance, positron emission tomography, single photon emission, computed tomography and ultrasonography, each with its own advantages and limitations. Of course the primary modalities that are made use of in different applications are computed tomography (CT) and magnetic resonance imaging (MRI). These imaging techniques comprise internal and external data of the patient's anatomy. Though, in dental field, in most of the cases of the routine clinical practice, only the external data of the patient's anatomy are needed. For thoses cases, the external data capturing and acquisition is done through laser surface digitizing. Acquired images can be used to develop a virtual model of the anatomical region of interest (ROI).

Computed Tomography

Computed tomography (CT) is accomplished by acquiring series of individual images representing cross-sections through the body, avoiding their superimposition. The principles of CT are based on the scanning and the transmittion of a beam of rays through the patient's body and their partial absorbtion from tissues with different density. The X-ray beam is ejected from a rotating X-ray tube and passes through the tissues in different projective directions. The amount of the not absorbed radiation or else the degree of X-ray attenuation, depended on the tissue composition and density, is detected from specific array detectors, located in a contralateral position relatively to the X-ray source (Spoor 2000). The measurement of the degree of X-ray attenuation for every tissue voxel is performed using an arbitrary grey scale, graded with 2000 (+1000, 0 –1000) numerical units, known as Hounsfield units. The value of +1000 represents the higher density in while color for the bones and the value of –1000 represents the lower density in black colour for the air.

CT possess no magnification errors caused by geometric distortions, though, despite the fact of the high degree of accuracy within the individual slices, it has relatively low between-slice accuracy even with relatively narrow collimation and no interslice gaps. The number of the detectors used as well as the elements they consist of are related to the in-plane resolution, while the depth reso-

Figure 4a. Roadmap of rapid prototyping

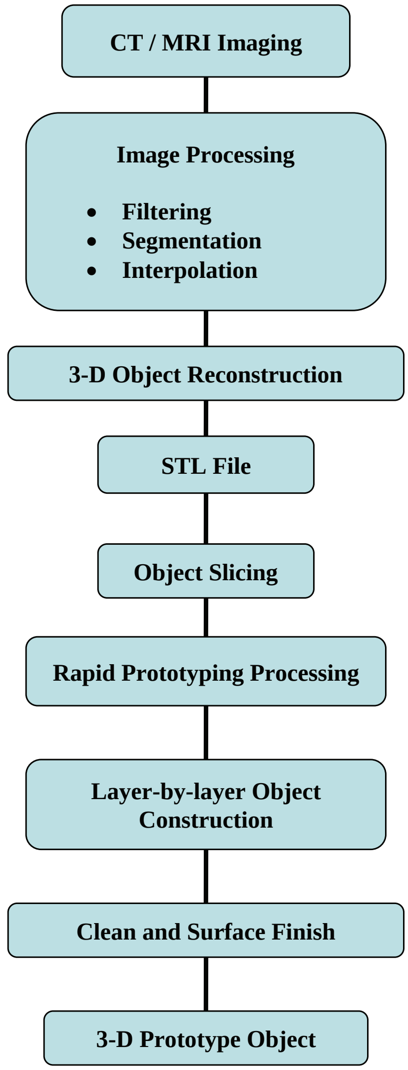

lution is dependent on the aperure of the X-ray source and the scanning period. The diagnostic value of the image obtained is characterized by factors such as the spatial resolution, uniformity, artifacts, signal- to- noise ratio, contrast and artifacts (Natali).

Magnetic Resonance Imaging (MRI)

MRI images can be obtained based on different tissue characteristics by varying the number and sequence of pulsed radio frequency fields in order to take advantage of magnetic relaxation properties of the tissues. The MRI signal is calculated for each pixel and associated voxel in a computer monitor using a grey scale with black representing the lowest and white the highest intensity. This signal or else called echo constitutes the emitted energy equivalent to the difference between the two energy states, picked up by a coil. Images can be reconstructed using information from two different relaxation process, known as T1

Figure 4b. The general process of medical RP model production.Choi J-Y, Choi J-H, Kim N-K, Kim Y, Lee J-K, Kim M-K, Lee J-H, Kim M-JInt. J. Oral Maxillofac Surg 2002; 31: 23–32.

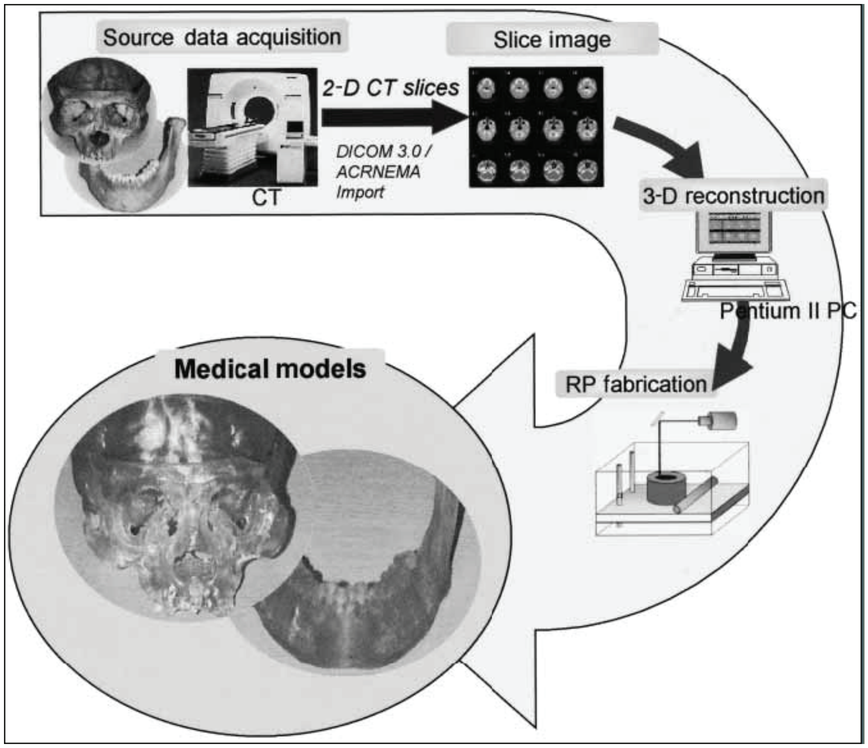

and T2. In T1-weighted images, fat gives a more intense signal than water and thus appears brigher, while T2-weighted images show the reverse pattern. Since the concentration of fat and water varies between different tissues, it is relatively straightforward to differentiate, by their echos, tissues with a sufficient number of protons (Stark, 2000; Gray, 2003).

CT and MRI are complementary techniques, whereas CT provides excellent visualisation of hard-tissues and MRI is the method of choise to investigate the soft-tissue systems. Consequently, MRI differs from CT in at least three points: (a) MRI measures the density of a specific nucleus, (b) the MRI measurement is volumetric and (c) MRI provides better images for soft tissues.

Integration of information between CT and MRI images will take it possible to develop more complex models, discriminating between hard and soft tissues.

Data and Image Processing

The patient's data captured from the aforementioned techniques are introduced as an input set of scenes into a computational inveronment, where image analysis and processing is applied, resulting in an output set of objects or modified scenes, with the wanted information defined and enhanced, whilst the unwanted information suppressed and/or extracted (Udupa, 1999). Considering image processing, a set of operations have been established in order to serve the most accurate anatomical 3d-representation, whom an accurate physical model or a tailored medical device will follow.

The sequence of the imaging operations begins with the delimitation of the volume (or region) of interest and the indentification of the range of the intensity of interest. During this procedure, in the given set of data scenes, the image space is reduced in dimensions and minimized to only the data of study, while every other irrelevant subject is precluded. This procedure results in output data scenes including only the information from which the desired anatomical model will derived and, consequently, the file of the stored data is significantly reduced (Schenone, 1999).

After obtaining the minimized data and the region of interest, improvement of image quality is performed, by supressing or eliminating the noise and other artifacts, from which every image modality suffers. This procedure is accomplished through filtering and smoothing techniques, by using different filters, the most common of which are the Gaussian and the median ones. Though, the sensitivity of those filters is not always ideal and suppression of desired data is often occured. In these cases, the minimization of negative effects is achieved by the integration of the personal knowledge to the algorithms activity.

Proceeding on the actual indentification and isolation of the tissues of interest from their backround, the phase of segmentation is performed (Fenster, 2005). Segmentation is an intermediate thought crucial stage for image analysis and significant precondition for every task supported (measurement, visualisation, registration, reconstruction and content-basd search) (Olabarriara, 2001). Segmentation is the interpretation of parts of image as objects and constitutes the process of partitioning images into constituent subregions through the extraction of boundary elements belonging to the same structure and their integration into a coherent and consistent model of the structure (McInerney, 1996). It is conducted in two phases, the recognition phase followed by the delineation one. In the recognition phase, a broad distinguishing of the desired anatomical structures is performed, while in the delineation phase, a precise anatomical registration is obtained, including the spatial extent and composition (Udupa, 2006).

The segmentation techniques are divided primarily in the classification-, region- and contour-based ones, each with its own advantages and limitations (Liew, 2006). In classification-based segmentation, voxels are classified and labeled as belonging to a particular tissue class according to a certain criterion. The simplest technique is based on thresholding (Kundu, 1990). Thresholding algorithm attempts to determine a threshold value which separates the desired classes (Suzuki, 1991).

Region-based methods are based on the image subdivision into regions, according to homogenious characteristics such as intensity or texture. Each of them may be classified as either inside or outside the target structure, and then break up the regions on the boundary between the two classifications into smaller regions and repeat the classification and subdivision on the new set of regions (Suetens 1993). This process can be repeated as many times as the user wishes, within the bounds of hardware limitations, in order to refine the calculated boundary. So, according to their function, region-based algorithms may be classified into those who: (a) merge pixels, (b) split image, (c) split-and-merge image in an iterative search scheme and, finally, in d) the watershed-based approach (Chang, 1994).

On the other hand, the contour-based approach rely on detecting edges in the image by classifying pixels using a numerical test for a property such as image gradient or curvature. In these techniques, a scene intensity threshold is specified and the surface that separates voxels with an intensity above the threshold from those with an intensity below the threshold is computed (Bomans, 1990).

The segmentation techniques are based on sophisticated algorithms that have been integrated in many commercial imaging and analysis systems. Though, despite the fact that accuracy, precision and efficiency is the optimal goal of every segmentation approach with validity and clinical applicability, there is no ideally reliable segmentation technique, since the algorithms suffer from variation due to the variation in the objects to be segmented and due to user' interaction (Fenster, 2006). Furthermore, the evaluation of the performance of segmentation algorithms is limited due to the poor methodology in training and testing them as well as due to the inability of comparing them between (Hoover, 1996). So, depending on the purpose of the segmentation process, a different metric variable is most significant and consequently needed than the others. As a result, finding the appropriate segmentation algorithm for a particular task as well as choosing the optimal parameters internal to the segmentation algorithm is still a challenge, rendering the fully automated segmentation and unsolved problem and difficult to be established (Kang , 2004). Manual segmentation is possible but is a time-consuming task and subject to operator variability. Finally, the human intervention is often demanded to initialise, check and correct the results produced form the method, establishing an interactive part, where different degrees of human assistance are combined with computational rational during the segmentation phases (semi-automated segmentation)) (Olabarriaga, 2001) .

Beyond segmentation, one of the most important phases of the biomedical image processing is image interpolation, through which the volume reconstruction is going to occur. Most 3-D biomedical images are sampled anisotropically, with the distance between consecutive slices significantly greater than the in-plane pixel size (Pan, 2004). Either prior to display and measurement or during these manipulations, the images must be transformed in order to compensate for this anisotropy and to convert the input data into output data of isotropic or of the desired level of discretization in any of the *n* dimensions (Grevera, 1998). This is achieved by using a pixel-by-pixel value interpolation to fill in the missing image information. More specific, the interpolation schemes are necessary to recover the missing contours in intermediate slices, in order to obtain an isotropic volume image (Morigi, 2004). Traditional interpolation algorithms can broadly be divided into two categories, which are the scene-based (image-based) and object-based (shape-based) (Frakes, 2008). The algorithms used in scene-based techniques determine pixel values for interpolated cross-sections directly from the density values of the given slices. The most commonly used scene-based methods are the straightforward nearest-neighbor, the linear interpolation of the grey intensity values and the spline-based interpolation. In object-based techniques, the interpolation is guided by object information extracted from the slices (Atoui, 2006). The most known technique of the latter class is the shape-based interpolation, according which the images are interpolated incorporating the correspondance in shape and position between objects on adjacent slices (Raya, 1990). Although, the scene-based algorithms have been used a lot the recent years, there is repeated evidence in the literature of the superior performance of the object-based interpolation. Though, object-based techniques are limitated by their high sensitivity in noise and their process methods over the scene-based time-consuming process (Mascarenhas, 2000).

After the accomplishment of the 3d object representation, the computational model must be interfaced to rapid prototyping. The interfacing of volume modeling to rapid prototyping is performed through its conversion into a stereolithography file (STL), which is a standard input format of almost all rapid prototyping systems. More specific, STL file consists of a mesh of connected triangular planar facets representing the outer skin of an object. Each facet is defined in terms of its vertices and a unit surface normal vector directed away from the interior part. The vertices of triangular facets are also ordered to indicate which side of the triangle contain the part mass (Jacob, 1999). STL files used in rapid prototyping systems must be valid to avoid failure in manufacturing. Invalid STL files may cause incosistencies of facet orientation and uncertainties in the system about which side of the object is the interior or the exterior one. Furthermore, irregularities in the solidified material, during processing, may cause structural problems in the final part and consequently resulting in uncontrolled shrinkage and surface warping (Ma 2001b). Beyond the direct conveyance of the model into the rapid prototyping procedure, the STL file may be conveyed indirectly to the rapid prototyping procedure, through a CAD package. CAD package constitutes a vector-based modeling environment, which relies on boundary representation, meaning that the solid object is defined by the surfaces which bound it. These surfaces are mathematically described using special polynomial functions such as non-uniform rational B-spline (NURBS) function, which represent arbitrary shapes using mathematical precision (Dimas, 1999). So, Inside a CAD environment, surface refinement, triangulation correction, editing and further manipulation of biomodels may be occurred as well as implant designing and design verification, prior to the rapid prototyping process (Ma, 2001a).

After the computer-aided image processing and the model manipulation to produce a STL file formatted solid model, a rapid prototyping procedure and apparatus are selected, by which the model will be sliced and the final anatomical part or device will be fabricated.

Typical Rapid Prototyping Systems

The construction of the 3-D object (physical model or device) obtained from the aforementionied process may be achieved through different rapid prototyping apparatus. Rapid prototyping techniques are very specialized technologies in terms of material processability and each technique requires a specific form of input material (Yeong, 2004). Though, the general building philosophy is common for all of them and is based on the model's decomposition into 2-D horizontal thin cross-sectional layer representation, on the implementation to the rapid prototyping machine and, finally, on the dimensionally accurate physical construction in an additive fashion of the model in a layer-by-layer way (Choi, 1997). Explicitly, starting from the bottom and building layers up, each newly formed layer adhers to previous in a pre-determined order, while each layer corresponds to each of the cross-sectional series. Rapid prototyping technologies may be classified, according to their methodology principles, into: (a) systems based on laser technology, (b) extrusion technology-based systems, (c) systems based on print technology and (d) assembly technology-based systems (Hutmacher, 2004). The most representative and commonly used in dentistry methods in each category will be discribed:

Systems Based on Laser Technology

Stereolithography

Stereolithography (SLA) is a photopolymerization technique, according which the optical energy is used to selectively solidify, by photocuring, seriate layers of liquid photopolymer resin, each of which represents a cross-sectional division of the model. The process involves an ultraviolet (UV) laser beam which is applied on the thin layer at the surface of the resin, in the direction of x and y, through a mirror. The mirror is computer controlled according to the computational model data sources. The solidification is performed in a vat of liquid resin, inside which there is an elevator holding the constructed model. After the accomplishment of every cured layer, the elevator lowers the already solid model along the z direction, so as the level covered the surface immediately above the model to be always liquid. The procedure is repeated until the full construction of the final part, when the whole model is raised up. The shelf-adhesive property of the material causes the layers to bond to one another and eventually form a 3-D object. Layers of sacrificial structures are simultaneously built up to fixture and support the growing shapes and are removed after the finishing of the process (Figure 4a) (Sachlos, 2003; Hutmacher, 2004; Stevens, 2008) .

Selective Laser Sintering

Selective laser sintering (SLS) is based on the interaction of a CO2 laser beam with seriate thin surfaces of thermoplastic powdered materials, after the application of which the neighboring particles reach the glass-transition temperature, get fused and form a solid mass. The energy of the laser beam is modulated to melt the powders only in selected areas defined by the object's geometry at the specific cross-section. The 3-D object is constructed in a fabrication piston, which secures the layer-by-layer building by lowering the model along the z-axis, after the accomplishment of each section. The powder supply is secured by a second delivery piston with opposite movement to the first, through a roller system. The fabrication chamber is maintained at a temperature just below the melting point of the powder so that heat from laser need only elevate the temperature slightly to cause sintering. As previously reported, the procedure is repeated until the full construction of the model. After the building process, the model is removed and submitted in post-processing procedures, including removal of the not scanned and fused powder or other manipulations depending upon the intended application (Figure 4b) (Berry, 1996; Leong, 2003; Hutmacher, 2004; Stevens, 2008).

Extrusion Technology-Based Systems

Fused Deposition Modeling

Another rapid prototyping constructing approach is fused deposition modeling (FDM). The mechanism by which this machine works is based on heating and pumping of the thermoplastic material, from which the 3-D object will be formed at one layer at time. Segments of a filament coil of the supplied material are introduced in a temperature-controlled head, which is stabilized in a stage, able to move in all, selected, diresctions, according to the programming of the computation data. Inside this head, the material starts to liquify and to extrud in a semiliquid state, through a nozzle, on the fabrication platform. The material is immediately solidified after beeing ejected from the nozzle and bonds to the layer below. Due to the time-consuming procedure of the material hardening and layer bonding, the resulted models from FDM require support structures, made of a different thermoplastic material, extracted from a second nozzle, which will be removed after the model accomplishment (Figure 4c) (Zein, 2002; Leong, 2003; Sachlos, 2003; Hutmacher, 2004;Peltola, 2008; Stevens, 2008) .

Systems Based on Print Technology

3-D Printing

One of the most investigated and used rapid prototyping technologies, especially in tisuue-engineering and drug-delivery applications, is 3-D printing (3-DP). The principles of operations are based in a ink-jet printing technology (ink-jet print head), according which deposits of "binder" solution are applied in a platform covered with powder, causing merging of the powder particles, through gluing, in a 2-dimensionally pre-defined way, on a stratification basis. Conceptually, any powdered material including polymers, metals or ceramics can be merged using this ink-jet system. The mechanism is based on the repeated cycles of cross-section reconstruction, securing by the cantrarily movement along the z-axis of two chambers. After the finifshing of each cross-section, the fabrication chamber inside which the model is constructed laid down the completed part and the other chamber supplies the surface above the completed part with material. The communication between the two chambers is done though a roller system, like in the FDM, which distributes and compresses the powder at the top of the fabrication chamber. After the bonder has dried in the powder bed, the finished component is retrieved and unbound powder is removed (Figure 4d) (Leong, 2003; Sachlos, 2003; Hutmacher, 2004; Ryan 2006; Stevens, 2008).

Assembly Technology-Based Systems

Shape Deposition Manufacturing

Despite the fact that all the rapid prototyping apparatus are based on additive layered manufacturing techniques, shape deposition manufacturing (SDM) combines the additive methodology with the material removal process of computer-numerically-controlled machines. The basic principle of SDM fabrication methodology is to deposit individual segments of a part, and of support material structure, as near-net shapes, then machined each to net-shape before depositing and shaping additional material. Beyond the contribution of rapid prototyping in reconstruction of model of high complexity, combines additive / substructive material processing enables the fabrication of heterogenious structures, permitting prefabricated components to be embedded within the growing shapes. The most significant advantage of the last application is that this technique employs the simultaneous addition of cells to the matrix during 3-D scaffold fabrication, innovating further the field of tissue engineering. Each prefabricated layer is first seeded with cells and biological factors, before the layers stacking up and final assembly. There are several materials which can be formed with SDM including metals, plastics, and ceramics, while several alternative processes are used in order to deposit these materials including extrusion, 2-part resin systems, hot wax dispention, photocurable dispention, microcasting, welding, and thermal spraying (Figure 4e) (Sachlos, 2003; Hutmacher, 2004).

Other Rapid Prototyping Methods and Future Directions

Despite the advantage that computer-controlled fabrication techniques of rapid prototyping have shown over the conventional, manual-based fabrication methods, each rapid prototyping apparatus performs its own unique limitations as far as concern the speed, the efficiency, the cost, the complexity of the control systems, the customization, the working materials, the auxialiary and / or supporting materials and, finally, the accuracy and the surface finish of the final products. So, even if rapid prototyping has already changed the way of medical approach, the presence of the above limitations leads to a continued research and developments that will help to improve and revolutionize manufacturing as it is known. So, beyond the known commercialized rapid prototyping systems, there are new developing innovations, some of the most recent are the two-photon polymerization process (TPP), the rapid freeze prototyping (RFP) and the multi-material laser-assisted densification (MMLD).

Two-Photon Polymeriazation Process

The TPP technique is a rapid micro-structuring technology for the fabrication of 3-D structures made of photosensitive materials having a resolution well beyond the diffraction limit, down to 100nm. Its principle is similar to the stereolithography, since both techniques use direct laser "recording" into a liquid volume of photosensitive material to induce a photochemical reaction and formation of polymolecules, leading to a solid mass. Though, in case of TPP, near-infrared laser pulses are used for curing of photosensitive materials. More specific, the TPP employs a two-photon absorption phenomenon, allowing energy deposition, inducing chemical reactions between starters molecules and monomers within a transparent matrix. The desired structures are fabricated by moving the laser focus in three dimensions within

Figure 5a. Stereolitography

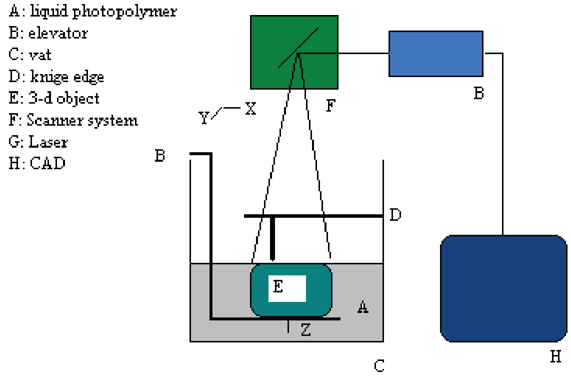

Figure 5b. Selective laser sintering

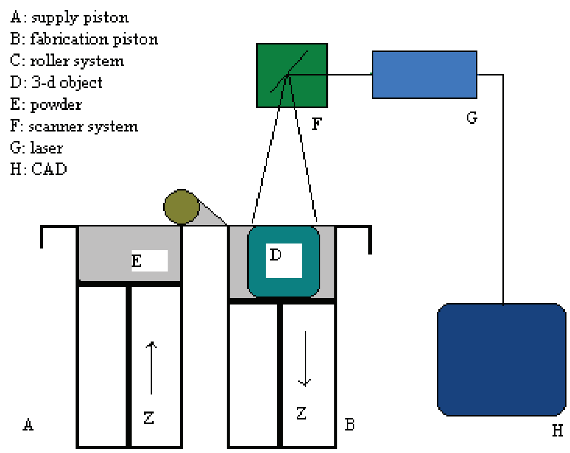

Figure 5c. Fused deposition modeling

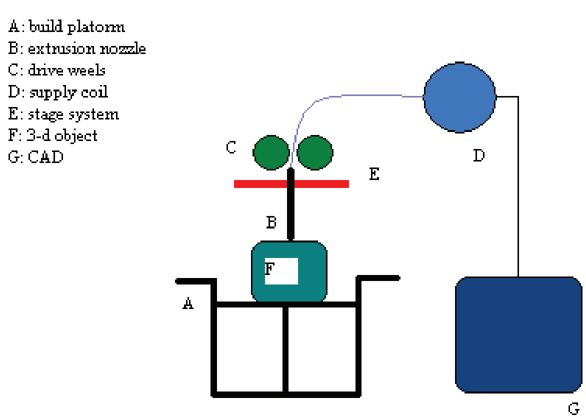

Figure 5d. 3-D printing

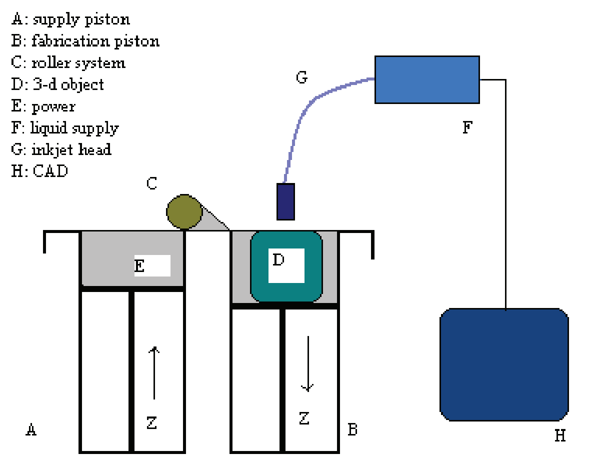

Figure 5e. Shape deposition manufacturing

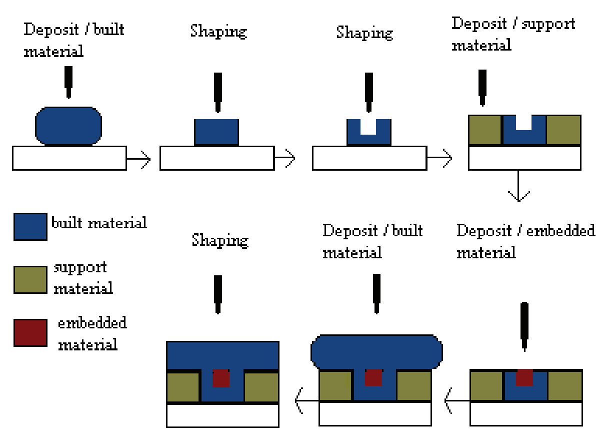

the matrix, by using a galvano-scanner and a micro-positioning system. The fabrication is not always patient- specific, however it is possible to fabricate any computer-designed 3-D structure, with design and material properties for a particular patient (Schlie, 2007; Peltola, 2008).

Rapid Freeze Prototyping

RFP is a novel, environmentally conscious method of solid freeform fabrication in a low-temperature environment, where 3-D objects are constructed through selectively water freezing into an iced substracte. The water is deposited in a layered manner, according which the one layer bonds to the previous through hydrogen bond. The process is done through the compbined function of a computer-pre-defined programming for the model slicing and a machine-setup, consisting of a pressurized water containment unit, an *X-Y* table to control the plate to obtain the correct part geometry, a *Z*-axis elevator for the successive layers, a micro-dispensing drop-on-demand nozzle and a freezer. This procedure has been used instead of the wax patterns in investment casting, especially in dental field, though the research is still in a preliminary phase (Leu, 2000).

Multi-Material Laser-Assisted Densification

MMLD is a new automated additive 3-D rapid prototyping technique which is used in the processing and construction of 3-D bi-material objects, directly from computer data sources, via moving laser beam. It is used instead of manual wax pattering of dental restorations and sintering of the porcelain-fused-to-metal in fixed prosthodontics, eliminating part-specific tooling, human intervention and burning-out procedure. This process is performed in two phases, in which, at first, dental ceramic and metallic powders are delivered through slurry approaches point-by-point to the desired location and, finally, once a layer (or a layer segment) is delivered, it is densified using a laser beam scanning in the desired pattern and with adjusted input power density depending on which powder material is under densification. Despite the fact that neither volumed experimental nor clinical data have been surfaced, it was found that that the temperature distribution, transient stress, residual stress and distortion of a multi-material component are dependent on the laser processing conditions as well as the material properties (Dai, 2005).

Selection Criteria

Despite the fact that rapid prototyping technology is a relatively new engineering task, firstly commercialized in 1980', it has become a continuously growing field with wide range of capabilities and acceptance, counting more than twenty systems worldwide. The uniqueness of each rapid prototyping system and their heterogeneity as far as concern the technology envelope and the material processability brings out benefits and limitations, which differentiate each apparatus' efficiency and suitability regarding specific application field. This makes the identification of the optimum and suitable rapid prototyping process to meet practitioners' requirements increasingly important as well as difficult (Byun, 2005). So, the selection of a rapid prototyping machine often constitutes a sophisticated and multi-factorial process, based on, mainly, benchmarking studies and, recently, on computer based selector programs. The main criteria incorporated for a pointed selection are the: (a) prize of the rapid prototyping machine, (b) dimensional accuracy along the X-Y and Z directions, (c) surface finish of the built part, (d) maximum dimensions of the part building envelope, (e) range or type of working materials, (f) range of layer thickness for part building, (g) speed and (h) availability of technology. Other secondary criteria mentioned are the laser or non-laser type, the size of machine and the office friendly or commercially type (Masood, 2002).

In dental field the biggest obstacles for rapid prototyping technologies are the restrictions set by the material selection, speed and cost (Leu , 2000). Most specific, SLA produces 3-D objects with high accuracy even in achieving small features, good surface finish and easy post-processing. Its restriction is the limited choise of photopolymerizable and biocompatible liquid polymer materials. The difficulty arising during the construction of plastic pattern of a removable partial denture using SLA was that mold cracking developed at the investing stage, resulting in small fins appearing on the divested casting. This was attributed to the expansion of the plastic pattern due to exothermic heat of the investment material during setting. So, the selection of other RP technologies to allow a plastic pattern to be replaced by a wax pattern may overcome this problem (Williams, 2004, 2006). Contrarily, SLS lacks in surface quality and detailed featuring compared to SLA, though the vast range of working materials (polysterene, nylon, wax etc) gives SLS a significant advantage. Furthermore, SLS has the potential of direct fabrication of metal framework, eliminating the intermediate pattern phase. Kruth et al. provide an example of a direct application of RP, particularly SLS, for the fabrication of metal-alloy frameworks for dental prosthesis (Kruth, 2005). Eggbeer et al. investigated the efficiency of using RP models as expendable casting models in the case of custom-made models of removable partial denture metal alloy frameworks (Eggbeer, 2005). RP models of the framework can be used as models for lost-wax casting of the actual framework with great success. FDM models are considered to have a lower quality and speed compared to SLA, though Wu et al, in a brechmark trial, has reported the possibility of fabrication of satisfactory titanium crown through FDM without porosity, with functional contours and smooth surface (Wu, 2001). FDM machine is more suited for placement in a hospital environment and the models derived are low-budget (Leu, 2000). As it is aforementioned, RFP and MMLD have been used instead of the wax patterns in investment casting, especially in dental field, though the research as well as the clinical performance is still in a preliminary phase.

Both SLA and FDM are methods of choise in surgical planning due to their ability to deposit materials with different colours as well as with translucency. This is quite beneficial since the use of different colours highlighs the critical structures, enhances the visualization of the complex model and helps the communication between the people get into the surgical operation. The use of tranculent material is used in the designing if guiding tempates during the surgical phase of dental implant insertion. Finally, FDM, SLS and 3DP are used in the production of biologically active implants mainly due to their capability of using versatile materials for the processes (Leu, 2000).

APPLICATIONS

Implant Dentistry

Fabrication of Surgical Guiding Template (Surgical Splints)

Endosseous dental implants image guided placement has undergone revolutionary development in the last five years, through the use of stereolithographic surgical splints. Its main goal is the accurate positioning of dental implants, completely correlated with the presurgical plan, resulting in improved functionality, aesthetics, biomechanical performance as well as minimal complications (Parel 2004). The protocole of the technique has been previously described for the construction of an optimum guiding template and an ultimate provisional fixed restoration prior the surgical phase for patients suffering from complete edentulism (Lal 2004, Papaspyridopoulos 2008).

According this protocole, the edentulous patient is provisionally treated with an optimum complete denture, based on which a radiographic template was fabricated (Figure 6a).

A scan tomography of the patient with the denture in place was performed and an image data set was acquired and transformed in the computational environment for further image processing. At this stage, the implant positions according to the virtual prosthetic restoration can be viewed, changed and selected (Figure 6b).

After the accomplishment of the image manipulation and the 3-D representation, the modified data are transfered through an STL format to the rapid prototyping process, where a stereolithograaphic model of the patient's jaw was constructed, based on which a patient-specific surgical template was fabricated (6c). Finally, the surgical phase may initiate and accomplished with high predictability, minimal complications and in less time.

Figure 6a. Duplicate dentures as radiographic templates. Papaspyridakos P, Lal K. J Prosthet Dent 2008;100:165-72.

Figure 6b. 3-D implant-planning. Papaspyridakos P, Lal K. J Prosthet Dent 2008;100:165-72.

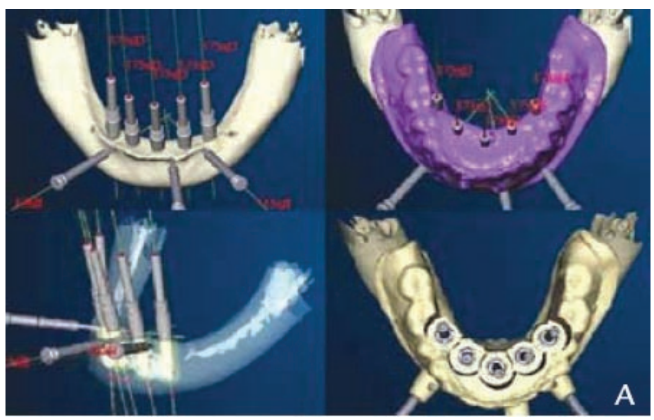

Figure 6c. Stereolithographic surgical template. Papaspyridakos P, Lal K. J Prosthet Dent 2008;100:165-72.

REFERENCES

Adam, F., Hammer, D. S., Pape, D., & Kohn, D. (2002). Femoral anatomy, computed tomography and computer-aided design of prosthetic implants. *Arch Orthop Trauma Surg*, *122*, 262-268.

Atoui, H., Miguet, S., & Sarrut, D. (2006). A fast morphing-based interpolation for medical images: application to conformal radiotherapy. *Image Anal Stereol*, *25*, 95-103.

Azari, A., & Nikzad, S. (2008). Computer-assisted implantology: historical backround and potential outcomes-a review. *The International Journal of Medical Robotics and Computer Assisted Surgery*, *4*, 95-104.

Berry, E., Brown, J. M., Connell, M., Craven, C. M., Efford, N. D., Radjenovic, A., & Smith, M. A. (1997). Preliminary experience with medical applications of rapid prototyping by selective laser sintering. *Med Eng Phys*, *19*, 90-96.

Bibb, R., & Brown, R. (2000). The application of computer aided product developoment techniques in medical modelling topic: rehabilitation and prostheses. *Biomed Sci Instrum*, *36*, 319-324.

Bibb, R., Eggbeer, D., Williams, R. J., & Woodward, A. (2006). Trial fitting of a removable partial denture framework made using computer-aided design and rapid prototyping techniques. Proceeding of the institution of mechanical engineers, Part H: *Journal of engineering in medicine*, *220*, 793-797.

Bill, J. S., & Reuther, J. F. (2004). Rapid prototyping in planning reconstructive surgery of the head and neck. Review and evaluation of indications in clinical use. *Mund Kiefer Gesichtschir*, *8*, 135-153.

Bomans, M., Hohne, K. H., Tiede, U., & Riemer, M. (1990). 3D segmentation of MR images of the head for 3D display. *IEEE Trans Med Imag*, *9*, 177–83.

Brown, G. A., Milner, B., & Firoozbakhsh, K. (n.d.). Application of computer-generated stereolithography and interpositioning template in acetabular fractures: A report of eight cases. *Journal of orthopedic trauma*, *16*, 347-352.

Bruant, J. S., Don, S. E., & Eiliam, B. S. (1995). Steeolithography in oral and maxillofacial operation planning. *International Journal of Oral Maxillofacial Surgery*, *24*, 98-103.

Byuan, H. S., & Lee, K. H. (2005). A decision support system for the selection of a rapid prototyping process using the modified TOPSIS method. *Int Adv Manuf Technol*, *26*, 1338-1347.

Cha, B. K., Lee, J. Y., Jost-Brinkmann, P. G., & Yoshida, N. (2007). Analysis of tooth movement in axtraction cases using three-dimensional reverse engineering technology. *European journal of orthodontics*, *29*, 325-331.

Chan, D. C. N., Frazier, K. B., Tse, L. A., & Rosen, D. W. (2003). Application of rapid prototyping to operative dentistry curriculum. *Journal of dental education*, *68*, 64-70.

Chang, Y. L., & Li, X. (1994). Adaptive image region-growing. *IEEE Trans on Image Processing*, *3*, 868-72.

Chen, D. T., & Zeltzer, D. (1992). Compuer animation of a biomachanically based model of muscle using the finite element model. *ACM Comput Graphics*, *26*, 89-98.

Choi, J. Y., & Choi, J. H., Kim, N. K., & Kim, Y. (2002). Analysis of errors in medical rapid prototyping models. *Int J Oral Maxillofac Surg*, *31*,23-32.

Choi, S. H., & Samavedam, S. (2002). Modelling and optimisation of rapid prototyping. *Computers in dentistry*, *47*, 39-53.

Chua, C. K., Leong, K. F., & Lim, C. S. (2003). *Rapid prototyping. Principles and applications.* World Scientific.

Connell, H. M., Statham, P. F., Collie, D. A., Walker, F. S., & Moos, K. F. (1999). Use of template for custom cranioplasty. *Phidias, EC Funded Network Project in Rapid Prototyping in Medicine, 2,* 7-8.

Da Rosa, E. L. S., Oleskovicz, L. C., & Aragao, B. N. (2004). Rapid prototyping in maxillofacial surgery and traumatology:case report. *Braz Dent J, 15,* 243-247.

Dean, D., Min, K. J., & Bond, A. (2003). Computer aided design of large-format prefabricated cranial plates. *Journal of craniofacial surgery, 14,* 819-832.

Di Giacomo, G. A., Cury, P. R., & Araujo, N. S. (2005). Clinical application of stereolithographic surgical guides for implant placement: preliminary results. *J Periodontol, 76,* 503-507.

Dimas, E., & Briassoulis, D. (1999). 3D geometric modelling based on NURBS : A review. *Advances in engineering software, 30,* 741-751.

Duret, F., Blouin, J. L., & Duret, B. (1988). CAD-CAM in dentistry. *J Am Dent Assoc, 227,* 715-720.

D'Urso, P. S., Atkinson, R. L., Lanigan, M. W., Earwaker, W. J., Bruce, I. J., Holmes, A., Barker, T. M., Effeney, D. J., & Thompsom, R. G. (1998). Stereolithographic (SL) biomodelling in craniofacial surgery. *British Journal Of Plastic Surgery, 51,* 522-530.

D'Urso, P. S., Earweaker, W. J., Redmond, M. J., Thompson, R. G., Effeney, D. J., & Tomlinson, F. H. (2000). Custom cranioplasty using stereolithography and acrylic. *British Journal of Plastic Surgery, 53,* 200-204.

Eggbeer, D., Bibb, R., & Williams, R. (2005). The compuer-aided design and rapid prototyping fabrication of removable partial denture frameworks. *Proc Inst Mech Eng, 219,* 195-202.

Erickson, D. M., Chance, D., Schmitt, S., & Mathis, J. (1999). An opinion survey of reported benefits from the use of stereolithographic models. *J Oral Maxillof Surg, 57,* 1040-1043.

Faber, J., Berto, P. M., & Quaresma, M. (2006). Rapid prototyping as a tool for diagnosis and treatment planning for maxillary canine impaction. *American Journal Of Orthodontics and Dentofacial Orthopedics, 129,* 583-589.

Fenster, A., & Chiu, B. (2005). Evaluation of segmentation algorithms for nedical imaging. *Proceeding of the IEEE, Engineering in medicine and biology, 27th annual conference,* (pp. 7186-7189).

Frakes, D. H., Dasi, L. P., Pekkam, K., Kitajima, H. D., Sundareswaran, K., Yoganathan, A. P., & Smoth, M. J. T. (2008). A new method for registration-based medical image interpolation. *IEEE transactions on medical imaging, 27,* 370-377.

Freed, L. E., & Vunjak-Novakovic, G. (1998). Culture of orgnized cell communities. *Adv Drug Deliver Rev, 33,* 15-30.

Giannatsis, J., & Dedoussis, V. (2007). Additive fabrication technologies applied to medicine and health care: a review. *Int J Adv Manuf Technol, 0268-3768* (Print) 1433-3015 (Online).

Gray, C. F., Redpath, T. W., Smith, F. W., & Staff, R. T. (2003). Advanced imaging:Magnetic resonance imaging in implant dentistry. *Clin Oral Implant Res, 14,* 18-27.

Grevera, G. J., & Udupa, J. K. (1998). An objective comparison of 3-D image interpolation methods. *IEEE trans on medical inaging, 17,* 642-652.

Guest, J. K., & Prevost, J. H. (2006). Optimizing multifunctional materials: Design of microstructures for maximized stiffness and fliod permeability. *International Jouran of solid and structures, 43,* 7028-7047.

Harris, J., & Rimmel, J. (2002). Can rapid prototyping ever become a routine feature in general dental practice? *Dent update, 29*, 482-486.

Heckmann, S. W., Winter, Meyer, M., Weber, H., & Wichmann, M. (2001). Overdenture attachment selection and the loading of implant and denture-bearing area.Part 2: A methodical study using five types of attachment. *Clin Oral Implant Res, 12*, 640-647.

Hieu, L. C., Bohez, E., Vander, S. J, Oris, P., Phien, H. N., Vatharaporn, E., & Binh, P. H. (2002a). Design and manufacturing of cranioplasty implants by 3-axis CNC milling. *Technology and Health Care, 10*, 413-423.

Hieu, L. C., Bohez, E., Vander Sloten, J., Phien, H. N., Vatcharaporn, E., Binh, P. H., An, P. V., & Oris, P. (2003). Design for medical rapid prototyping of cranioplasty implants. *Rapid Prototyping Journal, 9*, 175-186.

Hollister, S. J., Levy, R. A., Chu, T. M., Halloran, J. W., & Feinberg, S. E. (2000). Am image-based approach for designing and manufacturing craniofacial scaffolds. *Int J Oral Maxillfac Surg, 26*, 67-71.

Hollister, S. J., Maddox, R. D., & Taboas, J. M.(2002). Opitimal design and fabrication of scaffolds to mimic tissue properties and satisfy biological constraints. *Biomaterials, 23*, 4095-4103.

Hollister, S. J. (2005). Porous scaffold design for tissue engineering. *Nat Mater, 4*, 518-424.

Hollister, S. J., Lin, C. Y, Lin, C. Y., Schek, R. D., Taboas, J. M., Flanagan, C. L. Saito, E., Williams, J. M., Das, S., Wirtz, T., & Krebsach, P. H. (2004). Design and fabrication of scaffolds for anatomic bone reconstruction. *Med J Malaysia, 59*, 131-2.

Hollister, S. J., Lin, C. Y., Kang, H., & Adachi, T. (2008). *Computational design and simulation of tissue engineering scaffolds*. New York: Springer.

Hoover, A., Jean-Baptiste, J., Jiang, X., Flynn, P. J., Bunke, H., Goldgof, D. B., Bowyer, K., Eggert, D. W., Fitzgibbon, A., & Fisher, R. B. (1996). An experimental comparison of range image segmentation algorithms. *IEEE trans on pattern analysis and machine intelligence, 7*,673-689.

Hutmacher, D. W. (2000). Scaffolds in tissue engineering bone and cartilage. *Biomaterials, 21*, 2529-2543.

Hutmacher, D. W., Sttinger, & Risbud, M. V. (2004). Scaffold-based tissue engineering: rationale for compouter-aided design and solid free-form fabrication systems. *TRENDS in Biotechnology, 22*, 354-362.

Hutmacher, D. W., & Cool, S. (2007). Concepts of scaffold-based tisuue-engineering-the rational to use solid free-from fabrication techniques. *J cell Mol Med, 11*, 654-669.

Izatt, M. T., Thorpe, P. L., Thompson, R. G., D'Urso P. S., Adam C. J., Earweaker J. W. S., Labrom R. D., & Askin, G. N. (2007). The use of biomodelling in complex spinal surgery. *Eur Spine J, 16*, 1507-1518.

Jabero, M., & Sarment, D. (2006). Advanced surgical guidance technology: A review. *Implant dentistry, 15*, 135-142.

Jacob, G. G., Kai, C. C., & Mei, T. (1999). Development of a new rapid prototyping interface. *Computers in dentistry, 39*, 61-70.

Kang, Y., Engelke, K., & Kalender, W. A. (2004). Interactive 3D editing tools for image segmentation. *Medical image analysis, 8*, 35-46.

Klein, H. M., Schneider, W., Alzen, G., Voy, E. D., & Gunther, R. W. (1992). Pediatric craniofacial surgery. Comparison of milling and stereolithography for 3D model manufacturing. *Pediatr Radiol, 22*, 458-460.

Kohn, D. G., Sarmadi, M., Helman, J. I., & Kresbach, P. H. (2002). Effects of PH on human bone marrow stromal cells in vitro: Implications for tissue engineering of bone. *J Biomed Mater Res*, *63*, 567-576.

Kopp, K. C., Koslow, A. H., & Abdo, O. S. (2003). Predictable implant placement with a diagnostic/ surgical template and advanced radiographic imaging. *J Prosthet Dent*, *89*, 611-615.

Kruth, J. P., & Vandenbroucke, B., Van Vaerenbergh, J., & Naert, I. (2005). Digital manufacturing of biocompatible metal frameworks for complex dental prostheses by means of SLS / SLM. In *Virtual prototyping and rapid manufacturing-advanced research in visrtual and rapid prototyping. T*aylor & Francis, Londnon, (pp. 139-146).

Kundu, A. (1990). Local segmentation of biomedical images. *Computerized Medical Imaging and Graphics*, *14*, 173–83.

Lal, K., White, G. S., Morea, D. N., & Wright, R. F. (2006).Use of stereolithographic templates for surgical and prosthodontic implant planning and placement. Part I. The concept. *J Prosthodont*, *15*, 51-58.

Langer, R., & Vacanti J. P. (1993). Tissue engineering. *Science, 260*, 920-926.

Lee, S. J., Jung, I. Y., Lee, C. Y., Choi, S. Y., & Kum, K. Y. (2001). Clinical application of computer-aided rapid prototyping for tooth transplantation. *Dental Traumatology*, *17*, 114-119.

Leong, K. F., Cheah, C. M., & Chua, C. K. (2003). Solid freeform fabrication of three-dimensional scaffolds for engineering replacememnt tissues and organs. *Biomaterials*, *24*, 2363-2378.

Leu, M. C., Zhang, W., & Sui, G. (2000). An experimental and analytical study of ice: Part fabrication with rapid freeze prototyping. *CIRP Annals Manufacturing technoogy, 49*, 147-150.

Li, X., Wang, J., Shaw, L. L., & Cameron, T. B. (2005). Laser densification of extruded dental porcelain bodies in multi-material laser densification process. *Rapid prototyping journal, 1*, 52-58.

Lieu, Q., Leu, M., & Schmitt, S. (2006). Rapid prototyping in dentisry: Technology and application. *Int J Adv Manuf Technol*, *29*, 317-335.

Liew, A. W. C., & Yan, H. (2006). Current methods in the automatic tissue segmentation of 3D magnetic resonance brain images. *Current medical images reviews, 2*, 1-13.

Lin C. Y., Kikuchi, N., & Hollister, S. J. (2004a). A novel method for biomaterial scaffold internal archtecture design to match bone elastic properties with desired porosity. *J Biomech, 37*, 632-636.

Lin, C. Y., Hsiao, C. C., Chen, P. Q., & Hollister, S. J. (2004b). Interbody fusion cage design using integrated global layout and local microstructure topology optimization. *Spine*, *29*, 1747-1754.

Lohfeld, S., & McHugh, B. V. (2005). Biomodels of bone: A review. *Annals of Biomedical Engineering*, *33*, 1295-1311.

Ma, D., Lin, F., & Chua, C. K. (2001). Rapid prototyping applications in medicine. Part 1: NURBS-based volume modelling. *Int J Adv Manuf Technol*, *18*, 103-117.

Ma, D., Lin, F., & Chua, C. K. (2001). Rapid prototyping applications in medicine. Part 2: STL file generation and case studies. *Int J Adv Manuf Technol*, *18*, 118-127.

Mah, J., & Sachdeva, R. (2001). Comoputer-assisted orthodontic treatment. *Americal journal of orthodontics and dentofacial orthopedics, 120*, 85-87.

Mascarenas, N. D. A., Souza, I. A., Cruvinel, P. E., Biscegli, C. I., & Rosa, R. R. (2000). An estimation theoretic approach to 3-D image interpolation. *IEEE*, (pp. 163-169).

Masood, S. H., & Soo, A. (2002). A rule based expert system for rapid prototyping selection. *Robotics and computer integrated manufacturing, 18*, 267-274.

Mc Inerney, T., Terzopoulos, D. (1996). Deformabe models in medical image analysis: A survey. *Medical image analysis, 1*, 91-108.

Metzger, M. C., Majert-Hohlweg, B., Schon, R., Teschner, M., Gellrich, N. C., Schmelzeisen, R., &Gutwald, R. (2007). Verification of clinical precision after computer-aided recontruction in craniomaxilofacial surgery. *Oral Surg Oral Med Oral Pathol Oral Radiol Endod, 104*, e1-e10.

Mijagic, M., Fauquet, C., Galletti, C. Palot, C., Wiechmann, D., & Mah, J. (2005). Digital design and manufacturing of the lingualcare bracket system. *JCO, 34*, 375-382.

Milovanovic, J. (2007). Medical applications of rapid prototyping. *Mechanical Engineering, 5*, 79-85.

Morigi, S., & Sgaralli, F. (2004). 3D long bone reconstruction based on level sets. *Computerized medical Imaging and Graphics, 28*, 377-390.

Natali, A. N., & Viola, M. M. (2004). Computer tomography for virtual models in dental imaging. In *Dental biomechanics.* Taylor & Francis, London, (pp. 35-50).

Nizam, A., Gopal, R. N., Naing, L., Hakim, A. B., & Samsudin, A. R. (2006). Dimensional acuracy of the skulls models produced by rapid prototyping technology using stereolithography appararus. *Archives of orofacial sciences, 1*, 60-66.

Muller, A., Krishnan, K. G., Uhl, E., & `Mast, G. (2003). The application of rapid prototyping techniques in cranial reconstruction and preoperative planning in neurosurgery. *Journal of Craniofacial Surgery, 14*, 899-914.

Muller- Hartwich, R., Prager, T. M., & Jost-Brinkmann, P. G. (2007). SureSmile:CAD/CAM system for orthodontic treatment planning, simulation and fabriation of customized archwires. *Int J Comput Dent, 10*, 53-62.

Olabarriaga, S. D., & Smeulders, A. W. M. (2001). Interaction in the segmentation of medical images: A survey. *Medical image analysis, 5*, 127-142.

Otto, T., & De Nisco, S. (2002). Computer-aided direct ceramic restorations: A 10-year prospective clinical study of Cerec CAD / CAM inlays and onlays. *Int J Prosthodont, 15*, 122-128.

Otto, T., & Schneider, D. (2008). Long-term clinical results of chairside Cerec CAD / CAM inlays and onlays: a case series. *Int J Prosthodont, 21*, 53-59.

Pan, Z., Yin, X., & Wu, G. (2004). Segmentation –based interpolation of 3D medical images. *ICCSA, LNCS3044*, (pp. 731-740).

Papaspyridopoulos, P., & Lal, K. (2008) Complete arch implant rehabilitation using subtractive rapid prototyping and porcelain fused to zirconia prosthesis: A clinical report. *J Prosthet Dent 2008, (100), 165-172*.

Parel, S. M., & Triplett, R. G. (2004). Interactive imaging for implant planning, placement, and prosthesis construction. *J Oral Maxillofac Surg, 62*, 41-47.

Petzold, R., Zeilhofer, H. F., & Kalender, W. A. (1999). Rapid prototyping technology in medicine-basics and applications. *Computerized medical imaging and graphics, 23*, 277-284.

Pham, D. T., & Gault, R. S. (1998). A comparison of rapid prototyping technologies. *International journal of machine tools and manufacture, 38*, 1257-1287.

Rangert, B., Krogh P. H., Langer B., et al (1995). Bending overload and implant fracture: retrospective clinical analysis. *Int J Maxillofac Implants, 10*, 169-174.

Raya, S. P., & Udupa, J. K. (1990). Shape-based interpolation of miltidimensional objets. *IEEE trans on medical imaging, 1,* 32-42.

Reich, S., Wichmann, M., Nkenke, E., & Proeschel, P. (2005). Clinical fit of all-ceramic three-unit fixed partial dentures, generated with three different CAD / CAM systems. *Eur J Oral Sci, 113*, 174-179.

Robb, R. A. (1999). 3D visualization in biomedical applications. *Ann Reviews in Biomedical engineering, 01*, 377-399.

Ryan, G., Pandit, A., & Apatsidis, D. P. (2006). Fabrication methods of porous metals for use in orthopaedic applications. *Biomaterials, 27,* 2651-2670.

Sachlos, E., & Czernuszka, J. T. (2003). Making tissue enginnering scaffold work. Review on the application of solid freeform fabrication technology to the production of tissue engineering scaffolds. *European Cells and materials, 5,* 29-40.

Sarment, D. P., Sukovic, P., & Clinthorne, N. (2003). Accutacy of implant placement with a stereolithographic surgical guide. *Int J Maxillofac Implants, 18*, 571-577.

Schenone, A., Firenze, F., Acquarone, F., Gambaro, M., Maasulli, F., & Abdreucci, L. (1996). Segmentation of multivariate medical images via unsupevised clustering with 'adaptive resolution'. *Computerized madincal imaging and graphics, 20*, 119-129.

Schlie, S. (2007). Three-Dimensional Cell Growth on Structures Fabricated from ORMOCER® by Two-Photon Polymerization Technique. *Journal of Biomaterials Applications, 22*, 275-287.

Singare, S., Liu, Y., Li, D., Wang, J., & He, S. (2008).Individually prefabricated prosthesis for maxilla reconstruction. *J Prosthodont, 17,* 135-40.

Sigmund, O., & Toruato, S. (1997). Design of materials with extreme thermal explansion using a three-phase topology optimization method. *Journal of mechanics and physics, 45*, 1037-1067.

Spoor, F., Jeffery, N., & Zonneveld, F. (2000). *Imaging skeletal growth and evolution*. London: The linnean society of London.

Stark, D. D., & Bradley, W. G. (1999). *Magnetic resonance imaging.* St. Louis: C.V. Mosby.

Stevens, B., Yang, Y., Mohandas, A., Stucker, B., & Nguyen, K. T. (2008). A review of materials, fabrication methods, and strategies used to enhance bone regeneration in engineered bone tissues. *Appl Biomaterials, 85B*, 573-582.

Strub, J. R., Rekow, E. D., & Witkowski, S. (2006). Computer-aided design and fabrication of dental restorations. *J Am Dent Assoc, 137*, 1289-1296.

Suetens, P., Bellon, E., Vandermeulen, D., Smet, M., Marchal, G., Nuyts, J., & Mortelmans, L. (1993). Image segmentation : Methods and applications in diagnostic radiology and nuclear medicine. *European journal of radiology, 17*, 14-21.

Sun, W. (2002). *CT/MRI Based 3D reconstruction.* MEM Dept. Drexel University.

Sun, W., & Pallavi, L. (2002). Recent development on computer aided tissue engineering-a review. *Computer methods and programs in biomedicine, 67*, 85-103.

Sun, W., Drling, A., Starly, B., & Nam, J. (2004a). Computer- aided tissue engineering: overview, scope and challenges. *Biotechnol Appl Biochem, 39*, 29-47.

Sun, W., Starly, B., Drling, A., & Gomez, C. (2004b). Computer-aided tissue engineering: application to biomimetic modelling and design of tissue scaffolds. *Biotechnol Appl Biochem, 39*, 49-58.

Sun, Y. C., Lu, P. J., Wang, Y., Han, J. Y., & Zhao, J. J. (2007). Research and development of computer-aided design and rapid prototyping technology for complete denture. *Zhonghua Kou Qiang Yi Xue Za Zhi, 42*, 324-329.

Suzuki, H., & Toriwaki, J. (1991). Automatic segmentation of head MRI images by knowledge guided thresholding. *Computerized Medical Imaging and Graphics, 15*, 233-40.

Tan, K. H., Chua, C. K., Leong, K. F., Cheah, C. M., Gui, W. S., Tan, W. S., & Wiria, F. E. (2005a). Selective laser sintering of biocompatible polymers for application in tissue engineering. *Biomed Mater Eng, 15*, 113-124.

Tan, K. H., Chua, C. K., Leong, K. F., Naing, M. W., & Cheah, C. M. (2005b). Fabrication and characterization of polymer (ether-ether-ketone)/-hydroxiapatite biocomposite scaffolds using laser sintering. *Proc Inst Mech Eng Part, 219*, 183-194.

Terzopoulos, D., & Waters, K. (1990). Physically based facial remodeling, analysis and animation. *J Vis Compout Animation, 1*, 73-80.

Udupa, J. K. (1999). Three- dimensional visualization and analysis methodologies: A current prospective. *Radiographics, 19*, 783-806.

Udupa, J. K., Le BLANC, v. r., Zhuge, Y., Imielinska, C., Schmidt, H., Currie, L. M., Hirsch, B. E., & Woodburn, J. (2006). *Computerized medical imaging and graphics, 30*, 75-87.

Vacanti C. A. (2006). The history of tissue engineering. *J Cell Mol Med*, *10*, 569-576.

Vale, F. M., Castro, M., Monteiro, J., et al. (1997). Acrylic bone cement induces the production of free radicals by cultured human fibroblasts. *Biomaterials, 18*, 1133–5.

Vail, N. K., Swain, L. D., Fox, W. C., Aufdlemorte, T. B., Lee, G., & Barlow, J. W. (1999). Materials for biomedical application. *Materials and Design*, *20*, 123-132.

Webb, P. A. (2000).A review of rapid prototyping techniques (RP) in the medical and biomedical sector. *Journal of medical engineering and technology, 24*, 149-153.

Wierchmann, D., Rummel, V., Thalheim, A., Simon, J. S., & Wierchmann, L. (2003). Customized brackets and archwires for lingual orthodontic treatment. *Americal journal of orthodontics and dentofacial orthopedics, 124*, 593-599.

Williams, R. J., Bibb, R., & Rafic, T. (2004). A technique for fabricating patterns for removable partial denture frameworks using digitized casts and electronic surveying. *J Prosthet Dent, 91*, 85-88.

Williams, R. J., Bibb, R., Eggbeer, D., & Collis, J. (2006). Use of CAD/CAM technology to fabricate a removable partial denture framework. *J Prosthet Dent, 96*, 96-99.

Winder, J., & Bibb, R. (2005). Medical rapid prototyping technologies: State of the art and current limitations for application in oral and maxillofacial surgery. *J Oral Maxillofac Surg, 63*, 1006-1015.

Winder, R. J., McKnight, W., McRitchie, I., Montgomery, D., & Wulf, J. (2006). 3D surface accuracy of CAD generated skull defect contour. *Stud Health Technol Inform 119*, 574-6.

Wong, N., Huffer-Charchut, H., & Sarment, D .P. (2007). Computer-aided design / computer-aided manufacturing surgical guidance for placement of dental implant: case report. *Implant Dentistry, 16*, 123-130.

Wu, M., Tinschert, J., Augthun, M., Wagner, I., Schadlich-Stubenrauch, J., Sahm, P. R., & Spiekermann, H. (2001). Application of laser measuring, numerical simulation and rapid prototyping to titanium dental castings. *Dental Materials, 17*, 102-108.

Wurm, G., Tomancok, B., Holl, K., & Trenkler, J. (2004). Prospective study on cranioplasty with individual carbon fiber reinforced polymere (CFRP) implants produced by means of stereolithography. *Surg Neurol*, *62*, 510-521.

Yeong, W. Y., Chua, C. K., & Leong, K. F. Chandrasekaran, M. (2004). Rapid prototyping in tisue engineering: challenges and potential. *TRENDS in Biotechnology*, *22*, 643-650.

Zein, I. (2002). Fused deposition modelling of novel structure archtecture for engineering applications. *Biomaterials*, *23*, 1169-1185.

KEY TERMS

Accuracy: Accuracy of a segmentation technique refers to the degree to which the segmentation results agree with the true segmentation.

Bracket: An orthodontic device attached to an individual tooth to hold arch wires

Efficiency: Efficiency of the segmentation provides information on the practical use of the algorithm.

Fixed Partial Denture: Any dental prosthesis that is luted, screwed or mechanically attached or otherwise securely retained to natural teeth, tooth roots, and/or dental implant abutments that furnish the primary support for the dental prosthesis.

Guide Template: 1. A thin, transparent form duplicating the tissue surface of a dental prosthesis and used as a guide for surgically shaping the alveolar process 2. A guide used to assist in proper surgical placement and angulation of dental implants.

Implant: A prosthetic device made of alloplastic material(s) implanted into the oral tissues beneath the mucosal or/and periosteal layer, and on/or within the bone to provide retention and support for a fixed or removable dental prosthesis; a substance that is placed into or/and upon the jaw bone to support a fixed or removable dental prosthesis.

Investment Casting: A material consisting principally of an allotrope of silica and a bonding agent. The bonding substance may be gypsum (for use in lower casting temperatures) or phosphates and silica (for use in higher casting temperatures).

Object System: A collection of different objects.

Pixel: The 2-D analog of a voxel.

Precision: Precision of a segmentation algorithm provides information on the repeatability of the technique when used to segment a type of image.

Reliability: The ability of a system or component to perform its required functions under stated conditions for a specified period of time.

Removable Partial Denture: Any dental prosthesis that replaces some or all teeth in a partially dentate arch (*partial removable dental prostheses*) or edentate arch (*complete removable dental prostheses*). It can be removed from the mouth and replaced at will.

Scaffold: A supporting surface, either natural or prosthetic, that maintains the contour of tissue; a supporting framework.

Schene: Digital image.

Voxel: The volume elements into which a body region is virtually partitioned.

Wax or Acrylic Patterns: A form that is used to make a mold; a model for making a mold.

Chapter XVII
Unicode Characters for Human Dentition:
New Foundation for Standardized Data Exchange and Notation in Countries Employing Double-Byte Character Sets

Hiroo Tamagawa
The Japan Association for Medical Informatics, Japan

Hideaki Amano
The Japan Association for Medical Informatics, Japan

Naoji Hayashi
The Japan Association for Medical Informatics, Japan

Yasuyuki Hirose
The Japan Association for Medical Informatics, Japan

Masatoshi Hitaka
The Japan Association for Medical Informatics, Japan

Noriaki Morimoto
The Japan Association for Medical Informatics, Japan

Hideaki Narusawa
The Japan Association for Medical Informatics, Japan

Ichiro Suzuki
The Japan Association for Medical Informatics, Japan

ABSTRACT

In this chapter, the authors report the minimal set of characters from the Unicode Standard that is sufficient for the notation of human dentition in Zsigmondy-Palmer style. For domestic reasons, the Japanese Ministry of International Trade and Industry expanded and revised the Japan Industrial Standard (JIS) character code set in 2004 (JIS X 0213). More than 11,000 characters that seemed to be necessary for *denoting and exchanging information about personal names and toponyms were added to this revision, which also contained the characters needed for denoting human dentition (dental notation). The Unicode Standard has been adopted for these characters as part of the double-byte character standard, which enabled, mainly in eastern Asian countries, the retrieval of human dentition directly on paper or displays of computers running Unicode-compliant OS. These countries have been using the Zsigmondy-Palmer style of denoting dental records on paper forms for a long time. The authors describe the background and the application of the characters for human dentition to the exchange, storage and reuse of the history of dental diseases via e-mail and other means of electronic communication.*

INTRODUCTION

Computers store letters and other characters by assigning a number to each character (Kilbourne and Williams, 2003). The entire collection of characters is called *a character code set*. The character code set was established in Europe and America, and was gradually expanded together with the advent of computers. ASCII (American Standard Code for Information Interchange) (ANSI INCITS 4-1986, 1963) is one of the most popular and representative character code sets, and it is capable of encoding a maximum of 256 characters using one byte of information. All alphanumeric characters are covered by this code system, and ASCII has become the de facto worldwide standard due to its simplicity.

Together with the development of computers, a problematical point emerged in that the one-byte character set does not have the capacity to encode enough characters in countries such as Japan, China, Korea and other Asian countries which utilize ideographic writing systems (Hussein et al. 2004) . The majority of these countries employs writing systems based on the so-called Chinese characters and has their origins in long-standing Asian culture. Other glyphs, symbols and icons developed in the course of history of the individual countries are also used.

In order to circumvent the limitations of the ASCII character set, computer systems in these countries use two bytes for representing each character. Characters encoded using two-byte codes are called *double-byte characters* (Oram 1991). In double-byte character sets, each character is represented by two bytes, which enables the encoding of a maximum of 65536 (256x256) characters.

The design of Unicode (http://www.unicode.org/) is based on the simplicity and the consistency of ASCII; however, since it assigns between one and four bytes to each character, it goes far beyond the abilities of ASCII which is limited to encoding the Latin alphabet and a number of other characters, including those with diacritic marks used in European languages. Before Unicode was invented, there were hundreds of different encoding systems for assigning these numbers as single encoding could contain enough characters (http://en.wikipedia.org/wiki/Unicode). For example, the European Union alone requires several different encodings to cover all its languages and even for a single language like English, no single encoding was adequate for covering all the letters, punctuation, and technical symbols in common use.

Unicode has the explicit aim of transcending the limitations of traditional character encodings, such as those defined by the ISO 8859 standard (ISO/IEC 8859-11, 1999) , which are widely used in various countries of the world but remain largely incompatible with each other. In principle, Unicode encodes the underlying characters, graphemes and grapheme-like units rather than the variant glyphs (renderings) for such characters. In the case of Chinese characters, this sometimes leads to controversies over distinguishing the underlying character from its variant glyphs.

Unicode consists of a repertoire of about 100,000 characters, a set of code charts for visual reference, an encoding methodology, a set of standard character encodings, an enumeration of character properties such as upper and lower case, a set of computer files containing reference data, and a number of related items, such as character properties, rules for text normalization, decomposition, collation, rendering and bidirectional display order (for the correct display of text containing both right-to-left scripts, such as Arabic or Hebrew, and left-to-right scripts) (The Unicode Standard, 2006). Unicode also contains several characters, which enable the notation of human dentition and human tooth numbering. In this report, we refer to this as *dental notation*. As we describe in the next paragraph, there are three major notations for human dentition. In countries using double-byte character sets, the Zsigmondy-Palmer system (Zsigmondy, 1874) is the primary system for denoting or exchanging information concerning human dentition on paper media. In order to denote human dentition on computer displays or printers using double-byte characters, each of the companies producing computer systems for the dental industry developed user-defined characters using their original code system. The differences in these code systems obstructed the exchange of human dentition information via digital means. The difficulties arise from the fact that two encoding systems can use the same number for two different characters, or use different numbers for the same character.

Moreover, there are three major character sets in Japan (Shibano, 1999). One is JIS X 0208, standardized by the Japan Industrial Standard (JIS), the second is EUC-JP, which is popular among UNIX users, and the third is Shift-JIS. These encoding systems also conflict with one another. In the latest revision of the JIS character code set completed in 1983 (http://www.meti.go.jp/press/past/c60926e1.html), the external character code specification (user-defined characters) was revalidated since most computers were used as standalone machines, and networked computers were not dominant at that time. External character codes are used for displaying or printing glyphs and symbols on a monitor or a printer directly connected to the computer. However, the recent development of computer networks requires multi-industrial information exchange using standardized character code sets. A highly important point in the 1999 revision is that the external character code specification was abandoned (http://www.meti.go.jp/kohosys/press/0004964/index.html).

The field of dentistry is not an exception. From the beginning of the computerization of dentistry, Japan had adopted this external character code specification, especially in the dental insurance claim system. In order to denote and exchange electronic patient records on a network continuously, two major approaches have been taken. One is the typographical approach for a full notation of human dentition, and the other is the two-digit numbering system for human dentition..

MATERIALS AND METHODS

Dentists use several different dental notation systems for assigning information to a specific tooth on a paper medium. The three most common systems are the Universal numbering system (Ferguson 2005) (dental), the FDI World Dental Federation notation (Blinkhorn et al. 1998) , and the Zsigmondy-Palmer (The Unicode Standard, 2006) notation method.

Figure 1 shows these three major conventional methods for denoting human dentition. The Universal numbering system is a dental notation system for assigning information to a specific tooth, and is commonly used in the US. The uppercase letters A through T are used for primary teeth, and the numbers 1 - 32 are used for permanent

Figure 1. Tooth numbering systems for normal human dentition

Universal numbering system

*Permanent Dentition

1 2 3 4 5 6 7 8	9 10 11 12 13 14 15 16
32 31 30 29 28 27 26 25	24 23 22 21 20 19 18 17

*Deciduous Dentition

A B C D E	F G H I J
T S R Q P	O N M L K

The two-digit notation system developed by FDI

*Permanent Dentition

18 17 16 15 14 13 12 11	21 22 23 24 25 26 27 28
48 47 46 45 44 43 42 41	31 32 33 34 35 36 37 38

*Deciduous Dentition

55 54 53 52 51	61 62 63 64 65
85 84 83 82 81	71 72 73 74 75

Zsigmondy-Palmer notation

*Permanent Dentition

8 7 6 5 4 3 2 1	1 2 3 4 5 6 7 8
8 7 6 5 4 3 2 1	1 2 3 4 5 6 7 8

*Deciduous Dentition

E D C B A	A B C D E
E D C B A	A B C D E

teeth, where the tooth designated as "1" is the right maxillary third molar and the count continues along the upper teeth to the left side. Then the count begins at the left mandibular third molar, designated as number 17, and continues along the bottom row of teeth to the right side. Each tooth is assigned a unique number or letter, allowing for easier encoding using a keyboard (The Unicode Standard, 2006).

The FDI World Dental Federation notation is widely used by dentists internationally for assigning information to a specific tooth. Developed by the Fédération Dentaire Internationale (FDI), it is also known as the ISO-3950 notation. The

FDI system uses a two-digit numbering system, in which the first number represents the quadrant in which the tooth is located, and the second number represents the number of the tooth from the midline of the face. For permanent teeth, the upper right teeth begin with the number 1, the upper left teeth begin with the number 2, the lower left teeth begin with the number 3 and the lower right teeth begin with the number 4. For primary teeth, the sequence of numbers is 5, 6, 7, and 8 for the teeth in the upper left, upper right, lower right, and lower left quadrant respectively. From dentistry textbooks to insurance claims in every dental clinic, the Zsigmondy-Palmer notation is dominant in Japan (Huszár, 1989).

The Palmer notation (Palmer, 1891) is another system used by dentists to assign information to a specific tooth. Although allegedly superseded by the FDI World Dental Federation notation, it continues to be the preferred method used by the overwhelming majority of dental students and practitioners in the UK (Shibano, 1999). It was originally termed the "Zsigmondy system" after the Hungarian dentist Adolf Zsigmondy, who developed the idea in 1861, and makes use of a Zsigmondy cross to record the quadrants of the tooth positions (Charbeneau, 1975). Permanent teeth were numbered 1 to 8, and the primary dentition of children was depicted with a quadrant grid using the Roman numerals I, II, III, IV, V to number the teeth from the midline distally. The Palmer notation consists of the symbols (┘└ ┐┌), designating the quadrant in which the tooth is found, and a number indicating the distance from the midline. Permanent teeth are numbered 1 to 8, with deciduous teeth indicated by a letter (A to E). Hence, the left and the right maxillary central incisor would have the same number, "1"; however, the right one would have the symbol, "┘" underneath it and the left one would have "└". In Asian countries, the Zsigmondy-Palmer notation is dominant due to its ability to denote both the status and the position of the tooth.

Figure 2 is a typical front cover of a dental record in Japan, where the dental notation is written directly on the paper medium. Therefore, several symbols are needed for transferring tooth information via electronic media in order to utilize the capabilities of this notation.

The tooth numbering system developed by FDI is used in specialized fields such as epidemiological surveys, international comparisons

Figure 2. A typical front cover of a dental record in Japan

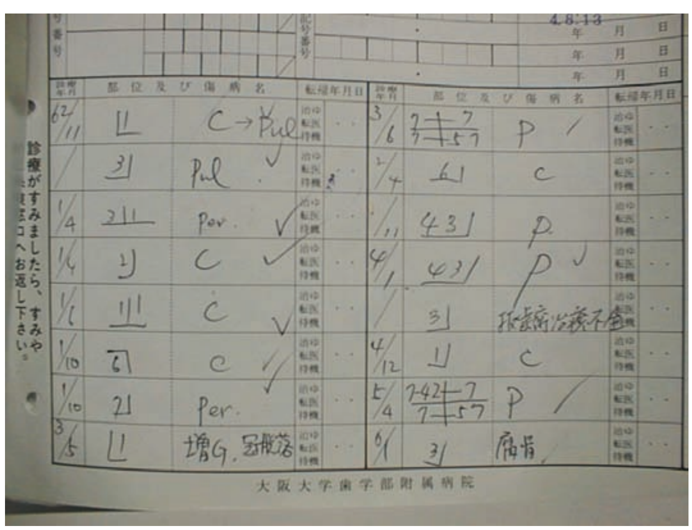

of dental diseases and data bank registrations for maxillo-facial diseases. In other words, the FDI method is not so popular in Japan. Therefore, as the first step of our study, we accumulated all the Japanese symbols concerned with the notation of dental information in the field of dentistry. Some symbols were built-in external characters in the dental hospital information systems, and others were font sets developed individually for the personal computers in dental clinics. The total number of characters was over 320.

The second step was to eliminate the symbols that can be denoted with combinations of conventional alphabetical characters such as (-), (+), (++) and so on. We eliminated the symbols that are closely related to the Japanese health care insurance system, such as circled hiragana and circled kanji, as they will disappear or change their typography when the health care system changes in the future. We also eliminated the symbols that are used rarely in Japan, such as the circled letters A to E for denoting abutment teeth of deciduous dentition.

The third step was grouping the characters. As a result, one group comprises symbols that might have a general application outside the field of dentistry. The next group contains the symbols for denoting the position of human dentition, such as upper jaw, lower jaw, right side of the jaw, left side and so on. The symbols in this group supply the simple numeric notation with additional information about the biological position of the tooth in the jaw. The last group comprises the symbols that denote non-natural human dentition, such as artificial teeth and supernumerary teeth, and other abbreviations. These symbols are used for data exchange in insurance claims.

The fourth step was considering the symbols for denoting the human dentition in one or three lines on monitors and printers, with the remark that one-line notations might save space on a paper medium or a monitor display. Finally, we selected a minimal set of thirty-one symbols.

RESULTS

Figure 3 shows the first group of sixteen numerical symbols enclosed in a circle or a double circle.

Although these signs are not specific to dentistry, we assigned a specific meaning to these modified numerical symbols in accordance with the dental insurance claim system in Japan.

A single-circled numeric indicates that the tooth is an abutment tooth for a bridge, while a double-circled one indicates that the tooth is an abutment tooth with pulp extirpated.

Figure 4 shows nine characters in three groups denoting artificial teeth, supernumerary teeth and an abbreviation for a group of teeth respectively. A triangle with a bar indicates an artificial spacer, especially on a denture, a circle with a bar indicates a supernumerary tooth, and a tilde with a bar indicates an abbreviation for a group of teeth.

Figure 3. The first group of symbols (circled and double-circled numerical symbols) of the proposed system

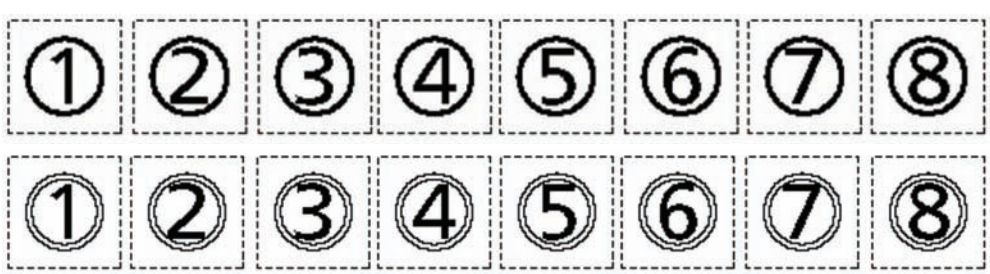

Figure 4. The second group of symbols, denoting artificial teeth, supernumerary teeth and an abbreviation for a group of teeth

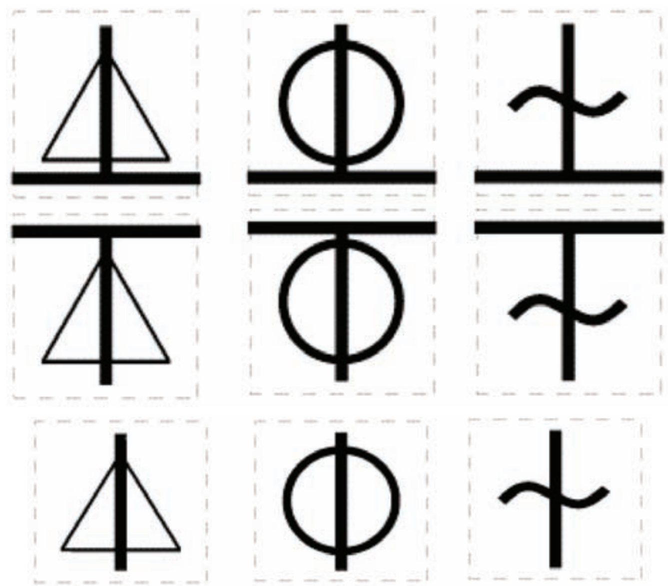

Figure 5. The third group of symbols, which are used for classifying the quadrants of the human jaw

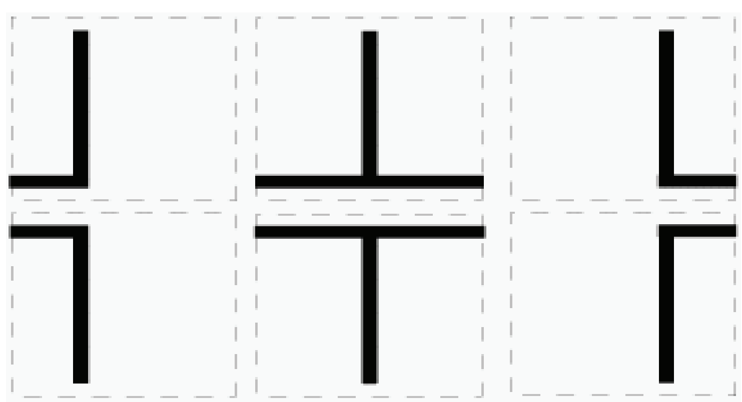

These symbols are not used by themselves but in combination with numerical symbols.

Figure 5 shows six characters used for classifying the quadrants of the human jaw. These symbols are used for clarifying the tooth position with respect to the upper, lower, left and right side of the jaw.

The Unicode system contains all symbols from Figure 3 to Figure 5.

Figure 6 shows a sample of the graphical user interface of a Japanese input method that enables the user to handle Unicode characters, where the user utilizes alphanumeric codes for referring to the symbols in the Unicode Standard table in their documents.

Figure 7 shows several examples of notations with combinations of numerical and Unicode symbols. The example on the first row denotes normal permanent dentition from the upper right

Figure 6. Character table of a Japanese input method

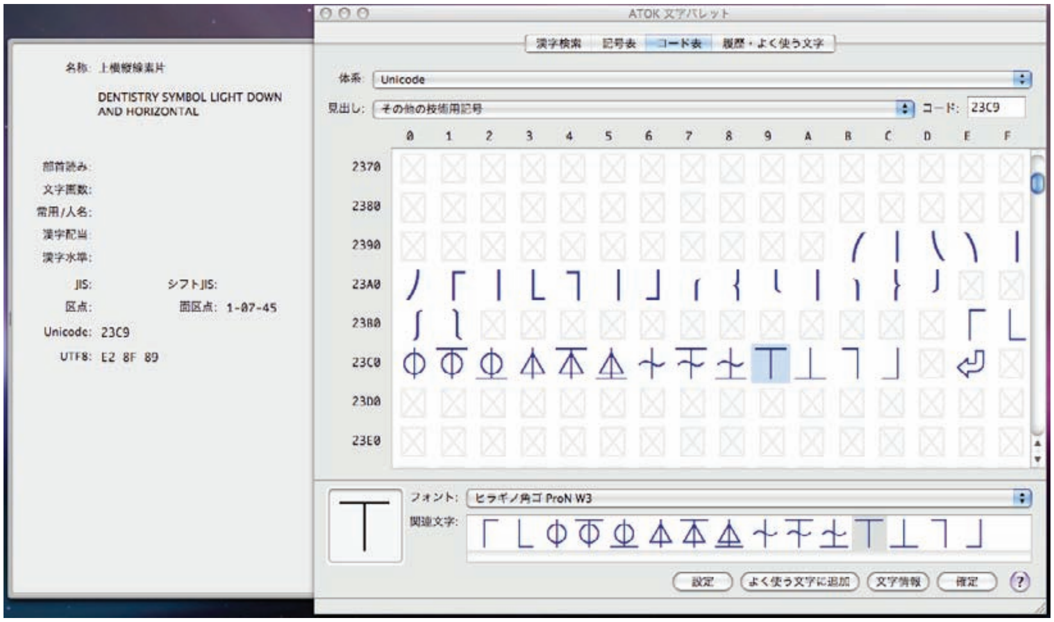

Figure 7. Notation examples indicating normal dentition and a fixed bridge

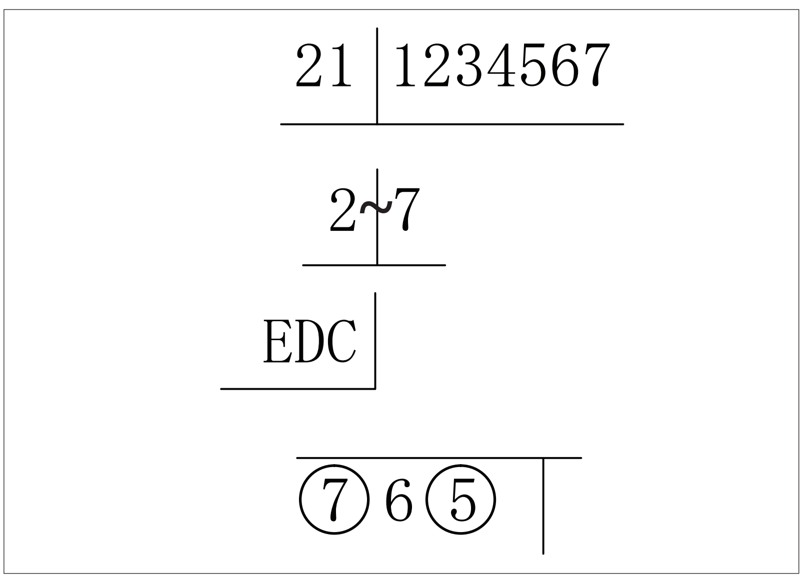

second incisor to the upper left second molar, while the one on the second row refers to the same dentition with the symbol for abbreviation. These two examples in fact indicate the same set of nine permanent teeth. Furthermore, the example on the third row denotes a right upper second deciduous molar, a first deciduous molar and a deciduous canine respectively. In the example on the fourth row, the combination of non-circled and circled numerical symbols indicates a permanent dentition with a fixed bridge as a whole. In insurance claims in Japan, this combination indicates that the right lower first molar is missing and the second premolar and the second molar are abutment teeth.

DISCUSSION

A committee of the American Dental Association (ADA) recommended the use of the Palmer notation method in 1947 (Huszár 1989); however, since this method required the use of specific symbols, it was difficult to implement using a keyboard. As a result, the association officially supported the universal system in 1968 (Ferguson 2005). After that, there was a sharp distinction between the information about the position and the status of the tooth in the dental notation. In this regard, we have described the symbols that enable the notation of both tooth position and related tooth information by virtue of the Unicode system. In this discussion, we describe the problems related to this notation system.

WHO has also developed a standardized data exchange format based on numerical symbols for each tooth that is specially designed for epidemiological use. This format has the advantage of being capable of transferring dentition data over a computer network. However, this information is difficult to visualize since it contains only numerical symbols that are surrounded by unrelated numerical information. Moreover, this system does not have any means of denoting supernumerary teeth.

The symbols in the Unicode Standard are originally derived from the concept in the Japanese insurance claim system that information about tooth position should not be separated from other information about the tooth such as disease name or history of dental treatment. In comparison with medical record systems, for example, internal medicine or pediatrics, it is a specific feature of dentistry to exchange information in digitized form. With some information about disease name, tooth position and treatment history, evidence of the daily treatment activities can be obtained.

As a result of their initial purpose and usage, the symbols contained traces of features specific to the Japanese insurance claim system. However, there is no difference in the way dentistry handles tooth data and other medical data. In order to decrease the influence of the insurance claim system, we have divided the symbols into four groups, where the symbols in the third group (Figure 5) have the potential to become part of a standardized data exchange format due to their simplicity. Moreover, the symbols in the third group provide a base for classifying the quadrants of the human jaw. By combining these symbols with numerical symbols, a clear distinction can be made between tooth data and other information. Also, it is possible to search websites for tooth position data by using a combination of symbols from the Unicode Standard and numerical symbols.

Figure 8 shows a screenshot of our hospital information system that reflects the Zsigmondy-Palmer notation and the treatment history. This format, a set of information such as date, tooth notation, disease name and treatment name, is one of the most typical formats of an electronic patient record in Japanese dentistry (http://law.e-gov.go.jp). However, there is a problem to overcome with respect to these symbols. For example, when the tooth notation continues onto a new line, the position of only the symbols for classifying the quadrants should be compensated on the lower line or the upper line in order to demonstrate the difference between the upper jaw and the lower jaw. Moreover, separated molars, dicuspidized premolars, deciduous abutment teeth with pulpectomy, implanted artificial teeth and transplanted natural teeth can not be denoted using the symbols in the Unicode table alone. However, other tooth notation systems, such as the Universal system and the FDI system, also lack this function.

Figure 8. A sample from an electronic patient record using the Zsigmondy-Palmer notation. It is an important part of the dental history of the patient.

As standalone computers gradually become more and more powerful, and as information technologies make the world an ever more connected place through the Internet, multimedia information is being sent through the Internet with surprising speed. There is a need for a new foundation for exchanging information concerning tooth notation, and the Unicode Standard is one of the good alternatives in this field.

REFERENCES

ANSI INCITS 4-1986 (1963). *American National Standard for Information Systems — Coded Character Sets — 7-Bit American National Standard Code for Information Interchange (7-Bit ASCII).* American National Standards Institute.

Blinkhorn, A., Choi, C., & Paget, H. (1998). An investigation into the use of the FDI tooth notation system by dental schools in the UK. *Eur J Dent Educ*, *2*(1), 39-41.

Charbeneau, G. T. (1975). *Principles and practice of operative dentistry*, 6. Philadelphia, PA: Lea and Febiger.

Ferguson, J. W. (2005). The Palmer notation system and its use with personal computer applications. *Br Dent J.*,*198*(9), 551-3.

http://en.wikipedia.org/wiki/Unicode

http://law.e-gov.go.jp/htmldata/S32/S32F03601000015.html (In Japanese)

http://www.meti.go.jp/kohosys/press/0004964/index.html (In Japanese)

http://www.meti.go.jp/press/past/c60926e1.html (In Japanese)

http://www.unicode.org/

Hussein, R., Engelmann, U., Schroeter, A., & Meinzer H. P. (2004): Internationalization of healthcare applications: a generic approach for PACS workstations. *Methods Inf Med.*, *43*(2), 133-40.

Huszár, G. (1989). The role of the life and works of Adolf Zsigmondy and Ottó Zsigmondy in the history of dentistry. *Fogorv Sz, 82*(12), 357-63.

ISO/IEC 8859-11 (1999): *8-bit single-byte coded graphic character sets, Part 11: Latin/Thai character set* (draft dated June 22, 1999; superseded by ISO/IEC 8859-11:2001, published Dec 15, 2001).

Kilbourne J., & Williams T. (2003). Unicode, UTF-8, ASCII, and SNOMED/CT. *AMIA Annu Symp Proc*. 2003; 892.

Oram, A. (1991). The hidden effects of computer engineering on user documentation. In T. T. Barker (Ed.), *Perspectives on software documentation, inquiries and innovations*. Amityville, NY: Baywood Press.

Palmer, C. (1891). Palmer's dental notation. *Dent. Cosmos, 23*(March), 194.

Shibano K., et al (1999): Approved minutes of the UTC 81 / L2 178 Joint Meeting Mission Viejo, CA –October 26-29.

The Unicode Standard, Version 5.0, Fifth Edition (2006). *The Unicode Consortium*. Addison-Wesley Professional, 27 October 2006. ISBN 0-321-48091-0

Zsigmondy A. (1874). A practical method for rapidly noting dental observations and operations. *Br. J. Dent. Science, 17,* 580.

KEY TERMS

ADA: American Dental Association

ASCII: American Standard Code for Information Interchange. The ASCII codeset contains a bit representation for each uppercase and lowercase alphabetic letter as well as punctuation, numbers, and control codes.

Character Code Set: A codeset, or coded character set, is a set of unambiguous rules that establishes a character set and the one-to-one relationship between each character in the character set and its bit representation.

Chinese Characters: Characters associated with an ideographic writing system such as Chinese, Japanese and Korean typically are encoded in more than one byte because the character repertoire has tens of thousands of characters.

Diacritic Marks: A diacritic, also called diacritical mark, point, or sign, is a small sign added to a letter to alter pronunciation or to distinguish between similar words.

Double-Byte Characters: A character set where each graphic character is encoded in two bytes

EUC-JP: Extended Unix Code (EUC) is a multibyte character encoding system used primarily for Japanese, Korean, and simplified Chinese. The structure of EUC is based on the ISO-2022 standard, which specifies a way to represent character sets containing a maximum of 94 characters, or 8836 (94^2) characters, or 830584 (94^3) characters, as sequences of 7-bit codes.

FDI: Fédération Dentaire Internationale

Graphemes: In typography, a grapheme is the fundamental unit in written language. Graphemes include alphabetic letters, Chinese characters, numerals, punctuation marks, and all the individual symbols of any of the world's writing systems.

Human Dentition: Dentition is the development of teeth and their arrangement in the mouth. The dentition can be expressed as a dental formula.

Ideographic Writing Systems: Ideographic writing systems consist of ideographs or pictographs that represent the meaning of a word, not the sounds of a language. Chinese and Japanese are examples of ideographic writing systems that are based on tens of thousands of ideographs.

ISO: The International Organization for Standardization. ISO is an international-standard-setting body composed of representatives from various national standards organizations.

ISO-3950: Also known as FDI World Dental Federation Two-Digit Notation

ISO 8859 Standard: While the bit patterns of the 95 printable ASCII characters are sufficient to exchange information in modern English, most other languages that use the Latin alphabet need additional symbols not covered by ASCII, such as ß (German), ñ (Spanish), å (Swedish and other Nordic languages) and ő (Hungarian). ISO/IEC 8859 sought to remedy this problem by utilizing the eighth bit in an 8-bit byte in order to allow positions for another 128 characters.

JIS: Japan Industrial Standard

JIS X 0208: JIS X 0208 is a Japanese Industrial Standard defining a set of kanji indexed by a pair of integers from 1 to 94 (this is known as the kuten pair of the kanji). This standard was previously known as JIS-C-6226.

JIS X 0213: JIS X 0213 is a Japanese Industrial Standard defining coded character sets for encoding the characters used in Japan. This standard extends JIS X 0208. The first version was published in 2000 and revised in 2004 (JIS2004). As well as adding a number of special characters, characters with diacritic marks, etc., it included an additional 3,625 kanji. The name of this standard is 7-bit and 8-bit double byte coded extended kanji sets for information interchange.

Palmer: C. Palmer

Shift-JIS: Shift JIS (also SJIS, MIME name Shift_JIS) is a character encoding for the Japanese language originally developed by a Japanese company called ASCII Corporation in conjunction with Microsoft and standardized as JIS X 0208 Appendix 1.

Technical Symbols: Technical symbols are related to and used in the various technical, programing language and academic professions. Miscellaneous Technical is a Unicode character block.

Tooth Notation: Associating information to a specific tooth. Three most commons systems are described in this paper.

Toponyms: Place-names. A toponym is a name of a locality, region, or some other part of Earth's surface, including natural features (such as streams) and artificial ones (such as cities).

Two-Digit Numbering System: Each quadrant of the mouth is assigned a number from 1 to 4 for the permanent teeth for example. One of eight teeth in the quadrant is assigned a number from 1 to 8. These two-digit represent the position of the teeth.

Unicode Character Code: In computing, Unicode is an industry standard allowing computers to consistently represent and manipulate text expressed in most of the world's writing systems. Unicode has its own character code.

Unicode-Compliant OS: Computer operation system that enables Unicode font sets so that applications on this OS handles almost all the language in the world. Mac *OS X* is *Unicode compliant* Windows based *Unicode compliant OS* are Windows 2000/XP/VISTA/2000 Server/2003 Server.

Universal Numbering System: One of simplified method of identifying teeth. It has been adopted by the American Dental Association and is in use by most general dentists today in the United States.

WHO: World Health Organization

Zsigmondy: Adolf Zsigmondy, Hungarian dentist

Chapter XVIII
Virtual Dental Patient:
A 3D Oral Cavity Model and its Use in Haptics-Based Virtual Reality Cavity Preparation in Endodontics

Nikos Nikolaidis
Aristotle University of Thessaloniki, Greece

Ioannis Marras
Aristotle University of Thessaloniki, Greece

Georgios Mikrogeorgis
Aristotle University of Thessaloniki, Greece

Kleoniki Lyroudia
Aristotle University of Thessaloniki, Greece

Ioannis Pitas
Aristotle University of Thessaloniki, Greece

ABSTRACT

The availability of datasets comprising of digitized images of human body cross sections (as well as images acquired with other modalities such as CT and MRI) along with the recent advances in fields like graphics, 3D visualization, virtual reality, 2D and 3D image processing and analysis (segmentation, registration, filtering, etc.) have given rise to a broad range of educational, diagnostic and treatment planning applications, such as virtual anatomy and digital atlases, virtual endoscopy, intervention planning etc. This chapter describes efforts towards the creation of the Virtual Dental Patient (VDP) i.e. a 3D face and oral cavity model constructed using human anatomical data that is accompanied by detailed teeth models obtained from digitized cross sections of extracted teeth. VDP can be animated and adapted to the characteristics of a specific patient. Numerous dentistry-related applications can be *envisioned for the created VDP model. Here we focus on its use in a virtual tooth drilling system whose aim is to aid dentists, dental students and researchers in getting acquainted with the handling of drilling instruments and the skills and challenges associated with cavity preparation procedures in endodontic therapy. Virtual drilling can be performed within the VDP oral cavity, on 3D volumetric and surface models (meshes) of virtual teeth. The drilling procedure is controlled by the Phantom Desktop (Sensable Technologies Inc., Woburn, MA) force feedback haptic device. The application is a very promising educational and research tool that allows the user to practice in a realistic manner virtual tooth drilling for endodontic treatment cavity preparation and other related tasks.*

INTRODUCTION

Creation of datasets comprising of digitized images of cross sections of the entire human body (as well as images acquired with other imaging modalities such as CT and MRI) has been a major breakthrough in biomedical imaging and related fields. The first such dataset was created as a result of the National Institute of Health (NIH) Visible Human Project (Ackerman, 1998; Banvard, 2002). Within this project, a male (1994) and a female (1995) cadaver were embedded in blue gelatin, frozen and sliced at 1 mm (0.33mm for the female cadaver) cryosections, thus producing two sets of transversal body slices. Each layer of the body was photographed at a resolution of 2048 x 1216 pixels and 24 bits color depth to create the Visible Human Male (VHM) and Visible Human Female (VHF) datasets. Axial MRI images of the head and neck, and longitudinal sections of the rest of the body as well as axial CT scans of the entire body were also produced. Recently, a Chinese project (Zhang et al., 2006) resulted in the creation of five Chinese Visible Human datasets, whose creators claim that consist of images of greater integrity and have better blood vessel identification than their US counterparts. Korean scientists have also completed the Visible Korean Human (VKH) project (Park et al., 2005). These Visible Human datasets (especially VHM, VHF) have given rise to a wide range of educational, diagnostic, treatment planning and virtual reality applications such as virtual anatomy and digital atlases, virtual endoscopy, surgery planning etc. Some characteristic examples are described in Robb and Hanson (2006).

Apart from medicine, digitized anatomical head images are also a valuable asset for dentistry. Such images can be used for the construction of 3D models for the anatomical education of dentistry students. In addition, such models can be incorporated in virtual reality applications that aim at familiarizing students with (virtual) dental instruments and their use in a number of dental procedures. Especially in the field of endodontics, the success of an endodontic therapy depends on many factors, two of them being the thorough knowledge of the internal tooth anatomy and the appropriate pulp cavity access. Indeed, the knowledge of tooth anatomy and good practice in dental drilling for cavity preparation are important parts of a dental student training that can help him/her learn how to achieve correct access of the root canal system during the endodontic therapy. Usually, dental students learn how to obtain root canal access on artificial teeth and jaws that are sometimes placed within a manikin head, using dental instruments and burs before, they perform this procedure on real patients.

Thus, novel educational tools that would help students in obtaining solid knowledge of the tooth anatomy and practicing pulp cavity access procedures are of great interest to the endodontics community. This chapter describes efforts towards this direction. More specifically, it deals with the creation of the Virtual Dental Patient (VDP), namely a 3D face and oral cavity model which was constructed using VHM anatomical data. This model is accompanied by detailed 3D teeth models obtained from digitized cross sections of a large number of extracted teeth (Lyroudia 2000, Lyroudia, et al. 2002). Using these models, students can get familiar with both the internal tooth anatomy and the anatomy of the maxillofacial region. The VDP can be adapted to the characteristics of a specific patient by using facial photographs or 3D surface data for this patient. It can be also animated so as to perform basic facial and head movements. The developed models have been used in a virtual tooth drilling system, whose aim is to aid dentists, dental students and researchers in getting acquainted with the handling of drilling instruments and the skills and challenges associated with cavity preparation procedures in endodontic therapy (Lyroudia et al 2002, Marras, et al. 2008). Virtual drilling can be performed within the VDP oral cavity, on 3D volumetric and surface models (meshes) of teeth. The dental bur is controlled by the Phantom Desktop (Sensable Technologies Inc., Woburn, MA) force feedback haptic device (Sensable Technologies Inc., 2006).

This chapter is organized as follows. Background work on this topic is described first. Then, the methodology used for the creation of a database of 3D surface and volumetric teeth models of various types is described. The construction of the face/oral cavity model and the adaptation, personalization and animation of the model are presented next, followed by a section detailing the virtual tooth drilling procedure. Directions for future work and conclusions are provided in the last two sections.

BACKGROUND

A number of commercially available 3D anatomical models (consisting mainly of triangle meshes) of the entire human body or its parts have been developed in the last years. These models have been constructed using a variety of approaches. 3D scanning of real body parts or anatomical casts (e.g. teeth of skeletal parts) followed by editing of the resulting models by experienced modelers/artists and doctors/dentists is such an approach. Manual delineation of organs/structures on each slice of a set of MRI/CT scans or cryosections from the Visible Human datasets, followed by surface reconstruction by triangulation and post-processing by artists/experts is another approach. Pictures from photographic illustrative atlases have also been used as source material for modeling. The triangle count of these models is usually high or very high and the degree of visual realism extremely good, enhanced, in most cases, by texture mapping. Usually, each organ is individually modeled and organs belonging to the same system are grouped together. Only a few models focus on areas that are of interest in dentistry and endodontics, such as the oral cavity and face/neck area. The uses for these models vary. Most of them are used for educational purposes and are usually incorporated in computer applications that allow the user to interact with the models (add or remove organs and systems, rotate them etc.). In such cases, the actual models are not directly available. Examples include the models in VH Dissector (Touch of Life Technologies Inc, Aurora, CO), 3D Head & Neck Anatomy for Dentistry (Primal Pictures LTD, London, UK) and Voxel-Man 3D Navigator (University Medical Center Hamburg-Eppendorf, Hamburg, Germany) applications. Others have been constructed for the production of educational videos, commercials, feature length films, medical illustrations, etc. These models are available for sale and are sometimes processed (skinned, rigged), so as to facilitate subsequent animation. The male and female anatomy collections (Zygote Media Group Inc, Lindon, UT) are examples of models in this category. Disadvantages of these models (at least for the scientific community) include their proprietary/commercial nature, the big polygon count that can hamper real-time animation attempts, and, the lack in most cases of anatomical landmarks among the vertices of the model.

In endodontics, the knowledge of the external and internal teeth morphology is essential for the clinical practitioner. 3D reconstruction methods, which result in 3D models that allow observations from arbitrary viewpoints, are gradually replacing the more limited 2D methods for the study of internal tooth morphology. At first, the 3D study of the teeth anatomy has been performed by 3D models created by tracing the contours of the teeth and the pulp chambers on the specimens serial cross sections (Berutti, 1993; Blasković-Subat et al., 1995; Hirano & Aoba 1995; Lyroudia et al., 1997a; Lyroudia et al., 1997b; Mikrogeorgis et al., 1999; Lyroudia, 2000; Han et al., 1998). The main disadvantage of this methodology is that the specimens have to be destroyed to prepare the cross sections and accurate images cannot be obtained because of the slice thickness.

The advanced X-ray computed transaxial microtomography, or microCT, has been used in the recent years as a good alternative. MicroCT is a non-invasive method that provides the ability to accurately visualize the root canal morphology, without resulting into teeth destruction (Nielsen et al., 1995; Rhodes et al., 2000; Bergmans et al., 2001). However, early studies using microCT were hampered by insufficient quality and resolution and projection errors (Nielsen, et al. 1995). Significant improvements in both software and hardware reduced section thickness to 81 micrometers (Rhodes, et al. 1999), 34 μm (Peters, et al. 2000) and 12.5 μm (Bergmans et al., 2003). The microCT technique, with a resolution of at least 100 μm, has proven to be useful as a non-destructive method for 3D reconstruction of teeth ex vivo (Oi et al., 2004; Plotino et al., 2006; Kim et al., 2007). Nevertheless, the prolonged scanning and reconstruction time -up to 4 hours per specimen (Nielsen et al., 1995; Rhodes et al., 2000) - comprise a factor that limits the efficiency of this method. Moreover, this method requires costly and sophisticated hardware and software that has to be supported and serviced by experienced personnel. Such conditions can be met only in well equipped and organised research centers (Rhodes et al., 2000; Stamm et al., 2003).

Several papers have reported the use of virtual reality technology in orthodontics (Carriere, J. and Carriere, L., 1995; Snow et al., 1996), restorative dentistry (Herder et al., 1996), orthognathic surgery (Wagner et al., 1997), implantology (Verstreken et al., 1996; Seipel et al., 1998), oral implant surgery (Kusumoto et al., 2006) and endodontics (Lyroudia et al., 2002) with encouraging results. Moreover, virtual-reality based cavity preparation training systems have been introduced in recent years, such as DentSim™ system (Denx Corp, Jerusalem, Israel) (Rose et al., 1999) and others (Ranta and Aviles, 1999; Wang et al., 2005; Yau and Hsu, 2006; Kim et al., 2005).

The DentSim™ system (Denx Corp, Jerusalem, Israel) (Rose et al., 1999) comprises of a real dental unit, a manikin head, a tracking system and software that allows student to view the results of his/her cavity preparation in the manikin head on 3D models on a computer monitor and compare them with the results of an optimal preparation. The system described in Ranta and Aviles (1999) involves a standalone 3D virtual tooth and a Phantom haptic device that enables the trainee to perform virtual drilling, while receiving appropriate force feedback. The system utilizes a stereoscopic display and a volumetric tooth representation, divided into different regions simulating different materials. The user can utilize a virtual pick to probe the tooth, a drill for cavity preparation and a carrier to fill the cavity with amalgam. In Wang et al. (2005), a triangular mesh is used for modeling the standalone tooth and the cutting tool is assumed to be represented by an analytical model (e.g. a sphere). A force model based on the penetration distance between the tool and the tooth is formulated and a local vertex deformation procedure is used to simulate material removal. The stability of the haptic simulation is also studied. In Yau and Hsu (2006), a 3D object modeling approach that utilizes surface elements (surfels) is utilized to model the tooth and the dental bur, in an effort to improve visual quality and rendering rate. A Boolean operator is used to determine surfels that have to be removed due to drilling. The method utilizes adaptive collision detection and an octree for storing the teeth data. In Kim et al. (2005), a volumetric tooth representation is utilized in a standalone virtual tooth drilling application. The tooth volumetric properties (stiffness, color) are contained into the volumetric representation and are used during the drilling procedure. The application can also generate simulated drill/tooth physical contact sound for increased realism. The application runs in a so-called multi-modal workbench that incorporates a stereo display, a Phantom haptic device, a SpaceMouse as a 6 DOF position device and an audio system. The three systems described in these papers operate on standalone teeth and the focus is on providing realistic material removal simulation as well as realistic haptic force rendering. In contrast, the dental drilling simulator described in this chapter incorporates the VDP 3D model of the maxillofacial region, the oral cavity and the teeth, so that dentistry students and researchers can get acquainted with the anatomy of the maxillofacial region and develop their dental drilling skills within a more realistic virtual environment.

3D TEETH RECONSTRUCTION

During the last ten years, our group has created a database of surface and volumetric 3D teeth models from different tooth categories. These models were generated from serial cross sections of properly prepared teeth and are part of the Virtual Dental Patient model. A description of these efforts and details regarding the creation procedure are provided in the following subsections.

Surface Reconstruction of Teeth

A database of teeth from different tooth categories was collected, prepared and reconstructed, using surface three-dimensional reconstruction from cross sections, as detailed in Lyroudia (2000). The first efforts towards this direction included the reconstruction of two C-shaped mandibular molars for the study of their internal morphology (Lyroudia et al, 1997a). Later on, reconstruction of two "double teeth" (Lyroudia et al, 1997b) and six teeth with morphological abnormalities (Mikrogeorgis et al, 1999) was performed. The steps that were followed in all these cases were the following:

- **Teeth preparation:** The teeth that were used were cleaned under running water and were placed in a 3% NaOCl solution for 24 hours. They were then embedded in a two-component polyester resin and numerous serial cross sections were taken from each specimen, by using a special microtome for hard tissues (Isomet, Buehler, Illinois, USA). The number of serial sections for each tooth depended on its size and shape, ranging between 12- 25 sections. The thickness of each section was 0.75-1mm.
- **Image digitization:** Indirect or direct digitization of the cross sections was performed using a stereoscopic microscope (Stemy SV8, Zeiss, Wetzlar or Stemi 2000-C, Zeiss, Wetzlar, Germany). During the indirect digitization, photographs of each section were taken and then digitized. The number of the photographs was different for each section depending on the size of the section.

Figure 1. Indirect digitization and collage of a number of grayscale images from a cross section of a maxillary molar.

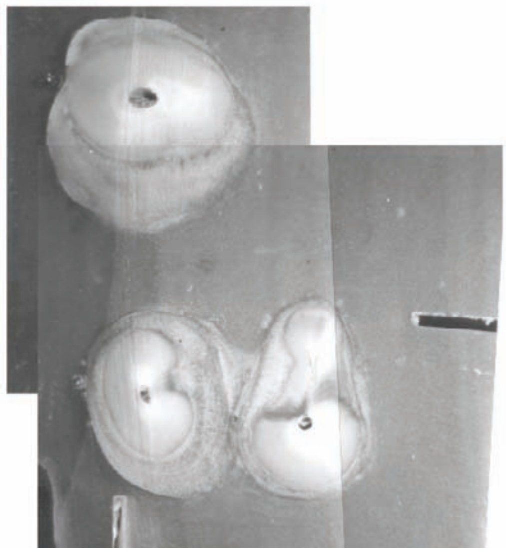

During direct digitization, the images of the sections were transferred directly, through a digital camera, in a personal computer.

- **Image mosaicing:** In order to obtain sufficient magnification, a number of overlapping photographs (indirect digitization) (Figure 1) or overlapping digital images (direct digitization) of the serial sections were taken. These were then assembled by using PhotoShop (Adobe Systems Inc.) in order to reconstruct the entire image of each section. Image registration techniques included in the software package EIKONA 3D (Alpha Tec Ltd, Thessaloniki, Greece) were used as well in order to create the image collage.
- **Alignment:** The acquisition procedure for the cross section images introduces alignment discrepancies between object profiles in consecutive cross sections. Although correlation-based automatic alignment techniques can be used, the results obtained might not be very accurate. Besides, the automatic alignment can produce artificial symmetry of the object under reconstruction. Therefore, the method that was selected was manual alignment involving two consecutive slices at each time. The two slices were displayed one atop the other, the upper image being displayed in a transparent mode. The user used the mouse to move (rotate, translate) the upper so image, so as to align it with the lower one. This procedure was applied repeatedly, until all images were aligned. The image registration techniques that were used in the mosaicing step were also applied in certain instances along with the above procedure for better slice alignment.
- **Contour following:** In order to proceed to the 3D surface reconstruction of the structure under study, one has to specify the contours delineating the objects of interest in each sec-

Figure 2. Contour following of the external and internal surfaces of the section of Figure 1

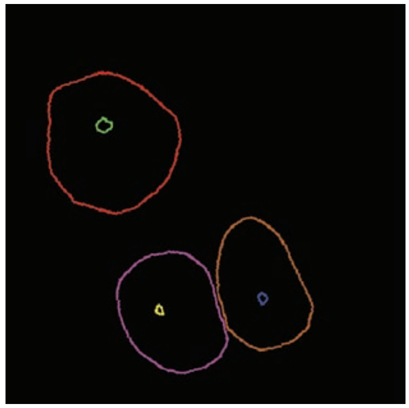

Figure 3. Three-dimensional surface reconstruction of a maxillary molar

tion image. This can be done either directly, using boundary/edge detection techniques or indirectly, by segmenting the objects of interest from the background. The method that was selected in most of the cases was manual contour following. An experienced user utilized the mouse to draw the boundaries of the objects of interest, namely the external surface of the tooth and the internal surface of the root canals (Figure 2). Different colors were used for the contours of different objects. The developed software allowed also contour corrections.

- **Contour matching-triangulation:** During this stage the user was asked to match the color-coded contours on pairs of sections, i.e., to specify the correspondences between contours. Branching was handled by matching two or more contours in one section with the same contour in the other section. Then, an automatic triangulation algorithm was used to reconstruct the object(s) surface. Objects were assigned a material and an opacity value by the user and triangles were shaded to produce the final tooth visualization (Figure 3). The visualized teeth can

Figure 4. Frame gallery showing the final set of tooth sections (after interpolation) used for the volume reconstruction of a maxillary premolar

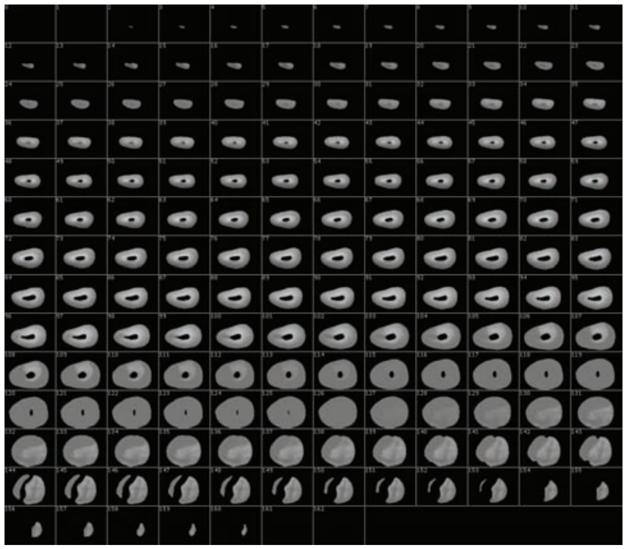

be cut using a cutting plane to reveal their interior structure. They can also be rotated or moved interactively, thus helping the viewer to understand their 3-D structure.

Volume Reconstruction of Teeth

Volumetric models were created for all teeth. The same teeth that were used for surface reconstruction were used for volume reconstruction as well. The steps up to (and including) contour following that were described in the previous subsection were applied in this case too. Since the pixel size within the resulting processed slices (depicting the segmented hard dental tissues) is different -actually smaller - from the spacing between two adjacent slices, interpolation of additional slices (Figure 4) in order to obtain an accurate, isotropic, volumetric description of the volume was performed. A binary, shape-based interpolation method using morphology morphing has been used for this purpose (Bors et al., 2002). This approach relies on erosions and dilations for morphing consecutive 2-D shape sets into one another. This morphing transformation is applied iteratively onto the sets obtained from the previous morphing, resulting into new intermediary sets. Eventually, these morphological transformations lead to sets which are closer in shape and size and finally, in their idempotency. The interpolation process is applied to all consecutive pairs of slices that form a tooth volume. Volume filtering that aimed at tooth surface smoothing was also applied. The resulting volumetric models (Figure 5) can be seen in a user-selected semi-transparent mode and be freely rotated and scaled for better viewing.

ANATOMICAL MODELING OF THE FACE AND THE ORAL CAVITY

In order to create a realistic face/oral cavity model for VDP, a large number of anatomically meaningful points were manually marked on various head tissues depicted on anatomical cryosections and computer tomography (CT) data of the Visible Human male cadaver. A sub-

Figure 5. Volume reconstruction of a maxillary premolar

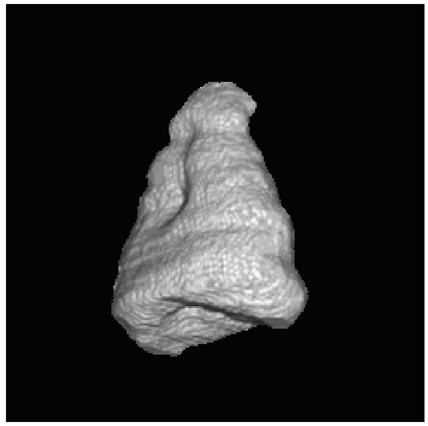

Figure 6. The VDP face/oral cavity 3D model

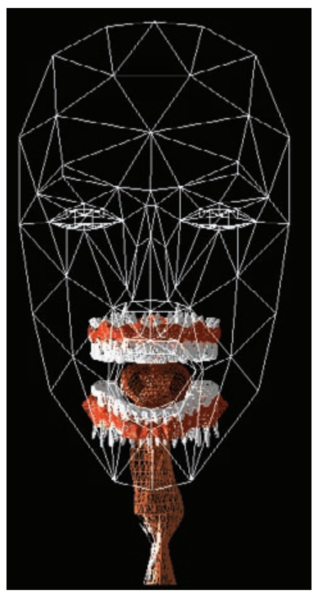

set of 377 section images corresponding to the head was used. The pixel spacing in the *X* and *Y* directions of these data is 0.33 mm, while that in the *Z* direction (distance between sections) is 1 mm. Hence, in order to create a 3D volume with isotropic voxels, we performed linear slice interpolation along the *Z* axis with a scale factor of 3. By employing simultaneously transversal, sagittal and coronal views of the head volume, we were able to visually identify the tissues and anatomical entities, which were our modeling targets. We have used the mouse to obtain the 3D coordinates of the internal or external points of interest in each rendered anatomical entity. In addition, we have used the part of the Visible Human CT dataset, which consists of scans of the frozen cadaver. These scans were used in order to identify bone structures, such as the mandible or palatal bones, since hard tissues are easier to distinguish in CT images. Appropriate scaling was applied in order to bring the CT data in the same scale as the corresponding anatomical data. The resulting 3D surface model consists of ten anatomical entities, namely, the external face area, the internal surface of lips and cheeks, the mandible, the tongue, the gums and the teeth of the upper and lower jaw, the larynx and, finally, the uvula (Figure 6). We have concentrated on modeling the inner surfaces of the human head in the area of the oral cavity, because our primary target is dental applications.

Each anatomical entity is represented as a separate triangular mesh, but various entities can be combined to build more complex structures, thus creating a hierarchical model. For example, the mesh that describes the mandible bone can be combined with the one that represents the gums and the teeth to form the lower jaw. This hierarchical structure facilitates the animation of the whole model by defining the interdependencies between parts. Moreover, it allows the selective visualization of a subset of these entities.

The constructed model is not an overly detailed one. It comprises of anatomically meaningful and important 3D points (landmarks) that capture only the essential elements of the geometry of the modeled anatomical structures. The number of points selected to define each structure was chosen to be the minimum number required to express the anatomical geometry of these parts, as well as their dynamics and functionality, in case of model animation. Moreover, only the external surface of the structures of interest has been modeled. These choices allow for model compatibility with the MPEG-4 external face models, ensure that the computational complexity for handling the model is sufficiently low and create a model comprising of anatomically meaningful landmarks, instead of an overly detailed model comprising of thousands of vertices, which might be good for artistic visualization/animation but not for the envisaged scientific applications.

During modeling, we assumed that any 3D surface of a prototype human head tissue has plane symmetry with respect to the *YZ* plane in the neutral posture and enforced this symmetry by proper modifications of the acquired 3D model points. This enforced symmetry of the head sur-

Figure 7. VDP model adaptation using two facial photographs

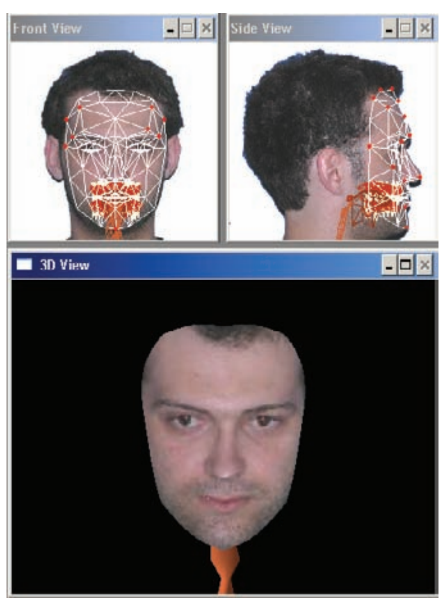

faces is obviously an idealization of the reality. However, it was adopted, since our aim was to create not a model of the Visible Human male head but a generic model.

In total, the model comprises of 1392 vertices and 2209 triangles. The model of the external face area was created by adapting the CANDIDE–3 3D face model (Ahlberg, 2001) to the NIH data. In essence, the created model is an extension of the CANDIDE-3 face model that includes the oral cavity. More details can be found in (Moschos et al., 2004).

MODEL ADAPTATION: PERSONALIZATION

The VDP generic facial and oral cavity 3D model can be adapted to the particular characteristics of an individual. This is achieved using a semi-automatic approach that utilizes two photographs of the person; a frontal one and a side one (Figure 7). The adaptation is supported by a 2D Finite Element Model (FEM). The selected adaptation approach offers speed, reliability and requires only a small amount of user interaction. The process consists of two steps as explained below.

In the first step, the facial model, which is overlaid on the two photographs, is being translated and scaled by the user so as to achieve a coarse alignment. The models of the oral cavity anatomical structures are also scaled and translated automatically in the same way as the facial model.

In the second step, the user performs a detailed adaptation and fitting of the 3D model on the photographs. This step involves a real-time 2D FEM method (Bathe, 1996). Essentially, the model 3D-mesh is represented as a system of springs that are deformed through user interaction. In more detail, the user moves with the mouse a small number (6-10) of mesh vertices so as to bring them into alignment with the corresponding points in the picture. For example, the user moves with the mouse the point of the 3D mesh that corresponds to the mouth corner and places it over the mouth corner of the person depicted in the photographs. Subsequently, the FEM moves the remaining vertices of the mesh, i.e., those that have not been placed by the user. Since this

Figure 8. Selection through a GUI of the teeth of the virtual patient that will be displayed

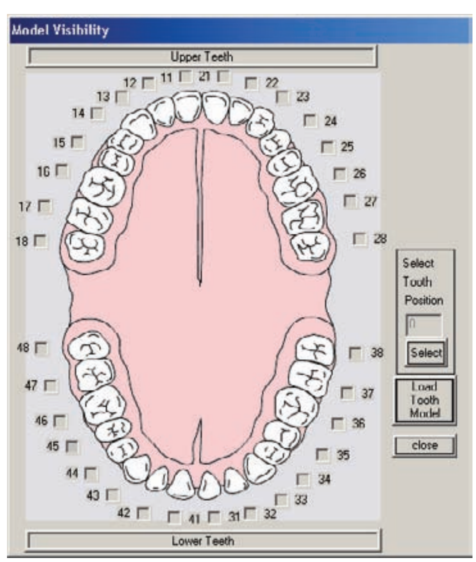

operation takes place in real time, the user can see the results of the interactive adaptation and proceed in corrections.

The FEM-based user-assisted adaptation is applied only on the facial part of the model, whereas the models of the oral cavity anatomical structures (palate, tongue, gums, teeth, etc) are translated and scaled according to the position and scale of the model mouth or the width of the jaws.

In addition, the user can opt to remove some of the teeth of the model. This feature can be used in order to create models of patients that lack some of their teeth. Selection of the teeth to be removed is performed through a graphic interface that depicts all teeth (Figure 8). The user can also select to render only certain parts of the model (face, gums, tongue etc.).

At the end of the adaptation procedure, additional realism can be achieved by applying the facial photographs on the 3D face model through texture mapping.

MODEL ANIMATION

The Virtual Dental Patient provides compatibility with the facial animation part of the MPEG-4 standard, in order to facilitate model animation. In more detail, the VDP includes a Face Animation Parameters (FAP) player that reads stored FAP files (files that describe the movement of certain points of the 3D model) and uses them to animate the model (Figure 9). For example, a file that instructs the model to open its mouth and protract its tongue can be applied. The user can save the model pose at certain instances of the VDP animation in VRML format.

Since the MPEG-4 facial animation standard deals only with facial movements, the VDP has to control the movement of the intraoral anatomical structures, which are not covered by the standard. More specifically, it controls the movement of the lower jaw, i.e., its rotation around the corresponding axis. The user specifies this axis during the model adaptation procedure described in the previous section. The movement of the vertex that represents the tip of the chin is used to control the angle of rotation of the jaw around this axis. The lower teeth, gum and tongue follow the rotation of the jaw. Furthermore, the VDP controls the horizontal movement of the lower jaw. In more detail, the influenced sub-models (teeth, gums, jaw, etc) are translated along the *X* axis for the same distance and direction as the tip of the chin.

During the animation, the curved Point-Normal triangles real time mesh subdivision technique (Vlachos, 2001) - i.e., a technique for

Figure 9. Frames extracted from an MPEG-4 video file

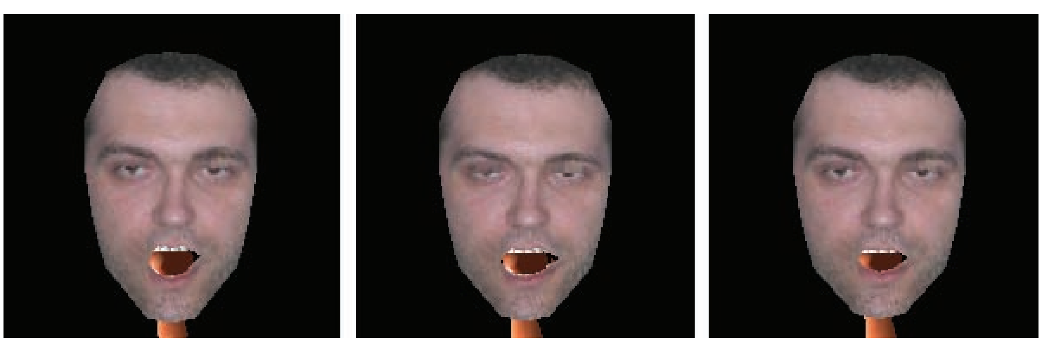

the generation of a more refined 3D model through the recursive subdivision of the initial triangles- is applied in order to improve the visual quality of the models and obtain smooth surfaces.

VIRTUAL TOOTH DRILLING

Based on the VDP model, a drilling application that allows the user to perform virtual drilling has been developed. Before drilling, the limited resolution (low triangle count) prototype of the virtual tooth, where drilling is to be performed, is replaced by a more detailed model within the oral cavity. In order to do so, the user provides the 3D volumetric (voxel-based) model of this tooth. As already mentioned above, this model is in the form of digitized serial cross sections, where the structures of interest (external tooth surface and root canals) have been segmented. The application loads the volumetric representation of the selected tooth and applies the Discrete Marching Cubes algorithm (Montani et al., 1994) in order to obtain its surface (mesh) representation and embed it in the face/oral cavity model. The insertion of this tooth in the VDP face/oral cavity model is performed in two steps:

Coarse automatic placement on the gums by utilizing information regarding the size of the teeth and the alveolus.

Manual adjustment, which is optional and can involve combinations of rotation, translation and scaling.

The volumetric tooth representation is required since the removal of tooth material that takes place during drilling is implemented as a series of mathematical morphology operations (namely erosions) on this representation. In more detail, the drilling operations are simulated using a series of successive erosions involving 3D structuring elements that represent the shape of drilling tools (dental burs) (Nikopoulos and Pitas, 1997). This approach can be used to implement drilling tools of almost all shapes. The application includes dental burs of four basic shapes, namely a spherical, a cylindrical, a cylindrical-conical and a conical one (Figure 10). The user can choose the desired drilling tool and set its shape-controlling parameters (for example, the radius of the spherical tool). The parameters of a drilling tool can be saved for future use. In addition, the application features a database of virtual dental burs, whose shape and dimensions correspond to commercially available ones.

Figure 10. A spherical virtual dental bur

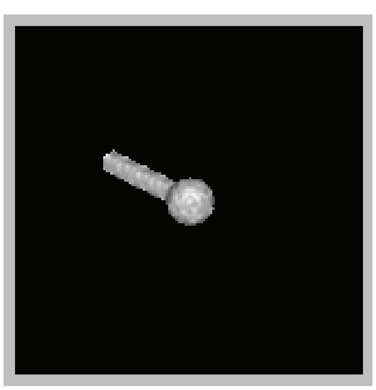

Figure 11. The Phantom Haptic Device

Two additional operations can be performed on the volumetric tooth model. The user can add material on the surface of the volume, an operation that is implemented through 3D dilations. He/she can also perform local smoothing of the volume surface. To do so, the user selects an appropriate smoothing window and moves the mouse or the haptic device (see below) over the surface, in areas that need to be smoothed.

The user can select to perform the dental drilling operation on a standalone volumetric model of a tooth, by using the mouse. However, for more realism, he/she can choose to perform drilling within the VDP oral and maxillofacial 3D model, on the surface model of the inserted tooth. In this case, the virtual dental bur can be controlled either by the mouse or by a haptic device. The Phantom Desktop six degrees of freedom positional sensing force feedback haptic device has been used for this purpose (Figure 11). The main component of this device is a serial feedback arm that ends with a stylus. Only three of the six degrees of freedom of the arm are active, providing translational force feedback along the three axes. Thus, while using the stylus for controlling the position and orientation of the virtual dental bur, the user senses contact / resistance forces during drilling (Figure 12). A realistic model of these forces is used. This model uses information from the volumetric representation (intensity, local surface gradients) in order to evaluate the components of the feedback force, namely the friction force, the compressive force and the viscosity friction (Lundin et al., 2002). The user-defined properties of the object (stiffness, static and dynamic friction) are involved in the evaluation of the force values. The stylus-controlled virtual dental bur is visible as a simple mesh model in the scene.

During the material removal operation, the application uses the internally available dual surface/volumetric representation of the tooth. This dual representation is necessary, since the SDK (Sensable Technologies Inc., Woburn, MA) (Sensable Technologies Inc., 2006) that has been used for handling the tool-tooth haptic interaction requires that the object is in a surface (mesh) representation whereas the proposed mathematical morphology-based material removal algorithm operates on the voxel-based teeth representation. The procedure is as follows. The position of the tip of the drilling tool (namely, the so-called haptic interface point) on the surface representation of the tooth is obtained through collision detection and is used to find the corresponding position on the tooth's volumetric representation. Then, 3D erosions are performed at this position of the volumetric model and the surface model is updated on the haptic device scene graph, so as to reflect

Figure 12. Using the phantom desktop haptic device with the virtual teeth drilling application

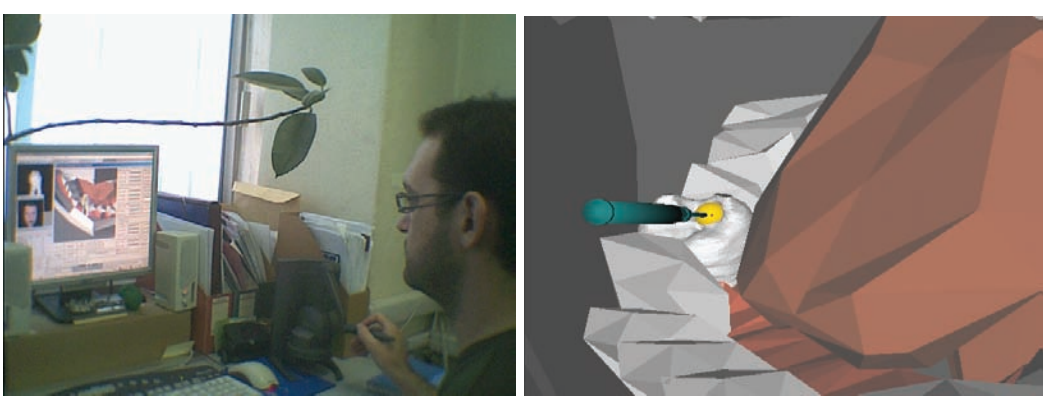

the induced surface changes. In order to reduce the update time, the fact that only local updating of the surface model is required is utilized. This is achieved by the local application of the Discrete Marching Cubes algorithm (Montani et al., 1994) on the area of the volumetric model that has been changed. The resulting surface patch is then used to substitute the corresponding existing patch on the surface tooth model. Another drilling variant is also available. This variant utilizes only the surface representation of the tooth. A method for computing consistent penetration depth information, in order to reduce collision response artifacts inherent to other existing penetration depth approaches is used. The method considers a set of surface vertices that are close to the bur surface to avoid discontinuous penetration depths. Furthermore the method incorporates a scheme that performs local surface subdivision or adjustment in order to cope with cases such as penetration in areas where the mesh is too coarse for good results to be achieved. The locally updated 3D surface patch is identical to the size and the shape of the bur tool.

The user can choose to "track" the performed drilling operations. In this case, a "history" of the performed operations is being kept and the user can undo a certain number of them. Thus, if an inexperienced user makes an error during the drilling procedure, he/she can undo his/her last drilling steps and continue towards the right direction. In addition, he/she can save the sequence of operations to a file and re-apply them on the same tooth at a later stage. Moreover, an instructor can use this feature in order to view off-line the drilling procedure as performed by a trainee and judge its skill level.

A drilled tooth can be saved either as a series of cross sectional images or in surface representation (namely, as a triangular mesh). The application supports the following mesh formats: VRML2, DXF and STL. The latter is a format used in stereo-lithography and can be given as input to a stereo-lithography device in order to construct a real 3D model of the tooth from the virtual model. An example of a virtual tooth that has been drilled with the developed application can be seen in Figure 13.

During drilling, the user can use active shutter glasses for stereo viewing and thus get a sense of depth in the scene. In addition, the user can choose to visualize certain parts of the model in a semi-transparent way (Figure 13c). This is a useful option and can be used, for example,

Figure 13. Volumetric (a) and surface (b) representation of a canine that has been drilled with the developed application; the semi-transparent model (c) of the same tooth that allows visualization of its root canal.

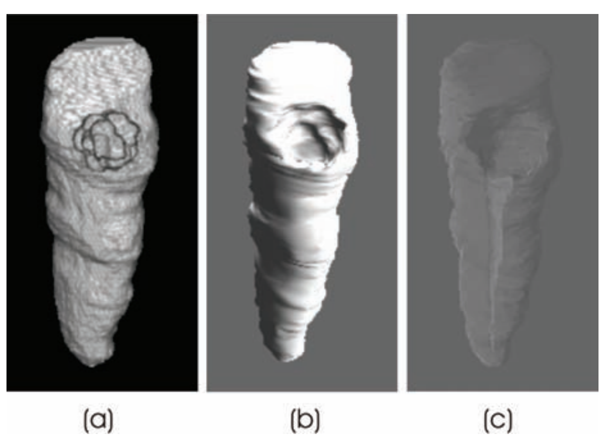

to allow the user to observe the anatomy of the root canals during the virtual preparation of the endodontic cavity.

FUTURE TRENDS

The use of 3D anatomical models and virtual reality technology in dental education and research is expected to increase in the near future, due to the many advantages that it offers. With respect to the Virtual Dental Patient model and the virtual dental drilling application presented in this chapter, a number of improvements and extensions are planned. These include their adaptation for use in other dentistry specialties, the development and implementation of more realistic and physically accurate material removal models for the drilling simulation and the creation of different bur types that are necessary in dental practice. Usability tests involving a large number of dental students and researchers that will make extensive use of VDP and the virtual drilling application will also be conducted. A small scale usability test involving a small number of dental students yielded very good results.

CONCLUSION

The Virtual Dental Patient is a novel 3D face and oral cavity model for dentistry and other related applications that has been created using Visible Human anatomical data. This model is accompanied by a database of detailed 3D teeth models obtained from digitized cross sections of a large number of extracted teeth. The model can be adapted to the characteristics of a specific patient using either facial photographs or 3D data and be animated using an MPEG-compatible facial animation.

The VDP has been utilized for the creation of a novel virtual tooth drilling application in the field of endodontics. Unlike most virtual drilling systems devised so far (that operate on standalone teeth and focus on realistic material removal simulation and realistic force rendering), in the new simulator, cavity preparation for the pulp cavity access is performed on teeth placed in their natural environment, i.e., within the oral cavity. The dental bur can be controlled by a haptic device that provides force feedback during the drilling operation and increases the level of realism and immersion. Drilling is performed on the VDP 3D volumetric/surface teeth models. Final results, i.e., drilled teeth models, as well as intermediate steps of the drilling procedure can be saved for future use or for inspection by an instructor.

In conclusion, the VDP and the dental simulator described in this chapter are promising educational and research tool that allow users to familiarize themselves with teeth and oral cavity anatomy and practice virtual tooth drilling for endodontic cavity preparation and similar tasks. Apart from its use as a training tool for students, the virtual drilling system can also assist experienced dentists in planning a tooth drilling intervention by getting familiar with the individual patient anatomy, identifying landmarks, planning the approach and deciding on the ideal target position of the actual clinical activity.

REFERENCES

Ackerman, M.J. (1998). The Visible Human Pproject. In *Proceedings of the IEEE*, 86(3), 504-511.

Ahlberg, J. (2001). *CANDIDE-3 – An updated parameterized face*. Technical Report No LiTH-ISY-R-2326, Department of Electrical Engineering, Linköping University, Sweden.

Banvard, R. (2002). The Visible Human Project Image Data Set: From Interception to Completion and Beyond. In *Proceedings of the CODATA: Frontiers of Scientific and Technical Data*.

Bathe, KJ. (1996). *Finite element procedures in engineering analysis*. Upper Saddle River, NJ: Prentice-Hall.

Bergmans, L. & Van Cleynenbreugel, J. & Beullens, M. & Wevers, M. & Van Meerbeek, B. & Lambrechts, P. (2003). Progressive versus constant tapered shaft design using NiTi rotary instruments. *International Endodontic Journal*, *36*(4), 288-295.

Berutti, E. (1993). Computerized analysis of the instrumentation of the root canal system. *Journal of Endodontics,* 19(5), 236-238.

Blasković-Subat, V. & Smojver, B. & Maricić, B. & Sutalo, J. (1995). A computerized method for the evaluation of root canal morphology. *International Endodontic Journal*, 28(6), 290-296.

Bors, A.G. & Kechagias, L. & Pitas, I. (2002). Binary morphological shape-based interpolation applied to 3-D tooth reconstruction. *IEEE Transactions on Medical Imagining*, 21(2), 100-108.

Carriere, J. & Carriere, L. (1995). Softlanding treatment through inverse anchorage and virtual reality. *Journal of clinical orthodontics,* 29(8), 479-86.

Han, K. & Lu, R.Q. & Ma, Y.H. & Lu, P.J. & Zhang, H. & Wang, W.B. (1998). Reconstruction of three-dimensional digital teeth. *The Chinese Journal of Dental Research*, 1(2), 22-25.

Herder, J. & Myszkowski, K. & Kunii, T.L. & Ibusuki, M. (1996). A virtual reality interface to an intelligent dental care system. *Studies in health technology and informatics*, 29, 400-410.

Hirano, Y. & Aoba, T. (1995). Computer-assisted reconstruction of enamel fissures and carious lesions of human premolars. *Journal of Dental Research*, 74(5), 1200-1205.

Kim, I. & Paik, K.S. & Lee, S.P. (2007). Quantitative evaluation of the accuracy of micro-computed tomography in tooth measurement. *Clinical Anatomy*, 20(1), 27-34.

Kim, L. & Hwang, Y. & Park, S.H. & Ha. S. (2005). Dental Training System using Multi-modal Interface. *Computer-Aided Design & Applications,* 2(5), 591-598.

Kusumoto, N. & Sohmura, T. & Yamada, S. & Wakabayashi, K. & Nakamura, T. and Yatani, H. (2006). Application of virtual reality force feedback haptic device for oral implant surgery. *Clinical Oral Implants Research*, 17(6), 708-713.

Lyroudia , K. & Samakovitis, G. & Pitas, I. & Lambrianidis, T. H. & Molyvdas, I. & Mikrogeorgis, G. (1997a). 3D Reconstruction of Two C-Shape Mandibular Molars. *Journal of Endodontics*, 23(2), 101-104.

Lyroudia, K. & Mikrogeorgis, G. & Nikopoulos, N. & Samakovitis, G. & Molyvdas, I. & Pitas I. (1997b). Computerized 3-D Reconstruction of two Double Teeth. *Endodontics and Dental Traumatology*, 13(5), 218-222.

Lyroudia, K. (2000). *Internal Tooth Morphology by using 3-D Reconstruction*. Thessaloniki, Greece.

Lyroudia, K. & Mikrogeorgis, G. & Bakaloudi, P. & Kechagias, E. & Nikolaidis, N. & Pitas, I.. (2002). Virtual Endodontics: Three-Dimensional Tooth Volume Representations and their Pulp Cavity Access. *Journal of Endodontics*, 28(8), 599-602.

Lundin, K. & Ynnerman, A. & Gudmundsson, B. (2002). Proxy based haptic feedback from volumetric density data. *EuroHaptics,* 104-109.

Marras, I. & Nikolaidis, N. & Mikrogeorgis, G. & Lyroudia, K. & Pitas, I. (2008). A Virtual System for Cavity Preparation in Endodontics. *Journal of Dental Education*, 72(4), 494-502.

Moschos, G. & Nikolaidis, N. & Pitas, I. (2004). Anatomically-based 3D face and oral cavity model for creating virtual medical patients. *IEEE International Conference on Multimedia and Expo (ICME)* 2, 867-870.

Montani, C. & Scateni, R. & Scopigno, R. (1994). Discretized Marching Cubes. *Proceedings of IEEE Conference on Visualization (Visualization '94)*, 281-287.

Nielsen, R. & Alyassin, A. & Peters, D. & Carnes, D. & Lancaster, J. (1995). Microcomputed tomography: an advanced system for detailed endodontic research. *Journal of Endodontics*, 21(11), 561–568.

Nikopoulos, N. & Pitas, I. (1997). An Efficient Algorithm for 3D Binary Morphological Transformations with 3D Structuring Elements of Arbitrary Size and Shape. *Proceedings of IEEE Workshop on Nonlinear Signal and Image Processing (NSIP'97).*

Oi, T. & Saka, H. & Ide, Y. (2004). Three-dimensional observation of pulp cavities in the maxillary first premolar tooth using micro-CT. *International Endodontic Journal*, 37(1), 46-51.

Park, J.S., Chung, M.S., Hwang, S.B., Lee, Y.S., Har, D.H., & Park, H.S. (2005). *V*isible Korean human: Improved serially sectioned images of the entire body. *IEEE Transactions on Medical Imaging*, 24(3), 352–360.

Peters, O.A. & Laib, A. & Rüegsegger, P. & Barbakow, F. (2000). Three-dimensional analysis of root canal geometry by high-resolution computed tomography. *Journal of Dental Research*, 79(6), 1405-1409.

Plotino, G. & Grande, N.M. & Pecci, R. & Bedini, R. & Pameijer, C.N. & Somma, F. (2006). Three-dimensional imaging using microcomputed tomography for studying tooth macromorphology. *Journal of the American Dental Association*, 137(11), 1555-1561.

Ranta, JF. & Aviles, WA. (1999). The Virtual Reality Dental Training System - Simulating Dental Procedures for the Purpose of Training Dental Students Using Haptics. *Proceedings of the Fourth PHANTOM Users Group Workshop*, 73-77.

Rhodes, J.S. & Ford, T.R. & Lynch, J.A. & Liepins, P.J. & Curtis, R.V. (1999) Micro-computed tomography: a new tool for experimental endodontology. *International Endodontic Journal*, 32(3), 165-170.

Rhodes, J.S. & Ford, T.R. & Lynch, J.A. & Liepins, P.J. & Curtis, R.V. (2000). A comparison of two nickel-titanium instrumentation techniques in teeth using microcomputed tomography. *International Endodontic Journal*, 33(3), 279-285.

Robb, R.A., & Hanson, D.P. (2006). Biomedical Image Visualization Research Using the Visible Human Datasets. *Clinical Anatomy*, 19(3), 240–253.

Rose, J.T. & Buchanan, J. & Sarrett, DC. (1999). Software reviews – the DentSim system. *Journal Dental Education, 63*(5), 421-423.

Seipel, S. & Wagner, I.V. & Koch, S. & Schneide, W. (1998). Oral implant treatment planning in a virtual reality environment. *Computer Methods and Programs in Biomedicine*, 57(1), 95-103.

Sensable Technologies Inc. (2006). Available from: http://www.sensable.com

Snow, M.D. & Graham, J.A. & Yates, W.J. (1996). Interactive computer technologies in dentistry. Virtual reality in orthodontics. *Studies in health technology and informatics*, 29, 411-422.

Stamm, T. & Kaup, M. & Hohoff, A. & Meier, T. & Meyer, U. (2003). Validity of a three-dimensional public-domain system for contemporary endodontic research. *Journal of Endodontics*, 29(12), 801-805.

Yau, H.-T. & Hsu, C.-Y. (2006). Development of a Dental Training System Based on Point-based Models. *Computer-aided design & applications*, 3(6), 779-787.

Verstreken, K. & Van Cleynenbreugel, J. & Marchal, G. & Van Steenberghe, D. & Suetens, P. (1996). Computer-assisted planning of oral implant surgery. An approach using virtual reality. *Studies in health technology and informatics*, 29, 423-434.

Vlachos, A. & Peters, J. & Boyd, C. & Mitchell, JL. (2001). Curved PN Triangles. *Proceedings of ACM Symposium on Interactive 3D Graphics.*

Wagner, A. & Rasse, M. & Millesi, W. & Ewers, R. (1997). Virtual reality for orthognathic surgery: the augmented reality environment concept. *Journal of Oral Maxillofacial Surgery*, 55(5), 456-62.

Wang, D. & Zhang, Y. & Wang, Y. & Lee, YS. & Lu, P. & Wang, Y. (2005). Cutting on triangle mesh: local model-based haptic display for dental preparation surgery simulation. *IEEE Transactions on Visualization and Computer Graphics*, 11(6), 671-683.

Zhang, S.X., & Heng, P.A., & Liu, Z.J (2006). Chinese visible human project. *Clinical Anatomy*, 19(3), 204-215.

KEY TERMS

3D Surface Model: A digital representation of a 3D object through its surface. The surface of the object is often defined by a polygon (usually triangle) mesh i.e., a collection of vertices, edges and faces.

3D Volumetric (Voxel-Based) Model: A digital representation of a 3D object through its volume, represented as a collection of voxels. A voxel is essentially the extension of a pixel in three dimensions and represents an elementary volume just as a pixel represents an elementary area in 2D data.

Haptic Device: An advanced user-machine interface that provides the sense of touch by applying forces, vibrations and/or motions to the user. Haptic devices can be used to assist in the creation or control of virtual objects or to enhance the remote control of machines.

MPEG-4 Standard: A collection of methods for the compression of audiovisual digital data developed by MPEG (Moving Picture Experts Group). MPEG-4 provides the technological elements enabling the integration of the production, distribution and content access paradigms in the fields of digital television, interactive graphics applications (synthetic content) and interactive multimedia.

Marching Cubes Algorithm: An algorithm initially published in 1987 by Lorensen and Cline for the extraction of a polygon mesh approximation of an isosurface from volumetric data. An isosurface is a surface that represents points of constant value within a volume. Many variants of the algorithms (such as the discrete marching cubes algorithm) have been proposed.

Mathematical Morphology: A theory for the analysis and processing of geometrical structures, usually applied in images (binary or grayscale) but applicable also to 3D volumetric data or other spatial structures. It is mainly based on set theory and topology. Common usages of mathematical morphology in images include edge detection, noise removal, image enhancement and image segmentation. The two most basic operations in mathematical morphology are erosion and dilation.

Mesh Subdivision: A common computer graphics technique used to add detail and smoothness to a polygon mesh by breaking into smaller pieces the polygons in the mesh.

Texture Mapping: A method used for adding detail to a 3D model by applying a separately defined texture or pattern on its surface, similar to applying wallpaper on a wall. Texture mapping does not affect the shape of the surface but only changes its colors. The most common texture mapping approach is to create a 2D image of the texture, often called a "texture map", which is then "wrapped around" the 3D object.

Virtual Reality: A form of human-computer interaction in which a real or imaginary environment is simulated and users are allowed to interact with it in real time and manipulate its components. Virtual reality is usually connected to the sense of immersion, i.e. the sense of actually being within the virtual environment. One of the ways to achieve immersion is by providing stimuli to more than one sensorial channels (visual, haptic, aural).

VRML (Virtual Reality Modeling Language): A standard file format for the representation of 3D interactive graphics.

Compilation of References

Abreu Jr., M., Tyndall, D. A., & Ludlow, J. B. (2001). Generation of TACT image slices using different reconstruction algorithms: Effects on natural caries detection. *Oral Surgery, Oral Medicine, Oral Pathology, Oral Radiology, and Endodontology, 92*, 576-581.

Abreu Jr., M., Tyndall, D. A., Ludlow, J. B., & Nortje, C. J. (2002). Influence of the number of basis images and projection array on caries detection using tuned aperture computed tomography (TACT). *Dentomaxillofacial Radiology, 31*, 24-31.

Ackerman, M.J. (1998). The Visible Human Pproject. In *Proceedings of the IEEE*, 86(3), 504-511.

ADA (2003). American Dental Association Survey Center. *Survey of dental practice*. Chicago: American Dental Association.

ADA (2004). *ADA Specification 1004 Computer Software Performance for Dental Practice Software*. [www page]. URL http://www.ada.org/prof/resources/standards/informatics_reports.asp

ADA (2005). *Health Insurance Portability and Accountability Act (HIPAA) [www page].* URL http://www.ada.org/prof/resources/topics/hipaa/index.asp

ADA (2006). *ADA Specification 1000: Standard Clinical Architecture for the Structure and Content for the Electronic Health Record*. [www page]. URL http://www.ada.org/prof/resources/standards/informatics_reports.asp

Adam, F., Hammer, D. S., Pape, D., & Kohn, D. (2002). Femoral anatomy, computed tomography and computer-aided design of prosthetic implants. *Arch Orthop Trauma Surg, 122*, 262-268.

Advanced Instruments. *QCount and Color QCount*. Retrieved March 23, 2008, from http://www.aicompanies.com/

Agrawal. (1998). Reconstructing the human body using biomaterials. *J Met*, 50(No. 1), 31.

Ahlberg, J. (2001). *CANDIDE-3 – An updated parameterized face*. Technical Report No LiTH-ISY-R-2326, Department of Electrical Engineering, Linköping University, Sweden.

Akca, K., & Iplikcioglu, H. (2001). Finite element stress analysis of the influence of staggered versus straight placement of dental implants. *Int J Oral Maxillofac Implants*, *16*(5), 722-730.

Akca, K., & Iplikcioglu, H. (2002). Finite element stress analysis of the effect of short implant usage in place of cantilever extensions in mandibular posterior edentulism. *J Oral Rehabil, 29*(4), 350-356.

Akca, K., Cehreli, M. C., & Iplikcioglu, H. (2002). A comparison of three-dimensional finite element stress analysis with in vitro strain gauge measurements on dental implants. *Int J Prosthodont*, *15*(2), 115-121.

Albrektsson, T., Sennerby, L., & Wennerberg, A. (2008). State of the art of oral implants. *Periodontol 2000, 47*, 15-26.

Alomari, Q. D., Reinhardt, J. W., & Boyer, D. B. (2001). Effect of liners on cusp deflection and gap formation in composite restorations. *Operative Dentistry, 26*, 406-411.

Alparone T., Baronti S., & Carla R. (1995). Two-dimensional rank-conditioned median filter. *IEEE Trans. Circuits Syst. II*, *42*(2), 130-132.

Andersen, A. H., & Kak, A. C. (1984). Simultaneous algebraic reconstruction technique (SART): A superior implementation of the ART algorithm. *Ultrasonic Imaging, 6*, 81-94.

Anderson, J.M. (2001). Biological responses to materials. *Annu Rev Mater Res*, *31*, 81–110.

Anonymous. (2008). *Poisson's ratio*. Retrieved July 18th, 2008 from the OLPC Wiki: http://en.wikipedia.org/wiki/Poisson_ratio

Anonymous. (2008). *Young's modulus*. Retrieved July 18th, 2008 from the OLPC Wiki: http://en.wikipedia.org/wiki/Young_modulus

ANSI INCITS 4-1986 (1963). *American National Standard for Information Systems* — *Coded Character Sets* — *7-Bit American National Standard Code for Information Interchange (7-Bit ASCII).*American National Standards Institute.

Arun, K. S., Huang, T. S., & Blostein, S. D. (1987). Least square fitting of two 3-D point sets. *IEEE Trans Patt Anal Machine Intell (PAMI), 9*, 698-700.

Atkinson, J. C., Zelle, G. G., & Shah, C. (2002). Electronic patient records for dental school clinics: More than paperless systems. *Journal of Dental Education*, *66*, 634-642.

Atmaram, G. H., Mohammed, H., & Schoen, F. J. (1979). Stress analysis of single-tooth implants. I. Effect of elastic parameters and geometry of implant. *Biomater Med Devices Artif Organs, 7*(1), 99-104.

Atoui, H., Miguet, S., & Sarrut, D. (2006). A fast morphing-based interpolation for medical images: application to conformal radiotherapy. *Image Anal Stereol, 25*, 95-103.

Azari, A., & Nikzad, S. (2008). Computer-assisted implantology: historical backround and potential outcomes-a review. *The International Journal of Medical Robotics and Computer Assisted Surgery, 4*, 95-104.

Bailit, H. L. (2003). Health services research. *Adv Dent Res, 17*, 82-85.

Balshi, S. F., Wolfinger, G. J., & Balshi, T. J. (2006). Surgical planning and prosthesis construction using computer technology and medical imaging for immediate loading of implants in the pterygomaxillary region. *Int J Periodontics Restorative Dent*. Jun, *26*(3), 239-47.

Bankman, I. A. (2000). *Handbook of medical imaging*, London: Academic press.

Banvard, R. (2002). The Visible Human Project Image Data Set: From Interception to Completion and Beyond. *Proceedings of the CODATA: Frontiers of Scientific and Technical Data*.

Bardosi, Z., & Pongracz, F. (2007). Flexible drill/endoscope calibration method for navigation. *Proc.of 4th International Conference on Computer Aided Surgery Around the Head*, Innsbruck, (pp. 11-13).

Barloworld Scientific. *Stuart SC6*. Retrieved March 23, 2008, from http://www.barloworld-scientific.com/

Baron, R. J. (2007). Quality improvement with an electronic health record: Achievable, but not automatic. *Ann Intern Med*, *147*, 549-552.

Barrett, J. F., & Keat, N. (2004). Artifacts in CT: Recognition and avoidance. *Radiographics, 24,* 1679-1691.

Bartolo, P. J., H. A. A., Rodrigo A. Rezende, Tahar Laoui and Bopaya Bidanda. (2008). Advanced process to fabricate scaffolds for tissue engineering. In P. B. Bopaya Bidanda (Ed.), *Virtual prototyping & Bio manufacturing in medical applications* (pp. 149-170). Springer.

Bathe, KJ. (1996). Finite Element Procedures in Engineering Analysis. Upper Saddle River, NJ: Prentice-Hall.

Bauer, J. C., & Brown, W. T. (2001). The digital transformation of oral health care: Teledentistry and electronic commerce. *J Am Dent Assoc*, *32*, 204-209.

Baumrind, S., & Frantz, R. C. (1971). The reliability of head film measurements. 1. Lamdmark identification. *American Journal of Orthodontics, 60,* 111-127.

Bausch, J. R., de Lange, K., Davidson, C. L., Peters, A., & de Gee, A.J. (1982). Clinical significance of polymerization shrinkage of composite resins. *Journal of Prosthetic Dentistry, 48,* 59-67.

Bazalova, M., Beaulieu, L., Palefsky, S., & Verhaegena, F. (2007). Correction of CT artifacts and its influence on Monte Carlo dose calculation. *Medical Physics, 34*(6), 2119-32.

Beaulieu, L, & Yazdi, M. (2006). Method and apparatus for metal artifact reduction in computed tomography. *Patent Pub. No.: WO/2006/039809 (US), PCT/CA2005/001582 (Int.)*

Benn, D. K., Kostewicz, S. H., Dankel, D. D., Segal, R., Schmidt, S. O., & Chardon, Z. (2000). Designing an electronic patient record with multiple real time decision support modules for managing diseases. *Proc AMIA Symp, 1168*.

Bergenholtz, G., & Spångberg, L. (2004). Controversies in endodontics. *Crit Rev Oral Biol Med*, *1, 15*(2), 99-114.

Bergmans, L. & Van Cleynenbreugel, J. & Beullens, M. & Wevers, M. & Van Meerbeek, B. & Lambrechts, P. (2003). Progressive versus constant tapered shaft design using NiTi rotary instruments. *International Endodontic Journal,* 36(4), 288-295.

Berry, E., Brown, J. M., Connell, M., Craven, C. M., Efford, N. D., Radjenovic, A., & Smith, M. A. (1997). Preliminary experience with medical applications of rapid prototyping by selective laser sintering. *Med Eng Phys*, *19*, 90-96.

Berti, G., Fingberg, J., Hierl, T., & Schmidt, J. G. (2004). An interactive planning and simulation tool for maxillo-facial surgery. In T. M. Buzug & T. C. Lueth (Eds.), *Perspectives in image-guided surgery* (pp. 872-879). World Scientific Publishing.

Berutti, E. (1993). Computerized analysis of the instrumentation of the root canal system. *Journal of Endodontics*, 19(5), 236-238.

Beyerer, J., & Leon, F. P. (2002). Die Radontransformation in der digitalen Bildverarbeitung. *Automatisierungstechnik, 50,* 472-480.

Bibb, R., & Brown, R. (2000). The application of computer aided product developoment techniques in medical modelling topic: rehabilitation and prostheses. *Biomed Sci Instrum, 36*, 319-324.

Bibb, R., Eggbeer, D., Williams, R. J., & Woodward, A. (2006). Trial fitting of a removable partial denture framework made using computer-aided design and rapid prototyping techniques. Proceeding of the institution of mechanical engineers, Part H: *Journal of engineering in medicine, 220,* 793-797.

Bill, J. S., & Reuther, J. F. (2004). Rapid prototyping in planning reconstructive surgery of the head and neck. Review and evaluation of indications in clinical use. *Mund Kiefer Gesichtschir, 8*, 135-153.

BioLogics. *AccuCount*. Retrieved March 23, 2008, from http://www.biologics-inc.com/

Biomaterials Properties Database (1996). University of Michigan, Copyright © Quintessence Publishing. http://www.lib.umich.edu/dentlib/Dental_tables/toc.html

Biomaterials Research http://www.biomaterials.group.shef.ac.uk/biomaterials/index.php

Biosurveillance Technical Committee (BTC) (2006). *Standards gap and overlap analysis biosurveillance use* *case: visit, utilization, and lab results data*. In: Office of the National Health Information Technology Coordinator, (Ed.), Evaluation of Standards Harmonization Process for HIT: Healthcare Information Technology Standards Panel.

Biosurveillance Technical Committee (BTC) (2006). *Selected standards.* In: Office of the National Health Information Technology Coordinator, editor. Evaluation of Standards Harmonization Process for HIT: Healthcare Information Technology Standards Panel.

Bird, M., & Gill, G. (1987). Individual differences and technology attributes: An examination of educational technology considerations related to trade and industry training. *Australian Journal of Educational Technology, 3*(2), 108–118.

Bishop C. (2006). *Pattern recognition and machine learning.* Springer Verlag.

Björk, A., & Skieller, V. (1983). Normal and abnormal growth of the mandible. A synthesis of longitudinal cephalometric implant studies over a period of 25 years. *European Journal of Orthodontics, 5,* 1-46.

Blasković-Subat, V. & Smojver, B. & Maricić, B. & Sutalo, J. (1995). A computerized method for the evaluation of root canal morphology. *International Endodontic Journal,* 28(6), 290-296.

Blinkhorn, A., Choi, C., & Paget, H. (1998). An investigation into the use of the FDI tooth notation system by dental schools in the UK. *Eur J Dent Educ, 2*(1), 39-41.

Bomans, M., Hohne, K. H., Tiede, U., & Riemer, M. (1990). 3D segmentation of MR images of the head for 3D display. *IEEE Trans Med Imag, 9,* 177–83.

Bookstein, F. (1991). *Morphometric tools for landmark data: geometry and biology.* Cambridge: Cambridge University Press.

Bookstein, F. L. (1996). Biometrics, biomathematics and the morphometric synthesis. *Bull Math Biol, 58,* 313-65.

Bookstein, F. L. (1997). Landmark methods for forms without landmarks: morphometrics of group differences in outline shape. *Medical Image Analysis, 3,* 225-243.

Borchers, L., & Reichart, P. (1983). Three-dimensional stress distribution around a dental implant at different stages of interface development. *J Dent Res, 62*(2), 155-159.

Bors, A.G. & Kechagias, L. & Pitas, I. (2002). Binary morphological shape-based interpolation applied to 3-D tooth reconstruction. *IEEE Transactions on Medical Imagining,* 21(2), 100-108.

Bouschlicher, M. R., & Rueggeberg, F. A. (2000). Effect of ramped light intensity on polymerization force and conversion in a photoactivated composite. *Journal of Esthetic Dentistry, 12,* 328-339.

Bowen, R. L. (1956). Use of epoxy resins in restorative materials. *Journal of Dental Research, 35,* 360-369.

Bowen, R. L. (1963). Properties of a silica-reinforced polymer for dental restorations. *Journal of the American Dental Association, 66,* 57-64.

Bowen, R. L. (1967). Adhesive bonding of various materials to hard tooth tissues. VI. Forces developing in direct-filling materials during hardening. *Journal of the American Dental Association, 74,* 439-445.

Broeren, J., Sunnerhagen, K., & Rydmar M. (2007). A kinematic analysis of a haptic handheld stylus in a virtual environment: A study in healthy subjects. *Journal of NeuroEngineering and Rehabilitation, 4*(13).

Brown, G. A., Milner, B., & Firoozbakhsh, K. (n.d.). Application of computer-generated stereolithography and interpositioning template in acetabular fractures: A report of eight cases. *Journal of orthopedic trauma, 16,* 347-352.

Brown, L. G. (1992). A survey of image registration techniques. *Computing Surveys, 24,* 325–76.

Bruant, J. S., Don, S. E., & Eiliam, B. S. (1995). Steeolithography in oral and maxillofacial operation planning. *International Journal of Oral Maxillofacial Surgery, 24,* 98-103.

Bundesamt für Strahlenschutz (2004). *Unterrichtung durch die Bundesregierung. Umweltradioaktivität und*

Strahlenbelastung im Jahr 2004 Bundesdruckerei Berlin, Germany.

Burdea, G. C., & Coiffet, P. (2003). *Virtual reality technology, (2nd Ed.) with CD-ROM*. New York: Wiley.

Butterworth, S. (1930). On the theory of filter amplifiers. *Wireless Engineer, 7*, 536–541.

Buurma, B., & Rutherford, R. B. (1999). Transplantation of human pulpal and gingival fibroblasts attached to synthetic scaffolds. *Eur J Oral Sci., 107*(4), 282-289.

Byuan, H. S., & Lee, K. H. (2005). A decision support system for the selection of a rapid prototyping process using the modified TOPSIS method. *Int Adv Manuf Technol*, *26*, 1338-1347.

Campbell, D. J. (2001). The use of cross-sectional spiral tomography in the placement of implants. *N Z Dent J*. Jun, *97*(428), 49-51.

Cannizzaro, G., Leone, M., & Esposito, M. (2007). Immediate functional loading of implants placed with flapless surgery in the edentulous maxilla: 1-year follow-up of a single cohort study. *Int J Oral Maxillofac Implants*. Jan-Feb, *22*(1), 87-95.

Carriere, J. & Carriere, L. (1995). Softlanding treatment through inverse anchorage and virtual reality. *Journal of clinical orthodontics*, 29(8), 479-86.

Cevidanes, L. H., Bailey, L. J., Tucker, S. F., Styner, M. A., Mol, A., Phillips, C. L., Proffit, W. R., & Turvey, T. (2007). Three-dimensional cone-beam computed tomography for assessment of mandibular changes after orthognathic surgery. *American Journal of Orthodontics and Dentofacial Orthopedics, 131*, 44-50.

Cha, B. K., Lee, J. Y., Jost-Brinkmann, P. G., & Yoshida, N. (2007). Analysis of tooth movement in axtraction cases using three-dimensional reverse engineering technology. *European journal of orthodontics*, *29*, 325-331.

Cha, J-Y., Mah, J., & Sinclair, P. (2007). Incidental findings in the maxillofacial area with 3-dimensional cone-beam imaging. *American Journal of Orthodontics and Dentofacial Orthopedics*, *132,* 7-14.

Chai, U. Dom, Ludlow, J. B., Tyndall, D. A., & Webber, R. L. (2001). Detection of simulated periodontal bone gain by digital subtraction radiography with tuned-aperture computed tomography. The effect of angular disparity. *Dentomaxillofacial Radiology, 30*, 92-97.

Chan, D. C. N., Frazier, K. B., Tse, L. A., & Rosen, D. W. (2003). Application of rapid prototyping to operative dentistry curriculum. *Journal of dental education, 68*, 64-70.

Chang, C. W., Hwang, Y. H., Grinshpun, S. A., Macher, J. M., & Willeke, K. (1994). Evaluation of counting error due to colony masking in bioaerosol sampling. *Appl Environ Microbiol, 60*(10), 3732-3738.

Chang, Y. L., & Li, X. (1994). Adaptive image region-growing. *IEEE Trans on Image Processing, 3*, 868-72.

Charbeneau, G. T. (1975). *Principles and practice of operative dentistry*, 6. Philadelphia, PA: Lea and Febiger.

Chasteen, J. E., Murphy, G., Forrey, A., & Heid, D. (2003). The Health Insurance Portability & Accountability Act and the practice of dentistry in the United States: Electronic transactions. *J Contemp Dent Pract* , *4*(4), 108-120.

Chattopadhyay, A., Arevalo, O., & Sohn, W. (2008). Understanding measurement of dental diseases and research participation in practice set-up. *Dent Clin North Am, 52*(2), 367-86.

ChemoMetec. *NucleoCounter*. Retrieved March 23, from http://www.chemometec.com/

Chen, D. T., & Zeltzer, D. (1992). Compuer animation of a biomachanically based model of muscle using the finite element model. *ACM Comput Graphics, 26*, 89-98.

Chen, R-S., Y.-J. C., Min-Huey Chen, Tai-Horng Young. (2007). Cell-surface interactions of rat tooth germ cells on various biomaterials. *Journal of Biomedical Materials Research Part A, 83*, 241–248.

Cheng, A. C., Tee-Khin, N., Siew-Luen, C., Lee, H., & Wee, A. G. (2008). The management of a severely resorbed edentulous maxilla using a bone graft and a CAD/CAM-guided immediately loaded definitive implant prosthesis: a clinical report. *J Prosthet Dent*., *99*(2), 85-90.

Choi, J. Y., & Choi, J. H., Kim, N. K., & Kim, Y. (2002). Analysis of errors in medical rapid prototyping models. *Int J Oral Maxillofac Surg, 31*,23-32.

Choi, S. H., & Samavedam, S. (2002). Modelling and optimisation of rapid prototyping. *Computers in dentistry, 47*, 39-53.

Christensen, G. E. (1994). *Deformable shape models for neuroanatomy*. DSc.-thesis, Server Institute of Technology, Washington University, Saint Louis.

Chua, C. K., Leong, K. F., & Lim, C. S. (2003). *Rapid prototyping. Principles and applications*. World Scientific.

Ciftci, Y., & Canay, S. (2000). The effect of veneering materials on stress distribution in implant-supported fixed prosthetic restorations. *Int J Oral Maxillofac Implants*, *15*(4), 571-582.

Clelland, N. L., Lee, J. K., Bimbenet, O. C., & Brantley, W. A. (1995). A three-dimensional finite element stress analysis of angled abutments for an implant placed in the anterior maxilla. *J Prosthodont*, *4*(2), 95-100.

Colifast. *Colifast Rapid Microcolony Counter*. Retrieved March 21, 2008, from http://www.colifast.no

Collins, D. L., Evans, A. C. (1997). Animal: validation and applications of nonlinear registration-based segmentation. *Int J Pattern Recogn Artificial Intelligence, 11*, 1271–94.

Connell, H. M., Statham, P. F., Collie, D. A., Walker, F. S., & Moos, K. F. (1999). Use of template for custom cranioplasty. *Phidias, EC Funded Network Project in Rapid Prototyping in Medicine*, *2*, 7-8.

Consultative Committee for Space Data Systems. (1999). *Reference model for an Open Archival Information System (OAIS)*, Red Book, Issue 1. CCSDS 650.0-R-1. Washington, D.C.: National Aeronautics and Space Administration. http://ssdoo.gsfc.nasa.gov/nost/isoas/ref_model.html

Cook, S. D., Klawitter, J. J., & Weinstein, A. M. (1981). The influence of implant elastic modulus on the stress distribution around LTI carbon and aluminum oxide dental implants. *J Biomed Mater Res*, *15*(6), 879-887.

Cook, S. D., Klawitter, J. J., & Weinstein, A. M. (1982). A model for the implant-bone interface characteristics of porous dental implants. *J Dent Res, 61*(8), 1006-1009.

Cook, S. D., Klawitter, J. J., & Weinstein, A. M. (1982). The influence of implant geometry on the stress distribution around dental implants. *J Biomed Mater Res, 16*(4), 369-379.

Craig, R.G., & Powers, J. M.(2002). *Restorative dental materials,* 11th ed.,Ed., Mosby, Inc., An Affiliate of Elsevier Science.

Csiszar I., (1991). Why least squares and maximum entropy? An axiomatic approach to inference for linear inverse problems. *Annals of Statistics*, *19*, 2032-66.

Cusack, C. M. (2008). Electronic health records and electronic prescribing: Promise and pitfalls. *Obstet Gynecol Clin N Am*, *35*(1) 63–79, ix.

D'Urso, P. S., Atkinson, R. L., Lanigan, M. W., Earwaker, W. J., Bruce, I. J., Holmes, A., Barker, T. M., Effeney, D. J., & Thompsom, R. G. (1998). Stereolithographic (SL) biomodelling in craniofacial surgery. *British Journal Of Plastic Surgery*, *51*, 522-530.

D'Urso, P. S., Earweaker, W. J., Redmond, M. J., Thompson, R. G., Effeney, D. J., & Tomlinson, F. H. (2000). Custom cranioplasty using stereolithography and acrylic. *British Journal of Plastic Surgery*, *53*, 200-204.

Da Rosa, E. L. S., Oleskovicz, L. C., & Aragao, B. N. (2004). Rapid prototyping in maxillofacial surgery and traumatology:case report. *Braz Dent J, 15*, 243-247.

Dahle, J., Kakar, M., Steen, H. B., & Kaalhus, O. (2004). Automated counting of mammalian cell colonies by means of a flat bed scanner and image processing. *Cytometry A*, *60*(2), 182-188.

Dansky, K. H., Gamm, L. D., Vasey, J. J., & Barsukiewicz, C. K. (1999). Electronic medical records: Are physicians ready? *J Healthc Manag, 44*, 440–54 [discussion: 454–5].

Dauvillier, B. S., Aarnts, M. P., & Feilzer, A. J. (2003). Modeling of the viscoelastic behavior of dental light-activated resin composites during curing. *Dental Materials, 19,* 277-285.

Dauvillier, B. S., Hübsch, P. F., Aarnts, M. P., & Feilzer, A. J. (2001). Modeling of viscoelastic behavior of dental chemically activated resin composites during curing. *Journal of Biomedical Materials Research, 58,* 16-26.

Davidson, C. L., & de Gee, A. J. (1984). Relaxation of polymerization contraction stresses by flow in dental composites. *Journal of Dental Research, 63,* 146-148.

Day, J. (2000) Cyberinfo: Privacy and personal health data in cyberspace. *J Contemp Dent Pract, 1,* 1-6.

Day, J. (2001) Privacy and personal health data in cyberspace: The role and responsibility of healthcare professionals. *J Contemp Dent Pract*, *1*(2), 02-06.

de Groot, R., Peters, M. C. R. B., de Haan, Y. M., Dop, G. J., & Plasschaert, A. J. M. (1987). Failure stress criteria for composite resin. *Journal of Dental Research, 66,* 1748-1752.

Dean, D., Min, K. J., & Bond, A. (2003). Computer aided design of large-format prefabricated cranial plates. *Journal of craniofacial surgery, 14,* 819-832.

Dee, S. W., Aas, R. S., Skjanes, K., Hermansen, L. F., Samset, I. D., Reitehaug, E., et al. (2000, Jan 1). *Development of a rapid system for monitoring total microbial load (HPC) in distribution systems and raw waters.* Paper presented at the Water Quality Technology Conference, Salt Lake City, UT.

Delany, J. (2004). Riding the wave of the future. Electronic patient charting debuts in student clinic. *Penn Dent J*, (pp. 2-5).

Delrose, D. E., & Steinberg, R. W. (2000). The clinical significance of the digital patient record. *J Am Dent Assoc*, *131*, 57S -60S.

Dhawan, A. P., Buelloni, G., & Gordon, R. (1986). Enhancement of mammographic features by optimal adaptive neighborhood image processing. *IEEE Trans. Med. Imag., MI-5,* 8–15.

DHHS (2008). Medical Privacy - National Standards to Protect the Privacy of Personal Health Information. [WWW page]. URL http://www.hhs.gov/ocr/hipaa/

DHHS (U.S. Department of Health & Human Services) (2004). The National Health Information Infrastructure (NHII 2002-2004) [WWW page]. URL. http://aspe.hhs.gov/sp/NHII/index.html

DHHS. (U.S. Department of Health and Human Services) (2001). *HIPAA Administrative Simplification, Proposed Security Rule*. [www page]. URL http://aspe.os.dhhs.gov/admnsimp/bannerps.htm#security

Di Giacomo, G. A., Cury, P. R., & Araujo, N. S. (2005). Clinical application of stereolithographic surgical guides for implant placement: preliminary results. *J Periodontol, 76*, 503-507.

Dimas, E., & Briassoulis, D. (1999). 3D geometric modelling based on NURBS : A review. *Advances in engineering software*, *30*, 741-751.

Director-General, Health Policy Bureau of Japan (1999). The Electronic Storage of Clinical Records. [www page]. URL http://www.medis.or.jp/2_kaihatu/denshi/file/e_notification990422.pdf

Dobbins, J. T., & Godfrey, D. V. (2003). Digital x-ray tomosynthesis: current state of the art and clinical potential. *Physics in Medicine and Biology, 48,* 65-106.

Dorsaz, P.-A., Dorsaz, L., & Doriot, P. A. (2000). The effect of image distortion on 3-D reconstruction of coronary bypass grafts from angiographic Views. *IEEE Transactions on Medical Imaging, 19,* 759-762.

Drevenstedt, G. L., McDonald, J. C., & Drevenstedt, L. W. (2005). The role of voice activated technology in today's dental practice. *J Am Dent Assoc*, *136*, 157-161

Dryden, I. L., & Mardia, K. V. (1998). *Statistical shape analysis.* Chichester, U.K.: John Wiley & Sons.

Duailibi, M. T., S. E. D., C.S. Young, J.D. Bartlett, J.P. Vacanti, and P.C. Yelick. (2004). Bioengineered teeth from cultured rat tooth bud cells. *J Dent Res 83*(7), 523-528.

Duret, F., Blouin, J. L., & Duret, B. (1988). CAD-CAM in dentistry. *J Am Dent Assoc, 227*, 715-720.

Duryea, J., Dobbins, J. T., & Lynch, J. A. (2003). Digital tomosynthesis of hand joints for arthritis assessment. *Medical Physics, 30,* 325-333.

Duyck, J., Van Oosterwyck, H., Vander Sloten, J., De Cooman, M., Puers, R., & Naert, I. (2000). Influence of prosthesis material on the loading of implants that support a fixed partial prosthesis: in vivo study. *Clin Implant Dent Relat Res, 2*(2), 100-109.

Eggbeer, D., Bibb, R., & Williams, R. (2005). The compuer-aided design and rapid prototyping fabrication of removable partial denture frameworks. *Proc Inst Mech Eng, 219*, 195-202.

Eick, J. D., & Welch, F. H. (1986). Polymerization shrinkage of posterior composite resins and its possible influence on postoperative sensitivity. *Quintessence International, 17,* 103-111.

Eisner, J., Chasteen, J., Schleyer, T., & Feldman, C. (1993). *The computer based oral health record: a new foundation for oral health information systems.* Chicago: American Fund for Dental Health.

Elefteriadis, J. N., & Athanasiou, A. E. (1996). Evaluation of impacted canines by means of computerized tomography. *International Journal of Adult Orthodontics and Orthognathic Surgery, 11,* 257-264.

Engelman, M. J., Sorensen, J. A., & Moy, P. (1988). Optimum placement of osseointegrated implants. *J Prosthet Dent, 59*(4), 467-73.

Eplee, H., Murray, B., Revere, J. H., Bollmann, F., Haddad, G., Klimek, J., Barna, S., Rhodes, G., Looki, T., Malone, A., Molvar, M., Pienkowski, B., Schoonheim, M., & Teravainen J. (2002). Electronic management systems. *Eur J Dent Educ, 6*(Suppl. 3), 152-160 File 16.

Erickson, D. M., Chance, D., Schmitt, S., & Mathis, J. (1999). An opinion survey of reported benefits from the use of stereolithographic models. *J Oral Maxillof Surg, 57,* 1040-1043.

Esposito, M., Hirsch, J-M., Lekholm, U., & Thomsen, P. (1998). Biological factors contributing to failures of osseointegrated oral implants. *Eur J Oral Sci, 106*(1), 527-52.

European Commission. (1995). Directive 95/46/EC. [www page]. URL www.cdt.org/privacy/eudirective/EU_Directive_.html

Ewers, R., Schicho, K., Undt, G., Wanschitz, F., Truppe, M., Seemann, R., & Wagner, A. (2005). Basic research and 12 years of clinical experience in computer-assisted navigation technology: a review. *International Journal of Oral and Maxillofacial Surgery, 34*, 1-8.

Faber, J., Berto, P. M., & Quaresma, M. (2006). Rapid prototyping as a tool for diagnosis and treatment planning for maxillary canine impaction. *American Journal Of Orthodontics and Dentofacial Orthopedics, 129,* 583-589.

Fano, U. (1947). Ionization yield of radiations. II. The fluctuations of the number of ions. *Phys. Rev.*, *72*, 26-29.

Farman, A. G., & Scarfe, W. C. (2006). Development of imaging selection criteria and procedures should precede cephalometric assessment with cone-beam computed tomography. *American Journal of Orthodontics and Dentofacial Orthopedics, 130,* 257-265.

Fawcett, T. (2003). *ROC graphs: Notes and practical considerations for data mining researchers.* Tech report HPL-2003-4. HP Laboratories, Palo Alto, CA.

FDA dental devices aproval Web site http://www.fda.gov/cdrh/index.html

Feilzer, A. J., De Gee, A. J., & Davidson, C. L. (1987). Setting stress in composite resin in relation to configuration of the restoration. *Journal of Dental Research, 66*, 1636-1639.

Fencil, L. E., & Metz, C. E. (1990). Propagation and reduction of error in three-dimensional structure determined from biplane views of unknown orientation. *Medical Physics, 17,* 951-961.

Fenster, A., & Chiu, B. (2005). Evaluation of segmentation algorithms for nedical imaging. *Proceeding of the IEEE, Engineering in medicine and biology, 27th annual conference,* (pp. 7186-7189).

Ferguson, J. W. (2005). The Palmer notation system and its use with personal computer applications. *Br Dent J.,198*(9), 551-3.

Ferreira, C. F. (2007). Biological tooth replacement and repair. *Journal of Oral Rehabilitation, 34*, 933-939.

Finkeissen, E., Weber, R., Haßfeld, S., Koke, U., & Wetter, T. (2002). AIDA - Experiences in compensating the mutual weaknesses of knowledge-based and object-oriented development in a complex dental planning domain. *Methods of Information in Medicine, 41*(2), 168-176.

Fitzpatrick, J. M., & West, J. B. (2001). The distribution of target registration error in rigid-body point-based registration. *IEEE Trans Med Imaging, 20*, 917–27.

Flores-Mir, C., Palmer, N. G,, Northcott, H. C., Khurshed, F., & Major, P. W. (2006). Perceptions and attitudes of Canadian dentists toward digital and electronic technologies. *J Can Dent Assoc, 72*(3), 243.

Fouad, A. F., & Burleson, J. (2003). The effect of diabetes mellitus on endodontic treatment outcome Data from an electronic patient record. *J Am Dent Assoc*, *134*, 43-51

Frakes, D. H., Dasi, L. P., Pekkam, K., Kitajima, H. D., Sundareswaran, K., Yoganathan, A. P., & Smoth, M. J. T. (2008). A new method for registration-based medical image interpolation. *IEEE transactions on medical imaging, 27*, 370-377.

Frederiksen, N. L. (1995). Diagnostic imaging in dental implantology. Oral Surg Oral Med Oral *Pathol Oral Radiol Endod*. Nov, *80*(5), 540-54. Review.

Freed, L. E., & Vunjak-Novakovic, G. (1998). Culture of orgnized cell communities. *Adv Drug Deliver Rev, 33*, 15-30.

Freydberg, B. K. (2001). Connecting to success: Practice management on the Net. *J Contemp Dent Pract, 3*(2), 050-061.

Frosio I., & Borghese N. A. (2008). Statistical based impulsive noise removal in digital radiography. *IEEE Trans. on Medical Imaging*

Frosio I., Abati S., & Borghese N. A. (2008) An expectation maximization approach to impulsive noise removal in digital radiography. *Int. J. Computer Assisted Radiology and Surgery.*

Frosio I., Ferrigno G., & Borghese N. A. (2006). Enhancing digital cephalic radiography with mixture models and local gamma correction. *IEEE Trans. Medical Imaging, 25*(1), 113-121.

Galletti.(1998). Artificial organs: Learning to live with risk. *Tech. Rev,* (pp. 34–40).

Ganz, S. D. (2007). CT-derived model-based surgery for immediate loading of maxillary anterior implants. *Pract Proced Aesthet Dent*. Jun, *19*(5), 311-8; quiz 320, 302.

Gardner, H. (1983). *Frames of mind: the theory of multiple intelligences.* New York: Basic Books.

Garnett, G., Huegerich, T., Chui, C., & He, W. (2005), A universal noise removal algorithm with an impulse detector, *IEEE Trans. Image Processing, 14*(11), 1747-1754.

Gautam, P., & Valiathan, A. (2008). Bio-smart dentistry: Stepping into the future! *Trends Biomater. Artif Organs, 21*(2), 94-97.

Gehrke, P., Dhom, G., Brunner, J., Wolf, D., Degidi, M., & Piattelli, A. (2006). Zirconium implant abutments: fracture strength and influence of cyclic loading on retaining-screw loosening. *Quintessence Int, 37*(1), 19-26.

Geman, S., & Geman, D. (1984). Stochastic relaxation, Gibbs distributions, and the Bayesian restoration of images. *IEEE Trans. Patt. Anal. And Mach. Intell., 6*(6), 721-741.

Giannatsis, J., & Dedoussis, V. (2007). Additive fabrication technologies applied to medicine and health care: a review. *Int J Adv Manuf Technol, 0268-3768* (Print) 1433-3015 (Online).

Glantz, P. O., Rangert, B., Svensson, A., Stafford, G. D., Arnvidarson, B., Randow, K., et al. (1993). On clinical loading of osseointegrated implants. A methodological and clinical study. *Clin Oral Implants Res*, *4*(2), 99-105.

Goff, S. (2004). The Computerized operatory. *Dental products report* [WWW page]. URL: http://www.dentalproducts.net

Goldberg, H. I., Ralston, J. D., Hirsch, I. B., Hoath, J. I., & Ahmed, K. I. (2003). Using an Internet comanagement module to improve the quality of chronic disease care. *Jt Comm J Qual Saf.*, *29*(9), 443-51.

Gonzalez, W. (2008). *Digital image processing.* 3rd edition. Prentice Hall.

Gordon, R., Bender, R., and Hermann, G. T. (1970). Algebraic reconstruction techniques (ART) for three-dimensional electron microscopy and X-ray photography. *Journal of Theoretical Biology, 29,* 471-481.

Grant, D. G. (1972). Tomosynthesis: A three-dimensional radiographic imaging technique. *IEEE Transactions on Biomedical Engineering, 19*, 20-28.

Gray, C. F., Redpath, T. W., Smith, F. W., & Staff, R. T. (2003). Advanced imaging:Magnetic resonance imaging in implant dentistry. *Clin Oral Implant Res, 14*, 18-27.

Green, S. R. (1996). Electronic vs. traditional recordkeeping. *Dent Econ*, *86*(8), 60-5.

Greenwood, S. R., Grigg, P. A., Vowles, R. V., & Stephens, C. D. (1997). Clinical informatics and the dental curriculum. A review of the impact of informatics in dental care, its implications for dental education. *Eur J Dent Educ*, *1*(4), 153-61.

Grevera, G. J., & Udupa, J. K. (1998). An objective comparison of 3-D image interpolation methods. *IEEE trans on medical inaging, 17,* 642-652.

Groenhuis, R. A. J., Webber, R. L., & Ruttimann, U. E. (1983). Computerized tomosynthesis of dental tissues. *Oral Surgery, 56,* 206-214.

Guest, J. K., & Prevost, J. H. (2006). Optimizing multifunctional materials: Design of microstructures for maximized stiffness and fliod permeability. *International Jouran of solid and structures, 43,* 7028-7047.

Gunz, P., Mitteroecker, P., & Bookstein, F. L. (2005). Semilandmarks in Three Dimensions. In D. E. Slice (Ed.), *Modern morphometrics in physical anthropology* (pp. 73-98). New York: Kluwer Academic / Plenum Publishers.

Halazonetis, D. J. (1994). Computer-assisted cephalometric analysis. *American Journal of Orthodontics and Dentofacial Orthopedics*, *105,* 517-521.

Halazonetis, D. J. (2001). Acquisition of 3-dimensional shapes from images. *American Journal of Orthodontics and Dentofacial Orthopedics, 119,* 556-560.

Halazonetis, D. J. (2004). Morphometrics for cephalometric diagnosis. *American Journal of Orthodontics and Dentofacial Orthopedics, 125,* 571-581.

Halazonetis, D. J. (2005). From 2D cephalograms to 3D computed tomography scans. *American Journal of Orthodontics and Dentofacial Orthopedics, 127,* 627-637.

Hamilton, J. (2005). Is the paperless practice possible?: A look at the ADA's electronic health record initiatives. *J Am Dent Assoc*, *136*, 161-162.

Hammond, P. (2008). The use of 3D face shape modelling in dysmorphology. *Arch Dis Child, 92*, 1120-1126.

Han, K. & Lu, R.Q. & Ma, Y.H. & Lu, P.J. & Zhang, H. & Wang, W.B. (1998). Reconstruction of three-dimensional digital teeth. *The Chinese Journal of Dental Research,* 1(2), 22-25.

Hansson, S. (2000). Implant-abutment interface: biomechanical study of flat top versus conical. *Clin Implant Dent Relat Res, 2*(1), 33-41.

Hansson, S. (2003). A conical implant-abutment interface at the level of the marginal bone improves the distribution of stresses in the supporting bone. An axisymmetric finite element analysis. *Clin Oral Implants Res, 14*(3), 286-293.

Hara, T., Takizawa, M., Sato, T., & Ide, Y. (1998). Mechanical properties of buccal compact bone of the mandibular ramus in human adults and children: relationship of the elastic modulus to the direction of the osteon and the porosity ratio. *Bull Tokyo Dent Coll, 39*(1), 47-55.

Harrell Jr., W. E., Stanford, S., & Bralower, P. (2005). ADA initiates development of orthodontic informatics standards. *Am J Orthod Dentofacial Orthop, 128*(2), 153-6.

Harris, J., & Rimmel, J. (2002). Can rapid prototyping ever become a routine feature in general dental practice? *Dent update, 29,* 482-486.

Hassan, H. et al. (2005) A volumetric 3D model of the human jaw. *Proceedings of 19th International Congress and Exhibition of CARS2005, Berlin, Germany, Elsevier ICS 1281,* 1244-49.

HealthGrades (2004). *Patient safety in American hospitals* [WWW page] URL http://www.healthgrades.com/media/english/pdf/HG_Patient_Safety_Study_Final.pdf

Heckmann, S. W., Winter, Meyer, M., Weber, H., & Wichmann, M. (2001). Overdenture attachment selection and the loading of implant and denture-bearing area.Part 2: A methodical study using five types of attachment. *Clin Oral Implant Res, 12,* 640-647.

Heid, D. W., Chasteen, J.,& Forrey, A. W. (2002) The electronic oral health record. *J Contemp Dent Pract., 15, 3*(1), 43-54.

Herder, J. & Myszkowski, K. & Kunii, T.L. & Ibusuki, M. (1996). A virtual reality interface to an intelligent dental care system. *Studies in health technology and informatics,* 29, 400-410.

Hierl, T., Wollny, G, Hendricks, J., Berti, G., Schmidt, J. G., Fingberg, J., & Hemprich, A. (2005). 3D-Analysis of soft tissue changes following maxillary distraction osteogenesis. In T. M. Buzug, K. Prüfer, K. Sigl, J. Bongarz, P. Hering, & G. Willems (Eds.), *Reconstruction of Soft Facial Parts.* Police and Research. Luchterhand Publishers. BKA Series 31-2.

Hierl, Th., Wollny, G., Schulze, F. P., Scholz, E., Schmidt, J. G., Berti, G., Hendricks, J., & Hemprich, A. (2006). CAD-CAM implants in esthetic and reconstructive craniofacial surgery. *J Comp Information Tech, 14,* 65-70.

Hieu, L. C., Bohez, E., Vander Sloten, J., Phien, H. N., Vatcharaporn, E., Binh, P. H., An, P. V., & Oris, P. (2003). Design for medical rapid prototyping of cranioplasty implants. *Rapid Prototyping Journal, 9,* 175-186.

Hieu, L. C., Bohez, E., Vander, S. J, Oris, P., Phien, H. N., Vatharaporn, E., & Binh, P. H. (2002). Design and manufacturing of cranioplasty implants by 3-axis CNC milling. *Technology and Health Care, 10,* 413-423.

Hildebolt, C. F., & Vannier, M. W. (1988). Three-dimensional measurement accuracy of skull surface landmarks. *Am J Phys Anthropol, 76,* 497-503.

Hill, D. L. G, Batchelor, P. G., Holden, M., & Hawkes, D. J. (2001). Medical image registration. *Physics in Medicine and Biology, 46,* R1–R45.

Hirano, Y. & Aoba, T. (1995). Computer-assisted reconstruction of enamel fissures and carious lesions of human premolars. *Journal of Dental Research,* 74(5), 1200-1205.

Hirsch, C., & John, M. (2003). Prävalenz kraniomandiblulärer Dysfunktion (CMD) bei Kindern und Jugendlichen. *Dtsch. Zahnärztl. Zeitschr, (DZZ),* 10, 589-92.

Ho, C. C., Wu, F. C., Chen, B. Y., Chuang, Y. Y., & Ouhyoung, M. (2005). Cubical marching squares: adaptive feature preserving surface extraction from volume data. *Computer Graphics Forum, 24,* 537-545.

Hoffmann, K. R., Wahle, A., Pellot-Barakat, C., Sklansky, J., & Sonka, M. (2000). Biplane x-ray angiograms, intravascular ultrasound, and 3D visualization of coronary vessels. *International Journal of Cardiac Imaging, 15,* 495-512.

Hoffmann, K. R., Williams, B. B., Esthappan, J., Chen, S.-Y. J, Caroll, J. D., Harauchi, H. et al. (1997). Determination of 3D positions of pacemaker leads from biplane angiographic sequences. *Medical Physics, 24,* 1854-1862.

Hollister, S. J. (2005). Porous scaffold design for tissue engineering. *Nat Mater, 4*, 518-424.

Hollister, S. J., Levy, R. A., Chu, T. M., Halloran, J. W., & Feinberg, S. E. (2000). Am image-based approach for designing and manufacturing craniofacial scaffolds. *Int J Oral Maxillfac Surg, 26*, 67-71.

Hollister, S. J., Lin, C. Y, Lin, C. Y., Schek, R. D., Taboas, J. M., Flanagan, C. L. Saito, E., Williams, J. M., Das, S., Wirtz, T., & Krebsach, P. H. (2004). Design and fabrication of scaffolds for anatomic bone reconstruction. *Med J Malaysia, 59*, 131-2.

Hollister, S. J., Lin, C. Y., Kang, H., & Adachi, T. (2008). *Computational design and simulation of tissue engineering scaffolds.* New York: Springer.

Hollister, S. J., Maddox, R. D., & Taboas, J. M.(2002). Opitimal design and fabrication of scaffolds to mimic tissue properties and satisfy biological constraints. *Biomaterials, 23*, 4095-4103.

Holmes, D. C., Haganman, C. R., Aquilino, S. A., Diaz-Arnold, A. M., & Stanford, C. M. (1997). Finite element stress analysis of IMZ abutment designs: development of a model. *J Prosthodont, 6*(1), 31-36.

Holmgren, E. P., Seckinger, R. J., Kilgren, L. M., & Mante, F. (1998). Evaluating parameters of osseointegrated dental implants using finite element analysis--a two-dimensional comparative study examining the effects of implant diameter, implant shape, and load direction. *J Oral Implantol, 24*(2), 80-88.

Honda, M. J., S. T., Yoshinori Sumita, Hiroshi Sagara, Minoru Ueda. (2007). The sequential seeding of epithelial and mesenchymal cells for tissue-engineered tooth regeneration. *Biomaterials*, 680-689.

Hoover, A., Jean-Baptiste, J., Jiang, X., Flynn, P. J., Bunke, H., Goldgof, D. B., Bowyer, K., Eggert, D. W., Fitzgibbon, A., & Fisher, R. B. (1996). An experimental comparison of range image segmentation algorithms. *IEEE trans on pattern analysis and machine intelligence, 7*,673-689.

Houston, W. J. B., Maher, R. E., McElroy, D., & Sherriff, M. (1986). Sources of error in measurements from cephalometric radiographs. *European Journal of Orthodontics, 8*, 149-151.

http://en.wikipedia.org/wiki/Unicode

http://law.e-gov.go.jp/htmldata/S32/S32F03601000015.html (In Japanese)

http://www.meti.go.jp/kohosys/press/0004964/index.html (In Japanese)

http://www.meti.go.jp/press/past/c60926e1.html (In Japanese)

http://www.unicode.org/

Huang, B. Y., Whittle, T., & Murray, G. M. (2006). A working-side chang to lateral tooth guidance increases lateral pterygoid muscle activity. *Arch Oral Biol. 5*(8), 689-96.

Huff, R., Dietrich, C. A., Nedel, L. P., Freitas, C., Comba, L. D., Olabarriaga, S. D. (2006). Erasing, digging and clipping in volumetric datasets with one or two hands. *VRCIA'06 Proceedings of the 2006 ACM int. conf. on Virtual reality continuum and its application*, *Hong Kong*, 271-278.

Humphries, S., Christensen, A., & Bradrick, J. (2006). Cone beam versus conventional computed tomography: comparative analysis of image data and segmented surface models. *International Journal of CARS (Computer Assisted Radiology and Surgery), Suppl. 1*, 398-400.

Hussein, R., Engelmann, U., Schroeter, A., & Meinzer H. P. (2004): Internationalization of healthcare applications: a generic approach for PACS workstations. *Methods Inf Med., 43*(2), 133-40.

Huszár, G. (1989). The role of the life and works of Adolf Zsigmondy and Ottó Zsigmondy in the history of dentistry. *Fogorv Sz, 82*(12), 357-63.

Hutmacher, D. W. (2000). Scaffolds in tissue engineering bone and cartilage. *Biomaterials, 21*, 2529-2543.

Hutmacher, D. W., & Cool, S. (2007). Concepts of scaffold-based tisuue-engineering-the rational to use solid free-from fabrication techniques. *J cell Mol Med, 11*, 654-669.

Hutmacher, D. W., Sttinger, & Risbud, M. V. (2004). Scaffold-based tissue engineering: rationale for compouter-aided design and solid free-form fabrication systems. *TRENDS in Biotechnology, 22*, 354-362.

Hwang, H. S., Hwang, C. H., Lee, K. H., & Kang, B. C. (2006). Maxillofacial 3-dimensional image analysis for the diagnosis of facial asymmetry. *American Journal of Orthodontics and Dentofacial Orthopedics, 130*, 779-785.

Hyvönen, N., Kalke, M., Lassas, M., Setälä, H., & Siltanen, S. (2008). Three-dimensional x-ray imaging using hybrid data collected with a digital panoramic device. *submitted (see http://www.siltanen-research.net/publications.html, June 2008).*

Institute of Medicine (IOM) (2000). *To err is human: Building a safer health system*. Washington DC: National Academy Press.

Iplikcioglu, H., Akca, K., Cehreli, M. C., & Sahin, S. (2003). Comparison of non-linear finite element stress analysis with in vitro strain gauge measurements on a Morse taper implant. *Int J Oral Maxillofac Implants, 18*(2), 258-265.

ISO/IEC 8859-11 (1999): *8-bit single-byte coded graphic character sets, Part 11: Latin/Thai character set* (draft dated June 22, 1999; superseded by ISO/IEC 8859-11:2001, published Dec 15, 2001).

Izatt, M. T., Thorpe, P. L., Thompson, R. G., D'Urso P. S., Adam C. J., Earweaker J. W. S., Labrom R. D., & Askin, G. N. (2007). The use of biomodelling in complex spinal surgery. *Eur Spine J, 16*, 1507-1518.

Jabero, M., & Sarment, D. (2006). Advanced surgical guidance technology: A review. *Implant dentistry, 15*, 135-142.

Jacob, G. G., Kai, C. C., & Mei, T. (1999). Development of a new rapid prototyping interface. *Computers in dentistry, 39*, 61-70.

Jaffe, M. J., & Rowlands, J. A. (1997). X-ray detectors for digital radiography. *Phys. Med. Biol., 42*, 1–39.

Janke, A. T. W. (2007). *Auswirkung nach dem DIR-System vermessener okklusal adjustierter Aufbißschienen auf die Stellung der Halswirbelsäule bei CMD-Patienten*. Krems: M.A.-theses.

Jeffcoat, M. K. (1993). Application of digital radiography to implantology. *J Dent Symp.* Aug, *1*, 30-3.

Jensen, M. E., & Chan, D. C. N. (1985). Polymerization shrinkage and microleakage. In G. Vanherle, & D.C. Smith (Eds.), *Posterior composite resin dental restorative materials* (pp. 243-262). Utrecht, The Netherlands: Peter Szulc Publishing Co.

John, J. H., Thomas, D., & Richards, D. (2003). Questionnaire survey on the use of computerisation in dental practices across the Thames Valley region. *British Dental Journal, 195*, 585-590.

Joos, U., Vollmer, D., & Kleinheinz, J. (2000). [Effect of implant geometry on strain distribution in peri-implant bone]. *Mund Kiefer Gesichtschir, 4*(3), 143-147.

Kaczmarz, S. (1937). Angenäherte Auflösung von Systemen linearer Gleichungen. *Bulletin international de l'Académie Polonaise des Sciences et des Lettres A, 35*, 355-357.

Kak, A. C., & Slaney, M. (1988). *Principles of computerized tomographic imaging.* New York: IEEE Engineering in Medicine and Biology Society.

Kak, A. C., & Slaney, M. (2001). *Principles of Computerized Tomographic Imaging.* Philadelphia, PA: Society of Industrial and Applied Mathematics.

Kanca, J. 3rd, & Suh, B. I. (1999). Pulse activation: reducing resin-based composite contraction stresses at the enamel cavosurface margins. *American Journal of Dentistry, 12*,107-112.

Kang, Y., Engelke, K., & Kalender, W. A. (2004). Interactive 3D editing tools for image segmentation. *Medical image analysis, 8*, 35-46.

Katsamanis, F., & Raftopoulos, D. D. (1990). Determination of mechanical properties of human femoral cortical bone by the Hopkinson bar stress technique. *J Biomech, 23*(11), 1173-1184.

Katsumata, A., Hirukawa, A., Okumura, S., Naitoh, M., Fujishita, M., Ariji, E., & Langlais R. P. (2007). Effects of image artifacts on gray-value density in limited-volume cone-beam computerized tomography. *Oral Surgery, Oral Medicine, Oral Pathology, Oral Radiology, and Endodontics, 104*, 829-836.

Katsumata, A., Hirukawa, A., Okumura, S., Naitoh, M., Fujishita, M., Ariji, E., & Langlais,R. P. (2007). Effects of image artifacts on gray-value density in limited-volume cone-beam computerized tomography. *Oral Surg Oral Med Oral Pathol Oral Radiol Endod, 104*, 829-36.

Kazandjian, S., Kiliaridis, S., & Mavropoulos, A. (2006). Validity and reliability of a new edge-based computerized method for identification of cephalometric landmarks. *Angle Orthodontist, 76*, pp. 619-24.

Kilbourne J., & Williams T. (2003). Unicode, UTF-8, ASCII, and SNOMED/CT. *AMIA Annu Symp Proc*. 2003; 892.

Kim, I. & Paik, K.S. & Lee, S.P. (2007). Quantitative evaluation of the accuracy of micro-computed tomography in tooth measurement. *Clinical Anatomy*, 20(1), 27-34.

Kim, L. & Hwang, Y. & Park, S.H. & Ha. S. (2005). Dental Training System using Multi-modal Interface. *Computer-Aided Design & Applications,* 2(5), 591-598.

Kim, S. (2004). Modern endodontic practice: Instruments and techniques. *Dent Clin North Am*, *48*(1):1-9.

Kinney, J. H., Marshall, S. J., & Marshall, G. W. (2003). The mechanical properties of human dentin: a critical review and re-evaluation of the dental literature. *Critical Reviews in Oral Biology and Medicine, 14*, 13-29.

Kitamura, E., Stegaroiu, R., Nomura, S., & Miyakawa, O. (2004). Biomechanical aspects of marginal bone resorption around osseointegrated implants: considerations based on a three-dimensional finite element analysis. *Clin Oral Implants Res, 15*(4), 401-412.

Kitamura, E., Stegaroiu, R., Nomura, S., & Miyakawa, O. (2005). Influence of marginal bone resorption on stress around an implant--a three-dimensional finite element analysis. *J Oral Rehabil, 32*(4), 279-286.

Klein, H. M., Schneider, W., Alzen, G., Voy, E. D., & Gunther, R. W. (1992). Pediatric craniofacial surgery. Comparison of milling and stereolithography for 3D model manufacturing. *Pediatr Radiol*, *22,* 458-460.

Kniss, J., Kindlmann, G., & Hansen, C. (2002). Multi-Dimensional Transfer Functions for Interactive Volume Rendering. *IEEE Transactions on Visualization and Computer Graphics, 8*, 270-285.

Kohn, D. G., Sarmadi, M., Helman, J. I., & Kresbach, P. H. (2002). Effects of PH on human bone marrow stromal cells in vitro: Implications for tissue engineering of bone. *J Biomed Mater Res, 63*, 567-576.

Kolehmainen, V., Siltanen, S., Järvenpäa, S., Kaipio, J. P., Koistinen, P., Lassas, M. et al. (2003). Statistical inversion for medical x-ray tomography with few radiographs: II. Application to dental radiology. *Physics in Medicine and Biology, 48*, 1465-1490.

Kolehmainen, V., Vanne, A., Siltanen, S., Järvenpäa, S., Kaipio, J. P., Lassas, M. et al. (2006). Parallelized Bayesian inversion for three dimensional dental x-ray imaging. *IEEE Transactions on Medical Imaging, 25*, 218-228.

Kopp, K. C., Koslow, A. H., & Abdo, O. S. (2003). Predictable implant placement with a diagnostic/surgical template and advanced radiographic imaging. *J Prosthet Dent, 89*, 611-615.

Korfage et al. (2005). Fiber-type Composition of the Human Jaw Muscles– (Part 2). Role of Hybrid Fibers and Factors Responsible für Inter-individual Variation. *J Dent Re.*, *84*(9), 784-93.

Korfage, J. A. M., Koolstra, J. H., Langenbach, G. E. J., & van Eijden, T. M. G. J. (2005). Fiber-type Composition of the Human Jaw Muscles - (Prat 1). Origin and Functional Significane of Fiber-type Diversity. *J Dent Res.*, *84*(9), 774-83.

Korioth, T. W. P., & Versluis, A. (1997). Modeling the mechanical behavior of the jaws and their related structures using finite element (FE) analysis. *Critical Reviews in Oral Biology and Medicine, 8*, 90-104.

Kragskov, J., Bosch, C., Gyldensted, C., & Sindet-Pedersen, S. (1997). Comparison of the reliability of craniofacial anatomic landmarks based on cephalometric radiographs and three-dimensional CT scans. *Cleft Palate Craniofac J, 34*, 111-116.

Krall, M. (1995). Acceptance and performance by clinicians using an ambulatory electronic medical record in an HMO. *Proc Annu Symp Comput Appl Med Care*, (pp. 708–11).

Krekmanov, L., Kahn, M., Rangert, B., & Lindstrom, H. (2000). Tilting of posterior mandibular and maxillary implants for improved prosthesis support. *Int J Oral Maxillofac Implants, 15*(3), 405-414.

Krol, D. M., Stump, L., Collins, D., Roumanis, S. A., & Radford, M. J. (2002). A qualitative analysis of medication use variance reports. *Jt Comm J Qual Improv.*, *28*(6), 316-23.

Krsek, P., Spanel, M., Krupa, P., Marek, I., & Cernochov, P. (2007). Teeth and Jaw 3D Reconstruction in Stomatology. *Medical Information Visualisation – BioMedical Visualisation, MediVis 2007*, 23-28.

Kruth, J. P., & Vandenbroucke, B., Van Vaerenbergh, J., & Naert, I. (2005). Digital manufacturing of biocompatible metal frameworks for complex dental prostheses by means of SLS / SLM. In *Virtual prototyping and rapid manufacturing-advanced research in visrtual and rapid prototyping. T*aylor & Francis, Londnon, (pp. 139-146).

Kukafka, R., Ancker, J. S., Chan, C., Chelico, J., Khan, S., Mortoti, S., Natarajan, K., Presley, K., & Stephens, K. (2007). Redesigning electronic health record systems to support public health. *J Biomed Inform*., *40*(4), 398-409.

Kumar, J. V. (2008). *Problems with use of PDA in oral health surveillance in New York State*. Unpublished personal communication.

Kumar, V., Ludlow, J., Cevidanes, L., & Mol, A. (2008). In vivo Comparison of Conventional and Cone Beam CT synthesized Cephalograms. *Angle Orthodontist, 78,* 873-879.

Kundu, A. (1990). Local segmentation of biomedical images. *Computerized Medical Imaging and Graphics, 14*, 173–83.

Kupeyan, H. K., Shaffner, M., & Armstrong, J. (2006). Definitive CAD/CAM-guided prosthesis for immediate loading of bone-grafted maxilla: a case report. *Clin Implant Dent Relat Res*., *8*(3), 161-7.

Kusumoto, N. & Sohmura, T. & Yamada, S. & Wakabayashi, K. & Nakamura, T. and Yatani, H. (2006). Application of virtual reality force feedback haptic device for oral implant surgery. *Clinical Oral Implants Research*, 17(6), 708-713.

Lai, H., Zhang, F., Zhang, B., Yang, C., & Xue, M. (1998). Influence of percentage of osseointegration on stress distribution around dental implants. *Chin J Dent Res, 1*(3), 7-11.

Lal, K., White, G. S., Morea, D. N., & Wright, R. F. (2006).Use of stereolithographic templates for surgical and prosthodontic implant planning and placement. Part I. The concept. *J Prosthodont, 15*, 51-58.

Lam, E. W., Ruprecht, A., & Yang, J. (1995). Comparison of two-dimensional orthoradially reformatted computed tomography and panoramic radiography for dental implant treatment planning. *J Prosthet Dent*. Jul, *74*(1), 42-6.

Lang, L. A., Kang, B., Wang, R. F., & Lang, B. R. (2003). Finite element analysis to determine implant preload. *J Prosthet Dent, 90*(6), 539-546.

Langer, R., & Vacanti J. P. (1993). Tissue engineering. *Science, 260*, 920-926.

Laurell, L., Lundgren, D., Falk, H., & Hugoson, A. (1991). Long-term prognosis of extensive polyunit cantilevered fixed partial dentures. *J Prosthet Dent, 66*(4), 545-552.

Laycock, S., & Day, A. (2003). Recent developments and applications of haptic devices. *Computer Graphics Forum*, *22*(2), 117–132.

Leake, J. L., & Werneck, R. I. (2005). The use of administrative databases to assess oral health care. *J Public Health Dent*, *65*(1), 21-35.

Lee, S. J., Jung, I. Y., Lee, C. Y., Choi, S. Y., & Kum, K. Y. (2001). Clinical application of computer-aided rapid prototyping for tooth transplantation. *Dental Traumatology, 17,* 114-119.

Lele, S., & Richtsmeier, J. T. (2001). *An invariant approach to statistical analysis of shapes.* London: Chapman and Hall-CRC press.

Leong, K. F., Cheah, C. M., & Chua, C. K. (2003). Solid freeform fabrication of three-dimensional scaffolds for engineering replacememnt tissues and organs. *Biomaterials*, *24*, 2363-2378.

Lester, H., & Arridge, S. R. (1999). A survey of hierarchical non-linear medical image registration. *Pattern Recognition*, *32*,129–49.

Letic, A., Crudo, V., & Abe, K. (2002).Tooth-germ morphogenesis signals for 3D tissue engineering scaffolds in oral reconstructions. *Tissue Engineering, 8*(6) Abs. O-118, 1165.

Letic, A., Crudo, V., & Abe, K. (2002a). Microspheres-based tissue engineering product for craniofacial bone reconstruction. *Tissue Engineering*, *8*(6) Abs. PP-169, 1234.

Letic-Gavrilovic, A., & Bakos, D. (2005). Membranes and bone substitutes in reconstructive surgery. Nova Science Publishers,Inc. USA. ISBN 1-59454-368-2, In B.M.Caruta, (Ed.), *Polymeric materials: New research*, (pp. 107-139).

Letic-Gavrilovic, A., Fini, M., Giavaresi, G., Giardino, R.,& Abe, K. (2001). Evaluation of composite collagen/hydroxy-apatite implantation and nerve growth factor (NGF) delivery on new bone ingrowth, *Acta Veterinaria, 51*(5-6), 299-310.

Letic-Gavrilovic, A., Piattelly, A., & Abe, K. (2000). Nerve growth factor beta (NGF beta) delivery via collagen/hydroxyapatite composite and new bone ingrowth. *J Mat Sci: Mat Med*, *14*, 1-8.

Letic-Gavrilovic, A., Scandurra, R., & Abe, K. (2000). Genetic potential of interfacial guided osteogenesis in implant devices *Dent Mater J, 19*(2), 99-132.

Letic-Gavrilovic, A., Todorovic, L. J., & Abe, K. (2004). Oral tissue engineering of complex tooth structure on biodegradable DLPLG/beta-TCP scaffolds. In N. Hasirci & V, Hasirci (Eds.), *Biomaterials: From molecules to engineered tissue*, (pp. 267-281). Kluwer Academic/Plenum Publishers, USA, .

Leu, M. C., Zhang, W., & Sui, G. (2000). An experimental and analytical study of ice: Part fabrication with rapid freeze prototyping. *CIRP Annals Manufacturing technoogy, 49*, 147-150.

Lewis, G. (1994). A parametric finite element analysis study of the stresses in an endosseous implant. *Biomed Mater Eng, 4*(7), 495-502.

Li, X., Wang, J., Shaw, L. L., & Cameron, T. B. (2005). Laser densification of extruded dental porcelain bodies in multi-material laser densification process. *Rapid prototyping journal*, *1*, 52-58.

Liang, H., Tyndall, D. A., Ludlow, J. B., and Lang, L. A. (1999). Cross-sectional presurgical implant imaging using tuned aperture computed tomography (TACT). *Dentomaxillofacial Radiology, 28*, 237.

Lieu, Q., Leu, M., & Schmitt, S. (2006). Rapid prototyping in dentisry: Technology and application. *Int J Adv Manuf Technol*, *29*, 317-335.

Liew, A. W. C., & Yan, H. (2006). Current methods in the automatic tissue segmentation of 3D magnetic resonance brain images. *Current medical images reviews, 2*, 1-13.

Lin C. Y., Kikuchi, N., & Hollister, S. J. (2004). A novel method for biomaterial scaffold internal archtecture design to match bone elastic properties with desired porosity. *J Biomech*, *37*, 632-636.

Lin, C. Y., Hsiao, C. C., Chen, P. Q., & Hollister, S. J. (2004). Interbody fusion cage design using integrated global layout and local microstructure topology optimization. *Spine*, *29*, 1747-1754.

Liu, J., Emken, J. L., Cramer, S. C., & Reinkensmeyer, D. J. (2005). Learning to perform a novel movement pattern using haptic guidance: slow learning, rapid forgetting, and attractor paths. In *Proc. of the 9th International Conference on Rehabilitation Robotics*, (pp. 37-40).

Liu, X., Wang, S., Sendi, L., & Caulfield, M. J. (2004). High-throughput imaging of bacterial colonies grown on filter plates with application to serum bactericidal assays. *J Immunol Methods, 292*(1-2), 187-193.

Lohfeld, S., & McHugh, B. V. (2005). Biomodels of bone: A review. *Annals of Biomedical Engineering, 33*, 1295-1311.

Lord, M. P. (1986). *Macmillan dictionary of physics.* London: The Macmillan Press Ltd.

Lorensen, W. E., & Cline, H. E. (1987). Marching cubes: A high resolution 3D surface construction algorithm. *Computer Graphics (SIGGRAPH '87 Proceedings), 21*, 163-169.

Lotz, J. C., Gerhart, T. N., & Hayes, W. C. (1991). Mechanical properties of metaphyseal bone in the proximal femur. *J Biomech, 24*(5), 317-329.

Lozanoff, S., & Diewert, V. (1989). A computer graphics program for measuring two- and three-dimensional form changes in developing craniofacial cartilages using finite element methods. *Comp Biomed Res, 22,* 63-82.

Lucy, L. (1974). An iterative technique for the rectification of observed distribution. *Astron. J., 79*, 745-754.

Ludlow, J. B., Davies-Ludlow, L. E., & Brooks, S. L. (2003). Dosimetry of two extraoral direct digital imaging devices: NewTom cone beam CT and Orthophos Plus DS panoramic unit. *Dentomaxillofacial Radiology, 32*, 229-234.

Ludlow, J. B., Davies-Ludlow, L. E., Brooks, S. L. & Howerton, W.B. (2006). Dosimetry of 3 CBCT devices for oral and maxillofacial radiology: CB Mercuray, NewTom 3G and i-CAT. *Dentomaxillofacial Radiology, 35*, 219-226.

Lundin, K. & Ynnerman, A. & Gudmundsson, B. (2002). Proxy based haptic feedback from volumetric density data. *EuroHaptics,* 104-109.

Lupovici, C., & Masanès, J. (2000). *Metadata for Long Term Preservation.* NEDLIB report series, 2. The Hague: Koninklijke Bibliotheek.. http://www.kb.nl/coop/nedlib/results/D4.2/D4.2.htm

Lyroudia , K. & Samakovitis, G. & Pitas, I. & Lambrianidis, T. H. & Molyvdas, I. & Mikrogeorgis, G. (1997). 3D Reconstruction of Two C-Shape Mandibular Molars. *Journal of Endodontics,* 23(2), 101-104.

Lyroudia, K. & Mikrogeorgis, G. & Bakaloudi, P. & Kechagias, E. & Nikolaidis, N. & Pitas, I.. (2002). Virtual Endodontics: Three-Dimensional Tooth Volume Representations and their Pulp Cavity Access. *Journal of Endodontics*, 28(8), 599-602.

Lyroudia, K. & Mikrogeorgis, G. & Nikopoulos, N. & Samakovitis, G. & Molyvdas, I. & Pitas I. (1997). Computerized 3-D Reconstruction of two Double Teeth. *Endodontics and Dental Traumatology,* 13(5), 218-222.

Lyroudia, K. (2000). *Internal tooth morphology by using 3-D Reconstruction.* Thessaloniki, Greece.

Ma, D., Lin, F., & Chua, C. K. (2001). Rapid prototyping applications in medicine. Part 1: NURBS-based volume modelling. *Int J Adv Manuf Technol, 18*, 103-117.

Ma, D., Lin, F., & Chua, C. K. (2001). Rapid prototyping applications in medicine. Part 2: STL file generation and case studies. *Int J Adv Manuf Technol, 18*, 118-127.

Ma, P. X., R. Z. (2001). Microtubular architecture of biodegradable polymer scaffolds. *J Biomed Mater Res, 56*, 469-477.

Ma, W.-Y., & Zhang, H. (1998). Content-based image indexing and retrieval. In B. Furht (Ed.), *Handbook of multimedia computing.* Boca Raton, FL: CRC Press.

MacGregor, D. G., & Halabisky, W. A. (1967). Electronic data processing in the storage and retrieval of dental patient file information. *J Dent Educ*, *31*(4), 499-507.

Maeda, M., Katsumata, A., Ariji, Y., Muramatsu, A., Yoshida, K., Goto, S., Kurita, K., & Ariji, E. (2006). 3D-CT evaluation of facial asymmetry in patients with maxillofacial deformities. *Oral Surgery, Oral Medicine, Oral Pathology, Oral Radiology, and Endodontics, 102*, 382-390.

Magni, A., de Oliveira Albuquerque, R., de Sousa, R. T., Hans, M. G., & Magnid, F. G. (2007). Solving incompatibilities between electronic records for orthodontic patients. *Am J Orthod Dentofacial Orthop*, *32*, 116-21

Magnusson, I., Clark, W. B., Marks, R. G., Gibbs, C. H., Manouchehr-Pour, M., & Low, S. B. (1988). Attachment level measurements with a constant force electronic probe. *Journal of Clinical Periodontology, 15*(3), 185-188.

Mah, J. K., Danforth, R. A., Bumann, A., & Hatcher, D. (2003). Radiation absorbed in maxillofacial imaging with a new dental computed tomography device. *Oral Surgery, Oral Medicine, Oral Pathology, Oral Radiology, and Endodontics, 96*, 508-513.

Mah, J., & Sachdeva, R. (2001). Comoputer-assisted orthodontic treatment. *Americal journal of orthodontics and dentofacial orthopedics, 120*, 85-87.

Maintz, J. B. A., & Viergever, M. A. (1998). A survey of medical image registration. *Med Image Anal*, *2*, 1–36.

Makela, T., Clarysse, P., Sipila, O., Pauna, N., Pham, Q. C., Katila, T., et al. (2002). A review of cardiac image registration methods. *IEEE Trans Med Imaging*, *21*, 1011–21.

Malo, P., Rangert, B., & Nobre, M. (2003). "All-on-Four" immediate-function concept with Branemark System implants for completely edentulous mandibles: a retrospective clinical study. *Clin Implant Dent Relat Res*, *5 Suppl 1*, 2-9.

Marchack, C. B. (2005). An immediately loaded CAD/CAM-guided definitive prosthesis: a clinical report. *J Prosthet Dent*. Jan, *93*(1), 8-12.

Marchack, C. B. (2007). CAD/CAM-guided implant surgery and fabrication of an immediately loaded prosthesis for a partially edentulous patient. *J Prosthet Dent*. Jun, *97*(6), 389-94.

Marchack, C. B. (2008). Complications of Computer-Aided-Design/Computer-Aided-Machining-Guided (NobelGuidetrade mark) Surgical Implant Placement: An Evaluation of Early Clinical Results. *Clin Implant Dent Relat Res.*

Marmitt, G., Friedrich, H., & Slusallek, P. (2006). Interactive Volume Rendering with Ray Tracing. *Eurographics State-of-the-Art Report 2006*, Vienna. Retrieved April 12, 2008, from http://graphics.cs.uni-sb.de/Publications/2006/eg2006star_vrt.pdf

Marras, I. & Nikolaidis, N. & Mikrogeorgis, G. & Lyroudia, K. & Pitas, I. (2008). A Virtual System for Cavity Preparation in Endodontics. *Journal of Dental Education*, 72(4), 494-502.

Mascarenas, N. D. A., Souza, I. A., Cruvinel, P. E., Biscegli, C. I., & Rosa, R. R. (2000). An estimation theoretic approach to 3-D image interpolation. *IEEE*, (pp. 163-169).

Masood, S. H., & Soo, A. (2002). A rule based expert system for rapid prototyping selection. *Robotics and computer integrated manufacturing*, *18*, 267-274.

Massie, T. H., & Salisbury, J. K. (1994). The PHANToM haptic device: A device for probing virtual objects. In *Proc. of ASME Winter Annual Meeting, Symposium on Haptic Interfaces for Virtual Environment and Teleoperator Systems*, (pp. 295-300).

Massler, M. & Schour, I. (1958). *Atlas of the Mouth*. Chicago: American Dental Association.

Mc Inerney, T., Terzopoulos, D. (1996). Deformabe models in medical image analysis: A survey. *Medical image analysis, 1*, 91-108.

Mehta, B. V., Rajani, S., & Sinha, G. (1997). Comparison of Figure processing techniques (magnetic resonance imaging, computed tomography scan and ultrasound) for 3D modeling and analysis of the human bones. *J Digit Imaging, 10*(3 Suppl 1), 203-206.

Mente, P. L., & Lewis, J. L. (1989). Experimental method for the measurement of the elastic modulus of trabecular bone tissue. *J Orthop Res, 7*(3), 456-461.

Meredith, N., & Setchell, D. J. (1997). In vitro measurement of cuspal strain and displacement in composite restored teeth. *Journal of Dentistry*, *25*, 331-337.

Merz, B. R., Hunenbart, S., & Belser, U. C. (2000). Mechanics of the implant-abutment connection: an

8-degree taper compared to a butt joint connection. *Int J Oral Maxillofac Implants, 15*(4), 519-526.

Metadata Engine Project: http://meta-e.uibk.ac.at/

Metz, C. E., & Fencil, L. E. (1989). Determination of three-dimensional structure in biplane radiography without prior knowledge of the relationship between the two views: Theory. *Medical Physics, 16,* 45-51.

Metzger, M. C., Majert-Hohlweg, B., Schon, R., Teschner, M., Gellrich, N. C., Schmelzeisen, R., &Gutwald, R. (2007). Verification of clinical precision after computer-aided recontruction in craniomaxilofacial surgery. *Oral Surg Oral Med Oral Pathol Oral Radiol Endod, 104,* e1-e10.

Mijagic, M., Fauquet, C., Galletti, C. Palot, C., Wiechmann, D., & Mah, J. (2005). Digital design and manufacturing of the lingualcare bracket system. *JCO, 34,* 375-382.

Miller, E. R., McCurry, E. M., & Hruska, B. (1971). An infinite number of laminagrams from a finite number of radiographs. *Radiology, 98,* 249-255.

Miller, J. H., & Thomas, J. B. (1976). The detection of signals in impulsive noise modeled as a mixture process. *IEEE Trans. on Communications,* (pp. 560-3).

Miller, M. C. Expanding dental practices with computer technology. *Dent Today.* 1995 Sep *14*(9), 72-81.

Milovanovic, J. (2007). Medical applications of rapid prototyping. *Mechanical Engineering, 5*, 79-85.

Min Lee, J. C. Y. D., Benjamin M. Wu. (2005). Scaffold fabrication by indirect three-dimensional printing. *Biomaterials. 26*, 4281-4289.

Misch, C. E. (1999). Implant design considerations for the posterior regions of the mouth. *Implant Dent, 8*(4), 376-386.

Mol, A. (2005). *Functional tissue engineering of human heart valve leaflets.* The Netherlands: Eindhoven University of Technology.

Momoi, Y., & McCabe, J. F. (1994). Hygroscopic expansion of resin based composites during 6 months of water storage. *British Dental Journal, 176,* 91-96.

Montani, C. & Scateni, R. & Scopigno, R. (1994). Discretized Marching Cubes. *Proceedings of IEEE Conference on Visualization (Visualization '94)*, 281-287.

Monteith, B. D. (1991). The electronic patient record and second generation clinical databases: problems of standards and nomenclature. *J Dent Educ, 55*(4), 246-52.

Mooney, D. J., C. P., James Piana, and Bruce Rutherford. (1996). Engineering dental pulp-like tissue in vitro. *Biotechnol. Prog., 12*, 865-868.

Morant, R. M., Eleazer, P. D., Scheetz, J. P., & Farman, A. G. (2001). Array-projection geometry and depth discrimination with tuned aperture computed tomography for assessing the relationship between tooth roots and the inferior alveolar canal. *Oral Surgery, Oral Medicine, Oral Pathology, Oral Radiology, and Endodontology, 2001*, 252-259.

Morigi, S., & Sgaralli, F. (2004). 3D long bone reconstruction based on level sets. Computerized medical Imaging and Graphics, 28, 377-390.

Morsi, Y. S., C. S. W. a. S. S. P. (2008). Conventional manufacturing processes for three-dimensional scaffolds. In P. B. Bopaya Bidanda (Ed.), *Virtual prototyping & Bio manufacturing in medical applications* (pp. 129-148). Springer.

Morton, D., Stanford, C. M., & Aquilino, S. A. (1998). Evaluation of resilient abutment components on measured strain using dynamic loading conditions. *J Prosthet Dent, 80*(1), 46-51.

Moschos, G. & Nikolaidis, N. & Pitas, I. (2004). Anatomically-based 3D face and oral cavity model for creating virtual medical patients. *IEEE International Conference on Multimedia and Expo (ICME)* 2, 867-870.

Moshiri, M., Scarfe, W. C., Hilgers, M. L., Scheetz, J. P., Silveira, A. M., & Farman, A. G. (2007). Accuracy of linear measurements from imaging plate and lateral cephalometric images derived from cone-beam computed tomography. *American Journal of Orthodontics and Dentofacial Orthopedics, 132,* 550-560.

Moskowitz, E. (2007). *Clinical Research in Dentistry.* N Y State Dent J, *73*(3), 4.

Moyers, R. E. (1988). *Handbook of orthodontics*. Chicago: Year Book Medical Publisher.

Mueller, K. (1998). *Fast and accurate three-dimensional reconstruction from cone-beam projection data using algebraic methods*. Dissertation, The Ohio State University.

Mueller, K., Yagel, R., & Wheller, J. W. (1999). Anti-aliased three-dimensional cone-beam reconstruction of low-contrast objects with algebraic methods. *IEEE Transactions on Medical Imaging, 18,* 519-537.

Muller-Hartwich, R., Prager, T. M., & Jost-Brinkmann, P. G. (2007). SureSmile:CAD/CAM system for orthodontic treatment planning, simulation and fabriation of customized archwires. *Int J Comput Dent*, *10*, 53-62.

Muller, A., Krishnan, K. G., Uhl, E., & `Mast, G. (2003). The application of rapid prototyping techniques in cranial reconstruction and preoperative planning in neurosurgery. *Journal of Craniofacial Surgery, 14,* 899-914.

Mupparapu, M. (2007). Remote access of electronic patient data with cellular wireless broadband technology. *Am J Orthod Dentofacial Orthop*, *132*, 260-5

Murray, G. M., Bhutada, M., Peck, C. C., Phanachet, I., Sae-Lee, D., & Whittle, T. (2007). The human lateral pterygoid muscle. *Arch Oral Biol.*, *52*(4), 377-80.

Murray, G. M., Phanachet, I., Uchida, S., &Whittle, T. (n.d.). The human lateral pterygoid muscle. A review of some experimental aspects and possible clinical relevance. *Austral dental Journal, 49*(1), 2-8.

Nagy, M., Hanzlicek, P., Zvarova, J., Dostalova, T., Seydlova, M., Hippman, R., Smidl, L., Trmal, J., & Psutka, J. (2008). Voice-controlled data entry in dental electronic health record. *Stud Health Technol Inform*, *136*, 529-34.

Naing, M. W., C. K. C. a. K. F. L. (2008). Computer aided tissue engineering scaffold fabrication. In P. B. Bopaya Bidanda (Ed.), *Virtual prototyping & Bio manufacturing in medical applications* (pp. 67-85). Springer.

Nair, M. K., Gröndahl, H.-G., Webber, R. L., Umadevi, P., & Wallace, J. A. (2003). Effect of iterative restoration on the detection of artificially induced vertical radicular fractures by Tuned Aperture Computed Tomography. *Oral Surgery, Oral Medicine, Oral Pathology, Oral Radiology, and Endodontology, 96,* 118-125.

Nair, M. K., Nair, U. P., Gröndahl, H.-G., & Webber, R. L. (2002). Accuracy of tuned aperture computed tomography in the diagnosis of radicular fractures in non-restored maxillary anterior teeth - an in vitro study. *Dentomaxillofacial Radiology, 31,* 299-304.

Nair, M. K., Nair, U. P., Gröndahl, H.-G., Webber, R. L., & Wallace, J. A. (2001). Detection of artificially induced vertical radicular fractures using tuned aperture computed tomography. *European Journal of Oral Sciences*, *109*, 375-379.

Nair, M. K., Seyedain, A., Agarwal, S., Webber, R. L., Nair, U. P., Piesco, N. P. et al. (2001). Tuned aperture computed tomography to evaluate osseous healing. *Journal of Dental Research, 80,* 1621-1624.

Nair, M. K., Seyedain, A., Webber, R. L., Nair, U. P., Piesco, N. P., Agarwal, S. et al. (2001). Fractal analyses of osseous healing using tuned aperture computed tomography images. *European Radiology, 11,* 1510-1515.

Nair, M. K., Tyndall, D. A., Ludlow, J. B., May, K., & Ye, F. (1998). The effects of restorative material and location on the detection of simulated recurrent caries. A comparison of dental film, direct digital radiography and tuned aperture computed tomography. *Dentomaxillofacial Radiology, 27,* 80-84.

Natali, A. N., & Viola, M. M. (2004). Computer tomography for virtual models in dental imaging. In Dental biomechanics. Taylor & Francis, London, (pp. 35-50).

Neutec Group. *Flash and Grow automatic colony counter*. Retrieved March 23, 2008, from http://www.neutecgroup.com/

Ngan, D. C., Kharbanda, O. P., Geenty, J. P., & Darendeliler, M. A. (2003). Comparison of radiation levels from computed tomography and conventional dental radiographs. *Australian Orthodontic Journal, 19,* 67-75.

NIDCR. (2008). NIDCR Awards Grants for New Practice-Based Initiative.) [WWW page]. URL http://www.

nidcr.nih.gov/Research/ResearchResults/ScienceBriefs/CurrentSNIB/PBRNOverviewClinicalResearch.htm

Nielsen, R. & Alyassin, A. & Peters, D. & Carnes, D. & Lancaster, J. (1995). Microcomputed tomography: an advanced system for detailed endodontic research. *Journal of Endodontics*, 21(11), 561–568.

Niinimäki, K., Siltanen, S., & Kolehmainen, V. (2007). Bayesian multiresolution method for local tomography in dental x-ray imaging. *Physics in Medicine and Biology, 52,* 6663-6678.

Nikopoulos, N. & Pitas, I. (1997). An Efficient Algorithm for 3D Binary Morphological Transformations with 3D Structuring Elements of Arbitrary Size and Shape. *Proceedings of IEEE Workshop on Nonlinear Signal and Image Processing (NSIP'97).*

Ning, P., & Bloomenthal, J. (1991). An evaluation of implicit surface tilers. *Computer Graphics, 13*(6), 33-41.

Niyazi, M., Niyazi, I., & Belka, C. (2007). Counting colonies of clonogenic assays by using densitometric software. *Radiat Oncol, 2*(4).

Nizam, A., Gopal, R. N., Naing, L., Hakim, A. B., & Samsudin, A. R. (2006). Dimensional acuracy of the skulls models produced by rapid prototyping technology using stereolithography apprarus. Archives of orofacial sciences, 1, 60-66.

Nunn, J. H., N. E. C., T. J. Gillgrass, R. S. Hobson, N. J. Jepson, J. G. Meechan, and F. S. Nohl. (2003). The interdisciplinary management of hypodontia: background and role of paediatric dentistry. *British Dental Journal 194*, 245–251.

O'Higgins, P. (1999). Ontogeny and phylogeny: some morphometric approaches to skeletal growth and evolution. In M.A.J. Chaplain, G.D. Singh, J.C. McLachlan (Ed.), *On growth and form. Spatiotemporal pattern formation in biology* (pp. 373-393). New York: John Wiley & Sons.

Oakley, C., & Brunette, D. M. (2002). The use of diagnostic data in clinical dental practice. *Dent Clin North Am*, *46*(1), 87-115.

Ogunbodede, E. O., Fatusi, O. A., Folayan, M. O., & Olayiwola, G. (2005). Retrospective survey of antibiotic prescriptions in dentistry. *J Contemp Dent Pract. 15, 6*(2):64-71.

Ohazama, S. A. C. M., Miletich, I., & Sharpe, P. T. (2004). Stem-cell-based tissue engineering of murine teeth. *J Dent Res, 83*(7), 518-522.

Oi, T. & Saka, H. & Ide, Y. (2004). Three-dimensional observation of pulp cavities in the maxillary first premolar tooth using micro-CT. *International Endodontic Journal,* 37(1), 46-51.

Olabarriaga, S. D., & Smeulders, A. W. M. (2001). Interaction in the segmentation of medical images: A survey. *Medical image analysis, 5*, 127-142.

Ono, I., Abe, K., Shiotani, S., & Hirayama, Y. (2000). Producing a full-scale model from computed tomographic data with the rapid prototyping technique using the binder jet method: a comparison with the laser lithography method using a dry skull. *J Craniofac Surg, 11*, 527-537.

Oram, A. (1991). The hidden effects of computer engineering on user documentation. In T. T. Barker (Ed.), *Perspectives on software documentation, inquiries and innovations.* Amityville, NY: Baywood Press.

Otsu, N. (1979). A thresholding selection method from gray-scale histogram. *IEEE Trans. on Systems, Man, and Cybernetics.*, *9*(1).

Otto, T., & De Nisco, S. (2002). Computer-aided direct ceramic restorations: A 10-year prospective clinical study of Cerec CAD / CAM inlays and onlays. *Int J Prosthodont*, *15*, 122-128.

Otto, T., & Schneider, D. (2008). Long-term clinical results of chairside Cerec CAD / CAM inlays and onlays: a case series. *Int J Prosthodont, 21,* 53-59.

Oxford Optronix. *ColCount.* Retrieved March 23, 2008, from http://www.oxford-optronix.com/

Oysaed, H., & Ruyter, I. E. (1986). Composites for use in posterior teeth: mechanical properties tested under dry and wet conditions. *Journal of Biomedical Materials Research, 20,* 261-271.

Pai, S. S., & Zimmerman, J. L. (2002). Health Insurance Portability and Accountability Act (HIPAA). Implications for dental practice. *Dent Today. 21*(10), 106-11

Palmer, C. (1891). Palmer's dental notation. *Dent. Cosmos, 23*(March), 194.

Pan, Z., Yin, X., & Wu, G. (2004). Segmentation –based interpolation of 3D medical images. *ICCSA, LNCS3044*, (pp. 731-740).

PANDORA project: http://pandora.nla.gov.au/pandora/

Panitvisai, P., Messer, H. H. (1995). Cuspal deflection in molars in relation to endodontic and restorative procedures. *Journal of Endodontics, 21,* 57-61.

Papaspyridopoulos, P., & Lal, K. (2008) Complete arch implant rehabilitation using subtractive rapid prototyping and porcelain fused to zirconia prosthesis: A clinical report. *J Prosthet Dent 2008, (100), 165-172.*

Papavasiliou, G., Kamposiora, P., Bayne, S. C., & Felton, D. A. (1996). Three-dimensional finite element analysis of stress-distribution around single tooth implants as a function of bony support, prosthesis type, and loading during function. *J Prosthet Dent, 76*(6), 633-640.

Papers from the Preservation (2000) conference and presentations from the Information Infrastructures for Digital Preservation workshop are available on the RLG Web site: http://www.rlg.org/events/pres-2000/

Parel, S. M., & Triplett, R. G. (2004). Interactive imaging for implant planning, placement, and prosthesis construction. *J Oral Maxillofac Surg, 62*, 41-47.

Park, J.S., Chung, M.S., Hwang, S.B., Lee, Y.S., Har, D.H., & Park, H.S. (2005). *V*isible Korean human: Improved serially sectioned images of the entire body. *IEEE Transactions on Medical Imaging*, 24(3), 352–360.

Parker, S. P. (Ed.). (1984). *McGraw-Hill dictionary of physics.* New York: McGraw-Hill Book Company.

Parker, S., Shirley, P., Livnat, Y., Charles Hansen, C., & Sloan, P. P. (1998). Interactive ray tracing for isosurface rendering. In *IEEE Visualization '98*, pp. 233–238.

Pearson, G. J., & Hegarty, S. M. (1989). Cusp movement of molar teeth with composite filling materials in conventional and modified MOD cavities. *British Dental Journal, 166,* 162-165

Penn, R. W. (1986). A recording dilatometer for measuring polymerization shrinkage. *Dental Material*s, (2), 78-79.

Perceptive Instruments. *Sorcerer Colony Counter.* Retrieved March 23, 2008, from http://www.perceptive.co.uk/

Perriard, J., Wiskott, W. A., Mellal, A., Scherrer, S. S., Botsis, J., & Belser, U. C. (2002). Fatigue resistance of ITI implant-abutment connectors: A comparison of the standard cone with a novel internally keyed design. *Clin Oral Implants Res, 13*(5), 542-549.

Persson, L. G., Lekholm, U., Leonhardt, A., Dahlen, G., & Lindhe, J. (1996). Bacterial colonization on internal surfaces of Branemark system implant components. *Clin Oral Implants Res, 7*(2), 90-95.

Peters, O.A. & Laib, A. & Rüegsegger, P. & Barbakow, F. (2000). Three-dimensional analysis of root canal geometry by high-resolution computed tomography. *Journal of Dental Research,* 79(6), 1405-1409.

Petrie, C. S., & Williams, J. L. (2005). Comparative evaluation of implant designs: influence of diameter, length, and taper on strains in the alveolar crest. A three-dimensional finite-element analysis. *Clin Oral Implants Res, 16*(4), 486-494.

Petzold, R., Zeilhofer, H. F., & Kalender, W. A. (1999). Rapid prototyping technology in medicine-basics and applications. *Computerized medical imaging and graphics, 23*, 277-284.

Pfister, A., R. D. L., Laib, A., Bner, U. H., Schmelzeisen, R., Lhaupt, R. M. (2004). Biofunctional rapid prototyping for tissue-engineering applications: 3D bioplotting versus 3D printing. *Journal of Polymer Science: Part A: Polymer Chemistry, 42,* 624-638.

Pham, D. T., & Gault, R. S. (1998). A comparison of rapid prototyping technologies. *International journal of machine tools and manufacture, 38*, 1257-1287.

Pierrisnard, L., Hure, G., Barquins, M., & Chappard, D. (2002). Two dental implants designed for immediate loading: a finite element analysis. *Int J Oral Maxillofac Implants, 17*(3), 353-362.

Pierrisnard, L., Renouard, F., Renault, P., & Barquins, M. (2003). Influence of implant length and bicortical anchorage on implant stress distribution. *Clin Implant Dent Relat Res, 5*(4), 254-262.

Plotino, G. & Grande, N.M. & Pecci, R. & Bedini, R. & Pameijer, C.N. & Somma, F. (2006). Three-dimensional imaging using microcomputed tomography for studying tooth macromorphology. *Journal of the American Dental Association,* 137(11), 1555-1561.

Pluim, J. P., Maintz, J. B., & Viergever, M. A. (2003). Mutual-information-based registration of medical images: a survey. *IEEE Trans Med Imaging, 22*(8), 986-1004. Review.

Pok, G., Liu J. C., & Nair A. S. (2003). Selective removal of impulsive noise based on homogeneity level information. *IEEE Trans. Image Processing, 12*(1), 85-92.

Polesel, V., Ramponi, G., & Mathews V. J. (2000). Image enhancement via adaptive unsharp masking. *IEEE Trans. Image Processing, 9*(3), 505-510.

Pongracz, F., & Bardosi, Z. (2007). Navigated drilling for dental implants based on virtual occlusion analysis: presentation of a new approach. *Proc.of 4th International Conference on Computer Aided Surgery Around the Head,* Innsbruck, (pp. 125-127).

Pongracz, F., & Bardosi, Z. (2006). Dentition planning with image-based occlusion analysis, *International Journal of CARS (Computer Assisted Radiology and Surgery), 1*(3), 149-156.

Pongracz, F., Bardosi, Z., & Szabo, L. (2005). Dentition planning for image-guided implantology. In *Proc. of CARS (Computer Assisted Radiology and Surgery), International Congress Series, Chicago, 1268,* (pp. 1168-1173).

Pongracz, F., Szabo, L., & Bardosi, Z. (2007). Planning and navigation tools for dental implantology. *Proc.of Automatisierungstechnische Verfahren für die Medizin Nr.267,* München, (pp. 41-42).

Pontes, F., Pontes, H., Adachi, P., Rodini, C., Almeida, D., Pinto, D. Jr. (2008). Gingival and bone necrosis caused by accidental sodium hypochlorite injection instead of anaesthetic solution. *Int Endod J, 41*(3), 267-70.

Preservation 2000: an International Conference on the Preservation and Long Term Accessibility of Digital Materials: http://www.ukoln.ac.uk/events/cedars-2000/

Press, W. H., Teukolsky, S. A., Vetterling, W. T., & Flannery, B. P. (1992). *Numerical Recipes in C. The Art of Scientific Computing.* Cambridge: Cambridge University Press.

Progen Scientific. *Schuett ColonyQuant automatic colony counter.* Retrieved March 23, 2008, from http://www.progensci.co.uk/

Project Prism: http://www.prism.cornell.edu/main.htm

Putman, M., Burton, R., & Nahm, M. H. (2005). Simplified method to automatically count bacterial colony forming unit. *J Immunol Methods, 302*(1-2), 99-102.

Rada, R. E. (1995). Document imaging and the patient chart: Envisioning the future for your practice. Ill *Dent J, 64*(3), 127-32.

Rangert, B., Krogh, P. H., Langer, B., & Van Roekel, N. (1995). Bending overload and implant fracture: a retrospective clinical analysis. *Int J Oral Maxillofac Implants, 10*(3), 326-334.

Rangert, B., Sennerby, L., Meredith, N., & Brunski, J. (1997). Design, maintenance and biomechanical considerations in implant placement. *Dent Update, 24*(10), 416-420.

Ranta, JF. & Aviles, WA. (1999). The Virtual Reality Dental Training System - Simulating Dental Procedures for the Purpose of Training Dental Students Using Haptics. *Proceedings of the Fourth PHANTOM Users Group Workshop*, 73-77.

Rantala, M., Vänskä, S., Järvenpäa, S., Kalke, M., Lassas, M., Moberg, J. et al. (2006). Wavelet-based reconstruction for limited-angle x-ray tomography. *IEEE Transactions on Medical Imaging, 25*, 210-216.

Raya, S. P., & Udupa, J. K. (1990). Shape-based interpolation of miltidimensional objets. *IEEE trans on medical imaging, 1*, 32-42.

Reddy, M. S., Mayfield-Donahoo, T., Vanderven, F. J., & Jeffcoat, M. K. (1994). A comparison of the diagnostic advantages of panoramic radiography and computed tomography scanning for placement of root form dental implants. *Clin Oral Implants Res.* Dec, *5*(4), 229-38.

Regber, K. (2002). *Auswirkungen eines Kaukrafttrainings auf die Kaumuskulatur.* Freiburg i.Br.: Inaugural-Dissertation.

Reich, S., Wichmann, M., Nkenke, E., & Proeschel, P. (2005). Clinical fit of all-ceramic three-unit fixed partial dentures, generated with three different CAD / CAM systems. *Eur J Oral Sci*, *113*, 174-179.

Reis-Schmidt, T. (2000). Clinical software & electronic charting--Essential tools. *Compend Contin Educ Dent*, *21*(5), 416-21.

Remmler, D., Olson, L., Duke, D., Ekstrom, R., Matthews, D., & Ullrich, C. G. (1989). Presurgical finite element analysis from routine computed tomography studies for craniofacial distraction: II. An engineering prediction model for gradual correction of asymmetric skull deformities. *Plast Reconstr Surg, 102,* 1395-1404.

Reynolds, P. A., Harper, J., & Dunne, S. (2008). Better informed in clinical practice - A brief overview of dental informatics. *British Dental Journal*, *204*, 313-317.

Rhodes, J.S. & Ford, T.R. & Lynch, J.A. & Liepins, P.J. & Curtis, R.V. (1999) Micro-computed tomography: a new tool for experimental endodontology. *International Endodontic Journal,* 32(3), 165-170.

Rhodes, J.S. & Ford, T.R. & Lynch, J.A. & Liepins, P.J. & Curtis, R.V. (2000). A comparison of two nickel-titanium instrumentation techniques in teeth using microcomputed tomography. *International Endodontic Journal,* 33(3), 279-285.

Richardson W. H. (1972). Bayesian-based iterative method of image restoration. *J. Opt. Soc. Amer., 62*, 55-59

Richter, E. J. (1998). In vivo horizontal bending moments on implants. *Int J Oral Maxillofac Implants, 13*(2), 232-244.

Ricketts, R. M. (1960). A foundation for cephalometric communication. *American Journal of Orthodontics, 46*, 330-357.

Rieger, M. R., Adams, W. K., & Kinzel, G. L. (1990). A finite element survey of eleven endosseous implants. *J Prosthet Dent, 63*(4), 457-465.

Rieger, M. R., Adams, W. K., Kinzel, G. L., & Brose, M. O. (1989). Finite element analysis of bone-adapted and bone-bonded endosseous implants. *J Prosthet Dent, 62*(4), 436-440.

Rieger, M. R., Mayberry, M., & Brose, M. O. (1990). Finite element analysis of six endosseous implants. *J Prosthet Dent, 63*(6), 671-676.

Ritter, A. B., S. R., & Michniak, B. B. (2005). Tissue Engineering. In S. R. Aurthur, B. Ritter, & B. B. Michniak (Eds.), *Biomedical engineering principles* (p. 596). CRC Press, Taylor & Francis Group.

Robb, R. A. (1999). 3D visualization in biomedical applications. *Ann Reviews in Biomedical engineering, 01*, 377-399.

Robb, R.A., & Hanson, D.P. (2006). Biomedical Image Visualization Research Using the Visible Human Datasets. *Clinical Anatomy,* 19(3), 240–253.

Rocci, A., Martignoni, M., & Gottlow, J. (2003). Immediate loading in the maxilla using flapless surgery, implants placed in predetermined positions, and prefabricated provisional restorations: a retrospective 3-year clinical study. *Clin Implant Dent Relat Res.*, 5(Suppl 1), 29-36.

Rogers, E. M. (2003). *Diffusion of innovations*, Fifth Edition. New York: Free Press.

Rose, J.T. & Buchanan, J. & Sarrett, DC. (1999). Software reviews – the DentSim system. *Journal Dental Education* 63(5), 421–423.

Roy, M. (2008). Your data breach was probably avoidable. *eWeek, 25*(19):24.

Ruttimann, U. E., Groenhuis, R. A. J., & Webber, R. L. (1984). Restoration of digital multiplane tomosynthesis by a constrained iteration method. *IEEE Transactions on Medical Imaging, 3*, 141-148.

Ryan, G., Pandit, A., & Apatsidis, D. P. (2006). Fabrication methods of porous metals for use in orthopaedic applications. *Biomaterials*, *27*, 2651-2670.

Sachlos, E., & Czernuszka, J. T. (2003). Making tissue enginnering scaffold work. Review on the application of solid freeform fabrication technology to the production of tissue engineering scaffolds. *European Cells and materials*, *5*, 29-40.

Sachlos, E., N. R., C. Ainsley, B. Derby, J.T. Czernuszka. (2003). Novel collagen scaffolds with predefined internal morphology made by solid freeform fabrication. *Biomaterials, 24*, 1487-1497.

Saeed, M., Rabiee, H. R., Kar, W. C., & Nguyen, T. Q. (1997). Bayesian restoration of noisy images with the EM algorithm. In *Proceedings of the ICIP 1997,* (pp. 322-5).

Sakaguchi, R. L. & Berge, H. X. (1998). Reduced light energy density decreases post-gel contraction while maintaining degree of conversion in composites. *Journal of Dentistry, 26*, 695-700.

Sakaguchi, R. L., Versluis, A., & Douglas, W. H. (1997). Analysis of strain gauge method for measurement of post-gel shrinkage in resin composites. *Dental Materials, 13*, 233-239.

Salo, S., Salo, H., Liisanantti, A., & Reponen, J. (2007). Data transmission in dental identification of mass disaster victims. *J Forensic Odontostomatol.*, *25*(1), 17-22.

Sanna, A., Molly, L., & Van Steenberghe, D. (n.d.). Immediately loaded CAD-CAM manufactured fixed complete dentures using flapless implant placement procedures: A cohort study of consecutive patients. *The Journal of Prosthetic Dentistry*, *97*(6), 331 – 339.

Sarment, D. P., Sukovic, P., & Clinthorne, N. (2003). Accutacy of implant placement with a stereolithographic surgical guide. *Int J Maxillofac Implants, 18*, 571-577.

Sato, Y., Shindoi, N., Hosokawa, R., Tsuga, K., & Akagawa, Y. (2000). A biomechanical effect of wide implant placement and offset placement of three implants in the posterior partially edentulous region. *J Oral Rehabil*, *27*(1), 15-21.

Sato, Y., Wadamoto, M., Tsuga, K., & Teixeira, E. R. (1999). The effectiveness of element downsizing on a three-dimensional finite element model of bone trabeculae in implant biomechanics. *J Oral Rehabil*, *26*(4), 288-291.

Satoh, T., Maeda, Y., & Komiyama, Y. (2005). Biomechanical rationale for intentionally inclined implants in the posterior mandible using 3D finite element analysis. *Int J Oral Maxillofac Implants*, *20*(4), 533-539.

Schenone, A., Firenze, F., Acquarone, F., Gambaro, M., Maasulli, F., & Abdreucci, L. (1996). Segmentation of multivariate medical images via unsupevised clustering with 'adaptive resolution'. *Computerized madincal imaging and graphics, 20*, 119-129.

Schleyer, T. (1995). *TEPR95 Proceedings*, (pp. 299-306). Newton, MA: Medical Record Institute.

Schleyer, T. K. (2004). Why integration is key for dental office technology. *J Am Dent Assoc*, *135*(Suppl), 4S-9S.

Schleyer, T. K. (2004). Should dentistry be part of the National Health Information infrastructure?. *J Am Dent Assoc*, *135*(12), 1687-95.

Schleyer, T. K., Thyvalikakath, T. P., Spallek, H., Torres-Urquidy, M. H., Hernandez, P., & Yuhaniak, J. (2006). Clinical computing in general dentistry. *J Am Med Inform Assoc*, *13*, 344-52.

Schleyer, T., & Spallek, H. (2001). Dental informatics. A cornerstone of dental practice. *J Am Dent Assoc, 132*(5), 605-13.

Schleyer, T., Spallek, H., & Hernandez, P. (2007). A qualitative investigation of the content of dental paper-based and computer-based patient record formats. *J Am Med Inform Assoc*, *14*, 515-526.

Schleyer, T., Speller, H., Battling, W. C., & Corby, P. (2003). The technologically well-equipped dental office. *J Am Dent Assoc*, *134* 30-41.

Schlie, S. (2007). Three-Dimensional Cell Growth on Structures Fabricated from ORMOCER® by Two-Photon Polymerization Technique. *Journal of Biomaterials Applications*, *22*, 275-287.

Schmuth, G. P. F., Freisfeld, M., Koster, O., & Schuller, H. (1992). The application of computerized tomography (CT) in cases of impacted maxillary canines. *European Journal of Orthodontics*, *14*, 296-301.

Schroeder, W., Martin, K., & Lorensen, B. (2006). *The visualization toolkit. An object-oriented approach to 3D graphics.* Clifton Park: Kitware

Schultheiss, D., D. A. B., Jorg Wefer, Udo Jonas. (2000). Tissue engineering from Adam to the zygote: Historical reflections. *World J Urol*, *18*, 84-90.

Schulze, R., Brüllmann, D. D., Röder, F., & d'Hoedt, B. (2004). Determination of projection geometry from quantitative assessment of the distortion of spherical references in single-view projection radiography. *Medical Physics*, *31*, 2849-2854.

Schulze, R., Heil, U., Weinheimer, O., Groß, D., Bruellmann, D. D., Thomas, E. et al. (2008). Accurate registration of random radiographic projections based on three spherical references for the purpose of few-view 3D reconstruction. *Medical Physics*, *35*, 546-555.

Schutze, H. J. (2001). Walk with a pen, or fly with a computer. Can electronic dentistry work for you? *N Y State Dent J*, *67*(10), 24-9.

Seipel, S. & Wagner, I.V. & Koch, S. & Schneide, W. (1998). Oral implant treatment planning in a virtual reality environment. *Computer Methods and Programs in Biomedicine*, 57(1), 95-103.

Sensable Technologies Inc. (2006). Available from: http://www.sensable.com

Sertgoz, A. (1997). Finite element analysis study of the effect of superstructure material on stress distribution in an implant-supported fixed prosthesis. *Int J Prosthodont*, *10*(1), 19-27.

Sertgoz, A., & Guvener, S. (1996). Finite element analysis of the effect of cantilever and implant length on stress distribution in an implant-supported fixed prosthesis. *J Prosthet Dent*, *76*(2), 165-169.

Sfikas, P. M. (2003). HIPAA security regulations. Protecting patients' electronic health information. *J Am Dent Assoc*, *134*, 640-643.

Shaughnessy, A. F., & Nickel, R. O. (1989). Prescription-writing patterns and errors in a family medicine residency program. *J Fam Pract*, *29*, 290–5.

Shelley, P. Q., Johnson, B. R., & BeGole, E. A. (2007). Use of an electronic patient record system to evaluate restorative treatment following root canal therapy. *Journal of Dental Education*, *71*, 1333-1339.

Shepp, L. A., & Vardi, Y. (1982). Maximum likelihood reconstruction for emission tomography. *IEEE Trans. Med. Imag.*, *1*, 113-122.

Shewchuk, J. R. (1994). An introduction to the conjugate gradient method without the agonizing pain. *Unpublished Work, (http://www.cs.cmu.edu/~quake-papers/painless-conjugate-gradient.pdf, June 2008).*

Shi, X.-Q., Han, P., Welander, U., & Angmar-Månsson, B. (2001). Tuned-aperture computed tomography for detection of occlusal caries. *Dentomaxillofacial Radiology*, *30*, 45-49.

Shibano K., et al (1999): Approved minutes of the UTC 81 / L2 178 Joint Meeting Mission Viejo, CA –October 26-29.

Shrimpton, P. C., Hillier, M. C., Lewis, M. A., & Dunn, M. (2003). Doses from Computed Tomography (CT) examinations in the UK – 2003 Review. *National Radiological Protection Board*. Retrieved March 16, 2008, from http://www.hpa.org.uk/radiation/publications/w_series_reports/2005/nrpb_w67.pdf

Siessegger, M., Schneider, B. T., Mischkowski, R. A., Lazar, F., Krug, B., & Klesper, B. (2001). Use of an image-guided navigation system in dental implant surgery in anatomically complex operation sites. *J Craniomaxillofac Surg*, *29*, 276-81.

Sigmund, O., & Toruato, S. (1997). Design of materials with extreme thermal explansion using a three-phase topology optimization method. *Journal of mechanics and physics*, *45*, 1037-1067.

Siltanen, S., Kolehmainen, V., Järvenpäa, S., Kaipio, J. P., Koistinen, P., Lassas, M. et al. (2003). Statistical inversion for medical x-ray tomography with few radiographs: I. General theory. *Physics in Medicine and Biology, 48,* 1437-1463.

Simmons, C. A., Meguid, S. A., & Pilliar, R. M. (2001). Differences in osseointegration rate due to implant surface geometry can be explained by local tissue strains. *J Orthop Res, 19*(2), 187-194.

Singare, S., Liu, Y., Li, D., Wang, J., & He, S. (2008). Individually prefabricated prosthesis for maxilla reconstruction. *J Prosthodont, 17,* 135-40.

Sittig, D. F., Kirshner, M., & Maupomé, G. (2003). Grand challenges in dental informatics. *Adv Dent Res, 17,* 16-19.

Slice, D. E. (2005). Modern morphometrics. In D. E. Slice (Ed.), *Modern morphometrics in physical anthropology* (pp. 1-45). New York: Kluwer Academic / Plenum Publishers.

Snow, M.D. & Graham, J.A. & Yates, W.J. (1996). Interactive computer technologies in dentistry. Virtual reality in orthodontics. *Studies in health technology and informatics,* 29, 411-422.

Snyder, T. L. (1995). Integrating technology into dental practices. *J Am Dent Assoc., 126,* 171-178.

Sone, S., Kasuga, T., Sakai, T., Kawai, T., Oguchi, K., Hirano, F. et al. (1995). Image processing in the digital tomosynthesis for pulmonary imaging. *European Radiology, 5,* 96-101.

Spatz, H. C., O'Leary, E. J., & Vincent, J. F. (1996). Young's moduli and shear moduli in cortical bone. *Proc Biol Sci, 263*(1368), 287-294.

Spoor, F., Jeffery, N., & Zonneveld, F. (2000). *Imaging skeletal growth and evolution*. London: The linnean society of London.

Stamm, T. & Kaup, M. & Hohoff, A. & Meier, T. & Meyer, U. (2003). Validity of a three-dimensional public-domain system for contemporary endodontic research. *Journal of Endodontics,* 29(12), 801-805.

Stark, D. D., & Bradley, W. G. (1999). *Magnetic resonance imaging.* St. Louis: C.V. Mosby.

Stegaroiu, R., Sato, T., Kusakari, H., & Miyakawa, O. (1998). Influence of restoration type on stress distribution in bone around implants: a three-dimensional finite element analysis. *Int J Oral Maxillofac Implants, 13*(1), 82-90.

Steinberg, A. D., Ashrafi, S., Žefran, M., & Kolesnikov, M. (2008). Facilitate learning periodontal probing skills by using a CD with 3D video recordings. *ADEA 85th Annual Session and Exhibition.*

Steinberg, A. D., Bashook, P. G., Drummond, J. L., Ashrafi, S., & Žefran, M. (2007). Assessment of faculty perception of content validity of PerioSim, a haptic-3D virtual reality dental training simulator. *Journal of Dental Education, 17,* 1574–1582.

Steinberg, A. D., Drummond, J. L., Bashook, P. G., Žefran, M., & Ashrafi S. (2006). Haptic 3D virtual reality dental training simulator reality validation. *Journal of Dental Research, 85*(A), 1264.

Stevens, B., Yang, Y., Mohandas, A., Stucker, B., & Nguyen, K. T. (2008). A review of materials, fabrication methods, and strategies used to enhance bone regeneration in engineered bone tissues. *Appl Biomaterials, 85B*, 573-582.

Strub, J. R., Rekow, E. D., & Witkowski, S. (2006). Computer-aided design and fabrication of dental restorations. *J Am Dent Assoc, 137,* 1289-1296.

Suetens, P., Bellon, E., Vandermeulen, D., Smet, M., Marchal, G., Nuyts, J., & Mortelmans, L. (1993). Image segmentation : Methods and applications in diagnostic radiology and nuclear medicine. *European journal of radiology, 17*, 14-21.

Suh, B. I., Feng, L., Wang, Y., Cripe, C., Cincione, F., & de Rijk, W. (1999). The effect of the pulse-delay cure technique on residual strain in composites. *Compendium of Continuing Education in Dentistry, 20*(2 Suppl), 4-12.

Sukovic, P. (2003). Cone beam computed tomography in craniofacial imaging. *Orthodontics & Craniofacial Research, 6*(Suppl 1), 31-36.

Suliman, A. A., Boyer, D. B., & Lakes, R. S. (1993). Interferometric measurements of cusp deformation of teeth restored with composite. *Journal of Dental Research, 72*, 1532-1536.

Sullivan, D. (2008). [Dental record systems]. Unpublished personal communication.

Sumita, Y., M. J. H., Takayuki Ohara, Shuhei Tsuchiya, Hiroshi Sagara, Hideaki Kagami, Minoru Ueda. (2006). Performance of collagen sponge as a 3-D scaffold for tooth-tissue engineering. *Biomaterials, 27*, 3238–3248.

Sun, W. (2002). *CT/MRI Based 3D reconstruction*. MEM Dept. Drexel University.

Sun, W., & Pallavi, L. (2002). Recent development on computer aided tissue engineering-a review. *Computer methods and programs in biomedicine, 67*, 85-103.

Sun, W., Drling, A., Starly, B., & Nam, J. (2004). Computer- aided tissue engineering: overview, scope and challenges. *Biotechnol Appl Biochem, 39*, 29-47.

Sun, W., Starly, B., Drling, A., & Gomez, C. (2004). Computer-aided tissue engineering: application to biomimetic modelling and design of tissue scaffolds. *Biotechnol Appl Biochem, 39*, 49-58.

Sun, Y. C., Lu, P. J., Wang, Y., Han, J. Y., & Zhao, J. J. (2007). Research and development of computer-aided design and rapid prototyping technology for complete denture. *Zhonghua Kou Qiang Yi Xue Za Zhi, 42*, 324-329.

Suryanarayanan, S., Karellas, A., Vedantham, S., Baker, S. P., Glick, S. J., D'Orsi, C. J. et al. (2002). Evaluation of linear and nonlinear tomosynthetic reconstruction methods in digital mammography. *Academic Radiology, 8*, 219-224.

Suryanarayanan, S., Karellas, A., Vedantham, S., Glick, S. J., D'Orsi, C. J., Baker, S. P. et al. (2000). Comparison of tomosynthesis methods used with digital mammography. *Academic Radiology, 7*, 1085-1097.

Suzuki, H., & Toriwaki, J. (1991). Automatic segmentation of head MRI images by knowledge guided thresholding. *Computerized Medical Imaging and Graphics, 15*, 233-40.

Swennen, G. R. J., Schutyser, F., & Hausamen, J. E. (2006). *Three-dimensional cephalometry. A color atlas and manual*. Berlin: Springer-Verlag.

Swennen, G. R., Schutyser, F., Barth, E. L., De Groeve, P., & De Mey, A. (2006). A new method of 3-D cephalometry Part I: the anatomic Cartesian 3-D reference system. *J Craniofac Surg, 17*, 314-325.

Synbiosis. *aCOLyte and ProtoCOL SR/HR*. Retrieved March 23, 2008, from http://www.synbiosis.com/

Szekely, D. G., Milam, S., et al. (1996). Legal issues of the electronic dental record: security and confidentiality. *J Dent Educ, 60*(1), 19-23.

Tada, S., Stegaroiu, R., Kitamura, E., Miyakawa, O., & Kusakari, H. (2003). Influence of implant design and bone quality on stress/strain distribution in bone around implants: a 3-dimensional finite element analysis. *Int J Oral Maxillofac Implants, 18*(3), 357-368.

Tan, K. H., Chua, C. K., Leong, K. F., Cheah, C. M., Gui, W. S., Tan, W. S., & Wiria, F. E. (2005). Selective laser sintering of biocompatible polymers for application in tissue engineering. *Biomed Mater Eng, 15*, 113-124.

Tan, K. H., Chua, C. K., Leong, K. F., Naing, M. W., & Cheah, C. M. (2005). Fabrication and characterization of polymer (ether-ether-ketone)/-hydroxiapatite biocomposite scaffolds using laser sintering. *Proc Inst Mech Eng Part, 219*, 183-194.

Tanabe, K. (1971). Projection method for solving a singular system of linear equations and its applications. *Numerische Mathematik, 17,* 203-214.

Tantbirojn, D., Versluis, A., Pintado, M. R., DeLong, R., & Douglas, W. H. (2004). Tooth deformation patterns in molars after composite restoration. *Dental Materials, 20,* 535-542.

Terzopoulos, D., & Waters, K. (1990). Physically based facial remodeling, analysis and animation. *J Vis Compout Animation, 1*, 73-80.

The Global Technology Revolution: Bio/Nano/Materials Trends and Their Synergies with Information Technology by 2015. (2001), RAND.

The Unicode Standard, Version 5.0, Fifth Edition (2006). *The Unicode Consortium*. Addison-Wesley Professional, 27 October 2006. ISBN 0-321-48091-0

Thevenaz, P., Ruttimann, U. E., & Unser, M. (1995). Iterative multi-scale registration without landmarks. In B. Werner (Ed.), *Proceedings of the 1995 IEEE International Conference on Image Processing (ICIP`95), III,* 228-231. Los Alamitos, CA, 23-26.

Third European Report on Science & Technology Indicators (2003) - Towards acknowledge-based economy. European Commission (EC).

Thurfjell, L., McLaughlin, J., Mattsson, J., & Lammertse, P. (2002). Haptic interaction with virtual objects: the technology and some applications. *Industrial Robot: An International Journal, 29*(3), 210-215.

Tikhonov, A. N. (1963). Solution of incorrectly formulated problems and the regularization method. *Soviet Mathematics - Doklady, 4,* 1035-1038.

Tsiklakis, K., Donta, C., Gavala, S., Karayianni, K., Kamenopoulou, V., & Hourdakis, C. J. (2005). Dose reduction in maxillofacial imaging using low dose Cone Beam CT. *European Journal of Radiology, 56,* 413-417.

Tuncelli, B., Poyrazoglu, E., Koyluoglu, A. M., & Tezcan, S. (1997). Comparison of load transfer by implant abutments of various diameters. *Eur J Prosthodont Restor Dent, 5*(2), 79-83.

Türp, J. C., & Schindler, H.-J. (2002). Zum Zusammenhangt zwischen Okklusion und Myoarthropathien. *Schweiz. Monatsschr. Zahnmed*, *113*(9), 403-11.

Tyndall, D. A., Clifton, L., Webber, R. L., Ludlow, J. B., & Horton, R. A. (1997). TACT imaging of primary caries. *Oral Surgery, Oral Medicine, Oral Pathology, Oral Radiology, and Endodontology, 84,* 214-225.

Udupa, J. K. (1999). Three- dimensional visualization and analysis methodologies: A current prospective. *Radiographics, 19,* 783-806.

Udupa, J. K., Le BLANC, v. r., Zhuge, Y., Imielinska, C., Schmidt, H., Currie, L. M., Hirsch, B. E., & Woodburn, J. (2006). *Computerized medical imaging and graphics, 30*, 75-87.

Ulrici, V. (1982). *Experimentelle Untersuchungen am Miniaturschwein (Mini-LEWE) zur Auswirkung von unilateralen Okklusionsstörungen auf die Kaumuskulatur (Ein Beitrag zur Ätiologie des Schmerz-Dysfunktions-Syndroms).* Leipzig: Dissertation zur Promotion A.

Ulrici, V. (1991). *Die Veränderungen des arthromuskulären Gleichgewichts im orofazialen Organ durch unilaterale Interferenzen. Eine tierexperimentelle Untersuchung am* Minischwein. Leipzig: Habilitationsschrift.

Umar, H. (2002). Capabilities of computerized clinical decision support systems: The implications for the practicing dental professional. *J Contemp Dent Pract*, 1(3), 027-042.

Umar, H. (2002). Clinical decision-making using computers: Opportunities and limitations. *Dent Clin North Am*, *46*(3), 521-38.

University of Glasgow, Humanities Advanced Technology and Information Institute, MPhil in Digital Management and Preservation. http://www.hatii.arts.gla.ac.uk/Courses/DigitalMPhil/

UNSCEAR, United Nations Scientific Committee on the Effects of Atomic Radiation. (2000). *Sources and effects of ionizing radiation, Report to the General Assembly, with scientific annexes*. Report Vol. I. Retrieved February 18, 2008, from http://www.unscear.org/unscear/en/publications/2000_1.html

Unterbrink, G. L., & Muessner, R. (1995). Influence of light intensity on two restorative systems. *Journal of Dentistry, 23,* 183-189. Händel, L. (1986). *Experimentelle Untersuchungen am Miniaturschwein (Mini-LEWE) zur Auswirkung unilateraler Okklusionsstörungen auf die Mjorphologie der Strukturen beider Kiefergelenke (Ein Beitrag zur Ätiologie des Schmerz-Dysfunktions-Syndroms).* Leipzig: Dissertation zur Promotion A.

v. Schilcher, C. (2004). *Die Position des Condylus mandibulare – Eine kritische Literaturübersicht.* Würzburg: Inaugural-Dissertation.

Vacanti C. A. (2006). The history of tissue engineering. *J Cell Mol Med, 10,* 569-576.

Vail, N. K., Swain, L. D., Fox, W. C., Aufdlemorte, T. B., Lee, G., & Barlow, J. W. (1999). Materials for biomedical application. *Materials and Design, 20,* 123-132.

Vale, F. M., Castro, M., Monteiro, J., et al. (1997). Acrylic bone cement induces the production of free radicals by cultured human fibroblasts. *Biomaterials, 18,* 1133–5.

Van Assche, N., van Steenberghe, D., Guerrero, M. E., Hirsch, E., Schutyser, F., Quirynen, M. & Jacobs, R. (2007). Accuracy of implant placement based on pre-surgical planning of three-dimensional cone-beam images: a pilot study. *Journal of Clinical Periodontology, 34,* 816-821.

Van Der Velden, U. (1979). Probing force and the relationship of the probe tip to the periodontal tissues. *Journal of Clinical Periodontology, 6*(2), 106–114.

van Lenthe, G. H., van den Bergh, J. P., Hermus, A. R., & Huiskes, R. (2001). The prospects of estimating trabecular bone tissue properties from the combination of ultrasound, dual-energy X-ray absorptiometry, microcomputed tomography, and microfinite element analysis. *J Bone Miner Res, 16*(3), 550-555.

Van Oossterwyck, H., Duyck, J., Vander Sloten, J., Van der Perre, G., Jansen, J., Wevers, M., et al. (2000). Use of microfocus computerized tomography as a new technique for characterizing bone tissue around oral implants. *J Oral Implantol, 26*(1), 5-12.

Van Oosterwyck, H., Duyck, J., Vander Sloten, J., Van der Perre, G., De Cooman, M., Lievens, S., et al. (1998). The influence of bone mechanical properties and implant fixation upon bone loading around oral implants. *Clin Oral Implants Res, 9*(6), 407-418.

van Rietbergen, B., Majumdar, S., Newitt, D., & MacDonald, B. (2002). High-resolution MRI and micro-FE for the evaluation of changes in bone mechanical properties during longitudinal clinical trials: application to calcaneal bone in postmenopausal women after one year of idoxifene treatment. *Clin Biomech (Bristol, Avon), 17*(2), 81-88.

van Rossen, I. P., Braak, L. H., de Putter, C., & de Groot, K. (1990). Stress-absorbing elements in dental implants. *J Prosthet Dent, 64*(2), 198-205.

Van Schaik, P., Turnbull, T., Van Wersch, A., & Drummond, S. (2004). Presence within a mixed reality environment. *CyberPsychology & Behavior, 7*(5), 540–552.

Van Steenberghe, D., Glauser, R., Blombäck, U., Andersson, M., Schutyser, F., Pettersson, A., & Wendelhag, I. (2005). A computed tomographic scan-derived customized surgical template and fixed prosthesis for flapless surgery and immediate loading of implants in fully edentulous maxillae: a prospective multicenter study. *Clin Implant Dent Relat Res.*, 7(Suppl 1), S111-20.

van Zyl, P. P., Grundling, N. L., Jooste, C. H., & Terblanche, E. (1995). Three-dimensional finite element model of a human mandible incorporating six osseointegrated implants for stress analysis of mandibular cantilever prostheses. *Int J Oral Maxillofac Implants, 10*(1), 51-57.

Vaubert, V. M., Moon, P. C., & Love, B. J. (1999). Extractable free monomers from self-cured dental sealants resulting from dispensing errors. *J Biomed Mater Res, 48*(1), 5-8.

Veitz-Keenan, A., Berkowitz, G. S., Brandes, I., Goldberg, K. L., Hamlin, D. A., Margolin, R., & Oen, K. (2007). Practice-based research networks. *N Y State Dent J, 73*(3), 14-15.

Ventres, W., Kooienga, S., Vuckovic, N., Marlin, R., Nygren, P., & Stewart, V. (2006). Physicians, patients, and the electronic health record: An ethnographic analysis. *Ann Fam Med*, *4*(2), 124–131.

Versluis, A., & Tantbirojn, D. (2006). Filling cavities or restoring teeth? *Journal of Dental Sciences, 1,* 1-9.

Versluis, A., Tantbirojn, D., & Douglas, W. H. (1997). Why do shear bond tests pull out dentin? *Journal of Dental Research, 76,* 1298-1307.

Versluis, A., Tantbirojn, D., & Douglas, W. H. (1998). Do dental composites always shrink toward the light? *Journal of Dental Research, 77,* 1435-1445.

Versluis, A., Tantbirojn, D., & Douglas, W.H. (2004). Distribution of transient properties during polymerization of a light-initiated restorative composite. *Dental Materials, 20,* 543-553.

Versluis, A., Tantbirojn, D., Pintado, M. R., DeLong, R., & Douglas, W. H. (2004) Residual shrinkage stress distributions in molars after composite restoration. *Dental Materials, 20,* 554-564.

Verstreken, K. & Van Cleynenbreugel, J. & Marchal, G. & Van Steenberghe, D. & Suetens, P. (1996). Computer-assisted planning of oral implant surgery. An approach using virtual reality. *Studies in health technology and informatics,* 29, 423-434.

Viceconti, M., Muccini, R., Bernakiewicz, M., Baleani, M., & Cristofolini, L. (2000). Large-sliding contact elements accurately predict levels of bone-implant micromotion relevant to osseointegration. *J Biomech, 33*(12), 1611-1618.

Vincent, L., & Soille, P. (1991). Watersheds in digital spaces: an efficient algorithm based on immersion simulations. *IEEE Trans. on Pattern Analysis and Machine Intelligence, 13*(6), 583-598.

Vlachos, A. & Peters, J. & Boyd, C. & Mitchell, JL. (2001). Curved PN Triangles. *Proceedings of ACM Symposium on Interactive 3D Graphics.*

Vogel, A., Jakstat, H., & Jüde, H.-D. (1990). Experimentelle Untersuchungen zum Einfluß der Registrierkraft auf das Ergebnis der Stützstiftregistrierung. *Dtsch. Stomatol., 40,* 363-65.

Wagner, A. & Rasse, M. & Millesi, W. & Ewers, R. (1997). Virtual reality for orthognathic surgery: the augmented reality environment concept. *Journal of Oral Maxillofacial Surgery*, 55(5), 456-62.

Wagner, E. H. (1998). Chronic disease management: what will it take to improve care for chronic illness? *Eff Clin Pract*., *1*(1), 2-4.

Walker, L., Enciso, R., & Mah, J. (2005). Three-dimensional localization of maxillary canines with cone-beam computed tomography. *American Journal of Orthodontics and Dentofacial Orthopedics, 128,* 418-423.

Walker, R. J. (2002). HIPAA strategy for dental Schools. *J Dent Educ*., *66*(5), 624-33.

Walther, W. (1998). Knowledge through documentation: From patients' data records to the basis of knowledge." *Int J Comput Dent*, *1*(1), 18-28.

Wang, D. & Zhang, Y. & Wang, Y. & Lee, YS. & Lu, P. & Wang, Y. (2005). Cutting on triangle mesh: local model-based haptic display for dental preparation surgery simulation. *IEEE Transactions on Visualization and Computer Graphics*, 11(6), 671-683.

Watanabe, F., Hata, Y., Komatsu, S., Ramos, T. C., & Fukuda, H. (2003). Finite element analysis of the influence of implant inclination, loading position, and load direction on stress distribution. *Odontology, 91*(1), 31-36.

Web Site Profiler: http://www.cs.cornell.edu/Courses/cs501/2000fa/project-folder/profiler.htmli2010: Digital Libraries Initiative http://ec.europa.eu/information_society/activities/digital_libraries/index_en.htm

Webb, P. A. (2000).A review of rapid prototyping techniques (RP) in the medical and biomedical sector. *Journal of medical engineering and technology, 24*, 149-153.

Webb, S. (1988). *The Physics of medical imaging.* Adam Hilger, Bristol-Philadelphia-New York, (pp. 29-32, 571-576).

Webber, R. L. (1994). Self-calibrated tomosynthetic, radiographic-imaging system, method and device. US Patent [5,539,637]. USA.

Webber, R. L. (1997). Self-contained tomosynthetic, radiographic-imaging system, method and device. US Patent [5,668,844]. USA.

Webber, R. L., & Messura, J. K. (1999, November 11). An in vivo comparison of diagnostic information obtained from tuned-aperture computed tomography and conventional dental radiographic imaging modalities. *Oral Surgery, Oral Medicine, Oral Pathology, Oral Radiology, and Endodontology., 88,* 239-247.

Webber, R. L., Horton, R. A., Tyndall, D. A., & Ludlow, J. B. (1997). Tuned-aperture computed tomography (TACT). Theory and application for three-dimensional dento-alveolar imaging. *Dentomaxillofacial Radiology, 26,* 53-62.

Weber, N. A. (2006). *Untersuchung zur Präzision des intraoralen Stützstiftregistrates bei der Ermittlung der zentrischen Kieferrelation verglichen mit der maximalen Interkuspidationsposition funktionsgesunder Probanden*. Münster: Inaugural-Dissertation.

Weinstein, A. M., Klawitter, J. J., & Cook, S. D. (1979). Finite element analysis as an aid to implant design. *Biomater Med Devices Artif Organs, 7*(1), 169-175.

Weiss, N. A. (2002). *Introductory statistics.* Addison Wesley, sixth edition.

WHO. (2006). *Electronic health records: Manual for developing countries.* WHO, Manila, Philippines.

Wierchmann, D., Rummel, V., Thalheim, A., Simon, J. S., & Wierchmann, L. (2003). Customized brackets and archwires for lingual orthodontic treatment. *Americal journal of orthodontics and dentofacial orthopedics, 124,* 593-599.

Williams, K. R., Watson, C. J., Murphy, W. M., Scott, J., Gregory, M., & Sinobad, D. (1990). Finite element analysis of fixed prostheses attached to osseointegrated implants. *Quintessence Int, 21*(7), 563-570.

Williams, R. J., Bibb, R., & Rafic, T. (2004). A technique for fabricating patterns for removable partial denture frameworks using digitized casts and electronic surveying. *J Prosthet Dent, 91,* 85-88.

Williams, R. J., Bibb, R., Eggbeer, D., & Collis, J. (2006). Use of CAD/CAM technology to fabricate a removable partial denture framework. *J Prosthet Dent, 96,* 96-99.

Williams, R. L., Srivastava, M., Conaster, R., & Howell, J. N. Implementation and evaluation of a haptic playback system. *Haptics-e, 3*(3).

Winder, J., & Bibb, R. (2005). Medical rapid prototyping technologies: State of the art and current limitations for application in oral and maxillofacial surgery. *J Oral Maxillofac Surg, 63,* 1006-1015.

Winder, R. J., McKnight, W., McRitchie, I., Montgomery, D., & Wulf, J. (2006). 3D surface accuracy of CAD generated skull defect contour. *Stud Health Technol Inform 119,* 574-6.

Wollny, G. (2004). Analysis of changes in temporal series of medical images. *MPI Series for Human Cognitive and Brain Sciences, 43.* Leipzig, Germany.

Wong, N., Huffer-Charchut, H., & Sarment, D .P. (2007). Computer-aided design / computer-aided manufacturing surgical guidance for placement of dental implant: case report. *Implant Dentistry, 16,* 123-130.

Wu, M., Tinschert, J., Augthun, M., Wagner, I., Schadlich-Stubenrauch, J., Sahm, P. R., & Spiekermann, H. (2001). Application of laser measuring, numerical simulation and rapid prototyping to titanium dental castings. *Dental Materials, 17,* 102-108.

Wu, T., Moore, R. H., & Kopans, D. B. (2006). Voting strategy for artifact reduction in digital breast tomosynthesis. *Medical Physics, 33,* 2461-2471.

Wu, T., Moore, R. H., Rafferty, E. A., & Kopans, D. B. (2004). A comparison of reconstruction algorithms for breast tomosynthesis. *Medical Physics, 31,* 2636-2647.

Wurm, G., Tomancok, B., Holl, K., & Trenkler, J. (2004). Prospective study on cranioplasty with individual carbon fiber reinforced polymere (CFRP) implants produced by means of stereolithography. *Surg Neurol, 62,* 510-521.

Yau, H.-T. & Hsu, C.-Y. (2006). Development of a Dental Training System Based on Point-based Models. *Computer-Aided Design & Applications,* 3(6), 779-787.

Yeong, W. Y., Chua, C. K., & Leong, K. F. Chandrasekaran, M. (2004). Rapid prototyping in tisue engineering: challenges and potential. *TRENDS in Biotechnology, 22,* 643-650.

Yongbin, Z., Lifei, Z., Zhu, X. R., Lee, A. K., Chambers, M., & Lei, D. (2007). Reducing metal artifacts in cone-beam CT images by preprocessing projection data. *Int. J. Radiation Oncology, Biology, Physics. 67,* 924-932.

Young, C. S., Rose Asrican, H. A., Ravens, M., Troulis, M. J., Kaban, L. B., Vacanti, J. P., & Yelick, P. C. (2005). Tissue-engineered hybrid tooth and bone. *Tissue Engineering, 11*(9/10), 1599-1610.

Young, C. S., Vacanti, J. P., Honda, M., Bartlett, J. D., & Yelick, P. C. (2002). Tissue engineering of complex tooth structures on biodegradable polymer scaffolds. *J Dent Res, 81*(10), 695-700.

Young, F. A., Williams, K. R., Draughn, R., & Strohaver, R. (1998). Design of prosthetic cantilever bridgework supported by osseointegrated implants using the finite element method. *Dent Mater, 14*(1), 37-43.

Yu, I. H., & Wong, Y. K. (2008). Evaluation of mandibular anatomy related to sagittal split ramus osteotomy using 3-dimensional computed tomography scan images. *Int J Oral Maxillofac Surg, 37,* 521-528.

Yuhaniak, I. J., Fernando, S., Schleyer, T., & Spallek, H. (2007). Speech recognition in dental software systems: Features and functionality. *Stud Health Technol Inform, 129*(Pt 2), 1127-31.

Zampelis, A., Rangert, B., & Heijl, L. (2007). Tilting of splinted implants for improved prosthodontic support: a two-dimensional finite element analysis. *J Prosthet Dent, 97*(6 Suppl), S35-43.

Zein, I. (2002). Fused deposition modelling of novel structure archtecture for engineering applications. *Biomaterials, 23,* 1169-1185.

Zhang, S.X., & Heng, P.A., & Liu, Z.J (2006). Chinese visible human project. *Clinical Anatomy,* 19(3), 204-215.

Zhang, W., X. F. W., J.G.C. Wolke, Z. Bian, M.W. Fan And J.A. Jansen. (2005). Differentiation ability of rat postnatal dental pulp cells in vitro. *Tissue Engineering, 11*(3/4), 357-368.

Zhang, Y. G., Chan, H.-P., Sahiner, B., Wei, J., Goodsitt, M. M., Hadjiiski, L. M. et al. (2006). A comparative study of limited-angle cone-beam reconstruction methods for breast tomosynthesis. *Medical Physics, 33,* 3781-3795.

Zhang, Y. G., Chan, H.-P., Sahiner, B., Wu, Y.-T., Zhou, C., Ge, J. et al. (2007). Application of boundary detection information in breast tomosynthesis reconstruction. *Medical Physics, 34,* 3603-3613.

Ziedses, B. G. (1932). Eine neue Methode zur Differenzierung in der Röntgenographie (Planigraphie). *Acta Radiologica, 13,* 182-192.

Zitova, B., & Flusser, J. (2003). Image registration methods: a survey. *Image Vision Comput, 21,* 977–1000.

Zsigmondy A. (1874). A practical method for rapidly noting dental observations and operations. *Br. J. Dent. Science, 17,* 580.

Zuiderveld, K. (1994). Contrast limited adaptive histogram equalization. In *Graphics gems IV,* (pp. 474-485): Academic Press Professional, Inc.

Zvárová, J., Dostálová, T., Hanzlícek, P., Teuberová, Z., Nagy, M., Pies, M., Seydlová, M., Eliásová, H., & Simková, H. (2008). Electronic health record for forensic dentistry. *Methods Inf Med, 47*(1), 8-13.

Zysset, P. K., Guo, X. E., Hoffler, C. E., Moore, K. E., & Goldstein, S. A. (1999). Elastic modulus and hardness of cortical and trabecular bone lamellae measured by nanoindentation in the human femur. *J Biomech, 32*(10), 1005-1012.

About the Contributors

Andriani Daskalaki presently works in the field of molecular medicine and bioinformatics at the Max Planck Institute for Molecular Genetics in Berlin. She completed her PhD in 2002 on working in the applications of photodynamic therapy in the area of oral medicine from the Free University of Berlin. She received a two-year DAAD scholarship (1996-1998) for her research in the field of PDT. Dr. Daskalaki received a MS in Medical Informatics from TFH Berlin with her work in "Development of a documentation software for robot-assisted intraoral operations" and a MS degree in bioinformatics with her work in "Variance analysis of multifactor models in gene expression experiments with application to the identification of genetic markers for hypertension." She received a poster prize for her participation in the International Photodynamic Association Meeting in Nantes. She is the editor of the "Handbook of Research on Systems Biology Applications in Medicine" and has presented many oral presentations at national and international meetings. She is a founding member and committee member of the Greek Dental Laser Association. Her research interest areas include systems biology, PDT, and laser applications in dentistry.

* * *

Hideaki Amano was graduated Hiroshima University in 1979. He obtained PhD in the field of pediatric dentistry from Hiroshima University, Japan. He achieved for hospital information system of Hiroshima university medical hospital as an associate professor. He is now a professor of team dentistry of Hiroshima University Faculty of Dentistry. His interest is in study on the three dimensional growth and development of the maxillo-facial complex and dental treatment for handicapped children.

Oscar Arevalo DDS, ScD, MBA, MS is the chief of the Division of Dental Public Health at the University of Kentucky College of Dentistry. His major interests include delivery and financing of dental care; program evaluation; educational, training, and workforce issues; and advocacy, implementation, and evaluation of oral health policy. Dr Arevalo is an active member of the American Association of Public Health Dentistry, Hispanic Dental Association and the American Public Health Association where has served as Scientific Chair of the Oral Health Section. He is a diplomate of the American Board of Dental Public Health.

N. Alberto Borghese is associate professor at the Department of Computer Science of the University of Milano, where he teaches the courses of intelligent dystems and robotics, and is the director of the Laboratory of Applied Intelligent Systems. He graduated with full marks and honors from Politecnico of Milano in 1984-85; he was visiting scholar at the Center for Neural Engineering of USC in 1991, at the Department of Electrical Engineering of Caltech in 1992, and at the Department of Motion Capture of Electronic Arts, Canada in 2000. His research interests include quantitative human motion analysis and modeling, statistical learning from data, applications to vision, graphics and medical imaging. He has coauthored more than fourty peer-reviewed journal papers and holds nine international patents.

Amit Chattopadhyay is assistant professor of Epidemiology and Dental Public Health at the University of Kentucky Graduate School, College of Public Health, and College of Dentistry. He has a broad variety of research interests and scientific publications as author/editor of several books and book chapters and as principal author in peer-reviewed journals of repute encompassing epidemiology; applied biostatistics; pathology; HIV/AIDS; cancer-precancer; clinical trials; and health economics. Alongside those areas, he is currently developing research in *in-silico* simulation of biological processes, disease etiology and outcomes; life-like cellular automaton; application of imputation models in public health and dentistry; ethics and philosophy.

Wei-Bang Chen is a PhD candidate in the Computer and Information Sciences Department at University of Alabama at Birmingham (UAB), Birmingham, AL, USA. He received his MS degree in genetics from National Yang-Ming University in Taipei, Taiwan in 1999 and a MS degree in computer sciences from UAB in 2005. His main research interests include bioinformatics, multimedia data mining, image processing, and computer vision. His current research involves microarray image and data analysis, biological sequence clustering, biomedical video and image mining, and spam image mining.

Domenico Ciambrone is the founder and CEO NRGSYS Software sas, responsible for technical and marketing strategies where he has acquired a strong experience over the Dicom standard, focused on medical imaging applications, with 3 products in portfolio already in worldwide distribution, and 2 more large products under development. Previously he had been IT manager at Alenia Aerospace spa, L'Aquila plant, designing, developing and managing the software infrastructure to support the entire production and test cycle within the L'Aquila plant. He was also the integration engineer at Italtel spa, responsible for setup of high performance measurement and test stations and for a specific collaboration project with Hughes Aircraft Co. (USA). He has a Degree in IT engineering from Milan Politechnic.

Tiago Araujo Coelho de Souza is a Fulbright/Capes scholar working in his Doctor of Public Health degree in the College of Public Health at the University of Kentucky, USA. Dr. Coelho de Souza has a Master degree in dentistry with focus in public health from the Federal University of Minas Gerais and a dental degree from the Federal University of Para, both in Brazil. Dr. Coelho de Souza worked as a dental public health professional with some indigenous groups at the Brazilian Amazon rainforest and as a UNESCO consultant at the Brazilian National Health Foundation (Funasa), Ministry of Health.

Iuri Frosio is an assistant professor at the Computer Science Department of the University of Milan, where he teaches computer science and programming. He received his MSc and PhD in biomedical engineering in 2002 and 2006, respectively, from the Politecnico of Milan, Italy. His research interests include medical image processing, virtual reality, artificial intelligence and human movement analysis. He is author or coauthor of nine peer-reviewed journal papers and holds four international patents.

Thomas Gäbler is an uppergraduate student of informatics at the University of Applied Sciences in Leipzig. Before that he studied surveying and mapping. Since 2006 he works within the Department of Maxillofacial and Facial Plastic Surgery at Leipzig University in the field of image analysis tools and software for surgical interventions. Here he learned to programme in VTK which he now uses for most of the tasks. Together with Daniel Kruber he is responsible for the software tool introduced in Chapter V.

Demetrios Halazonetis received his dental education at the University of Athens Dental School and his orthodontic training at the Orthodontic Dept. of Tufts University, where he also completed a Master's of Science course. He has been in private practice of orthodontics in Athens, Greece since 1987. In 1994 he obtained the Doctor of Odontiatriki degree (equiv. to PhD) from the University of Athens, and in 2002 was elected assistant professor at the same university, where he has been involved in research and teaching at the Orthodontic Dept. Dr. Halazonetis has published more than 40 scientific papers. He is the author of the *Viewbox cephalometric software* and associate editor of the *Am J Orthod Dentofacial Orthop.* His research interests and areas of expertise include cephalometrics and computed tomography applications (3D cephalometrics and treatment planning), geometric morphometrics and facial aesthetics.

Naoji Hayashi received a DDS from Osaka University, Japan in 1995. Since 1998, he was a research associate of Department of Preventive Dentistry, Osaka University Graduate School of Dentistry. He obtained a PhD in a field of epidemiology, from Osaka University in 2003. Since 2005, he is a research associate of division of medical information, Osaka University Dental Hospital with research interest of medical informatics.

Alexander Hemprich graduated in medicine and dentistry and is director of the Department of Oral and Maxillofacial Plastic Surgery at Leipzig University since 1994. His major interest lies in the rehabilitation of patients suffering from cleft lip and palate.

Jörg Hendricks graduated in medicine 2004 at Leipzig University and afterwards began to study dentistry. He is affiliated with the Department of Oral and Maxillofacial Plastic Surgery at Leipzig University since 2004. His main research interest lies in image analysis which was also his medical doctor´s thesis (analysis of midfacial distraction on the basis of new CT-investigation techniques). He now works on structural 3D craniofacial analysis and applications for dental and maxillofacial rigid and non-rigid registration techniques.

Thomas Hierl graduated in dentistry and medicine and holds the post of a senior consultant at the Department Maxillofacial and Facial Plastic Surgery at Leipzig University. His major interests lie in plastic and reconstructive surgery, esp. the rehabilitation of patients suffering from cleft lip and palate. In this field he received his PhD on midfacial distraction osteogenesis in 2002. Further research work concentrates on 3D image analysis, biomechanics of the midface and surgical planning software.

Yasuyuki Hirose was born in Tokyo, Japan in 1958. He studied at Kyushu Dental College in Fukuoka, Japan, where he graduated, then obtain his Dental Degree in 1984. He obtained PhD in the field of brain research, at Tokyo Medical and Dental University in Tokyo in 1988. He worked as an anesthetist and a system architect at Dental Hospital in that university until 1998. He is currently a professor and chair of Medical informatics, (Medical) Hospital, University of the Ryukyu in Okinawa, Japan, from 1998. He has contributed as an international expert of ISO/TC215, for WG1 from 1997 to 2003, now for WG4 from 2004 and for WG3 from 2007. He also contributed to JIS X 0213:2000 and to Unicode 3.2.0 in 2002 in technical symbols for dentistry. His research areas are the modeling of clinical thinking process, knowledge management, and the confidentiality control when accessing clinical data.

Masatoshi Hitaka studied at Kyushu Dental College in Fukuoka, Japan, where he graduated, then obtained his Dental Degree in 1978 and his PhD in the field of periodontology in 1986, and worked as an assistant professor of periodontology and endodontology until 2004. He is currently a general practitioner (periodontist) and working as a member of the society of dental hospital information system of Japan Association for Medical Informatics.

Heike Hümpfner-Hierl graduated in dentistry and medicine and is affiliated with the Department of Maxillofacial and Facial Plastic Surgery at Leipzig University since 2006. Her special interests lie in aesthetic and reconstructive surgery. Her research fields cover 2D and 3D facial analysis in cleft lip and palate patients, functional surgical outcome and sleep related breathing disorders. In 2007 she received the scientific prize of the German Cleft Lip and Palate Society for her research work on 2D facial analysis and surgical outcome after rhinoplasty in cleft lip and palate patients.

Maxim Kolesnikov received his Dipl.-Ing. degree in automation engineering from Moscow State Institute of Steel and Alloys in 2004 and the MS degree in electrical and computer engineering from the University of Illinois at Chicago in 2007. He is currently working toward the PhD degree in electrical and computer engineering at the University of Illinois at Chicago. His research interests include robotics and haptics with the emphasis on haptic rendering algorithms, applications of haptics to sensorimotor skill acquisition, collaborative haptics, haptic perception.

Daniel Kruber is an uppergraduate student of informatics at the University of Applied Sciences in Leipzig. Since 2006 he works within the Department of Maxillofacial and Facial Plastic Surgery at Leipzig University in the field of image analysis tools and software for surgical interventions. Here he learned to programme in VTK which he now uses for most of the tasks. Together with Thomas Gäbler he is responsible for the software tool introduced in Chapter V.

Anka Lectic, DDS, PhD, has collaborated with Royal Medical School, Histochemistry Department, London, Dental College - Biochemistry, Fukuoka, Japan and "La Sapienza" University Rome, Italy.. Dr. Letic has dedicated her research interest for over 20 years to the regulatory role of growth factors in morphogenesis and postnatal development. Recently, she is very active in cranio-facial surgery, researching the role of growth factors within the oral and maxillo-facial implantology area, interfacial guided osteogenesis and biocompatibility of biomaterials: Ti, hydroxyapatite/ PLLA, organic-inorganic composites as implants and bone fillers. She deposited Patent: "Process of production of hydroxyapatite/poly-L-lactide (HAp/PLLA) composite biomaterial in various shapes and compositions for bone tissue repair. Dr, Letic is member of four International Organization dealing with medical devices.

Kleoniki Lyroudia received the Diploma of Dentistry in 1980 and the PhD degree in 1982, both from the School of Dentistry of the Aristotle University of Thessaloniki, Greece. From 1980 until now she has worked in the Department of Endodontology, School of Dentistry, Aristotle University of Thessaloniki as a scientific co-operator, lecturer, assistant professor and associate professor. During her sabbatical leaves she has worked at the Dental School of Giessen, Germany (1985 and 1986) and the Dental School, University of Toronto, Canada, (1988 and 2002). She has also spent seven months in the University of British Columbia, Vancouver, Canada, working in the Department of Electrical Engineering on items related to dental informatics. Since 1989 she is in close co-operation with the Department of Informatics, Aristotle University of Thessaloniki, Greece, participating in a number of joint research efforts in topics related to dentistry and informatics. Prof. Lyroudia has published 60 journal papers and has over 80 conference presentations. She has worked in three-dimensional reconstruction of teeth (internal and external morphology), three-dimensional reconstruction of biological structures of the dental pulp and, recently, in virtual endodontics. She was scientific responsible for Aristotle University of Thessaloniki in a number of European Union research projects (TASTY, BIOPATTERN). She also has limited private dental practice in the field of Endodontics.

Marianthi Manda was born in Athens, Greece 1977. She currenlty conducts her PhD in biomaterials and biomechanics in the School of Dentistry, at the Aristotle Universtity of Thessaloniki, in Greece. She is a gratuade of School of Dentistry, at the National and Kapodistrian University of Athens. She otained the degree of Master of Scinece from the Aristotle University of Thessaloniki, completing her graduate studies at the department of Fixed Prosthesis and Implant Prosthodontics. Her research activity concentrates at the links of computer-aided design, bio-engineering and nanomechanics of biological structures and biomaterials in Prosthetic Dentistry.

Ioannis Marras was born in Karditsa, Greece in 1980. He received the BS degree from the Department of Informatics, Aristotle University of Thessaloniki, Greece in 2005. He is currently a researcher and teaching assistant and studies towards his PhD degree at the Artificial Intelligence Information Analysis (AIIA) Laboratory, Department of Informatics, Aristotle University of Thessaloniki. His current research interests lie in the areas of medical image analysis, signal and image processing and computer vision.

Georgios Mikrogeorgis received the Diploma of Dentistry in 1995 and the PhD degree in Endodontology in 2003, both from the School of Dentistry of the Aristotle University of Thessaloniki, Greece. Since 1995, he is a researcher and teaching assistant in the Department of Endodontology, School of Dentistry, Aristotle University of Thessaloniki. He has co-authored 1 book chapter, 17 journal papers and 22 congress presentations. Dr. Mikrogeorgis was the recipient of the Hellenic Society of Endodontics research scholarship in 2004, and the Hellenic Society of Endodontics Award in 2006.

Noriaki Morimoto was born in Japan in 1962. He studied at dental department of Hiroshima University, where he graduated, then obtain his Dental Degree in 1987. He obtained PhD in the field of effect of laser irradiation on orthodontic tooth movement research, at that University in 1993. He worked as an orthodontist and a system architect at dental hospital information system in that university until 1997. He is currently the chief of dental hospital information system society at Japan Association for

Medical Informatics. He is also a member of the committee concerning the standardization of a dental term in MEDIS-DC(Medical Information System Development Center).

Yos Morsi has wide-ranging internationally recognised expertise in the area of engineering simulation including laser diagnostics techniques and recently in the area of Bio-manufacturing and Tissue engineering. He is an active member in the research community, participating in the organisation of various international conferences on modelling and simulations, and heart valve research. His recent work is concentrated on the use of Fused Deposition Modelling (FDM) Rapid Prototyping technology to produce implantable scaffold templates for tissue generation.

Hideaki Narusawa was born in 1959. He achieved his diploma in dentistry in 1986 and PhD in 1990 in the field of conservative dentistry from Showa University, Japan. His main work is clinical education of general practice. His research work is to apply computer technology to dentistry. He is currently a lecturer of Conservative Dentistry of Showa University, Tokyo.

Nikos Nikolaidis received the Diploma of Electrical Engineering in 1991 and the PhD degree in Electrical Engineering in 1997, both from the Aristotle University of Thessaloniki, Greece. From 1998 to 2002 he was postdoctoral researcher and teaching assistant at the Department of Informatics, Aristotle University of Thessaloniki. He is currently an assistant professor in the same Department. Dr. Nikolaidis is the co-author of the book "3-D Image Processing Algorithms" (Wiley, 2000). He has co-authored 12 book chapters, 29 journal papers and 91 conference papers. His research interests include computer graphics, image and video processing and analysis, copyright protection of multimedia, computer vision and 3-D image processing. Dr. Nikolaidis is currently serving as associate editor for the *EURASIP Journal on Image and Video Processing*, the *International Journal of Innovative Computing, Information and Control* and the *Innovative Computing, Information and Control Express Letters.*

Shital Patel has a strong background in biotechnology. She has worked on a number of projects ranging from plant tissue engineering, molecular biology, genetics to clinical biochemistry. She is currently doing her PhD on Tissue Engineering of Heart Valve Leaflets under Prof. Morsi. She has participated in various international conferences and has received various awards and scholarships. She intends to move ahead in the field of biomedical sciences.

Ioannis Pitas received the Diploma of Electrical Engineering in 1980 and the PhD degree in electrical engineering in 1985 both from the Aristotle University of Thessaloniki, Greece. Since 1994, he has been a professor at the Department of Informatics, Aristotle University of Thessaloniki. From 1980 to 1993 he served as scientific assistant, lecturer, assistant professor, and associate professor in the Department of Electrical and Computer Engineering at the same University. He served as a visiting research associate or visiting assistant professor at several Universities. He has published 157 journal papers, 405 conference papers and contributed in 23 books in his areas of interest and edited or co-authored another 7. He has also been an invited speaker and/or member of the program committee of several scientific conferences and workshops. In the past he served as associate editor or co-editor of four international journals and general or technical chair of three international conferences. His current interests are in the areas of digital image and video processing and analysis, medical image analysis, multidimensional signal processing, copyright protection of multimedia and computer vision. Prof. Pitas is an IEEE Fellow and member of the National Research Council of Greece.

Ferenc Pongracz, after finishing his studies in Technical University of Budapest, has engaged in different fields of biomedical engineering. He spent the last 16 years with innovative research and development on image-guided surgical applications. Started with ARTMA Biomedical Inc, Vienna, Austria, he developed computer algorithm for augmented reality studies with magnetic digitizer (3Space™, Polhemus Inc., USA) and later with optical tracking devices (Polaris, Northern Digital Inc., Canada). He participated in developing the ARTMA Virtual Implant® software which was among the first applications focusing on use of active navigation in dental implantology. Recently, he worked as project leader with Albadent Inc., in Hungary to develop a new application (Dental Planner) which integrates novel functional principles in computerized dental implantology.

Arnold D. Steinberg completed his undergraduate studies in pre-dentistry at the University of Illinois at Chicago (UIC) and attended Northwestern University College of Dentistry where he received his DDS degree. He received the MS degree in biochemistry from the UIC College of Medicine. He was in part-time dental practice for over 30 years and was involved in a variety of research areas. He was a professor of Biochemistry at UIC and is currently a professor at the Department of Periodontics, UIC College of Dentistry. His current research interests include information technology in dentistry, creating interactive courses on CD-ROM, use of robotics and haptics technology in computer-based dental simulation programs.

Ichiro Suzuki graduated in 1981 from the Niigata University (Japan) and got a PhD in oral and maxillofacial surgery in 1985. Between 1985 and 2003 he was an assistant professor and a lecturer at the Department of Oral and Maxillofacial Surgery of Niigata University and University Dental Hospital. Since 2003 he is an associate professor at division of Community Health Promotion of Niigata University Medical and Dental hospital. His research interests cover the areas of medical and dental informatics, in particular regarding the hospital information system including EHR and the standardization in dental field. He also works on the regional medical liaison system.

Hiroo Tamagawa graduated from Osaka University (Japan) in 1979 and obtained his PhD in salivary research from Osaka University in 1986. From 1998 to 1990, he worked for Institute for Biomedical Research in University of Texas at Austin (U.S.A.) and researched epidemiological survey of Co-enzyme Q10. Since 1994, he works for division of interdisciplinary dentistry and division of medical information of Osaka University Dental Hospital, Japan, as an associate professor. He designed a hospital information system in Osaka University Dental Hospital. His interest covers the area of dental informatics, an application of information technology to dentistry and medicine, and ontology in medicine.

Daranee Tantbirojn is an assistant professor in the Division of Operative Dentistry, Department of Restorative Sciences, University of Minnesota School of Dentistry. She earned her DDS and Certificate in Operative Dentistry from Chulalongkorn University, Bangkok, Thailand. She pursued her MS in dental materials from the University of Alabama at Birmingham in 1991, and a PhD in oral biology/material sciences from University of Minnesota in 1998. Dr. Tantbirojn has taught dental materials, operative dentistry, and cariology at undergraduates and Advanced Training levels.

Antheunis Versluis is an assistant professor in the Minnesota Dental Research Center for Biomaterials and Biomechanics, Department of Restorative Sciences, University of Minnesota School of Dentistry. In

1988 he received his Ingenieur‘s degree in aerospace engineering at the Delft University of Technology, the Netherlands. In 1994 he received his PhD degree in numerical modeling and process analysis from the University of Greenwich, London, England for his research conducted at the University of Nijmegen, the Netherlands and the University of Minnesota, USA.

Andreas Vogel, adjunct professor, has attended School of Dentistry at the University of Leipzig, from 1967-72. Dr. Vogel’s diploma thesis was film documenting conditioned reflexes in rats. In post graduate, he attended the Department of Surgical Prosthetics and Facial Epithetics, University of Leipzig, in 1972 where his 1979 thesis explored blood flow measurement from the pulpa dentis by a nuclear diagnostic method. His 1986 postdoctorate work included the development of a nuclear method for registration of haemodynamic proceedings in small areas and implementation in the blood vessel system of the pulpa dentis. In 1987, he became assistant medical director and Facultas docendi in “Prosthetic dentistry.” He also founded the Institute for Medicine and Dental Technology GmbH Leipzig – IMD in 2002. And in 2003 he began his private practice. He has published and researched blood flow, ephitheses, masticatory muscles, temporomandibular joints, masticatory fores, relationship dentistry and tinnitus.

Gert Wollny studied mathematics at the University of Leipzig. After working as a software developer for a short time he joined the Max-Planck-Institute of Human Cognitive and Brain Sciences to work in image processing and in 2003 he received his PhD from the University of Leipzig on „The Analysis of Temporal Series of Medical Images“. Later he joined the group on Human Evolution of the MPI of Evolutionary Anthropology dedicating to image segmentation. Currently, Gert Wollny is with the Group of Biomedical Imaging Technologies at the ETSI Telecomunicación of the Universidad Politécnica of Madrid working in image registration.

Miloš Žefran completed his undergraduate studies in electrical engineering and mathematics at the University of Ljubljana, where he also received a MS degree in electrical engineering. He subsequently received a MS degree in mechanical engineering in 1995 and a PhD degree in computer science in 1996 from the University of Pennsylvania. From 1997 to 1999 he was a NSF postdoctoral scholar at the California Institute of Technology, after which he joined the Rensselaer Polytechnic Institute. Since 1999 he has been with the Department of Electrical and Computer Engineering at the University of Illinois at Chicago where he is currently an associate professor. His research interests are in robotics and control with applications to medical training, rehabilitation, and sensor networks.

Chengcui Zhang is an assistant professor of Computer and Information Sciences at University of Alabama at Birmingham (UAB) since August, 2004. She received her PhD from the School of Computer Science at Florida International University, Miami, FL, USA in 2004. She also received her bachelor and Master degrees in computer science from Zhejiang University in China. Her research interests include multimedia databases, multimedia data mining, image and video database retrieval, bioinformatics, and GIS data filtering. She is the recipient of several awards, including the IBM Unstructured Information Management Architecture (UIMA) Innovation Award, NSF IDBR Award, and UAB ADVANCE Junior Faculty Research Award from the National Science Foundation.

Index

E

F

G

H

O

P

R

S

T

U

V

W

X

Y

Z